PB85-235612

Proceedings of the 1982 Joint Symposium on Stationary Combustion NOx Control. Volume 2 Flue Gas Treatment, Fundamental Studies and Industrial/Commercial/Residential Applications

Acurex Corp., Mountain View, CA

Prepared for

Environmental Protection Agency
Research Triangle Park, NC

Jul 85

U.S. Department of Commerce
National Technical Information Service
NTIS

EPA/600/9-85/022b
July 1985

PROCEEDINGS OF THE 1982 JOINT SYMPOSIUM ON STATIONARY COMBUSTION NO_x CONTROL

PB85-235612

Volume II

Flue Gas Treatment, Fundamental Studies and Industrial/Commercial/Residential Applications

Symposium Cochairmen

Robert E. Hall and Dennis C. Drehmel, EPA
and
Michael W. McElroy, EPRI

Air and Energy Engineering Research Laboratory
Office of Research and Development
U.S. Environmental Protection Agency
Research Triangle Park, NC 27711

REPRODUCED BY
NATIONAL TECHNICAL
INFORMATION SERVICE
U.S. DEPARTMENT OF COMMERCE
SPRINGFIELD, VA. 22161

TECHNICAL REPORT DATA

(Please read Instructions on the reverse before completing)

1. REPORT NO. EPA/600/9-85/022b	2.	3. RECIPIENT'S ACCESSION NO. PB85 235612 /AS
4. TITLE AND SUBTITLE PROCEEDINGS OF THE 1982 JOINT SYMPOSIUM ON STATIONARY COMBUSTION NO_x CONTROL: Volume II. Flue Gas Treatment, Fundamental Studies, and Industrial/Commercial/Residential Applications		5. REPORT DATE July 1985 6. PERFORMING ORGANIZATION CODE
7. AUTHOR(S) Howard B. Mason, Compiler		8. PERFORMING ORGANIZATION REPORT NO.
9. PERFORMING ORGANIZATION NAME AND ADDRESS Acurex Corporation 555 Clyde Avenue Mountain View, California 94039		10. PROGRAM ELEMENT NO. 11. CONTRACT/GRANT NO. 68-02-3695
12. SPONSORING AGENCY NAME AND ADDRESS EPA, Office of Research and Development Air and Energy Engineering Research Laboratory Research Triangle Park, NC 27711		13. TYPE OF REPORT AND PERIOD COVERED Proceedings; 11/82-4/85 14. SPONSORING AGENCY CODE EPA/600/13

15. SUPPLEMENTARY NOTES AEERL project officers are Robert E. Hall (MD-65, 919/541-2477) and Dennis C. Drehmel (MD-4, 919/541-7505). EPRI project officer is Michael W. McElroy, 3412 Hillview Ave., Palo Alto, CA 94303.

16. ABSTRACT The proceedings document more than 50 papers describing recent advances in NOx control technology that were presented at the 1982 Joint Symposium on Stationary Combustion NOx Control. The papers covered the following topics: utility boiler field experience; NOx regulations; advanced combustion processes; NOx flue gas treatment; limestone injection SOx control; industrial process combustion; industrial, commercial, and residential systems; and fundamental combustion research.

17. KEY WORDS AND DOCUMENT ANALYSIS

a. DESCRIPTORS		b. IDENTIFIERS/OPEN ENDED TERMS	c. COSATI Field/Group	
Pollution	Flue Gases	Pollution Control	13B	
Nitrogen Oxides	Limestone	Stationary Sources	07B	08G
Boilers	Industrial Processes	Advanced Processes	13A	
Utilities				13H
Regulations			05D	
Combustion			21B	

18. DISTRIBUTION STATEMENT Release to Public	19. SECURITY CLASS (This Report) Unclassified	21. NO. OF PAGES 646
	20. SECURITY CLASS (This page) Unclassified	22. PRICE

EPA Form 2220-1 (9-73)

PREFACE

The 1982 Joint Symposium on Stationary Combustion NO_x Control was held November 1 through 4 in Dallas, Texas. This was the second symposium on NO_x control jointly sponsored by EPA and EPRI; the first was held in Denver in 1980. The symposium is a consolidation of EPRI's previous NO_x Control Technology Seminars and EPA's Symposia on Stationary Source Combustion. The objective of the symposium is to give attendees the opportunity to exchange information on the latest advances in combustion technology. Such an exchange of information contributes significantly to the development of cost-effective and reliable NO_x control systems.

Over 50 papers* were presented, beginning with an update of NO_x regulatory trends; focusing on development of control technology for coal-fired utility boilers, industrial power equipment, and process heaters; and discussing advances in fundamental combustion research. Speakers represented a wide variety of organizations including electric utility companies, manufacturers of utility boilers and process equipment, research and development groups conducting investigations sponsored by EPRI and EPA, as well as staff members of EPRI and EPA. Representatives from Japanese and West German utilities and boiler manufacturers provided status reports of activities in those countries, lending an international perspective to NO_x control issues.

Cochairmen of the symposium were Robert E. Hall and Dennis C. Drehmel of EPA, and Michael W. McElroy of EPRI. Introductory remarks were delivered by Robert C. Carr, program manager in the Air Quality Control Program of EPRI's Coal Combustion Systems Division, and the welcoming address was given by Frances Phillips, Deputy Regional Administrator for EPA Region VI. The Symposium Proceedings has been published in two volumes;

Volume I -- UTILITY BOILER APPLICATIONS

Session I:	NO_x Emissions Issues
Session II:	Manufacturer's Update of Commercially Available Combustion Technology
Session III:	Operational and Environmental Issues
Session IV:	Low-NO_x Combustion Development
Session V:	In-Furnace NO_x Destruction (Reburning)
Session VI:	Furnace Limestone Injection

Volume II -- FLUE GAS TREATMENT, FUNDAMENTAL STUDIES AND INDUSTRIAL/COMMERCIAL/RESIDENTIAL APPLICATIONS

Session VII:	Flue Gas Treatment
Session VIII:	Fundamental Combustion Studies
Session IX:	Stationary Engines and Industrial Process Systems
Session X:	Small Industrial, Commercial, and Residential Systems

* Portions of the work described in these proceedings were not funded by the U. S. Environmental Protection Agency; therefore, the contents do not necessarily reflect the views of the Agency and no official endorsement should be inferred.

CONTENTS

Paper | Page

PREFACE ii

INDTRODUCTORY REMARKS, Robert C. Carr, EPRI x

CLOSING REMARKS, Dennis C. Drehmel, EPA, IERL/RTP xiii

VOLUME I
UTILITY BOILER APPLICATIONS

SESSION I: NO_x EMISSIONS ISSUES
Chairman, Joshua S. Bowen, EPA, IERL/RTP

1 "Update on NO_x-Related Regulations," D. F. Walters 1-1

2 "A Utility Perspective on NO_x Control," C. H. Goodman 2-1

3 "Update on Acid Deposition," K. L. Demerjian (Abstract Only) 3-1

SESSION II: MANUFACTURERS' UPDATE OF COMMERCIALLY AVAILABLE COMBUSTION TECHNOLOGY
Chairman, David Eskinazi, EPRI

4 "Status of NO_x Controls for Riley Stoker Wall-Fired and Turbo-Fired Boilers," R. A. Lisauskas and A. H. Rawdon 4-1

5 "Foster Wheeler's Low NO_x Combustion Program Status and Developments," J. Vatsky 5-1

6 "Fossil Steam Generator NO_x Control Update," J. A. Barsin 6-1

7 "Status of Tangential Firing Low NO_x Technology", M. S. McCartney and R. J. Collette 7-1

(a) The information in this document has been funded wholly or in part by the United States Environmental Protection Agency. It has been subject to the Agency's peer and administrative review, and it has been approved for publication as an EPA document.

Paper Page

SESSION III: OPERATIONAL AND ENVIRONMENTAL ISSUES
Chairman, David G. Lachapelle, EPA, IERL/RTP

8 "Long Term Optimum Performance/Corrosion Tests of Combustion Modifications for Utility Boilers," J. M. Ferraro, P. S. Natanson, and R. M. Vaccaro . . . . 8-1[a]

9 "Analysis of Long-Term NO_x Emission Data From Pulverized Coal-Fired Utility Boilers," S. S. Cherry . . . . 9-1[a]

SESSION IV: LOW-NO_x COMBUSTION DEVELOPMENT
Chairman, G. Blair Martin, EPA, IERL/RTP

10 "NO_x Emissions Control With the Distributed Mixing Burner" Part I: "Field Evaluation on an Industrial-Size Boiler" B. Folsom, A. Abele, J. Reese and J. Vatsky . . . . 10-1[a]

Part II: "Thermal Environment and Heat Release Capacity Scaling" B. Folsom, R. Payne, A. Abelle and P. Nelson 10-23

11 "Part I: Evaluatiion of Tangential Fired Low NO_x Burner," Y. Takahashi, T. Sengoku, F. Nakashima, S. Kaneko, and K. Tokuda 11-1

"Part II: Feasibility Study of a Low-NO_x Retrofittable Firing System with U. S. Coals." A. Kokkinos, R. E. Donais, M. S. McCartney, and M. W. McElroy 11-26

12 "Low-NO_x Firing System for Tangentially Coal-Fired Utility Boilers -- Preliminary Testing," A. Kokkinos, R. D. Lewis, D. C. Borio, M. S. McCartney, J. M. Ferraro, and K. E. Keele. . 12-1[a]

13 "Economic and Engineering Analysis of Arch-Fired Furnaces," J. Vatsky and J. E. Cichanowicz. 13-1

14 "Status of Japanese Technical Development for Coal Combustion NO_x Control," Y. Nakabayashi, T. Miyasaka, and K. Mouri. . . . 14-1

(a) The information in this document has been funded wholly or in part by the United States Environmental Protection Agency. It has been subject to the Agency's peer and administrative review, and it has been approved for publication as an EPA document.

Paper Page

SESSION V: IN-FURNACE NO_x DESTRUCTION (REBURNING)
Chairman, Michael W. McElroy, EPRI

15 "Development of 'MACT' In-Furnace NO_x Removal Process for Steam Generators," Y. Takahashi, M. Sakai, T. Kunimoto, S. Ohme, H. Haneda, T. Kawamura, and S. Kaneko 15-1

16 "NO_x Reduction by Reburning with Gas and Coal -- Bench Scale Studies," S. L. Chen, W. C. Clark, M. P. Heap, D. W. Pershing, and W. R. Seeker. . . . . 16-1(b)

17 "Fuel Staging for Pulverized Coal Furnace NO_x Control," J. T. Kelly, R. L. Pam, and S. T. Suttmann. 17-1

18 "In-Furnace Control of NO_x Formation in Gas- and Oil-Fired Utility Boilers," L. J. Radak, A. Weir, Jr., B. G. Morton, M. N. Mansour, L. L. Smith, and S. E. Kerho 18-1

19 "A Review of In-Furnace NO_x Reduction and SO_x Reduction by Sorbent Injection," B. P. Breen and J. E. Gabrielson . . . . . 19-1(a)

SESSION VI: FURNACE LIMESTONE INJECTION
Chairman, James H. Abbott, EPA, IERL/RTP

20 "The Dry Additive Process for the Reduction of SO_2 Emission in Brown Coal Fired Boilers," 20-1

21 "Operation and Performance Report of the Steinmuller Low-NO_x SM-Burner and Its Potential Towards Utility Boiler SO_x Control via Sorbent Injection," M. Y. Chughtai, S. Michelfelder, and K. Leikert 21-1

22 "Low-NO_x Tangential System SO_x Control Through Sorbent Injection." S. Ohmine, R. J. Martin, J. T. Kelly, and E. K. Chu . . . . 22-1(a)

(a) The information in this document has been funded wholly or in part by the United States Environmental Protection Agency. It has been subject to the Agency's peer and administrative review, and it has been approved for publication as an EPA document.

(b) Although the information in this document has been funded wholly or in part by the United States Environmental Protection Agency, it does not necessarily reflect the views of the Agency and no official endorsement should be inferred.

Paper Page

23 "Feasibility of Furnace Injection of Limestone for SO_2 Control," A. Kokkinos, R. D. Lewis, D. C. Borio, A. L. Plumley, and M. W. McElroy 23-1

24 "IERL-RTP Research on Sulfur Capture in LIMB," R. H. Borgwardt, G. R. Gillis, and N. F. Roache . . . . 24-1(a)

25 "LIMB Testing: The Use of Dry Sorbents to Reduce Sulfur Oxide Emissions from Pulverized Coal Flames Under Low-NO_x Conditions," P. O. Case, M. P. Heap, R. Payne, and D. W. Pershing . . . . . 25-1(a)

VOLUME II
FLUE GAS TREATMENT, FUNDAMENTAL STUDIES AND INDUSTRIAL/COMMERCIAL/RESIDENTIAL APPLICATIONS

SESSION VII: FLUE GAS TREATMENT
Chairman, J. Edward Cichanowicz

26 "Economics of SCR Post Combustion NO_x Control Processes," J. E. Damon, R. W. Scheck, and J. E. Cichanowicz. 26-1

27 "Update on NO_x Flue Gas Treatment in Japan," Y. Nakabayashi, T. Miyasaka, K. Mouri, and K. Honda 27-1

28 "Evaluation of NO_x and NO_x/SO_x Flue Gas Treatment Technology for Coal-Fired Sources," J. D. Mobley and J. M. Burke . . . . . 28-1(a)

29 "Pilot-Scale Evaluation of Selective Catalytic Reduction for Coal-Fired Utility Boilers," G. H. Shiomoto, L. J. Muzio, and J. E. Cichanowicz 29-1

30 "Catalytic DeNO_x Demonstration System -- Huntington Beach Generating Station Unit 2," H. A. Kerry and A. Weir, Jr. 30-1

(a) The information in this document has been funded wholly or in part by the United States Environmental Protection Agency. It has been subject to the Agency's peer and administrative review, and it has been approved for publication as an EPA document.

Paper Page

31 "The Thermal DeNO$_x$ Demonstration Project," H. T. Dziegiel, T. B. Aure, and D. W. Anderson 31-1

32 "Current Status of Dry NO$_x$-SO$_x$ Emission Control Processes," S. M. Dalton 32-1

SESSION VIII: FUNDAMENTAL COMBUSTION STUDIES
Chairman, W. Steven Lanier, EPA, IERL/RTP

33 "The Influence of Scale and Fuel Properties on Fuel-Oil Atomizer Performance," W. R. Seeker, W. D. Clark, and G. S. Samuelsen . . . . 33-1(b)

34 "The Evolution of Fuel Bound Nitrogen During Heavy Oil Pyrolysis," S. P. Hanson, J. M. Bėer, and A. F. Sarofim 34-1

35 "Bench-Scale NO Emissions Testing of World Coals: Influence of Particle Size and Temperature," S. L. Chen, M. P. Heap, and D. W. Pershing . . . . 35-1(b)

36 "Correlation of NO$_x$ Emissions with Basic Physical and Chemical Characteristics of Coal," J. H. Pohl, S. L. Chen, M. P. Heap, and D. W. Pershing . . . . 36-1(b)

37 "Gas Phase Reaction Kinetics of NO$_x$ Formation from Fuel Nitrogen in Fossil Fuel Combustion," C. T. Bowman, R. K. Hanson, M. Louge, and A. Garman 37-1

38 "The Structure of Turbulent Diffusion Flames and Nitric Oxide Formation," J. E. Broadwell, P. E. Dimotakis, T. J. Tyson, C. J. Kau, and W. R. Seeker . . . . 38-1(b)

39 "Formation and Control of Pollutant Emissions During Stoker-Fired Coal Combustion," G. P. Starley, D. M. Slaughter, J. M. Munro, F. W. Bradshaw, G. Silcox, and D. W. Pershing . . 39-1(a)

(a) The information in this document has been funded wholly or in part by the United States Environmental Protection Agency. It has been subject to the Agency's peer and administrative review, and it has been approved for publication as an EPA document.

(b) Although the information in this document has been funded wholly or in part by the United States Environmental Protection Agency, it does not necessarily reflect the views of the Agency and no official endorsement should be inferred.

Paper Page

SESSION IV: STATIONARY ENGINES AND INDUSTRIAL PROCESS SYSTEMS
Chairman, Robert E. Hall, EPA, IERL/RTP

40 "Emulsion Fuel and Oxidation Catalyst Technology for Stationary Diesel Engines," J. H. Wasser . . . . 40-1(b)

41 "Emission Control Methods for Large Stationary Engines: Part I -- Combustion Modifications for Spark Gas Engines, Part II -- Combustion Modifications for Diesel Engines, Part III -- Catalytic NO_x Reduction by Ammonia," R. P. Wilson, Jr. . . . . 41-1(b)

42 "Application of Combustion Modification Technology for NO_x Control to Process Heaters," R. J. Tidona . . . . 42-1(a)

43 "NO_x Generation, Emission and Control from Cement Kilns in the United States," M. S. May 43-1

44 "Application of Combustion Modification Technology for NO_x Control to Cement Kilns," W. A. Carter and R. C. Benson . . . . 44-1(a)

45 "Development of a Low-NO_x Burner for Enhanced Oil Recovery," G. England, M. Heap, Y. Kwan, R. Payne, and D. Pershing . . . . 45-1(b)

46 "Environmental Assessment of Industrial Process Combustion Equipment Modified for Low-NO_x Operation," C. Castaldini, R. DeRosier, L. R. Waterland, and H. B. Mason . . . . 46-1(b)

SESSION X: SMALL INDUSTRIAL, COMMERCIAL, AND RESIDENTIAL SYSTEMS
Chairman, Michael C. Osborne, EPA, IERL/RTP

47 "Combustion Modifications for Coal-Fired Stoker Boilers," K. L. Maloney . . . . 47-1(a)

48 "Advanced Development of a Coal/Limestone Fuel Pellet for Industrial Boilers," B. W. Rising, H. N. Conkle, and R. D. Giammar . . . . 48-1(a)

(a) The information in this document has been funded wholly or in part by the United States Environmental Protection Agency. It has been subject to the Agency's peer and administrative review, and it has been approved for publication as an EPA document.

(b) Although the information in this document has been funded wholly or in part by the United States Environmental Protection Agency, it does not necessarily reflect the views of the Agency and no official endorsement should be inferred.

Paper | Page

49 "Low-NO_x Fiber Burner Application to Gas-Fired Firetube Boilers," J. P. Kesselring and W. V. Krill . . . . 49-1(b)

50 "Environmental Assessment of Industrial Boilers Firing Coal-Liquid Mixtures and Wood," L. R. Waterland, C. Castaldini, H. B. Mason, and R. DeRosier . . . . 50-1(b)

51 "Emission Characterization for A Residential Fluidized-Bed Wood-Chip Burner," R. S. Truesdale . . . . 51-1(a)

52 "Combustion Modification to Reduce Wood Stove Emissions," J. M. Allen and W. H. Piispanen . . . . 52-1(a)

APPENDIX A: LIST OF ATTENDEES A-1

(a) The information in this document has been funded wholly or in part by the United States Environmental Protection Agency. It has been subject to the Agency's peer and administrative review, and it has been approved for publication as an EPA document.

(b) Although the information in this document has been funded wholly or in part by the United States Environmental Protection Agency, it does not necessarily reflect the views of the Agency and no official endorsement should be inferred.

INTRODUCTORY REMARKS

By:

Robert C. Carr
Coal Combustion Systems Division
Electric Power Research Institute
3412 Hillview Avenue
Palo Alto, California 94304

On behalf of the Electric Power Research Institute, I would like to welcome everyone to Dallas for the second symposium and just make a few general comments on NO_x.

The EPRI perspective on this particular symposium is that it's certainly the most prestigious and most important symposium that relates to NO_x control in the industry. I think we have a unique conference. We have a very international flavor here. We have attendees from Japan, Germany, Canada, the Netherlands, France, and, of course, from all over the United States. This meeting brings together all the important people in NO_x control -- the users (utilities and other industries), the research specialists, the regulatory people, as well as the manufacturers. That's what makes this conference unique and allows us to exchange meaningful information.

The issue of NO_x control has been with us (when I say "us," I mean the industry and regulatory people) for some time. However, there are several issues that are now appearing on the horizon that promise to increase the pressure for broader NO_x control across the United States and, therefore, are accelerating the need for effective NO_x emissions control. The general category of concern is atmospheric loading of pollutants. The most potent example of that is acid precipitation or acid rain. Other concerns are atmospheric visibility, secondary particulate formation in the atomsphere, oxidants, and long-range transport. All of these may in fact require some form of NO_x control or NO_x may be implicated. With respect to the acid precipitation issue, this is perhaps the latest and certainly the most politically potent issue to face the utility industry because it may mean expanded retrofit NO_x emissions controls, particularly for the large coal-fired power plant population that we have. Although the role that NO_x would play in the acid rain legislation is not clear at this time, I think it is important that we clearly understand the options we have and anticipate the worst.

As a result of all these issues, a growing importance is being placed on NO_x control in the utility industry and in other industries as well. For most utilities, retrofit of coal-fired power plants for NO_x control is the major concern right now. There are fewer and fewer plants being constructed, and we don't anticipate any large growth of power plant construction in this decade. So most of the activity will be directed toward existing plants.

Since the last symposium, there have been some significant developments in the NO_x technology area such as combustion NO_x control via in-furnace destruction or reburning, continuing development of flue gas treatment (particularly in Japan), and furnace limestone injection for combined NO_x/SO_2 control. Many of these advancements are being spearheaded by the Japanese, who are clearly leaders in the NO_x area.

With respect to the electric utility industry, there are several concerns that must be addressed in NO_x control, many of which will be discussed at this meeting. I would like to make a few remarks about my perspective, and Charles Goodman from Southern Company Services will give a paper later this morning that will offer a more in-depth view of the utility perspective.

First, whatever we use, we want it to be simple, cheap, and reliable. I think the item of cost is particularly sensitive to the utility industry. It is due to the high cost of money and the long lead times required to build anything new. The utilities have a restricted capital investment capability currently which is very serious. It is difficult to raise front-end money for any new construction. Accordingly, the combustion control option for NO_x is the preferred one because of its simplicity and low cost, and because of the high NO_x removals we think we can achieve. Although the postcombustion control option does offer the potential of low NO_x, it also offers the certainty of high cost and perhaps even some reliability problems in the back end of the boiler. We think that the cost benefit of this option must be carefully weighed against incremental benefit in NO_x removals that may result. It is unclear at this time that the cost of postcombustion NO_x control justifies the incremental benefit.

Another area that is clearly important: you can't jeopardize operation of the boiler or the reliability of the steam generator. After all, this is the heart of the plant, and we don't want to make it any more complicated than it already is.

On the subject of cost, we think it is also important to combine environmental control technologies whenever you can. Adding a black box for every new pollutant species is very simple in concept, very expensive in practicality, and certainly not very creative. We think it is important whenever possible to combine processes; once again, to save the capital and also save operation and maintenance costs. I think the furnace limestone injection process (if it can be made to work and achieve the levels of SO_2 control we need) is certainly a candidate process that deserves a concerted amount of effort right now.

EPRI has the support of our utility advisory structure to pursue a vigorous NO_x R&D program, particularly in the retrofit area. Despite the uncertainties in the regulatory area, which we will hear about later, we are certainly supporting a major R&D effort in the development of retrofit NO_x controls for existing coal-fired power plants. Also, we are currently performing proof-of-concept work in the limestone injection area, and assuming that looks good, we anticipate a more comprehensive limestone injection program next year.

From my personal perspective, I would like to add a few other comments. I think we all recognize the importance of NO_x control in the utility industry. Of the three emissions we are trying to control -- particulate matter, SO_2, and NO_x -- I personally think that NO_x is the most difficult and most complicated. We have a reasonably good handle on particulate matter control now, and we are doing reasonably well with SO_2. I think NO_x in the future is going to be a big issue, and I don't think we are as far along as we would like to be. One of the reasons is that if you are going to control NO_x, you are talking about getting intimately involved with the processes occurring in the furnace: the fluid dynamics, thermodynamics, heat transfer, and chemistry. This makes it very difficult to scale up anything you do at a small scale, which is why I think NO_x control is more difficult than any of the other technologies we are dealing with. And the implications of a premature commercialization are extremely severe since we are dealing with the heart of the plant -- the boiler. I think these complexities are exemplified by the fact that in particulate matter we are pretty confident we can achieve 99.9 percent removals with new technologies. With SO_2 we are talking about 90 percent, and with NO_x we are talking about 80 percent.

The papers we are going to hear today and the rest of the week will demonstrate that we are making significant progress in NO_x control. The meeting agenda is divided into several distinct areas. We will hear updates of topics we have discussed before such as the status of regulations, combustion controls that are currently in place, and experience with flue gas treatment. We will also hear about some important new work: furnace limestone injection and in-furnace NO_x destruction or reburning. And there will be several papers describing fundamental combustion studies. I would like to emphasize the importance of the fundamental work. I think that this is where the new ideas and future developments are going to come from. Indeed the topics that are new sessions this time -- limestone injection and reburning -- were actually introduced in the fundamental sessions a few years ago. If you don't understand the fundamentals, it is a very difficult process to scale up and develop anything that is going to have widespread utilization.

With those remarks, I would like to close by again welcoming everybody. I am looking forward to an excellent symposium.

CLOSING REMARKS

By:

Dennis C. Drehmel
Special Projects Office
Industrial Environmental Research Laboratory
U.S. Environmental Protection Agency
Research Triangle Park, North Carolina 27711

This symposium dealt with NO_x control for stationary sources including power plants, process heaters, cement kilns, wood stoves, and industrial boilers. In addition, SO_x control was considered in conjunction with low-NO_x systems for utility and stoker boilers. For power plants, low-NO_x technology may be derived from new burner design or firing systems and from flue gas treatment. Concommitant SO_x control is achievable in the furnace with sorbent injection or downstream of the furnace with flue gas treatment. Presentations by boiler manufacturers confirmed that each had currently available burner and/or firing systems to achieve at least a 40 to 60 percent reduction in NO_x from levels before the advent of the New Source Performance Standards (NSPS). Some examples of these are the controlled combustion venturi burner, the controlled flow/split flame burner, the controlled mixing burner, and the low-NO_x concentric firing system. In addition, Southern California Edison reported on a fuel staging system called the ICNF (in-furnace control of NO_x formation) which reduced NO_x from 400 to as low as 130 ppm at the Alamedas No. 2 power plant. Other systems under development include the MHI series PM burner, the distributed mixing burner (DMB), the Foster Wheeler fuel-staged burner, the Babcock & Wilcox primary combustion furnace, and the MACT (Mitsubishi Advanced Combustion Technology).

The PM burner is an improvement in tangentially fired furnaces using a new arrangement of fuel, air, and flue gas recirculation ports. The idea is to introduce a concentrated fuel stream between two streams of recirculated flue gas to delay burning and provide a reducing atmosphere to convert fuel nitrogen to N_2. The DMB reduces NO_x also by establishing a fuel-rich region. This is accomplished in a wall-fired furnace by introducing less than theoretical air with the individual burners and the balance of the air through tertiary ports between the burners. The MACT, developed for tangential corner-fired furnaces, also uses a reducing zone, but in this case the zone is provided by firing a minority fraction of the fuel considerably above the main firing zone. As the NO_x formed in the main firing zone rises through the second burning zone it is reduced to N_2. Both PM burners and MACT allow lowering of stack NO_x to levels which are a 75 to 85 percent reduction from pre-NSPS levels. Incremental cost for a new application of PM burners was reported to be less than $5/kW.

Flue gas treatment for NO_x control included selective catalytic reduction (SCR), thermal deNO_x, and dry NO_x/SO_x control processes. The latter consists of carbon adsorption processes, electron beam irradiation processes, and copper oxide processes. Control efficiencies of NO_x in flue gas treatment processes are generally 90 percent, except for thermal deNO_x where 50 to 65 percent is typical. Reported costs of control were: SCR (Hitachi-Zosen), $53 to $95/kW; thermal de$NO_x$ (Exxon), $40/kW; carbon adsorption (Mitsui), $117/kW; electron beam (Avco-Ebara), $333/kW; copper oxide (Shell), $238/kW. Unfortunately, these costs are not exactly comparable because of differing assumptions and the fact that the latter three are also controlling 90 percent of the sulfur dioxide.

Control of SO_x is also possible by adding sorbent to the coal or by injection into the furnace. The former method is used by RWE (Rheinisch-Westfalisches Elektrizitatswerk) in tests burning brown coal. Brown coals range from 40 to 70 percent in moisture and hence produce a peak flame temperature of only 1,200°C. Under this condition, calcium hydroxide is an effective sorbent for SO_x when introduced with the coal. Information on the limestone injection method comes from work in Europe sponsored by Steinmuller and from work in the U.S. sponsored by EPA. In both, the percentage SO_x controlled increased with increasing fuel sulfur and with increasing sorbent addition rate. In both, the sorbent type and the fuel type were important, but the ranking differed. Differences appear to be dependent on the interaction of the furnace time/temperature profile and the inherent nature of the sorbent to develop surface area for reaction as it is initially exposed to temperature. It was reported that limes with extremely high surface areas (as much as 50 m^2/g) can be produced under the right time/temperature conditions and that the surface area will have a very strong influence on reactivity. The cost of SO_x control by means of sorbent injection at twice the theoretical addition rate was reported to be $21/kW.

Low-NO_x technology for other stationary sources parallels that for power plants. For process heaters, for example, the use of staged air was reported to reduce NO_x emissions by 60 to 71 percent. Similarly for enhanced oil recovery steam generators, the use of staged air allows operation with acceptable smoke and CO levels while limiting NO_x to below 85 ppm (at 3 percent O_2). For gas-fired firetube boilers, low-NO_x emissions have been achieved by ignition of premixed gas and air on a ceramic fiber matrix. Full load efficiency was 82.6 percent while NO_x emissions were lowered by 77 percent. Control of stationary engines was tested using exhaust gas recirculation, water/oil emulsions, stratified charge, and changed timing. NO_x could be reduced up to 50 percent by exhaust gas recirculation and up to 60 percent by the use of emulsions.

VOLUME II

FLUE GAS TREATMENT, FUNDAMENTAL STUDIES, AND INDUSTRIAL/COMMERCIAL/RESIDENTIAL APPLICATIONS

SESSION VII

FLUE GAS TREATMENT
Chairman, J. Edward Cichanowicz
EPRI

ECONOMICS OF SCR POST COMBUSTION
NO_x CONTROL PROCESSES

By:

J.E. Damon, R.W. Scheck
Stearns-Roger Engineering Corporation
4500 Cherry Creek Drive
Denver, Colorado 80217

And

J.E. Cichanowicz
Electric Power Research Institute
3412 Hillview Avenue
Palo Alto, California 94303

ABSTRACT

The capital and operating costs of the Selective Catalytic NO_x Reduction (SCR) process as applied to U.S. coal fired utility boilers have been items of considerable interest and controversy in recent years. Several studies have been issued by various entities which identify the costs of the SCR systems as they apply to U.S. utility boilers. However, due to differences in design criteria, economic premises and scopes of supply, these studies indicate a wide range of costs. This paper reviews three such studies (see References 1, 2 and 3) in order to reconcile these cost differences by establishing equivalent scopes of supply, design criteria and economic factors for each report reviewed. The operating and capital costs were then adjusted accordingly. The result is a cost comparison in which the SCR system cost differences as reported in the three studies are identified and explained. Updated capital costs and operating costs both in 1/1/83 dollars are reported in this paper. In addition other factors which could significantly increase these updated costs are reported in this paper.

INTRODUCTION

The purpose of this paper is to review the results developed in three studies concerning the economics of the Selective Catalytic NO_x Reduction (SCR) process to new coal fired utility boilers. The three reports are identified as References 1, 2 and 3 in this paper, and for expediency's sake will be referred to as follows:

- Reference 1 - EPRI/Stearns-Roger (S-R) Study,
- Reference 2 - EPRI/U.S. EPA/Tennessee Valley Authority (TVA) Study,
- Reference 3 - U.S. EPA/TVA Study.

The intent of this review is to examine the scope, the technical criteria and the economic premises of each of these studies in order to resolve the substantial differences between the capital and operating costs identified for the Hitachi-Zosen (H-Z) process, the SCR system common to each study.

BACKGROUND

The EPRI/S-R study was performed in late 1978 and early 1979 and was subsequently published in November 1982. This study reviewed the capital and operating costs of four different NO_x control systems to be installed on a new 500 (net) MW unit to be fired with Powder River Basin coal. The capital costs in this study were developed as a result of a preliminary engineering effort, for each system, which included the development of conceptual design drawings for each process. The Hitachi-Zosen (H-Z) system which is a SCR process is the system of interest in this paper because it is common to all the reports being reviewed. Several efficiency levels for NO_x control were reviewed in this report, but this paper will review only 90 percent NO_x reduction (i.e., Case 3) which is a common NO_x control level for all the studies.

The EPRI/U.S. EPA/TVA study was also performed in late 1978 and early 1979 and published in December, 1981. This report reviewed the capital and operating costs of a number of NO_x control systems, some of which were combined SO_x/NO_x removal systems. The report covered composite Air Quality Control Systems for a 500 MW (gross) coal fired power plant - that is the particulate control system, the flue gas desulfurization system as well as the NO_x control systems. The capital costs in this study were based upon an equipment list generated for the SCR system and its correlation with air quality control system cost data and TVA's design and construction experience. The Hitachi-Zosen system, with a 90 percent NO_x removal efficiency was singled out and costed in this study. This information provides the basis of comparison with the other reports being reviewed in this paper.

The U.S. EPA/TVA study was published in mid-1981 and contains updated information on the SCR systems. This report reviewed the capital and operating costs of a number of techniques and systems to control NO_x emissions from a 500 MW net coal fired power plant. Different NO_x emission reduction efficiencies were studied as well as combinations of the different systems to achieve the various NO_x removal levels. However, one control option was the separate use of the Hitachi-Zosen system at a 90 percent NO_x reduction efficiency. This study case is the basis of comparison with the other reports discussed in this paper. It should be noted that the capital costs in this study were based upon an equipment list generated for the SCR system and its correlation with air quality control system cost data and TVA's design and construction experience.

SELECTIVE CATALYTIC NO_x REDUCTION (SCR) PROCESS

Before proceeding with the comparisons of the various studies, a basic discussion of the SCR process is provided as a background. A schematic of the SCR process is shown in Figure 1. In this process, gaseous ammonia diluted with either air (i.e., below the flammability limit) or steam is injected, through a grid system, into the flue gas stream at the economizer exit of the boiler. The ammonia/flue gas mixture then travels to catalytic reactors (two for a 500 MW net unit) where the ammonia and NO_x interact, primarily, as shown in equations 1 and 2 below. The result is a substantial NO_x reduction at the exit of the reactor.

(1) $4\ NO + 4NH_3 + O_2 \longrightarrow 4N_2 + 6H_2O$

(2) $2\ NO_2 + 4NH_3 + O_2 \longrightarrow 3N_2 + 6H_2O$

As can be seen in the above equations, the stoichiometric $NH_3:NO_x$ mole ratio is approximately 1:1 considering that NO_x at the boiler outlet is generally assumed to be 95 percent NO and 5 percent NO_2. In actual practice this ratio may be 0.9 to 1.0 for a 90 percent removal efficiency based on the inlet NO_x concentration, assuming that a suitable catalyst volume has been provided to achieve this efficiency. If adequate catalyst volumes are not provided to achieve high efficiences, the result of increasing the $NH_3:NO_x$ mole ratio will be ammonia slip or breakthrough which is simply the flow of excess ammonia past the reactor(s) and on to the downstream equipment.

The ideal process temperature range is generally limited to 590°F to 750°F. Below the lower temperature there is danger of the formation of ammonium sulfates and bisulfates which can attack the catalyst surface. If the low temperature operation is continuous (i.e., 12 hours or more), this attack can permanently damage the catalyst. An economizer flue gas bypass (see Figure 1) is typically provided to raise the economizer exit flue gas temperature at low loads to an acceptable level and thereby overcome this problem in utility boiler applications. The economizer outlet temperature rarely exceeds 750°F at full load conditions. However, if exceeded, the NH_3 may disassociate and NO_x reduction process will be impaired; if temperatures exceed 900°F to 1000°F the catalyst may sinter and be permanently damaged.

The NO_x reduction efficiency of this process is dependent on the space velocity selected for the catalyst. The space velocity is basically the total flue gas volume per hour divided by the bulk volume of the catalyst, noting that the flue gas and catalyst volumes are generally stated in standard cubic feet or normal cubic meters for this purpose. The units of space velocity are reciprocal hours. The manufacturer in this report, Hitachi-Zosen, uses catalyst area velocity as an index of process efficiency. This index is basically, the standard flue gas volume entering the catalyst divided by the active catalytic area. This index is generally expressed in ft/hr. In general, reasonably low space velocities and/or area velocities are required for high process efficencies. This means that increased catalyst quantities are required for high NO_x reduction efficiences (e.g., 90%). It is important to note that increased quantites of catalyst are also required to control ammonia slip. That is, not only must a sufficient quantity of catalyst be provided to achieve the required NO_x reduction efficiency, but additional catalyst is generally required to insure the oxidation of excess ammonia used in the process to prevent excessive ammonia slip (i.e., typically less than 10 ppm.) The specific relationship of these indices and NO_x reduction efficiency is related to the proprietary catalysts used by the various SCR manufacturer's.

The catalyst used in these processes are either solid or surface coated catalyst on a substrate. Both are subject to erosion damage from fly ash in coal fired power plant flue gases, and the efficiency of the catalyst can be impacted over the long term (1 to 3 years). This loss of catalyst effectiveness will probably require the use of an excess of catalyst to maintain the required process efficency over an extended period of time. If this is the case, the capital and operating costs for the SCR process will be increased accordingly.

These catalysts also have the tendency to oxidize SO_2 to SO_3 which tends to react with the NH_3 carryover and for ammonium bisulfates (i.e., see equation 3) at the exit of the reactor.

$$(3)\quad NH_3 + SO_3 + H_2O \longrightarrow NH_4HSO_4$$

This substance has the tendency to condense in the intermediate baskets of a standard regenerative heater. This makes their removal by conventional soot blowing difficult. The result, particularly on high sulfur fuels, can be significant fouling of air heaters which will cause high draft losses and possibly unit load limitations. Frequent air heater water washings may be required. Japanese experience with SCR systems has led to the development of combined intermediate/cold end air heater baskets which have a heat transfer surface comfiguration which is conducive to cleaning by soot blowing. This combined section is longer than its conventional counterparts (the separate intermediate and cold end baskets in a standard regenative air heater). The result is more expensive air heaters which may reduce the ammonium bisulfate fouling. However, on high sulfur coals the effectiveness of this accommodation is still questionable.

The overall SCR operational experience on coal fired utility boilers is minimal. In Japan, Takahara Unit 1 (250 MW) is now testing the SCR process on coal. Initial results will be available in a companion paper in this session. In the U.S., three coal fired pilot plants are in operation, these are:

- The EPRI Arapahoe Test Facility at the Araphoe Power Plant of the
  Public Service Company of Colorado
  Size - 5000 scfm (2.5 MW)
  Supplier - Kawasaki Heavy Industries

- The U.S. EPA Pilot Plant at the Mitchell Station,
  Georgia Power Company
  Size - 0.5 MW
  Supplier - Hitachi Ship Building and Engineering Company

- The U.S. EPA Pilot Plant at the Big Bend Station of the Tampa Electric Company
  Size - 0.6 MW (Combined SO_x/NO_x Removal)
  Supplier - UOP Inc.

The only other U.S. experience is the SCR process installed on the Huntington Beach Unit 2 (107.5 net MW of flue gas capacity is being treated) of the Southern California Edison Company. This is an oil/natural gas fired unit, but the cost information on this project is now the best available in the U.S. for a full scale SCR system. This installation will be reviewed in a companion paper in this session.

SCOPE REQUIREMENTS AND COMPARISONS

The scope of any project will determine its capital costs, and these costs must be carefully assessed to provide a meaningful cost estimate. When establishing the scope of a new process it is important to establish the complete list of equipment and systems to be included. The use of equipment layout drawings such as shown in Figures 2 and 3 (taken from Reference 1) show a layout for the H-Z SCR System and provide the cost engineer with a complete view of the system and insures the inclusion of all equipment in the cost estimate. Therefore use of such drawings is well advised when developing the costs of new technology. This becomes especially important in studies such as those being reviewed in this paper. The reason being that capital costs are generally identified as the Total Process Cost (see Tables 3 and 3A.) This cost is increased by 50 to 56 percent to establish the Total Plant Investment (again see Tables 3 and 3A) which includes such items as general facilities, engineering fees, sales tax and project contengency. Once the Total Plant Investment (TPI) is established such items as (i.e., in this case) royalty allowances, preproduction costs, capital for initial supply inventories and initial catalyst cost are added to compute the Total Capital Requirement of the process. The point becomes that if the Total Process Capital (TPC) is not properly estimated, large errors in the Total Capital Requirement can result because it is heavily factored based on the TPC and the TPI. This is true even though this factoring is based on sound cost estimating techniques.

The Scope of Supply required (with foundations and supports) for an SCR system on a new unit should include the following:

1. An ammonia system which includes storage tanks, an unloading compressor and pump, a vaporizer, an ammonia injection grid as well as a steam or a compressed air system to provide a dilution medium for the ammonia.

2. Two reactors with ash hoppers are generally required for a 500 MW unit. This reactor system must include all flue gas duct work to and from the reactors as well as expansion joints and dampers. A

steam soot blower system should be provided at the inlet of each reactor.

3. A control system must be provided to control ammonia injection at the proper $NO_x:NH_3$ mole ratio and flue gas temperature.

4. An ash handling system must be provided for the two reactors to remove the ash collected in the reactors' hoppers.

5. An economizer bypass duct with control dampers will most likely be required for all SCR systems to maintain low load economizer exit flue gas temperatures above the minimum prescribed for this process.

6. Additional inlet particulate control system ducting will be required based on the spacing of the reactors (at least for the configuration assumed in Figure 1.) In the EPRI/S-R report, 120 feet of additional ducting was required.

7. The higher negative pressure incurred by the use of an SCR system prior to the Induced Draft Fans leads to increased structural support costs for the particulate control system and increased implosion prevention allowances in the boiler and flue gas circuit in general.

8. The incremental costs of larger Induced Draft Fans to support the SCR system should be included in the scope.

9. In recent years, a modified air heater design has been determined to be required for SCR systems. The incremental increased cost of this system should be included in the overall scope and costs of the SCR system.

All these items must be covered in order to establish a complete cost estimate for the SCR systems.

The EPRI/S-R report covered all of the items above except item 9 because at the time of this report the modified air heater requirement had not been determined.

The EPRI/U.S. EPA/TVA report covered most Scope of Supply items outlined above. However, since this report covered composite air quality control systems, certain items were excluded from the scope of SCR system and the separate cost of this system. Items 4 and 9 were not included, and items 6 and 7 were only partially considered. Again the modified air heater requirement was not defined at the time of this report.

The U.S. EPA/TVA report covered all items in the above scope except 4. Items 6 and 7 were only partially included. Again this was a comparative report of different systems and these costs were not identified for the isolated SCR system. However, the air heater modification requirement was known at the time of this report and was included.

The above discussion defines the differences in scope between the three studies under review for the common Hitachi-Zosen SCR system with a 90 percent NO_x removal efficiency. These differences have an impact on the capital and operating costs presented in each report, these impacts will subsequently be discussed and resolved.

DESIGN CRITERIA

The design criteria between the various studies have a significant impact when comparing costs. The capital costs indicated in the three studies for the Hitachi-Zosen SCR system with a 90 percent removal efficiency are as follows:

Study	$/kW[1]	Cost Date
EPRI/S-R	68 (net)[2]	7/1/79
EPRI/U.S. EPA/TVA	43.4 (gross)[2]	7/1/79
TVA/US EPA	50.9 (net)[3]	1/1/84

NOTES:

1) Based on a net or gross kilowatt capacity as indicated
2) Based in EPRI economic premises
3) Based on TVA economic premises

These costs while appearing very different are comparable when the technical design premises of each of the reports are examined. Table 1 shows a comparison of various "unadjusted" design parameters. The following significant differences occur and account for most of the cost differences in the three studies which were reviewed in this paper.

Unit Capacity

The 500 MW capacity for the EPRI/S-R, and the TVA/US EPA reports is a net rating. While this capacity is a gross rating for the EPRI/U.S. EPA/TVA report. This causes a cost difference of 9.6 percent between the $/kW costs shown for the EPRI/S-R and the EPRI/U.S. EPA/TVA studies for the H-Z system. The utility industry generally defines net capacity as gross capacity minus the average auxiliary power requirements to operate the plant. This definition is used in this context. While both $/net kilowatt or $/gross kilowatt are valid ways to express plant costs, the net or gross qualifiers should be applied to avoid errors in interpretation.

Volumetric Flue Gas Flow Rate and Coal Type

A $/kW cost value is somewhat misleading when costing air pollution control equipment because SCR systems are cost dependent on actual cubic feet per minute (ACFM) of flue gas flow which passes through them. The ACFM flow is dependent upon unit capacity, unit heat rate, the coal fired (especially where the percentage of moisture is high for the western U.S. coals), excess air levels and plant elevation. An examination of Table 1 shows significant differences in all these areas between all the reports being compared. The EPRI/S-R report has a flue gas ACFM flow 41 percent, and 35 percent higher than the EPRI/U.S. EPA/TVA and U.S. EPA/TVA reports, respectively. This is a significant factor in the cost differences as presented.

Uncontrolled NO_x Emissions

The amount of NO_x to be treated in moles/hour will have some impact on SCR system costs. The different levels shown in Table 1 have a small impact on the overall cost comparison.

Catalyst Volume

An extremely important design parameter is the volume of catalyst to be used for the 90 percent removal of NO_x. The EPRI/S-R and EPRI/U.S. EPA/TVA reports show comparable catalyst requirements when the ACFM differences between the two studies are considered. The U.S. EPA/TVA report shows a greatly reduced catalyst requirement even when compared to the EPRI/U.S. EPA/TVA report with a comparable ACFM flow. In this instance high space velocities resulting from catalyst improvements are predicated as the basis of the reduced catalyst usage and cost in the U.S. EPA/TVA report as compared to the other reports. However, it is important to note that cost estimates in all of the studies were based on the use of the catalyst designated as NOXNON 500 Type 3.

Economic Premises

Differing economic premises effect economic comparisons. The major differences in the economic premises for the various studies are the cost dates (see Table 2) for the Capital estimates and the O&M costs. True economic comparisons must have dollar values at the same point in time. Therefore the dates in the three studies must be equalized to make correct comparisons. Equalized and updated escalation and interest rates are also required.

The other differences between the various studies were minimal as shown in Table 2. The U.S. EPA/TVA report used a fixed charge rate somewhat lower than the other reports, as well as a longer center of gravity period. (The center of gravity date being the date at which 50 percent of the capital investment is expended in the project.)

The other differences between the reports are the unit costs for energy and materials, but these by themselves do not create large differences in the cost of the SCR systems. The annual hours of operation are also somewhat different and this does impact O&M cost comparisons.

The method of economic analysis used in the EPRI reports (and for this paper) is the EPRI Economic Premises, while the U.S. EPA/TVA reports use the TVA economic methodology. For purposes of this paper the overall system costs were compared, but not the methodology used to arrive at them. We would expect either method, when based on the same design criteria, scope of supply and similiar economic factors (see Tables 2 and 2A), to produce the same relative results.

UNADJUSTED ECONOMIC COMPARISONS

Tables 3 and 4 indicate the comparisons for capital and levelized operating costs, respectively, as they are reported in each study. As can be seen significant differences appear. However, these differences are created mainly by the scope, design and economic premise differences previously defined. It is interesting to note that the capital cost estimates in the EPRI/S-R and EPRI/U.S. EPA/TVA reports correlate very well on a $/ACFM basis (i.e., approximately 10 percent difference) even though they are different on a $/kW basis.

ADJUSTED SCOPE, DESIGN, AND ECONOMIC CRITERIA

In an effort to equalize the results presented in various reports being reviewed in this paper, the following adjustments were made to the scope, the design criteria and the economic premises of each of the reports.

The scope of supply of the EPRI/S-R study was expanded to include the incremental costs of the modified air heater design previously described. The scope of supply for the study EPRI/U.S. EPA/TVA was increased to include those items which previously defined as not or only partially included in this paper, including the modified air heater design. The scope of supply for the U.S. EPA/TVA was increased to include those items as previously defined as not or only partially included in this paper.

The design parameters in each of the reports were adjusted appropriately to remove the great differences as shown in Table 1A. Here it can be seen that the unit gross size was raised to 548 MW and the net rating was set at 500 MW. An appropriate turbine heat rate was established allowing for steam extraction for a flue gas indirect reheat system (50°F above saturation). Appropriate boiler efficiencies and fuel flow rates, based on the specific coals identified for each study, were established to develop appropriate flue gas flows for each report. In order to remove as many differences as possible, the excess air levels and plant ambient pressures were equalized. NO_x emissions from the boiler were set equal to the NSPS emission limits appropriate for the coal fired. The required NO_x removal efficiency was maintained at 90 percent in all cases. The $NH_3:NO_x$ mole ratio was equalized at 1:1 for all the studies. Finally, the cubic feet of catalyst required was modified for the increased or decreased ACFM flows developed in this adjustment process. The results of these adjustments were design conditons appropriate for a 500 net MW boiler using the coals identified in each report.

The economic premises for each report were adjusted as shown in Table 2A. As can be seen, the escalation and interest rates were updated and equalized for all the reports. All other parameters were also equalized for all the reports. The capital cost and the O&M cost dates were both set at 1/1/83.

The result of all these adjustments was a meaningful basis to compare the results of all three reports.

CAPITAL COST ADJUSTMENTS

The adjusted capital costs for all the processes are shown in Table 3A. The original capital costs of the EPRI/S-R and EPRI/U.S. EPA/TVA were escalated to the 1/1/83 date and adjusted for the new ACFM flow requirements. The EPRI/U.S. EPA/TVA report was further adjusted to include the added scope items previously defined. The U.S. EPA/TVA report costs were de-escalated to 1/1/83 dollars. The costs were also adjusted for the addition of previously mentioned scope items and for the adjusted ACFM flow rate.

The results of these adjustments in Table 3A indicate that the EPRI/S-R and EPRI/U.S. EPA/TVA reports have an excellent correlation, with the $/ACFM values being almost identical. The spread in the $ per net kilowatt value is 94.0 to 79.1 $/kW (net). The lower value being for the EPRI/U.S. EPA/TVA report, which is understandable due to the lower ACFM flow requirements of the Eastern coal used in this report as compared to that of the high moisture Powder River Basin coal used in the EPRI/S-R report. The $64.9 per net kW in the U.S. EPA/TVA report is somewhat lower than the previous reports. This results from the greatly reduced (i.e., approximately a 33 percent reduction) catalyst requirement indicated in this report, which in turn significantly reduced the cost for the reactors. It is important to note that the acceptability of the higher space velocity in this report, will have to be demonstrated, in terms of both NO_x reduction efficiency and NH_3 slip control, in order for this cost reduction to be valid.

O&M COST ADJUSTMENTS

Table 4A indicates the adjusted O&M costs, the first year mills/kWhr, and levelized mills/kWhr costs for each of the studies reviewed in this paper. The EPRI/S-R and the EPRI/U.S. EPA/TVA reports' O&M cost data were escalated per the adjusted economic factors (see Table 2A). In addition the catalyst replacement cost for each of these studies were revised per the adjusted ACFM requirements shown in Table 1A. The annual material and energy costs were also corrected per the adjusted unit costs shown in Table 2A. Finally the revised 1/1/83 capital costs were used for computing the annual fixed charges in these reports.

The annual O&M costs for the U.S. EPA/TVA report were recomputed in 1/1/83 dollars using the economic factors in Table 4A. The catalyst replacement cost was revised for the adjusted ACFM flow rate and de-escalated using a 6 percent rate (per this study's original design premises.) The annual material and energy costs were adjusted per the adjusted unit costs and for the increased operating hours indicated in Table 2A. A new annual net generating capacity was also used for adjusting the first year and levelized mills/kWhr costs.

The adjusted annual O&M cost comparison between the two EPRI reports indicates a very close correlation with the first year mills/kWhr costs being within 12 percent of one another, and the levelized mills/kWhr costs were (i.e., for a one year catalyst life) within 10 percent of one another. In both cases the levelized mills/kWhr dropped approximately 35 percent when a two year catalyst life was assumed, noting that this is not a statement on the guarantee life of the catalyst.

The adjusted differences of the first year mills/kWhr costs for the EPRI/S-R and the EPRI/U.S. EPA/TVA reports as compared to the U.S. EPA/TVA report are minus 26 percent and minus 17 percent, respectively. The adjusted differences of levelized mills/kWhr (i.e., for a one year catalyst life) for the EPRI/S-R and the EPRI/U.S. EPA/TVA reports as compared to the U.S. EPA/TVA report are minus 24 percent and minus 17 percent, respectively. The main reason for these differences is the greatly reduced catalyst loading indicated in the U.S. EPA/TVA report. A levelized mills/kWhr cost reduction for this latter report, when a 2 year catalyst life is assumed, is approximately 32 percent.

ADDITIONAL FACTORS AFFECTING COST

Although the three reports attempted to cover all the costs of SCR systems, certain costs associated with these systems remain to be identified. These are associated with the operation of the SCR system in conjunction with downstream air quality control equipment. Some of these unresolved issues are briefly discussed below.

Sulfur Content of the Coal will impact the cost of the SCR system. The SCR catalysts tend to oxidize SO_2 to SO_3, hence with high sulfur coals (e.g., the eastern coals in the TVA reports - see Table 1), this conversion can be fairly significant. The results can be significant formation of ammonium sulfate and air heater fouling. Experience at the EPRI Arapahoe test facility has shown this may be a problem even with the modified air heater design discussed in this report. The manufacturers of the SCR process feel this problem can be overcome by developing catalyst which will allow only minimal SO_2 conversion. Indications are that these catalysts may be more expensive than existing catalyst types and higher quantities may be required.

Ammonia Slip may be a problem in the use of the SCR systems. Indications from the Arapahoe test are that a 0.9 NH_3:NO_x mole ratio will give a 90 percent NO_x reduction. However, an increasing mole ratio up to 1.0 does not yield comparable NO_x reduction efficiencies, but does lead to increased ammonia slip. Ammonia slip is a problem because it contributes to air heater fouling and may be detrimental to air quality control equipment performance downstream of the SCR system. The degree of slip will be largely dependent upon the ability to control the NH_3:NO_x mole ratio. This in turn will depend upon the primary NO_x and NH_3 sensors used in the process control system. Since reliable sensors for control purposes do not exist, ammonia slip will most likely be a problem when attempts are made to achieve high NO_x reduction efficiencies.

The impact on other air quality control systems including waste disposal will also have to be carefully assessed to insure that additional costs are not incurred as a result of the use of SCR systems. The long term impacts on fabric filters, cold side electrostatic precipitators and wet or dry SO_2 scrubbers will require testing to ensure that there are no detrimental impacts on these systems. In addition, the potential utility user must be assured that waste disposal problems will not be increased by the occurrence of highly soluble ammonia compounds in the plant wastes or from possible hazards of catalyst disposal.

Catalyst space velocity requirements and life are still major areas of consideration in the use of SCR systems. Space velocities and the life of the catalyst will impact the first costs of SCR systems . If the cubic feet of catalyst required to achieve high NO_x reduction can be reduced in relation to a fixed flue gas flow rate, the overall catalyst cost can most likely be reduced, dependening on the material and processing requirements of the new catalyst. A quantitative illustration of the impact of lower catalyst costs is shown when comparing the levelized mills/kWhr (one year catalyst life) cost for the two TVA reports in Table 4A as compared with the EPRI/S-R study. The levelized cost of power is significantly reduced due to reduced catalyst cost volume and the resulting smaller reactor volumes. The SCR process cost is also significantly reduced when catalyst life is increased to 2 years in all cases examined in this paper. The reduction in levelized mills/kWhr in all cases ranged from 32 to 35 percent. The possible combined impact of improved catalyst and longer life is shown (see Table 4A) between the 1 year life catalyst levelized mills/kWhr cost for the EPRI/U.S. EPA/TVA report versus the 2 year catalyst life levelized mills/kWhr cost in the U.S. EPA/TVA report. The overall cost difference is minus 45 percent. This indicates that the first cost of the catalyst and the catalyst life are key items in determining the capital and operating costs of SCR system. Whether improved catalyst or increased catalyst life can be achieved still remain to be proven for the various coals burned in the U.S. However, increased life must be interpreted as the ability of the catalyst to facilitate long term high NO_x reduction efficiency which is minimally affected by the chemical and erosive impacts of fly ash as well as its long term ability to limit ammonia slip to 10 ppm. Finally, it should be remembered that coal sulfur content will effect the nature of the catalyst, and high sulfur coals may require more expensive catalysts which have the ability to retard the conversion of SO_2 to SO_3.

SUMMARY

This paper has reviewed and compared the economics of the application of the Selective Catalytic NO_x Reduction (SCR) process to U.S. coal fired boilers as presented in References 1, 2 and 3. Specifically, the Hitachi-Zosen SCR process with a 90 percent NO_x reduction was analyzed because this system was common to all three reports. At the outset it was recognized that the capital and operating costs identified in the three studies could not be compared until the scopes of supply, the design criteria and the economic premises for each were compared to identify their similarities and/or dissimilarities. This review indicated the following major differences:

- Two of the reports identified capital costs in \$/net kW while the other used \$/gross kW (see Table 3.)
- Large differences in the design flue gas volumetric flows were noted (see Table 1).
- Significant differences were noted in the scope of supply between the reports.
- Different capital and operating cost dates were used in the various studies.

These variations led to what appeared to be significant cost differences in the studies.

In order to correctly compare the reports the following steps were taken to reference these differences:

- A 548 MW gross and 500 MW net capacity was used to adjust the costs presented in each report.
- The flue gas flow rates (in ACFM) were adjusted for the above gross capacity and the unit heat rates based on the coals identified for each report. This adjustment included equalizing excess air levels and ambient air pressures (see Table 1A).
- A standard scope of supply was established and used for each study.
- One capital cost date (1/1/83) and one operating cost date (1/1/83) was used for each study.
- Updated, identical escalation and interest rates were used for each study (see Table 2A).

The capital and operating data which resulted from these adjustments are shown in Tables 3A and 4A with overall results summarized in the data shown below:

Report	$/Net kW	$/ACFM	First Year Mills/kWhr*	Levelized Mills/kWhr*
Cost Date	1/1/83	1/1/83	1/1/83	1/1/83
EPRI/S-R	94	15.93	6.87	12.59
EPRI/U.S. EPA/TVA	79	15.97	6.14	11.44
U.S. EPA/TVA	65	13.21	5.11	9.53

*Based on a one year catalyst guarantee life.

As can be seen, the capital costs shown for the EPRI reports on a $/kW (net) basis are somewhat different. The reason for this variation, is the difference (approximately 19%) in the adjusted flue gas flows used (see Table 3A) for these reports. However, on $/ACFM basis the two EPRI reports show an almost identical cost. The two TVA reports use nearly identical flue gas flows but have significantly different capital costs. This results in the significantly reduced catalyst requirements assumed in the U.S. EPA/TVA report, noting all these reports used Hitachi-Zosen's catalyst NOXNON 500 Type 3 in their cost analyses. The lower costs of this latter report could only be accepted when this reduced catalyst loading is demonstrated to be viable in achieving a 90 percent NO_x reduction efficiency while at the same time controlling NH_3 slip to 10 ppm or less.

The overall operating cost data for the adjusted study premises followed a pattern similiar to that of the capital costs. The first year and levelized mills/kWhr for the EPRI reports being within 12 percent of one another. The variation results from the previously discussed capital cost differences and the lower catalyst replacement costs of the EPRI/U.S. EPA/TVA report. The marked difference between the overall operating cost data in the TVA reports results from the significantly reduced catalyst costs identified in the U.S. EPA/TVA report. Again the viability of this reduced catalyst requirement will have to be demonstrated. Finally, the adjusted economic analyses of all the reports indicated that a 36 to 32 percent levelized mill/kWhr cost reduction could be expected if a two year catalyst guarantee life could be achieved. This statement assumes that the catalyst prices quoted in these studies would remain unchanged.

This paper focused upon the importance of scope supply, design criteria and design criteria when defining the capital and operating costs of SCR NO_x control systems. It has been shown that by establishing equivalent and consistent premises for the three reports reviewed in this paper, that what appear to be significant differences between these reports could be reconciled or readily explained. The authors of this paper would deem the adjusted capital and operating costs (see Tables 3A and 4A, respectively), shown for the two EPRI reports, to be representative of the range of SCR system costs for a 500 net MW coal fired boiler in the U.S. The U.S. EPA/TVA (see Tables 3A and 4A) costs can only be accepted when it is demonstrated that the reported reduced catalyst loading will both achieve the required 90 percent NO_x removal efficiency and control NH_3 slip to acceptable levels. Finally, future costs for the SCR systems can be expected to be higher than presented in this paper because the above studies account only for the installed costs of the SCR systems. Possible increased costs for SCR system impacts on particulate control, SO_2 control and waste disposal systems were not included.

REFERENCES:

1. EPRI/Stearns-Roger (S-R) Report: Technical and Economic Feasibility of Ammonia - Based Post Combustion NO_x Control; EPRI CS-2713, Project 783-2; Prepared by Stearns-Roger Engineering Corporation, Denver, Colorado; November, 1982.

2. EPRI/U.S. EPA/Tennessee Valley Authority (TVA) Report: Preliminary Economic Analysis of NO_x Flue Gas Treatment Processes Using TVA and EPRI Economic Premises; EPRI CS-2075, Project 783-3, Final Report; Prepared by TVA, Muscle Shoals, Alabama; December 1981.

3. U.S. EPA/Tennessee Valley Authority (TVA) Report: Evaluation of the Advanced Low-NO_x Burner, Exxon and Hitachi Zosen DeNO_x Processes; EPA 600/7-81-120, July 81; TVA/OP/EDT-81/28; Prepared by TVA, Muscle Shoals, Alabama; July 1981.

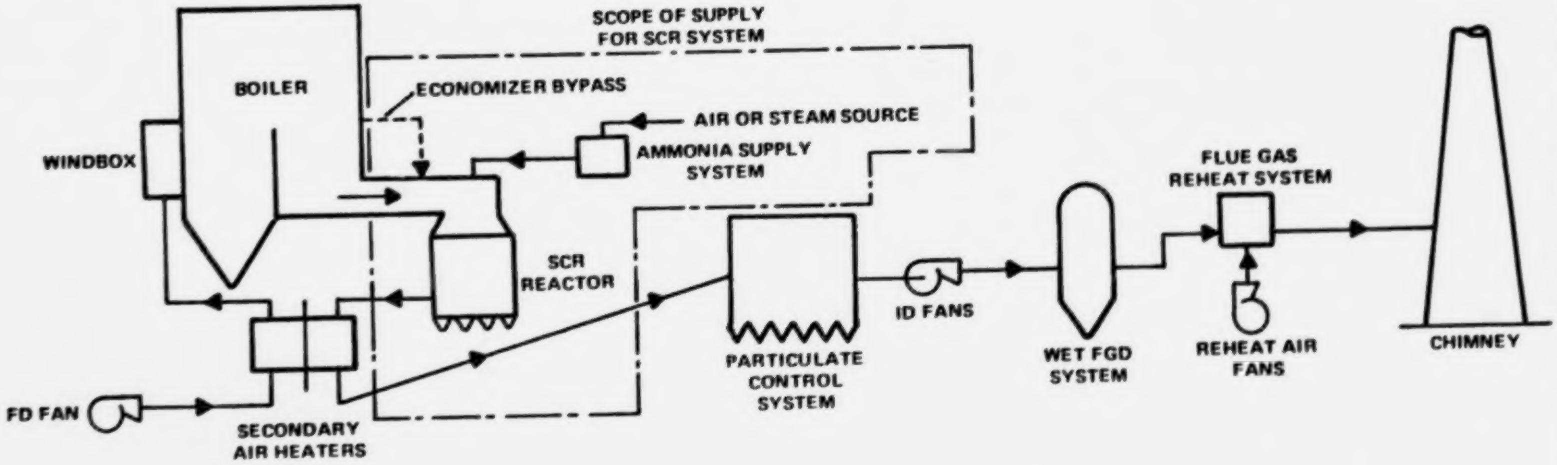
SCOPE OF SUPPLY
FOR SCR SYSTEM
BOILER
ECONOMIZER BYPASS
AIR OR STEAM SOURCE
WINDBOX
AMMONIA SUPPLY
SYSTEM
FLUE GAS
REHEAT SYSTEM
SCR
REACTOR
ID FANS
WET FGD
SYSTEM
REHEAT AIR
FANS
CHIMNEY
PARTICULATE
CONTROL
SYSTEM
FD FAN
SECONDARY
AIR HEATERS

FIGURE 1
PROCESS SCHEMATIC SELECTIVE CATALYTIC NO_x REDUCTION (SCR)

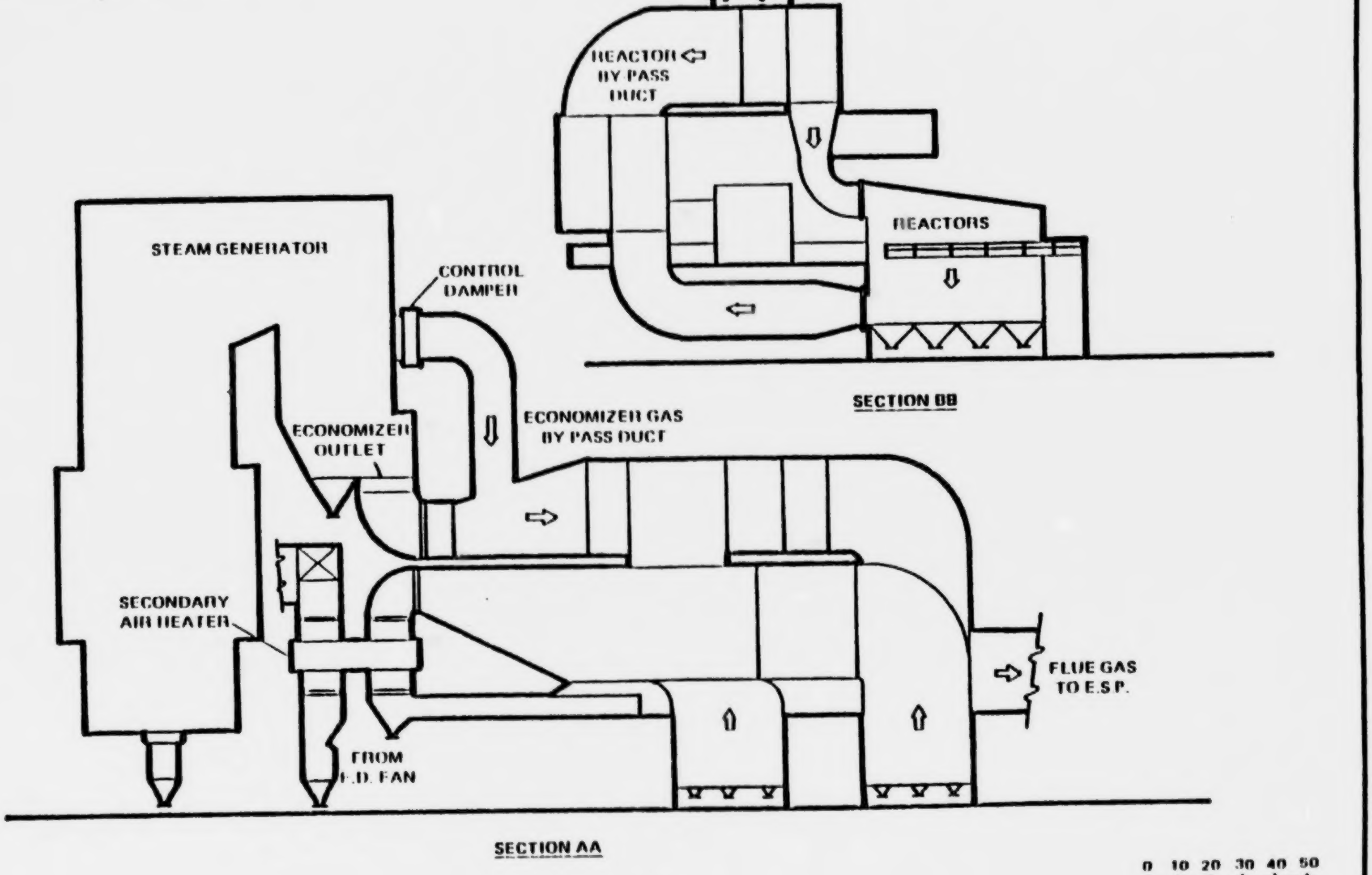

REACTOR BY PASS DUCT
REACTORS
SECTION BB
STEAM GENERATOR
CONTROL DAMPER
ECONOMIZER GAS BY PASS DUCT
ECONOMIZER OUTLET
SECONDARY AIR HEATER
FROM F.D. FAN
FLUE GAS TO E.S.P.
SECTION AA
0 10 20 30 40 50
GRAPHIC SCALE (FEET)

FIGURE 2
GENERAL ARRANGEMENT - ELEVATION OF HITACHI ZOSEN SYSTEM ON A 500 MW BOILER

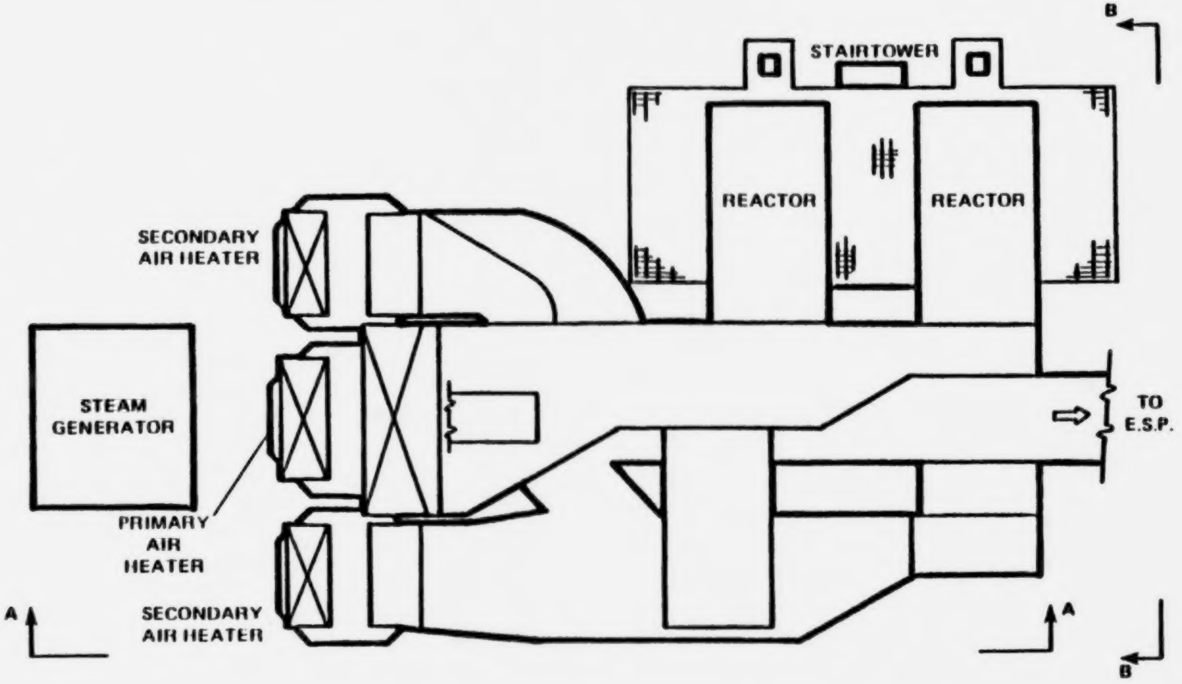
B
STAIRTOWER
REACTOR
REACTOR
SECONDARY AIR HEATER
STEAM GENERATOR
TO E.S.P.
PRIMARY AIR HEATER
SECONDARY AIR HEATER
A
A
B
0 10 20 30 40 50
GRAPHIC SCALE (FEET)

PLAN

FIGURE 3
HITACHI ZOSEN SYSTEM ON A 500 MW BOILER

TABLE 1
UNADJUSTED DESIGN PARAMETER COMPARISONS
HITACHI - ZOSEN PROCESS (90% NO$_x$ REMOVAL)

Report	EPRI/S-R Reference 1	EPRI/U.S EPA/TVA Reference 2	U.S. EPA/TVA Reference 3
Unit Data			
Unit Gross Capacity - MW	548	500	---
Unit Net Capacity - MW	500	---	500
Unit Gross Heat Rate - Btu/kWhr	9643	9000	---
Unit Net Heat Rate - Btu/kWhr	10569	Not Given	9500
Plant Elevation - Ft AMSL	1000	Sea Level	Sea Level
Ambient Pressure	14.2 psia	14.7	14.7
Coal Data			
Coal Source	Wyoming (Powder River)	Midwest - Bituminous	Eastern Bituminous
Coal HHV - Btu/lb	8020	10500	11700
Coal Moisture Content - Wt %	30.40	10.74	4.0
Coal Sulfur Content - Wt % (Wet)	0.48	3.12	3.40
Economizer Outlet Conditions			
Wet ACFM x 10^{-6}	3.036	2.146	2.249
Wet SCFM x 10^{-6}	1.258 (60°F)	0.958 (60°F)	1.0037 (60°F)
Temperature	700	705	705
Excess Air - °F %	24	20	20
Moisture - Vol %	13.09	9.48	4.0
SO_2 - lb/MMBtu	1.20	5.94	5.81
NO_x Data	Hitachi Zosen Case 3 90% Eff.	Hitachi Zosen 90% Eff.	Hitachi Zosen 90% Eff.
NO_x Emissions -			
lb/MMBtu (as NO_2)	0.47	1.01	0.40
Moles/hr (95% NO + 5% NO_2)	54.06	97.69	61.95
NH_3:NO_x Mole Ratio	1:1	1:1	1.1:1
Est. Catalyst Requirements - Ft^3*	17,000	14,000	10,734
Turbine Heat Rate - Btu/kWHr	8081	Not Given	Not Given
Boiler Efficiency - %	83.8	90.0	90.0

*NOXNON 500 Type 3, all cases.

TABLE 1A
ADJUSTED DESIGN PARAMETER COMPARISONS
HITACHI - ZOSEN PROCESS (90% NO_x REMOVAL)

Report	EPRI/S-R Reference 1	EPRI/U.S EPA/TVA Reference 2	U.S. EPA/TVA Reference 3
Unit Data			
Unit Gross Capacity - MW	548	548	548
Unit Net Capacity - MW	500	500	500
Unit Gross Heat Rate - Btu/kWhr	9643	9183	9183
Unit Net Heat Rate - Btu/kWhr	10569	10065	10065
Plant Elevation - Ft AMSL	1000	1000	1000
Ambient Pressure - psia	14.2	14.2	14.2
Coal Data			
Coal Source	Wyoming (Powder River)	Midwest - Bituminous	Eastern Bituminous
Coal HHV - Btu/lb	8020	10,500	11,700
Coal Moisture Content - Wt %	30.4	10.74	4.0
Coal Sulfur Content - Wt % (Wet)	0.48	3.12	3.40
Economizer Outlet Conditions			
Wet ACFM x 10^{-6}	2.9501	2.4737	2.4555
Wet SCFM x 10^{-6}	1.2224	1.0712	1.0633
Flue Gas Temperature - °F	700	700	700
Excess Air - %	20	20	20
Moisture - % (Vol)	13.46	9.48	4.0
SO_2 - lb/MMBtu	1.20	5.94	5.81
NO_x Data			
NO_x Emissions -			
lb/MMBtu (as NO_2)	0.5	0.6	0.6
Moles/hr (95% NO + 5% NO_2)	54.44	65.64	65.64
NO_x Removal Efficiency - %	90	90	90
NH_3:NO_x Mole Ratio	1:1	1:1	1:1
Est. Catalyst Requirements - Ft^3*	16,500	16,100	11,700
Turbine Heat Rate - Btu/kWHr	8081	8081	8081
Boiler Efficiency - %	83.8	88.0	88.0

*NOXNON 500 Type 3, all cases.

TABLE 2
UNADJUSTED ECONOMIC PARAMETERS COMPARISONS

Report	EPRI/S-R Reference 1	EPRI/U.S EPA/TVA Reference 2	U.S. EPA/TVA Reference 3
Cost Dates:			
Capital	7/1/79	7/1/79	7/1/82
Operating & Maintenance	7/1/79	7/1/80	1984
Minimum Annual Return (MAR) - %	10.0	10.0	10.0
Escalation Rate (e) - %	6.0	6.0	6.0
Fixed Charge Rate - %	18.0	18.0	14.7
Plant Life - Years	30	30	30
Interest During Construction - %	8	8	10
Center of Gravity Period - Years	1	1	1
Capital Recovery Factor	.10608	.10608	.106068
Present Worth Factor For Escalated Series[1]	17.7775	17.7775	17.7775
Levelized Factor[1]	1.886	1.886	1.886
Present Worth Factor For Escalated Series[2]	8.395	8.395	8.395
Levelized Factor[2]	0.891	0.891	0.891
NH_3 - \$/Ton	170.	186.	155.
Steam - \$/1000 lb	2.50		
- \$/MMBtu		2.81	2.70
Electricity - mills/kWhr	37.5	34.0	37.5
Annual Hours of Operation	6132	6132	5500

Notes: 1) For Annual Operating Costs over 30 years

2) For Biannual Replacement Costs over 28 years

TABLE 2A
ADJUSTED ECONOMIC PARAMETERS COMPARISONS

Report	EPRI/S-R Reference 1	EPRI/U.S EPA/TVA Reference 2	U.S. EPA/TVA Reference 3
Cost Dates:			
Capital	1/1/83	1/1/83	1/1/83
Operating & Maintenance	1/1/83	1/1/83	1/1/83
Minimum Annual Return (MAR) - %	12.5	12.5	12.5
Escalation Rate (e) - %	8.5	8.5	8.5
Fixed Charge Rate - %	15.3	15.3	15.3
Plant Life - Years	30	30	30
Interest During Construction - %	12.5	12.5	12.5
Center of Gravity Period - Years	1.5	1.5	1.5
Capital Recovery Factor	.12876	.12876	.12876
Present Worth Factor For Escalated Series[1]	18.50995	18.50995	18.50995
Levelized Factor[1]	2.314	2.314	2.314
Present Worth Factor For Escalated Series[2]	8.78160	8.78160	8.78160
Levelized Factor[2]	1.131	1.131	1.131
NH_3 - $/Ton	155.	155.	155.
Steam - $/MMBtu	3.75	3.75	3.75
Electricity - mills/kWhr	45.0	45.0	45.0
Annual Hours of Operation	5694	5694	5694

Notes: 1) For Annual Operating Costs over 30 years

2) For Biannual Replacement Costs over 28 years, where the Biannual Escalation rate is 17.7 percent and the biannual MAR is 26.6 percent.

TABLE 3
UNADJUSTED CAPITAL COST ESTIMATE COMPARISONS[1]
HITACHI - ZOSEN[2] PROCESS (90% NO_x REMOVAL)
(Thousands of Dollars)

Report	EPRI/S-R Reference 1 Table 5-5		EPRI/ U.S. EPA/TVA[3] Reference 2 Table 64		U.S. EPA/ TVA Reference 3 Table A-15
Cost Date	7/1/79		7/1/79		1/1/84
Reactors	1510$^{(4)}$	NH_3 Storage/Injection	950$^{(4)}$		840$^{(4)}$
Ductwork	3952	Reactor Section	6650		4195
Insulation	1571	Gas Handling	850		---
Ammonia System	308		---	Flue Gas Fans	3051
Air Preheater Design	---		---		585
Civil	1985		---		---
Elect/Inst.	534	Services, Utilities & Misc.	---		520
Fan/ESP Costs	1820		---		---
Indirect Costs	3050		---		---
Total Process Capital (TPC)	14,700		8450	Total Direct Investment	9191
(Cost $/kW)	(30)		(16.9)		(18.4)
General Facilities	740		450	Engineering Design & Supr.	643
Engineering & Fees - A/E	520		850	A/E Contractor	184
- Vendor	1825		---	Construction Expense	1471
Contingency - Project	2360		1700	Contractor Fees	460
- Process	2225		1250	Contingency	2390
Sales Tax	280		---		---
Total Plant Investment (TPI)	22,700		12,700	Total Fixed Investment	14,339
(Cost $/kW)	(45)		(25.4)		(28.7)
Royalty Allowances	355		300		458
Preproduction	652		1000	Allowance for Startup	1434
Inventory	198		100	Working Capital	522
Initial Catalyst	8050		6600		6473
AFDC	1815		1000		2237
Land	0		0		8
Total Capital Requirement (TCR)	33,800		21,700	Total Capital Investment	25,471
(Cost $/kW)$^{(5)}$	(68) per Net kW		(43.4) Per Gross kW		(50.9) Per Net kW
$/ACFM	11.13		10.11		11.33

Notes:
1) Comparisons of Capital Costs from Referenced Reports.
2) Dry Selective Catalytic NO_x Reduction (SCR) Process.
3) Based on EPRI Premises.
4) Costs refer to category to the nearest left of the number.
5) Based on a 500,000 kW net of gross capacity as indicated.

TABLE 3A
ADJUSTED CAPITAL COST ESTIMATE COMPARISONS[1]
HITACHI - ZOSEN PROCESS[2] (90% NO_x REMOVAL)
(Thousands of Dollars)

Report	EPRI/S-R Reference 1		EPRI/ U.S. EPA/TVA[3] Reference 2		U.S. EPA/ TVA Reference 3
Cost Date	1/1/83		1/1/83		1/1/83
Reactors	1874[4]	NH_3 Storage/Injection	1396[4]		863[4]
Ductwork	4905	Reactor Section	9791		4314
Insulation	1950	Gas Handling	1250		---
Ammonia System	382		---	Flue Gas Fans	3138
Air Preheater Design	732		614		609
Civil	2463		---		---
Elect/Inst.	662	Added Scope Costs	2248	Added Scope Items	2248
Fan/ESP Costs	2259		---	Services, Utilities & Misc.	670
Indirect Costs	3785		---		---
Total Process Capital Costs (TPC)	19012		15299	Total Direct Investment	11842
($/kW - Net)	(38.0)		(30.6)		(23.69)
General Facilities	951		765	Engineering Design & Supr.	829
Engineering & Fees - A/E	666		1530	A/E Contractor	237
- Vendor	2377		3059	Construction Expense	1895
Contingency - Project	3042	Combined Contingency	2295	Contractor Fees	592
- Process	2852		---		---
Sales Tax	380		306	Contingency (Overall)	3079
Total Plant Investment (TPI)	29280		23254	Total Fixed Investment	18474
($/kW - Net)	(58.6)		(46.5)		(36.9)
Royalty Allowances	475		543		592
Preproduction	849		1458	Allowance for Startup	1847
Inventory	244		62	Working Capital	602
Initial Catalyst	10389		9717		7266
AFDC	5761		4493		3647
Land	0		0		0
Total Capital Requirement (TCR)	46998		39527	Total Capital Investment	32428
($/kW - Net)[5]	(94.0)		(79.1)		(64.9)
$/ACFM	15.93		15.97		13.21

Notes:
1) Comparisons of Capital Costs from Referenced Reports.
2) Dry Selective Catalytic NO_x Reduction (SCR) Process.
3) Based on EPRI Premises.
4) Costs refer to category to the nearest left of the number.
5) Based on a 500,000 kW net capacity, all cases.

TABLE 4
UNADJUSTED ANNUAL REVENUE REQUIREMENTS
HITACHI - ZOSEN PROCESS (90% NO_x REMOVAL)
(Thousands of Dollars)

Report	EPRI/S-R Reference 1 Table 5-6 (Case 3)	EPRI/ U.S. EPA/TVA Reference 2 Table 71	U.S. EPA/TVA Reference 3 Table A-16
COST DATE	7/1/79	7/1/80	1/1/85
Operations	40	122.6	65.7
Maintenance	294	327.4	505.6
O&M Overhead	158	76.1	342.8
Total Operating & Maintenance (O&M)	492	526.1	914.1
Steam	67	19	145.4
Condensate	13	---	---
Electricity	727	470.5	611.7
Heat Credit	---	(87.9)	---
NH_3	445	1042.0	449.7
Catalyst Replacement	8050	6880.0	7479.6
Spent Catalyst Disposal	---	(260.0)	---
Total Variable O&M	9302	8064.5	8686.4
Total Annual O&M Costs	9794	8590.6	9600.5
Annual Fixed Costs	6084	3906.0	3744.2
Total First Year Costs	15878	12496.6	13344.7
kWhr/Year	3.066×10^9 (Net)	3.066×10^9 (Gross)	2.750×10^9 (Net)
First Year mills/kWhr	5.18	4.08	4.85
Levelized Annual O&M Cost	18741	16201.9	18106.5
Levelized Fixed Costs	6084	3906.0	3744.2
Total Annual Levelized Costs	24555	20107.9	21850.7
Levelized mills/kWhr 1-Year Catalyst Life	8.01	6.56	7.95
Levelized mills/kWhr 2-Year Catalyst Life	5.40	4.41	5.24
Reduction Percentage of Levelized mills/kWhr for 1-Year Versus 2-Year Catalyst Life	33%	33%	34%

TABLE 4A
ADJUSTED ANNUAL REVENUE REQUIREMENTS
HITACHI - ZOSEN PROCESS (90% NO_x REMOVAL)
(Thousands of Dollars)

Report	EPRI/S-R Reference 1	EPRI/ U.S. EPA/TVA Reference 2	U.S. EPA/TVA Reference 3
Cost Date	1/1/83	1/1/83	1/1/83
Operations	53	151	56
Maintenance	391	401	424
O&M Overhead	210	93	288
Total Fixed Operating & Maintenance (O&M)	654	645	768
Steam	99	23	221
Condensate	19	---	---
Electricity	787	605	830
Heat Credit	---	---	---
NH_3	431	492	492
Catalyst Replacement	10389	9717	7266
Spent Catalyst Disposal	---	---	---
Total Variable O&M	11725	10837	8809
Total First Year O&M Costs	12379	11482	9577
Annual Fixed Costs	7191	6006	4961
Total First Year Costs	19570	17488	14538
kWhr/Year (Net)	2.847×10^9	2.847×10^9	2.847×10^9
First Year mills/kWhr	6.87	6.14	5.11
Levelized Annual O&M Cost	28645	26569	22161
Levelized Fixed Costs	7191	6006	4961
Total Annual Levelized Costs	35836	32575	27122
Levelized mills/kWhr, 1-Year Catalyst Life	12.59	11.44	9.53
Levelized mills/kWhr, 2-Year Catalyst Life	8.27	7.40	6.51
Reduction Percentage of Levelized mills/kWhr for 1-Year Versus 2-Year Catalyst Life	34.3%	35.3%	31.7%

UPDATE ON NO_x FLUE GAS TREATMENT IN JAPAN

By:

Y. Nakabayashi, T. Miyasaka, K. Mouri
K. Honda
Electric Power Development Co., Ltd.
Tokyo, Japan

ABSTRACT

Results of research and development on Selective Catalytic Reduction carried out by EPDC have been reported at the two previous NO_x Symposia. This third report reviews the results of a SRC demonstration test at the No. 1 unit of Takehara Thermal Power Station (250 MW, Coal) performed over a one year period during 1981 and 1982.

The design of an SCR system for No. 3 unit of Takehara Thermal Power Station (700 MW, Coal), now under construction and trial operation, is also reported. In addition, the outline of research work for a new simultaneous De-NO_x/De-SO_x process is discussed.

INTRODUCTION

The development of De-NO_x flue gas treatment equipment for power generation boilers has ocurred rapidly in Japan. This De-NO_x equipment is now available for practical use, not only for gas and oil fired boilers but also for coal fired boilers, and, at this moment, new proposed coal fired thermal power plants are adopting this equipment.

The adoption of De-NO_x equipment has been discussed with local governments during the establishment of environment control agreements because combustion modification alone is not always sufficient to meet allowed NO_x emission levels. In areas with higher emission allowances it may be possible to build a coal thermal power station without De-NO_x equipment by the application of combustion modification technology, but most of the coal thermal power plants are required to install De-NO_x equipment. Table 1 shows the number of De-NO_x systems installed at coal fired thermal power stations in Japan.

In this context, it is felt that the chances for successful application of such equipment are greatest though cooperative development programs between Electric Power Companies and boiler manufacturers. As one example, EPDC conducted a demonstration test of Selective Catalytic Reduction (SCR) for one year at the 250 MW Takehara No. 1. After overcoming minor problems, the equipment is now used for commercial operation. The Takehara No. 3 unit (700 MW coal), which is now under trial operation (and expected to commence commercial operation in March, 1983), has SCR De-NO_x equipment for processing the entire flue gas stream.

This report discusses 1) results of the demonstration test at the Takehara No. 1 unit, 2) design of the Takehara No. 3 SCR system and 3) the test results of a new simultaneous De-NO_x/De-SO_x technology.

SCR DEMONSTRATION TEST

EPDC was commissioned by the government to install a demonstration SCR system designed for full capacity at the No. 1 boiler (coal-fired, 250 MWe) of the Takehara Power Plant. The design of the system was completed in 1978 and civil engineering, fabrication of equipment and installation were performed in 1979 and 1980. In 1981 the system was completed and connected to the power plant during an annual inspection shutdown, and a one year demonstration test was carried out until June 1982.

The specifications, test results, problems and countermeasures are explained as follows.

DEMONSTRATION SCR SYSTEM

The demonstration SCR system installed at the existing No. 1 unit of Takehara Station included the following major equipment with specifications given in Table 2:

- De-NO_x SCR equipment
- Hot-side electrostatic precipitator
- Induced draft fans
- De-nitrification equipment for waste water treatment
- Air preheater modifications

The flow diagram of this demonstration test plant is shown in Figure 1. This arrangement is generally called "low dust" SCR system. (LDSS)

TARGET PERFORMANCE OF DEMONSTRATION TEST

The target performance of the demonstration system is summarized as follows. This performance was considered possible based on the cooperative research work between EPDC and manufacturers.

• De-NO_x equipment	
De-NO_x efficiency	80% and over
Leakage ammonia	5 ppm and less
SO_3 conversion ratio	1% and below
• Hot-side ESP	
Dust concentration of outlet	100 mg/m^3N and less
• Bacteria N removal equipment	10 ppm and less

TEST RESULTS

The operation and performance of all equipment satisfied the guaranteed values as indicated in Table 3.

During the demonstration test period, equipment problems occurred down stream of the De-NO_x system but all problems were resolved during the test period. The details are explained as follows.

(1) Boiler

For the execution of demonstration test, a part of the economizer was removed in order to get the proper temperature at the De-NO_x equipment.

(2) De-NO_x equipment

The flue gas stream leaving the boiler is split into A and B ducts. A plate type De-NO_x catalyst is used in A train while the tubular type catalyst is used in B train. Both are selective catalytic reduction processes using ammonia injection.

The ammonia injection was commenced on July 1, 1981. The record of De-NO_x efficiency is shown in Figure 2 and discussed below.

(a) Particulars on A train De-NO_x equipment

The ammonia injection commenced on July 1, 1981, and after the various performance tests were carried out in the middle of July, 1981, the operation was continued at a De-NO_x efficiency of 80%.

At the plant shut down on Oct. 23, 1981 caused by a boiler outage, an open inspection of the SCR was carried out. Ash deposits from gas turbulence at the upper (inlet) end of catalyst (under the catalyst support beam) was observed. The deposit partly closed the gas flow. During the shut down period for boiler repair, a plate was installed under the catalyst support beam as a countermeasure. Thereafter, the operation was continued at 80% De-NO_x efficiency without any problem, and at the next open inspection of De-NO_x equipment on January 13, 1982, the effectiveness of the plate installment was confirmed. After the open inspection, the operation was continued at 80% De-NO_x ratio until the end of May, 1982, at which time the demonstration test was completed.

(b) Particulars on B train De-NO_x equipment

Same as A train, the ammonia injection was commenced on July 1, 1981, and various performance tests were conducted. Thereafter, the operation was continued at 80% De-NO_x efficiency. However, because of the adverse effect to the down stream equipment, ammonia injection rate was reduced or suspended temporarily for some period.

An open inspection was made during the plant shut down caused by boiler outage on October 23, 1981. Ash deposit on the upper (inlet) end of catalyst, situated under the catalyst support beam, partly plugged the gas flow, and the plugged area was much larger than A train (about 10% of the flow area).

Therefore, cleaning of ash deposit and installment of a plate to avoid gas turbulance were carried out during the shut down period for boiler repair. Also, at the open inspection of De-NO_x equipment executed on January 13, 1982, an additional plate under the catalyst support beam, soot blowing equipment and a flow adjusting grid at the top of first row of catalyst were installed. Inspection windows were also installed at each row of catalyst in order to inspect the inside during operation.

After that, while monitoring the condition of down stream equipment (such as plugging of air preheater and vibration of booster fan) ammonia injection rate was adjusted, and the operation was continued at 60 to 80% De-NO_x efficiency until the end of May, 1982.

At the annual inspection shut down in 1982, rearrangement of catalyst layers was performed to avoid the above ash deposit. Catalyst volume was also increased. The operation has been continued at 80% De-NO_x efficiency with good results after the annual shut down.

(c) Performance and reliability of De-NO_x equipment

The performance tests of De-NO_x equipment were conducted 4 times, namely middle of July, 1981, middle of November, 1981, end of January to beginning of February, 1982 and middle of May, 1982. Planned performance was confirmed. Table 4 shows the results of the 4 performance tests.

(3) Hot-side electrostatic precipitator

The hot-side electrostatic precipitator was specially installed for the SCR demonstration test because of the adoption of a low dust SCR system.

(a) Particulars on hot-side electrostatic precipitator operation

The hot-side electrostatic precipitaor commenced operation at the time of commencement of SCR operation, namely at the start-up after the annual shut down of June, 1981. The operation was continued until the completion of demonstration test without problems.

(b) Performance of hot-side electrostatic precipitator

As shown in table 3, the performance of the hot-side electrostatic precipitator fully satisfies the initial planned values.

(4) Air Preheaters

(a) Air preheater on A train

The A train air preheater started to operate from the day after annual inspection in June, 1981 and NH_3 was injected into SCR on July 1st, 1981.

3 to 4 ppm of NH_3 existed and 6 to 7 ppm of SO_3 existed in flue gas of air preheater inlet.

After operating about 2700 hours, an air preheater wash was executed while the boiler was shut-down for repair.

Gas draft loss was twice (110 mmAq) the initial value.

After washing of air preheater, air preheater operated favorably without problems until completion of demonstration test.

Gas draft loss trend is shown in Figure 3.

(b) B train air preheater

B train air preheater started at same time as A train.

4 to 5 ppm of NH_3 existed and about 10 ppm of SO_3 existed in flue gas of air preheater inlet.

Draft loss of B train air preheater was larger than A train air preheater and draft loss doubled in only 2 months. Therfore washing of air preheater was executed at an interval of once every 2 months.

This is mainly caused by higher NH_3 leakage level than A train. To avoid severe plugging of air preheater, NH_3 injection rate was reduced until annual inspection in end of March, 1982. At this inspection shut down, we decided to increase catalyst volume.

After this increase of catalyst volume, we achieved satisfactory continuous operation until completion of demonstration test with 80% De-NO_x efficiency and 2 to 3 ppm NH_3.

Gas draft loss trend is shown in Figure 3.

(c) Performance and Reliability of Air preheaters

Performance of air preheaters achieved initial planned value shown in Table 3.

Washing of air preheater under the condition of half-rung operation was executed to remove plugging compounds composed of ash, NH_3/SO_3 compounds. This was satisfactory to decrease draft loss.

Further expecting to reduce the washing intervals, modified soot blowers were installed in 1982's inspection.

After annual inspection, degree of plugging of air preheaters was relieved by means of above mentioned countermeasures and decrease of leakage NH_3. By September, 1982, significant draft increase was not observed and air preheaters have been favorably operating.

(5) Draft Fans

The induced draft fan (IDF) was added as part of the SCR modification while the booster fan (BUF) was original equipment.

(a) IDF operation

Slight vibration increase was experienced from the start of June 1981 to March, 1982. However this increase was within JIS allowable value and did not interfere with continuous operation.

(b) BUF Operation

Significant vibration increase was realized in about 1.5 month from 12/1000 mm to 55/1000 mm requiring that each fan of A train and B train be cleaned.

This vibration was caused by ash attached to fan blades. In 1982's inspection (March), countermeasures to resolve this trouble were as follows.

(1) Strength fan foundation.
(2) Coat B train fan blades

After execution of these countermeasures, vibration has not exceeded allowable value.

(c) Performance and reliability of fans

Performance was satisfactory.

On reliability, Problems of BUF vibration became acute. However this is caused by unbalance of blades caused by deposition and shedding of ash at the bolt fasteners for anti-errosion liners on blades.

At this moment, we believe that such a problem has been resolved by means of before mentioned countermeasures.

SUMMARIZED RESULT OF THIS DEMONSTRATION TEST

Following are our results of this demonstration.

- Established catalyst life greater than 1 year
- Specification of 5 ppm NH_3 leakage is not acceptable for stable continuous operation. Adequate value is less than 2.5 ppm.

DESIGN BASE FOR TAKEHARA NO. 1 SCR DEMONSTRATION AND NEW TAKEHARA NO. 3 UNIT

This section describes fundamental thought on design of the SCR demonstration plant at Takehara No. 1 unit and SCR of Takehara No. 3 unit. Test results of the pilot test and actual SCR experience of oil-fired boiler were incorporated in its design. This SCR design philosophy described below is from Babcock Hitachi Ltd. (BHK) who is one of the manufactures of the SCR for the demonstration plant and for No. 3 extension unit of Takehara Thermal Power Station.

DECISION OF CATALYST VOLUME (SV VALUE)

Results on catalyst fundamental characteristics obtained by pilot tests was considered in deciding SV value for achievement of our SCR specification. Those results are shown in Figure 4 - Figure 6.

SV value of Takehara No. 1 unit (demonstration plant) was decided as 2300 (1/hour) based on the dimension limitation of mounted catalyst block (described later) and results of pilot test data.

DECISION OF LINEAR VELOCITY (LV VALUE) AND PREDICTION OF DRAFT LOSS IN REACTOR

LV value is selected by the consideration for dust countermeasures of catalyst layer (such as dust deposition and dust errosion), allowed draft loss of SCR reactor and arrangement of catalyst block etc.

As Figure 7 shows, during pilot tests (LV = 4 m/s) no draft loss increase and remarkable performance was realized in long term test.

Then for SCR demonstration equipment of Takehara No. 1 unit, LV value of 4.8 m/s was selected, which is close to pilot test value. Planned draft loss in this case is 25 mmAq for catalyst layer and 55 mmAq for SCR reactor, including catalyst layer.

For Takehara No. 3 unit, errosion of catalyst is no problem remarkably even if LV value is same as value for SCR of oil fired boiler. Therefore, it becomes possible to design the Unit 3 reactor with LV value set at 7 m/s. In this case, 44 mmAq draft loss for catalyst layer will be predicted and 66 mmAq for reactor (including catalyst layer) will be also predicted. These values have enough margin against design allowance value of 100 mmAq and less.

CATALYST INSTALLATION

Figure 8 shows the installation of catalyst into SCR reactor. Namely, One "unit" of catalyst is made of several pieces of plate catalyst, and the larger "block" is made up of such units. This "block" is a basic component making up the catalyst layer in the reactor. This design enables mounting and extraction of catalysts in a short time.

NH_3 INJECTION DEVICE

If NH_3 is injected non-uniformly into catalyst layer disproportionately to the NO_x quantity in flue gas, NO_x performance is decreased because of un-balanced mole ratio of NH_3/NO_x in reactor. Thus, a multi-point injection array is used as shown in Figure 9.

R&D ON CONTINUOUS NH_3 MEASUREMENT INSTRUMENT

It is very important to continuously monitor leakage of NH_3 in order to 1) avoid adverse effect to downstream equipment such as air preheater, Fans, FGD etc. and 2) it is also very important in determining catalyst deterioration since increase of NH_3 can be observed in advance of $DeNO_x$ efficiency decrease.

Though we have standard measurement procedure fixed by Japan Industrial Standard (JIS K0099) for NH_3 concentration measurement, we have some troubles in measuring leakage NH_3 according to this standard because of interference from SO_3. To avoid this, we have introduced a modified procedure and are measuring leakage NH_3 concentration at outlet of SCR reactors at this moment.

Another continuous NH_3 measurement instrument was installed to Takehara's SCR demonstration test plant. This is an indirect measurement procedure using an NH_3 converter with a catalyst. Further, EPDC and Anritsu Electric Co., Ltd. has been executing joint research and development on a continuous NH_3 measurement instrument based on self-modulated derivative spectrometry of ultraviolet absorption to commercialize it for coal fired-boilers with SCR. The demonstration instrument was located at the outlet of the SCR at Takehara's SCR demonstration test plant in parallel with the instrument described before. This demonstration test is under execution. However, as this instrument is in successful operation, EPDC decided to introduce this to No. 3 unit of Takehara thermal power station based on the results at this moment.

Results from 6 months of testing, especially for the sampling system (a key element of this technique), is described below.

DEVELOPMENT OF OPTIMUM SAMPLING SYSTEM

- Temperature of sampling line

  Figure 10 shows temperature variation test of sampling line. No variation of output is observed with temperature variation above 350°C.

- Temperature of dust filter

  With less than 360°C at dust filter, NH_3 measured output decreases as temperature decreases. For more than 370°C, no outlet variation was observed as temperature varied.

  400°C is proper temperature at dust filter.

  This result is shown in Figure 11.

- Sampling gas volume

  More than 4 ℓ/min gas sampling volume is recommended because response time does not vary even if gas volume is increased.

  Response time of 90% is within 2 minutes. Figure 12 shows this result.

- Probe Temperature

  Output is stable at probe temperatures more than 380°C, as shown in Figure 13.

- Probe material

  Nickel alloy should be used for probe material.

- Confirmation of NH_3 losses in sampling line was done in comparative tests shown in Figure 14.

  NH_3 concentration measurements of standard gases injected through sampling line and bypass line were compared. No different value was observed, thereby verifying that no NH_3 loss occurs in this sampling system.

CONFIRMATION OF RELIABILITY OF MEASURED VALUE

- If correlation to manual analysis is demonstrated, leakage NH_3 trend will be accurate and reliable.

ITEMS TO BE CONFIRMED

- Confirmation of long-term stability and reliability
- Study of maintenance period.

CATALYST MANAGEMENT

It is very difficult to determine catalyst life at this moment because prediction method of catalyst life has not been established.

As catalyst deteriorates during long time use, it is essential to establish the method to measure the degree of catalyst deterioration.

One method of management (maintenance) of catalyst is described in this section. EPDC and other power companies have been executing cooperative efforts to establish a reasonable criterial for management of SCR catalyst maintenance.

For SCR at coal fired boilers, there is less actual experience at this moment. It is impossible to introduce key management method for SCR maintenance at this moment, but it will be very important to establish methods based on actual operation experience in future.

EVALUATION BY SAMPLE CATALYST

Catalyst test section is mounted to catalyst layer in SCR equipment. After this sample is extracted periodically from a reactor, activation of catalyst and physical characteristics such as specific surface area, pore distribution, strength etc. are measured under fixed conditions using a small scale measurement device in a laboratory. This is to check the degree of catalyst deterioration directly.

Especially, it is critical to check the K value coefficient of reactivity which is the index of catalyst activation.

PERFORMANCE CHECK ON ACTUAL OPERATION

Periodically, SCR operating conditions are repeated (same conditions such as gas temperature, NH_3 injection quantity etc.) and SCR performance is compared to the intitial or baseline data.

COMMERCIAL SCR PLANT OF TAKEHARA NO. 3 UNIT

No. 3 extention unit of Takehara Thermal Power Station entered into trial operation in October, 1982 and is scheduled to commence commercial operation in March, 1983.

This SCR equipment is the largest capacity installed in Japan. It is Low Dust SCR System (LDSS) and Figure 15 shows SCR flow diagram. Figure 16 shows the structure of reactor.

Table 5 shows planned operating conditions of this SCR equipment. These conditions are based on the results of SCR demonstration test described in Section 2.

COLD-SIDE SIMULTANEOUS NO_x/SO_x REMOVAL PROCESS

EPDC has been developing dry FGD, using activated char as SO_x adsorbent, jointly with Sumitomo Heavy Industries, Ltd. (SHI) since 1978.

Pilot test of this technology was completed in 1982 and on the basis of the results, EPDC started to construct Dry FGD demonstration equipment (300,000 Nm3/H capacity) at our Matsushima Thermal Power Station in 1981. This project is commissioned by MITI and this demonstration test is scheduled to start in September 1983.

As a result of this R&D, SHI established a new simultaneous De-NO_x/De-SO_x process at their laboratory, which is applicable at a temperature range of 130°-150°C.

EPDC performed R&D of this technology jointly with SHI, using 10,000 Nm3/H pilot test plant at Takehara Thermal Power Station. This 10,000 Nm3/H pilot plant is the same as used in the dry FGD development project.

One feature of this Dry FGD process is the injection of NH_3 before adsorption reactor. This has two merits as follows:

- Decrease of make-up quantity of activated char
- 30-40% De-NO_x efficiency at 130°C-150°C

Using the effect of De-NO_x above mentioned, an idea was introduced to improve De-NO_x efficiency. Figure 17 shows the cold-side simultaneous De-NO_x/De-SO_x process flow diagram.

This process combines two dry FGD in series, in which adsorbent is recycled in series or parallel among two reactors and regenerator. The concept of commercial plant is shown in Figure 18.

FEATURES OF COLD-SIDE DE-NO_x TECHNOLOGY

Expected characterties of this technology are as follows:

- 80% De-NO_x efficiency is expected.
- No adverse effect on down stream equipment
- Improvement of De-SO_x efficiency

RESULTS OF PILOT TEST

This test was conducted over 850 hours from March, 1982 to April 1982. Test items were as follows:

- Confirmation of application for coal fired boiler
- Confirmation of performance of De-NO_x/De-SO_x efficiency
- Confirmation of operation conditions

Test condition simulated the inlet condition of secondary reactor as follows:

SO_2	250 ppm
NO_x	240 ppm
Temperature	150°C

Under this flue gas condition, about 75% De-NO_x efficiency was obtained with NH_3 injection mole ratio of 2. Although almost 100% De-SO_x efficiency was obtained, the leaked NH_3 concentration of reactor outlet was remarkably high (20-30 ppm). We performed many parametric tests to obtain the characteristic simultaneous NO_x and SO_x removal. One result is shown in Figure 19.

We feel that if optimum inlet SO_x concentration, SV value and moving volume of activated char in reactor would be established, it can reduce leaked NH_3 and get the performance of 80% De-NO_x efficiency and almost 100% De-SO_x efficiency.

EVALUATION OF THIS TECHNOLOGY

In the case of 1st stage reactor, injected NH_3 as NO_x reduction agent contributes to SO_x removal reaction, but contribution to NO_x removal reaction is less because of high SO_x concentration. However, in the case of low concentration of SO_x (such as flue gas condition after 1st stage reactor), NH_3 has a higher effect on NO_x removal reaction, and overall De-NO_x efficiency would be much higher.

As this test was quite short, evaluation for commercial use was inadequate. Following items remains to be determined:

- Total system feasibility
- Long term stability and optimum conditions for operation

We are performing further feasibility studies with SHI.

CONCLUSION

The SCR demonstration plant at Takehara No. 1 and the SCR of Takehara's No. 3 unit are low dust SCR Systems (LDSS) having hot-side electrostatic precipitators upstream of SCR equipment. However, other power companies introduce High Dust SCR System (HDSS) which has cold-side ESP downstream of SCR equipment.

Both system have been commercialized for coal fired power plants in Japan. However, at this moment, no one can tell which system is most economic or has best reliability. EPDC is carefully evaluating both systems, looking at the actual data of SCR operation. EPDC is also using its best efforts to investigate other economical and reliable systems for coal fired power plants.

ACKNOWLEDGE

The authors acknowledge Babcock Hitachi K.K. and Sumitomo Heavy Industries for their cooperation in preparation of this paper.

REFERENCES

Y. Nakabayashi, status of R&D on NO_x removal in Japan and results of EPDC's R&D for De-NO_x Process Second EPRI NO_x Control Technology Seminar, Denver, Colorado, Nov. 1978.

T. Kimura, Y. Nakabayashi, K. Mouri, Overall Flue Gas Technology from Coal Fired Power Plant in Japan

ICCR 5th Conference Dusseldorf, Sept. 1980

Y. Nakabayashi, H. Yugami, K. Mouri Development of Flue Gas Treatment in Japan

Proceeding of the Joint Symposium on Stationay Combustion NO_x Control, Denver, Colorado Oct. 1980

Table 1 SCR for Coal Fired Boiler in Japanese Power Utilities Cos.

Power Company	Mfg	Power Station	Unit	SCR Capacity (MWe)	Start of operation	Efficiency (%)	Remarks
Hokkaido EPCO	BHK	Tomato-Atsuma	1	350x1/4	Oct. 1980	80	
Tohoku EPCO	BHK	Sendai	1	175	Mar. 1983	56 (80)	
	BHK	Sendai	2	175	Jun. 1983	56 (80)	
Tokyo EPCO	MHI	Yokosuka	1	265	Jun. 1985	Unfixed	Coal/oil or COM
	MHI	Yokosuka	2	265	Jun. 1985	Unfixed	ditto
Kansai EPCO	IHI	Himeji No. 1	1	33	Sep. 1982	-	
Chugoku EPCO	MHI	Shimonoseki	1	175	Apr. 1980	50	
	MHI	Shin-Ube	1	75	Mar. 1982	65	
	MHI	Shin-Ube	2	75	Jan. 1982	65	
	MHI	Shin-Ube	3	156	Nov. 1982	65	
Shikoku EPCO	MHI	Saijoo	1	156	Nov. 1982	65	
	IHI	Saijoo	2	250	Jan. 1984	-	
Kyushu EPCO	MHI	Minato	1	156	Mar. 1983	50	
		Matsuura	1	700	Jan. 1986	Unfixed	
EPDC	BHK/KHI	Takehara	1	250	Jul. 1981	80	
	BHK	Takehara	3	700	Mar. 1983	80	
	-	Matsuura	1	1000	-	-	
Joban Kyodo EPCO	MHI	Nakoso	8	600	Jan. 1983	50	Coal/oil
	IHI	Nakoso	9	375	Apr. 1983	-	Coal/oil
Sakata Kyodo EPCO	MHI	Sakata	1	156	Jun. 1984	35	
		Sakata	2	156	May 1985	35	
A	BHK	-	-	125	1984	65 (80)	
B	BHK	-	-	156	1984	65 (80)	
C	BHK	-	-	200	1984	60	
D	BHK	-	-	200	1984	60	

Table 2 The Specifications of Equipments at No. 1 Unit of Takehara Power Station

(1) Boiler (Existing)

Items	Specification	Remarks
Type	Subcritical Pressure Natural Circulation	Manufacturer Babcock Hitachi
Evaporation Capacity	810t/H	
Type of Combustion	Direct Combustion of Pulverized Coal	
Draft System	Balanced Draft	
Steam Pressure	176 kg/cm^2 G	Super Heater
Steam Temp.	571 C	Super Heater

(2) Hot Side ESP (New installed)

Items	Specification	Remarks
Type	Hot Side ESP Dry Type	Manufacturer Gadelius
Number	Two per Unit	
Gas Volume	397,000Nm^3/H	
Removal Efficiency	99.6%	Design
Gas Temp.	358 C	Design
Number of Compartment	2 Rooms and 3 Sections	
Size	16.4 m x 16.2 m x 14 m	(W x L x H)

(Continued)

(3) SCR (New Installed)

Equipment	SCR		NH	
Manufacturer / Items	Hitachi	K.H.I		Ube Kosan
Type	Vertical Fixed Bed	Ditto		High Pressure Storage Steam Heated Atomizing System
Number	1 unit	Ditto	Number	1 unit
Eff. (Target)	More than 80%	Ditto	Storage Capacity	75 t
Design Temp	350 C	Ditto		
Inlet NOx	300ppm	Ditto		
Inlet SOx	1,850ppm	Ditto		
Shape of Catalyst	Board	Pipe		
Size	8,000 x 10,800H	8,000 x 10,400H		

(4) Airpreheater (New Installed)

Items	Specification		Remarks
Type	Ljungstrom		Manufacturer Gadelius
Number	Two/Unit		
Capacity	(Gas side)	401,550 Nm^3/H	MCR
	(Air side)	324,700 Nm^3/H	MCR
Temp	(Gas side)	Input/Output 348 C/140 C	
	(Air side)	Input/Output 60 C/300 C	
Pressure Drop	Air side/Gas side 45mmAq/80mmAq		

(Continued)

(5) Fans

Items	Specification		Remarks
	I D F	F D F	
Type	Turbo FAN	Ditto	Manufacturer Hitachi Ltd
Number	Two per unit	Ditto	
Gas Volume	13,600 m^3/min	9,130 m^3/min	
Gas Temp	154 C	40 C	
Speed	900rpm	900rpm	
Motor Output	2,350 kW	1,350 kW	

(6) Wet F.G.D. (exsisting)

Items	Specification	Remarks
Type	Lime stone Gypsum	Manufacturer Babcock Hitachi Ltd
Number	1 unit	
Treated Gas Volume	800,000Nm^3/H	

(7) De-N (New Installed)

Items	Specification	Remarks
Type	Biological De-nitrate	Manufacturer Hitachi Zosen Ltd
Number	1 unit	
Treated Waste Water Volume	1,000 t/day	
N concentration outlet	10ppm and bellow	

Table 3 Guarantee And Actual Performance

Equipment	Items	Guarantee	Actual Performance	Remarks
SCR	Outlet NOx (ppm)	60ppm and bellow	58.2ppm/58.2ppm	Equivalent to 6%O_2
	DeNOx Eff.	More than 80%	80.7%/80.7%	
	Leakage NH_3	5ppm and bellow	3.4ppm/4.7ppm	Equivalent to 6%O_2
	SO_3 Conversion Ratio	1% and bellow	0.06%/0.68%	
	Draft Loss	85mmAq and bellow	32mmAq/62mmAq	
Hot Side ESP	Outlet	100mg/m^{3}N and bellow	29.7mg/m^{3}N/65.3mg/m^{3}N	
	Efficiency	More than 99.6%	99.62%/99.69%	
	Draft Loss	20mmAq and bellow	18mmAq/20mmAq	
Air Preheater	Outlet Temp. (Air-side)	312 ~ 297°C	304.3°C/300.8°C	
	Outlet Temp. (Gas-side)	153°C and bellow	142.8°C/141.6°C	
	Leakage Air Volume	35563~39820m^{3}N/H	30500m^{3}N/H/30890m^{3}N/H	
	Pressure Drop (Gas-side)	82.5mmAq	72mmAq/54mmAq	Equivalent to Gas Volume
	Pressure Drop (Air side)	44mmAq	35mmAq/31mmAq	Equivalent to Air Volume

Table 4 SCR Performance Tests Results

Items	Date	'81.7.19	'81.11.25	'82.1.27	'82.5.20	Remarks
DeNOx Eff	(%)	82.8	80.9	80.7	80.2	Equivalent to 6% O_2
Outlet NOx	(ppm)	51	56	58.2	64	
Leakage NH_3	(ppm)	2.1	3.3	3.4	3.0	
Inlet SOx	(ppm)	1540	1300	1285	1580	
Inlet SO_3	(ppm)	3.0	5.2	1.8	1.2	
Outlet SO_3	(ppm)	3.8	6.5	2.6	2.3	
SO_3 Conversion Ratio	(%)	0.05	0.1	0.06	0.07	

Items	Date	'81.7.10	'81.11.26	'82.1.27	'82.5.20	Remarks
DeNOx Eff	(%)	80.3	80.3	80.7	81.5	Equivalent to 6% O_2
Outlet NOx	(ppm)	72	57	58.2	58.6	
Leakage NH_3	(ppm)	0.6	4.9	4.7	5.0	
Inlet SOx	(ppm)	1540	1700	1282	1490	
Inlet SO_3 Inlet SO_3	(ppm) (ppm)	1.4 1.4	5.9 5.9	1.33 1.33	2 2.6	
Outlet SO_3	(ppm)	9.5	13.9	10.1	13.4	
SO_3 Conversion Ratio	(%)	0.53	0.47	0.68	0.75	

Table 5 Design Condition of S.C.R.

		Takehara No. 3 Unit
Boiler Spec	Type of Boiler	B&W Supercritical Pressure Reheat Type Up Boiler
	Rating Output	700 MW
	Fuel	Coal
Condition of Flue Gas	Gas Flow	2,230,000 Nm^3/h
	Gas Temperature	360 ~ 380 °C
	Inlet NOx Conc	250 ppm
	Inlet SOx Conc	1,000 ppm
	Dust Conc	100 mg/Nm^3
	S.V. Value	2,370 h^{-1}
	L.V. Value	6.9 m/S
	DeNOx Efficiency	(Target) 80 %
	Slip NH_3	~3 ppm
	SO_2 Conversion Rate	0.5 %
	Draft Loss	100 mmAq
	Manufacturer	BHK

Note: NOx and NH_3 concentration are based on the equivalent values of 6%O_2

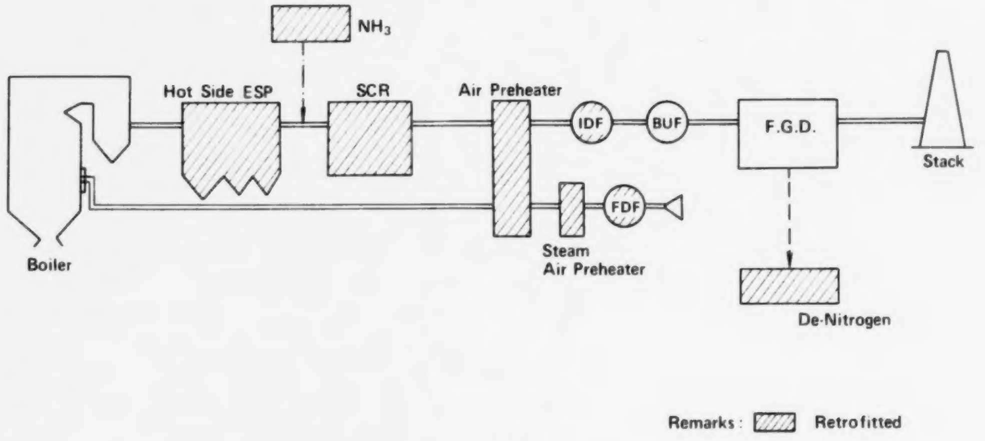
NH₃
Boiler
Hot Side ESP
SCR
Air Preheater
IDF
BUF
F.G.D.
Stack
FDF
Steam
Air Preheater
De-Nitrogen
Remarks: ▨ Retrofitted

Fig. 1 System Scheme

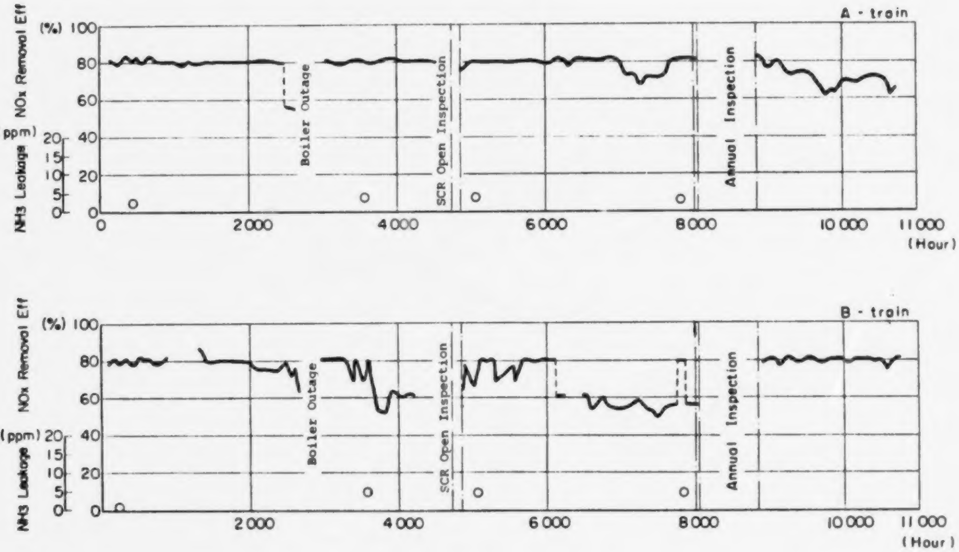

Fig. 2 Performance trend of SCR

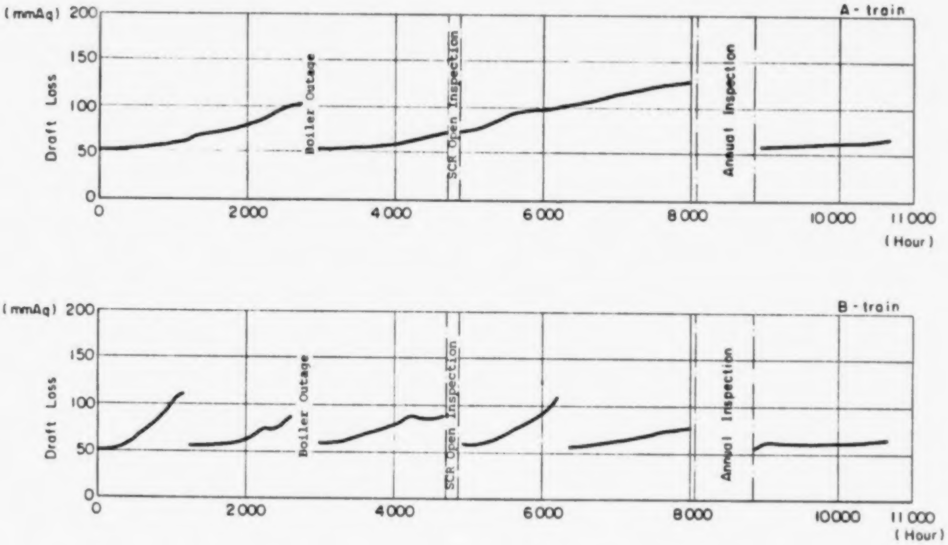

Fig. 3 Draft Loss trend & Air preheater

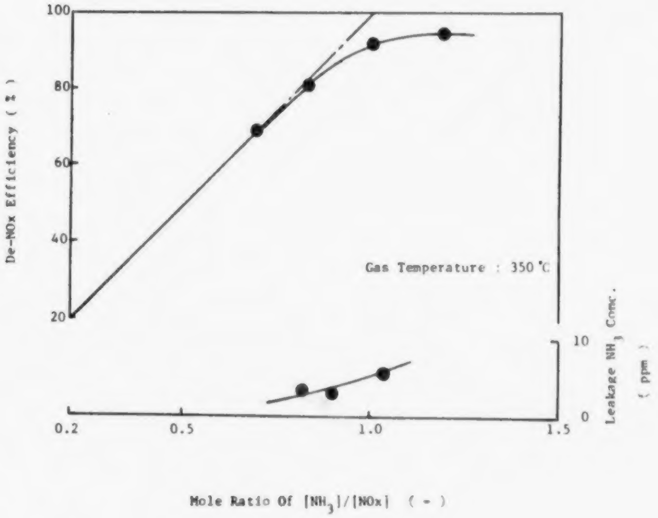

Fig.4 Characteristic Curves Of Mole Ratio Of $[NH_3]/[NOx]$ VS De-NOx Efficiency (Pilot Plant)

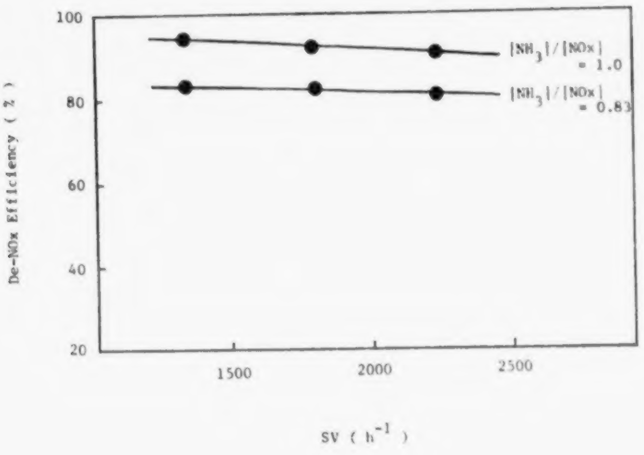

Fig.5 Characteristic Curves Of Space Velocity (SV) VS De-NOx Efficiency (Pilot Plant)

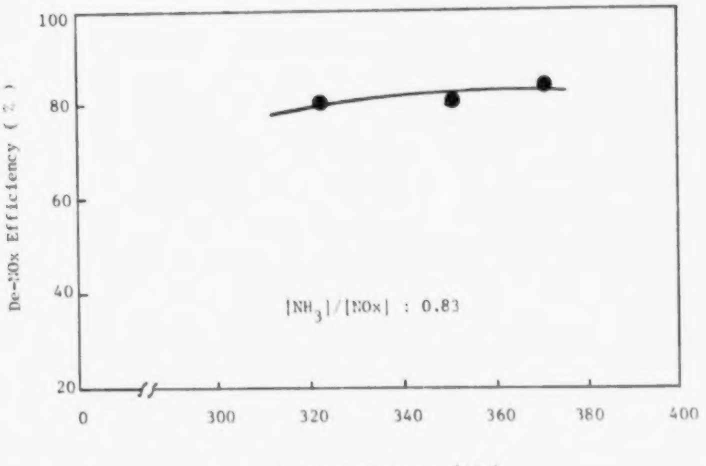

Fig.6 Characteristic Curve Of Gas Temperature VS De-NOx Efficiency (Pilot Plant)

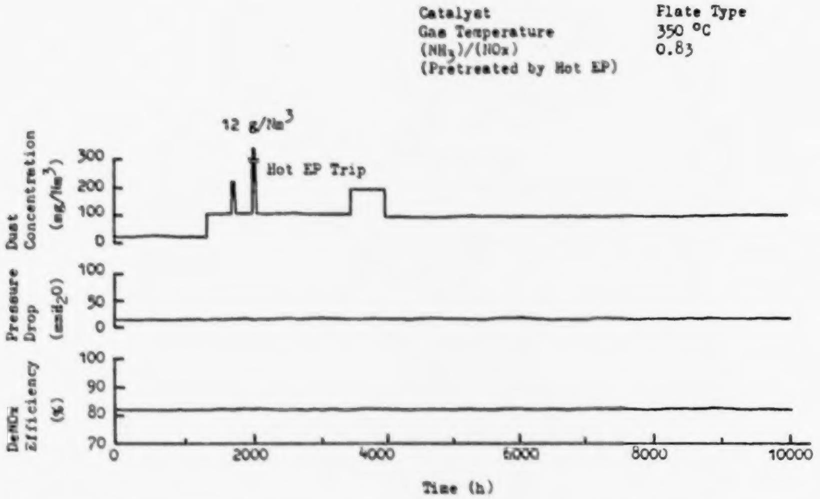

Fig. 7 Pilot Plant Test of Parallel Flow Reactor Treating Flue Gas from Coal-Fired Utility Boiler

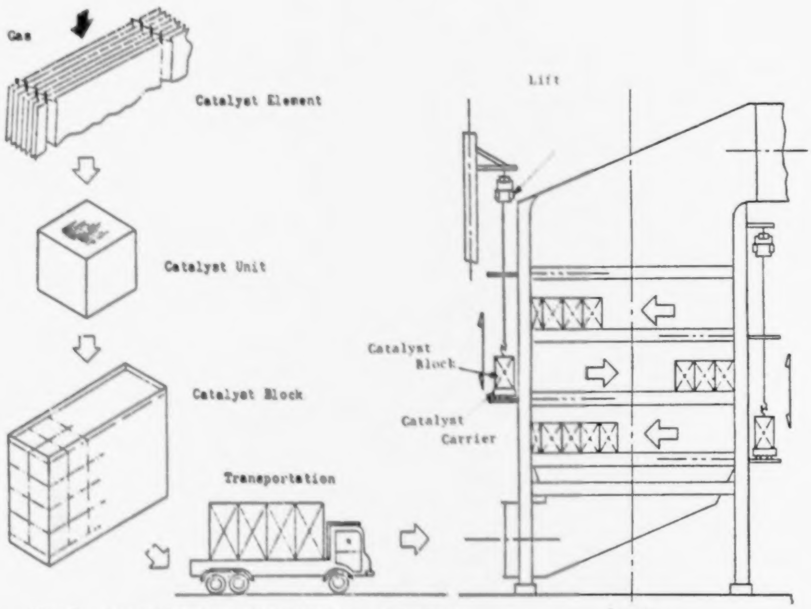
Gas
Catalyst Element
Catalyst Unit
Catalyst Block
Transportation
Lift
Catalyst Block
Catalyst Carrier
Loading

Fig. 8 Assembling and Loading Procedure of Catalyst

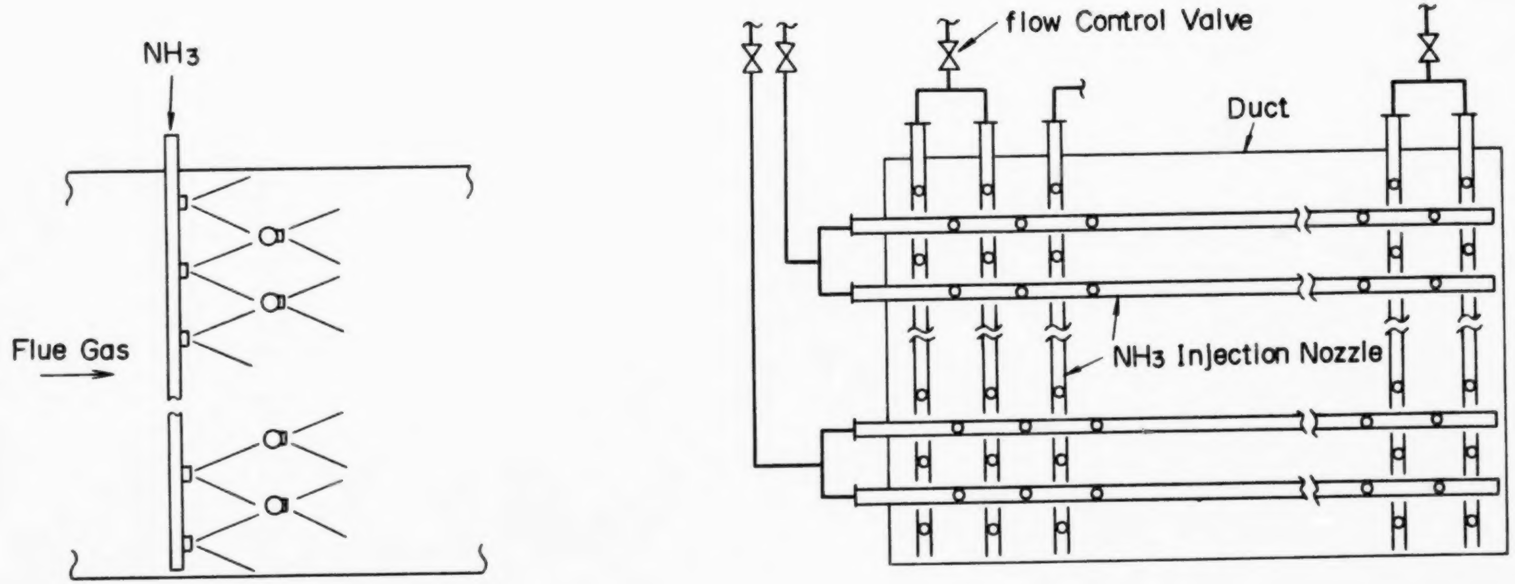
NH3
Flue Gas
flow Control Valve
Duct
NH3 Injection Nozzle

Fig. 9 Arrangement of NH_3 Injection Nozzle

(Takehara No.3 Unit)

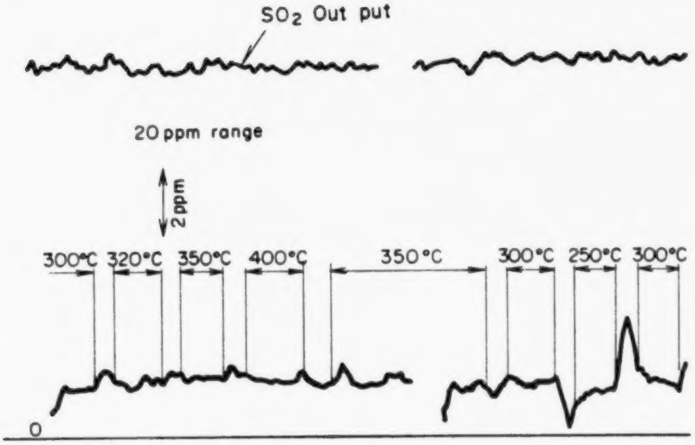

Fig. 10. Confirmation of Temperature at Sampling Line

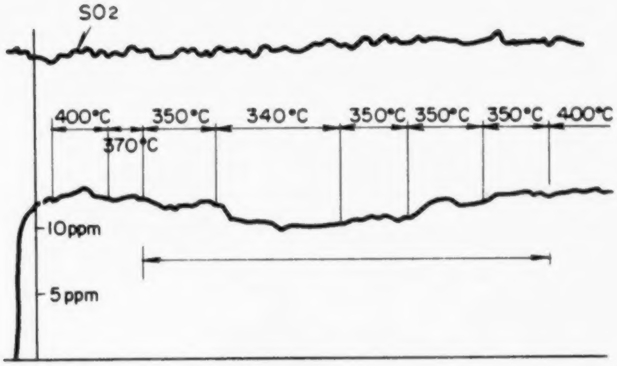

Fig. 11 Confirmation of Temperature at Dust Filter

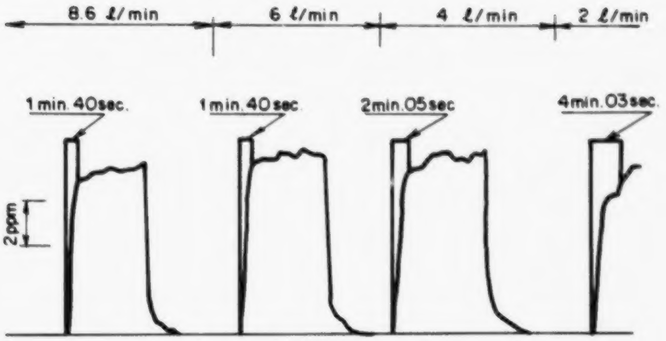

Fig. 12 Confirmation of Sampling Flow Rate

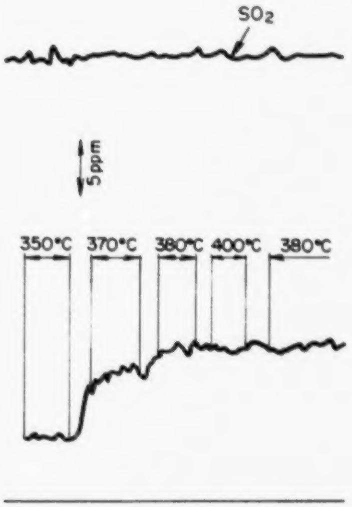

Fig. 13 Confirmation of Probe Temperature

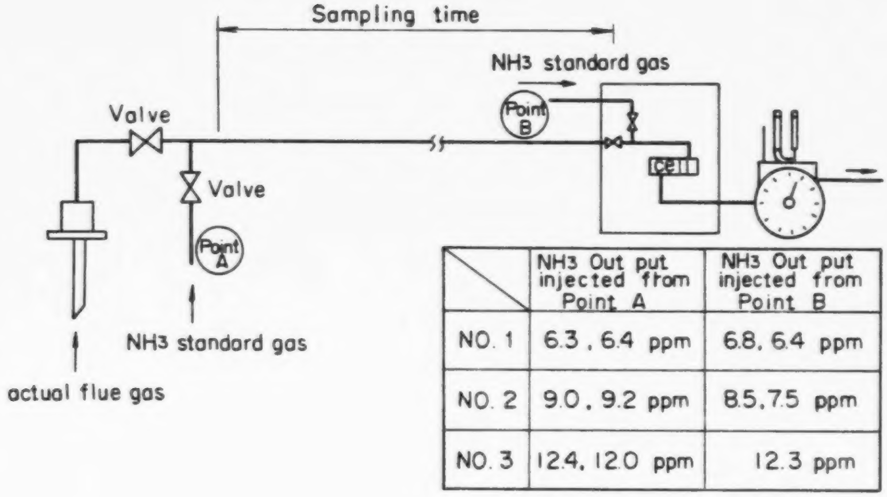
Sampling time
NH3 standard gas
Point B
Valve
Valve
cell
Point A
NH3 standard gas
actual flue gas

	NH3 Out put injected from Point A	NH3 Out put injected from Point B
NO. 1	6.3 , 6.4 ppm	6.8, 6.4 ppm
NO. 2	9.0 , 9.2 ppm	8.5, 7.5 ppm
NO. 3	12.4, 12.0 ppm	12.3 ppm

Fig. 14 Confirmation of NH_3 Losses in Sampling Line

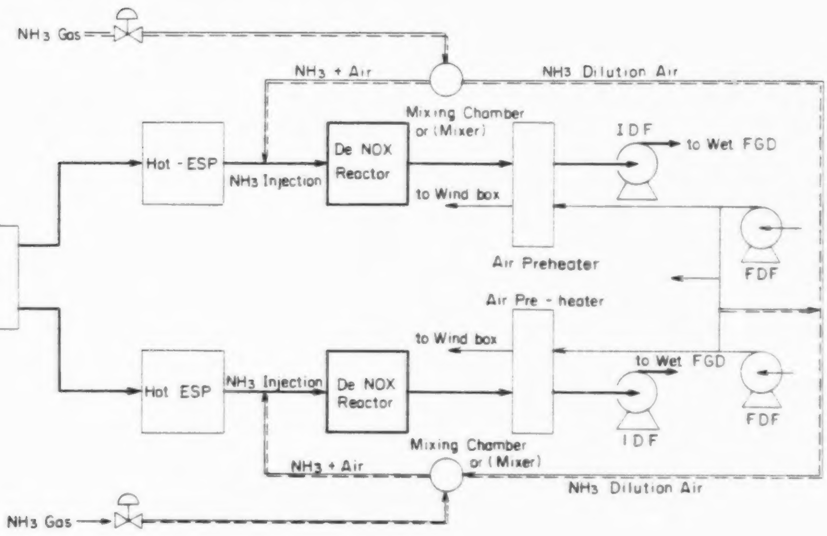
NH3 Gas
NH3 + Air
NH3 Dilution Air
Mixing Chamber or (Mixer)
Hot - ESP
NH3 Injection
De NOX Reactor
IDF
to Wet FGD
to Wind box
Boiler
Air Preheater
FDF
Air Pre - heater
to Wind box
to Wet FGD
Hot ESP
NH3 Injection
De NOX Reactor
FDF
IDF
Mixing Chamber or (Mixer)
NH3 + Air
NH3 Dilution Air
NH3 Gas

Fig.15 Flow Diagram of SCR Process

(Takehara No 3 Unit)

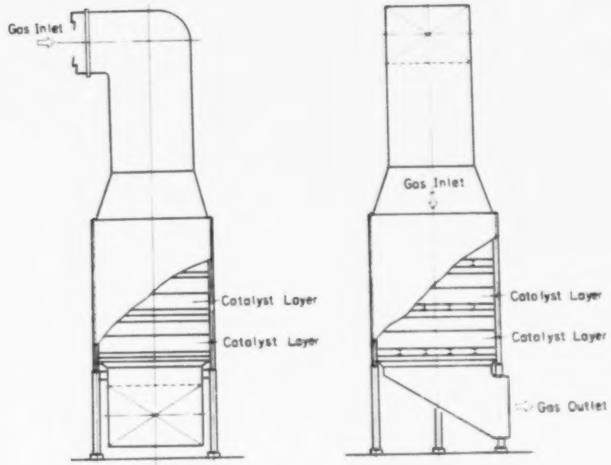
Gas Inlet
Catalyst Layer
Catalyst Layer
Gas Inlet
Catalyst Layer
Catalyst Layer
Gas Outlet

Fig.16 De-NOX Reactor
(Takehara No.3 Unit)

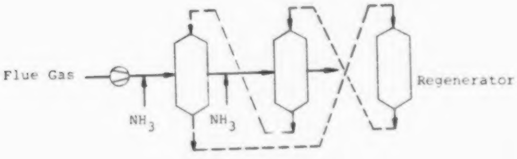
Flue Gas
NH_3
NH_3
Regenerator
DeSOx/DeNOx Reactor

(a) Activated Char Recirculation in Series Way

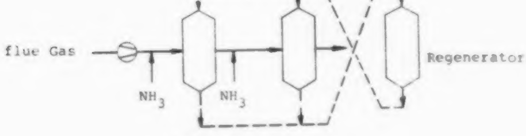
flue Gas
NH_3
NH_3
Regenerator
DeSOx/DeNOx Reactor

(b) Activated Char Recirculation in Parallel Way

Fig.17 Process Schemes of Cold-side Simultaneous NOx/SOx Removal

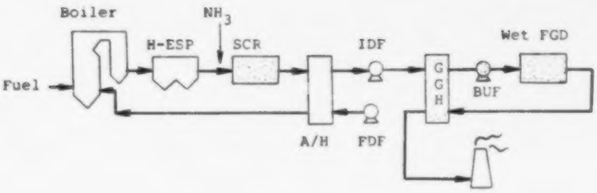
Boiler
NH_3
H-ESP
SCR
IDF
Wet FGD
Fuel
G G H
BUF
A/H
FDF

(a) Wet System (LDSS)

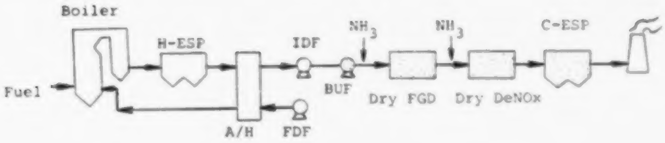
Boiler
H-ESP
IDF
NH_3
NH_3
C-ESP
Fuel
BUF
Dry FGD
Dry DeNOx
A/H
FDF

(b) Dry 2 Stage Simultaneous NOx/SOx Removal System

Fig. 18 Comparison of Dry and Wet De-NOx/De-SOx System

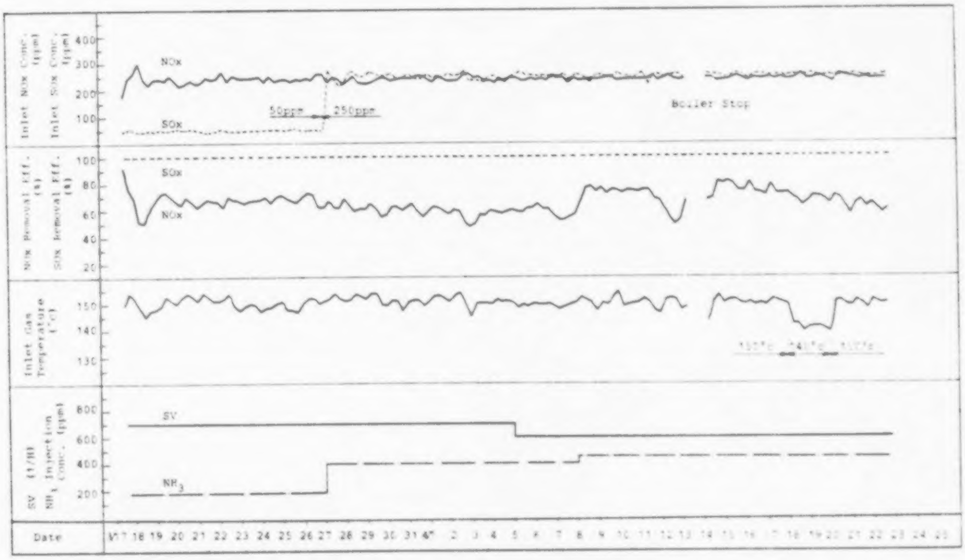

Fig. 19 Results of Pilot Test Operation

EVALUATION OF NO_x AND NO_x/SO_x FLUE GAS TREATMENT TECHNOLOGY FOR COAL-FIRED SOURCES

By:

J. David Mobley
Industrial Environmental Research Laboratory
U.S. Environmental Protection Agency
Research Triangle Park, North Carolina 27711
and
Jack M. Burke
Radian Corporation
Austin, Texas 78759

ABSTRACT

Nitrogen oxide (NO_x) emissions from stationary sources may be reduced by 80 to 90 percent through the application of selective catalytic reduction (SCR) of NO_x with ammonia (NH_3). For the most part, SCR has been developed and commercially applied in Japan. In the interest of evaluating SCR technology in the U.S., EPA has sponsored pilot-scale tests of two SCR systems treating flue gas from coal-fired boilers. The processes tested were the Hitachi Zosen process and the Shell Flue Gas Treatment (FGT) process, which also removes sulfur dioxide (SO_2). The results of those tests show that both processes tested are technically capable of reducing 90 percent of the NO_x in flue gas which contains the full particulate concentration from a coal-fired boiler; however, the performance of the Shell process was generally below this level. A sampling program conducted during the pilot plant tests showed no adverse secondary emissions from application of the SCR processes; however, high NH_3 and sulfur trioxide (SO_3) emissions are a concern due to their potential for causing operational problems in downstream equipment. Cost projections, which are based on pilot plant results, show that the Hitachi Zosen process combined with a conventional flue gas desulfurization process should cost less than the Shell process for control of both NO_x and SO_2 emissions.

EPA'S PILOT PLANT EVALUATIONS OF NO_x AND NO_x/SO_x FLUE GAS TREATMENT TECHNOLOGY

INTRODUCTION

In order to assess pollution control technology, EPA has sponsored research in many areas including flue gas desulfurization, particulate control, and combustion modifications. This research takes many forms ranging from theoretical studies to large-scale tests of new pollution control processes and techniques.

EPA's research activities have also addressed selective catalytic reduction (SCR) of nitrogen oxides (NO_x) with ammonia. As part of an effort to assess this technology in the United States, the EPA has sponsored pilot plant tests of two SCR processes. The processes tested were the Hitachi Zosen process and the Shell Flue Gas Treatment (FGT) process, which also removes SO_2. The tests were conducted using flue gas from two coal-fired boilers, and both pilot plants processed about 1600 Nm^3/hr of flue gas which is equivalent to 0.5 MW of electric generating capacity.

The EPA-sponsored evaluations were the first tests of the Shell FGT process for NO_x and SO_2 removal on a coal-fired boiler and the first coal-fired tests of the Hitachi Zosen process in the United States. Although the Hitachi Zosen process has been tested on coal in Japan, EPA felt that differences between the composition and properties of coals burned in Japan and those burned in the United States could affect the performance of the catalyst. As the results showed, fly ash properties at the United States test sites did affect operation of the Hitachi Zosen process, but did not impact operation of the Shell FGT process.

OBJECTIVES

The SCR pilot plant tests had several objectives. The primary one was to document the ability of each process to treat flue gas from a coal-fired boiler. Other objectives included evaluation of the processes' ability to reduce NO_x emissions by 90 percent for 90 days; measurement of emissions from the catalytic reactor of pollutants such as NH_3, SO_3, hydrocarbons, and CO; and measurement of the raw material and utility requirements of each process. Test programs were developed to meet these objectives, and the pilot plants were operated for nearly 2 years. During this period, several catalysts were tested over a wide range of operating conditions.

PROCESS DESCRIPTIONS

Hitachi Zosen Process

The Hitachi Zosen process uses ammonia (NH_3), added to the flue gas, to selectively reduce NO_x to molecular nitrogen (N_2) in a catalytic reactor. The overall chemical reactions are shown in Equations 1 and 2.

$$4\ NO(g) + 4\ NH_3(g) + O_2(g) \rightarrow 4\ N_2(g) + 6\ H_2O(g) \qquad (1)$$

$$2\ NO_2(g) + 4\ NH_3(g) + O_2(g) \rightarrow 3\ N_2(g) + 6\ H_2O(g) \qquad (2)$$

In the process, NH_3 is injected into flue gas which is at a temperature between 300°C and 400°C. The gas then passes through a catalytic reactor where the reactions (Equations 1 and 2) occur rapidly.

The pilot test unit of the Hitachi Zosen process was located at Georgia Power Company's Plant Mitchell Station in Albany, Georgia. The Hitachi Zosen pilot plant processed a 1600-2400 Nm^3/hr (1000-1500 scfm) slipstream of flue gas which was withdrawn between the economizer and the air preheater of the coal-fired Unit 3 at the Plant Mitchell Station. At this point, the flue gas contained the full particulate loading from the boiler. The slipstream from the boiler was first passed up through a flue gas heater for temperature control. NH_3 was then injected into the flue gas which flowed down through the reactor. After exiting the reactor, the gas passed through a cyclone particulate collector, a fan, and then returned to the boiler flue gas duct. The cyclone was included in the pilot unit to minimize abrasion in the fan.

Shell Flue Gas Treatment Process

The Shell FGT process differs in that it removes both SO_2 and NO_x. Copper supported on alumina is used as an SO_2 "acceptor." SO_2 and O_2 react with the acceptor as shown in Equation 3.

$$SO_2(g) + 1/2\ O_2(g) + CuO(s) \rightarrow CuSO_4(s) \qquad (3)$$

Copper oxide and, to a greater extent, the copper sulfate ($CuSO_4$) produced by the SO_2 acceptance reaction act as a catalyst for the reduction of NO_x by the injected NH_3 according to Equations 1 and 2.

As SO_2 is removed in the reactor, the acceptor becomes "loaded," and SO_2 emissions begin to increase. Once the time averaged SO_2 removal reaches the design level (i.e., 90 percent), flue gas flow to the reactor is shut off and the $CuSO_4$ and CuO are reconverted to Cu metal. In this regeneration step, a steam/hydrogen mixture is passed through the reactor, and a concentrated SO_2 stream is produced. The regeneration reactions are illustrated by Equations 4 and 5.

$$CuSO_4(s) + H_2(g) \rightarrow CuO(s) + SO_2(g) + H_2O(g) \qquad (4)$$

$$CuO(s) + H_2(g) \rightarrow Cu(s) + H_2O(g) \qquad (5)$$

The SO_2 produced by the regeneration of the acceptor can be further processed to recover the sulfur as sulfuric acid or elemental sulfur.

The Shell FGT pilot test unit was located at Tampa Electric Company's Big Bend Station in North Ruskin, Florida. The pilot plant processed a 1000 scfm (1600 Nm^3/hr) slipstream of flue gas which was withdrawn between the economizer and the air preheater of the coal-fired Unit 2. Flue gas from the boiler contained full particulate loading and was heated by in-line burners before entering the reactor. Flue gas flowed up through the reactor during acceptance of SO_2 and bypassed the reactor during the regeneration of the acceptor. During the program, some tests were conducted in which the reactor was fully loaded with SO_2, and NO_x was the only pollutant removed. While these tests were conducted, the reactor processed flue gas continuously.

RESULTS$^{(1,2)}$

The results of the pilot plant tests and subsequent data analysis can conveniently be divided into several categories, including: process performance, process energy requirements, process costs, and the flue gas impacts of the process. When added together, these results are indicative of the technical and economic feasibility considerations of applying these two SCR processes to coal-fired boilers. In the discussion which follows, the pilot plant test results are summarized separately for each of these categories.

Process Performance

The performance of the two pilot plants can best be summarized by the results of tests which were conducted to document the ability of the processes to reduce NO_x emissions by 90 percent over 90 days of continuous operation. In the case of the Shell FGT process, simultaneous SO_2 removal efficiency of 90 percent was also required.

Hitachi Zosen Process Performance--

The test results from the Hitachi Zosen pilot plant are presented in Figure 1. These results cover the period of May through October 1980, and represent over 3500 hours of operation. As illustrated by Figure 1, the Hitachi Zosen pilot plant met and exceeded the objectives of the test. During the first 90 days of operation, NO_x removal averaged over 90 percent. And, for the entire period of 160 days of continuous operation, the average NO_x reduction was 89.8 percent which is only slightly below the objective of 90 percent. Figure 1 also shows that in the range of 2100 to 2400 Nm^3/hr flow rate has essentially no effect on the NO_x removal efficiency of the process.

The results presented in Figure 1 indicate several things. They show that the Hitachi Zosen process is capable of treating flue gas from a coal-fired boiler for long periods of time while maintaining high NO_x reduction efficiencies. But they also show that the activity of the catalyst gradually declined over the period May through October. This indicates that additional catalyst may be required to maintain 90 percent reduction over a 1 year period of operation. However, a catalyst regeneration technique was tested which may make it possible to maintain 90 percent NO_x reduction without additional catalyst. Near the end of the test program, the catalyst was regenerated using an in situ, hot water washing technique. Following regeneration, the catalyst performance was essentially identical to that of fresh catalyst. Unfortunately, it was not possible to determine how long the effects of regeneration last or how many times the catalyst can be regenerated before a permanent loss of catalytic activity occurs. As a result, it is still uncertain if catalyst regeneration will permit the process to operate for 1 year at 90 percent NO_x reduction efficiency without the use of additional catalyst.

The results presented in Figure 1 are for Zosen's NOXNON 600 series catalyst. Prior to testing the 600 series catalyst, the pilot plant tested the 500 series catalyst which has smaller openings for gas passage. During the tests, the NOXNON 500 catalyst became plugged with fly ash after about 2000 hours of operation. This was evidenced by an increase in reactor pressure drop and a decline in NO_x reduction efficiency, and it was believed to result from the adhesiveness of the fly ash at high temperatures. Tests were conducted which compared fly ash properties from a power plant in Japan with the properties of fly ash from the Plant Mitchell power plant in the United States. At reactor operating temperatures, fly ash from Japan remained as a fine powder, but fly ash from Plant Mitchell agglomerated to form large lumps of material. This indicates a significant difference between a Japanese and United States coal-fired power plant and illustrates the need for test work in the United States.

In summary, the Hitachi Zosen tests indicated the need for a catalyst with larger gas passages to prevent catalyst plugging when treating flue gas from a coal-fired power plant in the United States. The tests did demonstrate that the process is capable of maintaining high NO_x reduction efficiencies for long periods of time. And, although catalyst activity gradually declined during the test program, it may be possible to maintain 90 percent NO_x reduction efficiency for a 1 year period with appropriate process design and operating considerations.

Shell FGT Process Performance--

The test results from the Shell FGT pilot plant are shown in Figure 2. These results are for tests conducted during June 1980, and they represent approximately 300 hours of operation in which flue gas was processed in the reactor. As Figure 2 illustrates, the Shell FGT process did not meet the objectives of the demonstration test. Although the SO_2 removal efficiency averaged 90 percent during the test, the NO_x reduction averaged only 70 percent. And the test lasted only 20 days rather than the scheduled 90 days.

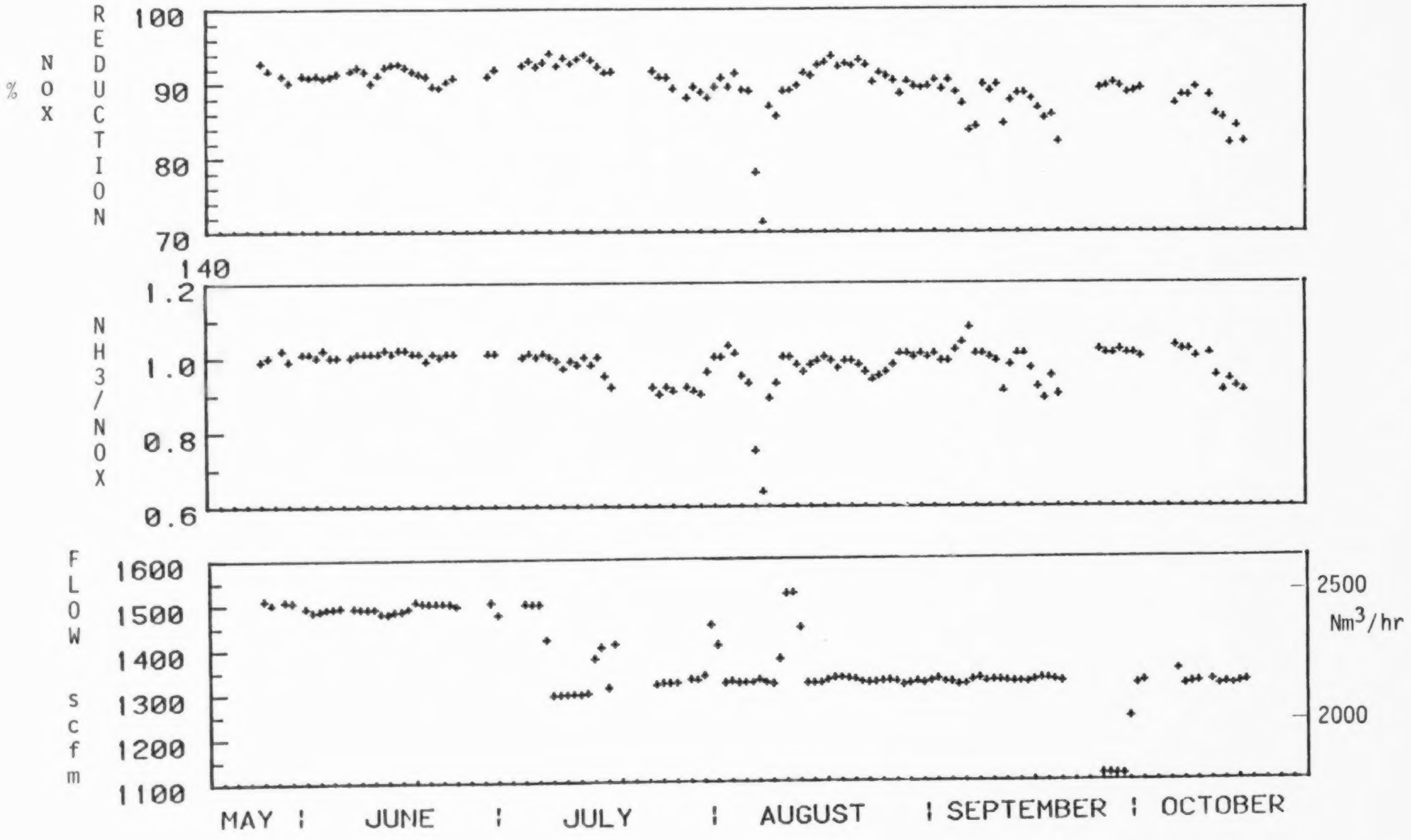

Figure 1. Pilot plant test results from the Hitachi Zosen process using NH_3 addition for NO_x reduction ( ).

The inability of the pilot plant to meet the test objective of simultaneously reducing NO_x and SO_2 emissions by 90 percent was due to the poor performance of the catalyst used in the process. With the reactor configuration used during the pilot plant tests, the NO_x reduction efficiency was low even when NH_3 was injected to give an NH_3 to NO_x ratio of 1.3. The NO_x reduction efficiencies of the pilot plant could be improved, but only at the expense of reduced SO_2 removal.

The results of the tests at the Shell FGT pilot unit did not demonstrate simultaneous reduction of NO_x and SO_2 emissions by 90 percent. However, the pilot plant test results can be extrapolated to identify conditions which will result in 90 percent reduction of both NO_x and SO_2 emissions. To achieve this level of emissions reduction, additional catalyst would have to be added to the reactor. Under the conditions at the pilot plant test site, 50 to 75 percent additional catalyst would have been required. While addition of catalyst is technically feasible, it would significantly increase the costs of applying the process. (An alternative method of improving NO_x reduction efficiency of the Shell FGT process was identified during the test program. The alternative method involved addition of processing steps to the SO_2-removal/NO_x-reduction cycle of the reactor. In a commercial design, the additional processing steps would require additional process equipment. This evaluation of the Shell FGT process did not consider the alternative method since sufficient information was not available to enable a cost estimate; however, the reader should be aware that the alternative method may be less costly than use of additional acceptor in the reactor.)

Another thing which was not attained during the tests with the Shell FGT process was the stability of the catalyst activity over a long period of time. Three catalysts were tested; of the three, the second processed flue gas for the longest period of time. Examination of the activity of this catalyst, as evidenced by its SO_2 removal efficiency, indicated that activity dropped after the catalyst's initial exposure to flue gas. The catalyst activity then stabilized and no measurable change in activity occurred over a 700 hour period. While this indicates that the catalyst activity appears stable for a coal-fired application, flue gas was not processed long enough to reach any conclusions.

Perhaps the most significant result of the tests with the Shell process was that no plugging of the reactor occurred. Flue gas was processed for a total of about 2000 hours and no increase in reactor pressure drop was recorded. This indicates that the parallel passage reactor design used in the pilot plant tests is well suited for application to coal-fired sources.

In summary, the tests of the Shell FGT process did not meet the objectives of the process to reduce emissions of both NO_x and SO_2 by 90 percent. However, the results can be extrapolated to identify a process design which will reduce NO_x and SO_2 emissions 90 percent. The test results did indicate that the parallel passage reactor design is well suited to coal-fired applications since no evidence of reactor plugging was found. But the test did not assess the long-term stability of the catalyst activity.

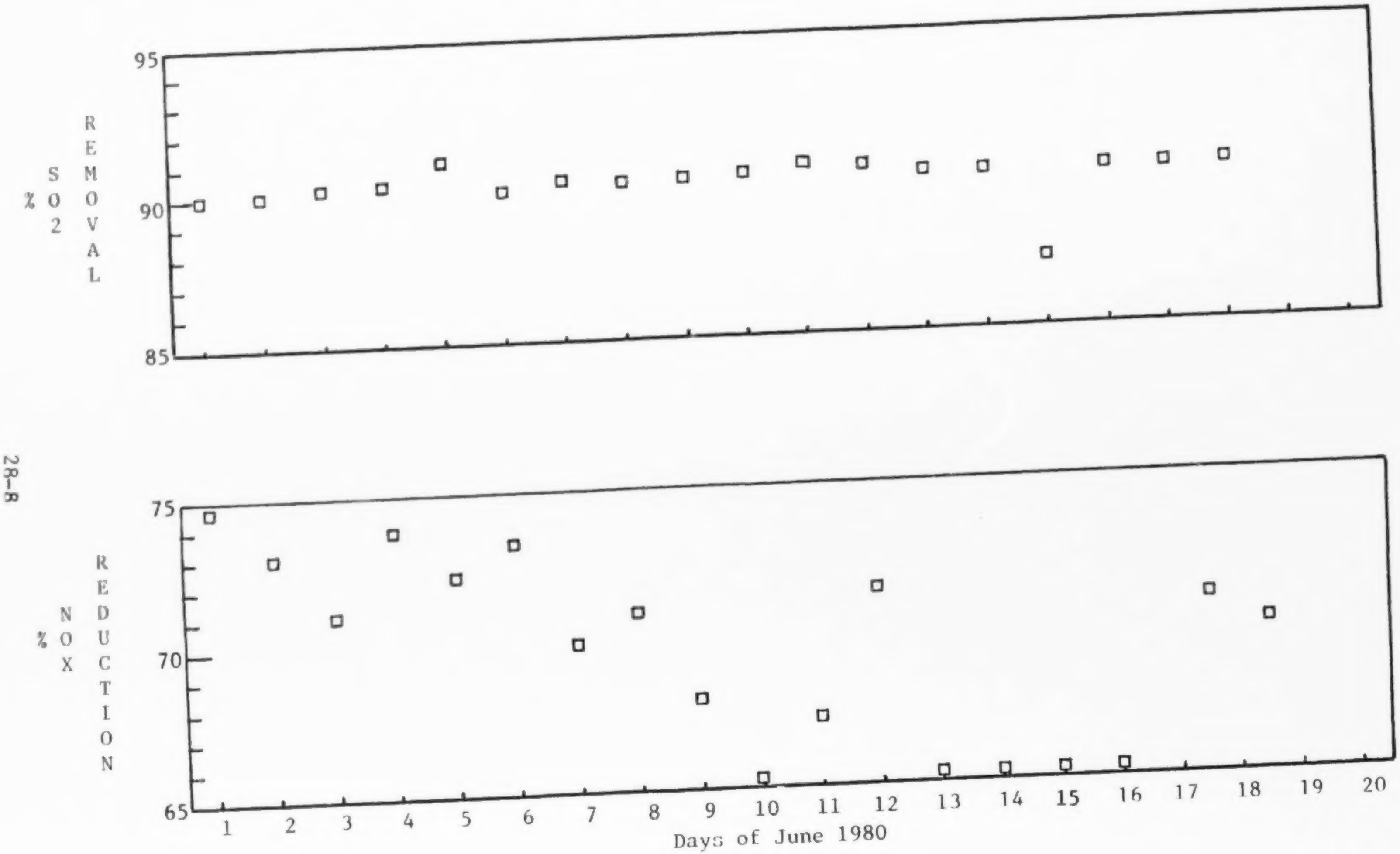

Figure 2. Pilot plant test results from the Shell Flue Gas Treatment process for SO_2 / NO_x removal from flue gas.

Process Energy Requirements

One of the key factors used by the EPA in evaluating any pollution control process is the fraction of the boiler's output which is required to operate the pollution control system. This is a measure of how much of the boiler's capacity does not generate electricity for sale and is thus one factor which contributes to the costs of applying a pollution control process.

As part of an evaluation of the pilot plant test results, the energy requirements of both the Hitachi Zosen and the Shell FGT processes were estimated. These estimates were made for a 500 MW application of each process, and they were based on measurements made during the tests as well as estimates made in a previous study.(3)

Since the Shell FGT process reduces emissions of both NO_x and SO_2 while the Hitachi Zosen process reduces only NO_x emissions, a direct comparison of process energy requirements is not meaningful. Instead, energy requirements for the Hitachi Zosen process and energy requirements for a flue gas desulfurization process were estimated and compared with the energy requirements for the Shell FGT process. The results of these estimates are presented in Table I, which identifies individual components and the overall process energy requirements as a percentage of the boiler's capacity.

As Table I shows, the Shell FGT process has an energy requirement equivalent to 5 percent of the boiler's capacity while the Hitachi Zosen combined with a flue gas desulfurization system required only 3.7 percent of the boiler's capacity. The principal difference between the energy demands of the two processes is the fuel energy requirement of the Shell FGT process.

TABLE I. COMPARISON OF HITACHI ZOSEN AND SHELL FLUE GAS TREATMENT PROCESS ENERGY REQUIREMENTS[a,b]

Energy Component	Hitachi Zosen[c]	Shell
Fuel	-	5.6
Steam	2.0	0.6
Electricity	2.0	2.0
Energy Credit	(0.3)	(3.2)
Total	3.7	5.0

[a] All energy requirements as percent of boiler capacity.

[b] 500 MW coal-fired boiler. Boiler thermal efficiency = 88%. Boiler heat rate = 9.5 MJ/kWh.

[c] Includes energy requirements for limestone flue gas desulfurization system.

The fuel energy consumed by the Shell process is equivalent to 5.6 percent of the boiler's capacity, and it is actually greater than the total process energy requirements. To some extent, the high fuel energy requirement of the Shell process is offset by the energy credit which results from application of the process. The energy credit is primarily the result of additional heat recovery in the air preheater due to lower permissible operating temperatures. Additional heat recovery is possible since samples collected during the pilot plant tests indicated that sulfur trioxide is removed from the flue gas in the reactor. This lowers the temperature at which sulfuric acid condenses (dew point), thus reducing the chance of corrosion in, or downstream of, the air preheater.

Another item of interest which is not shown in Table I is that the majority of the energy requirements shown for the Hitachi Zosen process are those of the flue gas desulfurization system: they are not associated directly with the SCR process. The estimated energy requirements of the Hitachi Zosen process alone are equivalent to only 0.3 percent of the boiler's capacity. These energy requirements result from compressed air and steam used for soot blowing and the electrical energy required to overcome the reactor pressure drop.

Process Costs

Estimates were prepared of total capital investment and annual revenue requirements for the Hitachi Zosen process and the Shell FGT process based on results from the pilot plant tests and estimates from a previous study.(3) These costs reflect the way each process was operated during the pilot plant test program, and they can be used to compare the two processes. However, since the Hitachi Zosen process does not remove SO_2, the costs of a flue gas desulfurization system(3) must be added to the Hitachi Zosen process cost estimate to make comparison with the Shell FGT process costs meaningful.

Table II contains the results of the cost estimates for the Hitachi Zosen and Shell processes and the cost estimate for a limestone flue gas desulfurization system. As shown, the Shell process costs are estimated to be significantly higher than the costs for the Hitachi Zosen process, including the costs of flue gas desulfurization. The capital investment for the Shell process is estimated to be $84.2 million or $168/kW of generating capacity. The capital investment for the Hitachi Zosen process including flue gas desulfurization is estimated to be $72.5 million or $145/kW of generating capacity. This indicates that the capital investment of the Shell process is over 15 percent higher than that for the Hitachi Zosen process. The primary reason for the Shell FGT process's being more expensive is the relatively poor NO_x reduction efficiencies attained by the process during the pilot plant tests.

TABLE II. ESTIMATED CAPITAL INVESTMENT AND ANNUAL REVENUE REQUIREMENTS FOR A 500 MW APPLICATION OF THE HITACHI ZOSEN AND SHELL FLUE GAS TREATMENT PROCESSES[a,b]

Cost Item	Hitachi Zosen Process			Shell Process
	HZ	FGD	Total	
Capital Cost	$22,100,000	$50,400,000	$72,500,000	$84,200,000
Annual Revenue Requirement	10,200,000	14,700,000	24,900,000	33,500,000

[a] A detailed breakdown of the Hitachi Zosen and Shell process cost estimates is included as an appendix to this paper.

[b] Basis for Estimates: 500 MW new coal-fired power plant burning 3.5 percent sulfur coal. Removal of both NO_x and SO_2 = 90 percent. Plant location in Midwestern United States. Project beginning mid-1977, ending mid-1980. Remaining life of power plant = 30 years. Plant on line 7000 hr/yr. Plant heat rate = 9.5 MJ/kWh.

Perhaps a more important measure of relative process costs is the annual revenue requirements of the processes. The revenue requirements represent the annual costs of process operation including raw material and energy requirements, depreciation, return on investment, and catalyst replacement. These revenue requirements are also presented in Table II. It should be noted that these costs are based on the assumption of a 1 year life for the catalysts used in both processes. As discussed earlier, this assumption cannot be verified by the pilot plant test results, but a 1 year catalyst life is typicallly guaranteed by process vendors.

As shown in Table II, the annual revenue requirements for the Shell process are estimated to be $33.5 million/year. This is over 30 percent greater than the annual revenue requirements for the Hitachi Zosen process which were estimated to be $24.9 million/year. Again, the principal reason for the difference between the annual revenue requirements for the two processes is the relatively poor performance exhibited by the Shell process during the pilot plant tests which indicated that a substantial increase in catalyst volume would be required to achieve 90 percent NO_x removal. Another significant difference is the relatively high energy requirements of the Shell process.

Overall, the results of the cost estimates indicate that the Shell FGT process requires a greater capital investment and has higher annual revenue requirements than the Hitachi Zosen process. However, the cost estimate was prepared only for a 500 MW coal-fired application with the requirements of 90 percent SO_2 and NO_x removal. The relative costs for the two processes could differ for other applications with different requirements.

Process Flue Gas Impacts

As part of the pilot plant tests, EPA conducted a sampling program designed to quantify process emissions of pollutants other than NO_x and SO_2. The objective of this sampling program was to determine if any adverse flue gas concentration impacts can result from application of SCR technology to a coal-fired source. Samples were collected at the inlet and outlet of the pilot plant reactors and analyzed for selected pollutants. Inlet and outlet samples were collected simultaneously, so that measured differences in pollutant concentration were due to changes across the reactors.

Table III identifies the specific pollutants measured and presents the results of the sampling program. As shown, the concentrations of some pollutants changed across the reactor while others did not. And in some cases, the concentrations of the pollutants were below the detection limits of the analytical techniques employed during the sampling program.

TABLE III. MEASURED CHANGE IN THE CONCENTRATIONS OF SELECTED POLLUTANTS ACROSS THE PILOT PLANT SCR REACTORS

	Hitachi Zosen Pilot Plant		Shell Flue Gas Treatment Pilot Plant	
Pollutant	Reactor Inlet Concentration	Reactor Outlet Concentration	Reactor Inlet Concentration	Reactor Outlet Concentration
Hydrogen Cyanide[a]	$<10\ \mu g/m^3$	$<10\ \mu g/m^3$	$<10\ \mu g/m^3$	$<10\ \mu g/m^3$
Nitrosoamines[a]	$<5\ \mu g/m^3$	$<5\ \mu g/m^3$	$<5\ \mu g/m^3$	$<5\ \mu g/m^3$
Carbon Monoxide	<0.017 %	<0.017 %	0.13 %	<0.017 %
Hydrocarbons (C_1-C_6)	<1.0 ppmv	<1.0 ppmv	28.5 ppmv	21.0 ppmv
Sulfur Trioxide	8.4 ppmv	20.7 ppmv	11.4 ppmv	0.1 ppmv
Ammonia	0	54.8 ppmv	0	15.3 ppmv

[a] Gas volume taken at 15.5°C, 1 atm, dry basis.

As illustrated in Table III, concentrations of hydrogen cyanide and nitrosoamines at the inlet and outlet of the pilot plant reactors were below the detection limits of the analytical techniques employed. In both cases, these concentrations are below the level which is considered safe for emissions from sources.

At the Hitachi Zosen plant, the concentrations of both CO and hydrocarbons were also below the detection limits of the analytical techniques. But at the Shell FGT pilot plant, the concentrations of these compounds were found to decrease across the reactor. This decrease represents an environmental benefit for the Shell process, and is believed to result from oxidation of these compounds in the reactor. It should be noted that the Hitachi Zosen reactor may also oxidize CO and hydrocarbons, but no conclusions can be drawn since these compounds were present in such low concentrations.

One of the most significant results of the emissions sampling program was the effect of the Hitachi Zosen and Shell processes on the concentration of SO_3 in the flue gas. As shown in Table III, SO_3 was produced in the Hitachi Zosen pilot plant reactor while the Shell FGT process removed SO_3 from the gas stream. These results are significant because of the effects SO_3 can have on equipment located downstream of an SCR reactor, especially the air preheater.

In the case of the Hitachi Zosen process, the increased SO_3 concentration raises the sulfuric acid dew point of the flue gas. This increases the potential for formation of ammonium sulfates. The net effect of increased flue gas SO_3 concentrations is to increase process costs. This is reflected in the cost estimates of air preheater modifications which include provisions for soot blowing, water washing, and periodic replacement of the air preheater elements.

In the case of the Shell process, removing SO_3 reduces the sulfuric acid dew point of the flue gas. This permits the air preheater to operate at lower temperatures without experiencing corrosion in the preheater or in downstream equipment. The result is additional heat recovery which lowers process energy requirements and thus process costs. The low SO_3 concentration at the reactor outlet also minimizes the potential for formation of ammonium sulfates.

Another significant result of the emissions sampling program is the measured NH_3 emissions from the processes. As shown in Table III, NH_3 emissions from the Hitachi Zosen process were over three times greater than the emissions from the Shell FGT process even though the NH_3/NO_x injection ratio was higher at the Shell pilot plant. This is due to the fact that the catalyst used in the Shell process promotes NH_3 oxidation while essentially no NH_3 oxidation occurred in the Hitachi Zosen process.

These results are significant since they indicate the potential for formation of ammonium sulfates downstream of the SCR reactors. Formation of ammonium sulfate is significant because it can result in corrosion and plugging of the air preheater and thus increase boiler operating costs. In the case of the Hitachi Zosen process, high NH_3 and SO_3 emissions indicate that a large quantity of ammonium sulfates can form downstream of the reactor. The Shell FGT process, on the other hand, has low emission rates of both NH_3 and SO_3. Thus, the potential for formation of ammonium sulfates is low.

CONCLUSIONS

Several important conclusions can be drawn from the results of the pilot plant test program. First, and most important, the test results show that both the Hitachi Zosen NO_x removal process and the Shell NO_x/SO_x control process are technically capable of achieving significant reductions of emissions from coal-fired boilers in the United States. Hitachi Zosen's NOXNON 600 catalyst and the Shell parallel passage reactor operated without fly ash plugging problems during the test program. The tests did show, however, that Hitachi Zosen's 500 series catalyst is prone to plugging. In contrast, tests by Hitachi Zosen in Japan reported that the NOXNON 500 catalyst treated flue gas from a coal-fired boiler for over 5000 hours without plugging problems. This difference between the properties of Japanese and United States coals points out the need for SCR test work when considering SCR process applications for untested coals.

In terms of performance, the Hitachi Zosen process met the test program objectives of 90 percent NO_x reduction for 90 days while the Shell FGT process did not. The Shell process did not meet the test program objectives because the catalyst performance was below expected levels and, therefore, the pilot plant reactor was undersized.

The pilot plant tests did not demonstrate a 1 year catalyst life, but the Hitachi Zosen catalyst did process flue gas for 6 months while averaging nearly 90 percent NO_x reduction. And although the Hitachi Zosen 600 series catalyst activity did decline during the test program, a regeneration technique was developed which restored catalyst activity to its original level. The performance of the Shell catalyst was quite stable during the test program, but the catalyst only processed flue gas for an equivalent of 3 months of operation. In both cases, a catalyst life of 1 year is typically guaranteed by the process vendors.

A comparison of the two processes, based on certain assumptions, shows that the Hitachi Zosen process combined with a flue gas desulfurization system has lower energy requirements and lower costs than the Shell FGT process. On the negative side, however, the Hitachi Zosen process has higher NH_3 and SO_3 emissions. Even so, it appears that the Hitachi Zosen process may cost less than the Shell FGT process for a 500 MW boiler burning high sulfur coal. The pilot plant tests show that it may be possible to achieve high NO_x and NO_x/SO_x control by use of FGT technology on coal-fired sources in the United States.

REFERENCES

1. J. M. Burke, Hitachi Zosen NO_x Flue Gas Treatment Process; Vol. 2, Independent Evaluation, Radian Corporation, EPA-600/7-82-057b, September 1982, U.S. Environmental Protection Agency, Research Triangle Park, NC.

2. J. M. Burke, Shell NO_x/SO_2 Flue Gas Treatment Process; Independent Evaluation, Radian Corporation, Draft Final Report, EPA/IERL-RTP-1377, January 1982, U.S. Environmental Protection Agency, Research Triangle Park, NC.

3. J. D. Maxwell, T. A. Burnett, and H. L. Faucett, Preliminary Economic Analysis of NO_x Flue Gas Treatment Processes, Tennessee Valley Authority, EPA-600/7-80-021 (NTIS PB 80-176456), February 1980, U.S. Environmental Protection Agency, Research Triangle Park, NC.

APPENDIX

CAPITAL INVESTMENT AND ANNUAL REVENUE REQUIREMENTS FOR FULL SCALE SYSTEMS

TABLE A-I. ESTIMATED CAPITAL INVESTMENT FOR A 500 MW APPLICATION OF THE SHELL FGT PROCESS[a]

Item	Investment, $	% of total direct investment
Direct Investment[b]		
NH_3 storage and injection	890,000	1.9
H_2SO_4 plant	7,172,000	15.2
Reactor section	27,455,000	58.1
Flow smoothing section	2,828,000	6.0
Steam naphtha reformer	4,698,000	9.9
Gas handling	1,546,000	3.3
Sub-total direct investment (DI)	44,589,000	94.4
Services, utilities (0.06) (DI)	2,675,000	5.6
Total direct investment (TDI)	47,264,000	100.0
Indirect Investment		
Engineering design and supervision	709,000	1.5
Architect and engineering contractor	177,000	0.4
Construction expense = $0.25\ (TDI \times 10^{-6})^{0.83}$	6,135,000	13.0
Contractor fees = $0.096\ (TDI \times 10^{-6})^{0.76}$	1,799,000	3.8
Total indirect investment (IDI)	8,820,000	18.7
Contingency = 0.2 (TDI + IDI)	11,217,000	23.7
Total fixed investment (TFI)	67,301,000	142.4
Other Capital Charges		
Allowance for start-up and modifications = (0.1) (TFI)	6,730,000	14.2
Interest during construction = (0.12) (TFI)	8,076,000	17.1
Total depreciable investment	82,107,000	173.7
Land	14,000	--
Working capital	2,051,000	4.4
TOTAL CAPITAL INVESTMENT	84,172,000	178.1

[a] Basis: 500 MW new coal-fired power plant, 3.5% sulfur coal, 90% NO_x removal, 90% SO_2 removal. Midwest plant location. Represents project beginning mid-1977, ending mid-1980. Average basis for scaling, mid-1979. Investment requirements for fly ash disposal excluded. Construction labor shortages with overtime pay incentive not considered.

[b] Each item of direct investment includes total equipment costs plus installation labor, and material costs for electrical, piping, ductwork, foundations, structural, instrumentation, and site preparation.

TABLE A-II. ESTIMATED AVERAGE ANNUAL REVENUE REQUIREMENTS FOR A 500 MW APPLICATION OF THE SHELL FGT PROCESS[a]

Item	Annual quantity	Unit cost, $	Annual cost, $	% of annual revenue required
Direct Costs				
Raw materials				
NH_3	7.875×10^6 kg	0.165/kg	1,299,500	3.88
Naphtha	39.773 m^3	132.1/m^3	5,254,000	15.69
Catalyst	--	--	12,600,300	37.63
Reformer catalyst	--	--	125,100	0.37
Total raw materials			19,278,900	57.57
Conversion costs				
Operating labor and supervision	29,200 labor hrs	12.50/labor hr	365,000	1.09
Utilities				
Naphtha	9,943 m^3	132.1/m^3	1,313,500	3.92
Steam	179,900 GJ	-1.896/GJ	341,200	1.02
Process water	8,078,000 m^3	0.01585/m^3	128,000	0.38
Electricity	68,859,000/kWh	0.029/kWh	1,996,900	5.96
Heat credit	1,047,500 GJ	-1.896/GJ	(1,986,000)	(5.93)
Maintenance			1,891,000	5.65
Analyses	4,380 labor hrs	17.00/labor hr	74,500	0.22
Total conversion costs			4,124,100	12.31
Total direct costs			23,403,000	69.88
Indirect Costs				
Capital charges				
Depreciation = (0.06) (total depreciable investment)			4,926,400	14.71
Average cost of capital = (0.086) (total capital investment)			7,238,800	21.62
Overheads				
Plant = (0.5) (conversion costs minus utilities)			1,165,300	3.48
Administrative = (0.1) (operating labor costs)			36,500	0.11
Marketing = (0.1) (sales revenue)			366,000	1.09
Total indirect costs			13,733,000	41.01
Spent catalyst disposal			11,400	0.03
Gross average annual revenue requirement			37,147,400	110.92
Byproduct Sales Revenue				
H_2SO_4	1.11×10^8 kg	-0.033/kg	(3,660,000)	(10.92)
TOTAL ANNUAL REVENUE REQUIREMENTS			33,487,400	100.00

[a] Basis: 500 MW new coal-fired power plant, 3.5% S coal. 90 percent NO_x reduction, 90 percent SO_2 removal. Midwest power plant location, 1980 revenue requirements. Remaining life of power plant = 30 years. Plant on line 7000 hr/yr. Plant heat rate = 9.5 GJ/kWh. Investment and revenue requirement for disposal of fly ash excluded. Total direct investment $47,264,000; total depreciable investment $82,107,000; and total capital investment $84,172,000.

TABLE A-III. ESTIMATED CAPITAL INVESTMENT FOR A 500 MW APPLICATION OF THE HITACHI ZOSEN PROCESS[a]

Item	Investment, $	% of total direct investment
Direct Investment[b]		
NH_3 storage and injection	645,000	5.5
Reactor section	8,632,000	73.4
Gas handling	351,000	3.0
Air preheater modifications	1,461,000	12.4
Sub-total direct investment (DI)	11,089,000	94.3
Services, utilities (0.06) (DI)	665,000	5.7
Total direct investment (TDI)	11,754,000	100.0
Indirect Investment		
Engineering design and supervision	274,000	2.3
Architect and engineering contractor	69,000	0.6
Construction expense = $0.25 (TDI \times 10^{-6})^{0.83}$	1,933,000	16.4
Contractor fees = $0.096 (TDI \times 10^{-6})^{0.76}$	625,000	5.3
Total indirect investment (IDI)	2,901,000	24.7
Contingency = 0.2 (TDI + IDI)	2,931,000	24.9
Total fixed investment (TFI)	17,586,000	149.6
Other Capital Charges		
Allowance for start-up and modifications = (0.1) (TFI)	1,759,000	15.0
Interest during construction = (0.12) (TFI)	2,110,000	17.9
Total depreciable investment	21,455,000	182.5
Land	5,000	--
Working capital	336,000	2.9
Royalty fee	300,000	2.6
TOTAL CAPITAL INVESTMENT	22,096,000	188.0

[a] Basis: 500 MW new coal-fired power plant, 3.5% sulfur coal, 90% NO_x removal. Midwest plant location. Represents project beginning mid-1977, ending mid-1980. Average basis for scaling, mid-1979. Investment requirements for fly ash disposal excluded. Construction labor shortages with overtime pay incentive not considered.

[b] Each item of direct investment includes total equipment costs plus installation labor, and material costs for electrical, piping, ductwork, foundations, structural, instrumentation, insulation, and site preparation.

TABLE A-IV. ESTIMATED AVERAGE ANNUAL REVENUE REQUIREMENTS FOR A 500 MW APPLICATION OF THE HITACHI ZOSEN PROCESS[a]

Item	Annual quantity	Unit cost, $	Annual cost, $	% of annual revenue required
Direct Costs				
Raw materials				
NH_3	5.25×10^6 kg	0.165/kg	866,300	8.47
Catalyst			5,125,000	50.14
Total raw materials			5,991,300	58.61
Conversion costs				
Operating labor and supervision	8,760 labor hrs	12.50/labor hr	109,500	1.07
Utilities				
Steam	86,700 GJ	1.896/GJ	164,400	1.61
Electricity	10,787,000 kWh	0.029/kWh	312,800	3.06
Heat credit	92,400 GJ	-1.896/GJ	(175,200)	(1.71)
Maintenance = (0.04) (TDI)			470,200	4.60
Analyses	2,920 labor hrs	17.00/labor hr	49,600	0.48
Total conversion costs			931,300	9.11
Total direct costs			6,922,600	67.72
Indirect Costs				
Capital charges				
Depreciation = (0.06) (total depreciable investment)			1,287,300	12.59
Average cost of capital = (0.086) (total capital investment)			1,900,300	18.59
Overheads				
Plant = (0.5) (conversion costs minus utilities)			314,700	3.08
Administrative = (0.1) (operating labor costs)			11,000	0.11
Total indirect costs			3,513,300	34.37
Spent catalyst disposal			(214,000)	(2.09)
TOTAL ANNUAL REVENUE REQUIREMENTS			10,221,900	100.00

[a] Basis: 500 MW new coal-fired power plant, 3.5% S coal. 90 percent NO_x reduction, 90 percent SO_2 removal. Midwest power plant location, 1980 revenue requirements. Remaining life of power plant = 30 years. Plant on line 7000 hr/yr. Plant heat rate = 9.5 MJ/kWh. Investment and revenue requirement for disposal of fly ash excluded. Total direct investment $11,754,000; total depreciable investment $21,455,000; and total capital investment $22,096,000.

PILOT-SCALE EVALUATION OF SELECTIVE CATALYTIC REDUCTION FOR COAL-FIRED UTILITY BOILERS

By:

G. H. Shiomoto and L. J. Muzio
KVB, Inc.
18006 Skypark Boulevard
Irvine, California 92714

and

J. Edward Cichanowicz
Air Quality Control Program
Coal Combustion Systems Division
Electric Power Research Institute
3412 Hillview Avenue
Palo Alto, California 94303

ABSTRACT

Ammonia-based selective catalytic reduction (SCR) has been proposed as a means of reducing NO_x emissions from coal-fired utility boilers well below current federal standards. EPRI is conducting a technical evaluation of the SCR process on a 5000 scfm pilot-scale facility at the EPRI Arapahoe Test Facility.

The pilot-scale system treats a 5000 scfm slipstream of flue gas (2.5 MWe equivalent) from Arapahoe Unit 4 which fires a western low sulfur coal. In addition to the SCR reactor, the system includes a regenerative air heater to assess impacts on air heater performance.

The results obtained during a one-year test program are presented. These include (1) the process performance (NO_x removal), (2) impacts of secondary emissions, including ammonia, SO_3, and ammonium/sulfate compounds, (3) impacts of increased SO_2 levels, (4) impacts on the air preheater due to deposit buildup, and (5) evaluation of the SCR process requirements, including the ammonia injection controls, and the performance and maintenance of flue gas monitoring systems.

INTRODUCTION

Post-combustion NO_x control methods have been proposed as a means to significantly reduce emissions from utility boiler systems. Flue gas treatment strategies generally offer an advantage of higher potential NO_x reductions than are currently available with combustion modifications. Much of the developmental work has been ongoing in Japan, in response to more stringent emissions standards. Natural gas- and oil-fired applications for the technology have been stressed, although coal-fired work is proceeding. Coal firing poses the additional problems associated with the presence of fly ash and higher levels of sulfur oxides in the combustion products.

One system of post combustion NO_x control is the selective catalytic reduction of NO_x with ammonia (SCR). The process involves the chemical reaction between NO_x and ammonia (NH_3) in the presence of a catalyst and at temperatures typical of those at the economizer exit (approximately 700°F). This system exhibits a high utilization of the injected ammonia reacting with NO_x to form water and nitrogen as the products. One side effect is the partial oxidation of SO_2 to SO_3, a minor gas species which can have serious influence upon corrosion and fouling of downstream equipment. In addition, small amounts of unreacted ammonia (NH_3 slip) can exit the catalyst bed.

EPRI operates a pilot-scale system at the Arapahoe Emissions Test Facility in Denver, Colorado, to gain coal-fired SCR experience. The catalyst is manufactured by Kawasaki Heavy Industries (KHI) and is considered representative of currently available SCR processes. The unit treats flue gases received from a slipstream diverted from a western coal-fired boiler operated by Public Service Company of Colorado (PSCo). The objectives of the test program included assessments of (1) the performance of the catalyst and (2) the impacts on equipment located downstream of the economizer and catalytic reactor, such as the air heater.

FACILITY DESCRIPTION

An outline of the SCR pilot plant, and the associated flue gas control and conditioning systems are shown in Figure 1. A 5000 scfm flue gas slipstream (approximately 2.5 MWe equivalent) was withdrawn from the economizer exit and passed through a flow measurement venturi. An electric heater provided temperature control, while a booster fan and damper arrangement controlled flow rate. The gas was transported to the vertical catalyst bed and flowed downward through three stages of catalyst. The treated flue gases then flow through the air preheater (APH) and return to the PSCo boiler system.

The NH_3 control system included preparation and injection, as well as the system demand and NH_3 flow measurement. Large portable tanks supplied liquid anhydrous NH_3 to the preparation system, where it was vaporized and controlled for pressure and temperature. The NH_3 vapor flow was measured prior to dilution with air and subsequent injection into the flue gas stream. The NH_3 was mixed with preheated air at a ratio of 1:20, which provided increased momentum for mixing with the flue gas stream. This mixture was injected just downstream of the booster fan and given sufficient time for thorough mixing prior to the entering catalyst reactor.

The catalyst consisted of homogeneous tubes (30 mm OD x 20 mm ID x 585 mm) with a hardening treatment used on the leading tube end to resist erosion. The main components of the catalyst were vanadium pentoxide and titanium dioxide. The tubes were arranged parallel to the gas flow and spaced to allow gas flow within and around the tubes. Each catalyst stage consisted of three layers or banks of tubes (Figure 2). Two assemblies of catalyst holders were used to closely fill the reactor cross section.

The APH located downstream of the catalyst bed was designed to be representative of utility practice (e.g. operating temperature, mass flow rate per unit area, sootblowing mass flux, and materials of construction). System controls were used to maintain the outlet gas temperature and the hot side air to gas differential pressure at typical values. The flue gas was cooled from a reactor exit temperature of approximately 670°F to approximately 300°F through the APH. Sootblowing schedules and other APH operating parameters were established based on manufacturer's recommendations in order to simulate typical utility operations. Three baskets arranged in a row from the hot to the cold end are referred to as the hot, cold-intermediate, and cold baskets, respectively. The basket element construction was conventional, however, the manner of material usage within the individual baskets was not. Each basket was constructed of separate layers of materials. The hot basket was constructed of corten and open hearth carbon steel, while the cold and cold-intermediate baskets utilized corten, enameled steel, and stainless steel. All of these materials are conventionally used in APH's, but with a varying resistance to corrosion. Late in the test program, a single piece cold/cold-intermediate basket was used, this was also constructed of the three materials.

Figure 1 also shows the auxiliary trace gas and ash injection systems. These were used in special short term tests to investigate the effects of higher ash loadings or high concentration of selected gas species on the catalyst operation.

TEST PROGRAM

In the course of the test program, both wet chemical and continuous analyzer sampling techniques were performed in NH_3 laden flue gas streams. NH_3 is a fairly reactive substance, resulting in a high potential for sampling interferences. The first phase of the test program included an investigation of potential sampling interferences when sampling for SO_3, sulfate and NH_3 (a detailed discussion of the sampling techniques will be deferred to in a later publication).

An outline of the test program is:

- Baseline Tests: Evaluation of the SCR catalyst with the systematic variation of the catalytic reactor operating parameters including inlet NH_3/NO_x mole ratio, flue gas flow rate and temperature. NO_x reduction efficiency, ammonia slip and SO_3 concentration were the primary parameters measured during this portion of the program.
- APH Evaluation: The APH performance evaluation was conducted concurrent with all phases of testing. The APH operating variables were held constant during the program (e.g., rotational speed, hot side ΔP, and exit gas temperature), so that effects of the variable catalyst operating conditions could be assessed.
- Off Design Operation: Later phases of the test program include system operation with enhanced levels of SO_2, CO, HC, and ash loading in the flue gas. These tests assessed the performance of the system at off design operating conditions.
- Transient Tests: A number of tests were conducted with the SCR system undergoing transient operating conditions. The focus of these tests was the evaluation of the NH_3 injection control system's ability to follow varying inlet conditions.

BASELINE TESTS

A summary of the SCR design conditions and the typical operations range are shown in Table 1. At these design conditions, the reactor was expected to produce a 90 percent NO_x reduction (η_{NO}) with no more than 1.0 NH_3/NO_x molar injection rate. The actual operating range was to some degree dependent upon the emissions of the boiler and deviated somewhat from the design point. Under normal conditions, full load boiler operation was held during testing. As shown, the only discrepancy was the NO_x level, which was significantly higher than the SCR design conditions. This change was ultimately reflected in the NH_3 injection rate and NH_3 slip. The PSCo boiler supplying the flue gas slipstream for the pilot plant burned a low sulfur western coal. A typical coal analysis is presented in Table 2.

Most of the data to be presented was obtained during the baseline test period, when a wide variety of operating conditions were explored. A single reactor flow and temperature operating point was used during a test day, with variation of the NH_3/NO_x as testing permitted. Exit NO_x levels were allowed to stabilize prior to the wet chemical and gaseous sampling. Once the baseline test matrix was complete, the reactor operation remained at base conditions of approximately 680°F, 5000 scfm at 0.9 to 0.95 NH_3/NO_x for long test periods while the test program shifted to other areas of interest. There was a slight difference in the reactor performance between the baseline testing and the tests where the reactor was allowed to equilibrate for 10 to 12 hours prior to sampling. The observed difference was slight in terms of NO_x

reduction efficiency, with the main impact being with the ammonia slip. This will be pointed out in the discussion of ammonia slip.

The η_{NO} versus NH_3/NO_x for 5000 scfm flow and temperatures of 580 and 680°F are shown in Figure 3. This relationship was fairly linear below an operating point of 0.9 NH_3/NO_x for the 680°F data. Above this point, the diminishing returns of additional ammonia injection were evident. The ammonia utilization (e.g., fraction of the injected ammonia that reacts with NO_x) was approximately 92.5 percent in the linear region of the curve, while the utilization fell off the higher operating ranges of NH_3/NO_x. The data indicated that 90 percent reduction at 1.0 NH_3/NO_x was met, although the data does exhibit some scatter. Error bars are included for data points in Figure 3. The η_{NO} was reduced at low temperature operation (580°F) with the average change in efficiency being 4 percent less than at 680°F.

The effect of flue gas flow rate upon η_{NO} was also studied; however the variation, if any, was within the data scatter of the 5000 scfm, 680°F tests. Curves for 2000, 3000, 4000, and 5000 scfm (corresponding to space velocities of 1300-3250 hr^{-1}) and temperatures of 580°F and 680°F showed very little variation from the data in Figure 3.

Ammonia slip (or unreacted NH_3 exiting the catalyst) was another important performance parameter which may have potential impact upon downstream equipment in the gas flow path or may ultimately be emitted from the system. The data for 680°F and 5000 scfm operation is shown in Figure 4. All data is presented as a percent of the injected (inlet) ammonia concentration, which indirectly normalizes the data to inlet NO_x concentration. The shaded bar represents the data obtained during the baseline test matrix. Reactor operation at 680°F showed a relatively constant NH_3 emission up to approximately 0.9 NH_3/NO_x. Above this point, the ammonia slip increased with increasing NH_3/NO_x ratio. This is consistent with the η_{NO} data presented earlier, which showed a flattening in the η_{NO} curve at this point. At high ammonia flow injection rates, more of the ammonia passed though unreacted while the NH_3 utilization decreases. With long-term equilibrium operation, the NH_3 slip was higher than the baseline data. This effect was thought to be the result of the catalyst material achieving an equilibrium of adsorbed NH_3 relative to the inlet NH_3 concentration.

Baseline NH_3 slip at 680°F operation as a function of flue gas flow rate is shown in Figure 5. The data scatter for 5000 scfm case is indicated with bars. Unlike η_{NO}, flow rate influenced NH_3 slip with reduced slip at lower flow rates. As flow was reduced, the NH_3 slip decreased, which corresponds to an increased residence time for reaction in the catalyst bed. Similar plots are shown for 580°F operation in Figure 6. In all cases, the NH_3 slip was higher at 580°F than comparable operation at 680°F.

A detrimental side reaction of the SCR technology is the catalytic conversion of SO_2 to SO_3 in the reactor. Minimizing the SO_2 to SO_3 conversion is one of the objectives in the design of a catalyst and can be altered by changing the catalyst formulation. The NH_3/NO_x operating point showed very little effect on the SO_2 to SO_3 conversion, but flue gas flow rate and temperature were influential factors. Figure 7 shows SO_3 concentration at the exit of the reactor as a function of flow rate, for the range of temperatures tested. For the 680°F operating point, the SO_3 concentration remained stable down to 4000 scfm, but thereafter began to rise appreciably. At 2000 scfm, the SO_3 conversion was approximately 3.1 percent (of the inlet SO_2 level), or over twice that at 5000 scfm. The same trend was observed for operation at 580°F although the SO_3 conversions were significantly lower. At 4000 or 5000 scfm and 580°F, SO_3 levels were close to boiler flue gas levels, indicating very little SO_2 to SO_3 conversion. The reduced flow rate provided increased residence time within the reactor, therefore greater time for the SO_2 to be catalytically converted to SO_3.

Reactor performance after approximately 8380 hours of NH_3 injection operation was documented to determine long term catalyst characteristics. No decrease in reactor NO_x reduction efficiency could be detected. NH_3 slip at at the reactor exit was higher than previous tests at similar conditions and averaged approximately 4.3 percent of inlet compared to ~3.3 percent measured early in the test program. The reason for the increase in NH_3 slip was not evident, but it did not seem to be reflected in the reactor efficiency. The SO_2 to SO_3 conversion was only slightly higher than previously, and averaged 1.4 percent of inlet SO_2 concentration.

Other long term reactor performance parameters showed no degradation. The pressure drop across the catalyst showed no significant increase throughout the one-year run time. Similarly, the periodic catalyst inspections showed no evidence of extensive ash buildup. Some ash deposition formed very early in the test program, and remained constant thereafter. Ash buildup was restricted to the bottom of the tube cases. Ash cones would form on top of the tube cross section, however, this buildup was temporary and could always be easily brushed or blown off. Very few tubes plugged and these were located along the edge of the catalyst bed, indicating flow distribution may be a factor.

Structural damage to the tubes did not occur during normal operation. Tubes occasionally slid out of the bottom of the cases due to slight misalignments of the bottom support grates. Most tubes would partially slide down to be supported by the next bank of tubes immediately below. The number of these tubes are a very small percentage of the total.

Erosion of the tubes was noted upon the first inspection, and throughout the program could be seen to gradually increase. Erosion was only noticed on the very top of the tubes, where the catalyst was hardened. The highest amount was at the very topmost case of stage 1, the first bank of tubes exposed to the flow. These tubes were also the closest to the reactor sootblowers. Correspondingly, the least amount of erosion was noted on the third stage. The erosion of the tube tops would typically start by pitting, which would frequently occur at the center of its cross section. The two edges of the tube sides were the last to erode. Upon first opening the reactor, the tube ends would be covered by a cone of ash, which concealed the eroded area. Once the ash was blown off, the indent on the top of the tube due to erosion could be seen. On a given bank of tubes, certain areas or groups of tubes seemed to erode at a higher rate than others. This was probably due to the flue gas flow streams or ash stratification within the reactor. No erosion could be detected along the side of the tube, although abrasion from the spacers could occasionally be seen. As time progressed, the amount of erosion increased. After approximately 6000 hours of operation, some "V" grooves were noted on the tube ends.

AIR PREHEATER PERFORMANCE

An important part of the test program was an assessment of how the catalytic reactor impacts air heater performance. This was accomplished during the test program by maintaining APH operating parameters constant (hot side ΔP, outlet gas temperature, and the sootblowing schedule) with varying reactor conditions. APH gas side ΔP was considered the most important parameter to continuously assess deposit formation in the air preheater elements. Basket inspection, basket weights, and deposit analysis were also used on a less frequent basis to provide additional information.

The change in NH_3, condensed ammonia species, and SO_3 concentration across the reactor exit and APH exit for base operating conditions are shown in Figure 8. Total ammonium consisted of gas phase NH_3 plus any condensed ammonium compounds or NH_3 absorbed on the fly ash. NH_3 predominates at the reactor exit, indicating that most of the total ammonium exists as gas phase NH_3 at reactor exit temperatures (approximately 670°F). The SO_3 level at the exit of the reactor is approximately 1.3 percent of the inlet SO_2 level due to the SO_2 to SO_3 conversion in the reactor. Upon passing through the APH the temperature dropped to 300°F and some species concentration changes were evident. The total ammonium level remained essentially constant across the APH, while the NH_3 level dropped significantly. This suggests that as the flue gas temperature dropped, a large portion of the gaseous NH_3 was absorbed by fly ash or condensed to form ammonium salts. A sizable decrease of SO_3 levels also occurred across the APH. The SO_3 levels at the APH exit were lower than the system inlet (boiler) levels (e.g., less than 0.5 ppm). The drop in SO_3 concentration also indicates that ammonium/sulfate compounds were formed in the APH, SO_3 was absorbed by fly ash, or that the SO_3 was being deposited in the APH basket elements. The constancy of total ammonium across the air preheater indicated that the amount formed by deposition could not be measured quantitatively through changes in NH_3 and NH_4^+ concentration.

Deposit or ash buildup within the APH baskets reduced the area available for gas flow, and resulted in higher gas side ΔP for a constant flow rate. While ΔP can be monitored continuously, it was not anticipated to be linearly related to the mass of deposit held within the baskets. It provided a good indicator of a steady state or rapid buildup of deposit formation, and has practical implications in terms of fan loads and cost impacts. Initial operation of the APH consisted of a baseline condition with the SCR reactor bypassed and then with the reactor in the flow path but no NH_3 injection. Both tests were run for three weeks and showed no tendency of an increase of the gas side ΔP. As soon as NH_3 injection was activated, a slow but steady increase in ΔP was noted. Gas side ΔP rose from an initial clean state of

4.0 in. H_2O to 5.6 to 5.8 in. H_2O after 3 to 4 weeks of operation (Figure 9a). After this point the ΔP appears to steady out, indicating an equilibrium between deposit formation and removal by sootblowing.

Inspections during the test runs showed the deposit accumulation to be restricted to the cold-intermediate and cold baskets. The hot baskets remained essentially clean, covered only by slight ash layer which could be easily brushed or blown off. Larger quantities of ash were present only where dropout occurred. Deposits were found at the interface between the two lower temperature baskets. The front (hot side relative to gas flow) of the cold-intermediate and rear (cold side) of the cold basket were relatively free of deposit accumulation. The heaviest accumulation occurred at the rear of the cold-intermediate and front of the cold baskets. Deposits seemed to extend approximately 4 to 10 inches into each basket, although this is difficult to accurately gauge given the limited access to the elements. Apparently, the hot basket and the leading edge of the cold intermediate basket were at a high enough operating temperature to prevent deposit formation. The cleanliness of the rear (the coldest) side of the cold basket suggest that the sootblowing was also a factor in the deposit location. The rearward face of the cold basket was closest to the cold side sootblowers. These sootblowers were operated at the highest frequency, on a schedule of once per 8-hour shift.

Other general observations showed that, for any given basket cross sectional face, deposition appeared to be heavier at the top (or further away radially from the APH centerline). Deposits were not always found over the entire basket cross section, and often were localized in patches. The occurrence of deposition did not appear to show any preference relative to the material of construction. Whenever present, the deposits were fairly uniform in appearance. In contrast to the grey fly ash, the deposits were of a dark black color, except when covered or mixed with ash. The buildup was almost crystal-like, with very small needles or peaks forming the surface. These black deposits were fairly hard and could not be easily blow or brushed off. When broken off the baskets, it was evident that the deposits contained a fair amount of fly ash. The black deposit seemed to act as a binder to form a matrix with the ash. A qualitative analysis showed the deposits to contain ammonium and were acidic.

Deposit samples were obtained during the various inspections and analyzed for sulfate and ammonium. The total sulfate content ranged from 25 to 32 percent with an average of 29.2 percent (by weight). A sample obtained from a disassembled basket was sent to a laboratory for analysis of ammonia, bisulfate and sulfate, and X-ray diffraction analysis for ammonium and sulfate compounds. The results are shown in Table 3. The ammonium and sulfate analysis were typical, but the X-ray data show large quantities of ammonium aluminum sulfate compounds. The calcium sulfate resulted from the normal combustion process as well as any SO_3 absorption into the ash. Ammonium sulfate was identified but in lesser magnitude to a whole array of ammonium iron sulfate compounds. Sulfates account for nearly one half of the deposit sample indicating the balance to be ash-related. The ammonium aluminum sulfate compounds account for ~42 percent of the deposit. In terms of mole percentages, these compounds can account for 90 percent of the sulfate, leaving the small balance to the calcium and other trace compounds. The aluminum in the deposits were probably obtained from the fly ash. Deposit samples taken from a single element material (corten, stainless or enameled steel) did not show any qualitative difference from one another. Once a layer or coating of deposit builds up, the element material would be masked from new deposit, indicating that the type of element would not be an important factor. Element material is most important with respect to corrosion resistance, a factor which could not be evaluated within the span of the test program.

In addition to the chemical analysis of the deposits, selected baskets were monitored for weight gain during an extended test run. These chemical analyses and the basket weight gain data were used to calculate a net deposition rate for ammonium and sulfate. The average weight gain was 7.2 lb/basket for a 50-day test. Assuming a constant flue gas flow of 5000 scfm on a 50-day operating period, a change of 0.27 ppm NH_4^+ across the reactor is sufficient to account for the weight gain. It should be stressed that these are net rates, and as calculated values reflect only that portion of sulfate and ammonium which were retained in the APH, and not that portion which may be collected and later removed by sootblowing. The weight gain and the calculated average deposition rates are consistent with the measurement of total ammonium concentrations that showed virtually no change between inlet and outlet of the APH.

Late in the test program, new one-piece cold/cold-intermediate baskets were installed in the APH. These were of similar construction and materials to the two separate baskets. The single piece design eliminated the basket interface and is a possible method to decrease deposit accumulation. All other APH parameters were held constant to allow comparison with the two piece baskets. Operation at base conditions and NH_3 injection raised the gas side ΔP from the initial 3.5 in. H_2O to 4.0 in. H_2O in three weeks (Figure 9b). Thereafter, the gas side ΔP was relatively steady for another two weeks. The use of the one-piece baskets seemed to reduce the final ΔP levels from 5.7 to 4.0 in. H_2O. This change was partially due to the lower initial ΔP of the clean baskets (4.0 versus 3.5) but also due to better cleanability, since the ΔP buildup from initial levels was also reduced. Without the interface between the baskets, where most of the deposits had previously formed, deposits on the new baskets could not be easily seen. Deposits could be detected within the center but quantity could not be distinguished. Very little deposit existed on either face of the one-piece baskets.

SO_2 INJECTION TEST

A number of tests were performed with trace gas and ash injection to the SCR flow system. One test which did show a large impact and could be potentially detrimental to a boiler system operation was the SO_2 spiking test. The SO_2 was injected just downstream of the NH_3 and boosted the SO_2 concentration to approximately 1400 ppm (3 percent O_2, dry) or about three times normal levels. Measurement of NH_3 and NH_4^+ were very similar to base conditions without SO_2 injection and no reduction of η_{NO} was detected. The

SO_2 to SO_3 conversion rate was reduced slightly (on a percentage rate compared to base conditions), but the actual SO_3 concentrations more than doubled to approximately 13 ppm (3 percent O_2, dry). SO_3 levels at the APH exit were essentially zero and similar to base data.

The rather high reactor exit levels of SO_3 resulted in fairly dramatic changes to the APH. The gas side ΔP is plotted versus time, for a test conducted with the original basket set (Figure 9c). At the beginning of the test, the APH had already operated for approximately two months at base conditions and the ΔP had increased from 4 to 5.8 in. H_2O. Deposits were undoubtedly present in the APH at the start of the SO_2 injection test. With SO_2 injection, the APH ΔP rose from 6 to 12 in. H_2O in ~3.5 days. The ΔP rose steadily during the period of SO_2 injection and was related to the enhanced SO_3 levels at the reactor exit since NH_3/NH_4^+ levels were essentially unaffected. After reaching a gas side ΔP of 12 in. H_2O, the SO_2 injection was stopped, and the system allowed to run at base conditions. Figure 9c shows that the gas side ΔP started a sizable reduction, although this test was cut short by system mechanical problems. Normal sootblowing schedules were held throughout the test period. A similar test was conducted with the one piece cold/cold-intermediate baskets showed similar results.

At the end of this test, an APH basket inspection was performed. A large quantity of deposits was found on the interface between the cold and cold-intermediate baskets. The majority of the additional deposits were found on the front of the cold basket. Some areas of the basket cross section were totally choked with deposit accumulation. Except for the quantity, the deposit was typical in appearance.

While quite startling, the very rapid rise in APH ΔP at high SO_2 levels should be evaluated with caution. The SO_2 levels to the reactor inlet were about three times above the design point. A SCR unit which would be installed on a boiler with comparable SO_2 levels would probably be supplied with a catalyst with a lower SO_3 conversion rate. However, these results do indicate additional constraints imposed on a boiler utilizing SCR, since even short-term (a few days) switches to higher sulfur fuels could result in detrimental APH operation. The rate of ΔP buildup and plugging was clearly not linear with the SO_3 concentration at the APH inlet. [Base reactor outlet SO_3 concentrations were typically 6-7 ppm (3 percent O_2 dry), while the SO_2 injection tests yielded ~12-13 ppm.] The buildup of deposits was probably a complex interaction between SO_3, NH_3 and NH_4^+ concentration, ash composition, sootblowing method and frequency, basket construction, and APH operating temperatures. The one parameter not explored extensively during these tests was APH sootblowing, which may offer a method to combat deposition through increased frequency or more efficient sootblowing methods.

TRANSIENT TESTS

The transient tests simulated SCR operation under typical boiler load fluctuations, and involved changing inlet conditions of temperature and flow rate. In addition, tests with variable inlet NH_3/NO_x were performed. The results showed that the NH_3 injection control systems (e.g., either controlling η_{NO} or inlet NH_3/NO_x ratio) were able to respond to the transient conditions without causing such adverse effects as abnormally high NH_3 slip, et cetera.

AMMONIA INJECTION CONTROL AND RELATED MEASUREMENT METHODS

There was perhaps no other system which was critical for proper operation of a SCR system, as the ammonia injection control. Efficient NO_x reduction and NH_3 utilization required that the amount of NH_3 injected was properly tailored to the system demands. Determination of the NH_3 requirements was provided by the measurement of various process parameters, but NH_3 flow measurement and system NO_x measurements were critical.

Two modes are available for the NH_3 flow control system. The system could be set to maintain a given NH_3/NO_x molar ratio or the NO_x reduction efficiency. Required inputs of flue gas flow rate and inlet NO_x concentration were used to control the NH_3 injection rate with NH_3/NO_x control. Inlet and outlet NO_x measurements were used to control NH_3 flow with η_{NO} control mode.

Accurate NH_3 flow measurement was required as an input to the NH_3/NO_x controller, and was necessary to accurately determine the operating point of the catalyst. The system used on the pilot plant was a thermal mass flowmeter. This instrument is perhaps appropriate for a research environment, where accurate data is required. A fairly clean ammonia supply is required by its principle of operation as the existence of condensed water or fine solids tend to build up and cause erroneous readings. The quality of NH_3 supply may become particularly sensitive for a utility application, since NH_3 costs will rise with grade, which in turn impacts operating costs. A system which is capable of measuring NH_3 flow in less than ideal environments would be more suitable to a utility use. Problems were initially encountered with the NH_3 flow measurement system on the pilot plant, resulting in system downtime. A utility application will require a NH_3 flow measurement system which stresses reliability and includes adequate filtering and heat tracing to preserve integrity.

Flue gas concentration of NO was also required to determine the NH_3 demand, or for η_{NO} determination. Inlet NO concentration is required on most conceivable NH_3 injection control modes. Inlet NO concentration measurement is fairly standard, however, a well designed system is required with careful attention paid to maximizing availability. Loss of this critical NO measurement used in NH_3 flow control will disable the SCR system unless the system is operated manually. Typically, utility practice puts a premium upon reliability and system availability, therefore NO_x monitors and sample systems require appropriate upgrading and redundant components to deliver the desired performance. This is in distinct contrast to currently used emission monitors which typically do not function in a control loop and thus a lower availability can be tolerated. The requirement of measuring exit NO_x is essentially no different than inlet NO_x measurement, however the presence of NH_3 slip and elevated SO_3 levels did create more problems. Increased frequency of plugging and corrosion in the sampling system are to be expected to some degree, requiring attention be paid to routine maintenance. In addition, there did appear to be a buildup of catalyst on the filter used to obtain a measurement sample. This resulted in a reduction in NO_x across the filter and indicated NO_x reduction higher than the actual.

CONCLUSIONS

1. The catalyst did meet its NO_x reduction requirements at design condition operation. No significant loss in reduction efficiency was noted during the catalyst life.

2. High levels of NH_3 slip and a reduced NH_3 utilization was observed for reactor operation above 0.9 NH_3/NO_x. Increased temperature reduces NH_3 slip and improved efficiency. Flue gas flow rate showed little significant effect upon η_{NO}, while increasing flow increased NH_3 slip. A measurable increase in NH_3 slip was noted after one year of catalyst operation.

3. SO_2 to SO_3 conversion occurred across the catalyst reactor. Either higher temperature and lower flue gas flow rate through the reactor raised the conversion rate.

4. Ash deposition in the catalyst bed was not a problem. Erosion of the tubes progressed with time, but was restricted to the leading tube edges.

5. The NH_3 slip and SO_3 concentration did promote APH deposit accumulation and resulted in higher gas side ΔP. Deposits accumulated in the interface between cold and cold-intermediate baskets. Use of a one piece (cold/intermediate) basket reduced the gas side ΔP slightly (net 1.5" ΔP). Deposits were composed of ammonium/aluminum/sulfate type compounds although the exact mechanism of their formation is unknown.

6. Enhanced inlet SO_2 levels did promote rapid deposit accumulation. However, these SO_2 levels were much larger than design levels.

7. Ammonia injection controls rely heavily upon NH_3 flow and NO_x concentration measurements. These systems must be upgraded and maintenance programs instituted to maintain availability required of utility systems.

ACKNOWLEDGMENTS

This program was conducted at athe EPRI Arapahoe Test Facility. The cooperation and assistance of the EPRI on-site personnel, Lou Rettenmauer and Richard Hooper, and the Kaiser Engineer operators and supervisors responsible for operating the pilot plant, were gratefully appreciated.

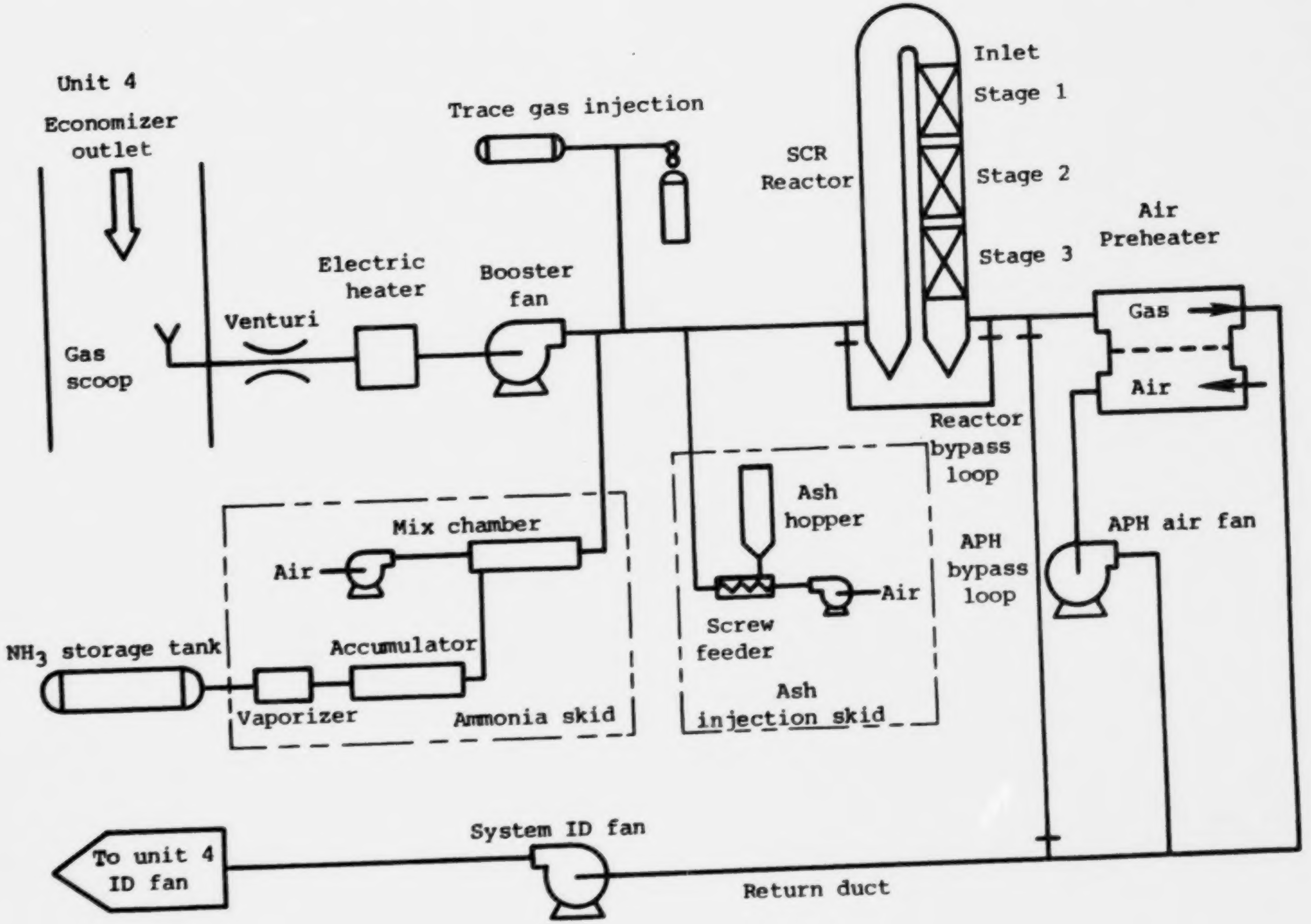
Unit 4
Economizer outlet
Gas scoop
Venturi
Electric heater
Booster fan
Trace gas injection
SCR Reactor
Inlet
Stage 1
Stage 2
Stage 3
Air Preheater
Gas
Air
Reactor bypass loop
APH bypass loop
APH air fan
Mix chamber
Air
Accumulator
NH_3 storage tank
Vaporizer
Ammonia skid
Ash hopper
Air
Screw feeder
Ash injection skid
System ID fan
To unit 4 ID fan
Return duct

Figure 1. IECPP test system.

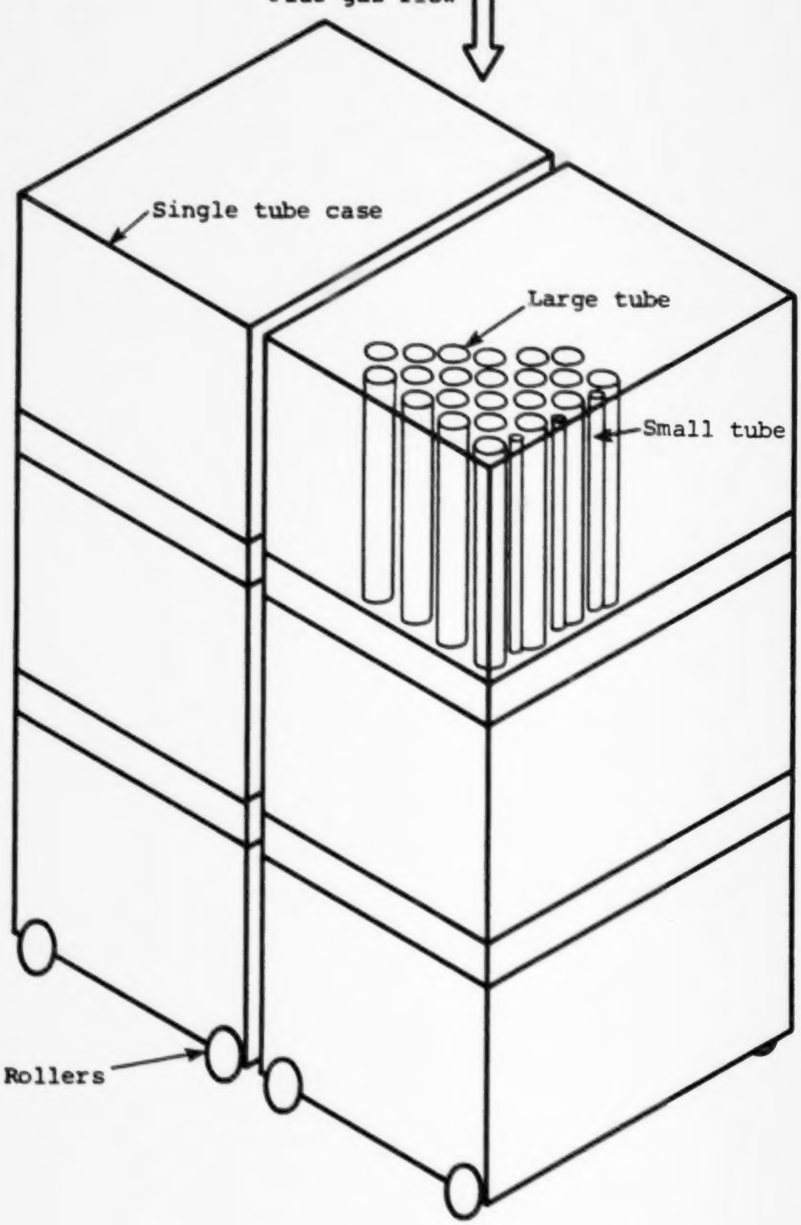
Flue gas flow
Single tube case
Large tube
Small tube
Rollers

Figure 2. Catalyst packing arrangement for a single reactor stage.

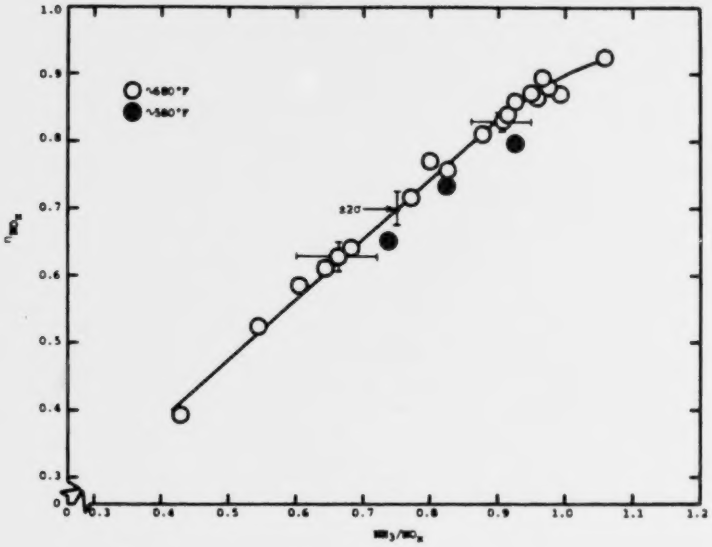

Figure 3. NO_x reduction efficiency, 5000 scfm (∿ 3250 hr^{-1}).

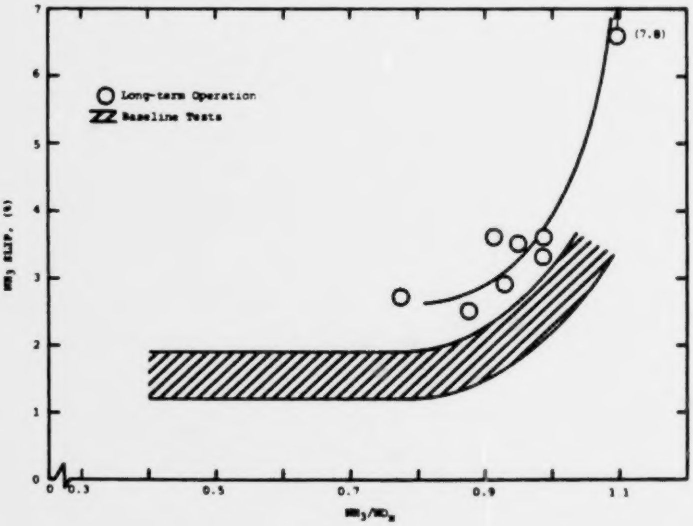

Figure 4. Ammonia slip, 5000 scfm (∿ 3250 hr^{-1}), ∿ 680°F temperature.

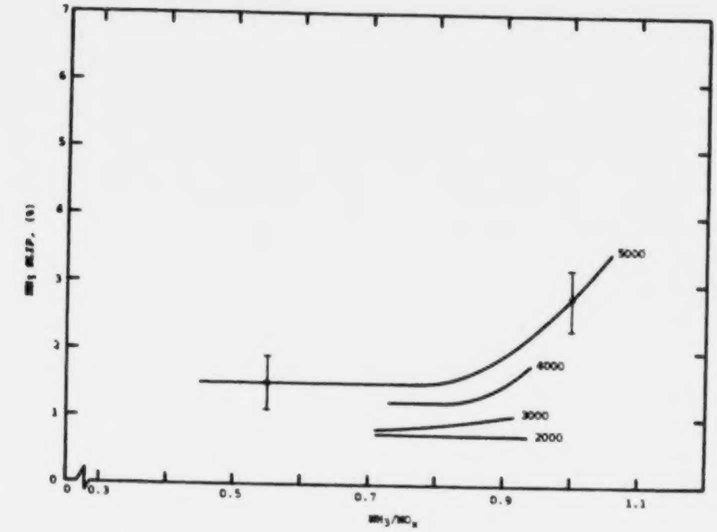

Figure 5. Ammonia slip, 680°F.

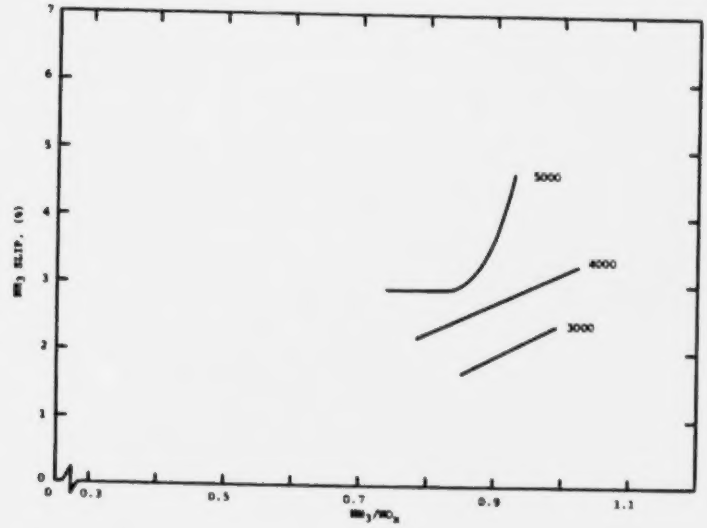

Figure 6. Ammonia slip, 580°F.

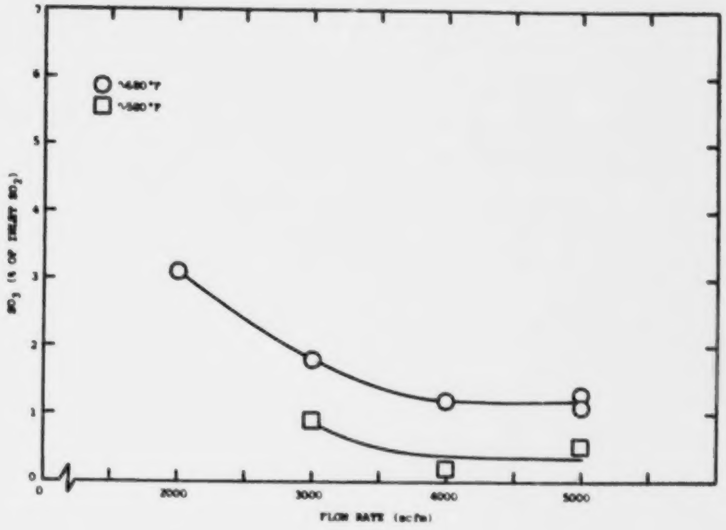

Figure 7. SO_2 to SO_3 conversion, 0.90 - 0.95 NH_3/NO_x

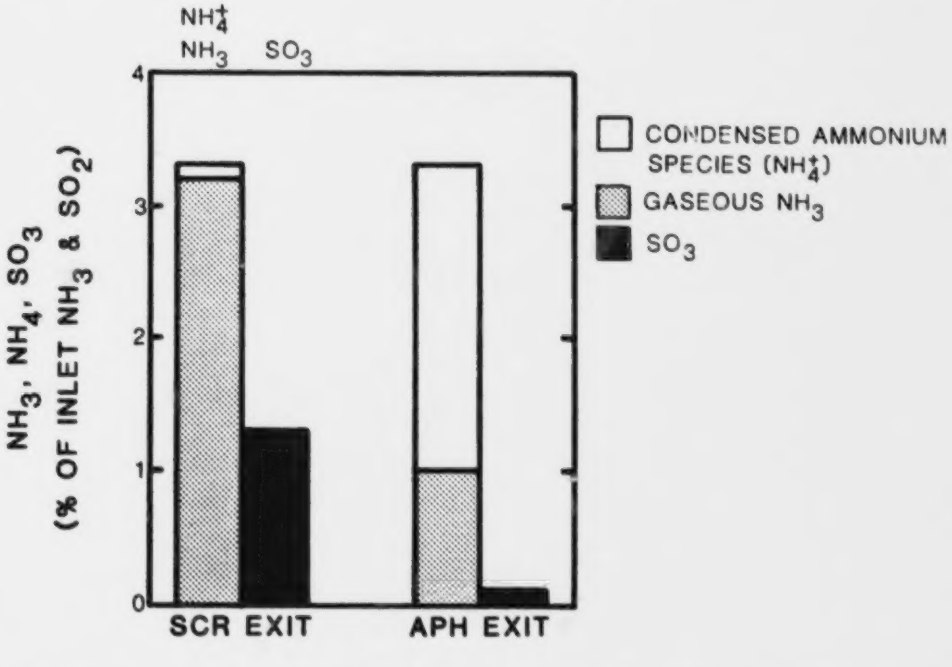

Figure 8. Base SCR operation - species profiles, 680°F, 5000 scfm, 0.93 NH_3/NO_x

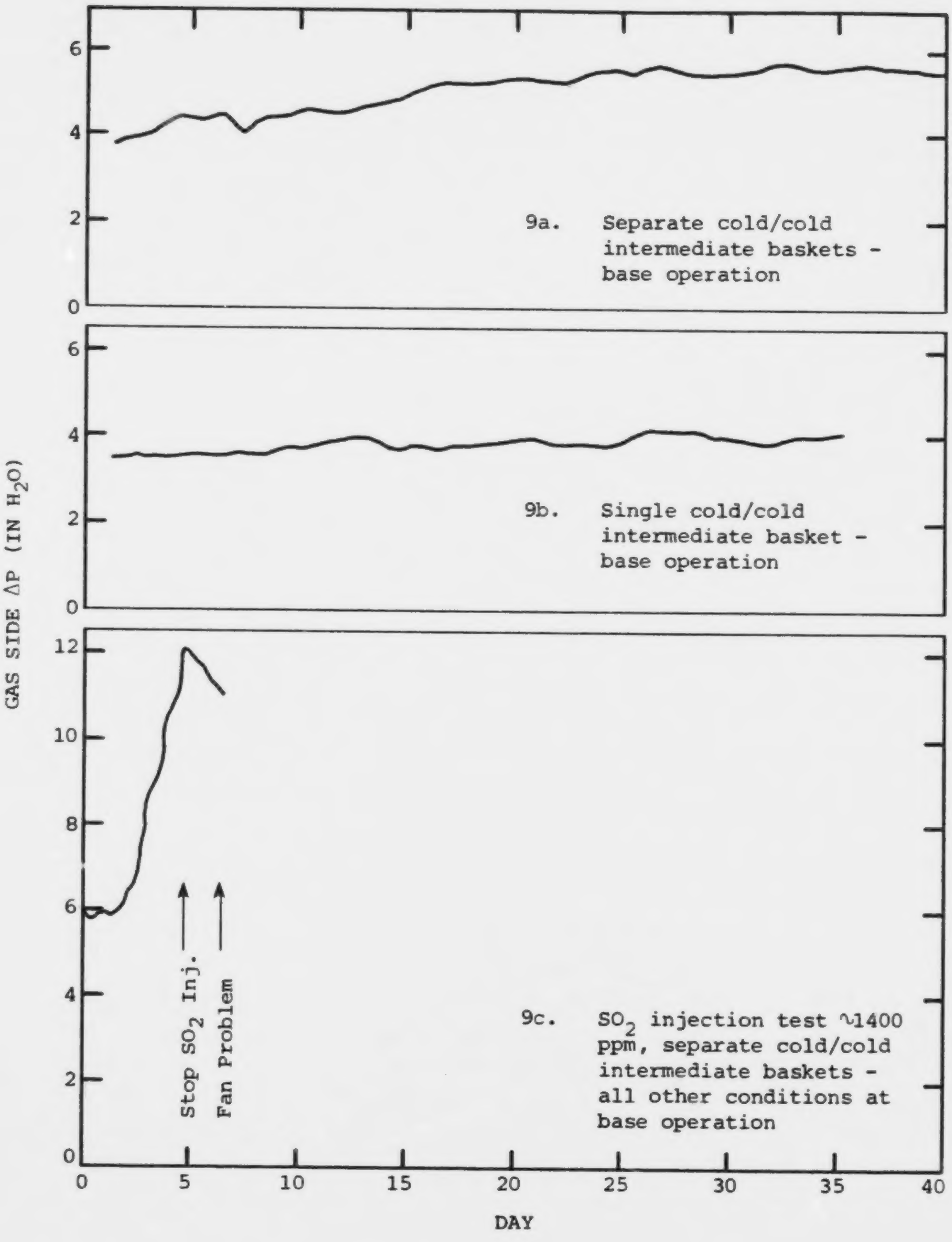

Figure 9. APH gas side ΔP - base operation & SO_2 injection tests.

TABLE 1. SCR DESIGN CONDITION AND TYPICAL OPERATING RANGE

Parameter	Design	Operating Range
Flow Rate (scfm)	5000	2000-5000
Flue Gas (Catalyst Temperature (°F)	680	580-750
NO_x (ppm, 5% O_2) [3% O_2, dry]	600 [740]	[~950]
SO_2 (ppm, 5% O_2) [3% O_2, dry]	350 [435]	[450]
SO_3 (3% O_2 dry)	--	~0.5
CO (ppm 5% O_2)	15	10-50
O_2 (%)	5	3-6
N_2 (%)	74	74
CO_2 (%)	11	13
H_2O (%)	9	7
Fly Ash (gr/scf)	3.3	~3

TABLE 2. TYPICAL COAL AND ASH ANALYSIS (ENERGY COAL)

Coal Analysis (As Fired)	
Proximate	
% Moisture	10.62
% Ash	8.28
% Volatile	36.33
% Fixed Carbon	44.77
Heating Value (Btu/lb)	11,132
Ultimate	
% Sulfur	0.54
% Carbon	63.41
% Hydrogen	4.47
% Nitrogen	1.56
% Chlorine	0.04
% Oxygen (Diff.)	11.08
Ash Analysis (Sample Not From SCR Reactor)	
L_1O_2	0.02
Na_2O	0.44
K_2O	1.1
MgO	1.7
CaO	6.0
Fe_2O_3	4.1
Al_2O_3	25.5
S_iO_2	56.2
T_1O_2	1.5
P_2O_5	1.2
SO_3	0.74
LOI	1.6

TABLE 3. APH BASKET DEPOSIT ANALYSIS

Species	Weight %
NH_4^+	2.72
Total $SO_4^=$	32.1
HSO_4^-	4.3*

X-ray Diffraction Analysis

$NH_4\ Al\ (SO_4)_2$	28.2
$NH_4\ Al\ (SO_4)_2 \cdot 12\ H_2O$	14.0
$CaSO_4$	4.4
$(NH_4)_3\ Fe\ (SO_4)_3$	
$(NH_4)_2\ Fe\ (SO_4)_2$	Identified in order of magnitude
$(NH_4)_2\ Fe\ (SO_4)_2 \cdot 2\ H_2O$	
$(NH_4)_2\ SO_4$	

---

*Due to presence of aluminum salts, the bisulfate determination is not certain.

CATALYTIC DENO$_x$ DEMONSTRATION SYSTEM HUNTINGTON BEACH GENERATING STATION UNIT 2

By:

Harold A. Kerry
Alexander Weir, Jr.
Southern California Edison Company
Research and Development
Rosemead, California

ABSTRACT

The Southern California Edison Company's 107.5 MW Selective Catalytic DeNO$_x$ System is being tested to develop performance and operational data on a post combustion NO$_x$ removal system. The unit was installed to demonstrate 90% NO$_x$ removal. Seven months of the planned one year program has been completed. This paper reviews operational data from the system.

INTRODUCTION

Southern California Edison Company is testing a full scale Kawasaki selective catalytic NO$_x$ reduction system on one half of the flue gas from the 215 MW, Unit 2 at the Huntington Beach Generating Station. The purpose is to develop cost, performance, and operational data on this post combustion NO$_x$ removal system. The unit was designed to achieve 90% NO$_x$ removal.

PROCESS DESCRIPTION

The NO$_x$ removal facility installed is a process in which nitrogen oxides in the boiler flue gas are lowered using ammonia as a chemical reducing agent. The reduction occurs in the presence of a catalyst at flue gas temperatures of 570° - 750°F (299 - 399°C). The flue gas is obtained after the economizer, but before the air preheater. No particulate removal is involved. Ammonia vapor, diluted with hot combustion air, is injected into the flue gas stream upstream of the reactor. The concept is shown in Figure 1. Nitrogen oxides are reduced by ammonia to nitrogen and water over the catalyst surface. The following reactions are postulated:

(1) $4\ NO + 4\ NH_3 + O_2 = 4\ N_2 + 6\ H_2O$
(2) $2\ NO_2 + 4\ NH_3 + O_2 = 3\ N_2 + 6\ H_2O$

It is believed that reaction (1) predominates since the flue gas NO/NO_2 ratio is very high. Thus, approximately one mole of ammonia is required for each mole of NO_x to be removed.

FACILITY DESCRIPTION

Existing Facility

Southern California Edison's Huntington Beach Generating Station consists of 4 units located on the coast at Huntington Beach, California. The flue gas stream of the 215 MW, Unit 2 is split into two streams after leaving the boiler, each stream with its own air preheater. One of these streams, approximately 500,000 CFM at 750°F (850,000 m^3/hr at 399°C) is fed to the NO_x removal facility for treatment. Typical flue gas emissions when operating on fuel oil are:

• NO_x Concentration	180-280 vppm at 3% O_2, dry
• SO_2 Concentration	70-140 vppm at 11% and 4% O_2
• Particulate Concentration	0.005 - 0.02 grains/SCF (11-46 mg/m^3)
• SO_3 Concentration	1-5 vppm

A typical load chart for a 24-hour period is shown in Figure 2.

Catalytic Reactor System

The reactor system consists of a reactor with catalyst, induced draft fan, dampers, and associated ducting and controls.

The reactor is designed for vertical flow and includes an inlet transition with guide vanes for proper flow distribution, a large rectangular section containing the catalyst beds, and an outlet transition duct. The catalyst modules are stacked two high and are supported by a "grating-type" floor. The catalyst is of the square-honeycomb type and was furnished by Kawasaki. Thirty-two catalyst elements are assembled in one basket or module to facilitate handling and minimize damage. The reactor contains 144 baskets and thus includes 4,608 catalyst elements. A damper is provided at the inlet and outlet duct of the reactor so that the reactor can be isolated from the boiler system. These dampers can also be used along with the reactor by-pass damper to regulate flue gas flow to the reactor during startup and shutdown to adjust the temperature rise of the reactor.

The induced draft fan, located downstream of the air preheater, is controlled by inlet vanes. The fan compensates for the added draft losses through the reactor system. A by-pass duct and damper as well as outlet dampers are provided. The fan may be isolated from the existing boiler system. The fan is designed to operate @ 371,800 CFM (632,500 m^3/hr) and 17 in. (430 mm) water gauge and directly driven by a 2,000 HP electric motor.

Ammonia Supply System

The ammonia supply system consists of a liquid anhydrous ammonia storage tank, ammonia vaporizer, and associated piping and controls.

The tank has a 12,000-gallon (45.4 m^3) capacity, which is adequate to support full load reactor operation in excess of 14 days. The tank is provided with one 25 kW electric-type vaporizer to insure an adequate ammonia vapor supply to the reactor system under low ambient temperature conditions.

Ammonia Dilution and Injection System

The ammonia dilution and injection system consists of an ammonia-gas dilution air blower, ammonia-flue gas mixer, and associated piping and controls. The system functions as follows:

The ammonia vapor from the storage tank flows to the ammonia gas dilution mixer through a pressure control valve and the ammonia flow control valve. The pressure control valve reduces the ammonia pressure to 30 psig (207 kPa). In the ammonia gas dilution mixer, the ammonia vapor is diluted with hot combustion air bled from the west-side air preheater. The hot combustion air is supplied to the mixer at approximately 600°F (316°C). A high pressure blower is utilized to boost the pressure of the hot combustion air from 13 in. (330 mm) to 40 in. (1016 mm) water gauge. From the ammonia gas dilution mixer the diluted ammonia is forwarded to the ammonia-flue gas mixer located in the flue gas duct upstream of the reactor. In the ammonia-flue gas mixer, the diluted ammonia is injected into the flue gas stream from the boiler economizer through a series of nozzles.

Control System

The major controls provided for operation of the reactor are the ammonia injection control system to maintain a set NO_x removal ratio, and an induced draft fan control system to maintain the proper flue gas flow through the reactor. The instrumentation for the control system is shown in Figure 3.

The ammonia injection is controlled by the ammonia flow control valve, which acts in response to the NO_x-ratio controller. Chemiluminescence NO_x monitors at the inlet and outlet of the reactor provides the NO_x content for the NO_x ratio controller. The chemiluminescence NO_x monitors are the heated type that accept hot-wet samples from heat traced sample systems. Other monitors are also provided for oxygen and sulfur dioxide at the reactor inlet and ammonia at the reactor outlet. In the ammonia monitor system, ammonia is converted to NO_x in a "catalytic ammonia to NO_x converter" and total NO_x is determined in another chemiluminescence NO_x monitor. The ammonia concentration is the difference between the outlet NO_x and the total nitrogen as NO_x in the ammonia-NO_x monitors. The ammonia monitor system is also the heated type that accepts hot-wet samples from the heat traced sample system. The ammonia monitor system has no control function but has an alarm for high ammonia. In addition to the reactor system monitors, monitors are provided down stream of the air preheater at the system stack for oxygen, NO_x and ammonia. These monitors are the dry sample type that accept chilled-dry samples. These measure stack emissions and have no control function.

The induced draft fan is used to control the flue gas flow through the reactor and balance the flow between the east and west air preheaters. Flue gas flow is controlled by the fan-inlet vanes, which act in response to a signal representing the difference between the actual flow through the reactor and one half of the total flue gas flow leaving the boiler. The reactor flue gas flow is monitored by an ANNUBAR flow indicator.

Arrangement

The reactor is located directly south of the unit and does allow for system expansion to treat all flue gas flow from Unit 2. The arrangement takes advantage of an existing duct elbow between the economizer outlet and inlet to the vertical shaft air preheater.

The existing west flue between the air preheater and stack was modified to incorporate the new induced draft fan, with bypass and isolation dampers, and to add a stub stack for monitoring visual opacity of treated flue gas.

TEST PROGRAM

The general objective of the test program is to verify and characterize the performance of selective catalytic NO_x removal systems, as well as assess the impact of such a system on steam generating plant operation and maintenance. To this end, the following major performance and operating parameters are to be determined during the test program:

a. NO_x removal efficiency as a function of the ammonia injection rate at various boiler operating conditions.

b. NH_3 slip (i.e., NH_3 concentration downstream of the reactor) and visual plume opacity at each test condition.

c. Catalyst performance deterioration versus service time. (This is a most important parameter, with a dominating impact on system operating cost.)

d. Operating factors such as system draft loss, ammonia usage and energy consumption.

e. Maintenance factors such as reactor and air preheater cleaning requirements due to deposits, such as, ammonia bisulfate.

f. Catalyst handling, replacement and disposal procedures.

g. Evaluation of ammonia injection controls, draft system controls, boiler protection controls and emission monitors and analyzers.

OPERATION

The catalytic deNO_x system was first put on line March 15, 1982. At that time, one month was planned for shakedown. However, seven months elapsed before shakedown, as originally planned, was completed. The initial three months of operations used low sulfur (0.25% S) oil fuel in the boiler and was characterized by moisture and SO_3 corrosion products accumulating in the monitor sample lines and monitors. This resulted in poor, or no, automatic control for NO_x removal facility. The initial problems were fairly typical of most startups and the control system was expected to be corrected with minor modifications. After much effort, however, the system still did not operate properly, and it was finally agreed, by all parties concerned, that the corrosion problems could not be simply corrected. A redesign of the sample line and monitor systems to convert them to a dry-chilled sample system was required. At the present time the redesign has been completed, and the modified equipment is being installed. During the subsequent four months of operation, gas fuel was used in the boiler. No corrosion products were observed in the sample lines since the sulfur-free fuel was used. However, some monitor instability was noted due to soot-like contaminants. It is hoped that the new dry sample system will prevent these soot-like contaminates from reaching the monitors.

Since startup, approximately 4,000 hours of catalyst reactor bed operation has been conducted with approximately 3,500 hours of NO_x reduction by ammonia injection. Because of the monitor problems, around-the-clock automatic operation has not been achieved. Automatic control for 90% NO_x removal has been achieved with reasonably good load tracking at one-half to full load and has been so operated on day shifts. At less than one-half load, automatic NO_x control operation results in unsatisfactory response from the control system and manual ammonia feed has been used.

Pressure drop (ΔP) across the reactor at maximum load is about 5 in. (127 mm) water gauge which is under the design maximum. No change in ΔP has been noted in the 4000 hours of operation. Temperature changes of the flue gas have been greater than anticipated. The temperature for gas is about 50°F (28°C) lower than oil and is frequently below the minimum set point, 570°F (299°C), for ammonia feed at minimum load.

Manual chemical evaluation tests were conducted to confirm the monitor indications. One series of these tests has been completed. The completed test results show the following:

	Experimental		
	Full Load 200,000 SCFM (322,000 Nm^3/hr)	Minimum Load 78,000 SCFM (125,000 Nm^3/hr)	Design Value
NO_x Inlet, vppm at 3% O_2, dry	215	240	
NO_x Outlet, vppm at 3% O_2, dry	23	19	
% NO_x Removal	89.2	92.7	90 min.
NH_3 Slip, vppm at 3% O_2, dry	9	8	10 max.

Thus far, the reactor outlet ammonia monitor system operation has also been inoperable, partially due to the above-mentioned monitor sample line problems and partially due to leaks around a quartz ammonia to NO_x catalyst tube used in the ammonia converter assembly. A metal catalyst tube will be substituted for the quartz tube to, hopefully, solve the leak problem and the converter will then be tested upon installation of the dry system.

The stack ammonia monitor system operation has been erratic due to drifts in the NO_x and the NH_3-NO_x monitor systems, low conversion efficiency of the ammonia to NO_x converter (about 30%) and a slow converter response (10-15 minutes to reach equilibrium). A metal catalyst tube was substituted for quartz in this sytem. The system, however, has been in operation only when gas fuel was used in the boiler and hence has not been subjected to the reaction products of ammonia and sulfur.

Although ammonia measurements with the existing system have been less than satisfactory, an initial lag in ammonia slip has been observed upon increase in ammonia feed before steady state ammonia slip occurs. This indicates that the ammonia is initially adsorbed on the catalyst until saturation is achieved. With decrease in ammonia feed, ammonia slip continues indicating desorption occurring. Because of this, adsorption-desorption characteristic, the ammonia slip at any load will depend on whether or not steady state conditions have been achieved. This would not be a problem on a commercial boiler, but may be on a utility boiler which is not base loaded.

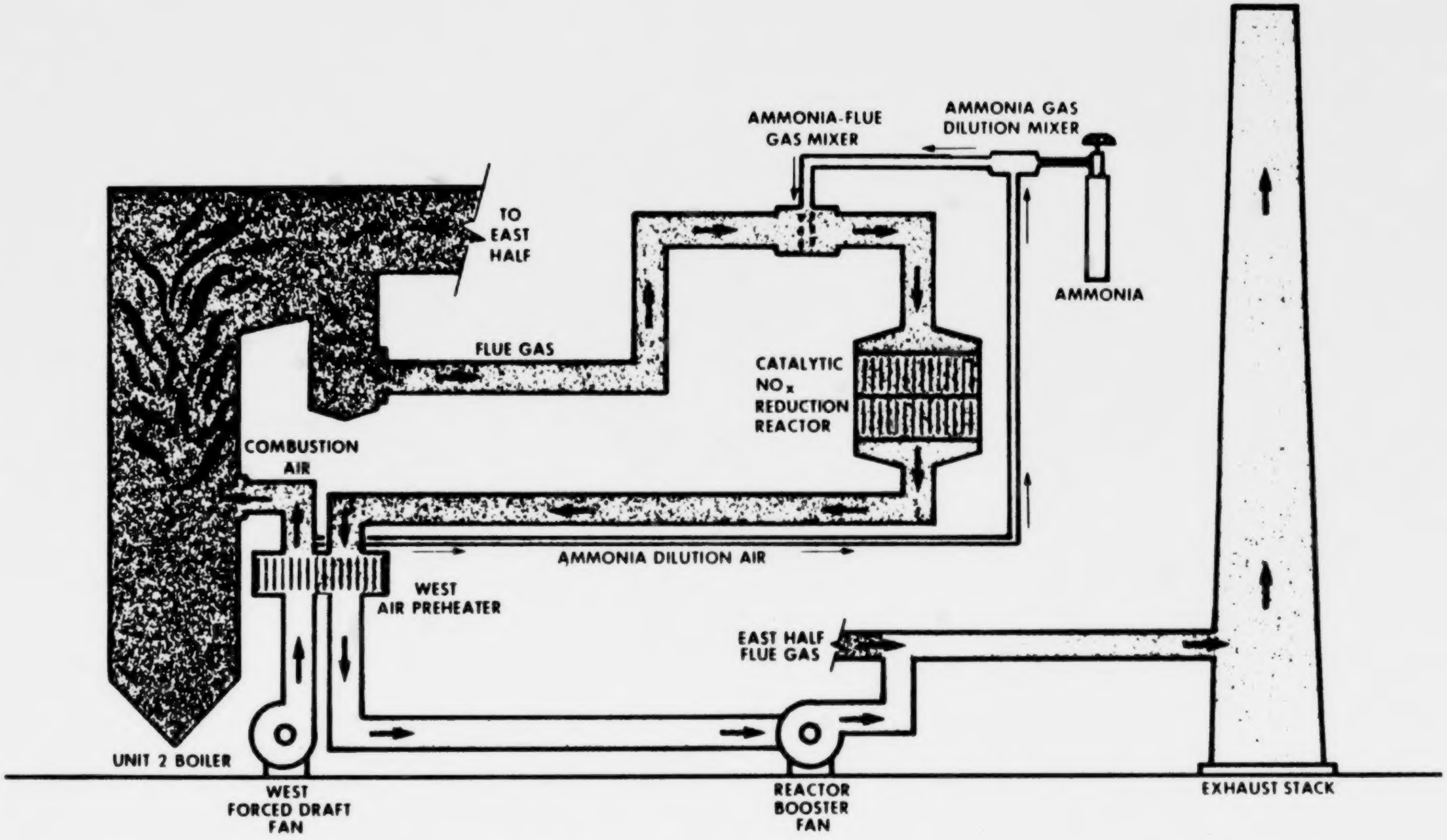
TO
EAST
HALF
AMMONIA-FLUE
GAS MIXER
AMMONIA GAS
DILUTION MIXER
AMMONIA
FLUE GAS
CATALYTIC
NO_x
REDUCTION
REACTOR
COMBUSTION
AIR
AMMONIA DILUTION AIR
WEST
AIR PREHEATER
EAST HALF
FLUE GAS
UNIT 2 BOILER
WEST
FORCED DRAFT
FAN
REACTOR
BOOSTER
FAN
EXHAUST STACK

Figure 1. Huntington Beach catalytic deNOx demonstration concept.

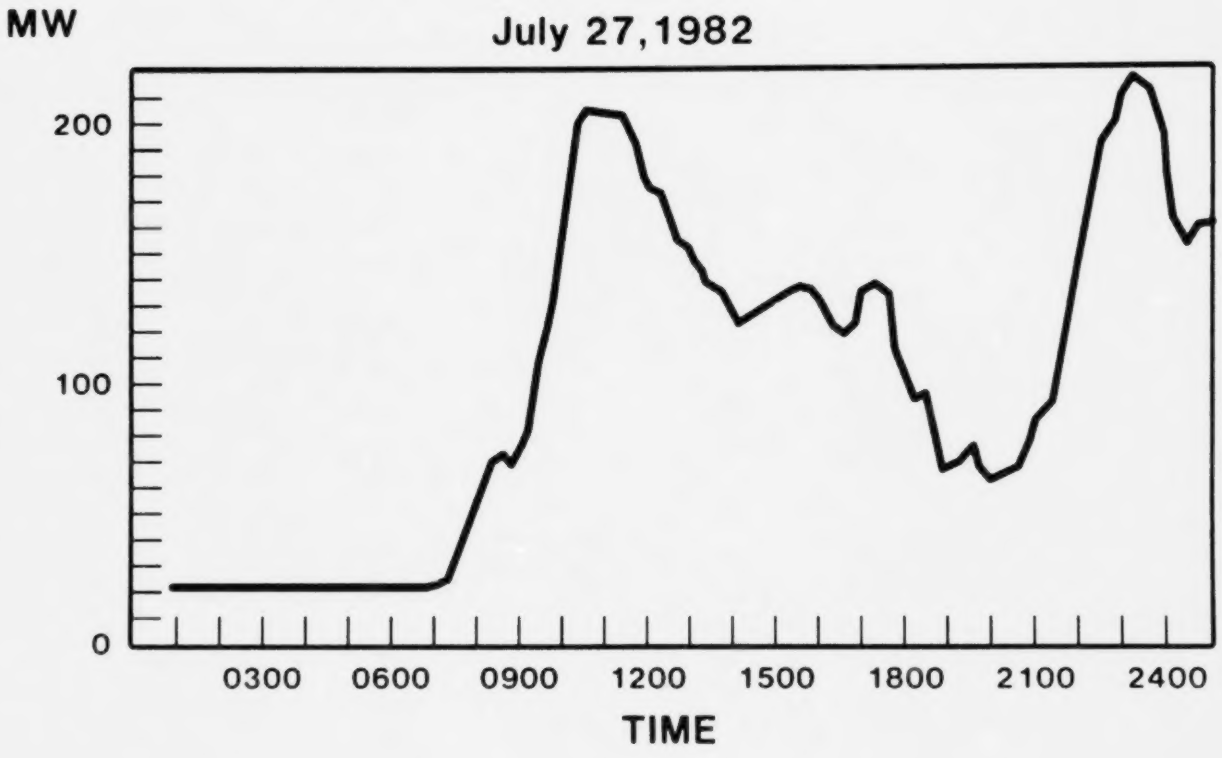

Figure 2. Huntington Beach unit 2 load.

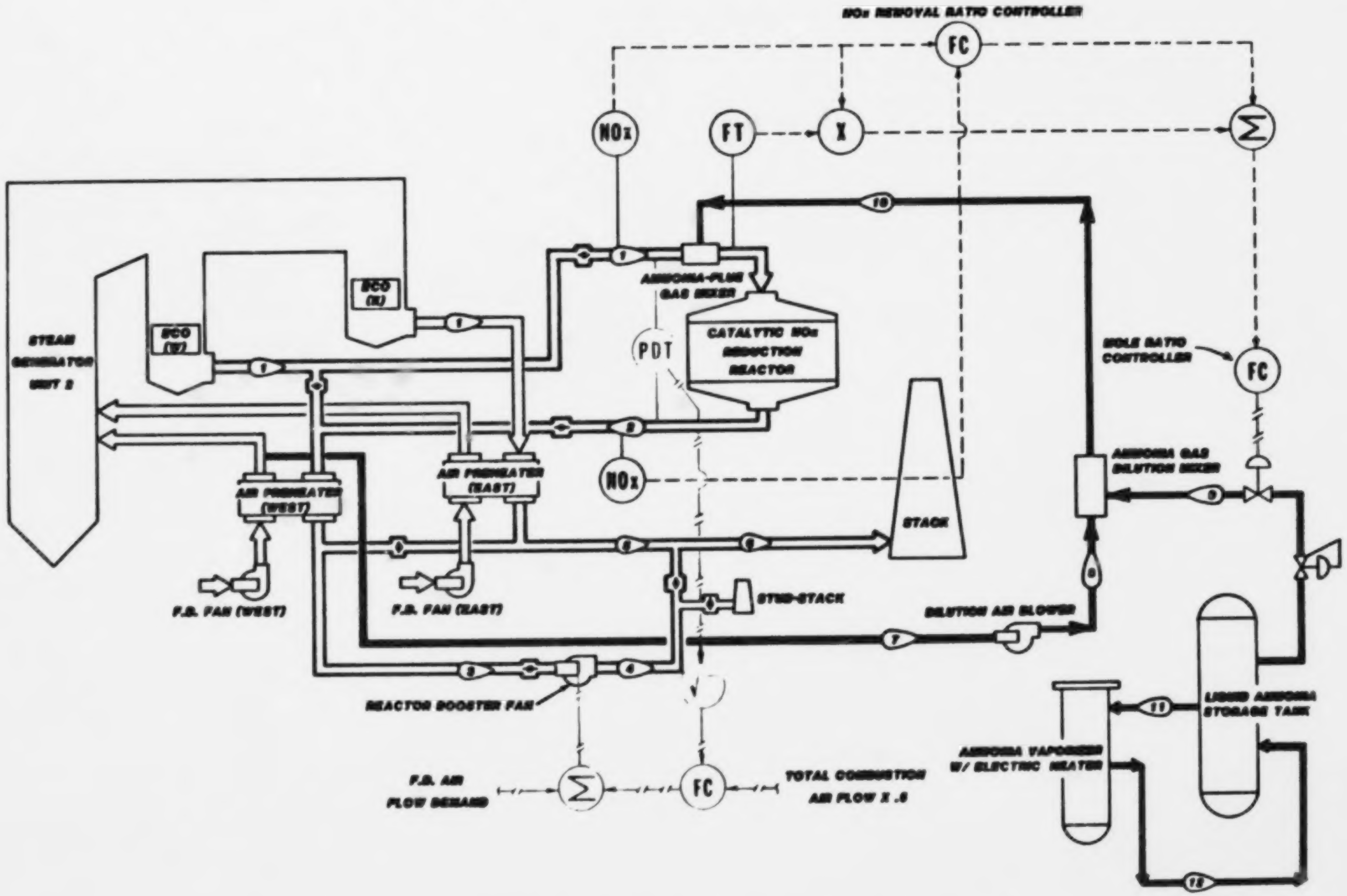
NOx REMOVAL RATIO CONTROLLER
FC
NOx
FT
X
Σ
STEAM GENERATOR UNIT 2
ECO (W)
ECO (E)
1
1
1
10
AMMONIA-FLUE GAS MIXER
CATALYTIC NOx REDUCTION REACTOR
PDT
2
NOx
MOLE RATIO CONTROLLER
FC
AMMONIA GAS DILUTION MIXER
9
AIR PREHEATER (WEST)
AIR PREHEATER (EAST)
5
5
STACK
8
STUB-STACK
F.D. FAN (WEST)
F.D. FAN (EAST)
DILUTION AIR BLOWER
7
3
4
REACTOR BOOSTER FAN
LIQUID AMMONIA STORAGE TANK
11
AMMONIA VAPORIZER W/ ELECTRIC HEATER
F.D. AIR FLOW DEMAND
Σ
FC
TOTAL COMBUSTION AIR FLOW X .6
12

Figure 3. Catalytic $deNO_x$ demonstration plant controls.

THE THERMAL DeNOx DEMONSTRATION PROJECT

By:

Henry T. Dziegiel, Tyrone B. Aure, David W. Anderson
Los Angeles Department of Water and Power
Power Design and Construction Division
P. O. Box 111, Room 604
Los Angeles, California 90051

ABSTRACT

In order to gather further information for pending regulatory proceedings, the Los Angeles Department of Water and Power undertook in 1978 a demonstration of Exxon Research and Engineering Company's patented Thermal DeNOx process. In this process, ammonia is injected into the boiler flue gas where the gas temperature is between 1600 deg F and 2200 deg F. At these temperatures, the ammonia reacts with the NOx to form nitrogen and water.

In the Department's demonstration, a full-scale Thermal DeNOx System was installed on Haynes Generating Station, Unit 4, which is a 235 MWe oil- and gas-fired unit. The system was started up in May 1982.

The Thermal DeNOx System uses a piping grid located in the flue gas stream just downstream of the secondary superheater to inject a mixture of ammonia vapor/compressed air. The grid is subdivided into six zones with independent ammonia injection controls for each zone.

A one-year test program on both fuel oil and gas is planned. Initial testing at full load on fuel oil has shown NOx reductions between 40 and 50 percent with ammonia breakthrough less than 65 ppm.

INTRODUCTION

In 1978, the Los Angeles Department of Water and Power (LADWP) undertook a demonstration of Exxon Research and Engineering Company's (ER&E) patented Thermal DeNOx process. The purpose of the demonstration was to acquire more information for pending regulatory proceedings, to analyze costs, and to test the reliability of the new technology. Thermal DeNOx is a selective noncatalytic reduction process that reduces the emission of oxides of nitrogen (NOx) from stationary combustion sources. In this process, ammonia (NH_3)

is injected into the boiler flue gas stream where the gas temperature is between 1600 deg F and 2200 deg F. At these temperatures, NH_3 reacts with NOx to form nitrogen and water.

LADWP's demonstration is the first full-scale test of the Thermal DeNOx process on a utility boiler in the United States. For this project, a full-scale system was installed on LADWP's Haynes Generating Station, Unit 4, located in Long Beach, California. Haynes Unit 4 is a 235 MWe oil- and gas-fired unit with a Babcock & Wilcox (B&W) boiler.

This paper reviews the process chemistry and describes the process flow diagram and the required equipment. In addition, the project organization, cost, and schedule are discussed.

The Haynes Unit 4 Thermal DeNOx System commenced operation in May 1982. A one-year test program on both fuel oil and gas is now in progress. Preliminary results of the test program are presented in this paper.

BASIC PROCESS CHEMISTRY

Essentially, Thermal DeNOx is a noncatalytic process based upon the selective reaction between NH_3 and the NOx in the hot flue gas. This reaction is dependent upon temperature and NH_3 residence time. The following two equations describe the generalized reactions for the Haynes Unit 4 demonstration:

$$NOx + NH_3 + O_2 + H_2O \longrightarrow N_2 + H_2O \quad (1)$$

$$NH_3 + O_2 + H_2O \longrightarrow NOx + H_2O \quad (2)$$

The NOx reduction shown in Equation 1 dominates over the range of temperature from 1600 deg F to 2200 deg F. Above 2200 deg F, the NOx production reaction shown in Equation 2 starts to dominate and the injection of NH_3 is counterproductive. Below 1600 deg F, the rate of both reactions becomes very low and the NOx reduction diminishes.

The NOx reduction is also dependent on the molecular ratio between NH_3 and initial NOx. As the NH_3 injection flow rate is increased, NOx reduction, shown in Equation 1, increases. However, the selective reactions do not continue to completion because of the short residence time at the required reaction temperature; therefore, the Thermal DeNOx process results in unreacted NH_3 being released from the boiler with the flue gas. This unreacted NH_3 is called NH_3 breakthrough and can be measured in the stack.

When using fuel oil to fire the boiler, the resultant flue gas contains small amounts of sulfur trioxide (SO_3). As the flue gas cools, some of the unreacted NH_3 combines with the SO_3 and water vapor (H_2O) to form ammonium sulfate [$(NH_4)_2SO_4$] and ammonium bisulfate (NH_4HSO_4).

PROCESS FLOW DIAGRAM

A simplified process flow diagram for the Haynes Unit 4 Thermal DeNOx System is shown in Figure 1.

The process equipment consists of the following three systems:

- NH_3 Supply System
- Air Supply System
- Injection Grid System

The NH_3 supply system includes a storage tank (containing anhydrous NH_3), two vaporizers, two superheaters, and an NH_3 flow control and metering station. The vapor pressure from the anhydrous NH_3 in the storage tank is used as the driving force to provide the flow of NH_3. During cold weather, the vaporizers add heat to maintain storage tank pressure. Condensation and/or freezing in the NH_3 supply is avoided by using a superheater to maintain the NH_3 temperature above 90 deg F. A control and metering station regulates both the pressure and flow rate of NH_3.

Before entering the injection grid, NH_3 is mixed with a compressed air stream from the air supply system. The air supply provides a dual function of cooling the injection grid and injecting the NH_3 into the boiler. The system consists of centrifugal air compressors and air heat exchangers that cool the compressor air to slow down disassociation of the NH_3 during injection.

The NH_3 and compressed air are distributed into the flue gas by the injection grid, which is a piping system located in the boiler flue gas stream just downstream of the secondary superheater (Figure 2). The injection grid consists of six zones, and the NH_3 injection rate can be individually controlled to each zone.

FACILITY DESCRIPTION

Haynes Unit 4 is a natural gas- and low sulfur fuel-oil-fired boiler manufactured by B&W and rated at 235 MWe. Unit 4 boiler has a single burner cavity and radiant heating section with the convection passes separated by a division wall and dual stacks. The back passes, which are located upstream of the air preheaters, are not divided; however, there are openings in the division wall for maintenance purposes. These openings allow limited mixing between the flue gases from the convection passes.

Table 1 shows the basic data for the Haynes Unit 4 boiler.

The existing NOx controls on Haynes Unit 4 include the following:

1. Off-Stoichiometric Firing - The burner firing pattern is varied by removing the flow of fuel to selected burners while still allowing the air to flow through the burner.

2. NOx Ports - These ports are open when firing gas and closed when firing oil. There are no intermediate positions.

3. Flue Gas Recirculation - The flue gas is recirculated into the bottom of the boiler below the burners. Though designed for use as a steam temperature control system, this system provides a minor amount of NOx reduction at the expense of boiler efficiency.

The Thermal DeNOx System equipment was erected adjacent to the boiler in an area approximately 120' x 80'. The arrangement of the DeNOx equipment is shown in Figure 3. Figure 4 is an aerial view of the NH_3 and air supply equipment.

The DeNOx retrofit uses a number of redundant systems to provide for increased system reliability. Above minimum unit load, the injection grid requires cooling by the compressed air. Three air compressors are provided; two are needed for the Thermal DeNOx process operation and one for standby. Dual NH_3 system equipment is provided for reliability.

The Haynes Unit 4 has an existing emission and efficiency monitoring system supplied by KVB that measures NOx, CO, excess O_2 and unit load. An 18-point sampling grid located upstream of the air preheaters allows measurement of the emissions at a matrix of locations.

SYSTEM COMPONENTS

The following is a description of each of the system's major components.

Ammonia Storage Tank (Figure 5)

The NH_3 storage tank is a 30,000-gallon, uninsulated carbon steel pressure vessel with a design pressure rating of 265 psig. The storage tank holds a minimum of 25,500 gallons of anhydrous NH_3. The operating pressure ranges between 50 and 150 psig.

NH_3 vapor pressure in the storage tank is the driving force for the NH_3 injection. The required NH_3 is supplied from the vapor space in the top of the tank. Excess flow and emergency shutoff valves are provided on the tank for safety.

Ammonia Vaporizers (Figure 6)

Two NH_3 vaporizers are provided. One is required for cool weather operation and one is a spare. Each is a carbon steel pressure vessel with a capacity of about 140 gallons. Both are equipped with an electrical immersion heater rated at 70 kW. The operational vaporizer is automatically turned on when the tank pressure falls below 50 psig. Both vaporizers are manifolded together and are fed by a common liquid NH_3 line. The heated NH_3 vapor flows through a common return line to the top of the NH_3 storage tank.

Superheaters (Figure 7)

Two superheaters are provided. One is required for operation and one is a spare. Each superheater consists of a 4 kW heater in a carbon steel vessel. They are located above the vaporizers between the storage tank and NH_3 flow control station at an elevation above the top of the tank. The superheater raises the NH_3 temperature to 90 deg F to eliminate condensation and/or freezing downstream of the pressure control valve.

Air Compressors (Figure 8)

Three identical 600-hp, single-stage centrifugal air compressors are used for grid cooling and NH_3 distribution. Each air compressor is capable of discharging 4,000 scfm of air at 25 psig. Two compressors are required during normal unit operation, and the third is a spare.

Air-Cooled Heat Exchangers (Figure 9)

Each air compressor is provided with an air-cooled heat exchanger containing two cooling coils to cool the compressor discharge air and compressor lube oil. The heat exchangers are forced-draft, finned-tube exchangers equipped with carbon steel tubesheets and box headers.

Ammonia Injection Grid

The injection grid is a piping grid divided into six individual zones connected to a common compressed air header. The grid is located downstream of the secondary superheater. Detailed design of the grid is considered proprietary by ER&E.

Ammonia Control Station (Figure 10)

A common pressure control station is provided with individual NH_3 flow control valves and flow measurement instrumentation for each grid zone.

Process Control

The process control is designed for automatic operation with the capability for NH_3/NOx optimization. The process control consists of a microprocessor and a programmable controller. ER&E's specifications required NH_3 stack monitors for optimization. However, based on a survey of available instruments, no reliable commercial NH_3 stack monitor was identified and this measurement was not included. Therefore, NH_3 breakthrough is measured by obtaining grab samples during the performance testing.

Other Equipment

In addition to the major process equipment, an NH_3 loading station, NH_3 area monitors, and instrument air dryers were required.

PROJECT ORGANIZATION

To accomplish this demonstration project, the LADWP obtained a process license from ER&E and contracted with them to provide the process design basis and injection grid design specifications.

LADWP contracted with KVB, Inc., of Irvine, California, for architectural and engineering services. The construction activities were performed by LADWP's construction organization except for the injection grid that was installed by B&W Construction Company.

The testing program is being conducted by KVB and LADWP personnel.

PROJECT COST AND CONSTRUCTION SCHEDULE

The Thermal DeNOx project was designed and constructed over a period of 40 months at a cost of $9,500,000 (actual dollars). Table 2 shows the project schedule from conceptual engineering through system start-up.

Table 3 shows the Thermal DeNOx project capital costs distribution. The costs are presented as actual dollars expended and are not corrected to current dollars.

PERFORMANCE TESTING

The Thermal DeNOx System was completed in May 1982. A one-year test program on both fuel oil and gas is now in progress. KVB has been contracted to conduct the performance testing.

During the performance testing, NOx emissions are measured by the emissions and efficiency monitoring system that was supplied by KVB and previously installed on Unit 4. NH_3 breakthrough is obtained on selected tests using grab samples from each stack and wet chemical analysis.

The performance test program is designed to satisfy the following requirements:

1. Determine if the process can meet ER&E's guaranteed 46-percent reduction of nitrogen oxides at full load using fuel oil with the NH_3 breakthrough below 65 ppm.
2. Satisfy the test requirements specified in the construction permit issued by the South Coast Air Quality Management District (SCAQMD).
3. Determine the system's operating characteristics at various loads with selected NH_3 injection rates.
4. Verify the automatic operation of the system during load changes.
5. Determine any long-term effects on the unit.
6. Determine long-term process efficiency.

Although the test data has not been completely analyzed at this time, the following discussion summarizes the initial results.

FUEL OIL PERFORMANCE

The tests for the guarantee showed that the system could achieve NOx emission reductions greater than ER&E's guarantee of 46 percent at full load. However, additional tests at full load showed a wide scatter of data for NOx reduction. Figure 11 shows the scatter of data for NOx reduction versus unit load.

Preliminary analysis of the test data reveals that the NOx reduction is complex and dependent upon several different factors at any given load. The main factor influencing NOx reduction is the molecular ratio of NH_3 to initial NOx. However, the percentage NOx reduction also appears to be affected by:

1. Initial NOx level in the flue gas - As the initial NOx level decreases, the rate of NOx reduction also decreases.

2. Increased excess oxygen - As the excess oxygen increases, the rate of NOx reduction decreases.

3. Distribution of NH_3 in grid - Because of the temperature variation across the boiler, the distribution of NH_3 between the six injection grid zones can alter the rate of NOx reduction.

The majority of tests indicate NOx reductions range between 40 and 50 percent at full load. Tests showing NOx reductions above 50 percent were for high initial NOx emissions.

The flue gas temperatures required to support the NOx reduction reaction vary with the boiler load. At 85- to 100-percent load, the flue gas temperatures are in the ideal range and the DeNOx system shows good performance of 40- to 50-percent reduction. As the load decreases, the temperatures decrease and the DeNOx system becomes less effective. At 60-percent load (140 MWe), the NOx reduction drops to approximately 25 percent, and at 50-percent load (115 MWe), the NOx reduction is below 20 percent.

GAS PERFORMANCE TEST

As shown in Figure 12, the gas tests also had some scatter of the data for a given load. The DeNOx system has a lower overall rate of NOx reduction with gas than with fuel oil. However, the NOx reduction efficiency is higher with gas and appears to be effective over a wider load range (e.g., 75-percent to 100-percent load).

NH_3 BREAKTHROUGH

The amount of NH_3 breakthrough is difficult to measure because a reliable commerical continuous monitor is currently unavailable. Therefore, the breakthrough was determined by obtaining grab samples from both stacks on selected test runs.

Figure 13 is a plot of the NH_3 breakthrough versus NOx reduction for fuel oil at unit load above 210 MWe, and Figure 14 is a similar plot for natural gas at unit load above 200 MWe. This is preliminary test data; additional tests are required before a final analysis can be completed.

INJECTION GRID DAMAGE AND SCALING

Inspection of the injection grid after approximately six months of operation revealed one length of grid pipe was broken off at the connection to the distribution header. Additionally, numerous grid supports have failed or have been distorted.

A detailed investigation is being conducted to determine the cause of the grid damage and method of repair.

In addition to the above grid damage, a brown scale is being deposited on the grid. A few nozzles have been plugged. Additional operation is needed to determine the impact of grid scaling on the grid's service life.

CONCLUSION

The Thermal DeNOx System appears to be capable of reducing NOx emissions between 40 and 50 percent at or near full load on fuel oil or gas. However, additional long-term testing is needed to determine the full potential of the system.

The DeNOx system is temperature-dependent and results vary for each application. Additional analysis and testing are required before conclusive results can be obtained.

The injection grid is located in a very harsh environment. The service life of the grid is questionable because of the damage observed after only six months of operation.

The injection grid cooling requirement increases the system's installed costs and creates an additional work load for operations and maintenance personnel. Also, because loss of grid cooling during operation requires a load reduction to prevent grid damage, the injection grid has a potential adverse impact on the unit's availability.

REFERENCES

1. Hurst, B. E., Schleckser, Jr., C. E., Exxon Research and Engineering Co., Applicability of Thermal DeNOx to Large Industrial Boilers. In: Proceedings of EPA-EPRI Joint Symposium on Stationary Combustion NOx Control, Denver, Colorado, 1980. 31 pp.

2. Hurst, B. E., Exxon Thermal DeNOx Process for Utility Boiler Applications. In: Proceedings of Joint ASME/IEEE Power Generation Conference, St. Louis, Missouri, 1981. 12 pp.

3. Exxon Research and Engineering Company, Improved Exxon Thermal DeNOx Process. Florham Park, New Jersey, undated. 4 pp.

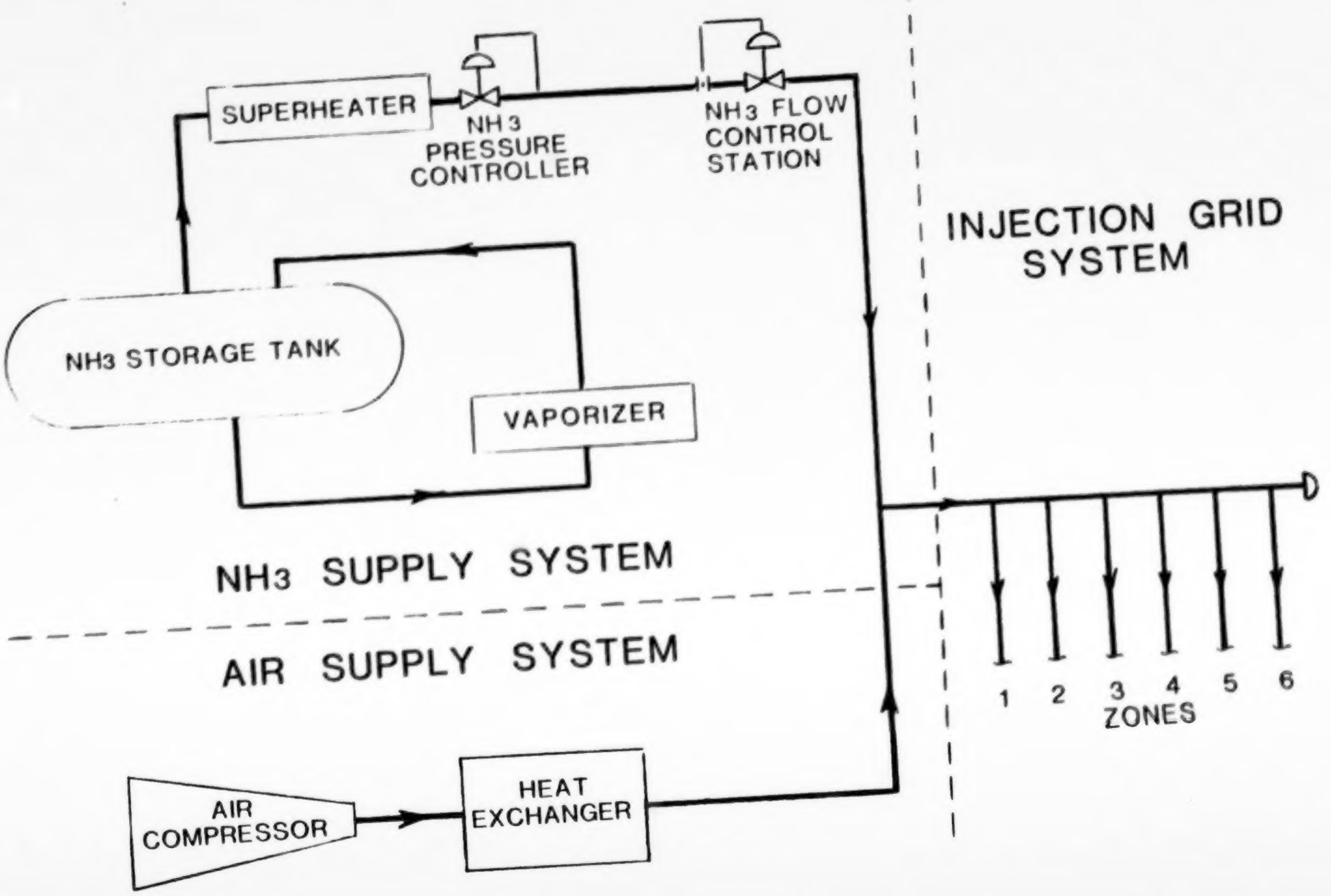

SUPERHEATER
NH3 PRESSURE CONTROLLER
NH3 FLOW CONTROL STATION
INJECTION GRID SYSTEM
NH3 STORAGE TANK
VAPORIZER
NH3 SUPPLY SYSTEM
AIR SUPPLY SYSTEM
1 2 3 4 5 6
ZONES
AIR COMPRESSOR
HEAT EXCHANGER

Figure 1. Thermal DeNOx System - Process Flow Diagram.

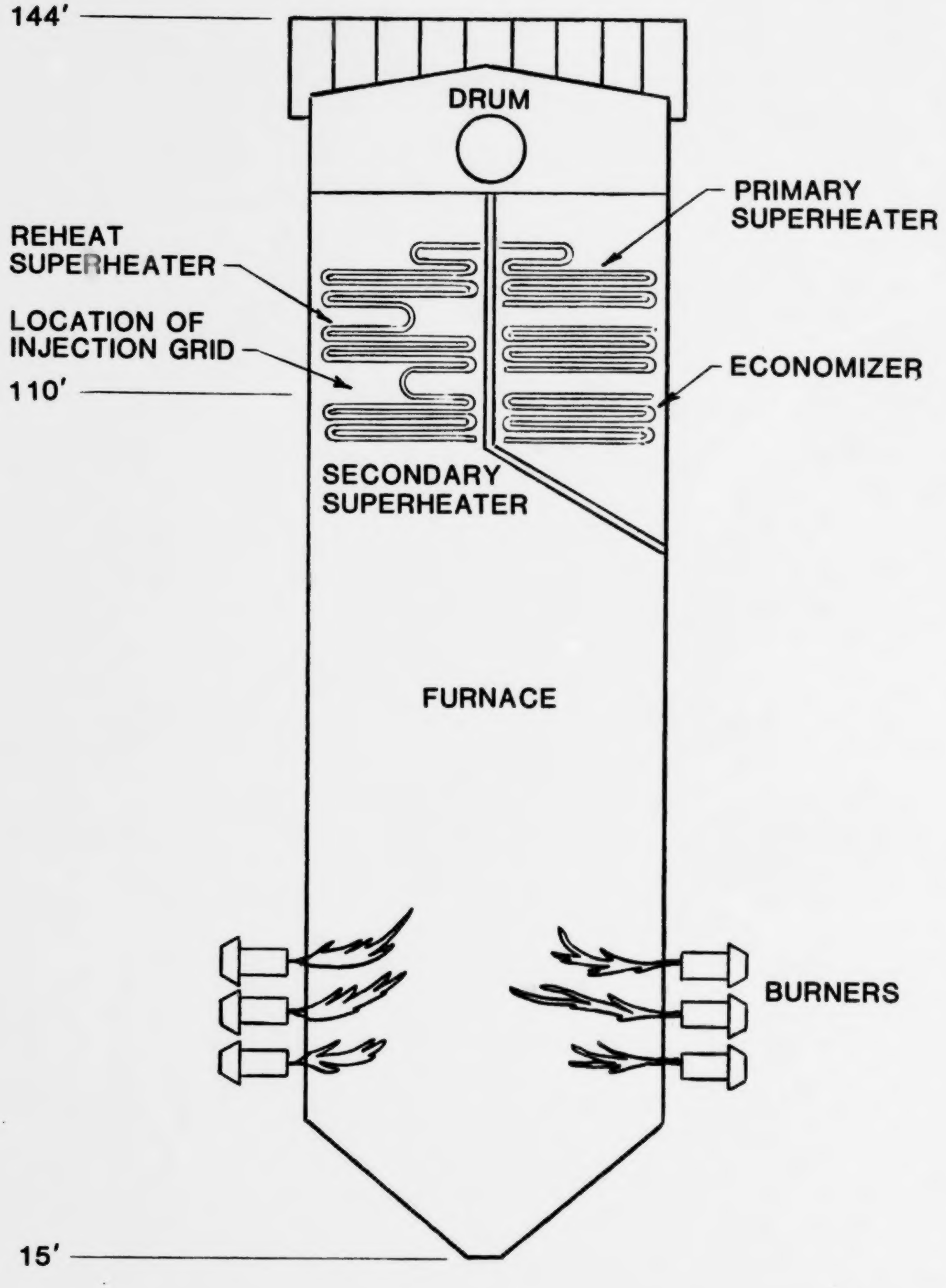
144'
DRUM
PRIMARY SUPERHEATER
REHEAT SUPERHEATER
LOCATION OF INJECTION GRID
110'
ECONOMIZER
SECONDARY SUPERHEATER
FURNACE
BURNERS
15'

Figure 2. Thermal DeNOx System - Location of Injection Grid.

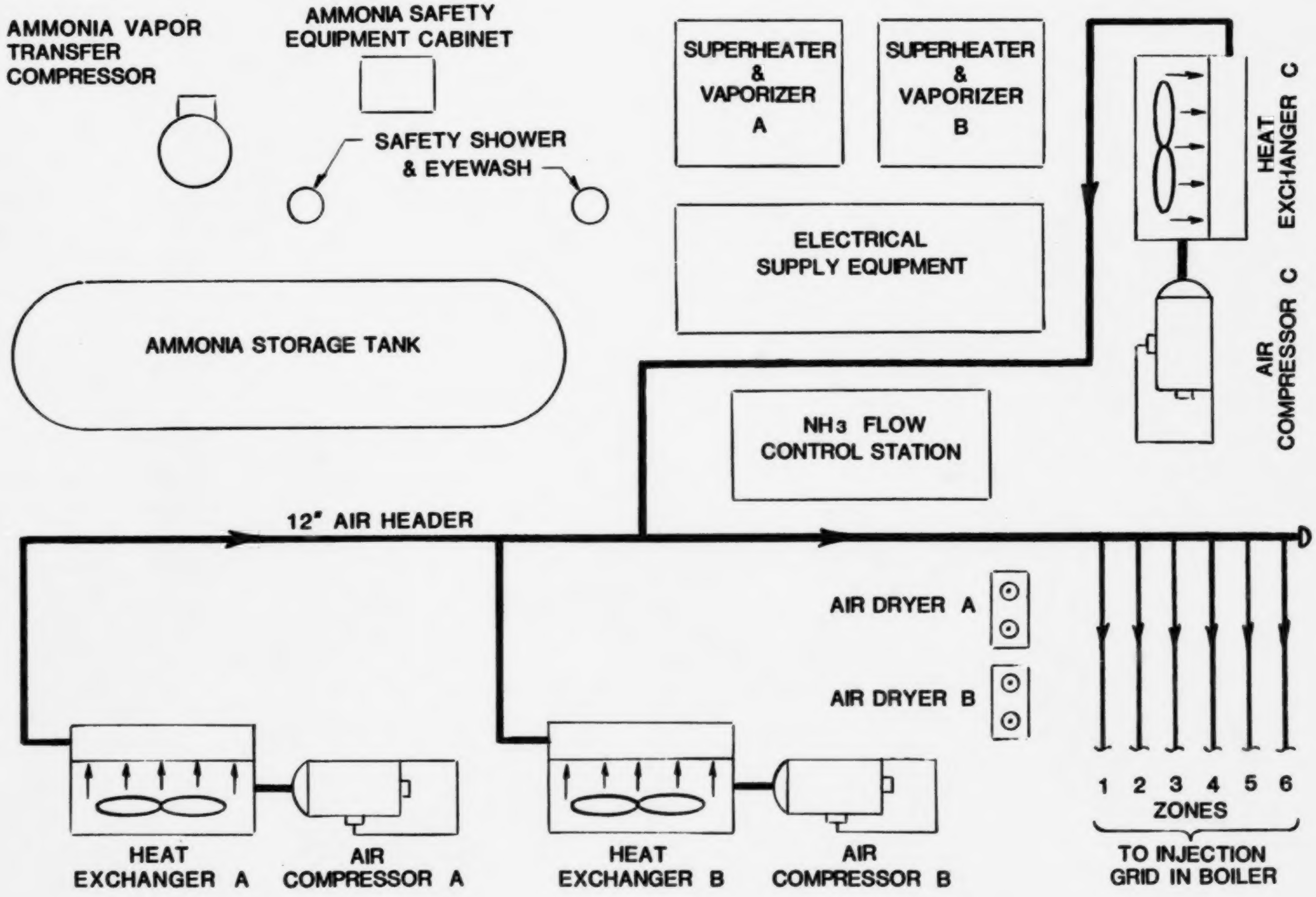
AMMONIA VAPOR TRANSFER COMPRESSOR
AMMONIA SAFETY EQUIPMENT CABINET
SAFETY SHOWER & EYEWASH
SUPERHEATER & VAPORIZER A
SUPERHEATER & VAPORIZER B
HEAT EXCHANGER C
ELECTRICAL SUPPLY EQUIPMENT
AIR COMPRESSOR C
AMMONIA STORAGE TANK
NH3 FLOW CONTROL STATION
12" AIR HEADER
AIR DRYER A
AIR DRYER B
HEAT EXCHANGER A
AIR COMPRESSOR A
HEAT EXCHANGER B
AIR COMPRESSOR B
1 2 3 4 5 6
ZONES
TO INJECTION GRID IN BOILER

Figure 3. Thermal DeNOx System - Equipment Arrangement.

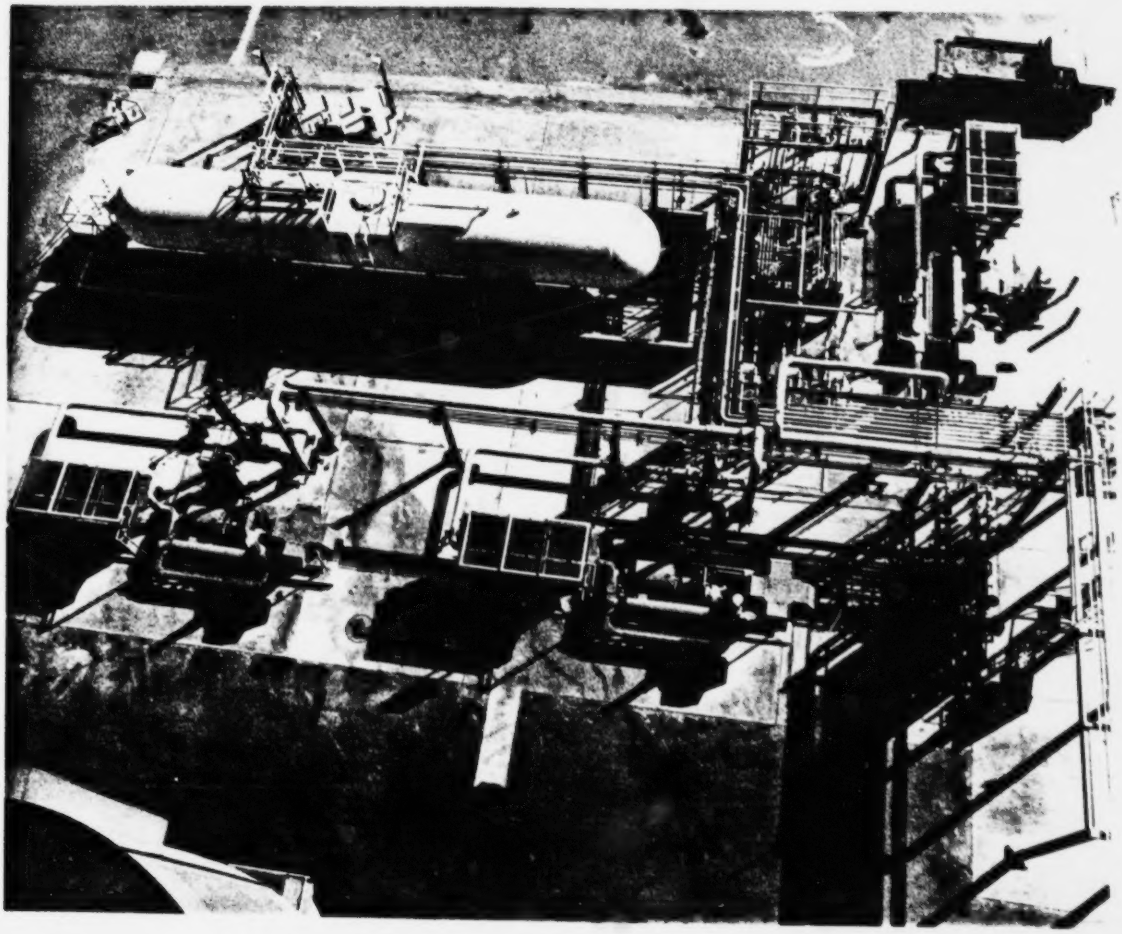

Figure 4. Thermal DeNOx System - Aerial View of the NH_3 and Air Supply Equipment.

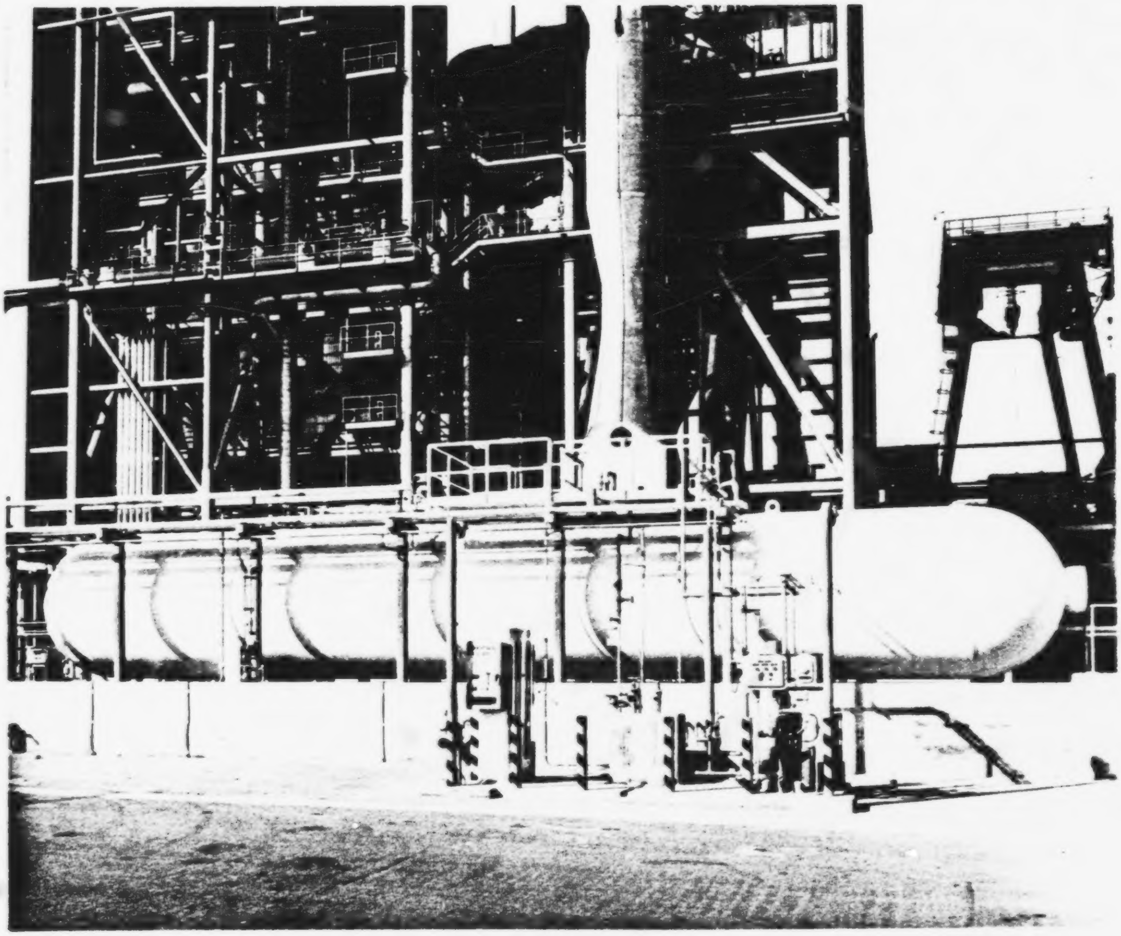

Figure 5. Thermal DeNOx System - Ammonia (NH_3) Storage Tank.

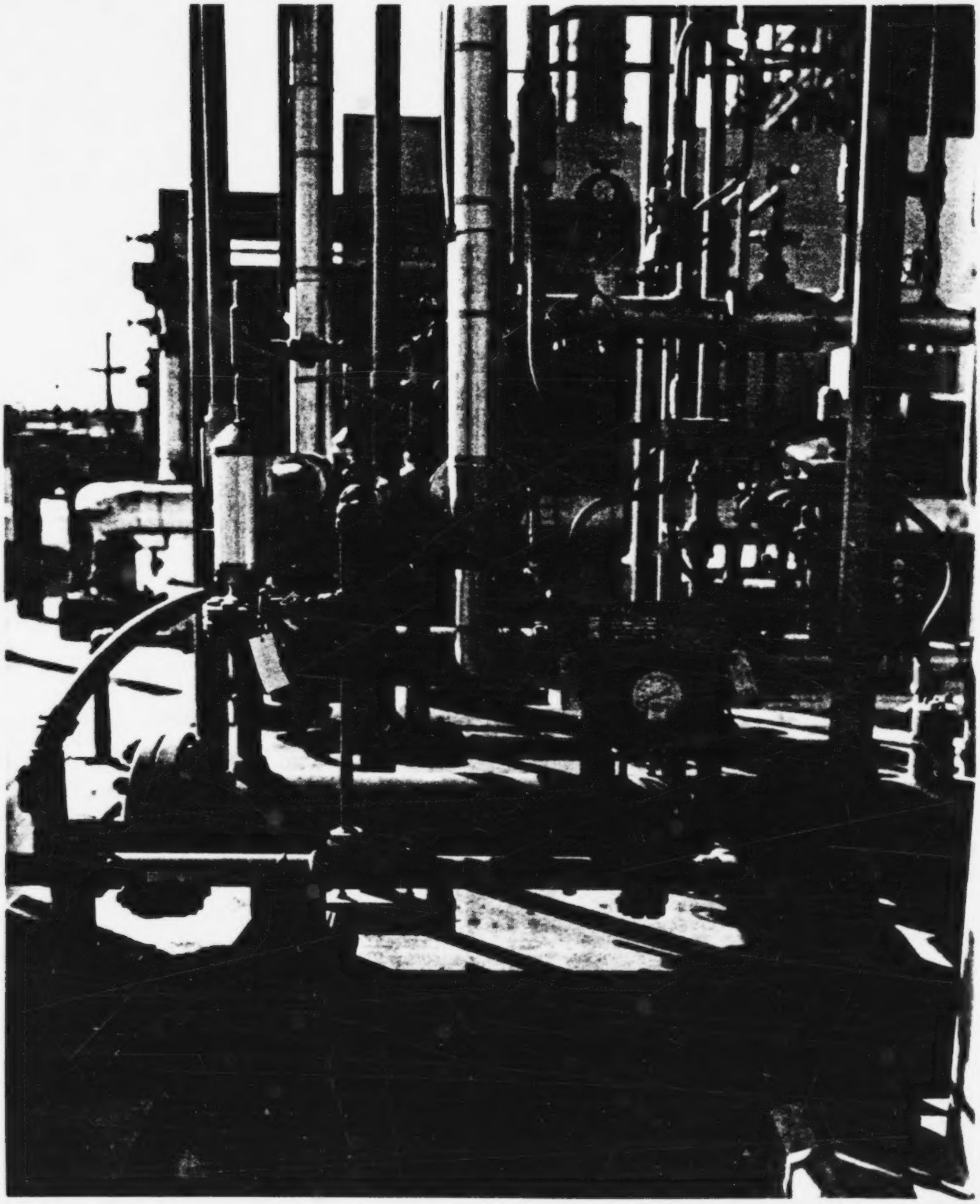

Figure 6. Thermal DeNOx System - Ammonia (NH_3) Vaporizer.

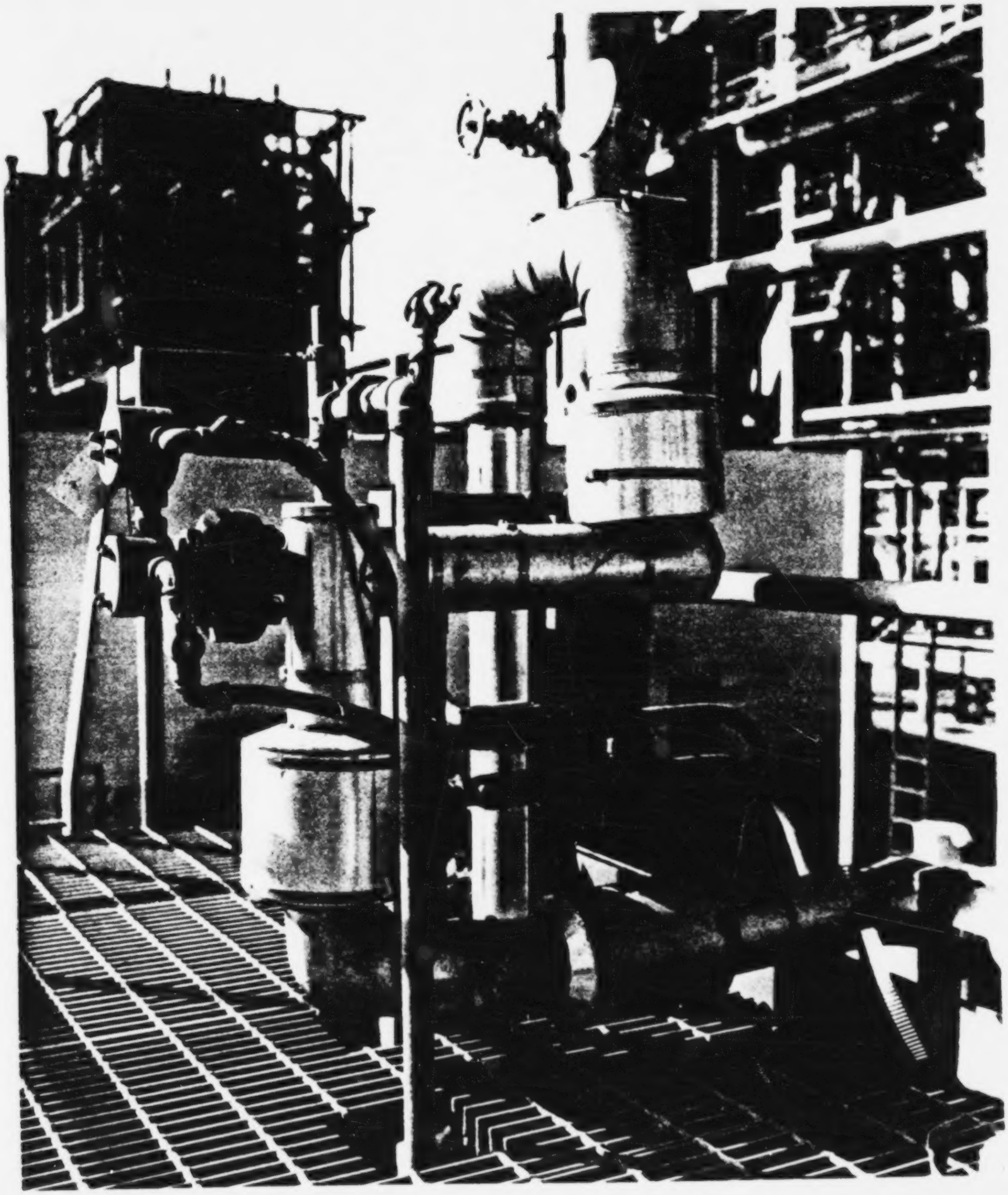

Figure 7. Thermal DeNOx System - Superheater.

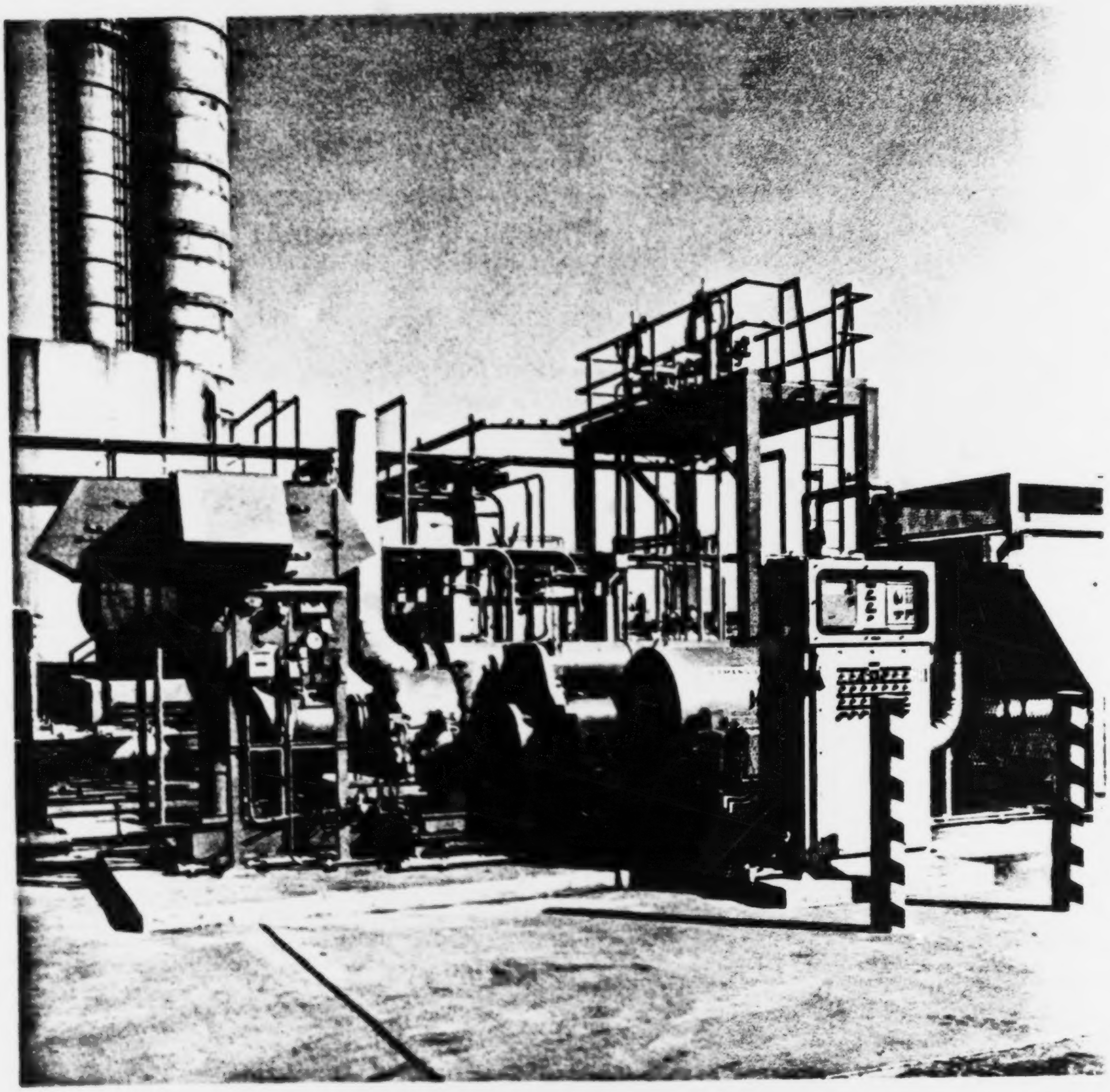

Figure 8. Thermal DeNOx System - Air Compressor.

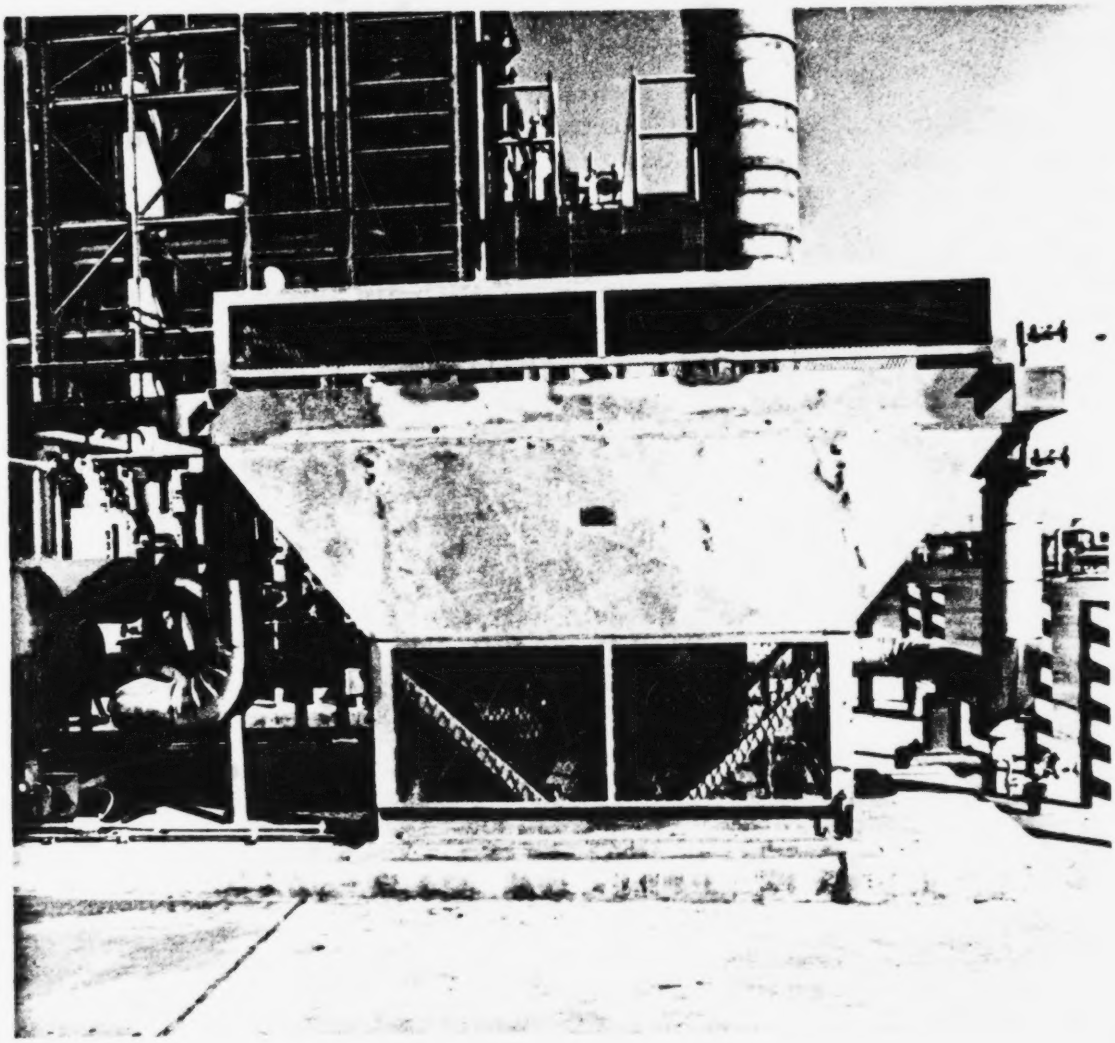

Figure 9. Thermal DeNOx System - Air-Cooled Heat Exchanger.

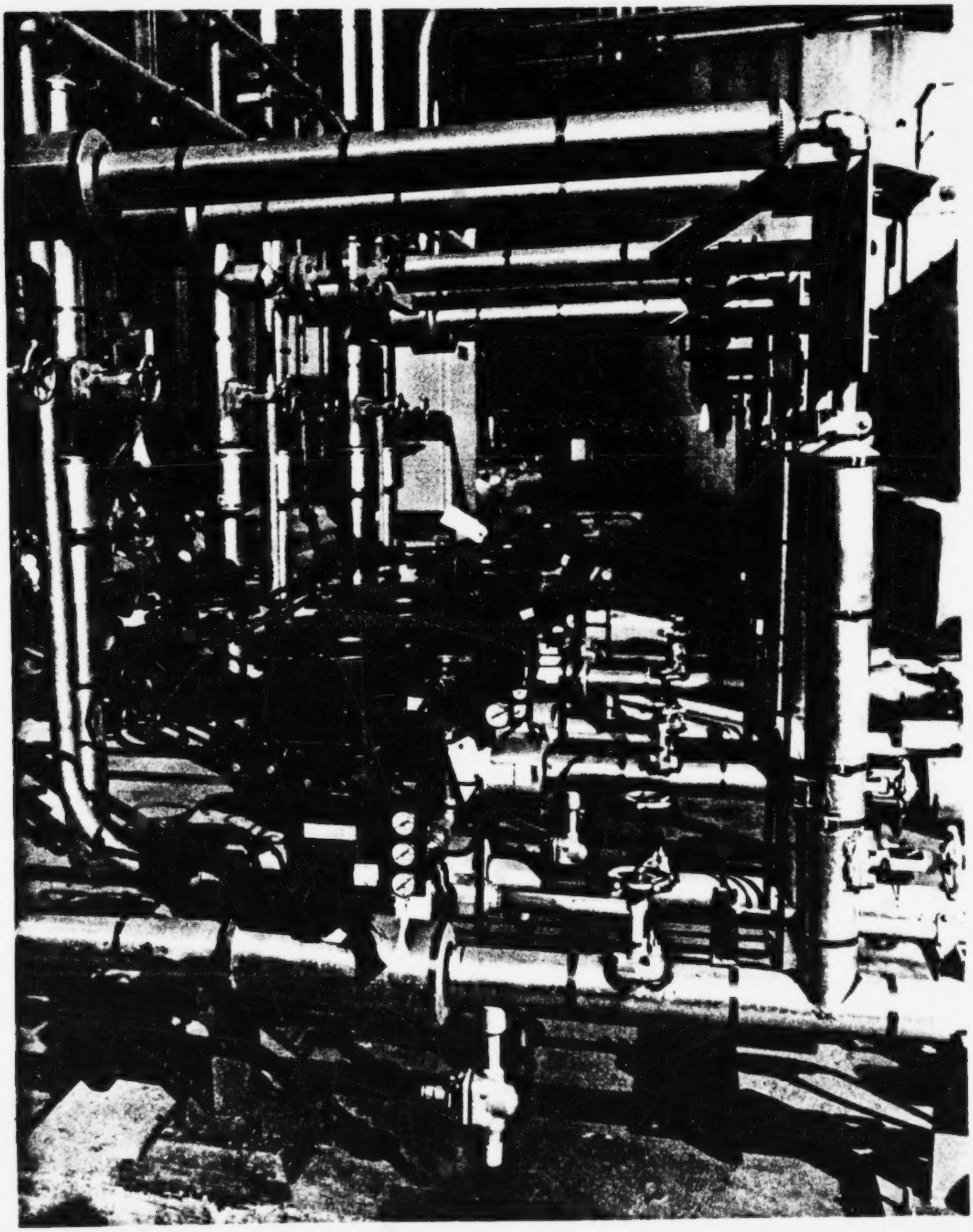

Figure 10. Thermal DeNOx System - Ammonia Control Station.

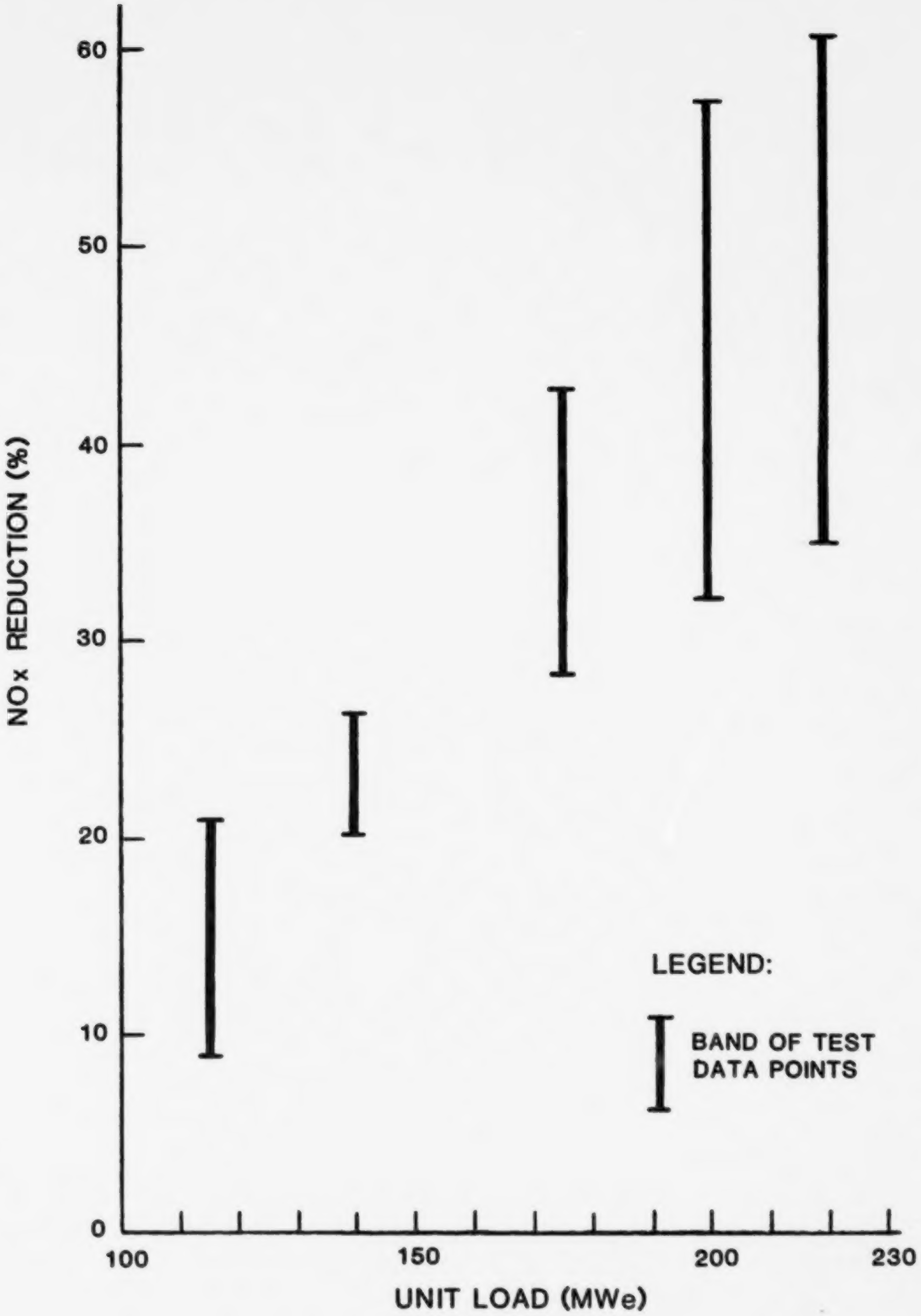

Figure 11. Thermal DeNOx Performance for Fuel Oil.

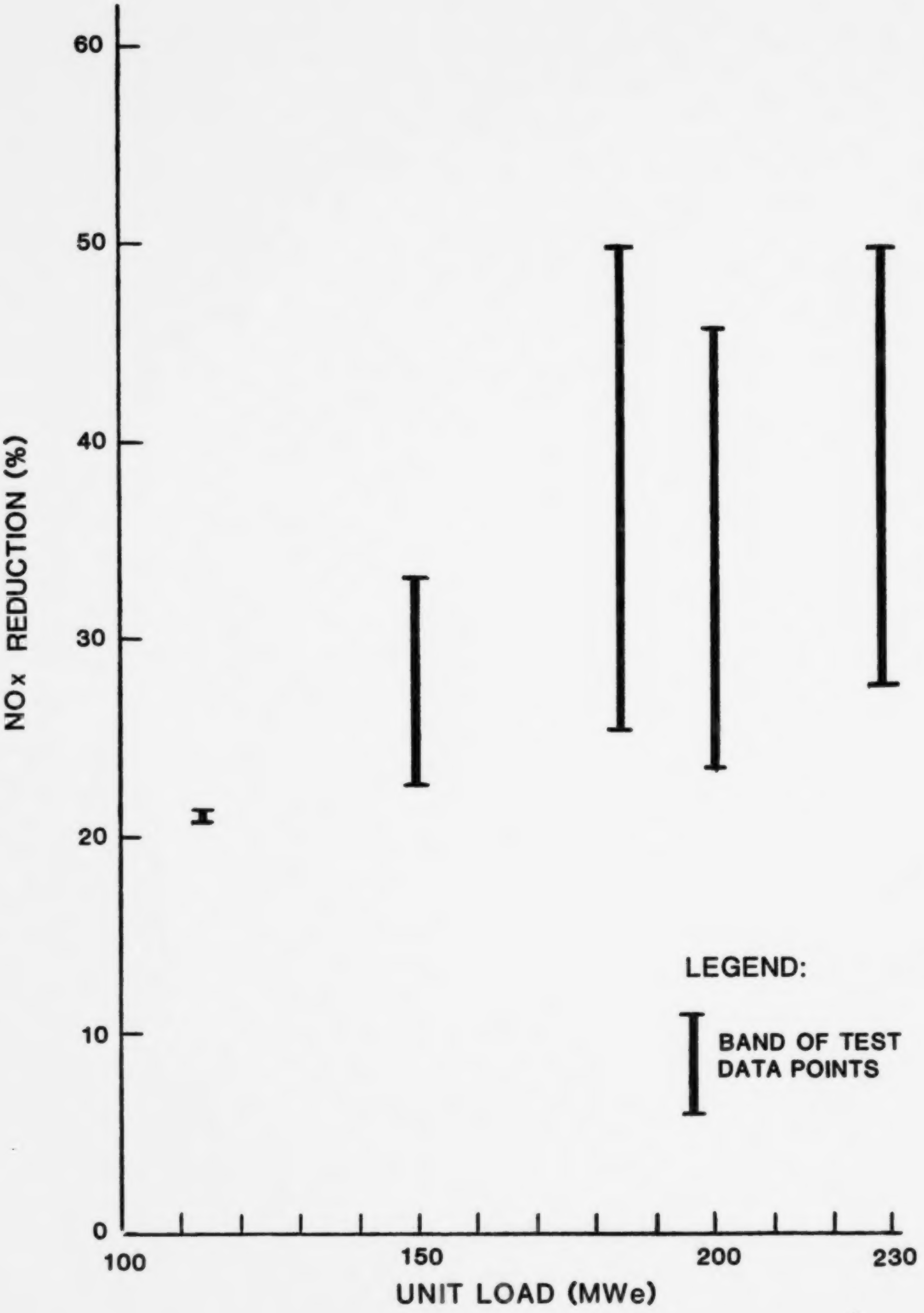

Figure 12. Thermal DeNOx Performance for Gas.

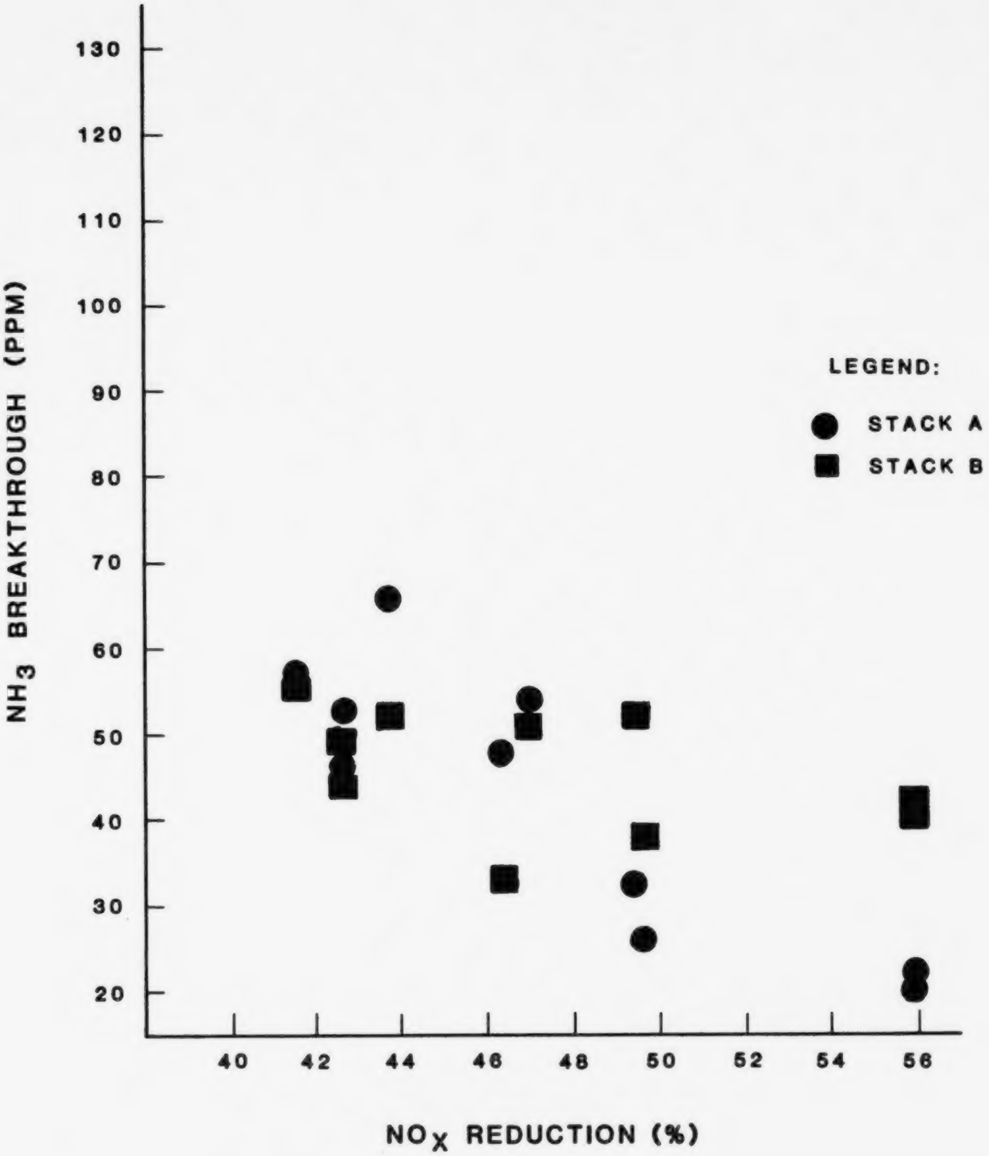

Figure 13. Ammonia (NH_3) Breakthrough for Oil Above 210 MWe.

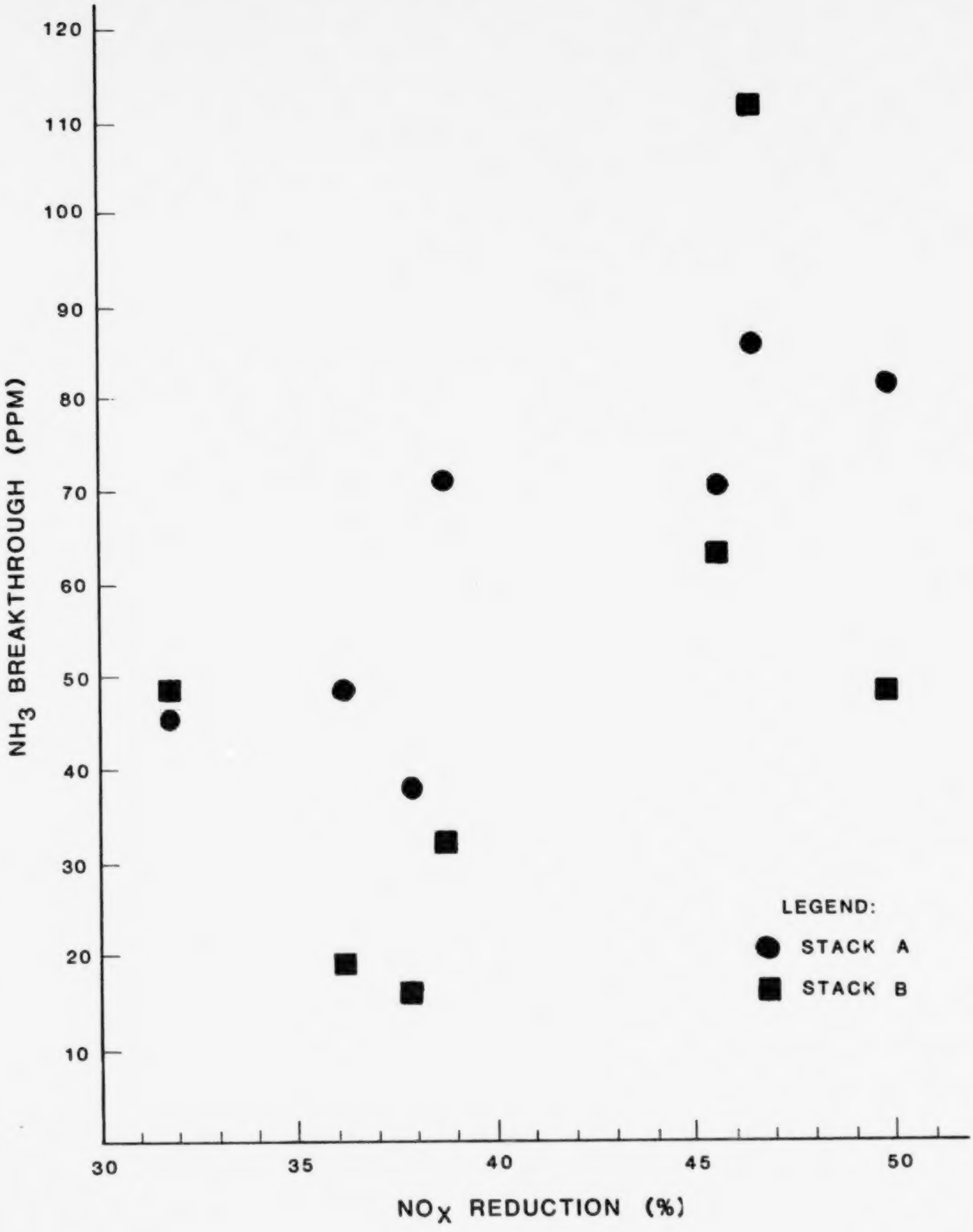

Figure 14. Ammonia (NH_3) Breakthrough for Gas Above 200 MWe.

TABLE 1. HAYNES UNIT 4 DATA*

Electrical Output	235 MWe
Boiler Type	Subcritical - Single Reheat
Steam Flow rate	1,575,000 LB/HR
Design Pressure	2325 psi
Superheater Outlet Pressure	2050 psi
High-Pressure Steam Temperature	1000 deg F
Reheat Steam Temperature	1000 deg F
Flue Gas Flow Rate	2,000,000 LB/HR at 3-4 percent O_2 dry
Flue Gas Temperature (in NH_3 Injection Zone)	1620-1900 deg F
NOx Concentration	190-220 PPMC at 3-4 percent O_2 dry
SO_3 Concentration	0.3-2.3 PPM at 3 percent O_2 dry
Particulate Concentration	0.0114 GR/DSCF
N_2O Concentration	43 PPM at 3-4 percent O_2 dry
SO_2 Concentration	125-150 PPM at 3 percent O_2

*All data are based on oil firing with full load.

TABLE 2: THERMAL DeNOx PROJECT SCHEDULE

Conceptual Engineering	January 1979
Boiler Temperature Profile Test	January 1979
Contract Executed	October 1979
Engineering Start	October 1979
Construction Start	January 1981
Air Compressor Start-Up	January 1982
Boiler Shutdown and Grid Installation	December 21, 1982 February 8, 1982
End of Construction	May 1982
NH_3 System Start-Up	May 1982

TABLE 3: THERMAL DeNOx PROJECT CAPITAL COSTS ($1,000)

Exxon License Fee	$ 400
Owner's Cost and Engineering	1,400
Architectural and Engineering Services	1,900
Material and Equipment	2,000
Construction	3,800
Total	$9,500

Installed Cost = $40/kW

CURRENT STATUS OF DRY NO_x-SO_x EMISSION CONTROL PROCESSES

By:

S. M. Dalton
Electric Power Research Institute
3412 Hillview Avenue
Palo Alto, California 94303

ABSTRACT

Combined NO_x-SO_x control techniques using a variety of complex chemical flue gas treatment processes have been proposed by a number of manufacturers. The wet chemical NO_x-SO_x processes are generally not economically competitive and development has shifted to dry NO_x-SO_x techniques. Three dry techniques that are currently being widely pursued as alternatives to wet FGD/selective catalytic reduction are discussed in some detail in this paper: the copper oxide processes, the carbon adsorption processes, and the electron-beam (E-beam) irradiation processes. There are at least five versions of the copper oxide process, eight versions of the carbon adsorption process with NO_x-SO_x reduction and two versions of the E-beam concept. All of these processes appear capable of achieving over 90% SO_2 removal and greater than 70% NO_x removal, although the power plant economic and operational impacts are not fully understood. None of the processes are in service commercially, though active development is underway in the U.S., Japan, and Germany.

NO_x-SO_x PROCESS STATUS

A number of simultaneous NO_x-SO_x removal processes have been developed in the past two decades. Early work included wet and dry scrubbing processes based on a variety of chemical reactions and unit operations. Today, dry combined processes that remove SO_x and NO_x simultaneously are being developed to compete with SO_x and NO_x removal done as independent steps. Three of the most advanced types of systems for combined dry SO_x-NO_x removal are copper oxide, carbon adsorption and electron-beam irradiation. This paper will discuss the status of systems using these three principals and will discuss one example of each system type in more detail. The developmental status, process description, performance data and relative costs will be summarized for each process example.

HISTORY OF NO_x-SO_x

Much of the early work in combined NO_x-SO_x processes evolved out of the initial work in wet scrubbing. Many early wet scrubbers for SO_2 were modified to try to sorb NO_x-usually as equal molar proportions of NO and NO_2. Unfortunately for wet scrubbers, the NO_x emissions from utility boilers are predominantly NO and in order to absorb have to be oxidized to reach equal molar proportions of NO and NO_2. This requires ozone, EDTA, $FeSO_4$, or other means to allow adsorption or to oxidize the NO. In addition, the co-absorption of NO and NO_2 is a slow process and required large absorbers with high pressure drop and many stages. When this was added to the complex chemistry of the process requiring many steps, the results were processes that could not compete economically with independent SO_x and NO_x control steps (such as conventional SO_x scrubbing plus catalytic NO_x removal).

A few systems were not limited by the chemistry and mass transfer limitations of wet scrubbers. All three concepts that are discussed in more detail in this paper do not suffer from this limitation. The dry copper oxide and carbon adsorption concepts have been proposed for NO_x and SO_x control in utilities for over ten years, and recent R&D work is bringing them closer to commercialization. The electron beam concept has been under development for a similar amount of time, though the proposed use on coal-fired utility boilers is recent.

GENERIC DESCRIPTION OF NO_x-SO_x CONCEPTS

Copper Oxide

The first generic process is copper oxide. Five systems are based on this generic process. The copper oxide processes depends on formation of copper sulfate to remove SO_2 followed by regeneration of sulfur (using reducing gas) and subsequent re-oxidation of the copper to copper oxide which is the active sorbent form. NO_x is catalytically reduced to N_2. The Shell flue gas treatment process (SFGT) and other several processes are based on the use of copper oxide as shown in Table 1, Reference 1. These include the Nippon Oil Company process (Japanese patent 7729469, March 5, 1977) and the U.S. Bureau of Mines Process, both of which use chemistry similar to the SFGT copper oxide process but are not as well developed. The Exxon Research Engineering processes uses a bed of CuO and Al_2O_3 to form sulfates. NO_x is reduced to N_2 in the presence of copper sulfate and ammonia. Though two U.S. Patents have been issued (4,001,376 and 4,039,478) Exxon has discontinued further development of this process.[1] The Houdry Chemicals Division of Air Products developed a fixed-bed mixture of copper and silica oxides (plus additive) that sorbed gas at 300oC (600oF) and regenerated H_2S using hydrogen. Houdry discontinued work in 1970. The Shell flue gas treatment (SFGT) process is based on copper oxide and is discussed in more detail later in this paper.

Carbon Adsorption

The second generic concept for NO_x-SO_x removal is use of carbon adsorption. At least eight carbon processes claim combined NO_x-SO_x removal as shown in Table 2. This is done via adsorption of SO_x on carbon followed by carbon cleaning (heating, washing, etc.). Carbon acts as a catalyst or has catalyst added so that ammonia addition promotes NO_x reduction to N_2. Carbon pores also catalize oxidation of SO_2 to SO_3 and react with water to form H_2SO_4 which is held in the pores until regeneration. This property allows high carbon loading with acid and reasonable system size.

The Bergbau-Forschung process received the most early attention in the U.S. primarily for SO_x control. It went through prototype testing in the U.S. at the Scholz plant of Gulf Power in the mid-1970s and at STEAG's station in Lunen, Germany in the mid-to-late 1970s. The first commercial plant is under construction in Mannhein West Germany. Most of the early work was centered around SO_x removal and only lab and pilot work has extended to NO_x removal. The process uses a moving bed adsorber with NH_3 injected upstream for NO_x removal. Hot sand is used to drive SO_2 off of the loaded carbon.

The Chemibau-Reinluft process uses a moving bed similar to the Bergbau-Forschung adsorber. The regeneration is by hot (385°C [750°F]) inert gas. Prototype testing in the 1960s has not led to commercial units.

In Japan, several manufacturers are working on carbon-type DESOX/DENOX processes. The Hitachi process adsorbs SO_2 in a dry carbon bed then washes H_2SO_4 out of the carbon with water. The dilute acid produced (10-20% H_2SO_4) is either concentrated or used to produce gypsum. Test units in Japan were from 2 MW to 150 MW on Tokyo Electric's oil-fired Goi and Kashima Stations. No data on commercial installations has been published in the U.S.

The Sumitomo process uses a moving bed adsorber similar to Bergbau-Forschung and regenerates with hot gas. SO_2 is converted to H_2SO_4 in an acid plant. Sumitomo began work in 1973 with bench work in 1974, and pilot plant work in 1976 on a 3.3 MW equivalent pilot plant. A test at the Takehara station reported results of 90-95% SO_2 removal and 30% NO_x removal at a space velocity of 500-900 hr^{-1}. Later results are not yet published. A demonstration plant with capacity to treat 300,000 Nm^3/hr will be constructed at Matsushima station in 1984(2).

The Takeda chemical process uses an adsorption step similar to the Bergbau-Forschung process and can either use washing or hot gas regeneration. Most recent tests have been done on a 33 MW equivalent plant treating gas from a sintering furnace.

The Unitika process uses fixed reactor beds instead of moving beds. The fixed beds are alternatively regenerated using hot inert gas. Most recent pilot tests have been conducted at the Union Glass Industry plant in Hirakata, Japan.

The only work done entirely in the U.S. is on the Westvaco activated carbon process. This uses a completely different mechanical design of the adsorption step--a multistage fluid bed. The regeneration step uses hydrogen to react with heated char and form H_2S and elemental sulfur at 524°C (1000°F). Pilot plant tests have been conducted on an oil-fired boiler, giving greater than 90% SO_2 removal. Though not tested, NO_x removal should be possible similar to other carbon processes. The process is not being actively commercialized.

The Mitsui-BF Dry DESOX-DENOX process is discussed in much greater detail in the section titled Mitsui-BF dry DESOX-DENOX process. It is an advanced example of the carbon adsorption dry DESOX-DENOX type systems.

Electron Beam Irradiation

The third generic concept that is receiving wide development attention is the electron beam (E-beam) irradiation concept. Two systems using electron beam technology both irradiate the gas using high energy electron "gun" accelerators to dissociate the gases to form free radicals. The two systems being developed differ in end-product, method of humidifying the gas and use of ammonia.(3) In the Avco-Ebara process, flue gas is humidified and cooled to about 79°C (200°F). The gas is irradiated in special reaction chambers by high energy electron beams in the presence of ammonia. SO_x and NO_x are then converted to ammonium sulfate and ammonium sulfate-nitrate. Particles are then collected, agglomerated and sized for eventual use as fertilizer. In the Research Cottrell process, a lime spray dryer is used to humidify the gas and remove some of the SO_x. This is followed by an E-beam chamber optimized for NO_x removal. Since no ammonia is used, the product is calcium sulfite and sulfate with some nitrates and it is not recovered. A fabric filter (or ESP) catches the spent by-product for disposal. Both systems are still at the pilot stage with a 1 $\frac{1}{2}$ MW Research Cottrell Avco-Ebara pilot being built at TVA and a 10 MW pilot being planned in Indiana. The Avco-Ebara system is discussed in detail in the section titled "Avco-Ebara Electron-Beam Process X" as an example of combined NO_x-SO_x E-beam processes.

SHELL FLUE GAS TREATMENT (SFGT) PROCESS

History and Process Description

The basic technology for the SFGT was developed by Shell Internationale Petroleum Maatschappij B.V. (SIPM) Den Haag, the Netherlands.(4) They began development in 1962. Laboratory and modeling work have been done to predict process performance. Early work was done for oil-derived flue gas. Pilot testing was done at Tampa Electric Company's Big Bend station on a 0.6 MW pilot plant using gas with and without fly ash. The gas was reheated to the proper reaction temperature. This work focused on mechanical and emission control performance. Projections of the acceptor/catalyst fouling rates and life were made. Full results of this testing are discussed in EPA's paper given at an earlier APCA meeting.

Experience on oil fuel is more extensive. A commercial system for combined NO_x-SO_x removal was installed at Showa Yokkaichi Sekiyu (SYS) refinery in Japan. The 40 MW equivalent system, installed in 1973, operates at 90% SO_2 removal and 40% NO_x reduction(1). The refinery already had reducing gas and Claus plant capability so the SFGT system was connected to those unit operations.

The SFGT process uses a fixed bed of copper oxide to sorb SO_2 from flue gas. A flow schematic is shown in Figure 1. Flue gas is passed through a set of specially designed, parallel passage, fixed-bed reactors which use a copper oxide on alumina sorbent for SO_2 removal. The reaction proceeds according to the following equation:

$$CuO(s) + SO_2(g) + 1/2O_2(g) \rightarrow CuSO_4(s) \qquad (1)$$

The reactor configuration was specifically designed to maintain catalyst stability and minimize pressure drop. A cyclical mode of operation using multiple reactors is employed. The system operates at about 385°C (750°F) in both sorption and regeneration steps.

When the majority of the copper in the reactor has been converted to copper sulfate, the flue gas is rerouted to another vessel and the spent vessel is purged in preparation for sorbent regeneration. The sorbent is regenerated by passing a dilute-reducing gas through the vessel.

Either hydrogen or methane can be used as the reducing agent. When methane is used, the regeneration reaction is:

$$CuSO_4 + 1/2CH_4(g) \rightarrow Cu(s) + SO_2(g) + 1/2CO_2(g) + H_2O(g) \qquad (2)$$

If hydrogen is used, reduction occurs by a variety of reactions:

$$CuSO_4(s) + 2H_2(g) \rightarrow Cu(s) + SO_2(g)\ 2H_2O(g) \qquad (3)$$

$$CuSO_4(s) + 4H_2(g) \rightarrow CuS(s) + 4H_2O(g) \qquad (4)$$

$$CuS_4(s) + H_2(g) \rightarrow Cu(s)\ 2H_2O(g) \qquad (5)$$

Sulfide formation is promoted by low temperature in the reactor. After regeneration, the reactor is purged and returned to flue gas service. In previous testing, cycle times of 40 to 80 minutes were measured.

There are several design options for concentrating and preparing the SO_2-regeneration gases for further processing. These options include water absorption/stripping (as shown in Figure 1), solvent adsorption, compression/condensation of water vapor, and complete liquefaction.

Conversion of the concentrated SO_2 to elemental sulfur can be accomplished by several technologies including the Allied Chemical, RESOX, BAMAG, or Claus processes. Most of these technologies also require a step to make reducing gas. Options for reducing gas include steam-methane or steam-naptha reforming and coal gasification.(1)

The CuO and $CuSO_4$ formed during oxidation and SO_2 acceptance act as catalysts for the reduction of NO_x by NH_3 addition. The acceptor is noncatalytic in the form of Cu. All reactions shown below are exothermic and raise flue gas temperature of 3°C (5°F)(4)

NO_x and NH_3 Reactions

$$6NO + 4NH_3 \rightarrow 5N_2 + 6H_2O \qquad (6)$$

$$4NO + 4NH_3 + O_2 \rightarrow 4N_2 + 6H_2O \qquad (7)$$

$$4NH_2 + 3O_2 \rightarrow 2N_2 + 6H_2O \qquad (8)$$

Shell Flue Gas Treatment Process Economics

The (SFGT) economics have been reviewed recently in a study by Stearns-Roger for EPRI.(4) The cost estimates in that report were based on mid-1978 dollars for a mid-1979 operating date. All costs in the summary cases in tables 3 and 4 were escalated to December 1982 dollars using EPRI's Technical Assessment Guide (TAG) economic premises. Table 3 shows capital cost estimates for various levels of NO_x control and Table 4 shows first year operating costs.

Process Limitations

The technical limits of the technology are:

- The process includes chemical processing steps that are more typical of a refinery--requiring additional operator training.
- Deposits in downstream ductwork and airheaters may require redesign of equipment.
- Excess moisture from tube leaks, condensation, or sootblowers can dissolve the soluble copper oxide/copper sulfate catalyst.
- Reducing gas is required necessitating reformer steps.
- Control and fire prevention methods will need special care during design and operation.
- The system is integrated with power plant heat recovery equipment and the SFGT cycle may be upset during power plant equipment malfunctions.
- Surge capacity is limited between SFGT acceptor/regeneration and Claus.
- NH_3 carry-over guarantees are not being made by UOP due to difficulty of measurement.

These technical limits are probably overshadowed by the regulatory requirements for NO_x control. Unless post-combustion NO_x control is required, the economics and complexity will probably not mean wide use of the SFGT process on utility boilers.

MITSUI-BF DRY DESOX/DENOX PROCESS

History and Process Description

Early development of the Mitsui-BF dry DESOX/DENOX process grew out of the work done by Bergbau-Forschung in Germany. The recent Japanese work included laboratory tests in 1980-1981 followed by absorber tests starting in early 1981.(5) A prototype by-product pilot plant was constructed in late 1981 and early 1982.

The Mitsui-BF process is divided into an adsorption section, a desorption section and a sulfur recovery section. The adsorber concept is similar to the Bergbau-Forschung with carbon regenerated by indirect heating. The rich SO_2 stream produced is partially reduced in a Mitsui-designed reduction reactor and the H_2S/SO_2 mixture is catalytically converted in a Claus reactor to elemental sulfur. This process is illustrated in Figure 2.

Adsorption/Regeneration Section. Flue gas enters the moving bed adsorbing system which holds activated coke. Since the optimum flue gas temperature for the process ranges from 120 to 140oC (248 to 284oF), which is usual with flue gas behind air-preheater, the process does not require preheating or precooling. The adsorption system consists of two vertically connected adsorbers where activated coke pellets flow downward by gravity from the top adsorber (second stage) to the bottom adsorber (first stage). Flue gas flows horizontally through the bottom adsorber (first stage) and goes into the top adsorber (second stage) via a duct. The first and second stage adsorber share the duty of SO_x removal and NO_x removal and both are fed ammonia. Chemical reactions in the adsorption section are as follows:

SO_2 removal

$$2SO_2 + O_2 + 2H_2O \rightarrow 2H_2SO_4 \qquad (9)$$

NO removal

$$4NO + O_2 + 4NH_3 \rightarrow 4N_2 + 6H_2O \qquad (10)$$

Competing ammonia reactions

$$NH_3 + H_2SO_4 \rightarrow NH_4HSO_4 \qquad (11)$$

$$2NH_3 + H_2SO_4 \rightarrow (NH_4)_2SO_4 \qquad (12)$$

Competing ammonia reactions 11 and 12 are favored kinetically and therefore ammonia injection with high SO_x levels results in lowered NO_x removal. The best NO_x removal occurs at low SO_x levels when the proper amount of ammonia is available to react with NO_x in contact with the coke. This is the reason the Mitsui-BF process uses two reactors. The lightly loaded coke that is most active for NO_x removal is in the second stage, where sulfuric acid, ammonium sulfate and bisulfate have not built up. As they become loaded, they are sent to the first stage for SO_x removal duty, where there is still enough activity to remove SO_x.

When high NO_x removal efficiency is required, it is necessary to increase ammonia feed to the second stage and consequently ammonia residual appears behind the adsorber. Test results show residual does not exceed 20 ppm at a NO_x removal efficiency of more than 80 percent. However, if treatment of the residual is required, the flue gas is sent through an extra adsorber which is smaller than the former ones and contains sulfuric acid rich activated coke from the first stage, to remove ammonia according to the rapid competing ammonia reactions.

Dust load in the flue gas behind these adsorbers is less than 30 mg/Nm^3-dry (.014 gr/scf) and it may be possible to send the flue gas to the stack without dust collectors. In the Mitsui pilot plant, a bag filter is provided in order to provide backup particulate control, and outlet dust load is less than 1 mg/Nm^3-dry (.5 x 10^{-3} gr/scf).

Activated coke saturated with sulfuric acid is discharged from the first stage adsorber by vibrating chute and sent to the desorber for regeneration. Activated coke is regenerated by indirect heating. The temperature of activated coke in the heat exchanger is maintained at 400±20°C (752±36°F). As a result of regeneration, concentrated gas with 20% SO_2 by volume is discharged from the desorber. Chemical reactions in the desorption section are as follows:

$$H_2SO_4 \rightarrow H_2O + SO_3 \qquad (13)$$

$$NH_4HSO_4 \rightarrow NH_3 + H_2O + SO_3 \qquad (14)$$

$$2SO_3 + C \rightarrow 2SO_2 + CO_2 \qquad (15)$$

$$3SO_3 + 2NH_3 \rightarrow N_2 + 3SO_2 + 3H_2O \qquad (16)$$

The regenerated activated coke is indirectly cooled by air and recycled to the adsorber.

Sulfur Recovery Section. As a tail-end process for SO_2 enriched gas treatment, the Mitsui pilot plant is provided with a sulfur recovery process. The process consists of conversion of some of the SO_2 to H_2S and subsequent Claus reaction. Two-thirds of the SO_2-enriched gas enters the coke reactor, and SO_2 is reduced to H_2S with steam and hot coke (coke breeze is used due to its low cost and availability). The temperature of the coke reactor is maintained between 650 to 950°C (1202 to 1742°F). H_2S from the coke reactor is mixed with the by-passed one-third of SO_2 gas and sent to subsequent Claus reactor. Many reactions occur in the coke reactor, but representative reactions can be written as follows:

$$C + SO_2 \rightarrow S + CO_2 \qquad (17)$$

$$C + H_2O \rightarrow H_2 + CO \qquad (18)$$

$$H_2 + S \rightarrow H_2S \qquad (19)$$

Claus reaction (in Claus stages):

$$2H_2S + SO_2 \rightarrow 3S + 2H_2O \qquad (20)$$

The tail gas from the Claus unit enters an incinerator to convert residual sulfur and H_2S to SO_2 and goes to the adsorber inlet or stack. To maintain high SO_2 removal efficiency without increasing running cost as a total system, the sulfur recovery process has to perform at high sulfur conversion efficiency. This is the reason Mitsui chose to develop the sulfur recovery process consisting of a coke reactor and Claus unit instead of more conventional processes.

Test Results

1. Typical NO_x-SO_x removal results are summarized in Table 5. Ammonia was injected to both first and second stages and the total molar amount did not exceed two times the inlet NO_x throughout these tests.

2. Figure 3 shows the effect of flue gas temperature on SO_2 and NO_x removal efficiency in the first stage. As flue gas temperature becomes higher, SO_2 removal efficiency decreases rapidly while NO_x removal efficiency increases slightly. NO_x removal efficiency in the first stage is also a function of ammonia feed, but this effect is not as significant as the temperature effect.

3. Figure 4 shows the relation between NO_x removal efficiency and flow rate of activated coke in the second stage. Since activated coke flows through both adsorbers in series, good NO_x removal efficiency in the second stage as shown in Figure 4 depends on good SO_2 removal efficiency in the first stage. This is because high SO_2 removal efficiency in the first stage is required to avoid competition for ammonia by SO_2.

A process material and energy balance is shown in Figure 5. The gas flow represents approximately a 350 MW plant with medium sulfur coals.

Mitsui-BF Process Economics

The Mitsui-BF dry DESOX-DENOX process represents an advanced design that has not yet been built at full scale. The developer, Mitsui, has provided EPRI with their estimate of cost for a DESOX-DENOX system on a 350 MWe (nominal) coal-fired power plant with the same material and energy balance as was shown in Figure 5. The basis of this estimate is not identical to others in this paper since it does not include owner costs such as land, interest during construction and project and process contingency, etc., in the same manner as the EPRI estimates. For example, EPRI's standard estimates usually show a higher ratio of indirect costs to direct cost. Reported initial capital charges for a 350 MW plant are:

	Million Dollars*	Million Yen
Direct (Including Initial Coke Charge)	37.5	9,932
Indirect	3.6	950
Total	41.1	10,882

Annual Operating Costs (First Year)

	Million Dollars	Million Yen
1. Fixed Costs	9.09	2411
2. Operating & Maint. Costs		
Labor	.20	54
Repair	1.23	325
Utility	5.37	1423
Other	.41	109
3. By-Product		
Sulfur Credit	(.37)	(98)
4. Overhead and Tax	.96	254
TOTAL First Year Costs	16.89	4,479

*Note conversion rate is 265.1 Yen/$ - costs not according to EPRI premises.

The technical limits of the carbon adsorption process are:

- Reduced NO_x removal with very high SO_2 inlet
- Potential for plugging of adsorber with ammonium salts
- Need to minimize ammonia breakthrough and carbon loss
- Reactor temperature control/hot spot and fire control
- Commercial adsorbent availability and cost
- Adsorbent attrition and consumption rate

The approach used by Mitsui (splitting the absorber bed functions) is an example of an approach being used to refine this well-established process concept.

AVCO-EBARA ELECTRON-BEAM PROCESS

History and Processes Description

Early development (from 1970) of the irradiation concept was done in Japan by Ebara in combination with the Japan Atomic Energy Research Institute(3). The original Ebara process concept evolved from a consideration of the reactions in photochemical smog. Batch-type tests using relatively low energy irradiation and long exposure times proved the formation of an aerosol was possible. From 1972-1974, small flow-type irradiation devices were used with a more powerful accelerator. The removal of SO_x and NO_x was good at the high irradiation rates and improved at lower temperature. From May 1974 to February 1977, a pilot plant with 1000 Nm^3/hr (625 scfm) was constructed and operated by Ebara. In the first half of the testing, unstable solid particles or a mixture of sulfuric and nitric acids was collected by an ESP. In the second half of the tests ammonia addition yielded a stable dry powdered product and improved SO_x and NO_x removal. The final stage of Japanese development included a 10,000 Nm^3/hr (6250 scfm) pilot plant built at an iron works in Japan and applied to sintering exhaust gas for one year (1977-1978) normal conditions were 200 ppm SO_x and 180 ppm NO_x, respectively. During this time, reported SO_2 removal efficiency exceeded 90 percent and NO_x removal exceeded 80 percent at 1.0 Mrad (equivalent to 10 J/g of gas or 4.54 KW-sec/lb). To maintain high efficiency, electron dose rates had to be uniform. Results of the large-scale Japanese test work are summarized in Figure 6 and 7 which show the SO_x and NO_x removal as a function of reaction temperature and absorbed energy.

Avco, the licensor and co-developer of this process in the U .S., has been actively pursuing a demonstration project in this country.[4] The process demonstration unit is expected to have a capacity of 32,000 Nm^3/hr or 20,000 scfm (about equivalent to 10 MWe gas flow). Avco has done laboratory work on the concept and has investigated U.S. markets for the by-product. The proposed full-scale demonstration has been supported by DOE and a group of Indiana utilities as well as the state of Indiana. Ebara is reportedly taking over U.S. development initiative and actively seeking funding.

The process steps include humidification and temperature control, ammonia addition, irradiation and by-product collection. This is shown schematically in Figure 8. The humidification vessel uses sprays to reduce bulk gas temperature to 79°C (200°F). Ammonia is added to make the by-product usable as ammonium sulfate and nitrate. The irradiation produces ozone and free radical intermediates, such as N, O, OH, HO_2. These combine to give sulfuric and nitric acids and ammonium salts. The overall process reactions can be summarized as:

$$\underset{(21)}{SO_2} + NO + NH_3 + H_2O \xrightarrow{O,\ OH,\ HO_2} (NH_4)_2\ SO_4 + (NH_4)_2\ SO_4 + 2NH_4NO_3$$

Water is required to give proper radical formation necessary for SO_x removal.

For simultaneous SO_x and NO_x removal the optimum process conditions are different. High NO_x removal (>90%) requires lower reaction temperature.

The electron beam irradiation step is at the heart of the design. Key design parameters are irradiation dosage, electron beam penetration, electron beam efficiency (absorbed energy vs. electrical power required), gas mixing, and reaction temperature. The reaction chamber designed to do this includes high voltage electron guns that discharge a beam of electrons into the gas through air cooled, thin titanium windows and sweeps the gas volume at a rate of 200 Hz. About 800 kW appears to be a good design value for the electron beam voltage because it will allow cable connections.(3) A detailed discussion of the process design and control variables is contained in references 3 and 6.

Avco-Ebara Process Economics

The economics of the Avco-Ebara process have been evaluated for EPRI by Bechtel Group, Inc., of San Francisco in Reference 3. This evaluation is based on December 1980 pricing and standard premises specified by EPRI. The costs have been escalated to December 1982 for presentation in this paper.

The capital costs are shown in Table 6 and first years costs in Table 7 along with unit rates for labor, utilities, and chemicals. Details are presented in Reference 3. Total levelized revenue requirement is 32.9 mills/kWh assuming no by-product credit. The study also prepared a comparison between conventional limestone and the Avco-Ebara process. This is shown below in December 1982 dollars.

Process	Total Capital Requirement ($/kW)	First-Year Operating Cost ($1000)	30-Year Levelized Revenue Requirement (mills/kWh)
Avco-Ebara	333.0	57,332	32.9
Wet Limestone	212.5	38,503	21.9

On the basis of the present state of development for, and the extent of experience with, the Avco-Ebara process and conventional wet limestone scrubbing, the levelized revenue requirement for the Avco-Ebara process without by-product credit is as much as 1.5 times greater than the levelized revenue requirement for conventional wet limestone scrubbing. In situations where postcombustion NO_x control is not required, the Avco-Ebara process becomes economically competitive with conventional wet limestone scrubbing only if a 58 $/ton net-back for the by-product can be obtained. In situations where postcombustion NO_x control is required, Bechtel estimates that the Avco-Ebara process, without by-product credit, may provide up to a 25 percent savings in the levelized revenue requirement over a combination of wet limestone scrubbing plus selective catalytic reduction.

Both versions of the electron beam technology represents an approach to combined NO_x-SO_x control based on novel physical and chemical steps. Technical limits of the technology are:

- For utility flue gas treatment, electron beam systems more powerful than present production models are required (High Voltage Engineering Corporation of Burlington, Massachussetts probably could supply these now);
- Proper control of humidification is required to prevent corrosion;
- The salability of by-products with and without fly ash will be critical to process economics;
- Coal-fired power plant flue gas has not been tested in the U.S., and a prototype is a necessary next step in development;
- A high ratio of electrical energy (versus steam or fuel) is required to supply auxiliary power needs.

The novel nature of this process means a prototype unit demonstration is an essential next step before commercial units are purchased.

CONCLUSIONS

All three dry generic NO_x-SO_x treatment processes discussed in this paper represent advanced methods of emission control.

All use ammonia and a common problem is ammonia monitoring, breakthrough and handling.

By-products and unit operations are not typical of utility plants. These by-products will require some special training and design considerations.

None of the processes have been tested at full-scale on coal-fired plants and commercial acceptance usually requires developers to complete this step before widespread use.

These processes are more complex mechanically than conventional wet scrubbing for SO_2, but may make inroads in the emission control market if more stringent NO_x control is required. Out of the many processes that have been proposed for dry, combined SO_x and NO_x control, these three generic concepts stand out as likely candidates for consideration on future plants.

ACKNOWLEDGEMENTS

I would like to acknowledge the efforts by Messrs. Kato and Kitamura of Mitsui in providing Mitsui-BF dry DESOX/DENOX process data for this paper. Additionally I would like to acknowledge the use of information in three draft EPRI reports, one prepared by Bechtel Energy, Inc. on the Avco-Ebara Process, one by Stearns-Roger Engineering on Postcombustion NO_x Processes, and one by Radian Corp. on the Status of FGD Processes. Information from these drafts was helpful in preparing this paper.

I would also like to thank Messrs. Cichanowicz and Morasky of EPRI for their assistance in preparing the paper and reviewing its accuracy.

REFERENCES

1. Radian Corporation, The Evaluation and Status of Flue Gas Desulfurization Systems (Draft); Palo Alto, RP982-28, June 1982.
2. Ando, J., SO_x and NO_x Removal for Coal-Fired Boilers in Japan; preprints of EPA/EPRI Flue Gas Desulfurization Symposium, Hollywood, Florida, May 1982.
3. Bechtel Group, Inc., A Preliminary Evaluation of the Avco-Ebara FGT Process (Draft); Palo Alto, California, RP982-27, September 1982.
4. Stearns-Roger Engineering Corporation, Technical and Economic Feasibility of Ammonia Based Postcombustion NO_x Control; Palo Alto, California, CS-2713, November 1982.

5. Personal Communication with Messrs. Kato and Kitamura, Mitsui Mining and Mitsui and Co., USA, September 14, 1982.

6. Shui, V. H., and Carlson, D. G., *Conversion of SO_x and NO_x to Fertilizer by Electron Irradiation*; AICHE National Meeting, Cleveland, Ohio, Paper No. 56F, August-September 1982.

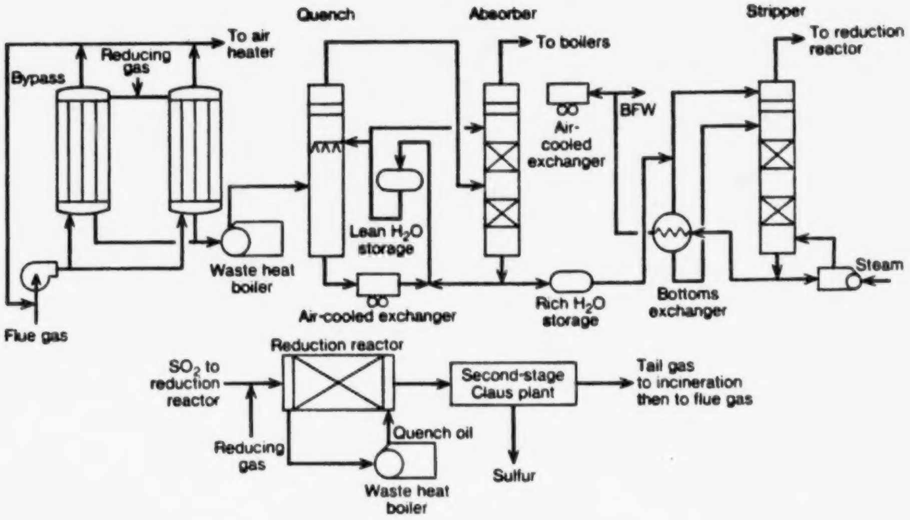
Quench
Absorber
Stripper
To air heater
Reducing gas
Bypass
To boilers
To reduction reactor
Air-cooled exchanger
BFW
Lean H_2O storage
Waste heat boiler
Air-cooled exchanger
Rich H_2O storage
Bottoms exchanger
Steam
Flue gas
Reduction reactor
SO_2 to reduction reactor
Second-stage Claus plant
Tail gas to incineration then to flue gas
Reducing gas
Quench oil
Waste heat boiler
Sulfur

Figure 1. Shell copper oxide process flow diagram. [1]

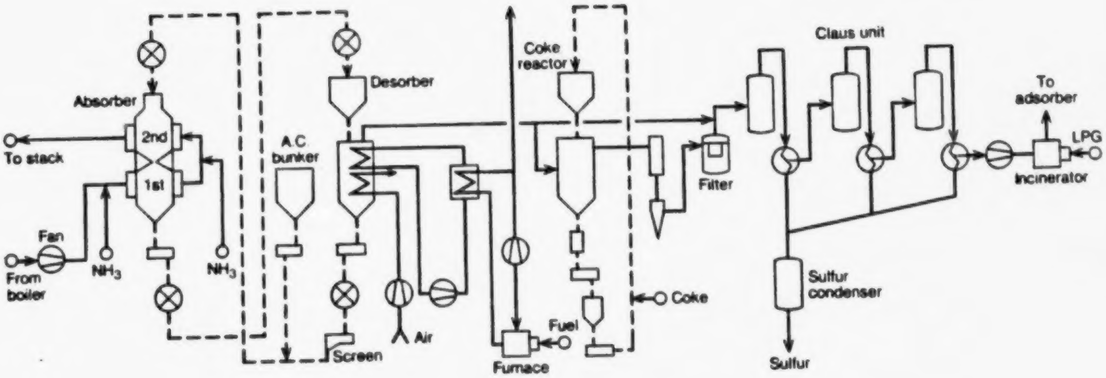
Absorber
2nd
1st
To stack
Fan
From boiler
NH_3
NH_3
A.C. bunker
Desorber
Screen
Air
Coke reactor
Furnace
Fuel
Coke
Filter
Claus unit
Sulfur condenser
Sulfur
To adsorber
LPG
Incinerator

Figure 2. Mitsui-BF dry desox denox process with sulfur recovery process. [5]

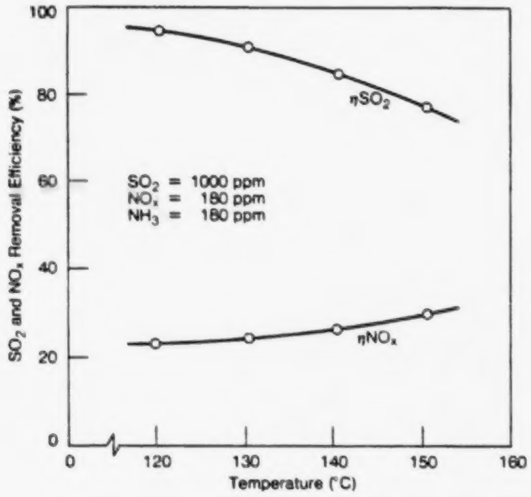

Figure 3. Effect of flue gas temperature on SO_2 and NO_x removal efficiency in the first-stage absorber (Mitsui-BF).

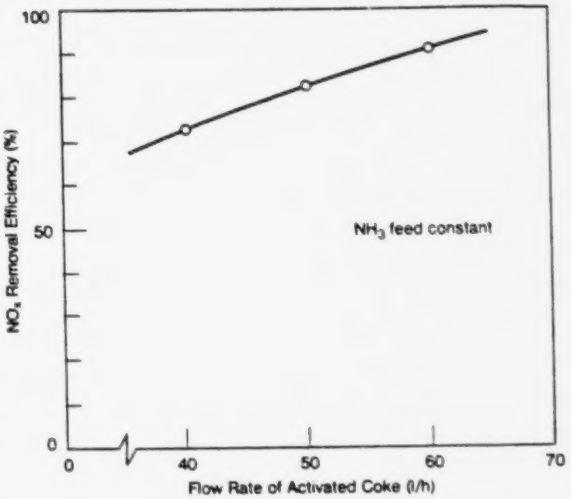

Figure 4. Relation between NO_x removal efficiency and flow rate of activated coke [illegible] the second stage adsorber Mitsui-BF.

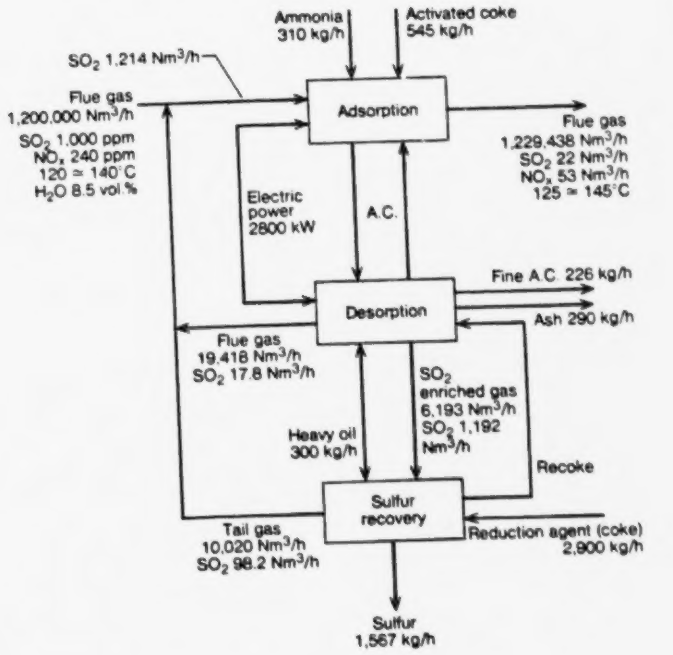

Ammonia
310 kg/h
Activated coke
545 kg/h
SO$_2$ 1,214 Nm^3/h
Flue gas
1,200,000 Nm^3/h
SO$_2$ 1,000 ppm
NO$_x$ 240 ppm
120 ≃ 140°C
H$_2$O 8.5 vol.%
Adsorption
Flue gas
1,229,438 Nm^3/h
SO$_2$ 22 Nm^3/h
NO$_x$ 53 Nm^3/h
125 ≃ 145°C
Electric
power
2800 kW
A.C.
Fine A.C. 226 kg/h
Desorption
Ash 290 kg/h
Flue gas
19,418 Nm^3/h
SO$_2$ 17.8 Nm^3/h
SO$_2$
enriched gas
6,193 Nm^3/h
SO$_2$ 1,192
Nm^3/h
Heavy oil
300 kg/h
Recoke
Sulfur
recovery
Tail gas
10,020 Nm^3/h
SO$_2$ 98.2 Nm^3/h
Reduction agent (coke)
2,900 kg/h
Sulfur
1,567 kg/h

Figure 5. Material and energy balance dry desox denox system with sulfur recovery for a power plant of 1,200,000 Nm^3/h flue gas (Mitsui-BF).

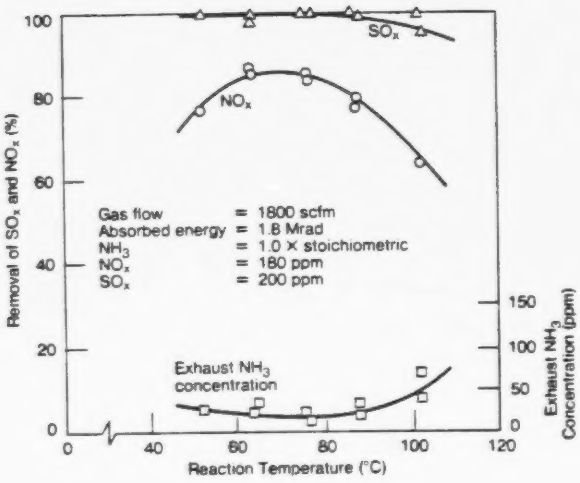

Figure 6. Removal of SO_x–NO_x and exhaust NH_3 concentration versus reaction temperature. [3]

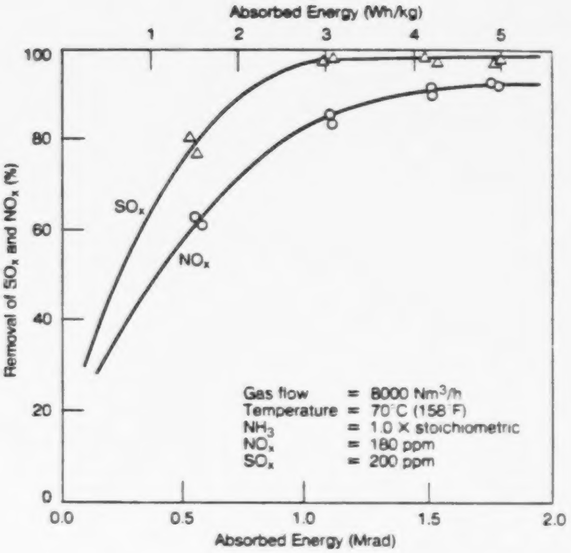

Figure 7. SO_x and NO_x removal versus electron dose Avco-Ebara. [3]

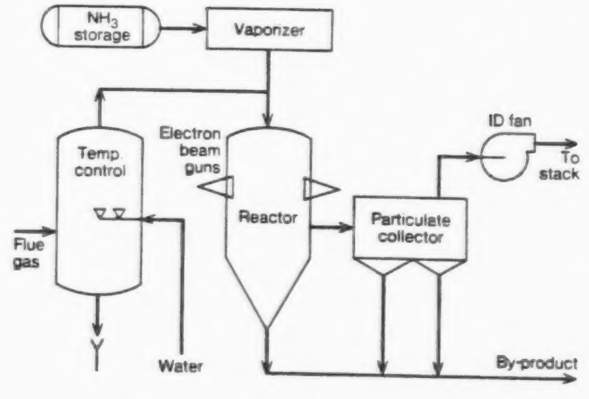
NH_3 storage
Vaporizer
Electron beam guns
Temp. control
Reactor
ID fan
To stack
Particulate collector
Flue gas
Water
By-product

Figure 8. E-beam SO_x/NO_x/particulate removal system schematic diagram. [6]

TABLE 1. COPPER OXIDE SORPTION SYSTEMS

Process	Type[a]	Status[b]	SO_2 Removal Capability[c]	Process Complexity[c]	NO_x Removal[d]	Particulate Removal	Clean Gas Required[d]	Subsystem Used[c]
BOM Copper Oxide	DR	E	M	M	?	N	Y or N	R
Exxon Copper Oxide	DR	CP	M	M	Y	N	Y	R
Houdry	DR	E	M	M	?	N	Y	R
Nippon Oil Copper Oxide	DR	?	?	?	?	?	?	?
Shell Copper Oxide	DR	P	M	M	Y	N	Y or N	R

Source: Ref. 1--Radian

---

a) W = Wet, D = dry, T = throwaway, R = regenerable.

b) C = commercial, CU = commercially used in other industries, CA = commercially available.
P = prototype, E = experimental CP = conceptual

c) H = high (95%), M = medium (80-95%), L = Low (<80%) for SO_2 removal.

d) Y = yes, N = no.

e) S = sulfur gas treatment, R = reducing gas production, W = waste and purge stream treatment, N = no.

TABLE 2. CARBON BASED SORPTION SYSTEMS

Process	Status[a]	SO_2 Removal Capability[b]	Commercial Technology Used[c]	Particulate Removal[c]	Subsystem Used[d]
Bergbau-Forschung	CA	H	Y	Y	R
Chemibau-Reinluft	P	H	Y	Y	R
Hitachi	P	H	Y	Y	N
Mitsui	P	H	Y	Y	S
Sumitomo	P	H	Y	N	S
Takeda	P	H	Y	Y	S
Unitka	E	H	Y	Y	S
Westvaco	E	H	N	Y	S

Reference 1-Radian

---

a) C = commercial, CU = commercially used in other industries, CA = commercially available.
P = prototype, E = experimental CP = conceptual

b) H = high (95%), M = medium (80-95%), L = Low (<80%) for SO_2 removal.

c) Y = yes, N = no.

d) S = sulfur gas treatment, R = reducing gas production, W = waste and purge stream treatment, N = no.

TABLE 3. CAPITAL COST ESTIMATE SHELL FGT PROCESS
($\$10^3$, Dec. 1982)

Case		1	2	3
NO_x Reduction %		67	83	90
Inlet NO_x, ppm		300	300	300
Reactors		2884	3171	3171
Ductwork		1827	1827	1827
Insulation		604	604	604
Ammonia Storage		423	582	503
UOP Package		8079	9105	9196
Flow Smoothing		1706	1706	1706
Claus Package		2265	2265	2265
Reformer Package		1691	1691	1691
Differential Costs		3624	3624	3624
Other Direct Costs		8101	8350	8365
Other Materials		1513	1561	1561
Field Labor		13450	13874	13878
Indirect Costs		8574	3843	18850
Process Capital		54741	57103	57241
(Cost $/kW)		(109)	(114)	(114)
General Facilities		2938	2860	2863
Engineering & Fees	o A/E	5764	5764	5764
	o UOP	17078	17078	17078
Contingency	o Project	12590	3154	13167
	o Process	5474	5718	5724
Sales Tax		1137	1199	1200
Total Plant Investment		99522	102876	103037
(Cost $/kW)		(199)	(206)	(206)
Royalty Allowance		227	257	257
Preproduction		5646	5871	5880
Inventory		486	524	529
Initial Catalyst		8003	9611	9611
Land		0	0	0
Total Capital Requirement		113,884	119,139	119,314
(Cost $/kW)		(227)	(238)	(238)

TABLE 4. FIRST YEAR O&M COSTS FOR 500 MW SHELL FGT PROCESS ($$10^3$, Dec. 1982)

Case	1	2	3
NO_x Reduction %	67	83	90
Inlet NO_x, ppm	300	300	300
Fixed O&M			
Operations	331	331	331
Maintenance	1616	1685	1685
O&M Overhead	977	1004	1004
TOTAL Fixed O&M	2924	3020	3020
Variable O&M			
Ammonia	498	619	664
Steam	80	83	83
Power	2718	3005	3005
Naphtha	1963	1963	1963
Sulfur Credit	(196)	(196)	(196)
Catalyst/Acceptor	8003	9611	9611
Reheat Credit	(1157)	(1157)	(1157)
TOTAL Varible O&M	14,223	16,242	16,287
Levelized Cost Mills/kWh	20.3	22.2	22.3

TABLE 5. TYPICAL PERFORMANCE DATA IN MITSUI-BF DRY DESOX/DENOX PILOT PLANT

Inlet Gas Condition									
Flue gas handled	Nm^3/hr (SCFM)	1000	(622)	1000	(622)	1000	(622)	1000	(622)
Temperature	°C (°F)	130	(266)	130	(266)	120	(248)	140	(294)
SO_2 concentration	ppm**	1000		1000		1000		1000	
NO_x concentration	ppm	180		180		180		185	
Behind first stage adsorber									
SO_2 concentration	ppm	90		90		60		180	
NO_x concentration	ppm	130		130		138		130	
Behind second stage adsorber									
SO_2 concentration	ppm	Trace		Trace		Trace		Trace	
NO_x concentration	ppm	48		25		28		13	
NH_3 residual	ppm	6		17		18		50	
Behind ammonia adsorber									
NH_3 residual	ppm	Trace		Trace		Trace		Trace	
Total SO_2 removal efficiency %		>98		>98		>98		>98	
Total NO_x removal efficiency %		78		86		84		93	

Reference 5-Ebara

---

*Water content in the flue gas is 10 percent

**SO_3 concentration is 10 ppm and total SO_3 removal efficiency is more than 98 percent.

TABLE 6. AVCO-EBARA PROCESS PROJECTED CAPITAL REQUIREMENTS

Unit Size (MW net)	2 x 500
Capacity Factor	65%
Coal Sulfur Content	4%
Pricing Level	December, 1982
SO_2 Emission Limit	1979 NSPS

Item	$/kW
Raw mateial receiving and storage	16.7
Flue gas treatment	80.0
Particulate removal credit	(18.3)
Reaction product separation and treatment	59.0
Flue gas supply	5.1
By-product storage	21.8
TOTAL process capital	164.3
General facilities @ 12.5% of 164.3	20.4
Engineering and home office fees @ 12.5% of 164.3	20.4
Project contingency @ 30% of 185	61.5
Process contingency @ 25% of 80.0 + 10% of 59.0	25.8
TOTAL plant cost	292.4
TOTAL plant investment	309.9
Royalty allowance @ 0.5% of 164.3	.84
Preproduction cost	13.0
Inventory and initial chemicals	9.6
Land	0
TOTAL capital requirement	333.34
Levelized fixed charges, mills/kWh:	9.4

TABLE 7. AVCO-EBARA PROCESS PROJECTED FIRST-YEAR OPERATING COSTS

Unit Size (MW net)	2 x 500
Capacity Factor	65%
Coal Sulfur Content	4%
Pricing Level	December 1982
SO_2 Emission Limit	1979 NSPS

Item	Unit	Unit Rate ($)	Annual Quantity	Annual ($000)
Operating labor	Manhour	18.45	40,000	738
Maintenance labor				3,081
Maintenance material				4,621
Admin./support @ 30% of (738 + 3081)				1,146
TOTAL Fixed O&M cost				9,586
Utilities				
Steam	10^3 lb	3.02	160,000	484
Water	10^3 gal	.6	164,000	99
Electricity[a]	kWh	.042	223.5×10^6	9,466
Fuel oil or natural gas	10^6 Btu	8.22	76,000	626
Chemicals				
Anhydrous ammonia	Ton	262	124,000	32,559
Kaolin	Ton	133	23,000	3,061
Other consumables (fixed allowance)				1,452
By-product	Ton		462,000	-
Total variable O&M cost				47,747
Total first-year operating cost				57,333
Levelized operating cost, mills/kWh: 23.5				

---

a) Annual quantity reflects a particulate removal credit of 735 kW.

SESSION VIII

FUNDAMENTAL COMBUSTION STUDIES

Chairman, W. Steven Lanier
EPA, IERL/RTP

THE INFLUENCE OF SCALE AND FUEL PROPERTIES ON FUEL-OIL ATOMIZER PERFORMANCE

By:

W. R. Seeker, W. D. Clark
Energy and Environmental Research Corporation
18 Mason
Irvine, CA 92714

G. S. Samuelsen
Mechanical Engineering
University of California, Irvine
Irvine, CA 92717

"Although the research described in this article has been funded wholly or in part by the United States Environmental Protection Agency through contract number 68-02-3633 to Energy and Environmental Research Corporation, it has not been subjected to the Agency's required peer and policy review and therefore does not necessarily reflect the views of the Agency and no official endorsement should be inferred."

ABSTRACT

The drop size produced by fuel-oil atomizers is of critical importance to the efficiency and pollutant emission performance of stationary sources burning liquid fuels. This study involved the investigation of the impact of nozzle scale and liquid properties on the drop size distribution produced by a variety of air-assist atomizers. A laser diffraction technique (Malvern) was employed in conjunction with photography, holography, and laser doppler velocimetry to measure drop size distribution as a function of nozzle operating conditions. Two spray rigs were employed that allowed testing of nozzles designed from 70,000 Btu/hr to 100 x 10^6 Btu/hr. Several liquids were utilized including water, No. 2 fuel oil, No. 6 fuel oil, and Hyvis polybutene that allowed a variation in viscosity from 1 cst to 50 cSt and tests were included using coal-oil and coal-water mixtures. Correlations of data with the design of the nozzle, liquid-to-air mass flow ratio, and viscosity were included.

INTRODUCTION

There are a wide variety of industrial applications of liquid combustion systems where the characteristics of the fuel injector determine performance. For example, the emission of NO_x and carbonaceous particulate from burning fuel oils in stationary sources is closely tied to the injector characteristics. The propensity to form cenospheres from fuel oils with high asphaltene content (Ref. 1) and soot from both petroleum and synthetic fuel oils (Ref. 2,3) has been found to be strongly dependent on droplet size. Results from EPA pilot-scale studies indicate that the emission of NO_x and smoke from oil-fired furnaces and boilers are influenced by the type of nozzle employed, the operating condition of the nozzle and the swirl of the primary air (Ref. 4,5). Even thermal NO_x from light fuels has been found to be dependent on droplet size (Ref. 6).

These data identify the need for characterizing those properties of the spray from fuel oil atomizers that likely dictate the amount of NO_x and carbonaceous particulate produced. The principal parameters controlled by the fuel injector are:

- Droplet Size. Small droplets have high surface-to-volume ratios which result in very high evaporation rates.
- Droplet Velocity. The droplet velocity determines the ballistic transport of the droplet in the near field of the flame.
- Fuel Distribution. The positioning of the fuel in the aerodynamic flow field generated by the burner determines many characteristics of the flame.

All of these parameters influence the mixing processes in the near field of the burner that bring the fuel into contact with the combustion air and recirculated products of combustion. It is likely that these mixing processes dictate the conversion of fuel-bound nitrogen to NO_x and the production of soot.

The most widely used type of nozzle for fuel-oil atomization is the air-blast or twin-fluid nozzle. The atomization process involves subjecting a relatively slow-moving oil stream to a high-velocity air or steam flow. There are a number of excellent reviews on the atomization of twin-fluid nozzles. Most notably the paper by Lefebvre (Ref. 7) presents a comprehensive review of various types of twin-fluid atomizers and their performance. The parameters of importance can be divided into those associated with the nozzle design and with the fuel properties. Lefebvre reviewed the impact on the droplet size distribution of geometry, flow rates, and fuel properties such as viscosity, density, and surface tension for two generic classes of twin fluid atomizers, plain jet and prefilming. The current work is designed to extend the available information to higher viscosities that are associated with heavy fuel oils, commercially available sub-scale and full-scale nozzles and complex liquid formulations such as coal-oil and coal-water mixtures. In the following sections, the methodology of characterizing of fuel-oil nozzles is discussed followed by a presentation and analysis of experimental results.

NOZZLE CHARACTERIZATION

A complete characterization of the performance of a nozzle requires spatial and temporal information on the flux of droplet size in the spray field produced by the nozzle. The general approach utilized in this study was to generate the spray field in a spray rig at ambient temperatures and to use a variety of diagnostic techniques to measure the flux of droplet sizes produced. A spray rig must meet several criteria for a study of stationary-source nozzle performance to yield useful information. The principal considerations are as follows:

- Control and measurement of important flow variables such as oil flow rate and air flow rate and pressure should be provided.

- Real fuels should be tested along with surrogates with similar properties in order to measure the atomization characteristics under conditions as close to the actual application as possible.

- Recirculation of droplets should be avoided since smaller droplets will preferentially be recirculated and thus bias the size distribution information.

- The spray rig should have optical access and both radial and axial movement capabilities since most of the modern diagnostic tools are optical techniques.

- The rig should be able to test a variety of nozzle scales since the impact of nozzle scale is of interest for subscale testing. This criteria might dictate the use of more than one rig in order to cover the range of nozzles used from subscale to full scale.

Two spray rigs are currently being used at EER in the Fundamental Combustion Research Program to investigate nozzle performance. The small spray rig is shown in Figure 1. The chamber was patterned after a firetube combustor at EER (also shown in Figure 1) with respect to the diameter and the ability to accommodate a variety of inlet geometries and swirl. The spray is directed downward in a plexiglass tube with an inner diameter of 0.61m and a height of 1.83m. Fuel oil is supplied to the nozzle through the use of a Zenith pump metering system which allows fine control of the flow rate between 1.06 to 10.6 liters/hr (0.18 to 2.8 gal/hr). The pump can be exchanged for a larger centrifugal pump for flow rates up to 79 liters/hr (20 gal/hr).

Two separate air flow systems are used--a primary flow and a screen air flow. The primary air is directed coaxially around the nozzle holder. The screen air is used to minimize the concentration of the fine mist of oil which can develop around the spray. The screen air flow is directed downward uniformly across the vessel diameter through the use of a perforated plate. The flows are supplied by two high-pressure blowers which allow flow rates to 22.9 m^3/min (810 CFM) for the primary air and up to 11.2 m^3/min (395 CFM) for the screen air. In the present configuration, these flow rates correspond to velocities up to 40.2 m/sec (132 ft/sec) for the primary and up to 0.67 m/sec (2.2 ft/sec) for the screen flow. The flow rates are measured using Barco venturis with the pressure drop measured with magnehelic differential pressure gauges. The venturis were chosen so as to minimize the pressure loss and to have as much of the presure head available from the blowers (15.2 cm H_2O from the primary blower and 25.4 cm H_2O from the screen air blower) at the spray rig. The exhaust from the rig is directed to a demister and then to the induced draft blower. The use of an ID blower allows the rig to be operated at slightly negative pressure. This feature is desirable in order to prevent fuel leakage and to be able to operate without windows.

The apparatus has six 7.62-cm (3-inch) diameter windows mounted horizontally at a height of 94 cm (37 inches) from the bottom of the plexiglass container. The window material is ground and polished Optosil 1 fused silica with better than schlieren quality homogeneity, low birefringence and a minimum number of bubbles. These characteristics are all necessary for high quality holography and photography. To allow for versatility in scattering angles and probing of portions of the spray, the windows are arranged at 45° and 30° from the cendral path. The windows are inset slightly from the container walls to prevent direct spray impingement and have a uniform flow velocity across their face to minimize droplet accumulation. Also, the windows can be easily removed for cleaning. The nozzle is positioned relative to the windows and optical systems by physically moving the nozzle holder/perforated screen air module. As designed, the axial position of the measurement can be varied from as close to the nozzle as allowed by the optical system to 76.2 cm away from the nozzle.

The large spray rig is patterned after the small rig and is shown in Figure 2. The chamber has an octagonal cross-section which is 1.5m across at the smallest dimension, is 2.4m (8 ft) tall and is constructed of aluminum. Large (60 cm x 90 cm) plexiglass windows are placed on two sides of the chamber for visual and photographic access. The chamber is mounted in an exhaust plenum which acts to distribute the exhaust to four ducts and serves as an oil reservoir. The exhaust is then directed to a demister and a high-pressure ID blower. The primary air blower can deliver up to 225 m^3/min (8000 cfm) and a variety of inlet geometries can be utilized from inlet quarls with and without swirl to perforated plate flow straighteners. The air flows were metered with venturis and the oil flow rate by a liquid rotameter. The oil and air flow rate capabilities of the large rig have been utilized to test nozzles up to 30 MW (100 x 10^6 Btu/hr).

DROPLET MEASUREMENT TECHNIQUES

A detailed nozzle characterization requires the measurement of droplet size distribution, droplet velocity, and droplet concentration throughout the spray field. The spray field produced by commercial fuel-oil nozzles is a difficult measurement environment even under ambient conditions. The typical spray field contains a high concentration of droplets on the order of 1000 droplets/cm^3 that can severely limit the applicability of certain droplet sizing techniques. Also, the size distribution produced can be very broad. It is necessary to be able to measure from 1 to 1000 μm to cover the full range of expected droplet sizes. This requires the instrument to have three decades of dynamic range. Finally, it is necessary to be able to isolate the measurement to certain regions of the spray if spatial information is required.

The first phase of the FCR program involved selection or development of the appropriate diagnostic techniques to allow a full characterization of fuel-oil nozzles. This involved first reviewing the available diagnostic techniques and actual in-house testing of a variety of techniques. It became evident that no one technique could supply all the information required, but rather a methodology was required which utilized a variety of techniques selected to give tha type of information required as determined by the application. As background for the methodology employed, methods available for acquisition of nozzle characterization are summarized in the following section.

Mechanical Versus Optical

Droplet sizing was first conducted using mechanical techniques. Optical methods were later introduced with the application of photographic techniques to spray analyses. Now, with the advent and advance of laser technology, the optical methods have expanded in number with a continual expansion in capability.

Mechanical methods include (1) droplet impaction on glass slides coated with such materials as oil, grease, soap, plastic film, and magnesium oxide (e.g., Refs. 8-11); (2) droplet impaction on an immersion fluid that is immiscible with the sampled droplet (e.g., Ref. 12); (3) freezing of atomized droplets (e.g., Ref. 13); (4) the use of molten wax as the atomizing fluid and the subsequent solidification and collection of wax particles (e.g., Ref. 14); and (5) aerodynamic separation of collected sprays (e.g., Ref. 15). All these techniques require some means, usually tedious and time-consuming, of counting and sizing the collected droplets. In addition, the local flowfield and droplet properties can be perturbed by the collection techniques employed. Finally, the data cannot be readily resolved spatially nor temporally, and the velocity of individual droplets cannot be obtained.

Optical sizing techniques have four distinct advantages over mechanical techniques—they are nonintrusive and perturb neither the flow nor droplet conditions, measurements can be made in-situ, the droplet properties can be measured in relatively short periods, and droplet velocities can be obtained. From the variety available, optical techniques can be classified into two general groups: visualization and light scattering.

Optical Visualization Techniques

High-speed photography has been used to measure size distributions in sprays and thereby avoid local perturbation by an intrusive probe (e.g., Ref. 16-19). However, photography is not readily capable of giving the temporal distribution of the droplet sizes produced by the atomizer. In addition, the perceived size distribution is biased to the small particles. This is a result of the spray ballistics. The large droplets maintain a velocity after leaving the atomizer that is higher than the velocity of the smaller drops. As a result the number concentration of the smaller droplets is disproportionately biased to a higher percentage. It is necessary to convert the apparent spatial distribution to the true distribution by multiplying the number of droplets of any given size by the droplet velocity for that size.

Analyses of spray photographs are also compromised by the interpretation of the depth of field. The question arises as to whether blurred images outside the field of focus should be counted. There is a tendency to count large droplets over a greater depth of field than would be covered when counting smaller droplets. One approach to this problem is to observe Fresnel diffraction rings around droplet images. The width of the diffraction ring can be correlated to the position of the droplet in the field of focus. The rejection or acceptance of a droplet, then, can be based on the appearance of the rings.

Holography. Holography has been used successfully in dilute spray systems in both isothermal (Ref. 20) and reacting flows (Ref. 21). An advantage over photography is the provision of a 3-D recording which removes the field of depth uncertainty but still leaves the ambiguity associated with defining a sample volume for droplet sizing.

In dense sprays of the type encountered in boilers, the utility of holography is uncertain. In order for drops to be reconstructed clearly, the coherent light diffracted by each drop must pass unobstructed to the film plane. In dense sprays, secondary scattering of the light diffracted from the original source can occur and thereby create a hologram with ill-defined droplets.

As with photographic techniques, the analysis of holograms is tedious and dependent on judgment. Image analyzers have been employed to extract droplet size information (e.g., Ref. 22), but the judgment of an operator is still required to determine which images are in focus and how many are not.

Flash TV. A high-speed flash-illuminated, television recording instrument has been designed (Ref. 23) and used (e.g., Ref. 24) to measure local size distributions and, by spatial traverse, size distributions of whole sprays. A high-intensity (xenon) lamp is flashed at a preset frequency in the range from 100 to 1000 times with a 0.5 microsecond duration. The light is focused at a point in the spray producing a sampling volume, typically 10 mm^3. The illuminated droplet is transmitted to a 525-line TV camera Vidicon using appropriate optics.

The focus of the droplet is assessed electronically and rejected if not within prescribed constraints. The drop is then sized by the number of lines intercepted on the photosensitized surface of the Vidicon. The resolution is typically 4 μm. Sized particles are then classified into six size ranges and stored on magnetic tape. The tape can substantially be fed for computer manipulation of the data, including various mathematical and statistical operations.

Optical Light Scattering Techniques

Light scattering methods can be divided into two categories, those that measure the light from a collection of particles in a collimated laser beam, and those that measure the light scattered from a highly focused laser beam by individual particles. A primary example of the former is the angular light distribution produced by droplets scattering light in the forward direction by diffraction. The primary example of the latter are droplets scattering light from an optical fringe produced by interferometry.

Diffraction. The standard example of droplet sizing using diffractive scattering is a technique described by Dobbins, et al. (Ref. 18). The method is based on the forward scattering of a parallel beam of monochromatic light which has passed through a spray. The Sauter mean diameter is directly dependent upon the angular distribution of the light intensity. The technique has been applied satisfactorily to a number of practical problems (e.g., Refs. 25-28) to recover the spray Sauter mean diameter as a function of nozzle operating condition.

Although the angular distribution of the light intensity does not allow a distribution of droplet size to be inferred, the angular distribution of light energy can be related to distribution (Ref. 29). It is this method that is employed commercially in the Malvern instrument that will be subsequently tested in this study.

Interferometry. Interferometry utilizes a laser beam split into two parallel beams of equal intensity. The sampling volume is formed by focusing the two beams at a point. The intersection of the two beams establishes an interference fringe pattern (i.e., a row of equally-spaced columns of light varying in intensity in a Gaussian distribution). A droplet passing through the columns of light scatters light from each column in succession. Because the spacing between the columns can be calculated from the angle of intersection and the wavelength of the incident light, the velocity of the droplet passing through the fringe is a function of the frequency ("doppler signal") of the scattered light.

The relative amplitude modulation of the doppler signal is referred to as the visibility of the droplet producing the signal. The amount of modulation is a function of the particle size relative to the fringe spacing; i.e., a function of d/δ, where d is the particle diameter and δ is the fringe spacing (Ref. 30).

Bachalo (Ref. 31) expanded the concept of visibility by utilizing light scattered in angles away from the forward direction. The net effect is to (a) reduce the size of the measurement volume, (b) reduce the background noise, and (c) increase the size limits over which the technique can be used. Rather than measuring the diffractive component of light scattered in the forward direction, the technique relies on the measurement of the reflected and refracted light, and is based on the measurement of the relative phase shift that occurs when two light waves pass through the droplets following different paths.

EXPERIMENT APPROACH

The approach adopted in the present study was to obtain spray measurements under ambient conditions in the small spray rig using three separate techniques:

- Interferometry
- Holography
- Diffraction

Interferometry is a point measurement technique and was selected because of the potential to (1) measure simultaneously droplet size and velocity, and (2) resolve spatially droplet size and velocity distributions. Holography provides an instantaneous, three-dimensional "picture" of the droplet field and was selected as a check for the interferometric and diffraction techniques. Diffraction was selected because, although velocity and spatial resolution are not provided, the technique has been extensively tested (e.g., Ref. 28) and is relatively fast in providing processed data. In addition, because diffraction was employed in previous EPA studies at the International Flame Research Foundation (Ref. 26), the adaptation of diffraction to the present study had the added advantage of providing a check on reproducibility between two laboratories.

A Sonicore Type 052 nozzle was selected for testing which had a rated capacity of 1.9 liters/hr (0.5 gal/hr). The IFRF study included some limited data on the 052 model using the laser diffraction technique. The diffraction measurements were performed using the Malvern Model 1800. The interferometry measurements utilized an SDL Model VP1001 processor and optical system and was performed by SDL personnel. The interferometry system is described in detail elsewhere (Ref. 32). Later measurements were repeated by EER personnel using developed optics and the SDL processor. The holography measurements were also performed using an SDL Holocamera operated by SDL personnel which is described elsewhere (Ref. 33). Subsequent measurements have used a shadowgraph and high-speed shadowgraph techniques developed previously for the study of reacting pulverized-coal particles (Ref. 34).

Measurements were taken at a variety of operating conditions and positions within the spray field. The major difficulty in directly comparing the results from the three techniques was the different formats of the results. For example, the interferometry technique output was typically frequency data with diameter-class-size dependent on the range of particle sizes measured. On the other hand, the Malvern diffraction technique yielded Rosin-Rammler data in the form of logrithmic class cutoffs. These differences necessitated some manipulation of the data in order for a direct comparison to be made. An example of the data is plotted on a common basis of fractional weight versus droplet diameter in Figure 3 for one nozzle operating condition. The agreement between holography and diffraction is excellent in both the maximum droplet size present and the location of the peak in the distribution. The principle disagreement occurs at small droplet sizes which are below the resolution limit of holography. For these conditions, the resolution limit was estimated to be 20 μm. On the other hand, the agreement between diffraction or holography and the interferometry technique is poor. The dynamic range for these tests was selected to be 8.8 to 88 μm; thus, it is not surprising that the interferometry technique did not measure large droplets. However, the discrepancy between the diffraction and interferometry data at small droplets sizes is unclear.

The principal conclusion from the first phase of this study (Ref. 32) was that despite the fact that interferometry has a high potential for making the measurements required for completely characterizing nozzle performance, there are several considerations which restrict its use. Principally, the limited dynamic range dictates that multiple measurements are required in order to cover the broad size distribution typically encountered in sprays. Also, the high droplet densities produced by larger nozzles can result in multiple scattering problems unless special precautions are taken to minimize probe volume sizes. Finally, since the technique supplies measurements at a single point, a large number of measurements are required to completely characterize a spray field. These limitations result in the interferometry data being very tedious to take and difficult to interpret.

The diffraction technique was found to supply a rapid and accurate measurement of the droplet size distribution produced by fuel oil nozzles. The major limitations involved with its use was under conditions whose strong velocity gradients exist such as near the nozzle exit. The measured mean droplet size was found to be strongly dependent on distance in these regions; likely due to the preferential deceleration of smaller droplets. This restriction implies that measurement can only be performed in regions away from the nozzle exit where all droplet sizes have relaxed to a common velocity.

The methodology developed for the complete characterization of fuel-oil nozzles involves the use of a variety of diagnostic techniques. The principal diagnostic is the laser diffraction measurement which yields a rapid characterization of droplet size distribution. It can yield spatial information if masking techniques or deconvoluting techniques (Ref, 35,36) are applied. For fuel distribution measurements the preferred technique is high-speed shadowgraph techniques (Ref. 32) which can yield qualitative information on droplet concentration, flow direction and velocity. Where detailed measurements are required, the LDA/Interferometry may have some application.

NOZZLE PERFORMANCE

There are a variety of twin-fluid fuel-oil nozzles currently available, each having different configurations. In Figure 4 is shown schematics of three nozzles that have been characterized using the laser diffraction technique. In the Delavan nozzle, an oil stream is directed down the center of the nozzle with a relatively low velocity. This oil stream is broken into droplets with a high-velocity sheet of air which enters over a distributor at the tip of the nozzle. The Y-jet nozzle has the same basic "plain jet" atomization process as the Delavan. For the Y-jet, the oil flow is divided into twelve separate streams, each of which is subjected to a high-velocity cross flow of air from separate air jets. The Sonicore nozzle represents a second class of nozzles similar to the prefilming type of nozzle utilized in some aircraft engines. The air is conveyed down the center core of the nozzle and the fuel oil is introduced downstream of the throat of a converging-diverging section. The atomization occurs as the sheet of oil is subjected to the high-velocity air stream. The Sonicore nozzle also includes a resonator cap which is designed to enhance atomization by reflecting shockwaves from the expanding air stream. However, little difference has been determined in the measured size distribution when the resonator cap was removed.

The important design features which govern the spray quality of twin-fluid atomizers are as follows:

- Type of atomization; e.g., plain jet or prefilming
- Mass ratio of air flow to liquid flow
- Air velocity
- Nozzle scale

Of these, the most important has been found to be the air velocity (Ref. 7) which is determined by the nozzle design and the air/liquid mass flow ratio. Spray quality data for ten different commercial nozzles are shown in Figure 5 as measured with the laser diffraction technique both at IFRF (Ref. 26) and at EER (Ref. 32). These include nozzles up to 15 MW in size. Although there is a large variation among the various nozzles, the generally strong dependence on the mass ratio is obvious. The differences between the correlations are likely due to the different air velocities caused by the differences in nozzle design.

The relationship between nozzle design and velocity determines the required atomizer pressure drop.

Larger nozzles are typically operated at lower air/oil mass ratios due to the very large energy required to achieve high velocities and high air/oil mass ratios, and hence do not achieve high atomization quality. This is shown in Figure 6 for the Sonicore nozzle at three scales from 20 kW (0.5 g/sec) to 15 MW (280 g/sec). The small nozzles can achieve high quality atomization by using low air-to-liquid gas ratios, but these ratios would be restrictively high for larger scales. These data also suggest that there is a dependence on scale which cannot be accounted for by velocity and air/oil ratio. This observation is consistent with previous results for prefilming nozzles which have found that atomization quality decreases with increasing scale (Ref. 7).

In addition to nozzle design, liquid properties such as viscosity, density, and surface tension strongly impact atomization quality. For fuel oils, the most important of these is viscosity due to the wide variation that can occur between fuel types. For example, the viscosity of a number 2 fuel oil can be as low as 6 cSt, while a number 6 fuel oil can have viscosities in excess of 10,000 cSt. The impact of viscosity on two different nozzles, the Sonicore and Delavan is shown in Figure 7. The increase in viscosity results in larger droplet sizes and is consistent with a power dependence on mean droplet diameter of .4.

The atomization of mixtures such as coal-oil and coal-water mixtures is not well understood. These will likely have complex liquid properties which will have an uncertain effect on the mechanisms of atomization. Also, the presence of the size distribution of solid particles further complicates the problem. A comparison of the atomization quality for coal-water and coal-oil mixtures with a fuel oil is supplied in Figure 8 for the Delavan nozzle. High atomization quality can be achieved for these mixtures only at very high air flow rates. Both an increase in the coal particle size and an increase in the mass loading of solids were found to be detrimental to atomization quality. More research is required to quantify the impact of these parameters and to optimize the design of nozzles for the efficient atomization of these mixtures.

SUMMARY

The present study was undertaken to characterize the performance of commercially available fuel oil nozzles on real fuels at a variety of scales. The measurements are necessary to the exploration of pollutant formation in combustors and boilers operating on both conventional and alternative fuels. The characterization methodology developed and tested utilized specially designed spray rigs and optical diagnostic techniques for measurement of droplet size, velocity, and fuel distribution. Laser diffraction and high-speed shadowgraph techniques were found to be the most appropriate techniques for testing large-scale (up to 30 MW) nozzle performance. Laser interferometry (LDA/visibility) was found to have severe limitations for such measurements but may be necessary where detailed point measurements of velocity and size are required. Using the laser diffraction technique, the atomization quality produced by a variety of twin-fluid fuel-oil nozzles was found to be most dependent on the mass ratio of fuel to air utilized by the nozzle and the viscosity of the liquid fuel. For mixtures of pulverized solids and liquids, the atomization quality was found to be dependent both on the mass loading and on the size distribution of the solid phase.

ACKNOWLEDGEMENTS

This work is supported by the EPA under the Fundamental Combustion Research Applied to Pollution Formation Program, Contract 68-02-3633. Steve Lanier is the EPA project officer. The technical assistance of P. Sampson and R. Garcia is gratefully acknowledged.

REFERENCES

1. Goldstein, H. L. and G. W. Siegmund. Factors Affecting Particulate Emission From Combustion of Residual Fuel Oil. Proceedings of 1st Chemical Congress of North American Continent, American Chemical Society, Mexico City, 1975.

2. Kramlich, J. C., G. S. Samuelsen, and W. R. Seeker. Carbonaceous Particulate Formation from Synthetic Fuel Droplets. Fall Meeting of the Western States Section of the Combustion Institute, Paper No. WSS/CI 81-52, 1981.

3. Kramlich, J. C., R. Payne, and G. E. England. Soot Formation from Synthetic Fuel Droplets. 183rd National Meeting, American Chemical Society, Las Vegas, 1982.

4. England, G. C., M. P. Heap, R. T. Horton, D. W. Pershing, and G. Flament. The Control of Pollutant Formation in Fuel Oil Flames--The Influence of Oil Properties and Spray Characteristics. In: Proceedings of the Third Stationary Source Combustion Symposium; Volume II. Advanced Processes and Special Topics, EPA-600/7-79-050b, 1979. p. 41.

5. Heap, M. P., D. W. Pershing, G. C. England, J. W. Lee, S. L. Chen. The Influence of Fuel Characteristics on Nitrogen Oxide Formation--Bench-Scale Studies. In: Proceedings of the Third Stationary Source Combustion Symposium; Volume II. Advanced Processes and Special Topics, EPA-600/7/79-050b, 1979. p. 3.

6. Nazami, A. A. and N. P. Cernansky. A Monodisperse Spray Combustion System and the Measurement of Oxides of Nitrogen. The Spring Meeting of the Western States Section of the Combustion Institute. Boulder, Colorado, WSS/CI Paper No. 78-37, 1978.

7. Lefebvre, A. H. Airblast Atomization. Prog. Energy Combust. Sci., 6:233-261, 1980.

8. Kuhn, R. Atomization of Liquid Fuels. NACA Technical Memorandum 329-331, 1925.

9. Lee, D. W. The Effect of Nozzle Design and Operating Conditions on the Atomization and Distribution of Fuel Sprays. NACA Report 425, 1925.

10. Nukiyama, S., and Y. Tanasawa. An Experiment on the Atomization of Liquid by Means of an Airstream. Transactions of the Society of Mechanical Engineers, 4, S-13, 1938.

11. Woolridge, A. L. A Photographic Technique for the Determination of Sizes of Liquid Droplets. CWL Special Publication 3-6, U.S. Army Chemical Warfare Laboratories, 1959.

12. Tate, R. W. Immersion Sampling of Spray Droplets. AIChE Journal 7: 574, 1961.

13. Taylor, E. H., and D. B. Harmon. Measuring Drop Sizes in Sprays. Industrial and Engineering Chemistry, 46, 1955.

14. Joyce, J. R. The Wax Method of Spray Particle Size Measurement. Tech. Rept. I. C. T./7, Shell Petroleum Co., Ltd., London, England, 1946.

15. May, K. R. The Cascade Impactor: An Instrument for Sampling Coarse Aerosols. Journal of Scientific Instrumentation, 22:187, 1945.

16. Stubbs, H. E., and J. L. York. Photographic Analysis of Sprays. Transaction of the American Society of Mechanical Engineers, 74:1157, 1952.

17. DeCorso, S. M. A Photographic Method of Determining the Drop-Size Distribution of a Spray. Research Report 8-0524-R32, Westinghouse Research Laboratories, Pittsburgh, PA, 1958.

18. Dobbins, R. A., L. Crocco, and L. Glassman. Measurement of Mean Particle Sizes of Sprays from Diffractively Scattered Light. AIAA Journal, 1:1882, 1963.

19. Ingebo, R. D. Atomization, Acceleration, and Vaporization of Liquid Fuels. Sixth Symposium (International) on Combustion, The Combustion Institute, New York, 1957. p. 684

20. Polymeropoulos, C. E., and V. Sernas. Measurement of Droplet Size and Fuel-Air Ratio in Sprays. Combustion and Flame, 29:123, 1977.

21. Webster, R. P., R. P. Weight, and E. Archenhold. Holographic Size Analysis of Burning Sprays. Combustion and Flame, 27:395, 1976.

22. Feinstein, S. P., and M. A. Girard. Feasibility of Automated Drop-Size Distributions from Holographic Data Using Digital Image Processing Tech. niques. AIA Paper 79-0297, presented at the 17th Aerospace Sciences Meeting, New Orleans, 1979,

23. Simmons, H. C., and D. L. Lapera. A High-Speed Spray Analyzer for Gas Turbine Fuel Nozzles. Paper presented at ASME Gas Turbine Conference, Cleveland, March, 1969.

24. Simmons, H. C. The Correlation of Drop-Size Distributions in Fuel Nozzle Sprays. Journal of Engineering for Power, 99(3):309, 1977.

25. Flament, G., and R. Payne. Effects of Fuel Properties and Atomization Parameters on NO_x Control for Heavy Liquid Fuel-Fired Package Boilers. Final Report, Subcontract EER-8317-1 (Energy and Environmental Research Corporation), IFRF Doc. No. 3130110.

26. Payne, R., G. Flament, S. Michelfelder, and G. C. England. Characterization of Fuel Atomizers Using a Laser Diffraction Droplet Size Analyzer. VDI-Berichte, Number 346:103-110, 1979.

27. Tishkoff, J. M., D. C. Hammond, and A. R. Chraplyvy. Diagnostic Measurements of Fuel Spray Dispersion. Presented at the ASME Winter Annual Meeting, Paper 80-WA/HT-3J, 1980.

28. Negus, C., and B. J. Azzopardi. The Malvern Particle Size Distribution Analyzer: Its Accuracy and Limitations. Harwell Report AERE-R 9075, 1978.

29. Swithenbank, J., J. M. Beér, D. S. Taylor, D. Abbot, and G. C. McCreath. A Laser Diagnostic Technique for the Measurement of Droplet and Particle Size Distribution. University of Sheffield, Department of Chemical Engineering and Fuel Technology Report HIC 245. 1976

30. Farmer, W. M. The Interferometric Observation of Dynamic Particle Size, Velocity, and Number Density. Ph.D. Thesis, University of Tennessee, 1973.

31. Bachalo, W. D. Method for Measuring the Size and Velocity of Spheres by Dual-Beam Light-scatter Interferometry. Applied Optics, 19: 363, 1980.

32. Seeker, W. R. and G. S. Samuelsen. Spray Characterization. Volume III, Section IV, Final Report Contract 68-02-2631. U.S. Environmental Protection Agency, Research Triangle Park, North Carolina, 1982.

33. Samuelsen, G. S., J. D. Trolinger, M. P. Heap, and W. R. Seeker. Observations of the Behavior of Coal Particles During Thermal Decomposition. Combustion and Flame, 40:7-12, 1981.

34. Seeker, W. R., and M. P. Heap. The High Temperature Decomposition and Combustion of Pulverized Coal. Volume II, Section III. Final Report, Contract 68-02-2631. U.S. Environmental Protection Agency, Research Triangle Park, NC, 1982.

35. Yule, A.J., C. AH Seng, P. G. Felton, A. Ungut, and N. A. Chigier. A Laser Tomographic Investigation of Liquid Fuel Sprays. Eighteenth Symposium (International) on Combustion. The Combustion Institute, Pittsburgh, PA, 1981. pp. 1501-1510.

36. Hammond, D. C. A Deconvoluting Technique for Line-of-Sight Optical Scattering Measurements in Axisymmetric Sprays. Publication GMR-3361. General Motors Research Laboratory, Warren, Michigan, 1980. Accepted for publication in Applied Optics.

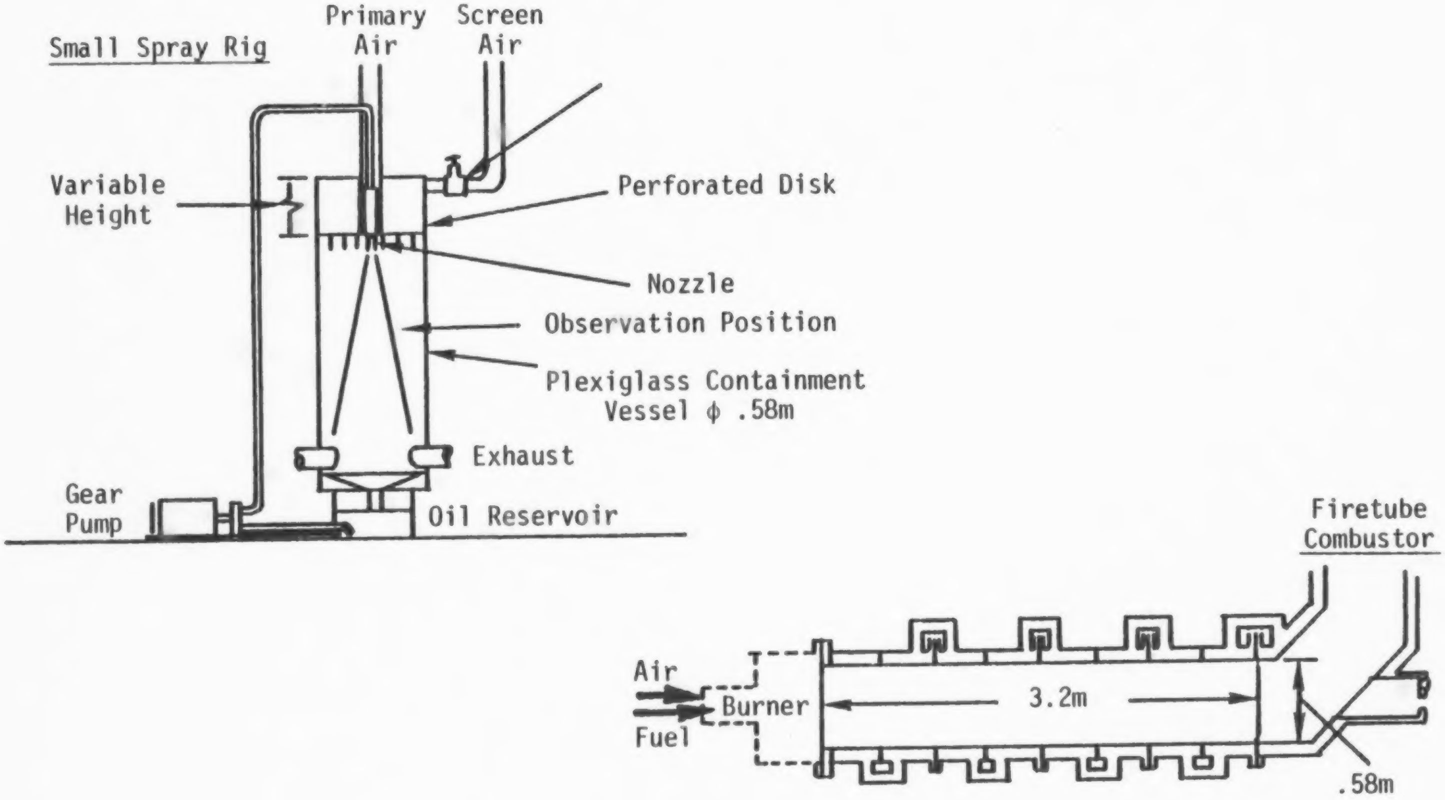
Small Spray Rig
Primary Air
Screen Air
Variable Height
Perforated Disk
Nozzle
Observation Position
Plexiglass Containment Vessel ϕ .58m
Exhaust
Gear Pump
Oil Reservoir
Firetube Combustor
Air
Fuel
Burner
3.2m
.58m

Figure 1. Schematic of small spray rig for characterizing fuel oil nozzles up to 3 x 10^6 Btu/hr and EER firetube combustor.

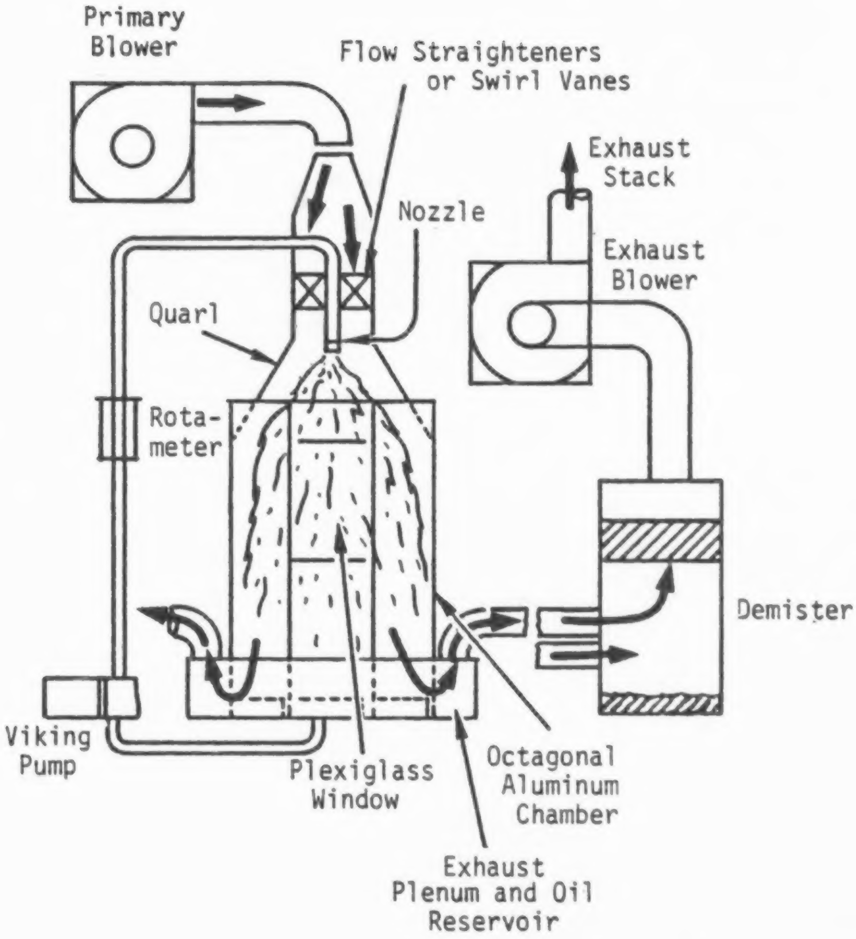
Primary Blower
Flow Straighteners or Swirl Vanes
Exhaust Stack
Nozzle
Exhaust Blower
Quarl
Rota-meter
Demister
Viking Pump
Plexiglass Window
Octagonal Aluminum Chamber
Exhaust Plenum and Oil Reservoir

Figure 2. Large spray rig facility for nozzle characterization up to 100×10^6 Btu/hr.

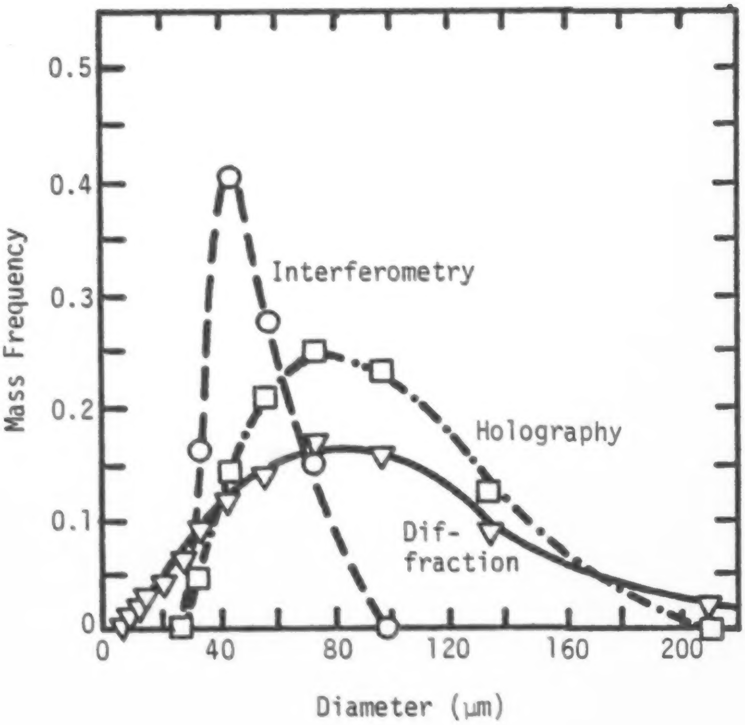

Figure 3. Interferometric, diffraction, and holographic data--weight density atomizing pressure (1.34 atm, 20 cm from nozzle).

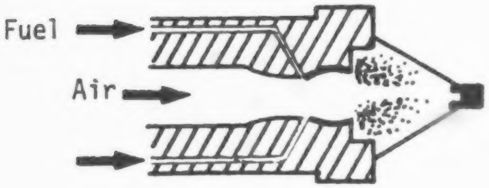

Sonicore

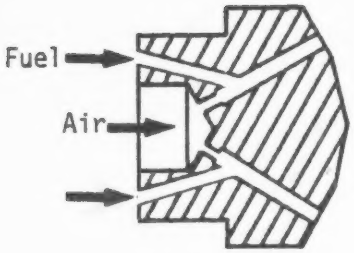

Y-Jet

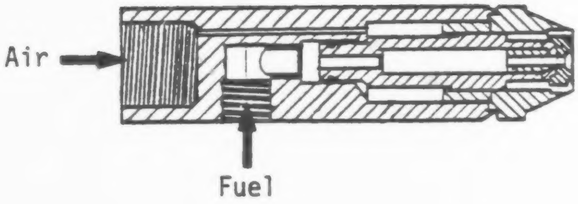

Delavan

Figure 4. Schematics of three twin-fluid nozzles characterized.

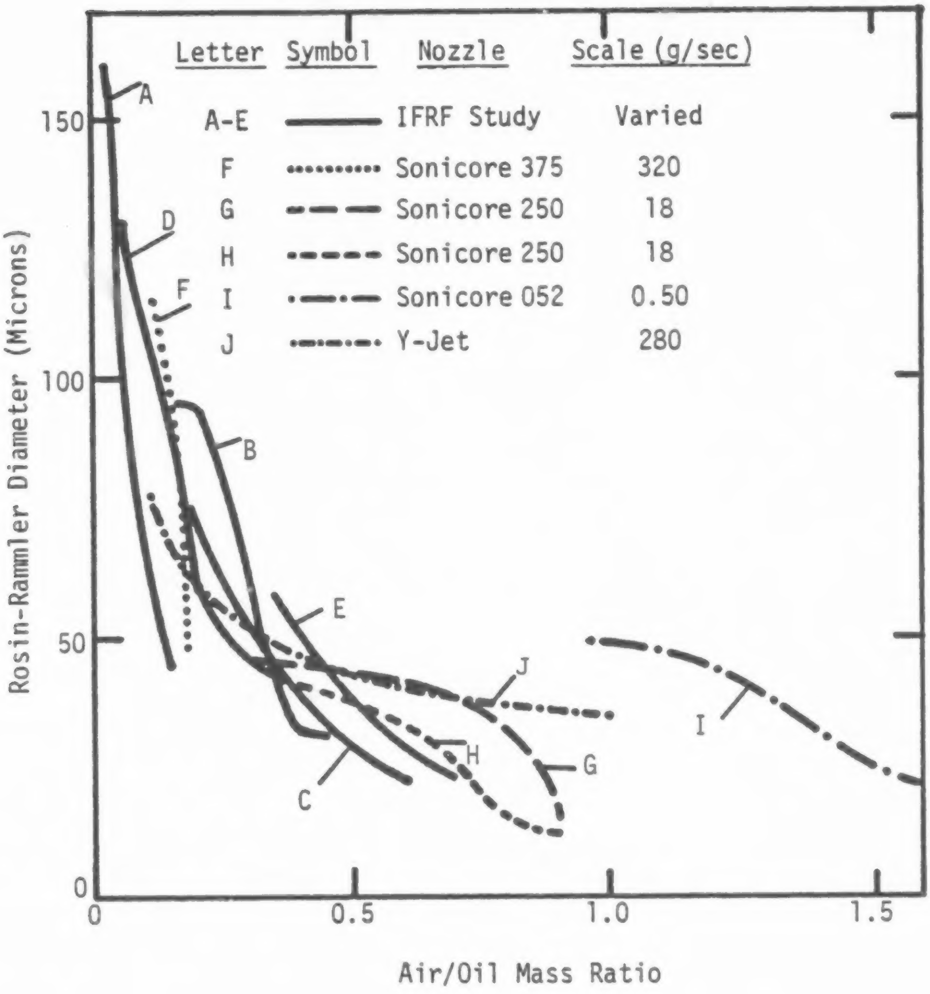

Figure 5. Influence of mass ratio of atomizing air to liquid flow on atomization quality of ten twin-fluid nozzles (No. 2 fuel oil, 5 cSt viscosity).

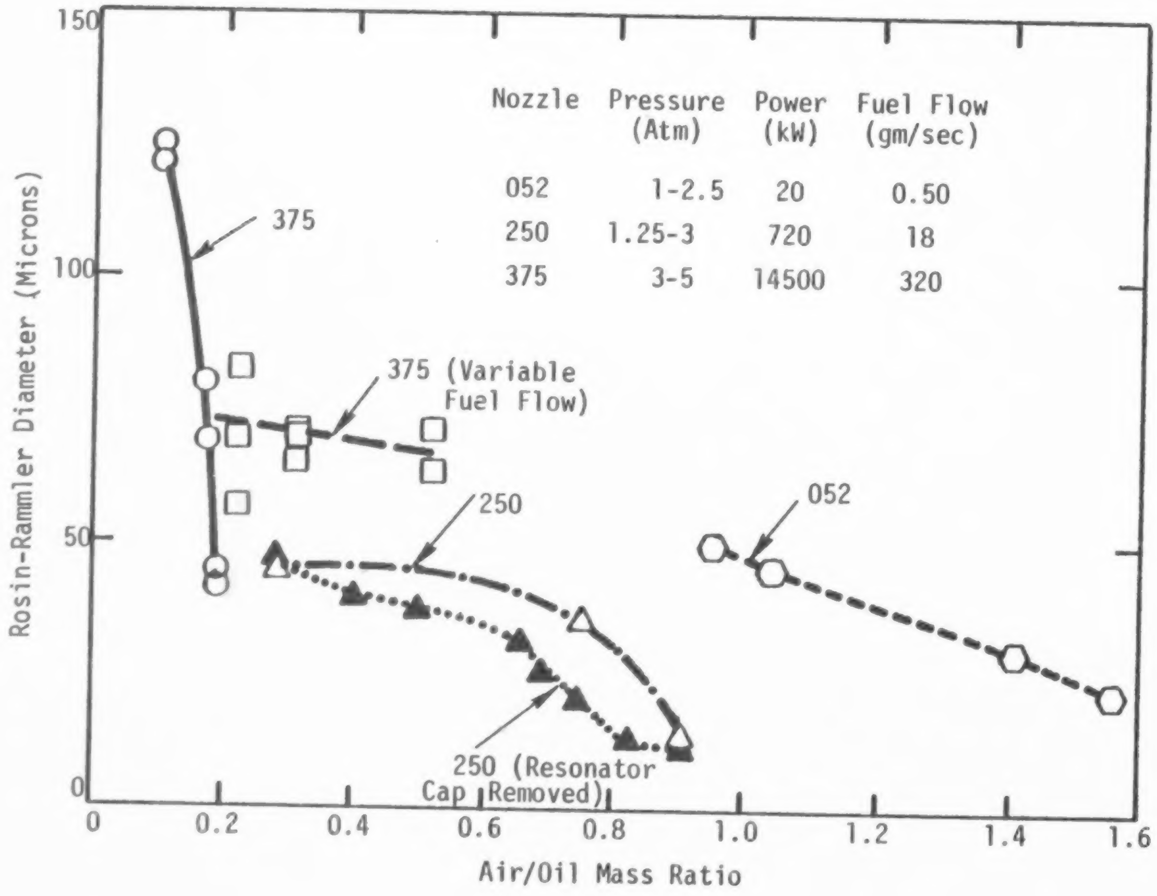

Figure 6. Influence of Sonicore nozzle scale on atomization quality (No. 2 fuel oil).

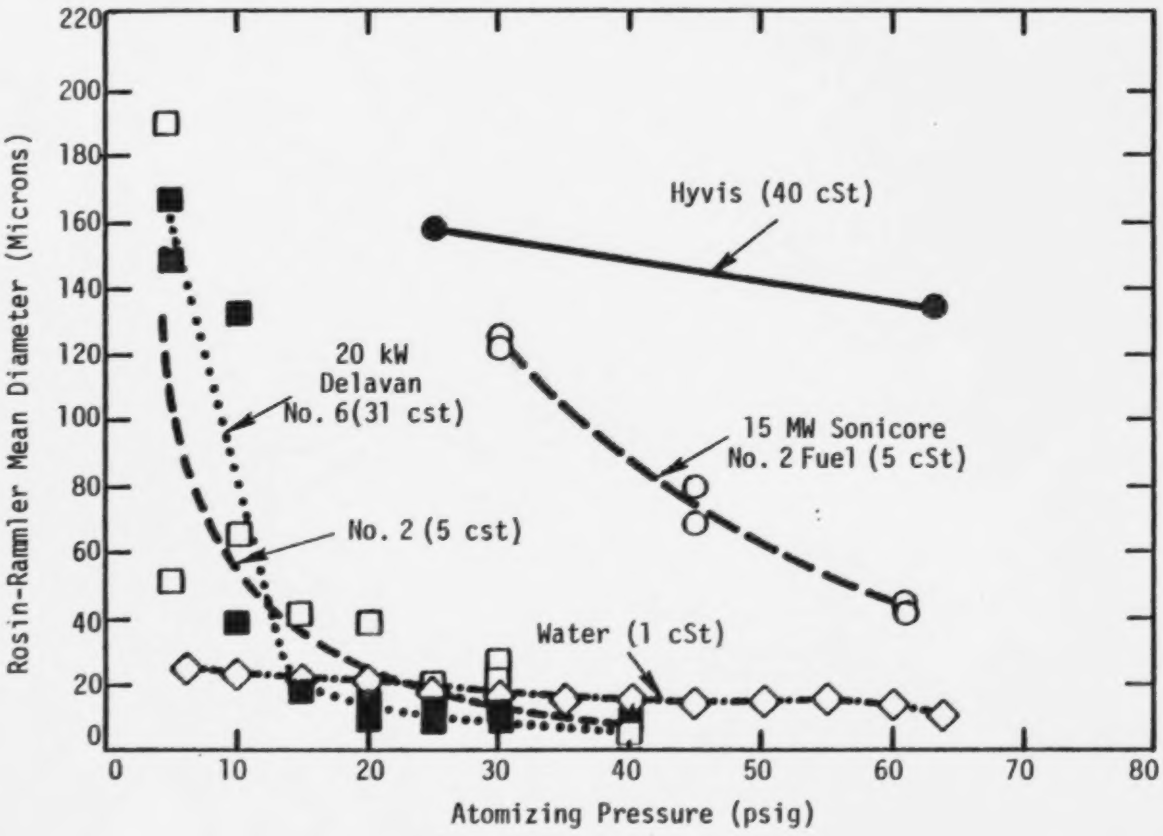

Figure 7. Influence of viscosity of atomization quality from 15 MW Sonicore and 20 kW Delavan nozzles.

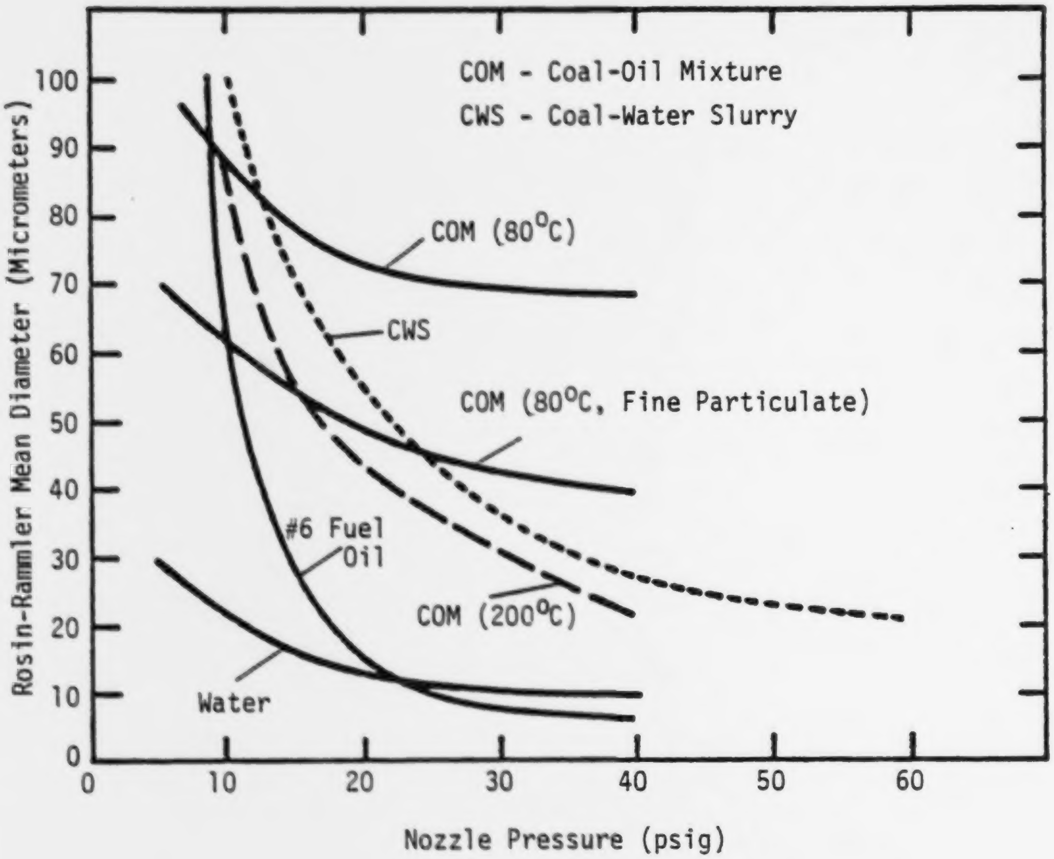

Figure 8. Influence of fuel formulation on atomization quality from Delavan nozzle (Model 30610-8, temperature denotes slurry temperature at nozzle exit, oil slurries differ by fineness of particulate phase).

THE EVOLUTION OF FUEL BOUND NITROGEN DURING HEAVY OIL PYROLYSIS

By:

S. P. Hanson, J. M. Beér, and A. F. Sarofim
Department of Chemical Engineering
Massachusetts Institute of Technology
Cambridge, MA 02139

"Although the research described in this article has been funded wholly or in part by the United States Environmental Protection Agency through contract or grants 805552030 and CR80-884801 to the Massachusetts Institute of Technology, it has not been subjected to the Agency's required peer and policy review and therefore does not necessarily reflect the views of the Agency and no official endorsement should be inferred."

ABSTRACT

The evolution by fuel oils of nitrogeneous species during pyrolysis of droplets 150 μm in diameter at furnace temperatures of 1000, 1200 and 1400 K were compared with the evolution of nitrogen during equilibrium distillation. For equilibrium conditions, the nitrogen evolution from a Gulf Coast No. 6 and Indo-Malaysian No. 6 oils lagged the total mass evolution, indicating that the nitrogen is in high molecular weight compounds. For shale oil, the nitrogen evolution paralleled the mass evolution suggesting the nitrogen compounds were distributed throughout the mass spectrum. Under rapid heating in the furnace, significant departure from equilibrium distillation was observed. For the Gulf Coast No. 6 and the later stages of distillation of the Indo-Malaysian oil, the nitrogen evolution was much more rapid than under equilibrium conditions. For the shale oil, following an initial nitrogen-free mass evolution, the nitrogen loss was in proportion to the mass loss. The departure from equilibrium distillation can be explained in terms of diffusional effects within the vaporizing droplets.

INTRODUCTION

The viability of staged combustion for control of NO_x emissions during the combustion of nitrogen-containing oils depends upon the release of nitrogen in the fuel-rich stage. Inasmuch as the nitrogen in residual fuel oils has a low volatility, there is a concern that the nitrogen may be retained in an unburned, possibly coked, residue from the first fuel-rich stage and be converted to nitric oxide with a relatively high efficiency in the fuel lean second stage. The present study of the evolution of fuel bound nitrogen during the vaporization of fuel droplets has been motivated by this concern.

The evolution of fuel-nitrogen from multicomponent fuel droplets is controlled by the coupling of transport processes in the gas and liquid phases through the thermodynamic equilibria between phases. The objective of this investigation has been to identify those factors of significance during the vaporization of multicomponent fuel droplets to show how these factors may influence the rate of evolution of nitrogenous species from heavy fuel oils. Experiments were performed(1) in a laminar flow drop-tube furnace, Fig. 1, on a linear array of 150 μm diameter fuel particles. The conditions to which the particles were subjected conformed to those found in the first stage of a multi-staged combustor.

Data on the evolution of fuel-nitrogen and rates of vaporization in an inert atmosphere at temperatures between 1000 K and 1400 K were obtained for a raw Paraho shale oil, a Gulf Coast No. 6 petroleum fuel oil, and Indo-Malaysian No. 6 Petroleum fuel oil. The evolution of fuel-nitrogen and residual carbon-to-hydrogen ratios of vaporizing droplet arrays of these fuels were compared with similar data obtained from equilibrium batch distillation experiements. It was found that the fuel-nitrogen evolution from vaporizing droplets differs significantly from that found from equilibrium batch distillation. The difference is due to diffusional resistance in the interior of the droplets which modifies the liquid surface composition, thereby changing the contribution of fuel components in the vapor phase.

The nitrogen evolution from droplets of fuels which contain their nitrogen primarily in the heavier fuel components was greater than batch distillation nitrogen evolution at equivalent extents of vaporization. However, for fuels in which the nitrogen content is associated with the intermediate molecular weight fuel species, the nitrogen evolution from vaporizing droplets is retarded in comparison to batch distillation nitrogen evolution, and the degree of retardation is temperature dependent. The observed behaviors during droplet vaporization result from an initial preference for the evolution of light, volatile, mobile components followed by an accelerated evolution of heavy fuel species. The extent of vaporization at which the change of preference occurs depends upon the fuel composition and the rate of vaporization.

RESULTS

The compositions and other properties of the heavy fuel oils are presented in Table 1. The carbon-to-hydrogen atomic ratio for the petroleum-based fuels and the shale oil are all about 0.6. The nitrogen content is particularly high for shale oil, 2.21% by weight, and lowest for the Indo-Malaysian petroleum fuel oil, 0.23% by weight.

Equilibrium Distillation Results

The Gulf Coast No. 6 petroleum, the Indo-Malaysian No. 6 petroleum, and the raw Paraho shale oil have boiling curves, Fig. 2, that range mostly between 600 K and 800 K for the first 80% extent of vaporization. The low initial boiling point of the Gulf Coast No. 6 petroleum fuel oil, and more rapid temperature increase is indicative of a broader spectrum of chemical species than associated with the Indo-Malaysian No. 6 petroleum fuel oil, and the shale oil.

The carbon-to-hydrogen atomic ratio of the fuel residue, normalized with respect to the carbon-to-hydrogen atomic ratio of the original fuel, offers an indication of the composition of the vaporized material. The normalized carbon-to-hydrogen atomic ratio for the petroleum fuel oils and the shale oil, Fig. 3, shows that the Gulf Coast No. 6 petroleum fuel oil undergoes a continual loss of the relatively lighter species, in agreement with the large and steep temperature change of its boiling curve, Fig. 2. The Indo-Malasian No. 6 petroleum fuel oil exhibits a similar behavior, but to a lesser degree, in agreement with its boiling curve. The raw Paraho shale oil, which has a boiling curve similar to the Indo-Malaysian No. 6 petroleum fuel oil, shows no tendency to increase its carbon-to-hydrogen atomic ratio during the course of equilibrium distillation.

Figure 4 shows the fractional evolution of nitrogen during the course of equilibrium atmospheric distillation for the petroleum fuel oils and shale oil. The Gulf Coast No. 6 petroleum and Indo-Malaysian No. 6 petroleum fuel oils have almost identical nitrogen evolutions, the bulk of their nitrogen being retained in the residue. Thus the nitrogen is primarily associated with the heavy species in these fuels. The raw Paraho shale oil evolves its nitrogen in proportion to its mass. Thus the nitrogen is either broadly distributed with respect to species molecular weight; or associated with intermediate molecular weight species in a mixture of many species, each in low concentration; or associated with a mixture of species having a narrow spectrum of molecular weights. The first of these descriptions is correct, as supported by shale oil analyses(2).

Furnace Pyrolysis Results

Due to the possibility of internal boiling it is not practical to use particle size as a measure of mass when dealing with heavy fuel oils. Shale oil is a typical example. When 150 micrometer droplets of shale oil are injected into the helium atmosphere of the laminar flow furnace at 1000 K, they are seen to swell to three times their original diameter, Fig. 5, even though 50% of the mass has been vaporized.

The spatial mass variation, obtained when sampling, must be correlated against the particle velocity history in order to yield the temporal variation in mass for a vaporizing particle. The velocity is determined, because of the highly ordered droplet array used for these experiments, by the particle injection frequency. The interdrop spacing is a function of the vaporization rate of the particle array, it being observed that the array initially increases its interdrop spacing as vaporization begins, and thereafter, gradually adjusts the interdrop spacing as the rate of vaporization and mass of the particles change. Thus the maximum residence time in the test zone of the furnace is determined by the injection frequency and vaporization rate of the array, given a constant initial particle size. The particular velocity variation along a vaporizing droplet array is a function of fuel type, rate of particle generation, furnace temperature, and furnace gas composition.

Figure 6 shows the velocity profiles of the fuels investigated. The injection velocities differ in order that stable droplet arrays may be generated with each fuel. The increase in velocity for increasing furnace temperature is seen to be only slight when compared at a single furnace location. However, the integrated effect of this velocity difference may reduce residence times at 1400 K to 90% that at 1000 K. The Gulf Coast No. 6 petroleum is remarkable for its initially rapid vaporization, Fig. 7. The Indo-Malaysian No. 6 petroleum fuel oil and the raw Paraho shale oil have similar behaviors matching that typically observed for heavy fuels.

The Gulf Coast No. 6 petroleum fuel oil shows little change in its carbon-to-hydrogen content, Fig. 8, except at high temperatures and large extents of vaporization. The Indo-Malaysian No. 6 petroleum shows no variation in carbon-to-hydrogen ratio after an initial increase. The raw Paraho shale oil is strongly temperature dependent with respect to the carbon-to-hydrogen ratio of the vaporizing droplet array, becoming carbon rich to greater degrees and at lower extents of vaporization with increasing furnace temperature. This above behavior is completely different from that observed for equilibrium bulk distillation.

The Gulf Coast No. 6 petroleum evolves nitrogen from a rapidly vaporizing droplet array in proportion to the mass vaporized, Fig. 9, without any apparent dependence on temperature. The Indo-Malaysian No. 6 petroleum, Fig. 10, exhibits an initial evolution of nitrogen free material, following which a rapid increase in nitrogen evolution occurs at about 20% extent of vaporization, which eventually lessens until the nitrogen is evolved at rate approximately proportional to the mass evolved. The raw Paraho shale oil has a temperature dependent nitrogen evolution, Fig. 11. At furnace temperatures below 1000 K, the fractional evolution of nitrogen is similar to that for equilibrium bulk distillation. However, as the furnace temperature increases, a progressively larger amount of nitrogen free mass is evolved. Thereafter the nitrogen appears to be evolved in proportion to the mass vaporized.

DISCUSSION

When considering the evolution of fuel nitrogen during the vaporization of heavy fuel oils it must be remembered that the nitrogen is associated with many fuel components all of which are contributing to the total nitrogen evolution to some extent. The molecular weight of the compound in which the nitrogen is found influences the ability of the nitrogen to escape in several ways: the higher the molecular weight, the less volatile is the compound relative to the other fuel components at the surface and the less mobile is the compound relative to the other fuel components within the droplets; also, for a given nitrogen content, the mass of the fuel with which the nitrogen is associated increases.

The equilibrium batch distillation of a fuel reveals the nitrogen evolution under well mixed conditions. Data of this sort is often used as an indication of the nitrogen evolution from atomized fuels, however, it is better used as the vaporization rate limited case of droplet vaporization, i.e. internal mixing is rapid compared to the rate of droplet vaporization. The evolution of nitrogen from a rapidly vaporizing droplet does not match equilibrium nitrogen evolution after the initial few percent extent of mass evolution. This is because internal mixing is not rapid for droplets having diameters of the order of 100 micrometers, undergoing vaporization at rates typical of practical combustion systems(3). The differentiation of fuel species, over that affected by volatility differences, represented by the equilibrium distillation data, is due to diffusional resistance in the liquid phase, and droplet surface regression.

Temperature gradients within vaporizing fuel droplets are small, but concentration gradients cannot be neglected ($Le>20$). The droplet temperature is not constant with time but follows the surface temperature which is affected by the changing surface composition. For a 100 micrometer kerosene fuel droplet, the temperature lag was found to be about 2 Celcius degrees(4), but for heavy fuel oils the lag would be greater, and subject to abrupt changes in surface temperature. Nevertheless, once vaporization has begun the heat capacity of the droplet is small compared to the latent heat content of the vaporized material. Thus the rate of vaporization is controlled by gas phase energy transport processes, whereas the evolution of a particular fuel component is determined by liquid phase mass transport processes modified by surface regression and component volatility at the droplet surface. The resultant evolution of fuel-nitrogen is the summation of the evolution of nitrogenous components, and is therefore highly dependent upon the nitrogen distribution among the fuel components.

The Gulf Coast No. 6 petroleum and Indo-Malaysian No. 6 petroleum fuel oils have most of their nitrogen associated with heavy fuel components and during equilibrium batch distillation retain much of this nitrogen in a non-distillate residue. The carbon-to-hydrogen ratio gradually increases due to the progressive loss of the lighter fuel components. The nitrogen evolution from the vaporizing droplet array is greatly in excess of the equilibrium values. The Gulf Coast fuel oil uniformly evolves its nitrogen with mass, and the Indo-Malaysian fuel oil, after an initial evolution of nitrogen free mass, behaves similarly. The carbon to hydrogen ratios of the fuel droplets do not vary significantly except for an initial rapid increase for the Indo-Malaysian fuel oil, which corresponds to the evolution of nitrogen free material. Apparently, after an initial period of conditioning, during which light fractions are vaporized a surface composition is established having a higher temperature and higher concentration of heavy molecular weight compounds than the average composition would dictate. The higher relative volatility of the heavy species at the surface allows the nitrogenous compounds to be evolved together with the other fuel components, thus preventing the formation of a non-distillable nitrogen-rich concentrate. Pyrolysis of the nitrogen-containing compounds may contribute to the increase in relative volatility.

The raw Paraho shale oil presents a case in which the nitrogen species are distributed among the intermediate and heavy molecular weight fuel species. The broad distribution of nitrogen results in the uniform nitrogen evolution with mass during equilibrium batch distillation. The presence of a light nitrogen free fraction is not evident from batch distillation results. This is as a consequence of simultaneous evolution of a portion of the intermediate molecular weight nitrogenous compounds, caused by the similarity of, or strong interaction between the fuel species as evidenced by an invariant carbon-to-hydrogen ratio. The nitrogen evolution from a vaporizing droplet at 1000K is almost identical to the equilibrium evolution presumably due to the fuel species similarity or strong interactions. However, with increasing furnace temperature, the effects of diffusional resistance become evident, and light nitrogen free material is initially evolved until a surface composition is attained that permits the nitrogenous compounds to be evolved. The evolution of each nitrogenous compound is diffusionally limited to a different extent, thus although the nitrogen is evolved in proportion to the mass, the contributions of the nitrogenous compounds in the vapor differ from batch distillation composition and also differ with vaporization rate as reflected in a temperature dependent variation of carbon-to-hydrogen ratios for the droplet residues.

Confirmation of the importance of diffusion within the droplets was obtained by setting up model experiments with n-dodecane doped with pyridine, acridine, and quinoline. The system was selected because it was amenable to theoretical analysis(3). The theoretical analysis which took into account the concentration gradients within the droplets was able to satisfactorily describe the experimental results, as shown in Fig. 12. Of particular note, are the data on the quinoline doped oil, which shows the characteristic behavior observed with the Malaysian No. 6 oil of first evolving a relatively nitrogen free fraction and then showing a rapid evolution of nitrogen species greatly in excess of that expected from equilibrium distillation.

CONCLUSIONS

The evolution of fuel-nitrogen from vaporization droplets of heavy fuel oils departs significantly from the equilibrium batch distillation nitrogen evolution. The differences observed in the nitrogen evolution of vaporizing droplets as opposed to equilibrium batch distillation are attributable to diffusion limitation in the liquid phase.

The extent to which diffusion limitation plays a role is influenced by the rate of vaporization and the volatility of each nitrogen containing compound with respect to all other fuel components. During the initial stages of vaporization the lower molecular weight compounds have enhanced evolutions, but after some extent of vaporization, determined by the fuel properties and environmental conditions, the heavier molecular weight compounds are evolved at accelerated rates.

A Gulf Coast No. 6 petroleum fuel oil, and Indo-Malaysian No. 6 petroleum fuel oil, all of which have most of their nitrogen content bound to the higher molecular weight fuel components, display rates of nitrogen evolution that were greater than equilibrium distillation results would suggest. The carbon to hydrogen ratio of the fuel residues, which was found to increase during the course of equilibrium distillation, remains uniform with increasing extent of droplet vaporization, thereby inhibiting the formation of a nitrogen rich non-distillable residue which would form a char.

Raw Paraho shale oil which has its nitrogen associated primarily with the intermediate molecular weight fuel species, exhibited an initial nitrogen free weight loss associated with the vaporization of a light fraction. This initial loss of light fraction increased with increasing rate of vaporization. When nitrogen evolution from these fuels commences, it is in proportion to the weight loss, paralleling equilibrium nitrogen evolutions but originating at a higher extent of vaporization due to the initial nitrogen free weight loss.

The retardation in nitrogen evolution from the shale oil is not so great that detrimental effects preclude staged combustion as a method to control fuel-nitrogen conversion to nitric oxide. On the other hand, the Gulf Coast No. 6 and Indo-Malaysian No. 6 petroleum fuel oils behave, both with respect to nitrogen evolution and the tendency to char formation, such that staged combustion appears to be an appropriate method to handle them.

ACKNOWLEDGMENTS

The authors wish to express their thank for the financial support of the work discussed in this paper under EPA Grants No. 805552030 and CR80-884301. The authors wish to acknowledge fruitful discussions with the project monitor W.S. Lanier.

REFERENCES

1. Hanson, S.P. The Evolution of Fuel Nitrogen During the Vaporization of Heavy Fuel Oil Droplet Arrays. Sc.D. Thesis, M.I.T., 1982.
2. Mezey, E.J., Singh, S., and Hissong, D.W. Fuel Contaminants, (Vol 1). Battelle Columbus Laboratories, Report No. EPA-600/2-76-177a, 1976.
3. Hanson S.P., Beer, J.M., and Sarofim, A.F. Non-Equilibrium Effects in the Vaporization of Multicomponent Fuel Droplets. 19th Symposium (International) on Combustion, The Combustion Institute, 1982.
4. Fong, L. S.B. Thesis, M.I.T., Cambridge, MA, 1980.

	(i)	(ii)	(iii)
Ultimate Analysis, %			
Carbon	88.29	87.50	83.63
Hydrogen	12.31	12.41	11.81
Nitrogen	0.44	0.23	2.21
Sulfur	0.47	0.22	0.69
Oxygen	0.86	1.04	1.18
Ash	0.01	0.04	0.09
Water and Sediment	none		1.6
Flash Point, °C	149	99	102
Pour Point, °C	8	16	29
Gross Heat of Combustion, MJ/kg	43.89	44.36	42.86
Specific Gravity @ 15°C	0.9309	0.9230	0.9279

Table 1. Fuel Properties of (i) Gulf Coast No. 6 Petroleum Fuel Oil, (ii) Indo-Malaysian No. 6 Petroleum Fuel Oil, (iii) Raw Paraho Shale Oil

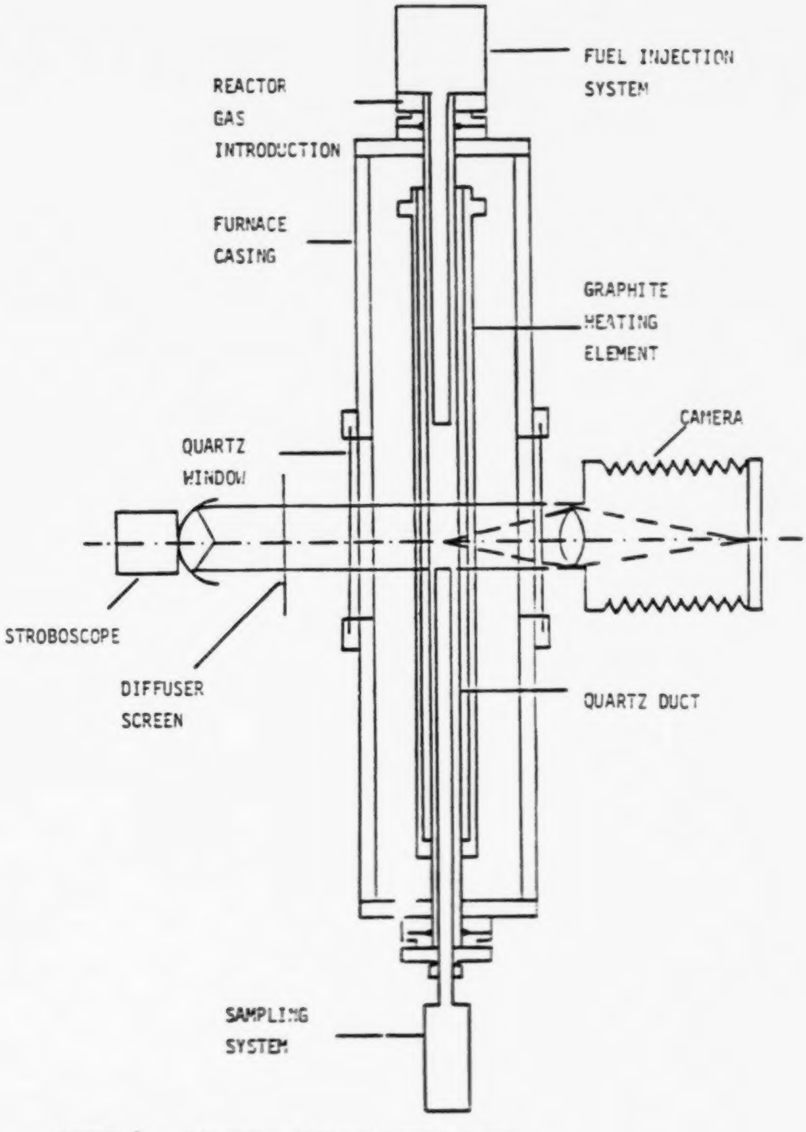
FUEL INJECTION SYSTEM
REACTOR GAS INTRODUCTION
FURNACE CASING
GRAPHITE HEATING ELEMENT
CAMERA
QUARTZ WINDOW
STROBOSCOPE
DIFFUSER SCREEN
QUARTZ DUCT
SAMPLING SYSTEM

FIGURE 1 Schematic of Experimental System

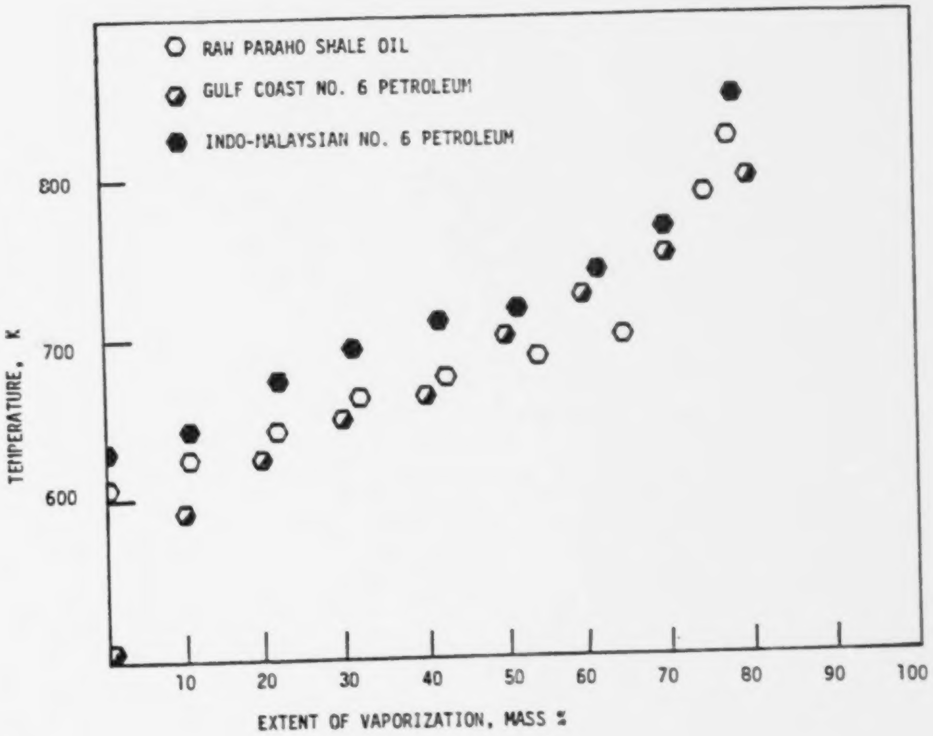

Figure 2 Engler-Type Boiling Point Curves of Gulf Coast No. 6 Petroleum Fuel Oil, Indo-Malaysian No. 6 Petroleum Fuel Oil, and Raw Paraho Shale Oil

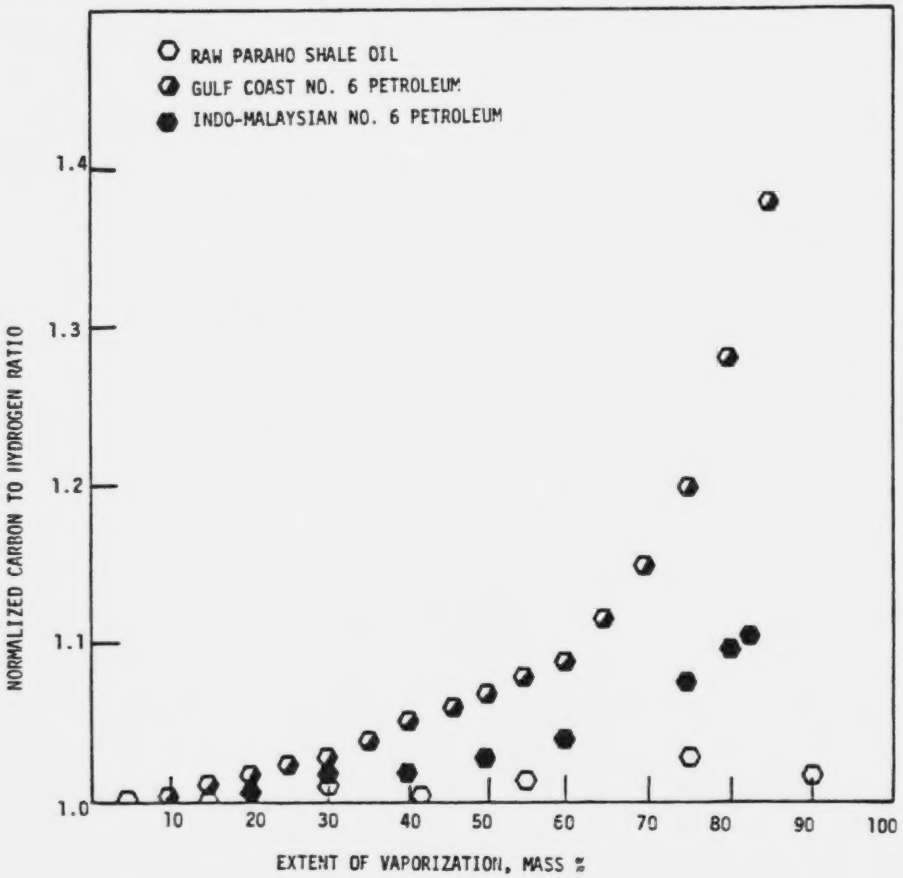

Figure 3 Normalized Carbon to Hydrogen Atomic Ratios of Fuel Residues During Equilibrium Batch Distillation of Gulf Coast No. 6 Petroleum Fuel Oil, Indo-Malaysian No. 6 Petroleum Fuel Oil, and Raw Paraho Shale Oil

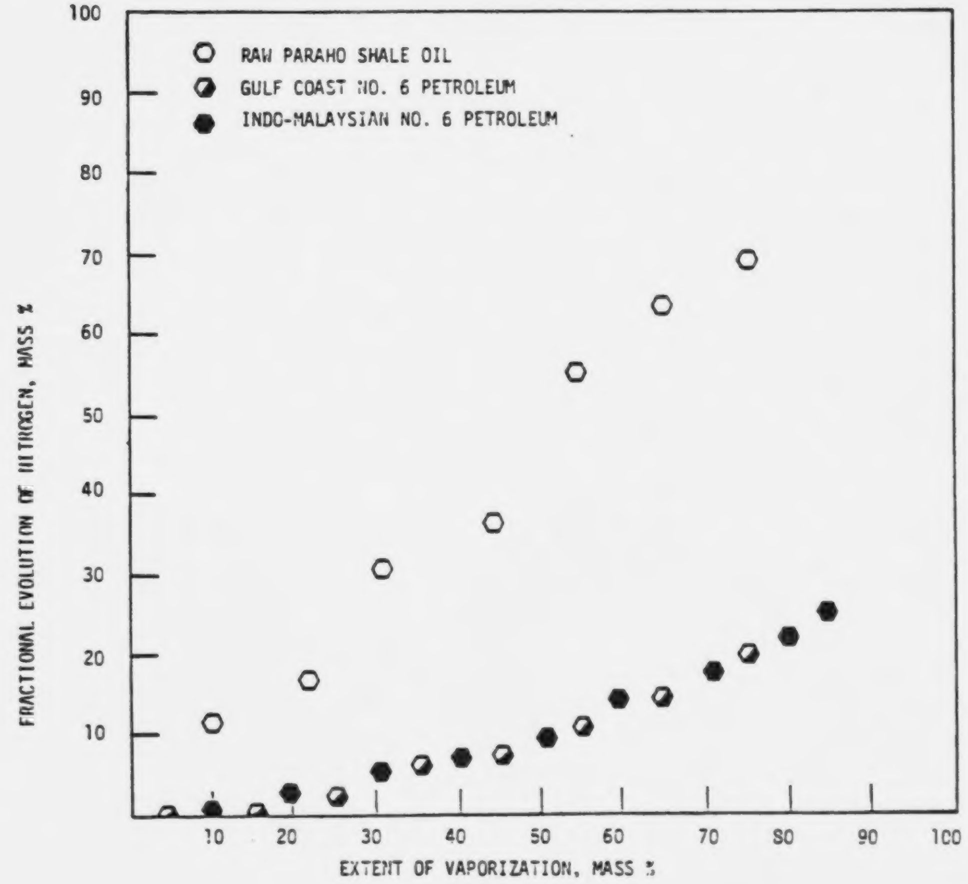

Figure 4 Nitrogen Evolution During Equilibrium Batch Distillation of Gulf Coast No. 6 Petroleum Oil, Indo-Malaysian No. 6 Petroleum Fuel Oil, and Raw Paraho Shale Oil

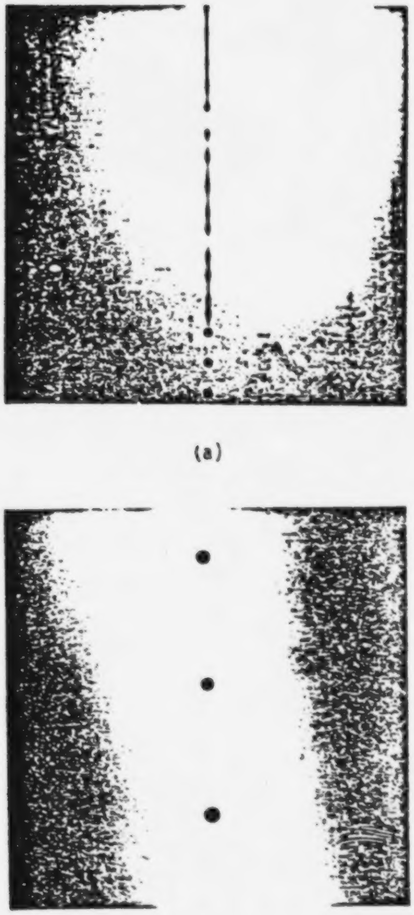

(a)

(b)

Figure 5 Raw Paraho Shale Oil Droplets Vaporizing in Helium Atmosphere at 1000 K (a) At Point of Introduction, 150 μm Diameter, (b) 115 ms Residence Time, 50 % Mass Loss, 450 μm Diameter

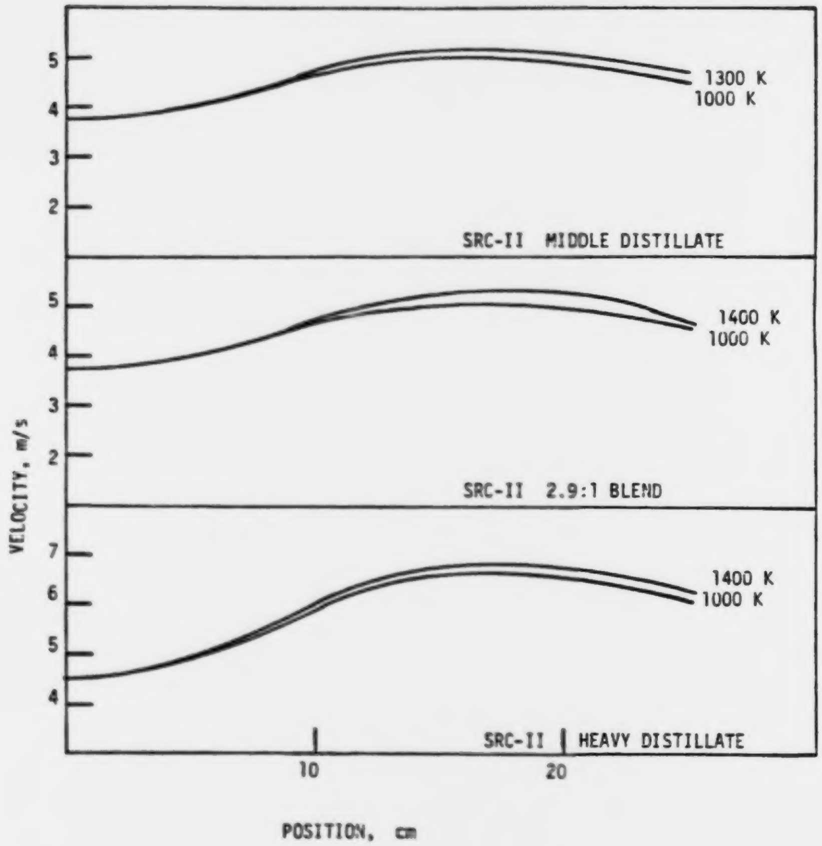

Figure 6 Particle Velocity versus Position in Furnace for 150 μm Droplet Arrays of SRC-II Middle Distillate Fraction, SRC-II Heavy Distillate Fraction, and SRC-II 2.9:1 Blend Middle and Heavy Distillate Fractions

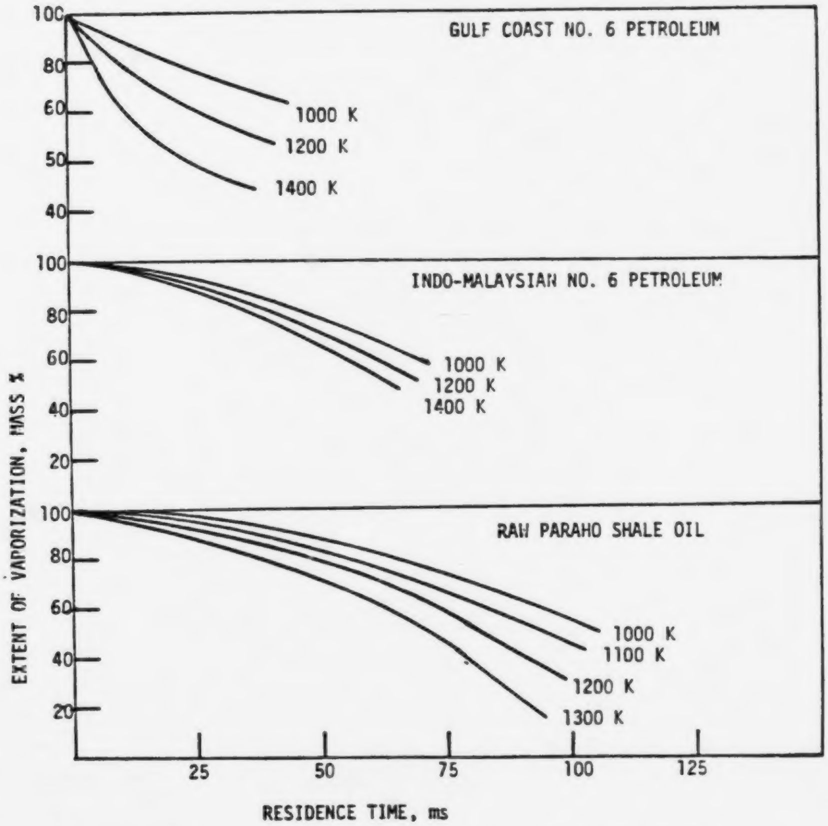

Figure 7 Extent of Vaporization versus Residence Time in Furnace for 150 μm Droplet Arrays of Gulf Coast No. 6 Petroleum Fuel Oil, Indo-Malaysian No. 6 Petroleum Fuel Oil, and Raw Paraho Shale Oil

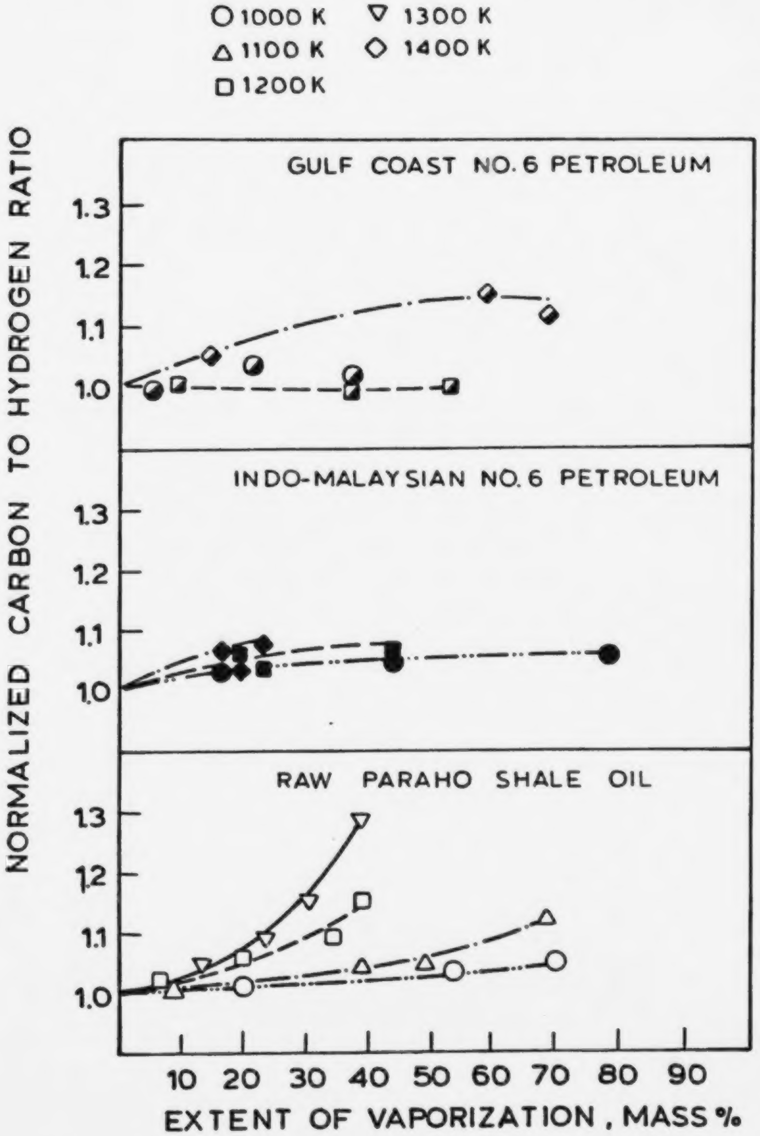

Figure 8. Normalized Carbon to Hydrogen Atomic Ratios of Fuel Residues from Pyrolysing 150 μm Droplet Arrays of Gulf Coast No. 6 Petroleum Fuel Oil, Indo-Malaysian No. 6 Petroleum Fuel Oil and Raw Paraho Shale Oil.

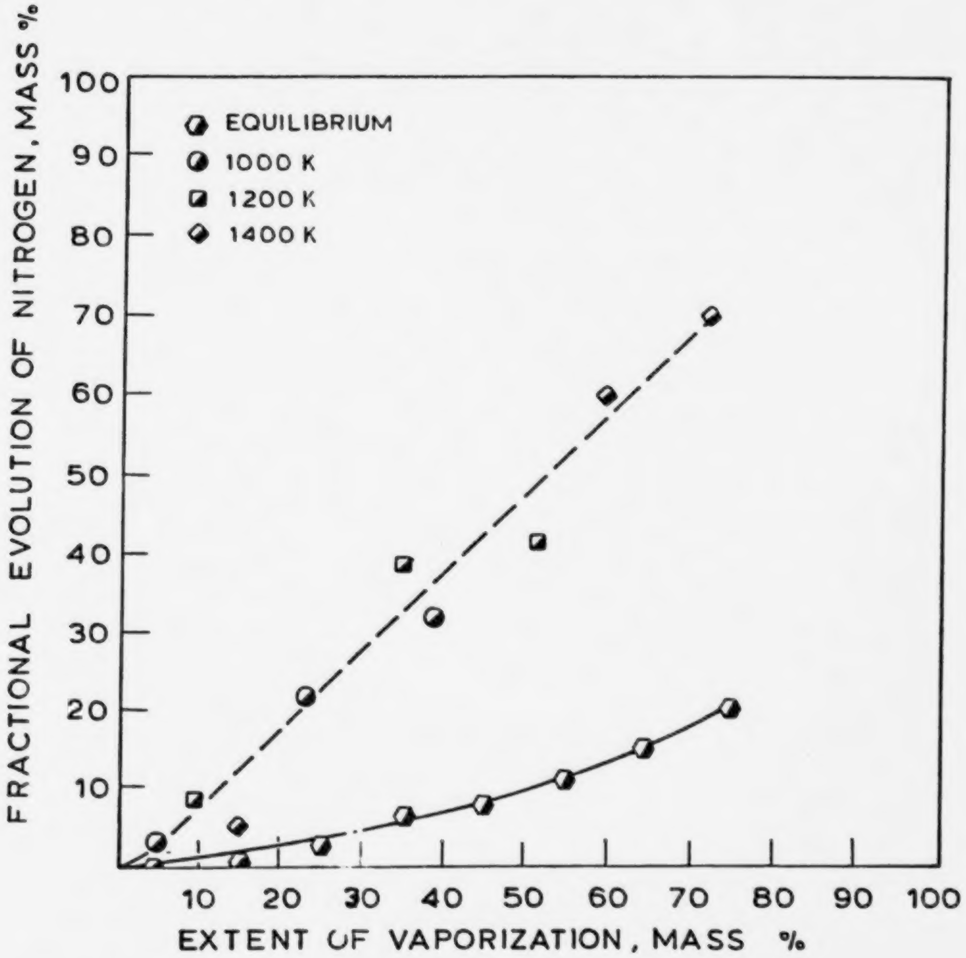

Figure 9. Nitrogen Evolution from Pyrolysing 150 μm Droplets Arrays of Gulf Coast No. 6 Petroleum Fuel Oil.

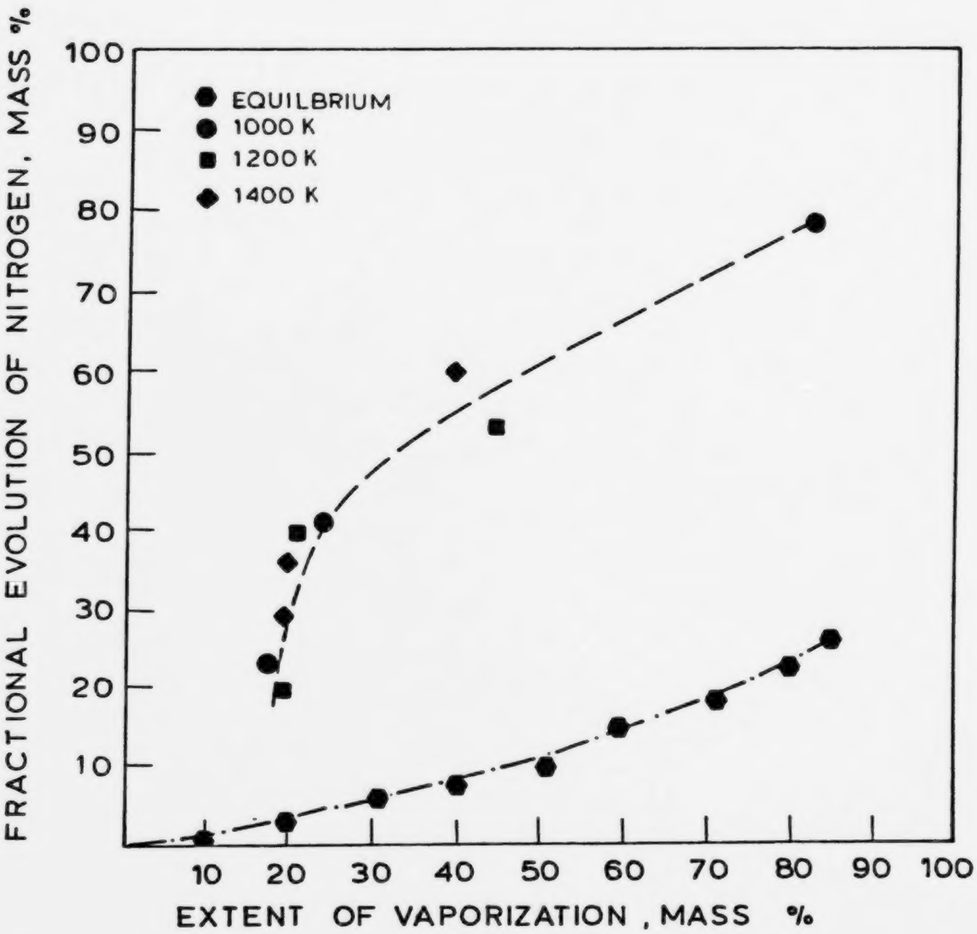

Figure 10. Nitrogen Evolution from Pyrolysing 150 μm Droplets Arrays of Indo-Malaysian No. 6 Petroleum Fuel Oil.

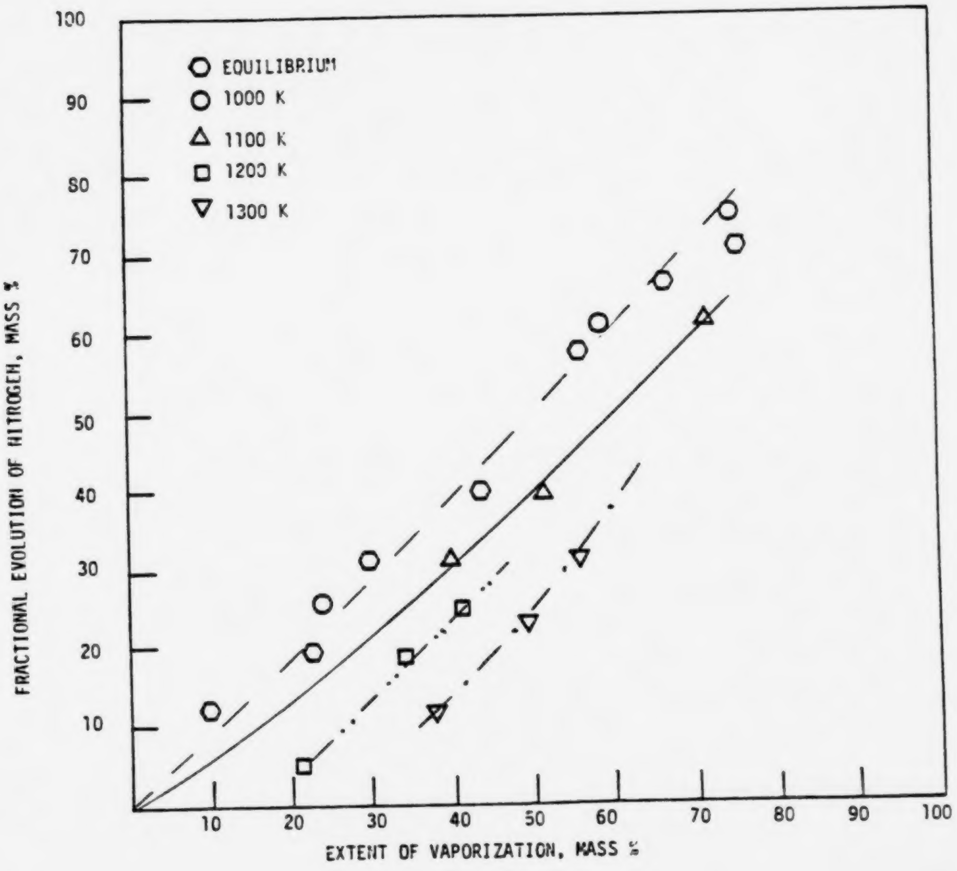

Figure 11 Nitrogen Evolution from Pyrolysing 150 µm Droplet Arrays of Raw Paraho Shale Oil

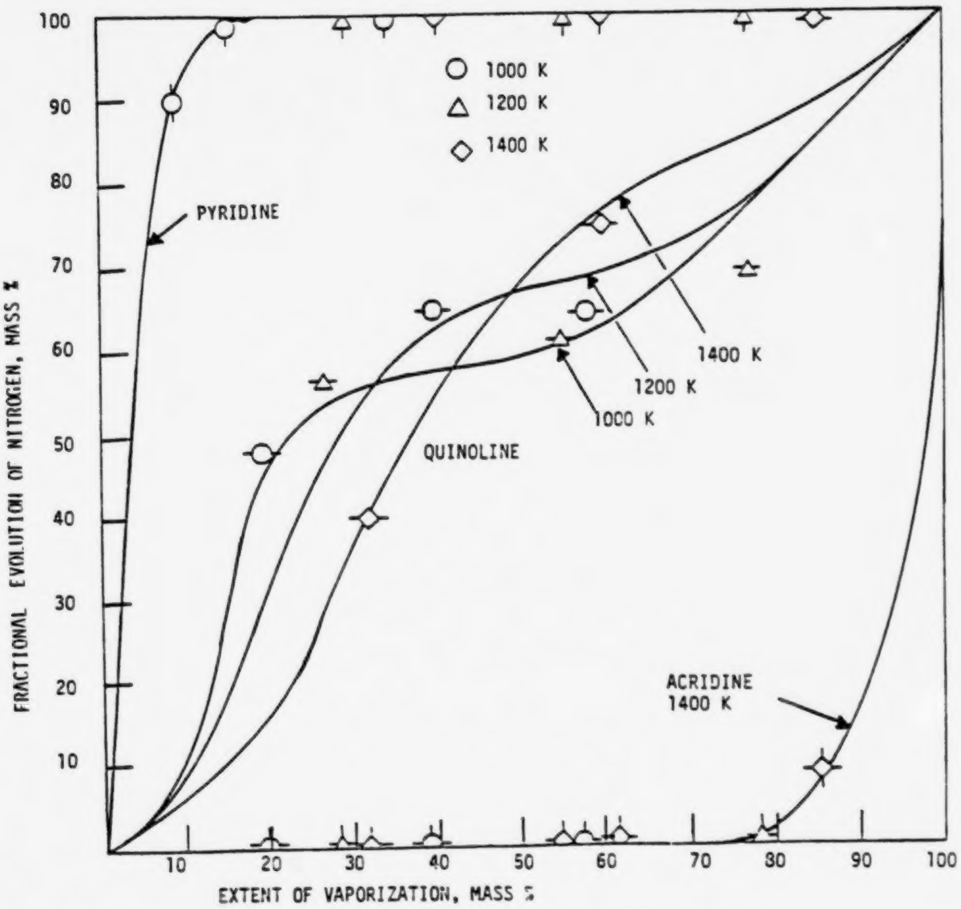

Figure 12 Nitrogen Evolution from Pyrolysing 150 μm Droplet Arrays of n- Dodecane Dopes with Pyridine, Quinoline or Acridine (Data Points are Experimental, Solid Lines are Calculations from Theory)

BENCH-SCALE NO EMISSIONS TESTING OF WORLD COALS: INFLUENCE OF PARTICLE SIZE AND TEMPERATURE

By:

S. L. Chen, M. P. Heap, D. W. Pershing
Energy and Environmental Research Corporation
18 Mason
Irvine, CA 92714-4190

"Although the research described in this paper has been funded wholly or in part by the United States Environmental Protection Agency through contract #68-02-2667 to Energy and Environmental Research Corporation, it has not been subjected to Agency review and therefore does not necessarily reflect the views of the Agency and no official endorsement should be inferred."

ABSTRACT

This paper describes results from a research project supported by the U.S. Environmental Protection Agency and the International Energy Agency (for Canada, Denmark, and Sweden) in which forty-eight coals from North America, Europe, Asia, South America and Australia were burned in a 21 kW_t refractory-lined tunnel furnace to determine the effects of burner configuration, particle size and temperature on NO emissions under normal (excess air) and staged combustion conditions. Fuel NO was determined under excess air conditions by replacing the combustion air with an $Ar/O_2/CO_2$ mixture. Under excess air conditions increasing flame temperature and decreasing particle size both increased NO emissions with rapidly mixed flames because both changes enhanced the evolution of fuel-nitrogen from the coal particle. Conversely, with axial diffusion flames, increasing temperature or decreasing particle size was found to be beneficial because both changes promoted the evolution of fuel nitrogen species within the fuel-rich flame core. With staged combustion increasing heat extraction generally reduced exhaust NO emissions via a complex mechanism. Reducing second-stage flame temperatures had little effect on the concentration and speciation of the gaseous nitrogen species leaving the first stage, and on the conversion of solid phase nitrogen in the second stage. However, it dramatically decreased the second-stage conversion of gas phase nitrogen intermediates to exhaust NO. The controlling mechanism appears to be selective NO reduction by NH_i species. The effectiveness of increased heat extraction rate was also found to depend heavily on the coal composition.

INTRODUCTION

The development of NO control strategies for coal-fired boilers has received considerable attention over the past decade. Pilot-scale studies (1) established that fuel/air mixing controlled by burner design dictated the formation of NO in pulverized coal flames and that rapid mixing of coal volatiles and air promoted NO formation. Bench-scale and research studies further established the significance of fuel nitrogen oxidation (2), the factors controlling fuel nitrogen evolution (3,4), and conditions that affect NO formation from pulverized coal under fuel-rich conditions (5,6). Burner designs have been demonstrated at various scales (7,8,9), which are capable of minimizing emissions from field operating boilers and more advanced combustion control techniques have been proposed which will substantially change state-of-the-art boiler designs (10). However, little information is currently available regarding the relationship of fuel properties to the influence of combustion conditions on NO_x formation and control.

Pulverized-coal combustion produces nitric oxide by the fixation of molecular nitrogen (thermal NO) and by the oxidation of coal-bound nitrogen (fuel NO). Thermal NO formation is known to be extremely temperature dependent; however, the key parameter controlling fuel NO formation from a given coal is the gas-phase reactant stoichiometry. Excess oxygen promotes fuel NO formation. When a pulverized coal particle is injected into a flame, it decomposes and the fuel-bound nitrogen splits between the char and the volatile fractions. The volatiles are composed of tars and light gases, and the tars further decomposed after ejection from the coal particle producing gas-phase nitrogen compounds and soot. Char nitrogen is defined as that which is associated with a solid, either as a pyrolysis product of the tars or as the original coal char; gas-phase volatile nitrogen is that which is produced from the volatile coal fractions and reacts in the gas phase forming N_2, NO, HCN, or NH_3.

This paper summarizes some of the results from a study which investigated the impact of combustion conditions and coal properties on the fate of both char and volatile (fuel-bound) nitrogen under excess air and fuel-rich (staged) conditions. A total of 48 coals from five continents were burned in a 21 kW_t refractory-lined tunnel furnace using air and nitrogen free mixtures as the oxidant. Exhaust and in-flame measurements were made to quantify the relationship between coal properties and thermal environment in terms of the amount and speciation of volatile and char nitrogen at the exit of the first stage and the conversion of the fuel nitrogen fragments in the second stage.

EXPERIMENTAL FACILITIES

Bench-Scale Reactor

The experimental reactor, illustrated in Figure 1, is a refractory-lined, down-fired tunnel which consists of six separate sections. Each section is made up of an outer steel shell and three layers total thickness of 28 cm of refractory insulation. The main combustion chamber is 15.2 cm in diameter. The furnace entry (top section) consists of a 30.5-cm-long refractory quarl that diverges gradually from 5.1 cm to the full 15.2 cm diameter. The long quarl helps to eliminate recirculation and improves the one-dimensionality of the flow field. Sampling or air/additive injection can be achieved through the access ports located at different axial positions.

All of the experiments for the excess air screening studies were conducted with the straight tunnel configuration shown in Figure 1. During the latter phases of the program, the top four sections of the furnace were modified to facilitate the measurement of in-flame species concentrations, and to permit the investigation of the effects of heat extraction under staged combustion conditions. The modified furnace sections, as shown in Figure 2, include:

1. A removable radiation shield upstream of the staging/cooling position to minimize the effects of downstream parameters (e.g., wall temperature) upon upstream conditions.

2. Two refractory sections with removable coils to allow cooling of first- and/or second-stage combustion products.

3. A removable staging choke to insure isolation of the first stage.

4. A removable air ring for second stage air injection.

Bench-Scale Burners

Pulverized coal supplied from a twin screw feeder is transported by primary air to the burner on top of the furnace. The burners used in this study have been described elsewhere (11). They are of two basic types: a premixed and a diffusion burner. In the premixed burner, primary air and the pulverized coal are injected radially outward through six 0.32 cm holes (at a 30° angle with the vertical) into a premixing chamber. The preheated main combustion air is injected radially inward into the chamber in six round jets opposing the coal jets. This burner produces predominantly one-dimensional flow with negligible backmixing. Ignition in the mixing chamber is prevented by water-cooled tubes which separate the mixing chamber from the hot furnace.

The coal plus transport air can also be supplied to the diffusion burner where variable swirl is achieved by dividing the main combustion air into two streams: one which flows axially, parallel to the injector, and the other which flows through swirl vanes (11). Swirling all the combustion air and injecting the coal-plus-transport-air through a 1.9 cm O.D. injector with six 0.48 cm diameter holes spaced radially at the tip produces a short, intensely backmixed flame termed a "radial diffusion flame." Conversely, an axial diffusion flame is obtained with a single-hole, parallel injector (1.12 cm diameter hole). In the axial mode, the combustion air is also added through swirl vanes to provide a stable ignition zone at the injector.

Measurement Systems and Analytical Methods

Flue gas sampling was conducted with a stainless steel water-cooled probe (jacketed with cooling water) and the following gas species were measured continuously by the method indicated:

- NO - chemiluminescence
- O_2 - paramagnetism
- CO/CO_2 - nondispersive infrared

In-flame gas samples were taken with a water spray probe. The probe is made of four concentric stainless steel tubes. The outside diameter of the probe is 3.2 cm and the sample flow passage is 1.26 cm in diameter. Water spray at the tip of the probe provides rapid quenching of the oncoming combustion products. The sample train for in-flame measurements is shown in Figure 3. Samples could be directed to either side of the system; i.e., dry measurements of NO, CO/CO_2, and O_2 species or wet measurements of NH_3 and HCN species. Gas-phase HCN and NH_3 species were collected in a gas washing unit which consists of an impinger in series with a bubbler containing a fritted glass cylinder. The sample solutions were subsequently analyzed for CN and dissolved ammonia using specific ion electrodes.

An elbow-shaped water-quench probe was used for collecting in-flame solid samples isokinetically. This probe is similar to the water-spray probe except that the water-cooling jacket has been replaced with a layer of insulating ceramic fiber which minimizes thermal disturbances resulting from the cooling probe. The collected solid samples were analyzed for C, H, N, and ash content with a Perkin-Elmer elemental analyzer. Detailed measurements of exhaust solids loading and composition were not made. However, mass balance calculations indicated that carbon burnout exceeded 95 percent.

FUELS

All the coals were pulverized to 65 percent through 200 mesh (U.S. standard sieve, 74 micron) for the fuel screening studies. The principal properties of the coals used in this study are shown in Table 1; complete fuel analysis data for all 48 coals is available elsewhere (11). All of the fuel composition data were determined by an independent laboratory.

PARTICLE SIZE

The influence of particle size on NO formation under both staged and excess air conditions was investigated by burning a high-volatile bituminous coal, Coal Valley, Canada (▲), with different size distributions obtained by mechanical sieving. These results are summarized in Figures 4, 5, and 6. Figute 4 shows the particle size distribution of the various size cuts. The weight-mean particle diameter determined using the Rosin-Rammler distribution was 69 microns for the normal cut, 141 microns for the coarse cut and

39 microns for the fine cut particles. Figure 6 shows the fuel NO emissions resulting from the combustion of these three different size-range particles under three different mixing conditions. (Fuel NO was isolated by replacing the combustion air with an artificial oxidant mixture containing 21 percent O_2, 18 percent CO_2, and the balance Ar.) In premixed and radial diffusion flames, the coarse particles produced much lower amounts of fuel NO than the fine particles, whereas in axial diffusion flames, fine particles produced lower fuel NO than coarse particles. This can be attributed to differences in volatile and char-nitrogen distribution resulting from different particle heating rates and subsequent distribution resulting from different particle heating rates and subsequent volatile evolution. (Smaller particles favor increased nitrogen evolution early in the flame front.) Thus, it appears that decreasing particle size increases NO emissions with rapidly mixed flames because it enhances the evolution of fuel nitrogen in an oxygen-rich region. Conversely, with axial diffusion flames decreasing particle size is beneficial because it promotes the evolution of fuel nitrogen within the fuel-rich flame core where the formation of N_2 is favored. Further, the data indicate that the conversion of fuel nitrogen from smallest particles is much more strongly influenced by the burner mixing than the large particle conversion.

Figure 5 shows the influence of coal particle size on exhaust NO emissions for the Coal Valley sub-bituminous coal under staged combustion conditions. Decreasing the mean particle size from 69 microns (normal) to approximately 39 microns (fine) significantly decreased the minimum emission level. This behavior is in direct agreement with the axial diffusion flame results and is again believed to be because with the small particles more nitrogen can be driven out of the solid phase into the fuel-rich, first stage where N_2 formation is favored. This effect is analogous to that observed previously by England, et al, (12) for heavy liquid fuel oils and it could be particularly significant in a staged combustion system with a small primary zone residence time.

THERMAL ENVIRONMENT - EXCESS AIR COMBUSTION

Figures 7 and 8 summarize the data from a series of tests investigating the influence of thermal environment on fuel NO formation under excess air conditions. In these experiments flame temperature was varied by changing the CO_2/Ar ratio in the artificial oxidant; in all cases the inlet O_2 was 21 percent. Detailed flame temperature measurements were not attempted, but the theoretical flame temperatures are shown in parentheses to provide a measure of the potential changes in the particle environment. Fuel NO formation in the premixed flames (Figure 7) increased with increasing local temperature. However, the opposite effect was observed with the axial diffusion flames as shown in Figure 8; fuel NO formation decreased slightly with increasing particle temperature. Pohl and Sarofim (3) have shown that increasing pyrolysis temperature can increase volatile nitrogen yield. Therefore, increasing the local temperature in a premixed flame probably results in increased fuel NO formation because it enhances the evolution of volatile nitrogen in oxygen rich zones. Conversely, with axial flames, the increased evolution occurs within fuel-rich zones where N_2 formation is favored and overall fuel NO formation is reduced according to the following reaction scheme based on the work of Haynes (13), Morley (14), and Fenimore (15):

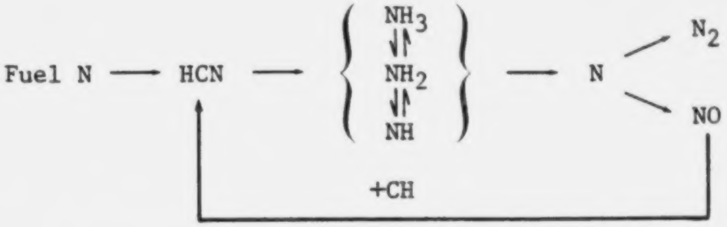

THERMAL ENVIRONMENT - STAGED COMBUSTION

The temperature profile in a staged combustion system can have a strong influence on the effectiveness of this control technique. In liquid fuel-fired systems, it is desirable to have a nearly adiabatic first-stage (12) and in pulverized coal flames, increasing primary zone temperature should reduce exhaust NO because it:

- Increases volatile nitrogen release
- Accelerates the rate of TFN (NO + NH_3 + HCN)
- Reduces the amount of char nitrogen

However, previous experimental studies (10,16) have indicated that increased heat extraction decreases exhaust NO. To investigate this effect, a series of experiments was conducted in which the first stage of the reactor system was significantly cooled by inserting water-cooling coils along the walls. (See Figure 2 for the details of this configuration.) A suction pyrometer was used to define the impact of this cooling on the bulk gas temperature at the end of the first stage for the Coal Valley sub-bituminous coal. At a first stage stoichiometry of 0.6, the gas temperature was reduced approximately 200 K; at SR_1 = 0.9, the temperature reduction was 150 K. Figure 9 shows the corresponding NO emissions measured in the exhaust for this test sequence, and indicates that increasing the rate of heat extraction in the first stage significantly decreased the exhaust NO_x at all stoichiometries studied.

First-Stage Processes

Figure 10 presents data on the impact of the time/temperature history on the gas-phase and solid-phase nitrogen species at the exit of the first stage. These results indicate that for the Coal Valley coal, increasing the rate of first stage heat extraction had relatively little effect on the intermediate gas-phase species and on the amount of nitrogen retained in the solid phase. These data suggest that the large reduction in the exhaust emissions (Figure 9) is not due to changes in the "fuel" entering the second stage; rather, it must be the direct result of a major change in the second stage processes.

Solid Nitrogen Conversion

To investigate the influence of first stage cooling on solid (char) nitrogen conversion, experiments with the COED char/C_3H_8 fuel burning in argon/oxygen were conducted. Again, the first stage exit temperature was decreased approximately 200 K with a wall cooling coil. Figure 11 shows the exhaust NO emission results from this test sequence. The emissions data indicate that at $SR_1 = 0.9$ cooling increased exhaust NO by 37 ppm, and this is directly attributable to a measured increase in first stage NO of 47 ppm. At lower stoichiometries, no effect was observed. Thus, it appears that increasing the heat extraction rate does not affect the oxidation of solid-phase nitrogen in the second stage flame.

TFN Conversion

The influence of first stage cooling on gas-phase TFN (TFN = NO + NH_3 + HCN) conversion in the second stage was investigated by studying staged propane/ammonia flames. Figure 12 summarizes these data and indicates that when the first stage stoichiometry is relatively lean ($SR_1 \geq 0.75$) and NO is the dominant TFN species, temperature appears to have little effect on second stage TFN conversion. This is in direct agreement with previous excess air studies on the influence of temperature on fuel nitrogen conversion. However, when HCN and NH_3 are the dominant species under richer conditions, decreasing the temperature of the second-stage flame (by cooling in the first stage)

Figure 12 summarizes these data and indicates that when the first stage stoichiometry is relatively lean ($SR_1 \geq 0.75$) and NO is the dominant TFN species, temperature appears to have little effect on second stage TFN conversion. This is in direct agreement with previous excess air studies on the influence of temperature on fuel nitrogen conversion. However, when HCN and NH_3 are the dominant species under richer conditions, decreasing the temperature of the second stage flame (by cooling in the first stage)

dramatically decreased TFN conversion. In these experiments, there was no solid phase, so this effect must have been associated with a change in gas-phase chemistry. Because the propane/NH_3 results (Figure 12) suggested that the form of the TFN species was of primary importance, a special series of experiments was conducted with the Utah coal. Alternatively, NO or NH_3 was injected into the second stage flame (with the staging air) and the effect of cooling was studied. These results are summarized in Figure 13. When the added fuel nitrogen was in the form of NO (circles), the thermal environment had essentially no effect on the conversion (retention) of the fuel nitrogen in the second stage flame. However, when NH_3 was added, a significant thermal effect was observed at all stoichiometries (triangles). These results strongly suggest that the reduction in exhaust NO emissions with increased heat extraction is directly associated with selective reduction of first stage NO by NH_3 in the second stage flame. The concentrations and thermal conditions (1150 K at the second stage inlet) are essentially analogous to those required for external "thermal de-NO_x" (17). The overall chemistry of this reaction is believed to be:

$$NO + NH_3 + 1/4\ O_2 \longrightarrow N_2 + 3/2\ H_2O$$

where the principal elementary step is:

$$NO + NH_2 \longrightarrow N_2 + H_2O$$

Coupling With Fuel Chemistry

Figure 14 shows the influence of heat extraction rate on the Canadian lignite coal. These data (typical of low rank coals) show that increasing heat extraction only reduced exhaust NO at high stoichiometries ($SR_1 > 0.7$). Figure 14 also presents detailed in-flame measurements. Increased cooling had little effect on TFN; however, at rich conditions ($SR_1 < 0.7$) it increased the carry-over of solid nitrogen. Thus, decreased emission associated with a reduced gas-phase conversion was somewhat mitigated by an increased contribution from char nitrogen. Figure 15 shows typical results for the high volatile bituminous coals. At high stoichiometric ratios ($SR_1 > 0.7$) reducing first stage temperature increased first stage NO. Thus, there was essentially no effect of decreasing temperature on exhaust NO at $SR_1 > 0.7$ because of a decrease in the first stage NO decay rate and the low NH_3 concentrations.

CONCLUSIONS

The results of this investigation with coals from five continents indicate that fuel properties and thermal environment can have a major influence on NO formation under both staged and excess air combustion conditions. Both parameters can alter the fraction of the fuel nitrogen evolved with the hydrocarbon volatiles and the local temperature strongly influences both the kinetics of NO reduction by hydrocarbons and NH_3.

Under excess air conditions, increasing flame temperature and decreasing particle size both increased NO emissions with rapidly mixed flames because both changes enhanced the evolution of fuel-nitrogen from the coal particle. Conversely, with axial diffusion flames, increasing temperature or decreasing particle size was found to be beneficial because both changes promoted the evolution of fuel nitrogen species within fuel-rich flame core.

Increasing the rate of heat extraction from a staged combustion system generally reduces exhaust NO emissions via a complex mechanism. Reduced second stage flame temperatures had little effect on solid-phase nitrogen conversion, but they dramatically decrease gas-phase TFN conversion due to a shift in controlling flame chemistry. If the reactants are cooled sufficiently to bring the bulk gas temperature at the first stage exit to approximately 1200 K, it is possible to obtain selective NO reduction (by NH_3) in the second-stage flame zone and, therefore, reduce the exhaust NO emissions by 5 to 35 percent. However, the effectiveness of this concept is strongly dependent on the combustor design (first-stage temperature profile and residence time) and fuel chemistry. Increasing heat extraction appears to be most favorable with low-rank coals, because they produce large amounts of NH_3 and relatively less first-stage NO. Conversely, high-rank coals (e.g., Russia) may be less influenced by the cooling in the first stage because they produce relatively little NH_3. Additionally, first stage cooling may decrease the rate of TFN decay in the fuel-rich zone and, hence, increase both the TFN and char nitrogen carry-through into the second stage. Finally, because of the extremely low temperatures required for the selective NO + NH_3 reaction, carbon burnout in the second stage may be a significant problem.

ACKNOWLEDGMENTS

This work was supported under United States Environmental Protection Agency (EPA) Contract 68-02-2667, and Contract 68-02-3658 which was funded by the International Energy Agency (IEA). The contracting countries of IEA were Canada, Denmark, and Sweden. The EPA Project Officers were G. Blair Martin and Dennis C. Drehmel. The authors are pleased to acknowledge the contributions of their colleagues, R. J. Samuel in conducting the experiments, and R. K. Nihart in performing the chemical analyses.

REFERENCES

1. Heap, M. P., T. M. Lowes, and R. Walmsley. Emission of Nitric Oxide from Large Turbulent Diffusion Flames. In: Fourteenth Symposium (International) on Combustion, The Combustion Institute, Pittsburgh, Pennsylvania, 1973. p. 883.

2. Pershing, D. W., and J. O. L. Wendt. Pulverized Coal Combustion: The Influence of Flame Temperature and Coal Composition on Thermal and Fuel NO_x. In: Sixteenth Symposium (International) on Combustion, The Combustion Institute, Pittsburgh, Pennsylvania, 1977. p. 389.

3. Pohl, J. H., and A. F. Sarofim. Devolatilization and Oxidation of Coal Nitrogen. Sixteenth Symposium (International) on Combustion, The Combustion Institute, Pittsburgh, Pennsylvania, 1977. p. 491.

4. Solomon, P. R., and M. B. Colket. Coal Devolatilization. In: Seventeenth Symposium (International) on Combustion, The Combustion Institute, Pittsburgh, Pennsylvania, 1979. p. 131.

5. Wendt, J. O. L., D. W. Pershing, J. W. Lee, and J. W. Glass. Pulverized Coal Combustion: NO_x Formation Mechanisms Under Fuel-Rich and Staged Combustion Conditions. In: Seventeenth Symposium (International) on Combustion, The Combustion Institute, Pittsburgh, Pennsylvania, 1979. p. 77.

6. Rees, D. P., L. D. Smoot, and P. O. Hedman. Nitrogen Oxide Formation Inside a Laboratory Pulverized Coal Combustor. In: Eighteenth Symposium (International) on Combustion, The Combustion Institute, Pittsburgh, Pennsylvania, 1980. p.

7. Barsin, J. A. Pulverized Coal Firing NO_x Control. In: Proceedings of Second NO_x Control Technology Seminar, Electric Power Research Institute, Palo Alto, California, 1979.

8. Vatsky, J. Experience in Reducing NO_x Emissions in Operating Steam Generators. In: Proceedings of Second NO_x Control Technology Seminar, Electric Power Research Institute, Palo Alto, California, 1979.

9. Heap, M. P., and B. A. Folsom. Optimization of Burner/Combustion Chamber Design to Minimize NO_x Formation During Pulverized Coal Combustion. Chapter 11, EPA Project Decade Monograph on Coal Combustion, EPA/IERL, Research Triangle Park, North Carolina, in press.

10. Johnson, S. A., P. L. Cioffi, T. M. Sommer, and M. W. McElroy. The Primary Combustion Furnace System: An Advanced Low NO_x Concept for Pulverized Coal Combustion. In: Proceedings of Second NO_x Control Technology Seminar, Electric Power Research Institute, Palo Alto, California, 1979.

11. Chen, S. L., M. P. Heap, D. W. Pershing, and G. B. Martin. Influence of Coal Composition on the Fate of Volatile and Char Nitrogen During Combustion. In: Nineteenth Symposium (International) on Combustion, The Combustion Institute, Pittsburgh, Pennsylvania, 1983.

12. Pershing, D. W., J. E. Cichanowicz, G. C. England, M. P. Heap, and G. B. Martin. The Influence of Fuel Composition and Flame Temperature on the Formation of Thermal and Fuel NO_x in Residual Oil Flames. In: Seventeenth Symposium (International) on Combustion. The Combustion Institute, Pittsburgh, Pennsylvania, 1978.

13. Haynes, B. S. Reactions of Ammonia and Nitric Oxide in the Burnt Gases of Fuel-Rich Hydrocarbon-Air Flames. Combustion and Flame 28, 1977. p. 81.

14. Morley, C. The Mechanism of NO Formation from Nitrogen Compounds in Hydrogen Flames Studied by Laser Fluorescence. In: Eighteeenth Symposium (International) on Combustion, The Combustion Institute, Pittsburgh, Pennsylvania, 1981. p. 23.

15. Fenimore, C. P. Reactions of Fuel-Nitrogen in Rich Flame Gases, Combustion and Flame 26, 1976. p. 249.

16. Chen, S. L., M. P. Heap, D. W. Pershing, and G. B. Martin. The Fate of Coal Nitrogen During Combustion. Fuel, Vol. 61, 1982.

17. Lyon, R. K. Method for the Reduction of the Concentration of NO in Combustion Effluents Using Ammonia. U.S. Patent No. 3,900,554, 1975.

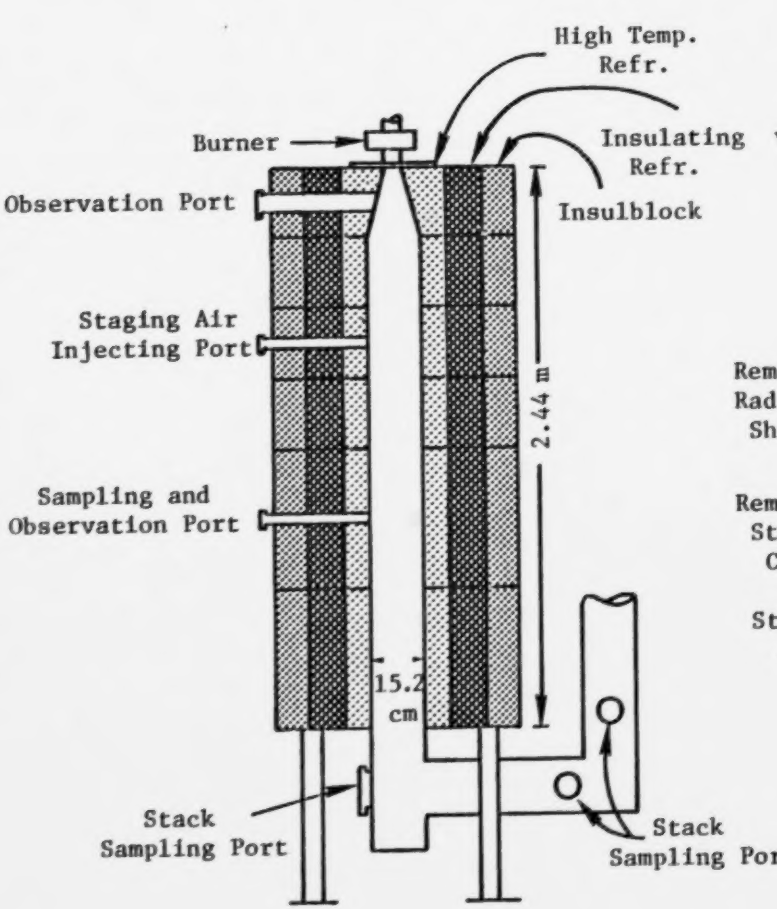
High Temp.
Refr.
Burner
Insulating
Refr.
Insulblock
Observation Port
Staging Air
Injecting Port
2.44 m
Sampling and
Observation Port
15.2
cm
Stack
Sampling Port
Stack
Sampling Ports

Figure 1. Bench-scale reactor used for excess air studies.

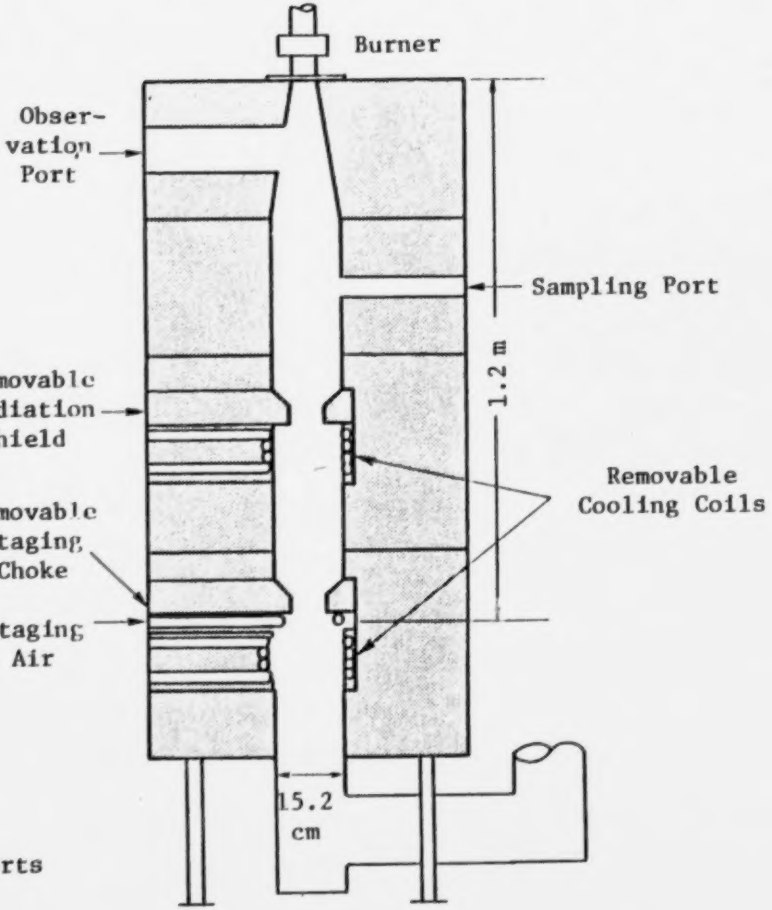
Burner
Obser-
vation
Port
Sampling Port
1.2 m
Removable
Radiation
Shield
Removable
Cooling Coils
Removable
Staging
Choke
Staging
Air
15.2
cm

Figure 2. Modified furnace sections for staged combustion studies.

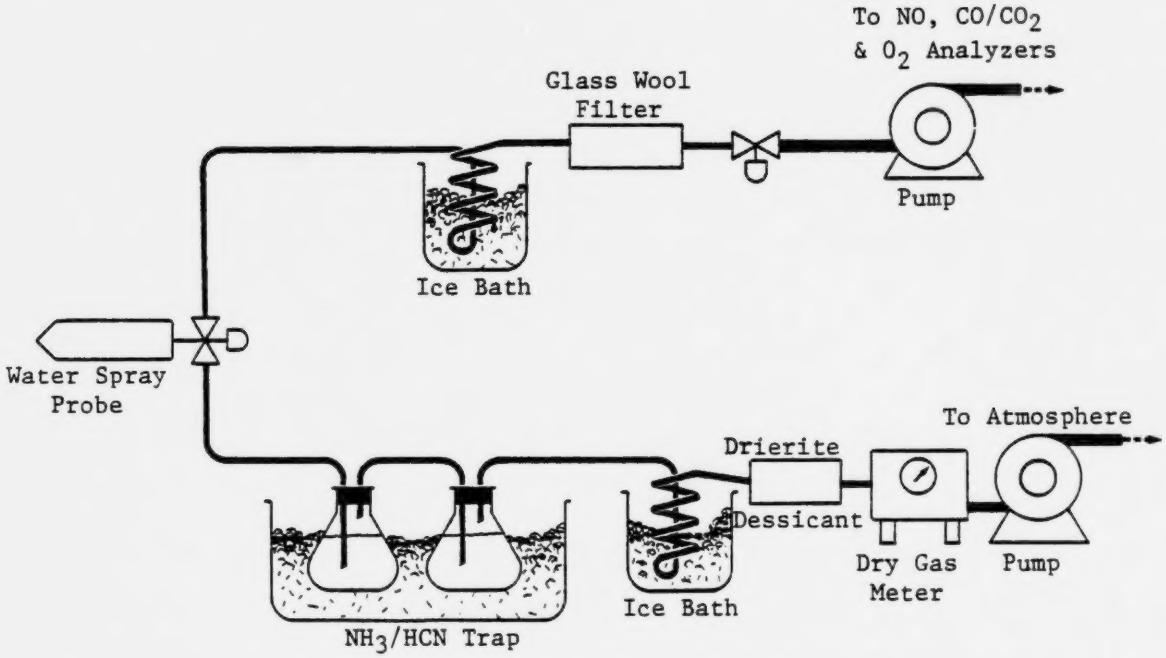
To NO, CO/CO2
& O2 Analyzers
Glass Wool
Filter
Pump
Ice Bath
Water Spray
Probe
To Atmosphere
Drierite
Dessicant
Dry Gas
Meter
Pump
Ice Bath
NH3/HCN Trap

Figure 3. Sample train for in-flame measurements.

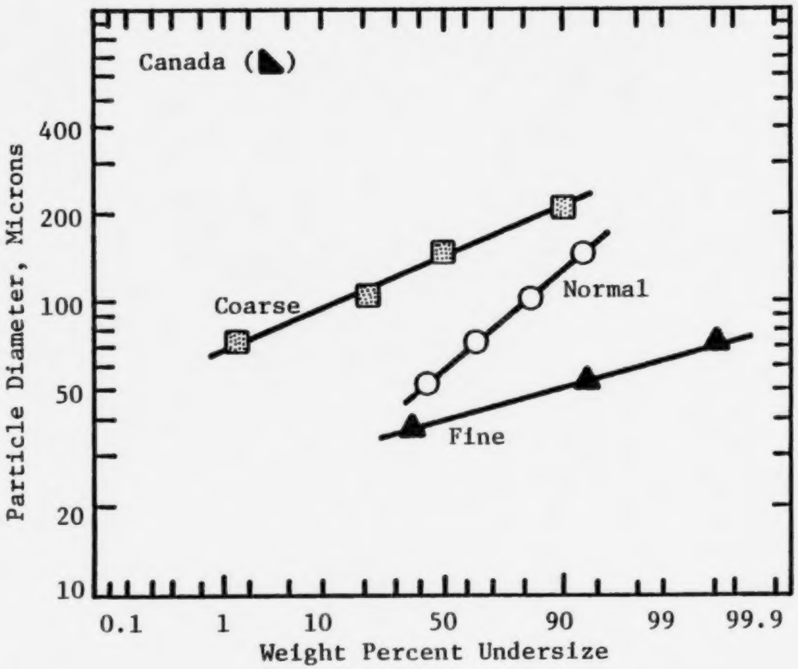

Figure 4. Particle size distribution.

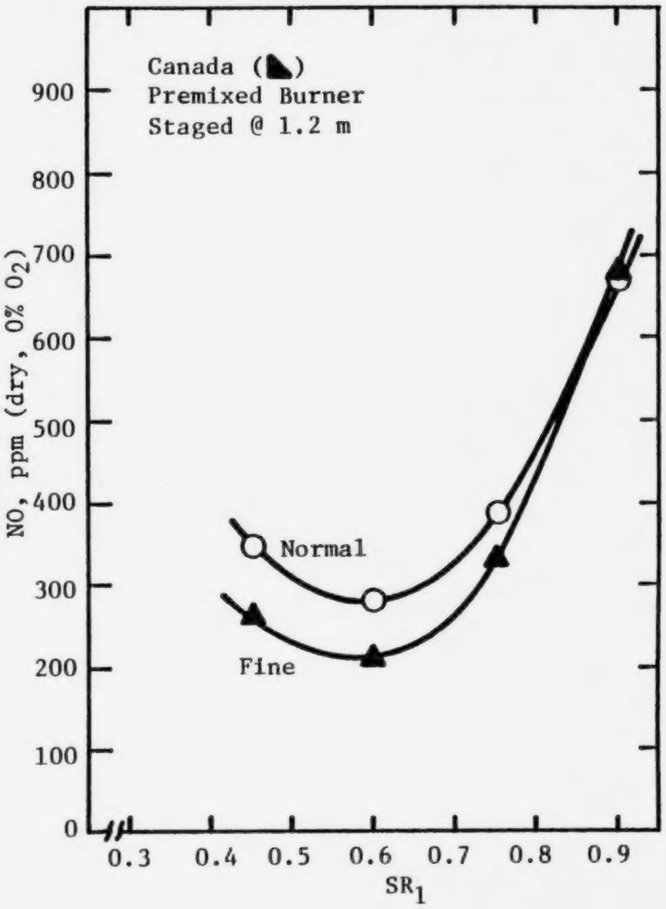

Figure 5. Influence of particle size on exhaust NO emissions

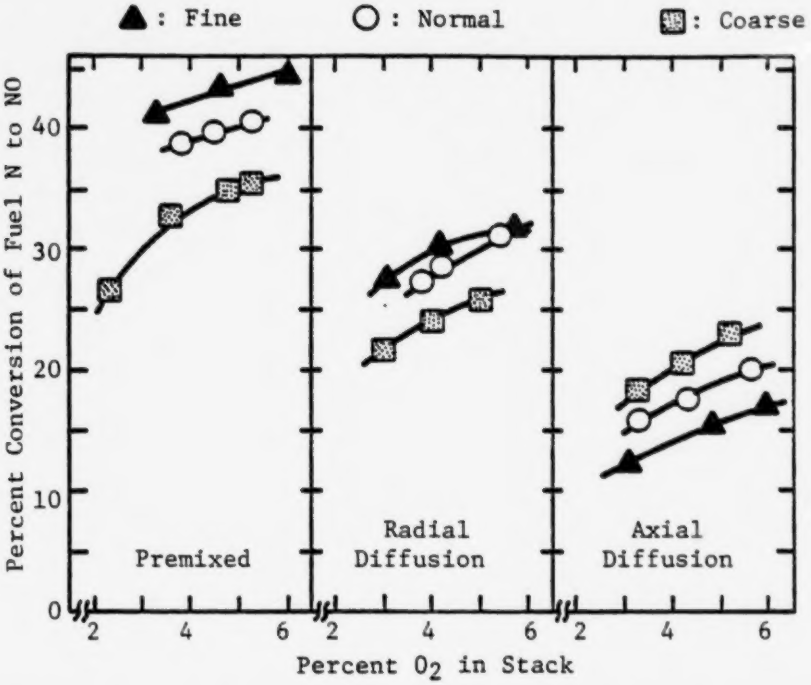

Figure 6. Influence of particle size. (Exhaust emissions, excess-air conditions, Canadian bituminous coal, ◣).

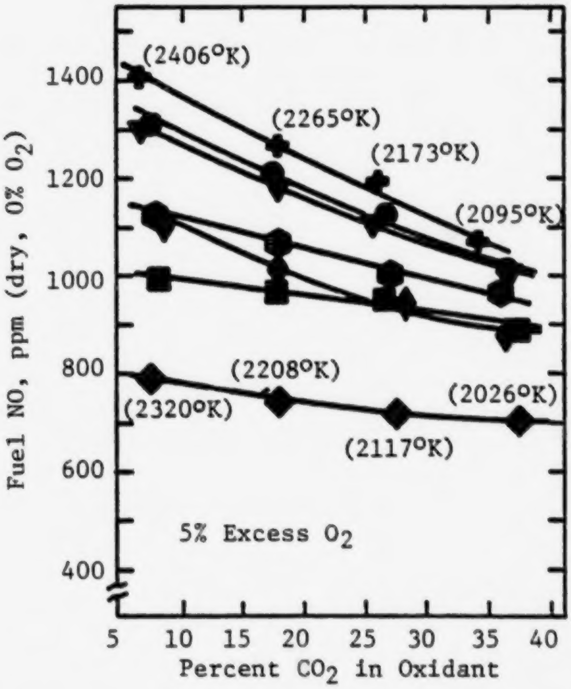

Figure 7. Influence of thermal environment: Premixed burner. (Exhaust emissions, excess-air conditions, see Table 1 for symbol key).

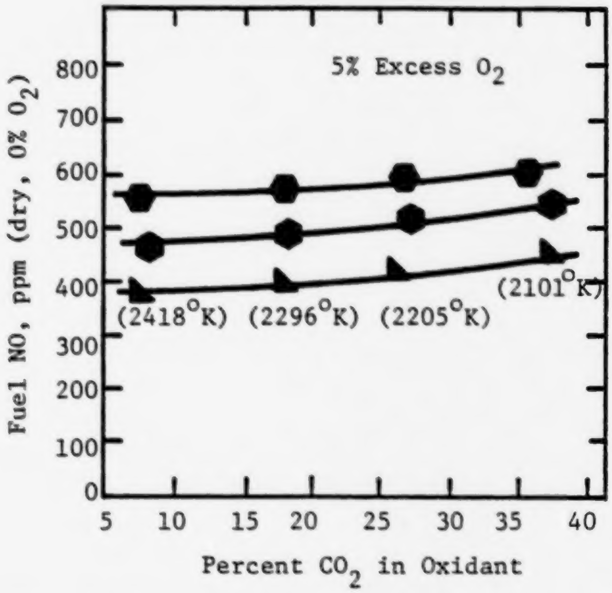

Figure 8. Influence of thermal environment: axial diffusion burner. (Exhaust emissions, excess-air conditions, see Table 1 for symbol key.)

Open Symbols: Normal
Closed Symbols: First-Stage Cooling

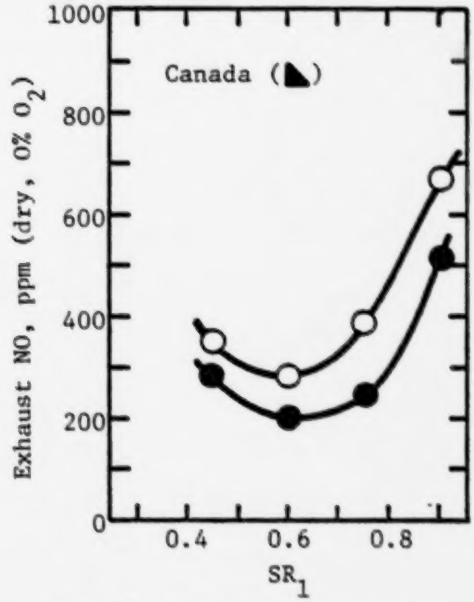

Figure 9. The impact of first-stage heat removal. (Staging at 1.2m, 5% overall excess O_2).

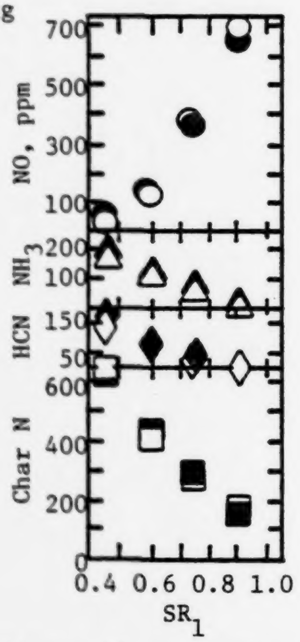

Figure 10. Nitrogen species at first stage exit (1.2m).

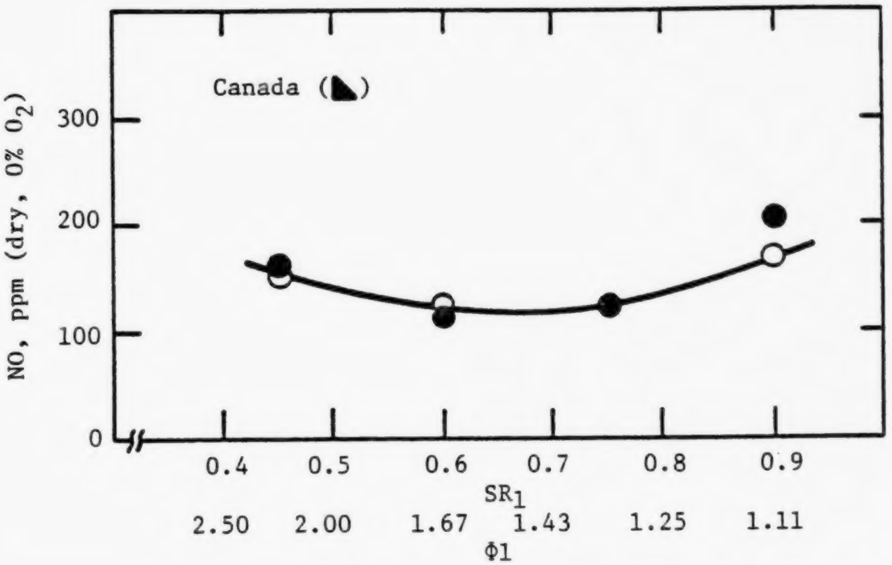

Figure 11. Influence of first-stage cooling on solid nitrogen conversion. (Staging at 1.2m, 5% overall excess O_2).

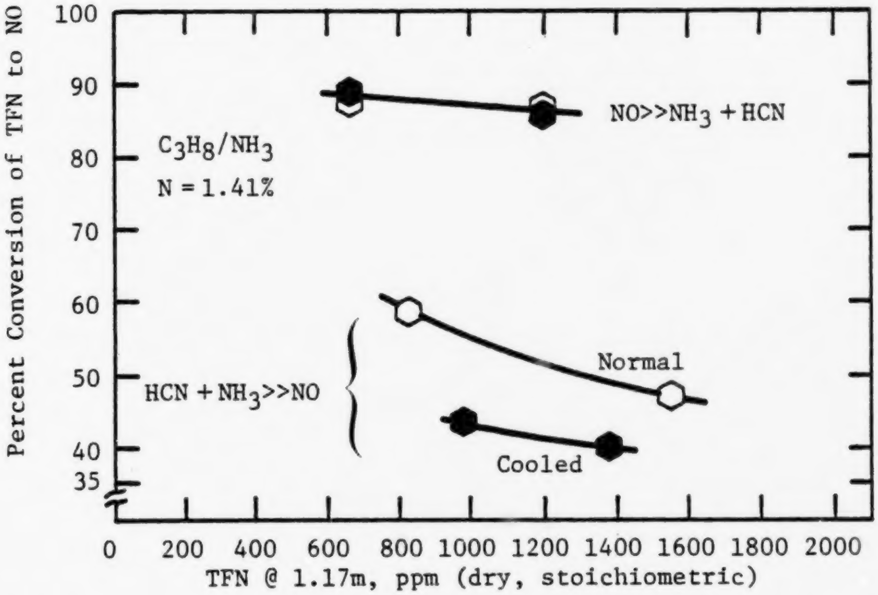

Figure 12. Influence of cooling on second-stage TFN conversion--C_3H_8/NH_3 flames. (Conversion based on HCN, NH_3, and NO measurements in furnace exhaust.)

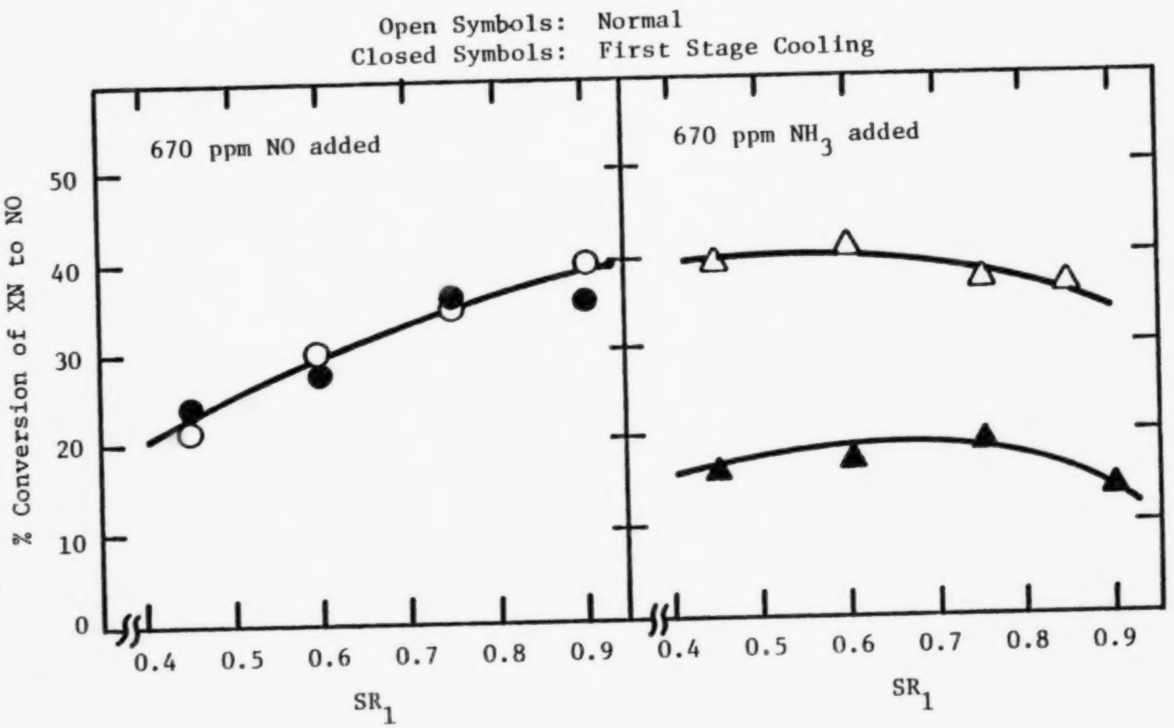

Figure 13. Influence of cooling on second-stage TFN conversion. (Based on HCN, NH_3, and NO measurements at 1.2m, flow rate of added N species, and exhaust NO measurements.)

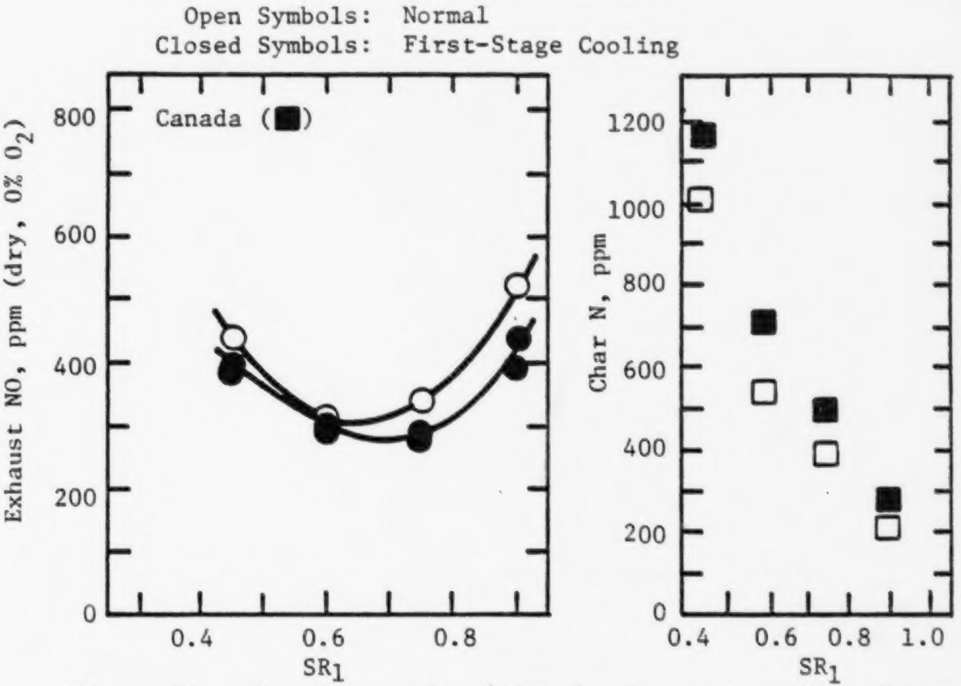

Figure 14. The impact of cooling for low-rank coals. (Staged combustion, 5% overall excess O_2.)

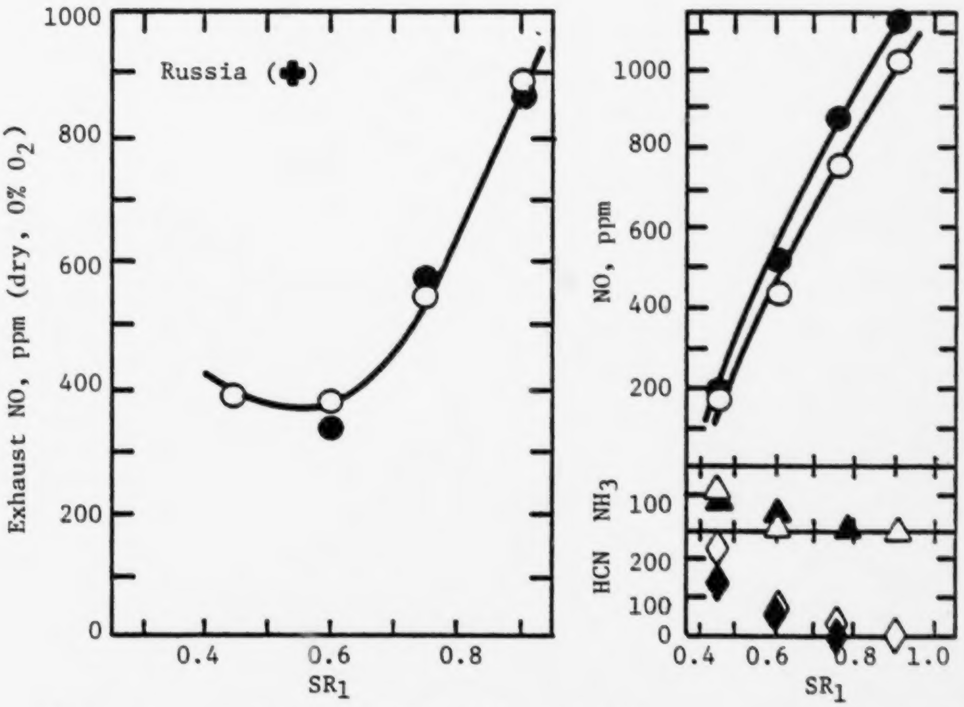

Figure 15. The impact of cooling for high-rank coals. (Staged combustion, 5% overall excess O_2.)

TABLE 1. FUEL ANALYSIS

Fuel Symbol	⊠	○	◆	■	◣	⬢	●	⬣	✚	▼	♦
Fuel Source	Coed Char	Price Utah	Canada	Canada	Canada	Blended U.S./Canada	Canada	Canada	Russia	England	Australia
Proximate Analysis (% as received)											
Moisture	3.24	6.39	30.07	27.05	6.62	3.62	1.03	0.87	2.09	3.23	3.20
Ash	14.07	7.40	14.27	9.69	11.18	10.73	18.51	6.94	18.19	16.36	16.40
Volatile Matter	7.73	38.89	28.19	29.59	33.52	34.53	30.26	34.10	28.38	26.99	27.46
Fixed Carbon	74.96	47.32	27.47	33.67	48.68	51.12	50.20	58.09	51.34	53.42	52.94
Ultimate Analysis (% Dry)											
Carbon	77.03	73.17	54.55	59.33	67.93	71.21	67.31	78.80	68.45	69.54	66.34
Hydrogen	1.71	5.55	3.03	3.82	4.21	4.73	4.85	5.26	4.34	4.39	3.99
Nitrogen	1.67	1.54	0.64	1.06	0.94	1.19	1.42	1.68	2.00	1.51	1.53
Sulfur	2.67	0.66	0.93	0.42	0.27	1.20	2.37	1.88	0.59	0.68	0.60
Ash	14.54	7.90	20.41	13.28	11.97	11.13	18.71	7.00	18.58	16.90	16.94
Oxygen	2.38	11.18	21.50	21.49	14.68	10.54	5.34	5.38	6.04	6.98	10.60
Heating Value Btu/lb	12,105	12,340	6,107	7,488	10,811	11,882	11,862	14,000	11,597	11,719	11,725
Classification (ASTM D388)		High Volatile B Bituminous	Lignite A	Sub-bituminous C	High Volatile C Bituminous	High Volatile B Bituminous	High Volatile A Bituminous	High Volatile A Bituminous	High Volatile A Bituminous	High Volatile B Bituminous	High Volatile A Bituminous
Pyrolysis HCN Yield (equivalent ppm)		1,267		434	675				740		921
Modified ASTM Char N (equivalent ppm)		1,762		1,221	918				1,895		1,668

CORRELATION OF NO_x EMISSIONS WITH BASIC PHYSICAL AND CHEMICAL CHARACTERISTICS OF COAL

By:

J. H. Pohl, S. L. Chen, M. P. Heap, D. W. Pershing
Energy and Environmental Research Corporation
18 Mason
Irvine, California 92714

"Although the research described in this article has been funded wholly or in part by the United States Environmental Protection Agency through contract numbers 68-02-3633, 68-02-2667 and 68-02-3658 to Energy and Environmental Research Corporation, it has not been subjected to the Agency's required peer and policy review and therefore does not necessarily reflect the views of the Agency and no official endorsement should be inferred."

ABSTRACT

The properties of the coal as well as combustor design and operation influence NO_x emissions from combustors. Reliable methods of predicting dependence of NO_x emissions on coal properties are needed so that utility operators can select fuels which comply with regulations, boiler manufacturers can design boilers for different coals, and the Environmental Protection Agency can establish reasonable emission goals for different coals.

To accomplish this, a correlation which accounts for combustor conditions and fuel properties is required. This paper reviews existing information and condludes that information is unavailable to simultaneously correlate both combustor conditions and coal properties with NO_x emissions. Experiments are needed to measure the nitrogen devolatilization rate and oxidation and reaction rate of char nitrogen under conditions applicable to pulverized coal flames for a range of coals.

In the absence of correlations between fuel properties and combustor conditions and NO_x emissions, correlations of NO_x emissions with fuel properties for controlled combustor conditions are extremely useful. Correlations have been developed which correlate NO_x emissions with coal properties for a premixed coal flame, a radial diffusion coal flame, an axial diffusion flame, and an optionally staged flame. These correlations are more accurate and require only knowledge of the proximate and nitrogen analyses and are therefore thought to be more useful than previous expressions which required more extensive experimentation on the coals. These correlations show that coal nitrogen has the largest influence on the amount of NO_x emitted but that volatile matter has a secondary influence. Differences between the expressions confirm that high-volatile matter produces high NO_x in unstaged flames but low NO_x in staged ones.

INFLUENCE ON NO_x EMISSIONS

The amount of NO_x formed in combustors depends on the design and operation of the combustor and the properties of the fuel. It is the sum of contributions from oxidation of fuel nitrogen, oxidation of molecular nitrogen through the extended Zeldovich mechanism, and production of prompt NO by reactions of fuel fragments with molecular nitrogen(1). Oxidation of fuel nitrogen contributes some 35-80 percent (2,3) of the NO produced in pulverized-coal combustors. The remainder is largely the result of molecular nitrogen oxidation by oxygen containing radicals. Prompt NO_x accounts for less than 10 ppms and is usually unimportant in practical combustors. This paper concentrates on the contribution of fuel nitrogen since that is a major, difficult-to-control source of the nitrogen oxides. However, other sources of NO_x will become more important when NO_x derived from fuel nitrogen is successfully reduced.

The amount of nitrogen oxide formed in boilers depends on boiler design parameters, boiler operation, and fuel properties. Figure 1 summarizes field data on these effects. Dotted lines indicate the data is limited and the position of the lines is uncertain. The influence of boiler design on NO_x production can be mostly accounted for by the firing method and the burner zone heat release rate. These are combined into a single design parameter in Figure 1 for boilers operated near full load at 18-25 percent excess air (3-4 percent dry O_2 in the stack). The major operating variables which alter NO_x emissions are level of excess air and air staging. NO_x emissions from unstaged boilers are shown in Figure 1a and from staged in Figure 1b. The variation in NO_x emissions with nitrogen convert of the fuel shows the influence of fuel properties on emissions. The concentration of nitrogen in the fuel will be shown later to be a major, although not the only, influence of fuel properties on NO_x emissions.

Figure 1 shows major features of NO_x emissions. First, the method of firing the coal (and burner zone heat release rate) have a major influence and can account for a factor of 2 to 7 in NO_x emissions. Second, NO_x emissions may differ by a factor of 2 for coals with high fuel nitrogen content. Third, staging the air in the combustor reduces NO_x emissions for all methods of firing:

- Wet bottom boilers by 10-15 percent
- Arch-fired boilers by 5-20 percent
- Cyclone boilers by 10-30 percent
- Opposed-fired boilers by 20-30 percent
- Wall-fired boilers by 20-50 percent
- Tangentially-fired boiler by 30-50 percent
- Turbo®-fired boilers by 30-50 percent

Third, the NO_x emissions from boilers show unexplained differences in NO_x

emissions of a factor of 2-3 which may be caused by variation in design, operation, and/or fuel properties.

Data from field and pilot-scale tests confirm that fuel properties have a large influence on the emissions of NO_x from boilers. Field tests show 200-300 ppm (3% O_2) differences in NO_x emissions attributable to fuel properties (3,13,17). Controlled pilot-scale tests designed to identify the influence of fuel properties on NO_x emissions show differences of 150-500 ppm (0% O_2)(18,19). Figure 2 shows the results of pilot-scale combustion trials conducted at Energy and Environmental Research Corporation by Chen(18,20,21). These tests isolated the influence of mixing and fuel properties on NO_x emissions. The tests are conducted in a 70,000 Btu/hr refractory-lined furnace with variable heat extraction(22). Coal was injected through the three configurations shown in Figure 2. Ar/CO_2 mixtures were used to simulate air oxidation in the unstaged and air in the staged tests. These configurations approximate mixing limitation of the practical-firing methods shown in Figure 1. The nozzle in Figure 2a produces a uniform heterogeneous mixture of coal and air prior to combustion and represents the limit of intensely mixed flames produced with high swirl. The nozzle shown in Figure 2b requires radial mixing of fuel and air and can approximate the mixing conditions of wall-fired and opposed-fired units. The nozzle shown in Figure 2c has slower axial mixing promoted by low swirl in the secondary air. Mixing in this nozzle can approximate early mixing in tangentially-, arch-, and Turbo®-fired flames. Emissions for unstaged conditions are higher for rapidly mixed flames by 300-600 ppm (0%, O_2, dry). However, the emissions of NO_x vary by as much as 400 ppm (0%, O_2, dry) for fixed nitrogen content of the fuel and mixing conditions.

Successfully establishing the minimum achievable emission of NO_x and achieving that level will require improved understanding of the influence of boiler design, boiler operation, and fuel properties on NO_x emissions. Considerable work has been done to identify the influence of design and operating parameters on NO_x emissions(2-17,19,23-26). This work continues and will eventually lead to minimization of the influence of design and operating conditions on NO_x emissions for a given fuel. However, reliable methods of predicting or easily measuring the minimum level of nitrogen oxides achievable with different fuels are needed so that utility operators can select fuels which comply with regulations, boiler manufacturers can design boilers for particular fuels or a range of fuels, and the Environmental Protection Agency can set reasonable emission standards and goals for the range of fuels existing in the United States.

This paper uses information from the literature to establish a correlation which predicts the relative dependence of nitrogen oxides emissions on fuel properties. The mechanism of conversion of fuel nitrogen to products is critically reviewed, unimportant reactions are eliminated, noncontrolling reactions are combined, a predictive equation is formulated, numerical values of the constants are specified as accurately as possible from available data, and research needed to improve the predictive capabilities of the correlation are recommended.

MECHANISM FOR CONVERSION OF FUEL NITROGEN TO NITROGEN OXIDES

The mechanism for conversion of fuel nitrogen to products is complicated by potential branching points and transformation and interactions between solids, gases, and liquids. A mechanism is shown schematically in Figure 3. Nitrogen is partially removed from the coal as the temperature is increased. This can happen in a number of ways:

- Nitrogen contained in the original structure is ejected as relatively large molecules, possibly as tar.
- Smaller nitrogen-containing molecules are formed by thermal decomposition and are ejected from the coal.
- Secondary reaction products are produced from reaction of nitrogen released within the pores of the coal.

Once the nitrogen is released from the coal the compounds can react with one another, solid surfaces, or gas-phase products of combustion. The end result is production of nitrogen oxides and molecular nitrogen. The removal of nitrogen from the char is kinetically controlled(27-29) and a fraction of the nitrogen remains to be burned as part of the char in pulverized-coal furnaces. The char nitrogen is oxidized to nitrogen oxide which will react further with gas molecules and solid surfaces within and outside the char particle. The overall conversion of fuel nitrogen to NO_x can be expressed as

$$\frac{NO}{\text{Fuel N}} = \overbrace{\alpha\left[\overset{\text{Tar}}{\beta(1-\phi_1)} + \overset{\text{HCN}}{(\beta_2+\beta_1\phi_1)(1-\phi_2)} + \overset{NH_3}{\phi_3(\beta_3+\beta_1\phi_1\phi_2\ \beta_2\phi_2)}\right]}^{\text{Volatile Conversion}} + \overset{\text{Char Conversion}}{\left[(1-\alpha)\gamma\eta_2\right]} \qquad (1)$$

where greek letters represent the fractional splits shown in Figure 3. This expression is more detailed than previously presented(27) but may simplified by eliminating and combining unimportant and noncontrolling terms.

The expression can also be used to account for the influence of combustor conditions on ultimate conversion by expressing each of the factors as fundamental or semiempirical functions of combustor conditions. A simple example is expression of the initial split of nitrogen between the char and volatiles as

$$\alpha = \frac{N_{volatile}}{FN} = 1 - e^{-\int_0^t e^{-E/RT}dt} \qquad (2)$$

where the devolatilization rate is independent of the surrounding atmosphere and is first order in char nitrogen concentration. This accounts for the influence of time/temperature history of the combustor on NO_x production.

This work seeks to produce a manageable expression for conversion of fuel nitrogen to NO_x. To accomplish this, each step in the mechanism is evaluated using existing data to eliminate and simplify expression (1) as possible.

Devolatilization of Fuel Nitrogen

The emission of nitrogen oxides produced from burning coal nitrogen strongly depends on the extent of devolatilization from the coal. Four pieces of indirect evidence support this:

1. Difference in NO_x emissions with coal characteristics(3,13,17-22).
2. Differences in conversion of fuel nitrogen to NO_x between coal and char(26-29).
3. Differences in NO_x emission caused by changes in the first stage temperature(2,18,20,21,24).
4. Difference in NO_x emission between low- and high-volatile coals(18, 19,24).

Unfortunately, none of the available data directly proves that the division of nitrogen between the char and volatile matter influences the emissions of nitrogen oxides. The first piece of evidence could be caused by many coal properties although the rate of fuel nitrogen evolutions seems to be the most likely. The second argument strongly supports influence of volatile fuel nitrogen on NO_x emissions. However, the results might be influenced by other changes, such as slower nitrogen evolution rates for low nitrogen chars. Argument 3 supports the contention, but higher temperatures will also alter gas kinetics. Argument 4 is strongly in favor of the hypothesis, but different coals may have differences other than the volatility of fuel nitrogen. Nonetheless, the extent of fuel nitrogen devolatilization should influence NO_x emissions; much evidence supports this hypothesis, and little evidence contradicts.

In spite of this, the rate of devolatilization of coals has been reported to be independent of coal type(27,30). Pohl and Sarofim(27) used a time-resolved disperse-phase reactor and found that the rate constant for nitrogen devolatilization at all extents of reaction(31) to be within a factor of 6 for the Savage Montana lignite and the Pittsburgh Seam #8 bituminous coals. The difference was attributed to experimental uncertainty but only two coals were investigated and no firm conclusions can be reached. Solomon and Colbet(30) measured the rate constant for nitrogen evaluation from 12 bituminous coals and one lignite using a hot screen integral reactor. Their results also showed a factor of 6 difference in the rate constant for nitrogen evolution for different coals for initial use were as secondary nitrogen release. A difference of a factor of 6 in the rate constant for evolution of nitrogen will mean the difference between devolatilizing 40 or 94 percent of the nitrogen in the coal. Better data on devolatilization of fuel nitrogen is required before the influence of coal properties on evolution of nitrogen and production of NO_x can be resolved.

The extent of fuel nitrogen devolatilization depends on the devolatilization temperature, time, possibly heating rate, but not strongly on the atmosphere. Some have suggested that evolution of fuel nitrogen obtains an asymptotic value which depends only on temperature(30). If true for the conditions of pulverized flames, Equation (2) could be expressed as a function of the highest temperature in the combustor. However, no asymptotic values of char nitrogen are observed at the conditions of pulverized flames(27) nor at longer heating times when the data is critically evaluated(30). The extent of nitrogen evolution must then be a function of the time/temperature history in the combustor.

The rate of heating the coal may alter the devolatilization of nitrogen from the coal. Evidence for the influence of heating rate on nitrogen evolution is limited and was obtained outside conditions in pulverized-coal combustors. Available data indicates that heating rate does alter the ultimate yield of volatile nitrogen at a given temperature(32). However, data obtained at pulverized-flame conditions suggest that heating rate is unimportant above 10^4 C/sec(33).

The atmosphere surrounding the coal should not alter the rate of nitrogen evolution. However, data is very limited, taken outside the range of conditions in pulverized-coal combustor, and may be contradictory(22 and 39). Here we assume that the atmosphere does not seriously alter the rate of nitrogen evolution from the coal, but further experiments are required to establish this.

Most of the rate constants reported for nitrogen evolution from coal may be invalid at the conditions of pulverized-coal flames. Several rate constants for nitrogen evolution from coal have been reported(27,30,39) and others can be extracted from reported data. The data used to extract rate constants for nitrogen evolution has been obtained in dispersed reactors(27) or heated grids(30,32,34-36). Care must be used in interpreting the results from both reactors.

Rate constants derived from data taken with the heated grid were unable to predict behavior of pulverized-coal flames(37). A number of potential errors are associated with use of the hot-wire experiments to derive devolatilization rate constants:

- Maximum achievable temperatures are less than 1500 to 1800 depending on the grid material compared to maximum flame temperatures of 2200°K.
- Heating rates used were less than 10^3°K/sec while heating rates in pulverized flames are 10^4-10^6°K/sec.
- Compensation for reaction during heating and cooling are difficult, although not always important.
- Temperature measurements can be inaccurate(38).

Most important, poor time resolution makes the study of devolatilization reactions by the hot-screen apparatus difficult. Early work used the hot-screen apparatus as an integral reactor with reaction times between 5 and 80 seconds. Devolatilization rate constants were extracted using a first-order rate expression from the amount of the nitrogen removed at the end of the reaction. The devolatilization of nitrogen does not follow a simple first-order rate expression(27,30,31). In fact, the rate of reaction falls progressively below a first-order reaction as the reaction progresses(31). The rate constant for nitrogen evolution has been correlated as a first-order reaction at different extents of nitrogen removal(31), although only the rate constant extrapolated to the onset of reaction was reported(27). Interpretation of the results from hot-screen experiments as an integral reactor will therefore yield an average rate constant for the extent of reaction. This rate constant will vary with the time chosen in the experiment and will always underestimate the extent of nitrogen devolatilization at the short times important in pulverized-coal flames.

Later time-resolved measurements were attempted using the hot-screen apparatus(34). The gases were collected in an IR cell and changes in compositions of the gases were measured using a Fast Fourier Transform infrared spectrometer capable of a measurement every 200 milliseconds(38). Resolution of 200 milliseconds is insufficient to observe the fast devolatilization of nitrogen at high temperatures(27), actual time resolution is considerably broadened by transport and dispersion of the products, and the nitrogen balance is inadequate since the tar (but not nitrogen concentration of the tar) and HCN are the only nitrogen products which can be measured. Use of the hot-screen apparatus is therefore limited for measuring rate constants of nitrogen evolution applicable to pulverized-coal flames.

The dispersed-phase reactor is more applicable to measuring the rate of nitrogen evolution under simulated combustion conditions but will also result in uncertainties. First, the reactor is more difficult to construct and operate than a hot-screen apparatus. Second, particle temperatures are difficult to measure and were estimated in the past(27,31,33). Gas products are difficult to measure, have a residence time which depends on the time of evolution and the gas residence time of the system, and have rarely been measured(27,28,39). In spite of these limitations, the dispersed-phase reactor appears to be the only device capable of simulating combustion conditions(34) and providing the time resolution necessary to measure the rate of fuel nitrogen evolution.

Devolatilized Fuel Nitrogen Compounds

The distribution of fuel nitrogen among gas-phase compounds does not appear to influence the conversion of fuel nitrogen into nitrogen oxides. The amount of NH_3, HCN, and nitrogen present in the tar are known to vary with coal type(18,28,30-32,35,36,38) and combustor conditions(31). Ammonia can account for as much as 14 percent of the nitrogen in the first stage of staged lignite flames but accounts for less than 1 percent in flames burning high-volatile A and high-rank coals under the same conditions. The amount of nitrogen oxide exiting the first stage can account for as much as 15 percent of the nitrogen in anthracite flames but less than 5 percent in lignite flames. Hydrogen cyanide can account for 15 percent of the nitrogen in high-volatile A and B coal flames but less in higher and lower rank coal flames(18). The variation in exit NO emission can be explained without reference to the distribution of nitrogen between compounds in the gas phase. Knowledge of this distribution is therefore concluded to be unnecessary to estimate the influence of coal properties on NO_x emissions.

NO_x emissions appear to depend on the amount of nitrogen evolved into the gas phase and the conditions of the gas phase, but not the concentration of individual species in the gas phase. This allows Equation (1) to be simplified to the expression of Pohl and Sarofim(27):

$$\frac{\text{NO}}{\text{Fuel NO}} = \alpha\eta_1 + (1 - \alpha)\,\eta_2 \qquad (3)$$

Oxidation of Char Nitrogen

Oxidation of the nitrogen contained in the char could ultimately control NO_x emission. This will occur when conversion of volatile nitrogen to NO_x is controlled to low levels. In these cases, oxidation of nitrogen in the char will be a major source of NO_x. Estimates show that oxidation of the nitrogen in the char can contribute between 10 and 90 percent of the NO_x formed in coal flames. The amount depends on flame temperature and fuel equivalence ratio(27,28) and properties of the char(39). Little data exists on conversion of char nitrogen to NO_x and discrepancies exist in the data which does exist. Figure 4 shows that the nitrogen released from the char at the condition of pulverized flames will be 15 to 25 percent converted to NO_x. The extent of this conversion depends on temperature, fuel equivalence ratio, and probably characteristics of the char. All measurements indicate that production of NO_x is lower under fuel-rich conditions. Pershing and Wendt(2) found a stronger dependence on fuel equivalence ratio than did Pohl and Sarofim(27) and Song, et al.(28). The data of Pershing and Wendt and Song, et al., indicate high temperatures can reduce the formation of NO_x from nitrogen in the char. Pohl and Sarofim's data is consistent in magnitude with Pershing and Wendt's but is inconsistent with the temperature-dependence shown by the data of Song, et al. The existing data is sufficient to qualitatively establish that conversion of nitrogen in the char to NO_x depends on combustor conditions but is inadequate to determine quantitatively the influence of temperature, fuel equivalence ratio, and char properties on conversion of char nitrogen to NO_x.

A model has been proposed which includes the major features controlling conversion of char nitrogen in the coal(39). The model was based on the recently demonstrated premise that nitrogen and carbon in the char are oxidized in proportion to their molar concentration(40). Rate constants and pore structures derived from char combustion studies(41) can then be used to describe the oxidation of nitrogen in the char. Homogenous reduction of the nitrogen oxide can be estimated using a model similar to the one developed by Wendt and Schultze. In this model, nitrogen oxides which escape the pores can be further reduced by reaction in the gas phase.

Homogenous Gas-Phase Reactions

Nitrogen compounds released from the coal or char react in the gas phase to form nitrogen oxides and molecular nitrogen. Ample evidence shows that conversion of the nitrogen compounds to nitrogen oxides depends strongly on the fuel equivalence ratio(42-44), the concentration of fuel nitrogen in the gas phase(42,43), weakly on temperature(42-47), and not on the structure of the fuel nitrogen compound(42,46,48).

A sequence of overall reactions can then be written to explain the conversion of fuel nitrogen in the gas phase.

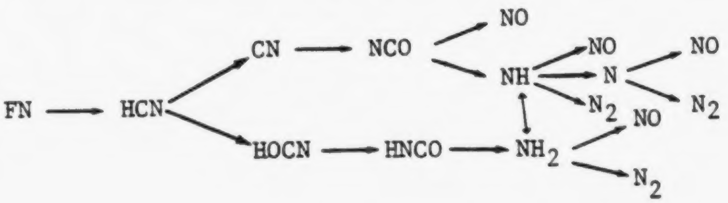

Evidence supports the following sequence of reactions:

- Fuel nitrogen is rapidly, irreversibly, and quantitatively converted to HCN.
- HCN is irreversibly converted to NCO(45,50) or HOCN(47,51) through a rate-controlling step.
- HOCN and NCO rapidly interchange with one another and react to form NH_i species.
- The NH_i species are equilibrated among themselves and, except possibly N, and provide the branching point for production of NO or N_2.
- The oxidizer and NH_i species which provide the branching point are uncertain(1,42-51). In spite of this, equilibration among the NH_i and oxygen species allows expressions to be written for conversion of fuel nitrogen.

The efficiency of conversion of gas-phase fuel nitrogen to nitrogen oxides can be expressed simply. The expression results from integrating the ratio of the rate of NO formation to the rate of fuel nitrogen depletion over the life of the fuel nitrogen compounds. The first such expression(42) was derived from the following reactions.

$$I + O_x \quad k_4 \ldots \quad NO + \ldots \tag{4}$$

$$I + NO \quad k_5 \ldots \quad N_2 \ldots \tag{5}$$

Dividing the two rates and integrating over the life of the fuel nitrogen species yields

$$\frac{[NO]}{X} = 1 - \exp\frac{-[NO] + [N]}{2X} \tag{6}$$

where X is an empirical derived parameter which was thought to be,

$X = \dfrac{k_4[OX]}{k_5}$, and was found to be 2-3 times the equilibrium concentration of [OH] in rich flames.

Fenimore refined expression (6) in later papers. He presented evidence in 1976(43) that the nitrogen intermediate is NH_2 and correlated the oxidant with the equilibrium concentration of hydroxyl radical. The following expression for α, the fraction conversion of fuel nitrogen, was derived from available data

$$\alpha = 0.56 \frac{[H_2O]^2}{[H_2]} \exp{-20\text{kcal}/RT} \tag{7}$$

where $[H_2O]/[H_2]$ has replaced $[OH]^2$ equ. However, this correlation for α had an average discrepancy of 88 percent.

Fenimore made minor modification to the expression for α in 1979(44). He presented evidence that NH_2 is the most important amine intermediate, and correlated α with the concentration of water

$$\alpha = 700[H_2O]^{exp}-50kcal/RT \tag{8}$$

The three expressions for α developed by Fenimore correlate the data with similar accuracy. However, expression (8) is more convenient to use since the concentration of H_2O can be estimated easily and accurately in flames.

In the cases where gas-phase chemistry controls, conversion of fuel nitrogen can be estimated from knowledge of the exit temperature, water analysis of the coal including hydrogen in the coal, a fuel nitrogen analysis, and use of equations (8) and (6). Conditions may also exist when conversion of fuel nitrogen is partially or completely controlled by devolatilization of the fuel nitrogen, gas-phase reactions in the pores, or by quenched reactions. An expression for the extent of devolatilization of fuel nitrogen was derived in expression (2). A first-order devolatilization process has been assumed in Equation (2) but any fundamental or empirical expression could be used. The amount of volatile nitrogen calculated in expression (2) can be used in place of the original fuel nitrogen in expression (6) to calculate conversion of fuel nitrogen to NO_x.

Reaction of char nitrogen in pores is more difficult to estimate. First, the residual nitrogen left in the char must be estimated by expression (2). The gas-phase concentration inside the pores must usually be estimated using a pore model such as derived by Wendt and Schulze(39). Reactions of the gases inside the pores can be estimated from reaction mechanisms(39). Nitrogen oxides which exit the pores can react further in the gas phase.

In some cases, conversion of fuel nitrogen may be controlled by quenching before the nitrogen compounds have completely reacted. Typically, coals burned in air contain a nitrogen oxide equivalent (0% O_2, dry) of 1500-5000 ppm as fuel nitrogen. This is considerably above the equilibrium value of nitric oxide at pulverized-flame conditions, approximately 1000 ppm. Fuel nitrogen compounds must continue to react and to reduce the summation of fixed nitrogen concentration to the equilibrium value. The level of fixed nitrogen in these cases will be higher although similar to the equilibrium value when the gases are quenched too rapidly.

Heterogeneous Reaction of Fuel Nitrogen

Solid surfaces have the potential to catalyze reduction of nitrogen oxides. The phenomena was first recognized in a fluid-bed combustor(52). Previous work had been done on the use of carbonaceous substances for destruction of nitrogen oxides in automobile exhausts(53,54). Subsequently, the importance of heterogeneous reactions(28,29,55-59) in pulverized-coal systems was investigated.

Examination of the kinetic mechanism shows that heterogeneous reduction of nitrogen is of minor importance in pulverized flames. The homogenous rate(44) of reaction of amine species to N_2 at 2000°K, 5×10^{-6} g/cc of char with 20 m^2/g, and 1 ppm of amine species is 300 times faster than destruction of NO by heterogeneous reactions(29,59) with the char. This is a conservative estimate since flame temperatures are above 2000°K only briefly in pulverized-coal flames, the heterogeneous reaction has a large activation energy, the particle loading will be less outside the flame region, and the specific surface area could be lower or higher by a factor of 10. The rate constant used was derived using a value of 20 m^2/g(59), but because of the uncertainties surface areas should be considered part of the rate constant. The concentration of active amine species in pulverized coal flames is on the order of 10's of ppm(60), but the concentration of individual amine species can be about 1 ppm(47,50).

The heterogeneous reduction of nitrogen oxides can be important when the homogenous reactions are inactive. The homogenous reactions will be slow when quenched, when the system has approached equilibrium, or when a reactant is depleted. The heterogeneous reactions will be quenched more rapidly than the homogenous ones because of the long larger activation energy and will not contribute to destruction of NO in quenched gases. Destruction by heterogeneous reaction cannot be important near equilibrium because no net destruction occurs. Heterogeneous destruction of NO can become important when a reactant necessary for homogenous destruction is depleted. In this case, the net destruction of NO in pulverized-coal flames by heterogeneous reactions could approach 25 percent(29). Fuel nitrogen destruction is constrained at these conditions by equilibrium to a conversion of about 35 percent, but this will usually be achieved by faster homogenous reactions in the active parts of the flame.

The available experimental data indicates that heterogeneous reactions of nitrogen oxides are unimportant in coal flames(56). Recently, a heterogeneous rate constant was derived by burning a char from a Utah bituminous coal under conditions where homogenous reactions to destroy NO were unimportant. The derived rate constant was larger but of similar mganitude to those derived by others. This large heterogeneous rate constant was used to predict the destruction of fuel nitrogen in a coal flame of the bituminous coal. Heterogeneous destruction could account for a 20 percent reduction in NO_x while homogenous reactions accounted for 50 percent reduction. Homogenous and heterogeneous reduction will not be additive since depletion of reactants by the faster homogenous reactions will reduce the amount of NO destroyed by the heterogeneous rates. Destruction of NO by heterogeneous reactions, then, seems to be of minor importance in pulverized-coal flames.

REQUIRED WORK

Available data does not allow formulation of an accurate correlation of conversion of fuel nitrogen to NO_x. Therefore, further experiments are required. Data are inadequate in two areas:

1. Rate constants for devolatilization of nitrogen from different coals applicable to pulverized-coal flames.
2. Rate of oxidation of the residual char nitrogen.

The first is the most important and experiments are urgently needed. The second is poorly defined, currently of less importance than the first, but will become more important when current levels of nitrogen oxide are reduced.

The experiments which can determine the rate constant for devolatilization of nitrogen are limited and difficult. The nitrogen devolatilization rate constant must be determined within a factor of two so that the fraction of nitrogen evolved can be predicted within an absolute fraction of oil. In addition, the experimental conditions must be the same as those of a pulverized-coal flame. This will require:

- Dispersed-phase pulverized coal
- Heating rates greater than 10^4 °K/sec
- Measure particle temperatures of 1000-2200°K
- Times of 2-1000 milliseconds with resolution of 1 milliseconds

Collection of the entire char in a stream of hot, rapidly-flowing gas in a reactor with cold walls will satisfy these conditions. Cold walls, or shielding, is required to optically measure particle temperatures in devolatilization experiments.

The experiment needed to measure the oxidation rates of char nitrogen can be simpler because char oxidation does not depend on rapid heating, the reaction mechanism is better understood and simpler, and the time constants are longer. Fluid beds, packed beds, thermal gravimetric balances, and flow reactors have all been successfully used to measure the rate of char oxidation over a wide range of chars, temperatures, and oxygen partial pressures(41). Experiment and theory have not been adequately developed to measure, account, and correct for the reactive internal surface areas of chars. Future experiments must adequately account for the surface area available for oxidation and the dithermal restrictions of the char.

CONTROLLED MIXING CONDITIONS

Correlations of NO_x emissions with fuel properties for controlled mixing conditions are valuable when correlation cannot be developed to account for the influence of combustor conditions. The previous section has shown that insufficient information is available to correlate NO_x with combustor conditions. In such cases, correlation of coal properties with NO_x emission from combustor with controlled mixing conditions can:

- Rank coals for NO_x emission for different controlled mixing conditions.
- Identify the coal properties which most strongly influence NO_x emissions.
- Indicate the most effective means of controlling NO_x emissions for coals under controlled mixing conditions.

The controlled mixing conditions shown in Figure 1 result in greatly different levels of NO_x emissions. Figure 6 shows that conversion of char nitrogen (solid symbols) is constant for all three mixing conditions, 25 percent, but that conversion of volatile nitrogen depends on the mixing condition. This is not surprising, since conversion of char nitrogen depends on the conditions inside the char particle and the atmosphere surrounding the char particle in the long burnout stage. These conditions are similar for the three flames studied. The conversion of volatile nitrogen depends on the oxygen available in the early regions of the flame and strongly depends on mixing conditions. Premixed flames will have the most radial diffusion flames intermediate, and axial diffusion flames the least oxygen available to oxidize fuel nitrogen. This trend is clearly shown in Figure 5. The slight decrease in conversion of gas-phase nitrogen corresponds with increasing excess air for the premixed flame is thought to be insignificant, although a slight decrease could be expected from lowering the temperature in the premixed case. Conversion of coal nitrogen in these experiments is controlled by mixing of the gas phase.

Correlations

A correlation of fuel properties with NO_x emissions has been successfully developed previously for the controlled mixing conditions shown in Figure 2(18,20,21). This correlation is used to measure volatile HCN and char nitrogen to correlate NO_x emissions with coals for conditions of Figure 2 and measured distribution of nitrogen leaving the first stage of a two-stage combustor to correlate the minimum NO_x emissions. The new correlations uses the same form but has improved over the old one by

- Using the proximate and coal nitrogen analyses instead of requiring that volatile HCN and char nitrogen and nitrogen distribution in the combustor be measured.
- Slightly improving explanation of the variability in NO_x emissions from $v^2 = 0.85$ to $v^2 = 0.90$.
- Allowing the correlation to be extended to coals for which HCN and char nitrogen data were unavailable so that now fuels from peat to anthracite have been correlated.
- Eliminating the need for measurements at the first stage of two-stage combustors to correlate minimum NO_x emissions.

The new correlations predict the NO_x emission extremely well for the premixed and radial diffusion flame, well for the minimum NO_x emissions from staged flames, and adequately for the axial diffusion flame.

Premixed Flame

Nitrogen oxides from the premixed flame can be correlated with the coal nitrogen, volatile matter of the coal, and the fixed carbon content of the coal. The data was correlated with

$$NO = 285 + 1280\left(\frac{N_o}{1.5}\right) + 180\left(\frac{VM}{40}\right)\left(\frac{NO_{eq}}{3200}\right) - 840\left(\frac{FC}{60}\right)\left(\frac{NO_{eq}}{3200}\right) \qquad (9)$$

where N_o is percent nitrogen in the fuel (daf). VM is percent volatile matter in the coal (daf), FC is fixed carbon in the coal (daf), and NO_{eq} is the NO equivalent of fuel nitrogen in the coal on a zero percent O_2, dry basis.

Fixed carbon and volatile matter are not independent, but inclusion of both explains an additional 5 percent of the variability and so both terms have been retained. Equation (9) correlates the NO_x emission from the premixed flame with a coefficient of determination, $r^2 = 0.9$ for 20 coals and $r^2 = 0.75$ for 46 coals. Figure 6a shows the error of fit. The predicted NO_x is within 50 ppm except for three coals, □-Beulah, ◁-Hardin, and △-Savage. These are all lignite coals from the North Great Plain region. The volatile matter of these coals is difficult to measure, is suspected of part of the error in prediction, and is being verified. The correlation is considered good and applicable to predicting NO_x emissions from the premixed flame.

Equation (8) reveals the properties of the coal which most influence NO_x emissions. For an average coal the constant term adds 400 ppm, the nitrogen concentration of the coal adds 1300 ppm, the volatile matter of the coal adds 200 ppm and the fixed carbon (a measure of char nitrogen) subtracts 800 ppm for a total of 1100 ppm. The nitrogen in the coal has the largest influence on NO_x emissions, but the volatile matter has a secondary influence.

Radial Diffusion Flame

The NO_x emissions from the radial diffusion flame were correlated with fuel properties with $r^2 = 0.9$ for 20 coals using the same form of equation as used for the premixed flame.

$$NO = 340 + 835\left(\frac{NO}{1.5}\right) + 20\left(\frac{VM}{40}\right)\left(\frac{NO_{eq}}{3200}\right) - 395\left(\frac{FC}{60}\right)\left(\frac{NO_{eq}}{3200}\right) \qquad (10)$$

Figure 6b compares the predicted versus estimated NO_x emissions. All predicted and measured values are within 70 ppm NO_x. Five costs have error on the order of 50-80 ppm. These coals all have either high or low volatile matter.

The absolute NO_x emissions of the radial diffusion flame are lower than in the premixed flame. The difference can be seen in equation 10 where for an average coal the constant term contributes 300 ppm, the coal nitrogen 800 ppm, the volatile matter only 20 ppm, and the fixed carbon removes 400 ppm. This results in NO_x emission of about 700 for an average coal. The volatile nitrogen is converted to N_2 with greater efficiency in the radial diffusion flame because of more restricted oxygen availability.

Axial Diffusion Flame

Development of a correlation of NO_x emission with coal properties for the axial diffusion flame presented special problems. A correlation equation of the same form as equations (9) and (10) was tried but the coefficient of determination, $r^2 = 0.55$ for 20 coals was considerably less than for the premixed and radial diffusion flames. The axial diffusion flames had a relatively long ignition delay. This ignition delay depended on coal type and allowed considerable mixing of oxidant with the fuel prior to ignition. This behavior is shown in Figure 7. As expected, the premixed flame produced the highest NO_x emissions, but the radial diffusion and unstabilized axial diffusion flame produced similar emissions indicating similar mixing conditions. However, the axial diffusion flame showed greatly reduced emissions when

25 percent propane was used to stabilize the flame near the nozzle. Correlations of NO_x emissions from the axial diffusion flame is then expected to depend on coal properties which control emissions, typically total enthalpy of the released volatile matter, as well as the coal properties which normally influence NO_x emission. In light of this, the poorer correlation is expected.

Mimimum Staged NO_x Emissions

The minimum NO_x emissions from a flame burning a coal is of prime impo-tance is selecting coals, designing boilers, and setting standards. The minimum NO_x emitted from a staged flame can be as little as one-third that emitted from an intensely mixed flame. Figure 8 shows the difference between premixed staged and unstaged flames. The staged flame still shows variations in emissions between coals with the same nitrogen content of 100 ppm. The form of Equations (9) and (10) was used to correlate NO_x emissions from the staged flame resulting in

$$NO = 150 + 80\left(\frac{N_o}{1.5}\right) - 30\left(\frac{VM}{40}\right)\left(\frac{NO_{eq}}{3200}\right) + 100\left(\frac{FC}{60}\right)\left(\frac{NO_{eq}}{3200}\right) \qquad (11)$$

Figure 9 shows the correlation of NO_x emissions for 20 coals. The correlation had a coefficient of determination of $r^2 = 0.71$. Slightly better correlations were obtained used expressions with different forms, but the improvements did not justify abandoning the form used for the other flames. An extremely important point is the sign change in the contribution of volatile matter between Equations (9) and (10), and Equation (11). This means that in volatile nitrogen contributes to an increase in NO_x emissions in the unstaged flames but to a decrease in staged flames. This is perfectly reasonable and shows that volatile nitrogen can be forced towards N_2 under staged conditions.

CONCLUSIONS

Emissions of NO_x could be correlated with fuel and combustor conditions if the rate of evolution of the volatile and char and the reactions of the char nitrogen in the char particles were known. This is not the case and experiments are needed to determine the rate of nitrogen devolatilization from the coal and the rate of oxidation and reaction of char nitrogen. In the absence of such knowledge, empirical correlations of NO_x emission with coal properties for controlled mixing experiments can be most useful. Excellent correlations for nitrogen oxide emission with coal properties were developed for several controlled mixing experiments in this paper. These showed that the emissions of NO_x can be correlated with proximate and nitrogen analyses, the amount of fuel nitrogen is the major contribution to NO_x emission, but that volatile nitrogen is a secondary contribution. The results also showed that high-volatile nitrogen will produce high NO_x emissions in unstaged flames but low NO_x emissions in staged flames.

ACKNOWLEDGEMENTS

This work has been supported by the U.S. Environmental Protection Agency under Contract 68-02-3633. The bench-scale experimental results were obtained under Contracts 68-02-2667 and 68-02-3658 which were funded by the EPA and the International Energy Agency (for Canada, Denmark, and Sweden). The authors also wish to acknowledge the assistance and guidance given by the project officers W. Steven Lanier, G. Blair Martin, and Dennis C. Drehmel, and the computational assistance provided by Greg P. Stacley of the University of Utah.

REFERENCES

1. Hayhurst, A. N., and I. M. Vince. Nitric Oxide Formation from N_2 in Flames: The Importance of Prompt NO. Progress in Energy and Combustion Science, 6(1), 1980. p. 35-51.

2. Pershing, D. W., and J. O. L. Wendt. Pulverized Coal Combustion: The Influence of Flame Temperature and Coal Composition on Thermal and Fuel NO_x. In: Proceedings of the Sixteenth Symposium (International) Combustion, The Combustion Institute, Pittsburgh, Pennsylvania, 1977. pp. 389-399.

3. Marshall, J. J., and A. P. Selker. The Role of Tangential Firing and Fuel Properties in Attaining Low-NO_x Operation for Coal-Fired Steam Generation. In: Proceedings, Second NO_x Control Technology Seminar, EPRI. FP-1109-SR, Electric Power Research Institute, Palo Alto, California. pp. 5-1 - 5-28.

3. Bartok, W., A. R. Crawford, and G. J. Piegari. Systematic Field Study of NO_x Emission Control Methods for Utility Boilers. U.S. Environmental Protection Agency, Research Triangle Park, North Carolina, NTIS PB 210 739, 1971. 159 pp.

5. Crawford, A. R., E. H. Manny, and W. Bartok. Field Testing: Application of Combustion Modifications to Control NO_x Emissions from Utility Boilers. U.S. Environmental Protection Agency, Research Triangle Park, North Carolina, NTIS PB-237 344, 1974. 151 pp.

6. Cato, G. A., H. J. Buening, C. C. DeViro, B. G. Morton, and J. M. Robinson. Field Testing: Application of Combustion Modification to Control Pollutant Emissions from Industrial Boilers. Phase I. U.S. Environmental Protection Agency, Research Triangle Park, NC, NTIS PB 238 920, 1974. 204 pp.

7. Christiano, J. P., and R. V. Crume. NO_x Standards of Performance for New Lignite-Fired Steam Generators. In: Proceedings Technology and Use of Lignite, Grand Forks Energy Research Center, Grand Forks, North Dakota, GFERC/IC-77/1, 1977. pp. 274-284.

REFERENCES (Continued)

8. Crawford, A. R., E. H. Manny, and W. Bartok. Field Testing: Application of Combustion Modification to Power Generating Combustion Sources. In: Proceedings of the Second Stationary Source Combustion Symposium, Volume II. Utility and Large Industrial Boilers. U.S. Environmental Protection Agency, Research Triangle Park, North Carolina, EPA-600/7-77-073b, 1977. pp. 3-40.

9. Ctvrtnicek, T. E., and S. J. Rusek. Cyclone Boilers--Their NO_x Emissions and Population. In: Proceedings of the Second Stationary Source Combustion Symposium, Volume II. Utility and Large Industrial Boilers. U.S. Environmental Protection Agency, Research Triangle Park, North Carolina, EPA-600/7-77-073b, 1977. pp. 123-141.

10. Maloney, K. L., and P. L. Langsjoen. Westen Industrial Boilers. In: Proceeding of the Second Stationary Source Combustion Symposium, Volume II. Utility and Large Industrial Boilers. U.S. Environmental Protection Agency, Research Triangle Park, North Carolina, EPA-600/7-77-073b, 1977. pp. 163-208.

11. Chichanowicz, J. E., M. W. McElroy, L. J. Muzio, T. W. Sonnichsen, and G. H. Shiomoto. NO_x Emissions Characteristics of Down-Fired, Sequential Air Addition Furnaces. In: Proceedings, Second NO_x Control Technology Seminar, Electric Power Research Institute, Palo Alto, California, EPRI FP-1109-SR, 1979. pp. 12-1 - 12-20.

12. Crawford, A. R., E. H. Manny, and W. Bartok. Control of Utility Boiler and Gas Turbine Pollutant Emissions by Combustion Modification--Phase I. U.S. Environmental Protection Agency, Research Triangle Park, North Carolina, NTIS PB-281-078, 1978. 140 pp.

13. Rawdon, A. H., R. A. Lisankas, and F. J. Zone. Design and Operation of Coal-Fired Turbo Furnaces for NO_x Control. In: Proceedings, Second NO_x Control Technology Seminar, The Electric Power Research Institute, Palo Alto, California, EPRI FP-1109-SR, 1979. pp. 6-1 - 6-9.

14. Thompson, R. E. Nitric Oxide Controls for Coal Fired Utility Boilers from an Applications Viewpoint. In: Proceedings: Second NO_x Control Technology Seminar. Electric Power Research Institute, Palo Alto, California, EPRI FP-1109-SR, 1979. pp. 9-1 - 9-27.

15. Brandt, J., R. Bruchhaus, K. Hein, J. J. Homburg, J. Jacobs, M. Karschner, H. Kremer, R. Quack, R. A. Riedlinter, R. Telöken, and K. Than. Minderungstechnologie für NO_x-Emissionen Steinkohlengefeuerter Grosskraftwerke. Technischwissschaftliche Berichte Wärmekraftwerke, Heft 8, VGB Technische Vereinigung der Grosskraftwerkhetreiber E. V. Essen, Federal Republic of Germany, 1980. 325 pp.

16. Sonnichsen, T. W., and J. E. Cichanowicz. NO_x Emissions Characteristics of Arch-Fired Furnaces. In: Proceedings of the Joint Symposium on Stationary Combustion NO_x Control, U.S. Environmental Protection Agency, Research Triangle Park, North Carolina, IERL-RTP. 1087, 1980. pp. 152-.

REFERENCES (Continued)

17. Barsin, J. A. Fossil Steam Generator NO_x Control Update. In: Proceedings of the Joint Symposium on Stationary Combustion NO_x Control, IERL-RTP-1087, U.S. Environmental Protection Agency, Research Triangle Park, North Carolina, 1980. pp. 69-93.

18. Chen, S. L., M. P. Heap, and D. W. Pershing. The Fate of Volatile and Char Nitrogen During Combustion of U.S. and World Coals. Presented at the Nineteenth International Symposium on Combustion, Haifa, Israel, August 1982.

19. Kawamura, T., and D. J. Frey. Current Developments in Low-NO_x Firing Systems. In: Proceedings of the Joint Symposium on Stationary Combustion NO_x Control, IERL-RTP-1087, V. U.S. Environmental Protection Agency, Research Triangle Park, North Carolina, 1980. pp. 94-129.

20. Heap, M. P., D. W. Pershing, G. C. England, J. W. Lee, and S. L. Chen. The Influence of Fuel Characteristics on Nitrogen Oxide Formation--Bench-Scale Studies. In: Proceedings of the Third Stationary Source Combustion Symposium; Volume II. Advance Processes and Special Topics. The U.S. Environmental Protection Agency, Research Triangle Park, North Carolina, EPA-600/7-79-050b, 1979. pp. 3-39.

21. Chen, S. L., M. P. Heap, D. W. Pershing, R. K. Nihart, and D. P. Rees. Fate of Coal Nitrogen During Combustion. In: Proceedings of the Joint Symposium on Stationary Combustion NO_x Control, EPA, IERL-RTP-1086, IV, U.S. Environmental Protection Agency, Research Triangle Park, North Carolina, 1981. pp. 154-180.

22. Pershing, D. W., J. E. Cichanowicz, G. C. England, M. P. Heap, and G. B. Martin. The Influence of Fuel Composition and Flame Temperature on the Formation of Thermal and Fuel NO_x in Residual Oil Flames. In: Proceedings of the Seventeenth Symposium (International) on Combustion, the Combustion Institute, Pittsburgh, Pennsylvania, 1978. pp. 715-726.

23. Heap, M. P., T. M. Lowes, R. Walmsley, and H. Bartelds. Burner Design Principles for Minimum NO_x Emissions. In: Proceedings, Coal Combustion Seminar, U.S. Environmental Protection Agency, Research Triangle Park, North Carolina, NTIS PB-224-210, 1973. pp. 141-171.

24. Heap, M. P., T. J. Tyson, G. P. Carrer, and T. M. Lowes. The Optimization of Burner Design Parameters to Control NO_x Formation in Pulverized Coal and Heavy Oil Flames. In: Proceedings of the Stationary Source Combustion Symposium, U.S. Environmental Protection Agency, EPA-600/2-76-152b, Research Triangle Park, North Carolina, 1976. pp. II-197 - II-237.

25. Brown, R. A., H. B. Mason, and P. Neubauer. Investigation of Staging, Parameter for NO_x Control in Both Wall and Tangentially Coal Fired Boilers. In: Proceedings of the Second Stationary Source Combustion Symposium, Volume III. The U.S. Environmental Protection Agency, EPA 600/7-77-073c, Research Triangle Park, North Carolina, 1977. pp. 141-192.

REFERENCES (Continued)

26. Vatsky, J. Experience in Reducing NO_x Emission in Operating Steam Generators. In: Proceedings, Second NO_x Control Technology Seminar, EPRI-FP-1109-SR, Electric Power Research Institute, Palo Alto, California, 1979. pp. 7-1 - 7-17.

27. Pohl, J. H., and A. F. Sarofim. Devolatilization and Oxidation of Coal Nitrogen. In: Proceedings of Sixteenth Symposium (International) on Combustion, The Combustion Institute, Pittsburgh, Pennsylvania, 1977. pp. 491-501.

28. Song, Y. H., J. H. Pohl, J. M. Beér, and A. F. Sarofim. Nitric Oxide Formation During Pulverized Coal Combustion. Combustion Science and Technology, 28:31-39, 1982.

29. Song, Y. H., J. M. Beér, and A. F. Sarofim. Reduction of Nitric Oxide by Coal Char at Temperatures of 1250 K-1750 K, Combust. Sci. Technol., 25, 1981. pp. 237-240.

30. Solomon, P. R., and M. B. Collet. Evolution of Fuel Nitrogen in Coal Devolatilization, Fuel, 57, 1978. p. 749-755.

31. Pohl, J. H. Fate of Coal Nitrogen. ScD Thesis, Massachusetts Institute of Technology, Cambridge, Massachusetts, 1976. 430 pp.

32. Blair, D. W., and J. O. L. Wendt. Formation of NO_x and Other Products from Chemically Bound Nitrogen in Coal Combustion, DOE/ET/11314-T1, U.S. Department of Energy, Morgantown, West Virginia, 1980. 280 pp.

33. Kobayashi, H. Devolatilization of Pulverized Coal at High Temperatures. Ph.D. Thesis, Massachusetts Institute of Technology, Cambridge, Massachusetts, 1976. 423 pp.

34. Freihaut, J. D., and D. J. Seery. Method for Characterization of Coal During Thermal Decomposition. In: Final Report, Fundamental Combustion Research Applied to Pollution Formation, Volume III, W. R. Seeker, M. P. Heap, and T. J. Tyson, U.S. Environmental Protection Agency, Research Triangle Park, North Carolina, EPA-68-02-2631, 1982. pp. II-1 - VI-3.

35. Blair, D. W., J. O. L. Wendt, W. Bartok, Evolution of Nitrogen, and Other Species During Controlled Pyrolysis of Coal. In: Proceedings of Sixteenth Symposium (International) on Combustion, The Combustion Institute, Pittsburgh, Pennsylvania, 1976. pp. 475-489.

36. Solomon, P. R., and R. M. Carangelo. Pyrolysis/FTIR Study of EER Coals. Prepared for Energy and Environmental Research Corporation, Irvine, California, 1981. 62 pp.

37. Kau, C. J., and T. J. Tyson. Numerical Model for Two-Phase One-Dimensional Flow Reactor. Internal Report Energy and Environmental Research Corporation, Irvine, California, March 1982.

REFERENCES (Continued)

38. Freihaut, J. D., M. F. Zabielski, and D. J. Seery. Reaction-Induced Temperature Deviations During Coal Devolatilization in a Heated Grid. In: ACS Division of Fuel Chemistry Preprints 27(2), 1982. pp. 89-98.

39. Wendt, J. O. L., and O. E. Schulze. Effect of Diffusion--Reaction Interactions on Fuel Nitrogen Conversion During Coal Char Combustion. Paper presented at Eastern States Section of the Combustion Institute, Silver Spring, Maryland, 1974. 24 pp.

40. Song, Y. H., J. M. Beér, and A. F. Sarofim. Oxidation and Devolatilization of Nitrogen in Coal Char. Combustion Science and Technology, 28, 1982. pp. 177-183.

41. Smith, I. W. The Intrinsic Reactivity of Carbons to Oxygen. Fuel, 57, 1978. pp. 409-414.

42. Fenimore, C. P. Formation of Nitric Oxide from Fuel Nitrogen in Ethylene Flames. Combust. Flame 19(2), 1972. pp. 289-296.

43. Fenimore, C. P. Reactions of Fuel-Nitrogen in Rich Flame Gases. Combustion and Flame, 26, 1976. pp. 249-256.

44. Fenimore, C. P. Studies of Fuel Nitrogen Species in Rich Flames Gases. In: Proceedings, Seventeenth (Inrernational) Symposium on Combustion, The Combustion Institute, Pittsburgh, Pennsylvania. 1979. pp. 661-671.

45. Morley, C. The Formation and Destruction of Hydrogen Cyanide from Atmospheric and Fuel Nitrogen in Rich Atmospheric-Pressure Flames. Combustion and Flame, 27, 1976. pp. 189-204.

46. Haynes, B. S. Reactions of Ammonia and Nitric Oxide in the Burnt Gases of Fuel-Rich Hydrocarbon-Air Flames. Combustion and Flame, 28, 1977. pp. 81-91.

47. Morley, C. The Mechanism of NO Formation from Nitrogen Compounds in Hydrogen Flames Studied by Laser Fluorescence. In: Proceedings Eighteenth Symposium (International) on Combustion. The Combustion Institute, Pittsburgh, Pennsylvania, 1981. pp. 23-32.

48. Turner, D. A., R. L. Andrews, and C. W. Siegmund. Influence of Combustion Modifications and Fuel Nitrogen Content on Nitrogen Oxides Emissions from Fuel Oil Combustion. AIChE Symposium Series 126, 68, 1972. pp. 55- .

49. Kau, C. J., and T. J. Tyson. A Computer Program for General Flame Analysis. Energy and Environmental Research Corporation, Irvine, California, 1981. 70 pp.

REFERENCES (CONCLUDED)

50. Mulvihill, J. N., and L. F. Phillips. Breakdown of Cyanogen in Fuel-Rich $H_2/N_2/O_2$ Flames. In: Proceedings, Fifteenth Symposium International) on Combustion. The Combustion Institute, Pittsburgh, Pennsylvania, 1.

51. Haynes, B. S. The Oxidation of Hydrogen Cyanide in Fuel-Rich Flames. Combustion and Flame, 28, 1977. pp. 113-121.

52. Pereira, F. J., J. M. Beér, B. Gibbs, A. B. Hedley. NO_x Emissions from Fluidized-Bed Coal Combustors. In: Proceedings of the Fifteenth Symposium (International) on Combustion, The Combustion Institute, Pittsburgh, Pennsylvania, 1974. pp. 1149-1156.

53. Shelef, M., and K. Otto. Simultaneous. Catalytic Reaction of O_2 and NO with CO and Solid Carbon. Journal of Colloid and Interface Science, 31, 1972. pp. 73- .

54. Edwards, H. W. Interaction of Nitric Oxide with Graphite. AIChE Symposium, Series No. 126, 68, 1972. pp. 91- .

55. Levy, J. M., L. K. Chan, A. F. Sarofim, and J. M. Beér. No. 1 Char Reactions at Pulverized Coal Flame Conditions. In: Proceedings of Eighteenth Symposium (International) on Combustion, The Combustion Institute, Pittsburgh, Pennsylvania, 1981. pp. 111-120.

56. Glass, J. W., and J. O. L. Wendt. Mechanisms Governing the Destruction of Nitrogenous Species During the Fuel Rich Combustion of Pulverized Coal. In: Proceedings of the Nineteenth Symposium (International) on Combustion, The Combustion Institute, Haifa, Israel, 1982. 26 pp.

57. De Soete, G. G. Mechanisms of Nitric Oxide Reduction on Solid Particles. Fundamental Combustion Research Applied to Pollution Formation, Volume II. W. R. Seeker, M. P. Heap, and T. J. Tyson, U.S. Environmental Protection Agency, Research Triangle Park, North Carolina, EPA-68-02-2631, 1982. 227 pp.

58. De Soete, G. G., Ch. Giorgetti, and A. Querad. Mechanism of Nitric Oxide Reduction on Solid Particles. Part II. Comparative Study of Coal and Char Particles. Fundamental Combustion Research Applied to Pollution Formation, Volume II, W. R. Seeker, M. P. Heap, and T. J. Tyson, U.S. Environmental Protection Agency, Research Triangle Park, North Carolina, EPA-68-02-2631, 1982. pp. 228-423.

59. Song, Y, H. Fate of Fuel Nitrogen During Pulverized Coal Combustion. ScD. Thesis, Massachusetts Institute of Technology, Cambridge, Massachusetts, 1978. 316 pp.

60. Michel, J. B., and R. Payne. Detailed Measurement of Long Pulverized Coal Flames for the Characterization of Pollutant Formation. International Flame Research Foundation, Doc. nr. F09/a/23, IJmuiden, The Netherlands, 1980. 92 pp.

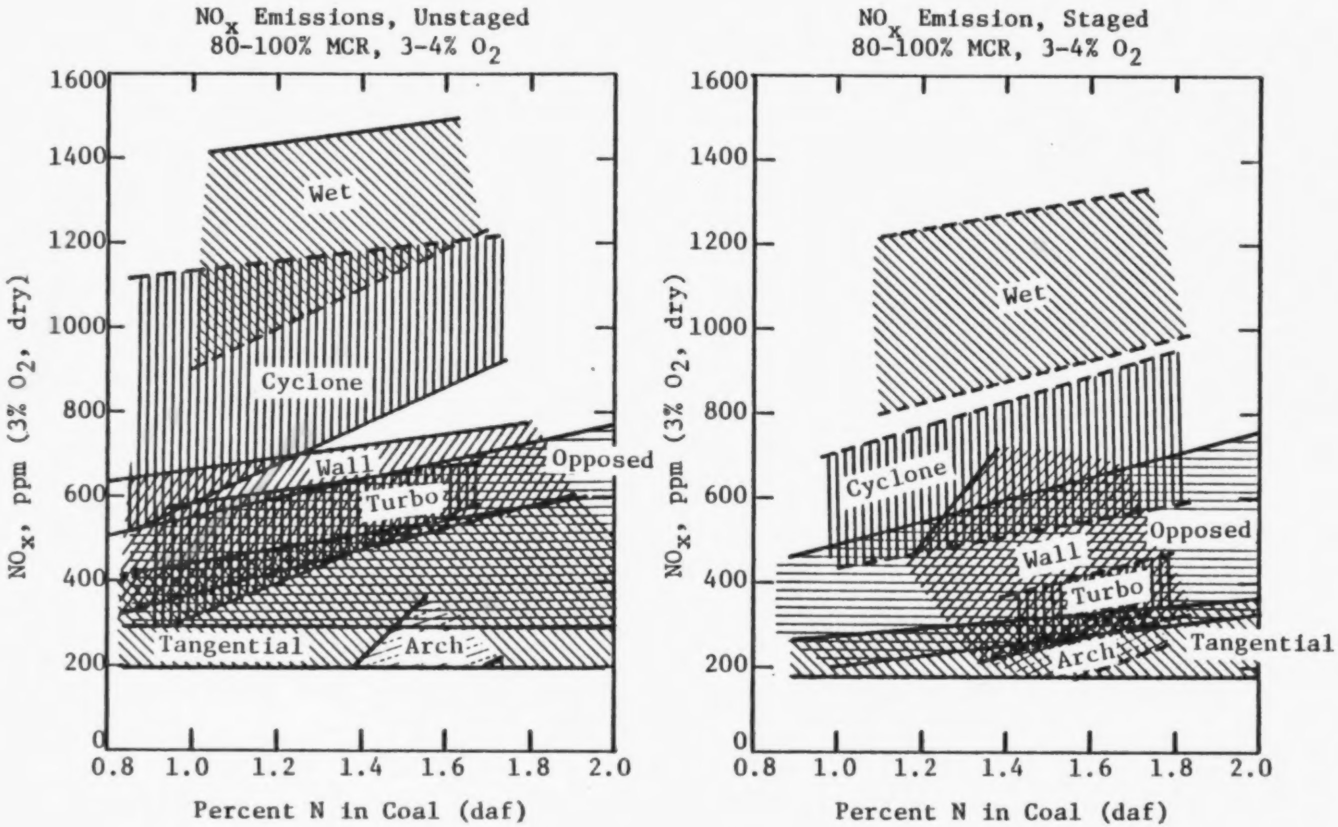
NO$_x$ Emissions, Unstaged
80-100% MCR, 3-4% O$_2$

NO$_x$ Emission, Staged
80-100% MCR, 3-4% O$_2$

a. Unstaged

b. Staged

Figure 1. NO$_x$ emissions from operating boilers 4-16.

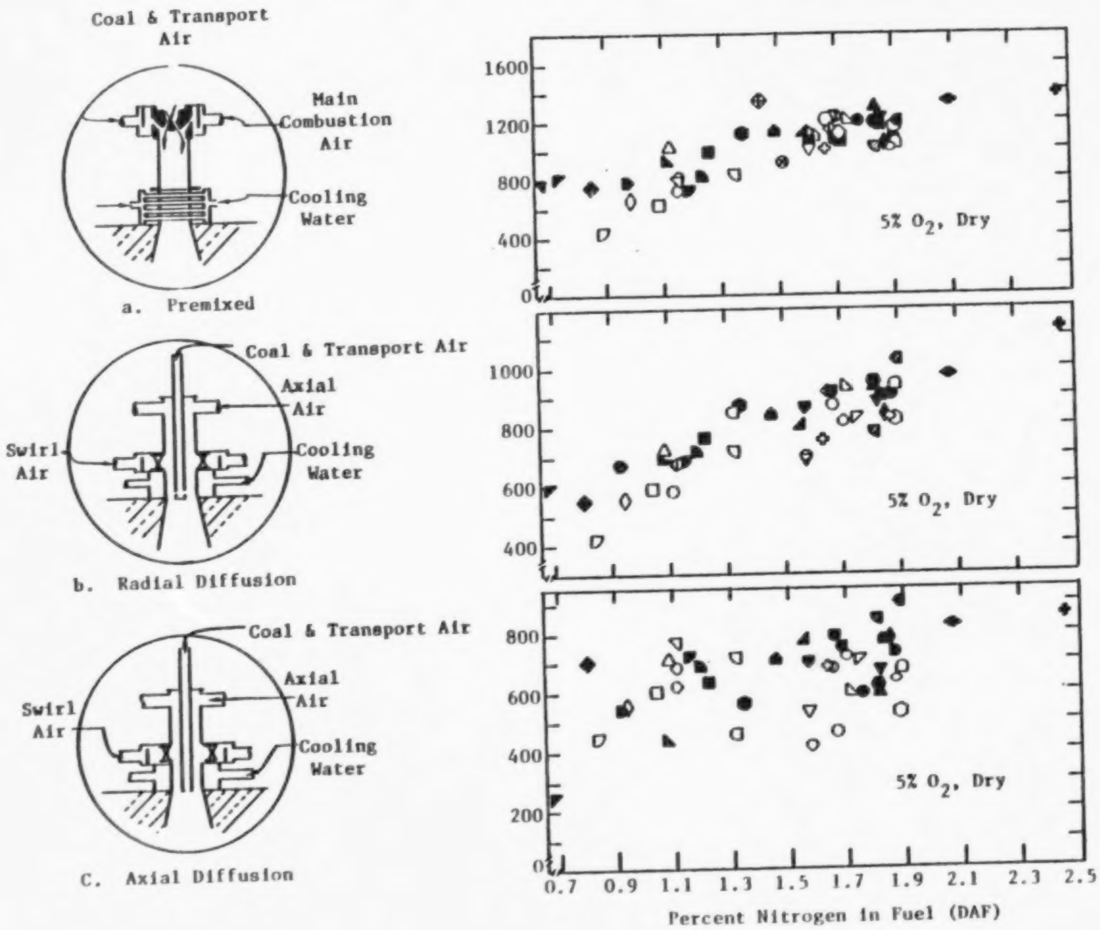

Figure 2. Influence of mixing and fuel nitrogen content on NO_x emissions.

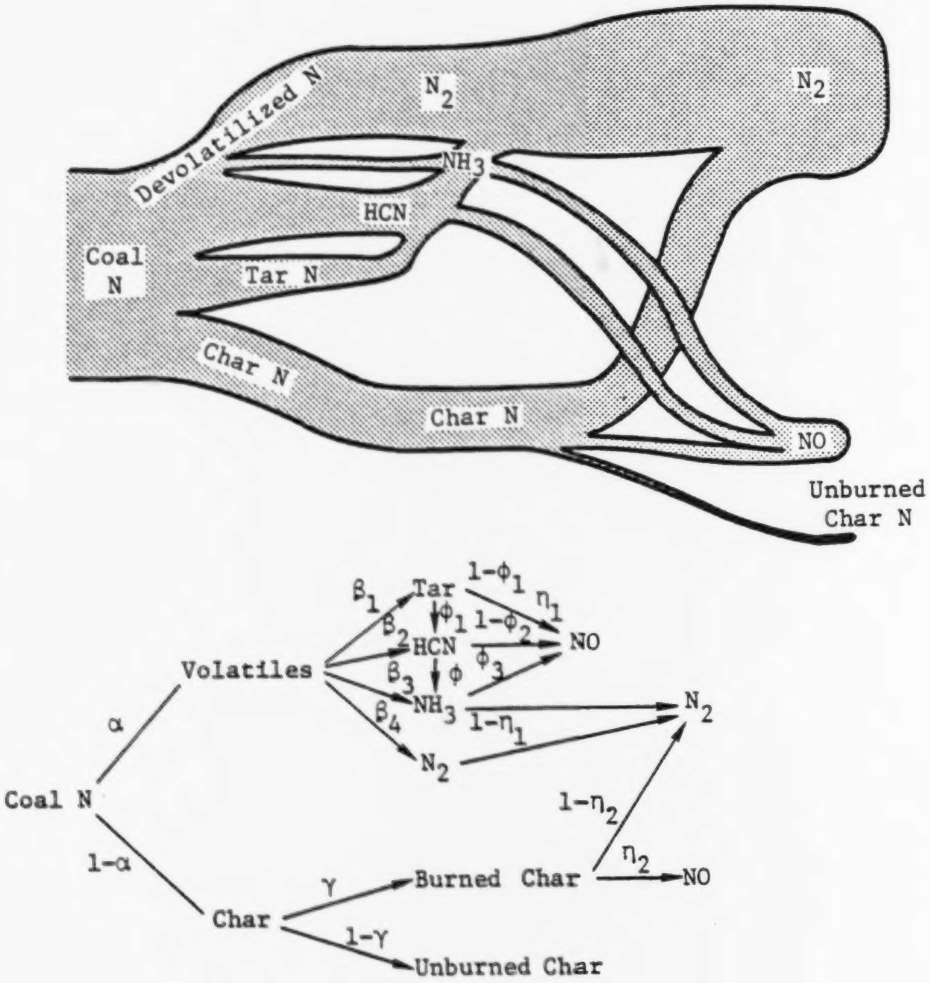

N2
N2
Devolatilized N
NH3
HCN
Coal N
Tar N
Char N
Char N
NO
Unburned Char N
Tar
HCN
NH3
N2
NO
N2
Volatiles
Coal N
Char
Burned Char
Unburned Char
NO
α
1-α
β1
β2
β3
β4
φ1
φ
1-φ1
1-φ2
φ3
η1
1-η1
1-η2
η2
γ
1-γ

Volatile Conversion

Tar HCN NH_3

$$\frac{\text{NO}}{\text{Fuel N}} = \alpha[\beta_1(1-\phi_1) + (\beta_2+\beta_1\phi_1)(1-\phi_2) + \phi_3(\beta_3+\beta_1\phi_1\phi_2+\beta_2\phi_2)]$$

Char Conversion

$$+ \ [(1-\alpha)\gamma\eta_2]$$

Figure 3. Fate of fuel nitrogen.

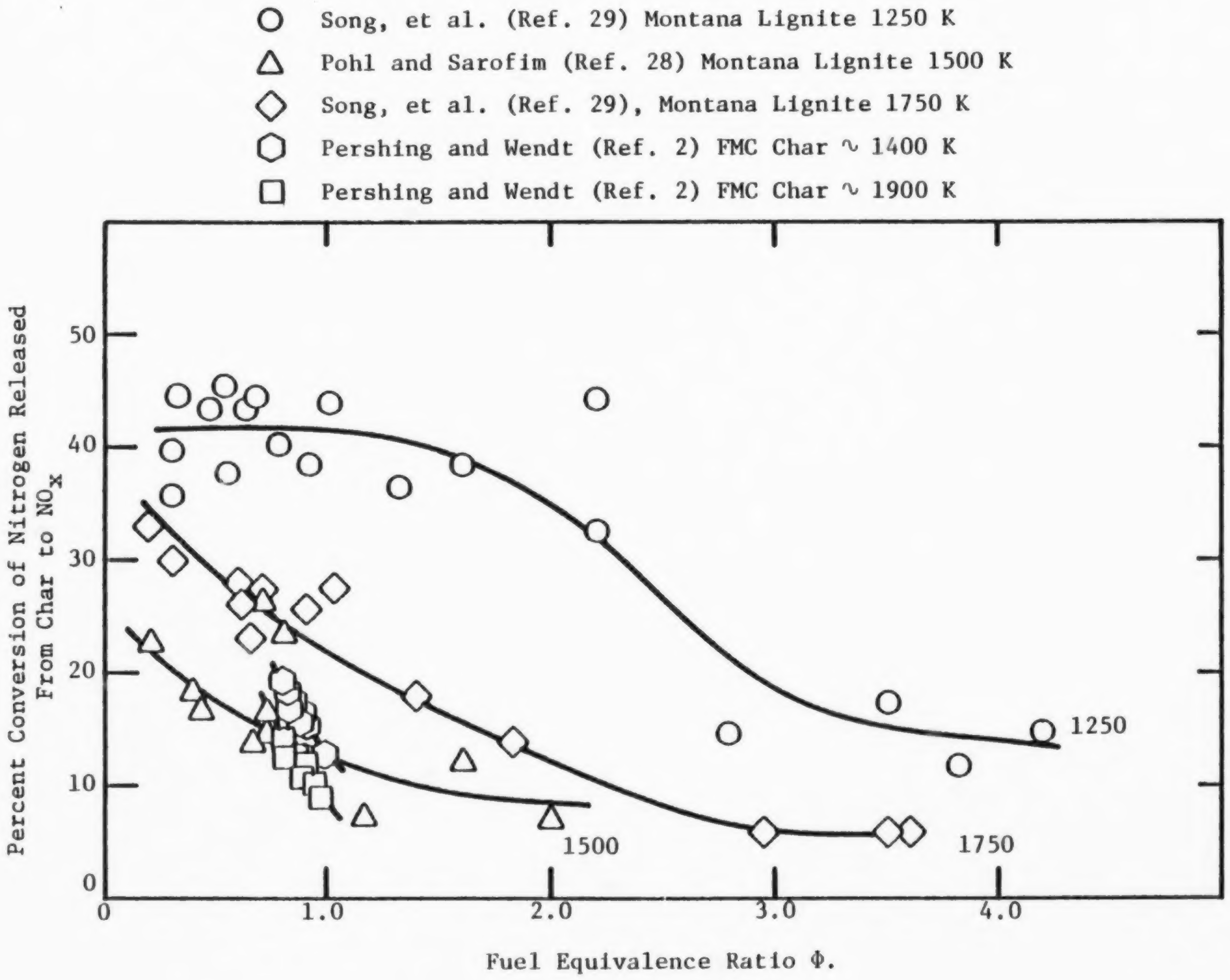

Figure 4. Conversion of char nitrogen to NO$_x$.

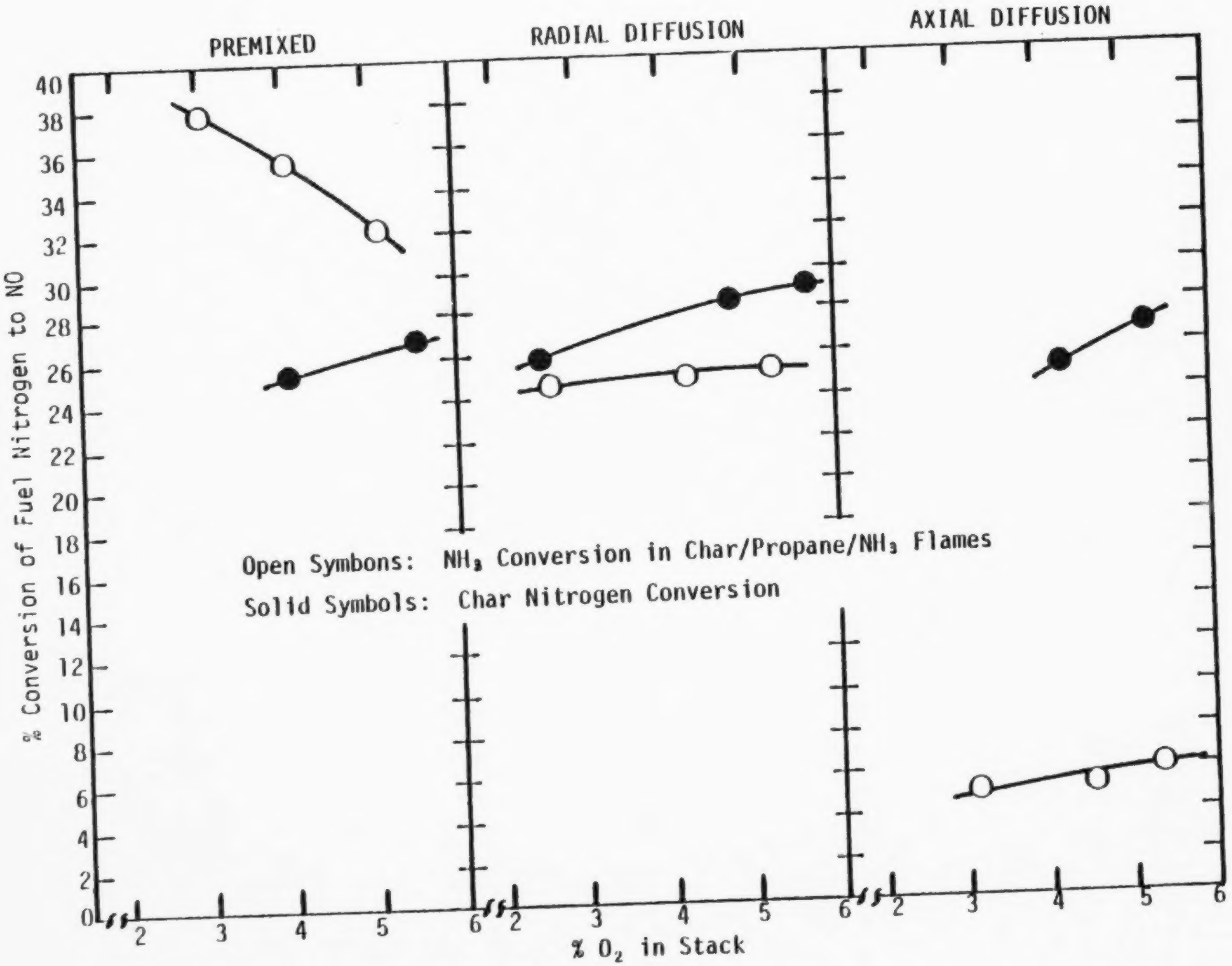

Figure 5. Effects of mixing condition on volatile and char nitrogen conversion.

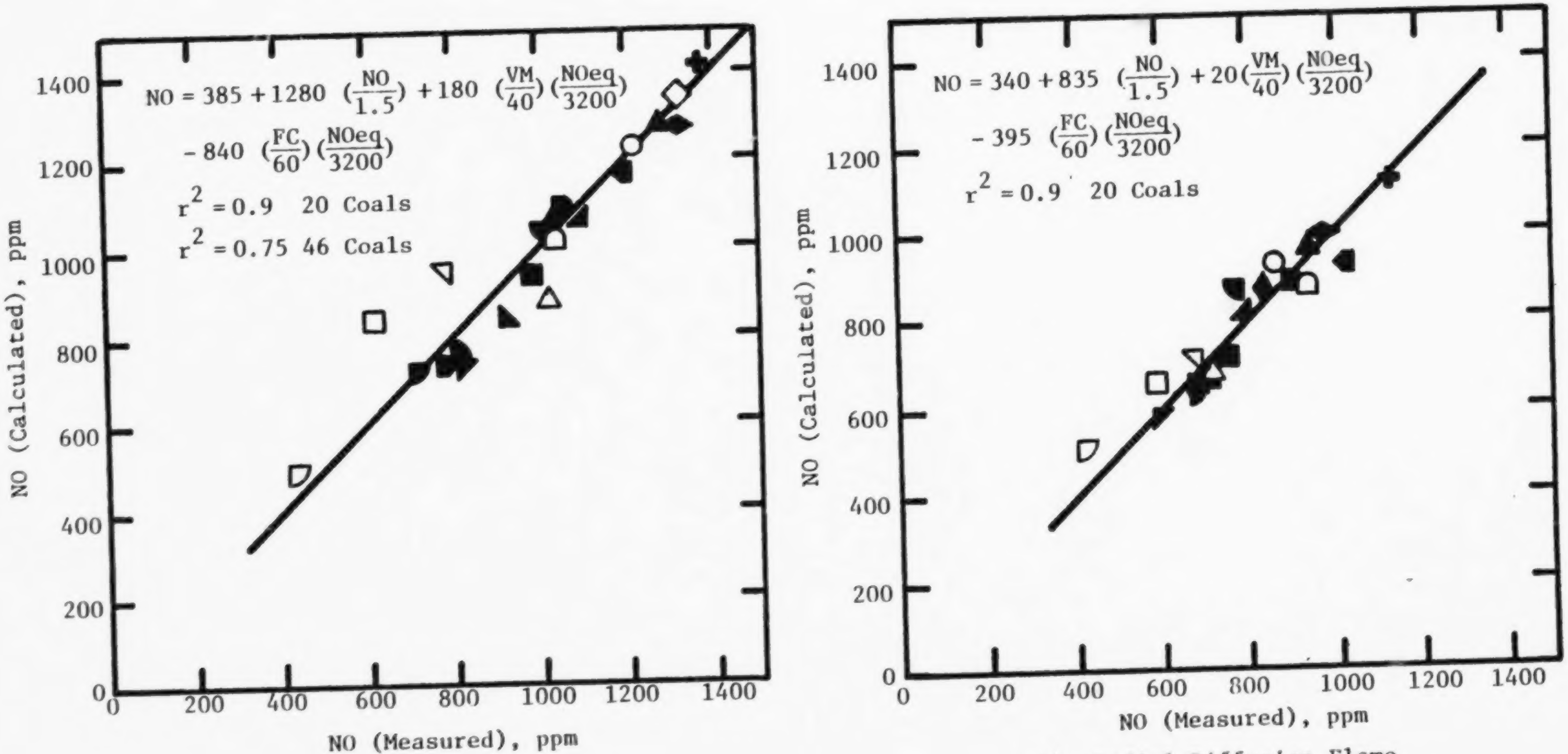

a) Premixed Flame

b) Radial Diffusion Flame

Figure 6. Empirical correlation of fuel properties with NO_x emissions.

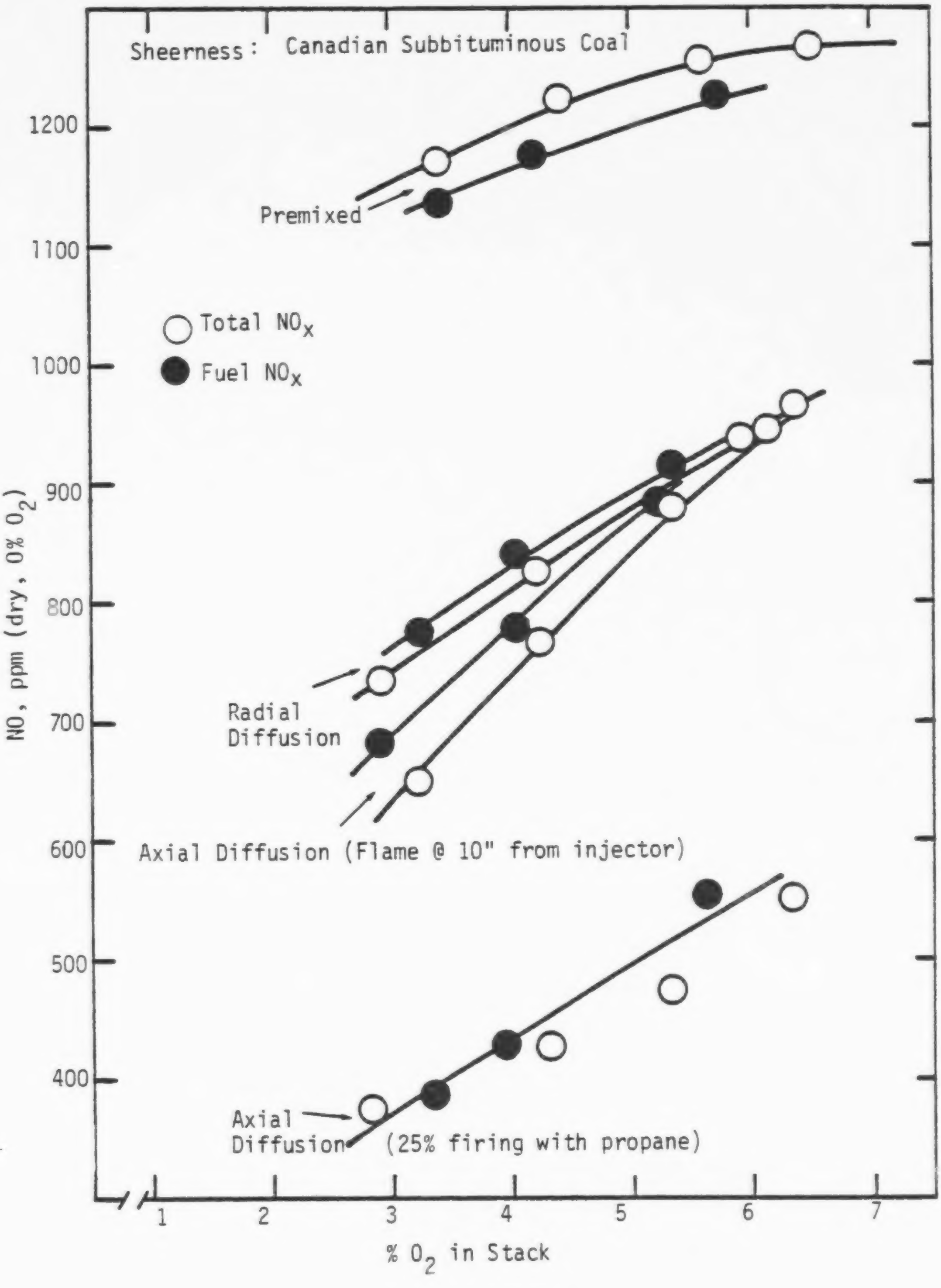

Figure 7. Influence of injector on NO_x emissions.

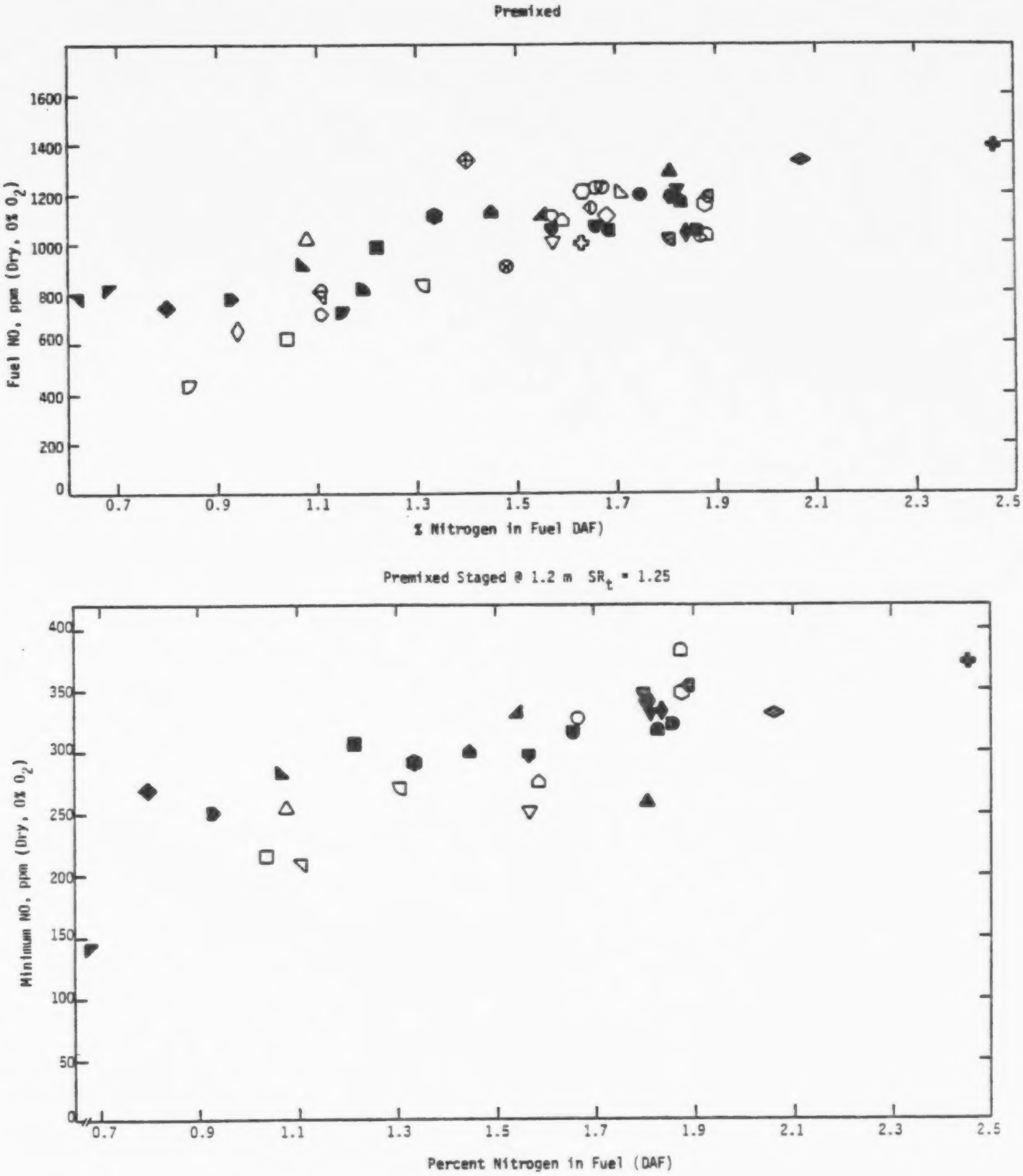

Figure 8. Minimum NO_x emission achieved by staging.

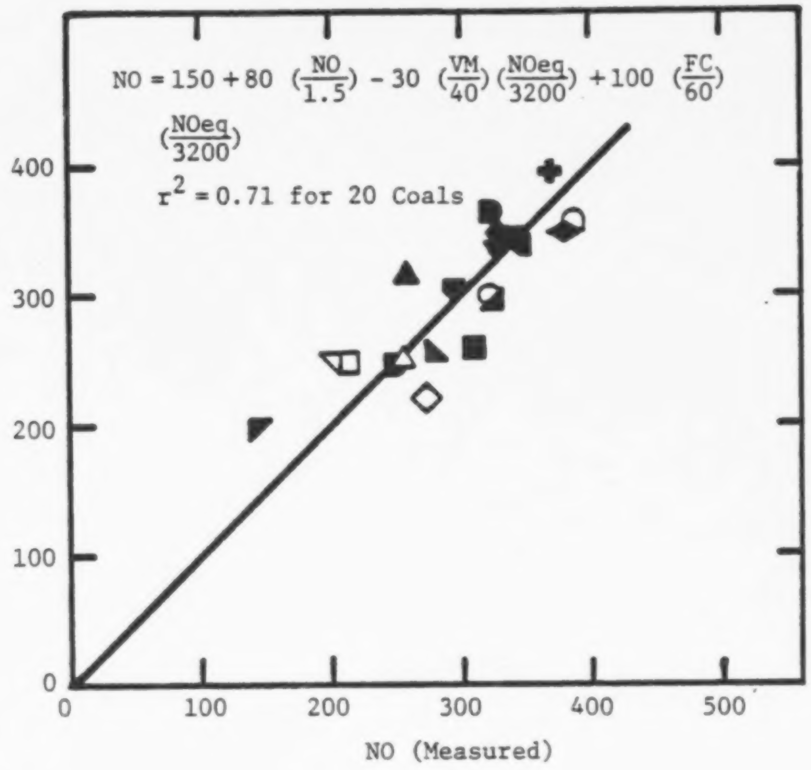

Figure 9. Empirical correlation of minimum NO_x emissions with fuel properties.

GAS PHASE REACTION KINETICS OF NO_x FORMATION FROM FUEL NITROGEN IN FOSSIL FUEL COMBUSTION

By:

C. T. Bowman, R. K. Hanson, M. Louge and A. Garman
Department of Mechanical Engineering
Stanford University
Stanford, California 94305

"Although the research described in this article has been funded wholly or in part by the United States Environmental Protection Agency through cooperative agreement #807942-01 to Stanford University, it has not been subjected to the Agency's required peer and policy review and therefore does not necessarily reflect the views of the Agency and no official endorsement should be inferred."

ABSTRACT

A combined experimental and analytical study of the gas-phase reaction kinetics of fuel nitrogen species under conditions simulating the primary zone of staged fossil fuel combustors is in progress. Two related problem areas are addressed in this program:

1. The reaction mechanism for conversion of cyano species to amine species for conditions appropriate to fossil fuel combustion.
2. The role of hydrocarbon species in the post-combustion gases on fuel nitrogen chemistry.

The experimental program is being carried out in a shock tube and in a flat flame burner facility. Various optical diagnostic and probe techniques are used to monitor the concentrations of imporant species during the course of reaction. Measured concentration profiles are used to infer information on the fuel nitrogen reaction mechanism and kinetic parameters.

INTRODUCTION

Several methods for reducing NO_x emissions from fossil-fuel-fired combustion equipment currently are under investigation. One of the more promising methods is staged combustion (controlled fuel-air contacting). Studies of staged combustion of fossil fuels have shown that there are optimum first-stage conditions, in terms of stoichiometry and temperature, for NO_x reduction. Some recent results showing the effects of first-stage stoichiometry on overall NO_x emissions and on nitrogenous species concentrations at the end of the first stage in a pulverized fuel combustor are shown in Figure 1. The occurrence of a minimum in overall NO_x emissions for a rich first stage, which exceeds predicted equilibrium values, indicates the role of gas-phase fuel nitrogen reactions in NO_x emissions from fossil fuel flames and emphasizes the importance of developing appropriate kinetic models for fuel nitrogen chemistry in rich hydrocarbon-air flames.

Recent studies of fuel nitrogen chemistry in combustion gases have elucidated the essential features of the reaction mechanism and suggest that the reaction proceeds as indicated below.

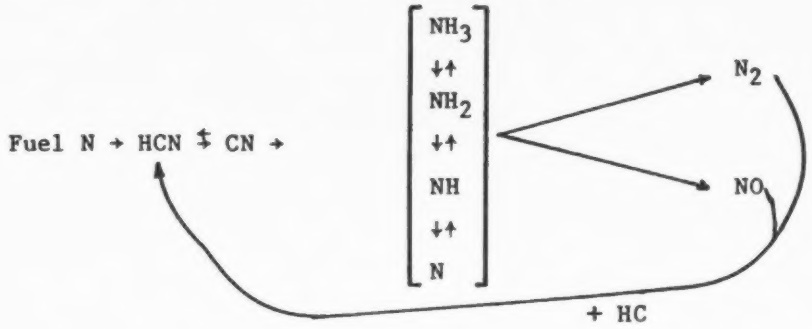

While there is a general consensus on the main features of the mechanism, the present understanding of the detailed reactions involved is deficient in several important respects. These kinetic uncertainties are evidenced by the failure of existing fundamental kinetic models to predict some significant experimental observations on the fate of fuel nitrogen species in fuel-rich combustion.

Experimental studies of the fate of nitrogenous species in fuel-rich premixed hydrocarbon-air combustion have been carried out, and several kinetic models hae been proposed to fit the experimental data. These kinetic models have had some success in modeling NO and ΣCN and ΣNH_i profiles in moderately-rich hydrocarbon-air flames. However, significant departures between existing kinetic model predictions and measured concentration profiles hae been reported in very fuel-rich flames, suggesting that some key reaction steps are missing in these models or that kinetic parameters for important reactions are not known to sufficient accuracy.

Some aspects of the fuel nitrogen reaction mechanism have been studied in detail. The reactions of NH_i species which lead to formation have been and are the subject of numerous investigations, and the mechanism for formation of CN from HCN is under investigation at Stanford University and other laboratories. However, relatively little information is available on the reactions involved in the conversion of cyano species to amines under fuel-rich conditions and the role of hydrocarbon species in the fuel nitrogen reaction mechanism still is unclear. We are investigating these two areas, and the present paper reports initial results from this study.

Reaction Mechanism for Conversion of Cyano Species to Amine Species

The mechanism for conversion of HCN and CN to NH_i is largely unsubstantiated, as direct experimental data either to identify critical intermediate species or to specify kinetic parameters of critical reactions are unavailable. However, it is fairly certain that reactions involving NCO can play a key role. Hence, our work dealing with HCN/CN → NH_i conversion focuses on detailed studies of reactions forming and removing NCO. Shock tube techniques with simple gas mixtures are used to effectively isolate the elementary reactions of interest.

Preliminary studies have shown that a principal step for CN removal is

$$CN + O \rightarrow CO + N$$

Hence, a determination of the kinetic parameters of this reaction is required as a first step in the study of the HCN/CN → NH_i conversion mechanism. To this end mixtures of cyanogen (C_2N_2), nitrous oxide (N_2O) and Argon (Ar) were shock-heated and the CN concenration was measured as a function of time using an ultraviolet absorption technique, Figure 1. A typical plot of the CN concentration as a function of time is shown in Figure 2. Kinetic modeling has shown that the initial stages of reaction are described by the following elementary steps,

$$N_2O + M \rightarrow N_2 + O + M \tag{1}$$

$$C_2N_2 + O \rightarrow CN + NCO \tag{2}$$

$$CN + O \rightarrow CO + N \tag{3}$$

$$NCO + O \rightarrow CO + NO \tag{4}$$

These modeling studies also have shown that measurement of the maximum CN concentration and the time required to achieve this maximum will yield values for the rate coefficients of both Reaction (2) and Reaction (3).

Before making these measurements, a precise determination of the rate coefficient of Reaction (1) was made, since this reaction governs the production of O-atoms which oxidize the CN and NCO. In this study, mixture of N_2O and Ar were shock-heated and the N_2O concentration was measured as a function of time using an infrared emission technique. From these measurements the following expression for k_1 was determined in the temperature range 1650-2200K.

$$k_1 = 6.9 \times 10^{23}\ T^{-2.5} \exp(-32710/T)\ \text{cc/mole.s}$$

Preliminary results from the $C_2N_2/N_2O/Ar$ experiments have yielded the following values for the rate coefficients for Reactions (2) and (3) at 2030K,

$$k_2 \simeq 4 \times 10^{11}\ \text{cm}^3\text{/mole.s}$$

$$k_3 \simeq 1.6 \times 10^{13}\ \text{cm}^3\text{/mole.s}$$

Further experiments are in progress to refine these values and extend the temperature range of the measurements.

In addition to the above work, we have developed tunable infrared laser absorption methods for measurement of CO and NO to complement the CN measurement. Application of the laser absorption method to measure CO in the $C_2N_2/N_2O/Ar$ experiments indicates that CO probably is formed in a vibrationally-excited state by the exothermic reaction

$$CN + O \rightarrow CO + N \qquad (3)$$

Kinetic modeling is in progress to confirm this finding and also to verify the value of k_3 obtained from the CN absorption measurements.

The tunable laser also will be used to measure NO to allow a determination of k_4, although the accuracy of this measurement will be reduced due to interference from other NO producing reactions.

When experiments using $C_2N_2/N_2O/Ar$ mixtures are complete, additional experiments will be performed using $C_2N_2/O_2/Ar$ mixtures. In this system the dominant reactions are

$$C_2N_2 + M \rightarrow CN + CN + M \qquad (5)$$

followed by

$$CN + O_2 \rightarrow NCO + O \qquad (6)$$

$$C_2N_2 + O \rightarrow CN + NCO \qquad (2)$$

$$CN + O \rightarrow CO + N \qquad (3)$$

$$NCO + O \rightarrow CO + NO \qquad (4)$$

Assuming k_2 and k_3 are known, measurement of CN will allow a determination of the rate coefficient for Reaction (6), which is expected to be another reaction of importance in the conversion of cyano to amine compounds.

Role of Hydrocarbon Species in Fuel Nitrogen Chemistry

Haynes, 1977, and Malte, et al., 1976, have observed significant hydrocarbon concentrations in the combustion products of rich hydrocarbon-air flames. A particularly important question concerns the mechanism underlying this hydrocarbon "break-through" and the subsequent effect on the HCN - NH_i chemistry. Several studies have shown that the presence of hydrocarbons in rich combustion gases can lead to NO formation.

The mechanism for this NO formation is uncertain, but several investigators have postulated that hydrocarbon radicals react with N_2 to produce HCN

$$CH + N_2 \rightarrow HCN + N$$

which subsequently oxidizes to form NO. Malte, et al., 1976, proposed a reaction between hydrocarbon radicals and NO which also forms HCN, e.g.,

$$CH + NO \rightarrow HCN + O$$

$$CH_2 + NO \rightarrow HCN + OH$$

Hence, there exists the possibility that hydrocarbon radicals in the post-flame zone can be a source for NO and also destroy NO. Since hydrocarbon radicals compete for available radicals in the post-flame zone, the presence of hydrocarbons may indirectly impact the fuel nitrogen chemistry by affecting the O-H radical pool.

We are investigating the role of hydrocarbon species in the fuel nitrogen reaction mechanism in atmospheric and low-pressure premixed rich $H_2/O_2/Ar$ flames seeded with hydrocarbons and with either NH_3 or NO. The experimental technique employed is a modification of the flame perturbation method developed by Dixon-Lewis (1967). In this approach, a trace amount of a perturbing species, for example NH_3 or NO, will be added to a rich hydrogen flame. The fate of the added fuel nitrogen species in the flame is determined by probe sampling. In addition, the effect of the added nitrogen species on the O-H radical pool is inferred from an optical measurement of OH. This flame in turn will be perturbed by the addition of a trace amount of a hydrocarbon species, such as C_2H_4, and the effects of this additive on the fuel nitrogen and O-H radical pools determined. In addition, the fate of the added hydrocarbon species is inferred from a measurement of stable hydrocarbon species.

A schematic diagram of the premixed flat flame burner facility is shown in Figure 4. The burner system is mounted on an optical table, and the burner is translated relative to the table surface by a stepping motor, facilitating axial traverses above the burner surface with fixed optics and probes. A DEC-MINC 11 minicomputer has been interfaced with the burner facility. This computer serves to acquire and reduce gas sampling data on-line and also to control burner position. Available gas sampling instrumentation includes Beckman NDIR analyzers for CO and CO_2, a TECO chemiluminescent NO_x analyzer, Orion ion analyzers for ΣCN and ΣNH, and a Perkin-Elmer Sigma 1 gas chromatograph for measurement of stable hydrocarbons and N_2.

An initial series of experiments was carried out to validate the gas sampling techniques in atmospheric-pressure C_2H_2-air flames. The flame conditions duplicated those used by Haynes, 1975. A typical comparison of the NO, ΣCN, and ΣNH_i and total be fixed nitrogen, $TFN = NO_x + \Sigma CN + \Sigma NH_i$, profiles obtained in the present study with those reprted by Haynes is shown in Figure 5. The present NO and ΣNH_i measurements are in excellent agreement with the results of Haynes. However, the present ΣCN measurements, and hence TFN, are higher than reported by Haynes. Two possible reasons for this discrepancy are the slightly lower flame temperature employed in the present study and the lower HCN recoveries obtained when using buffered solutions in the bubblers as was done by

Haynes. Alternative methods for ΣCN determination, including gas chromatography and optical techniques, currently are being used to evaluate the ion analyzer method.

When these diagnostic evaluation experiments are completed, work will begin on the flame perturbation experiments.

REFERENCES

Chen, S. L., Heap, M. P., Pershing, D. W., Nihart, R. K. and Rees, D. P. (1980), "The Influence of Fuel Composition on the Formation and Control of NO_x in Pulverized Coal Flames," Paper 80-13, Western States Section, Combustion Institute Meeting, Irvine, CA.

Dixon-Lewis, G. and Williams, A. (1967), "Some Observations on the Combustion of Methane in Premixed Flames," Eleventh Symposium (International) on Combustion, p. 951.

Haynes, B. S. (1975), "The Formation and Behavior of Nitrogen Species in Fuel Rich Hydrocarbon Flames," Ph.D. Thesis, University of New South Wales, Australia.

Haynes, B. A. (1977), "Reactions of Ammonia and Nitric Oxide in the Burnt Gases of Fuel-Rich Hydrocarbon-Air Flames," Comb. and Flame 28, p. 81.

Malte, P. C., Halgren, C. A., Monteith, L. E., Corlet, R. C. and Pratt, D. T. (1976), "The Fate of Organic Nitrogen in Jet-Stirred Combustion," Paper 76-31, Western States Section, Combustion Institute Meeting, LaJolla, CA.

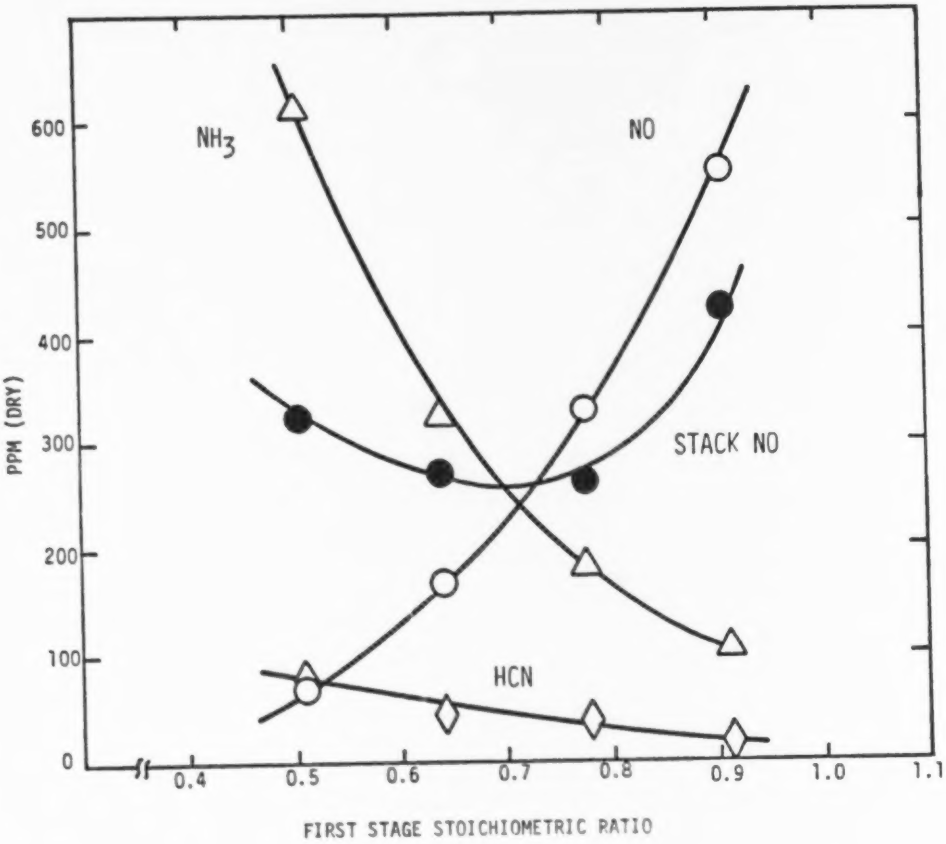

Figure 1. Influence of first stage stoichiometry on nitrogen species distribution in staged combustion of pulverized coal (Chen, et al., 1980).

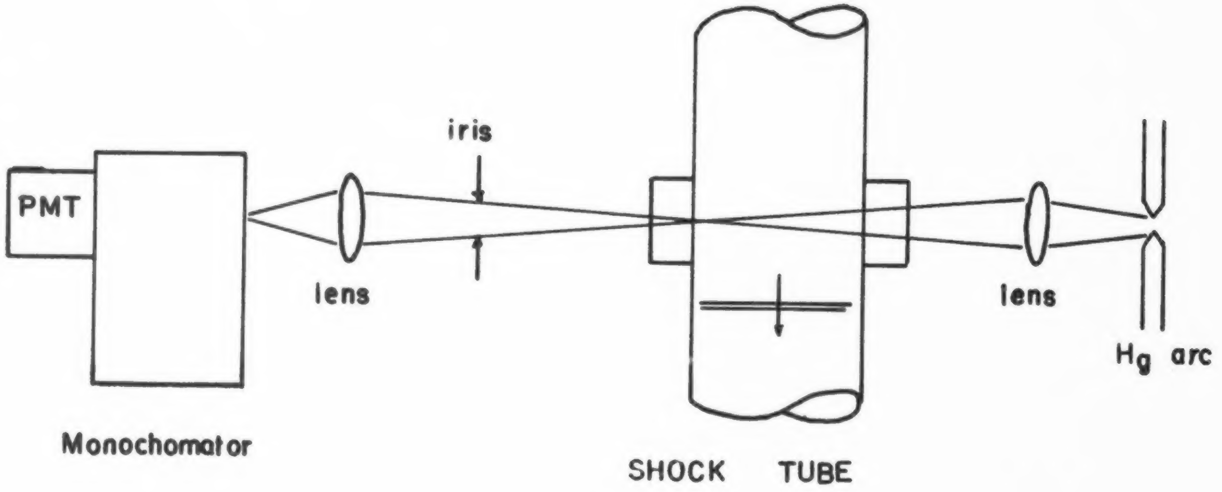
iris
PMT
lens
lens
Hg arc
Monochomator
SHOCK TUBE

Figure 2. CN absorption diagnostic - optical arrangement.

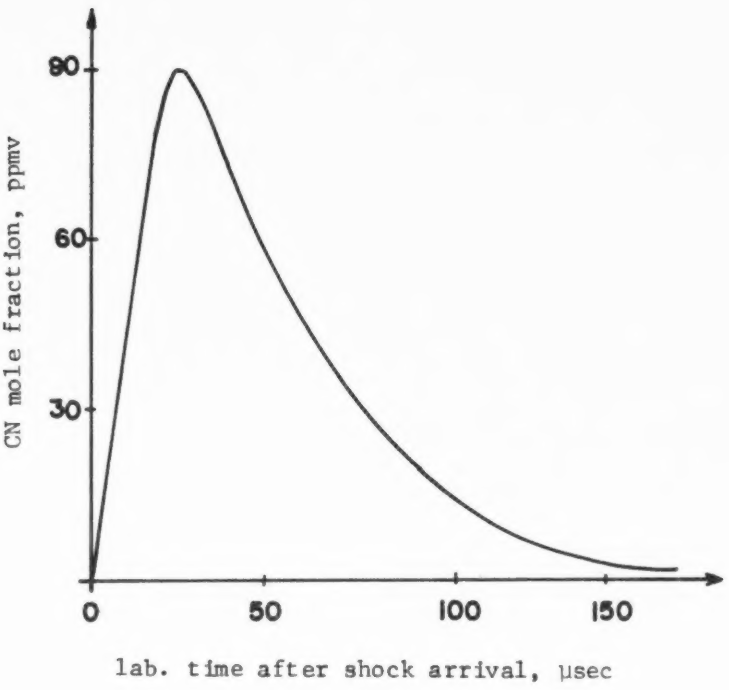

Figure 3. Typical CN absorption profile; T = 2000 K, p = 0.5 atm
Initial mixture: $C_2N_2/N_2O/Ar$ = 3/12/985.

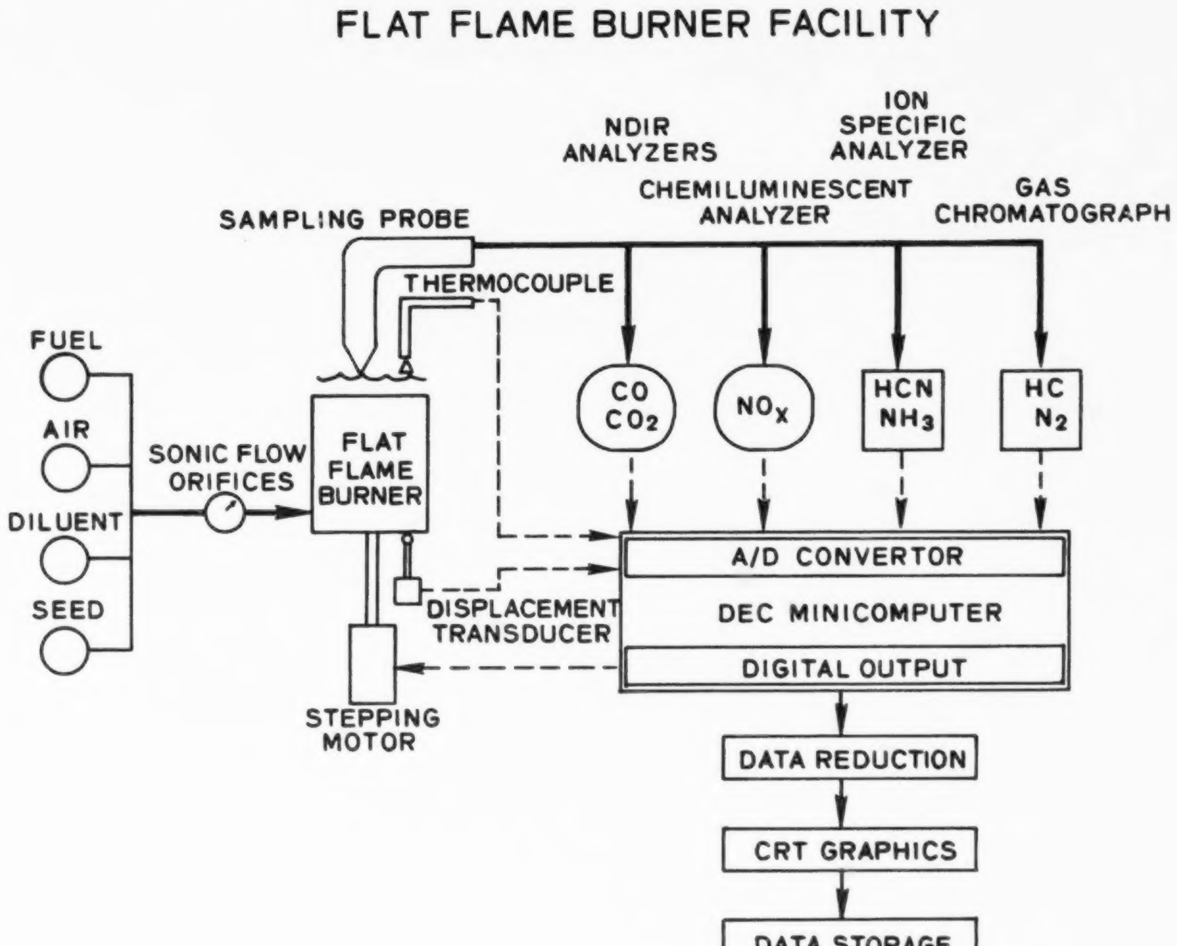
FLAT FLAME BURNER FACILITY
NDIR ANALYZERS
ION SPECIFIC ANALYZER
CHEMILUMINESCENT ANALYZER
GAS CHROMATOGRAPH
SAMPLING PROBE
THERMOCOUPLE
FUEL
AIR
DILUENT
SEED
SONIC FLOW ORIFICES
FLAT FLAME BURNER
CO CO_2
NO_x
HCN NH_3
HC N_2
A/D CONVERTOR
DEC MINICOMPUTER
DIGITAL OUTPUT
DISPLACEMENT TRANSDUCER
STEPPING MOTOR
DATA REDUCTION
CRT GRAPHICS
DATA STORAGE

Figure 4. Flat flame burner facility.

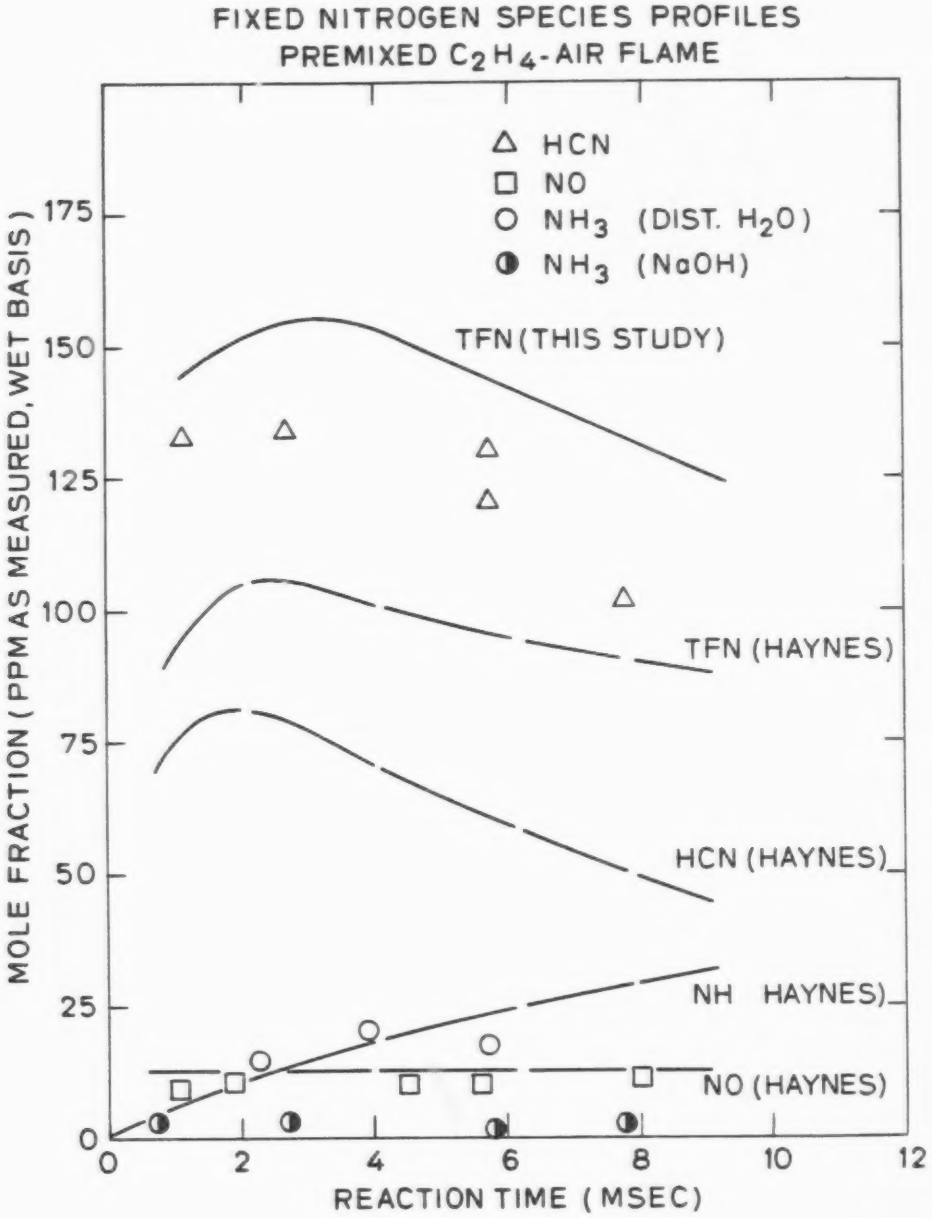

Figure 5. Fixed nitrogen profiles in a rich C_2H_4-Air flame.

THE STRUCTURE OF TURBULENT DIFFUSION FLAMES AND NITRIC OXIDE FORMATION

By:

J. E. Broadwell
TRW Corporation
Space and Technology Group
Redondo Beach, California 90278

P. E. Dimotakis
California Institute of Technology
Graduate Aeronautical Laboratory
Pasadena, California

T. J. Tyson, C. J. Kau and W. R. Seeker
Energy and Environmental Research Corporation
18 Mason
Irvine, California 92714

"Although the research described in this article has been funded wholly or in part by the United States Environmental Protection Agency through contract number 68-02-3633 to Energy and Environmental Research Corporation, it has not been subjected to the Agency's required peer and policy review and therefore does not necessarily reflect the views of the Agency and no official endorsement should be inferred."

ABSTRACT

The purpose of the present study was to develop an understanding of the mechanisms controling nitric oxide generation in gas-fired turbulent diffusion flames discharging into air and to formulate a model describing these processes. A coherent flame concept of turbulent mixing was utilized wherein large-scale structures are responsible for air entrainment into the fuel jet. The large-scale structures subsequently cascade to smaller scales before homogenization of the fuel and air occurs. Support for the developing conceptual model arises from isothermal turbulent water jet mixing studies underway at Caltech. They were carried out in the large water facility using a newly developed technique for determining the extent of molecular mixing from the appearance or disappearance of molecules which fluoresce. The conceptual model was expressed in a simple mathematical form and utilized for the prediction of NO from H_2 and CH_4 jet flames. The model provides an explanation for the observed dependence of nitric oxide generation on the jet Reynolds number.

INTRODUCTION

Many practical combustion devices rely upon turbulent mixing for fuel air contacting; and, in most instances, it controls the heat release rate and therefore the combustion intensity. In particular, the characteristics of one of the simplest industrial flames, gaseous turbulent jet diffusion flames, are dominated by the fuel air mixing process. The performance of these flames which have direct application as industrial flares is determined by the entrainment of air into the fuel jet and the microscopic mixing of molecules of fuel and air; i.e., the turbulent mixing processes. The ignition and stability of the flame, the formation of trace pollutants such as NO, the combustion efficiency of the flame, and flame quenching phenomenon are all related to the specific thermal and chemical environment within the flame which in turn is controlled by the physical turbulent mixing processes. Other more complex combustion devices such as pulverized-coal burners involve the same basic mixing processes as jet gas flames along with the complications of two-phase transport and heat release.

Understanding the physics of turbulent mixing is necessary to:

- Make and interpret satisfactory measurements in many combustion systems.
- Make intuitive predictions concerning the effects of parameter variations on the performance of combustion systems.
- Develop effective models of practical combustion devices.

The purpose of this paper is to summarize the efforts being carried out in the EPA's Fundamental Combustion Research Program (FCR) to develop this understanding. There are two major tasks, one of which is being carried out at Caltech which involves an experimental study of a turbulent jet issuing into a quiescent environment (typical of flare flame). In the second task, a simple model of pollutant formation in jet flames is under development at TRW in conjunction with EER based upon the experimental observations. The FCR effort to date has concentrated on one of the simplest mixing systems; however, the development of an understanding of even the simplest mixing processes will have implications to all turbulent-mixing-dominated processes.

THE PHYSICS OF TURBULENT MIXING

The rate of mixing and reaction in a turbulent environment is much faster than rates due to molecular diffusion because of the ability of turbulence to rapidly transport and mix properties. For example, the combustion rate in an industrial flare is orders of magnitude larger than the corresponding rates in a laminar candle flame. Laminar transport is controlled by diffusional processes and it is tempting to treat the diffusive nature of turbulent flames by using an effective or "eddy" diffusivity. Much of the current modeling efforts involves this gradient diffusion concept. However, it is well accepted (Ref. 1) that the gradient diffusion approach is a simplifying artifice which does not necessarily represent the true nature of turbulence.

Many attempts have been made to extend the gradient diffusion approach to the prediction of complex turbulent phenomena. These have included different averaging techniques (e.g. Favre), multi-equation transport models deduced from higher moments of the Reynolds' time-averaged Navier-Stokes equations, the use of scalar invariants, and the statistical manipulation of assumed probability density-functions (pdf's) to obtain distributions of joint pdf's.

The modern view of turbulent transport, based upon experimental evidence obtained over the last few years, is very much at odds with the gradient diffusion model. In order for the gradient diffusion model to be self consistent, the scale of turbulent motions must be small compared to the distance that the diffusing quantities, such as concentration, change significantly. However, there is strong experimental evidence (Ref. 2), that the basic transport mechanism is associated with long lifetime coherent elements of fluid (eddies) which develop as a consequence of unstable inviscid motion. The coherent flame model was developed by Broadwell (Ref. 2) in order to account for these observed mixing processes.

According to the coherent flame model (Ref. 2), turbulent mixing begins with the entrainment of air into the jet. Empirically, it has been found that this entrainment rate is determined by the jet momentum and is linear with distance. The entrainment takes the form of large-scale inviscid intertwining of fuel and air; i.e., air is carried into the jets in large-scale eddies. The large eddies cascade to many smaller eddies due to the dissipative nature of turbulence until they are small enough for the reactants to molecularly diffuse across the scale. The final small scale, or "Kolmogorov's micro-scale," is the smallest turbulent scale at which point viscosity smooths out velocity fluctuations. Reactions of fuel and air can occur in two distinct regions. One is on the very thin diffusive interface between fuel and air on the large structures. The other path is at the small scale when the entrained air has been homogenized with the fuel. The bulk of the reactions proceeds at the microscale due to the relatively small amount of surface area available for reactions on the large structures. Because the reactants are finally homogenized by molecular diffusion, the reactions are expected to occur at stoichiometric conditions similar to a laminar diffusion flame.

EXPERIMENTAL

The FCR program has sponsored the present experiments underway at Caltech concerning the entrainment, mixing, and chemical reaction of turbulent jets with stationary reservoir fluid. They were carried out in a large water facility using a newly developed technique for determining the extent of molecular mixing and monitoring the chemical environment of a particular mixing and reacting species on a molecular scale. The experiments utilize dyes which fluoresce when excited by the 5145 Angstrom line from an argon ion laser and have the property that the fluorescence can be suppressed or induced by a particular chemical environment. Water soluble fluorescein was used in the present investigations which has the property that it will not fluoresce in an acid (low pH environment) but will fluoresce if the (local) pH exceeds a given threshold value. This transition is reversible and occurs over a very narrow range of mixture ratio as well as on a very short time scale. These properties provide a means of determining fluid which has been molecularly mixed with at least a certain volume ratio of the other reactant as a function of time and space. In other words, the extent of mixing on a molecular scale can be directly monitored.

This diagnostic technique is ideal for measuring the distribution of product (defined in this operational way) in a turbulent reacting flow, with a spatial and temporal resolution that is unachievable by conventional means. In addition, the fact that the laser excitation can be arranged by appropriate optics to be confined to a particular line or plane, allows the measurements to be realized over the whole illuminated plane (or line) at once. Such measurements are best described as field measurements, as opposed to point measurements, and they provide information about both the large and small scales of turbulence, the dynamics of which are ultimately responsible for bringing the two chemicals into molecular contact. In addition, and also important in the context of this investigation, by controlling the concentrations of the reacting species (say, aqueous solutions of an acid and base), the fluorescence threshold can be crossed at any volume ratio ϕ of reservoir fluid to jet fluid. This allows the effects of equivalence ratio on the turbulent reaction process to be investigated directly.

The pH-sensitive fluorescent dye can be used to mark jet fluid which has not yet mixed with reservoir fluid in at least a predetermined ratio or fluid which has mixed with reservoir fluid in excess of a predetermined ratio. Specifically, for each value of mixture ratio of jet fluid and reservoir fluid there is a unique pH value; and for every pH value there is a unique fluorescence intensity. Using a base solution (high pH) containing a small amount of fluorescent dye as a jet fluid and an acid solution (low pH) as the reservoir fluid, allows the jet fluid to be viewed. In other words, an element of jet fluid will fluoresce as it exits the jet nozzle and continue to fluoresce as it mixes with reservoir fluid until it reaches a particular mixture ratio, at which point the fluoresce of that element will abruptly stop. The mixture ratio at which the fluorescence transition occurs may be selected by the experimenter by simply selecting the concentration of the corresponding acid and base solutions. In this way, jet fluid which has not yet mixed with reservoir fluid to at least a given ratio may be labeled. On the other hand, if an acid solution containing a small amount of fluorescent dye is used as the jet fluid and a base solution as the reservoir fluid, then the jet fluid will not fluoresce as it exits the nozzle and will fluoresce only after it has mixed with a sufficient amount of reservoir fluid, thus marking fluid which has mixed with reservoir fluid in excess of a given ratio.

A thin plane of laser light was formed by an appropriate combination of spherical and cylindrical optical elements, thus allowing a slice through the turbulence to be recorded. A 3-Watt (Coherent Radiation CR-3) argon ion laser beam was passed through a collimating lens, the focal length of which was chosen to place the waist of the beam near the center of the reservoir tank. The beam was then turned vertically upward by a right-angle prism and finally passed through a cylindrical lens to spread the beam in one dimension. The resulting laser sheet entered the reservoir through a circular window at the bottom of the tank. The arrangement of the optical elements is depicted in Figure 1. This optical method has been documented previously (Ref. 3).

It is recognized that this technique does not account for the density changes that would accompany combustion. These experiments are therefore to be viewed as a first step, the purpose of which is to investigate the validity of the new ideas in the simplest circumstances. The effects of heat release and resulting density changes can be studied in a subsequent investigation in combustion of gaseous reactants. The basic ideas suggested by these investigations should remain applicable in such an environment.

Experiments were made using the fluorescence in three different ways:

1. Nonreacting Jet: (Water soluble) fluorescein was mixed with the jet fluid at a neutral pH ($6 < pH < 7$) which fluoresced, with the reservoir also at a neutral pH. Figure 2 shows a typical photograph for this case, which represents the dilution of the original dyed jet fluid by the entrained reservoir fluid. In this case, the fluorescence intensity is a local measure of the jet fluid concentration on the plane of symmetry of the jet.

2. Product Formation: Fluorescein was premixed with acidic jet fluid (low pH) which was discharged into a basic reservoir (high pH). In this arrangement, the mixed fluid fluoresces when sufficient reservoir fluid mixes on a molecular scale with the jet fluid. When the mixture reaches the threshold composition, as preset by the selected concentration of the jet and reservour fluids, it fluoresces marking the resulting "product" of the chemical reaction corresponding to the selected equivalence ratio ϕ (defined here as the volume of reservoir fluid required to neutralize a unit volume of jet fluid). Typical data are depicted in Figure 3.

3. Mixing Length: Fluorescein was mixed with a basic jet fluid (high pH) which discharged into an acidic reservoir (low pH). In this case, the jet fluid ceases to fluoresce when it has mixed with a certain amount of reservoir fluid, corresponding, as before, to the selected equivalence ratio. The resulting data allow the "flame length" to be measured directly. Typical data using this arrangement are depicted in Figure 4.

These photographs, and numerous others, corroborate the basic ideas discussed in the previous section. In the nonreacting jet (Figure 2), the feature which is particularly noteworthy is the deep penetration of the reservoir fluid into the jet, indicating the presence of large-scale structures. This same feature is also obvious in the reacting jets (Figure 3 and 4). The visualization of product formation in Figure 3 supplies additional support to the emerging model. There is evidence of no molecular mixing for several diameters downstream of the jet entrance. Molecular mixing is first evident on the edge of the jet associated with the thin interface between the reservoir and jet fluids. However, the bulk of the molecular mixing begins throughout the jet at one axial location when the large structures cascade down to smaller structures and homogenization occurs.

Data such as that shown in Figure 4, can be used to measure the distance at which every element of jet fluid has molecularly mixed with the reservoir fluid. This molecularly mixed length is analogous to the flame length in jet diffusion flames. As the Reynolds number is increased, the "flame length" measured in jet diameters increases until under turbulent conditions the flame length reaches an asymptotic value. This is true for all diffusion flames and true for the mixing length data measured from these photographs. This observation can be explained by the model of turbulent mixing presented above. When the jet disappears (or when all fuel has burned) every element of jet fluid is molecularly mixed with the required parts of reservoir fluid. The required reservoir fluid (or air) is entrained into the jet at some upstream location and the two fluids subsequently intertwine on an ever decreasing scale-cascade to the Kolmogorov scale. Once at that scale, homogenization occurs by diffusion across the scale. It can be shown (see Ref. 2) that at high Reynolds numbers the time to diffuse across the Kolmogorov scale is very short compared to the large-scale breakdown time. Thus, the mixing time is controlled by the slower entrainment-breakdown time; and, further, since this is independent of Reynolds number (Ref. 1) the mixing time is independent of Reynolds number.

Other observations on these flame length data are also explainable by the coherent flame model. In particular, the flame length has been found to be linear with ratio of fuel to air required to burn the fuel (the equivalence ratio) (Ref. 4 and 2). These observations, along with data obtained in shear layers can argue strongly against the validity of the turbulent gradient diffusion model and lend support to the emerging coherent flame model.

MODEL FORMULATION

The formulation of the model which makes use of the concepts of turbulent mixing discussed above is detailed elsewhere (Ref. 2 and 5) and will only be outlined in this section. The first analytical calculations to be performed involve the formation of NO in turbulent diffusion flames which involves relatively slow chemical reactions. The discussion to this point has dealt with situations in which the chemical reaction rates are fast relative to mixing and in which, therefore, the reaction rate is controlled by the entrainment rate. However, the same basic notions about molecular mixing also apply to these slower reactions.

The approach is to follow a unit mass of fuel as it leaves the nozzle and mixes with air at the rate of entrainment of air. At any given time, the mass of fuel and the air entrained up to that point are undergoing the cascade to smaller scales or have reached the smallest Kolmogorov scale. For simplicity, reaction taking place on the interface of the large structures will be ignored because it is small relative to that taking place as the fuel and air are homogenized at the small scale. Fast flame reactions are completed when the fuel and air are homogenized by molecular diffusion in the small scale flamelet. However, slow reactions take place in two environments: the first involves the homogenizing flamelet as the fuel and air finally diffuse together at stoichiometric conditions and the second is in the flame core as a homogenized packet of fuel and air entrains more air and cascades to smaller scales.

The model is formulated as two interacting reactors as shown in Figure 5. The reactors A and B together contain a unit mass of fuel to which air is added at the entrainment rate. Reactor B represents the flamelet wherein reactions occur at stoichiometric conditions. Reactor A represents the flame core which takes place at variable stoichiometry depending on the distance from the jet entrance. These concepts were implemented by taking reactor B to be a well-stirred reactor and reactor A to be a plug-flow reactor.

The critical parameters required by the model are as follows:

1. Stoichiometry. The reactions in the flamelet are assumed to take place at

stoichiometric conditions since the final homogenization process is by molecular diffusion. The reactions in the flame core reactor occur under rich conditions throughout the flame zone as determined by the mass interchange rates.

2. Residence times: The residence time in the flamelet reactor (B) is taken to be the time to diffuse across the microscale. Relating the scale to known quantities and relating it to clock time (Ref. 2) yields

$$\tau = \beta \, 4K_2 \left(\frac{\rho_m}{\rho_o}\right)^{1/4} \frac{t}{\sqrt{Re_o}} ,$$

where Re_o is the initial Reynolds number based on the jet diameter, K_2 is a constant which relates the entrainment rate to distance which was found empirically ($K_2 = 0.16$), ρ_m is the mean mixture density, and ρ_o is the initial density. The parameter β is an unknown proportionality constant that will be selected upon comparison with experimental data. The success of the modeling approach is determined by the ability to choose a single valued constant to fit a variety of data.

3. Mass Interchange Rate: The interchange rates between the two reactors is determined by the entrainment rate of air into the flame and the requirement that reactions in the flamelet occur at stoichiometric conditions. The rate of entrainment is obtained from the empirical relationships of Ricou and Spalding (Ref. 6). The flow rate from A to B is then set by the requirement to carry enough unburned fuel into B to react stoichiometrically.

4. Radiation Heat Transfer: The temperature of the flamelet and flame core is critical to the rate of formation of thermal NO. Without radiation losses, this temperature would be the adiabatic flame temperature. The model as formulated uses an optical thin calculation and requires an independent assessment self-absorption of the flame in order to determine the radiative heat loss. A single parameter, α, is used as the multiplicative correction to gas radiative heat transfer based on an optical-thin approximation and is thus a measure of the flame self-absorption. Figure 6 demonstrates the impact of this parameter on the temperature profile in an H_2/air flame.

The computer code has been developed for the interacting well-stirred and plug flow reactors. The highlights of the physical and mathematical aspects of the code are as follows:

- Implicit finite difference method for solving time-dependent governing equations (continuity, species and energy conservation equation, and equation of state).
- Fully detailed kinetic mechanisms (see Ref. 7 for details of kinetics).
- JANAF tables for calculations of thermochemical properties of each species.
- Optical-thin approximation considering only gas to ambient radiative heat transfer with correction for self-absorption.

The details of the developed computer code are also supplied elsewhere (Ref. 8).

RESULTS

The hydrogen turbulent diffusion flame data of Bilger and Beck (Ref. 9) provide an ideal test of the model. The measurements include detailed measurements of the nitric oxide field of a vertical hydrogen flame in still air. These flames had high Froude numbers (10^6) but were still strongly impacted by buoyancy effects. However, at constant Froude number the main reactant and product concentrations gave axial profiles which were similar and independent of Reynolds number.

Figure 7 shows the results of NO measurements on the hydrogen flame axis for a constant Froude number of $.6 \times 10^6$ and variable Reynolds number from 1500 to 12000. The principle feature of these data is the dependence on Reynolds number; or, in other words, the lack of Reynolds similarity. These results at constant Froude numbers indicate that the normalized peak NO mass fraction or the emission index has an inverse square root dependence on Reynolds number. Also shown in Figure 7 are the computed results using a 0.7 correction factor to optical-thin radiation heat transfer and the best fit to the data for the proportionality constant β. The model predicts the position and peak value of NO adequately and thus correctly predicts the Reynolds number dependence. At lower Reynolds number where the model is not expected to be as applicable, the predicted peak NO position is not in as good agreement with the experimental data. At longer axial distances the agreement between the predicted and experimental results are also not as good. The reason for this discrepancy is unclear due to the fact that after the peak, the NO reactions are frozen due to lower temperature and the declining profile is due to dilution by continuing air entrainment. Thus, if the peak is matched, the dilution by entrainment should be adequately predicted. The experimental data at X/D_o of 140 appears to be inconsistent with this dilution rate.

Predictions have been also made on the NO emission indices for CH_4/air turbulent diffusion flames. Experimental data for free CH_4/air turbulent diffusion flames with NO measurements are very scarce. Recently Peters and Donnerhack (Ref. 10) have reported their experimental data on NO in CH_4/air flames. However, the experiment was performed in a co-flowing fuel-air system. The overall equivalence ratio of all flames was maintained at a constant value of 0.63 by varying air and CH_4 flow rates. The size of the flame tube (external air tube) was fixed while the fuel nozzle diameter was varied. These flames are confined in nature, which limits the free supply of air for macroscopic entrainment. The pressure gradient which occurs as a result of confinement could cause flow recirculation which in turn would affect the patterns of macroscopic entrainment and microscopic mixing. Techniques for treating confined flow are beyond the scope of this paper. For the purpose of this report, we have selected only the flames from Peters and Donnerhack's data which are least affected by confinement. These flames are from the smallest fuel tubes which also have the highest fuel jet velocities and the lowest air velocities. The parameters of these flames and the emission indices are presented along with the results from the numerical model in Table 1. The predicted emission indices are within 15 percent of the measured value.

As a final example of the application of the analytical approach, the model has been used to predict the impact of mixing rate of a secondary fuel on the effectiveness of reburning for NO_x reduction (see Reference 11). In the reburning process, a small amount of fuel is added to the lean exhaust products from the main burner zone in order to effect a reduction in the NO level. Typically 10-20 percent of the fuel to the boiler must be supplied as reburning fuel to achieve a 50 percent reduction in overall NO. A slower mixing rate of this reburning fuel could potentially offer a locally rich environment for NO reduction while maintaining an overall stoichiometry at the end of the reburning zone near unity. Offsetting this advantage is the possibility of setting up too-rich an environment in the early stages of the flame, giving rise to poor conversion of NO to N_2. In order to examine this issue, a simple numerical experiment was constructed as follows (see Figure 8).

Hot products from the primary combustion zone with 10 percent excess air were reburned and held for a total residence time, including mixing, of 0.5 sec. The jet Reynolds Number was held at a value of 10,000 while the initial jet velocity and diameter were varied (consistent with this Reynolds Number) to give mixing times from less than 0.05 sec to 0.3 sec. Over this range of mixing times the overall reburning stoichiometry was varied between 0.9 and 0.99. The reduction of NO was observed as a function of these parameters.

Figure 9a shows the influence of mixing rate on nitrogen conversion for a reburning equivalence ratio, ϕ_{RB}, of 1.10. This, by definition, is the ratio of reburning fuel to available oxygen in the combustion products normalized by the value of this ratio for complete combustion. A ratio of 1.10 implies then that the reburning fuel is 10 percent in excess of that required to burn out the excess O_2 in the product. In this specific instance the excess O_2 is 2 percent, the initial combustion product temperature is 2300 F, the initial NO level is 300 ppm, and the reburning fuel contains one percent HCN to simulate a reburning fuel containing fuel nitrogen. The NO conversion to XN, without regard to the fate of the reburning fuel nitrogen, is given by the upper curve (Figure 9a). With characteristic chemical reaction time for NO reduction on the order of 0.1 seconds, the process is clearly mixing controlled for $\tau_{mix} \geq 0.1$ sec. In this regime the flame provides a sufficiently rich environment for effective NO reduction even though the overall reburning conditions are near stoichiometric.

The bottom curve in Figure 9a shows the conversion of the reburning fuel nitrogen. Here the chemical time constant is on the order of 0.3 sec and hence effective conversion through mixing control is achieved only for mixing times of 0.3 sec or greater. For this example, the net conversion of both NO and reburning fuel nitrogen is given by the middle curve. The NO conversion dominates this combined process in this example because of the high initial NO of 300 ppm and the low reburning fuel flow associated with near stoichiometric conditions.

Figure 9a shows the total nitrogen conversion (including both NO and reburning fuel nitrogen) as a function of the reburning equivalence ratio, ϕ_{RB}. The results are presented for both situations with and without the presence of reburning fuel nitrogen and for the two limits of fast ($\tau_{mix} = 0.01$ sec) and slow ($\tau_{mix} = 0.3$ sec) mixing. It can be seen that in the absence of reburning fuel nitrogen slow mixing is favorable for $\phi_{RB} \leq 1.37$. For richer overall conditions, it is preferable to have the entire process occurring at those conditions rather than a portion of the process at the less favorable, extremely rich conditions induced by delayed mixing. This threshold ϕ_{RB} moves to 1.45 when reburning fuel nitrogen is present, as the HCN conversion process favors richer conditions.

The essential conclusion to be drawn from Figure 9 is that in order to achieve effective reburning with a minimum of reburning fuel, the mixing time must be greater than approximately 0.2 seconds.

CONCLUSIONS

A model has been formulated that describes, in a simple way, chemical reactions in turbulent fuel jets discharging into air. The model deals with both fast and slow reactions and is therefore applicable to nitric oxide generation processes. A basic aspect of the model is that molecular mixing which precedes the reaction does not take place as a consequence of the "turbulent diffusion" of the reactants towards each other down concentration gradients. Instead, fuel and air are entrained throughout the jet, intertwine in large-scale inviscid motions, and mix molecularly at the interfaces and as the mixture is homogenized at the Kolmogorov scale. This view of the mixing process leads to a model in which the state of the fuel-air mixture is independent of the radial coordinate. The usual bell-shaped distributions arise solely from the radial variation in the ratio of pure air to the fuel-air mixture.

The model has been applied to hydrogen and methane jet flames discharging into air. The results in both cases are in good agreement with several sets of measurements. In particular, the model appears to explain satisfactorily the dependence of nitric oxide generation rate on Reynolds number. The model has also been used to predict the impact of mixing rate of the secondary fuel on the effectiveness of the reburning process for in-furnace NO_x reduction. Further development and refinement of the model requires a better understanding of the physical mixing process in turbulent jets. This work is continuing in both the theoretical and experimetnal efforts at Caltech and TRW in conjunction with EER via the EPA's Fundamental Combustion Research program.

ACKNOWLEDGEMENTS

This work is supported by the EPA under the Fundamental Combustion Research Applied to Pollution Formation Program, Contract 68-02-3633. Steve Lanier is the EPA Project Officer.

REFERENCES

1. Tennekes, H. and J. L. Lumley. A First Course in Turbulence. The MIT Press, Cambridge Massachusetts, 1972.

2. Broadwell, J. E. A Model of Turbulent Diffusion Flames and Nitric Oxide Generation Part I. Final Report 68-02-3633, U.S. Environmental Protection Agency, Research Triangle Park, North Carolina, To be submitted to Jnl of Fluid Mech. 1982.

3. Dimotakis, P. E., R. C. Miake-Lye, and D. A. Papantoniou. Structure and Dynamics of Round Turbulent Jets. Graduate Aeronautical Laboratory of California Institute of Technology. GALCIT Report FM 82-01. Pasadena, California, 1982.

4. Hottel, H. C. Burning in Laminar and Turbulent Fuel Jets. Fourth (International) Symposium on Combustion. The Williams and Wilkins, Co. Baltimore, Maryland, 1953. pp. 97.

5. Tyson, T. J., C. J. Kau, and J. E. Broadwell. A Model of Turbulent Diffusion Flames and Nitric Oxide Generation, Part II. Final Report Contract 68-02-3633, U.S. Environmental Protection Agency, Research Triangle Park, North Carolina. To be submitted to Jnl of Fluid Mech., 1982.

6. Ricou, F. P. and D. B. Spalding. Measurements of Entrainment by Axisymmetric Turbulent Jets. Jnl Fluid Mech., 11:21, 1961.

7. Seeker, W. R. and M. P. Heap. Fundamental Combustion Research Applied to Pollutant Formation, Volume 1B, Gas Phase Chemistry. Final Report Contract 68-02-2631. U.S. Environmental Protection Agency, Research Triangle Park, North Carolina, 1982.

8. Tyson, T. J., M. P. Heap, and W. R. Seeker. Fundamental Combustion Research Applied to Pollution Formation, Volume IV, Engineering Analysis. Final Report Contract 68-02-2631. U.S. Environmental Protection Agency, Research Triangle Park, North Carolina, 1982.

9. Bilger, R. W. and R. E. Beck. Further Experiments on Turbulent Jet Diffusion Flames. Fifteenth (International) Symposium on Combustion, The Combustion Institute, Pittsburgh, PA, 1974. pp. 541.

10. Peters, N. and S. Donnerhack. Structure and Similarity of Nitric Oxide Production in Turbulent Diffusion Flames. Eighteenth (International) Symposium on Combustion, The Combustion Institute, Pittsburgh, PA, 1981. pp. 33.

11. Chen, S. L., W. C. Clark, M. P. Heap, D. W. Pershing, and W. R. Seeker. NO_x Reduction by Reburning with Gas and Coal--Bench Scale Studies. The EPA/EPRI Joint Symposium on Stationary Combustion NO_x Control. Dallas, Texas 1982. Session IV.

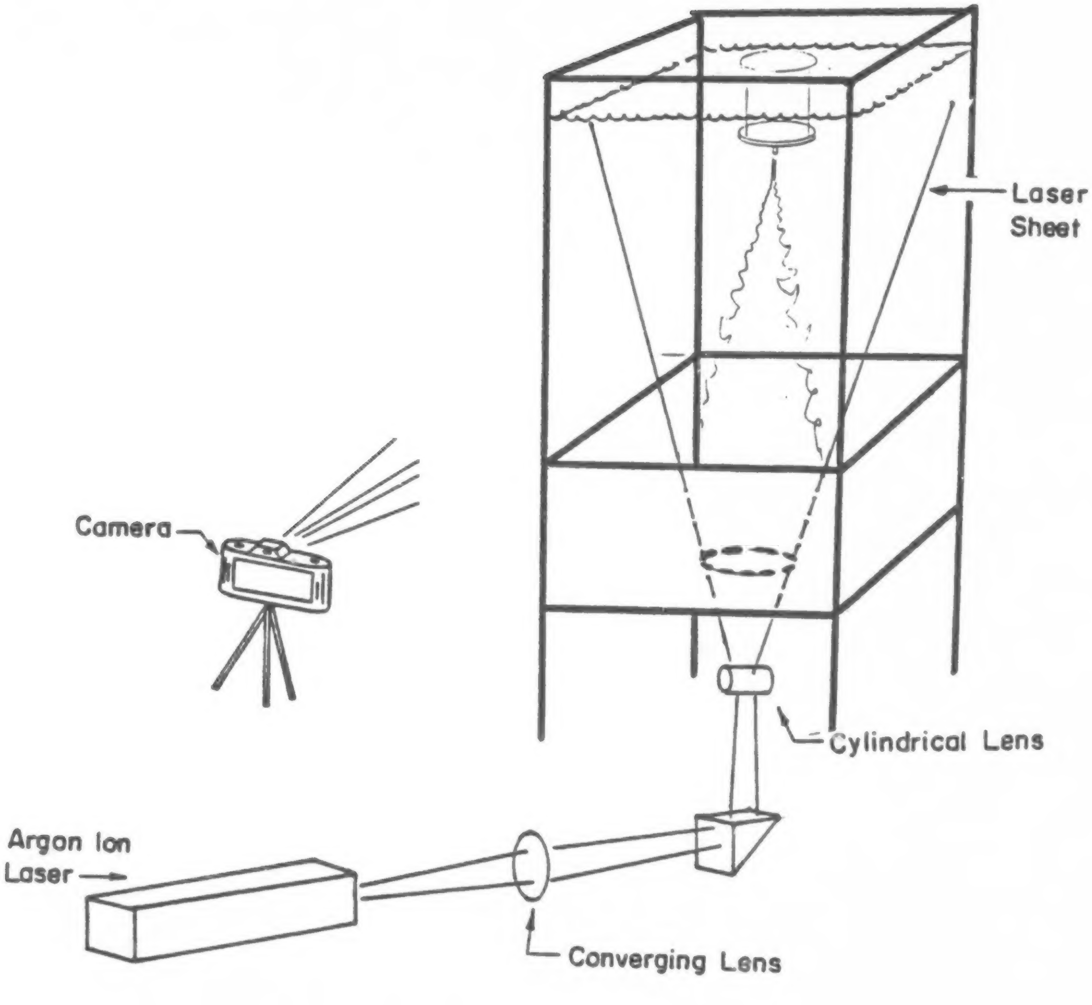
Laser Sheet
Camera
Cylindrical Lens
Argon Ion Laser
Converging Lens

Figure 1. Laser-induced fluorescence laser sheet optics.

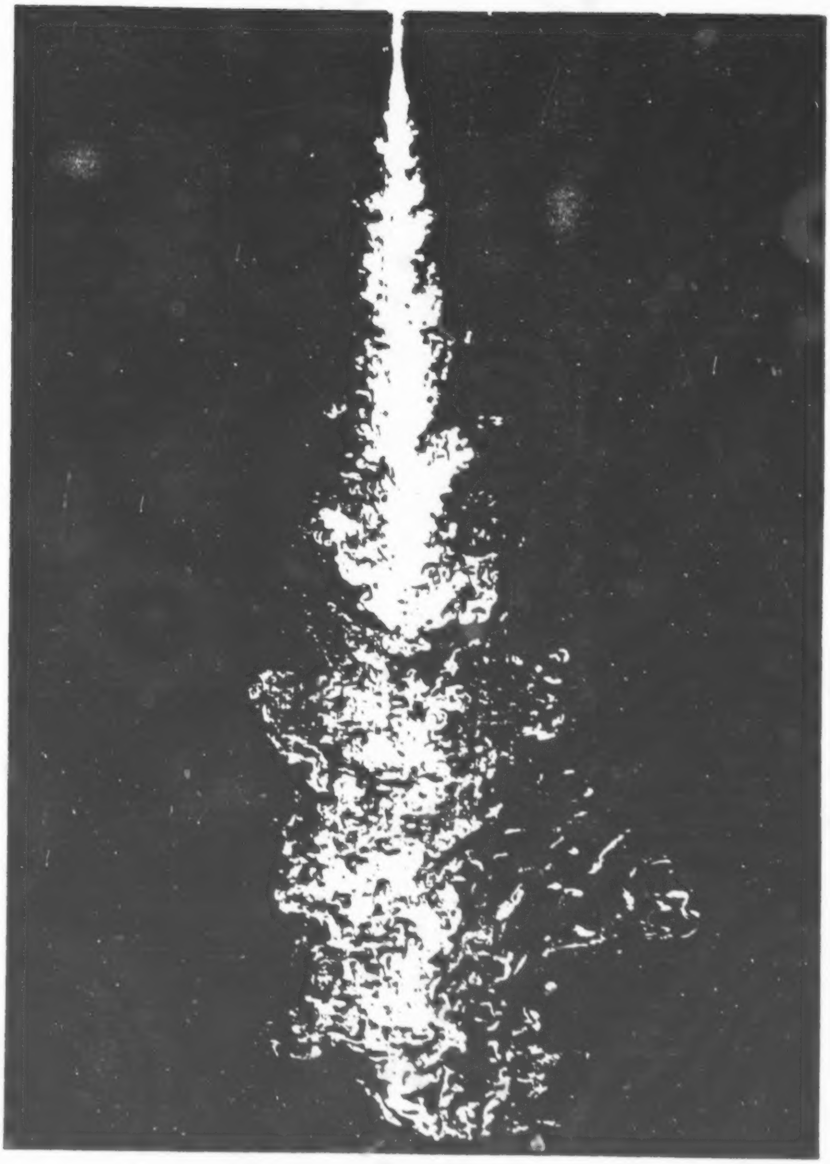

Figure 2. Nonreacting jet fluid concentration on the plane of symmetry of a turbulent jet (Re = 10,000).

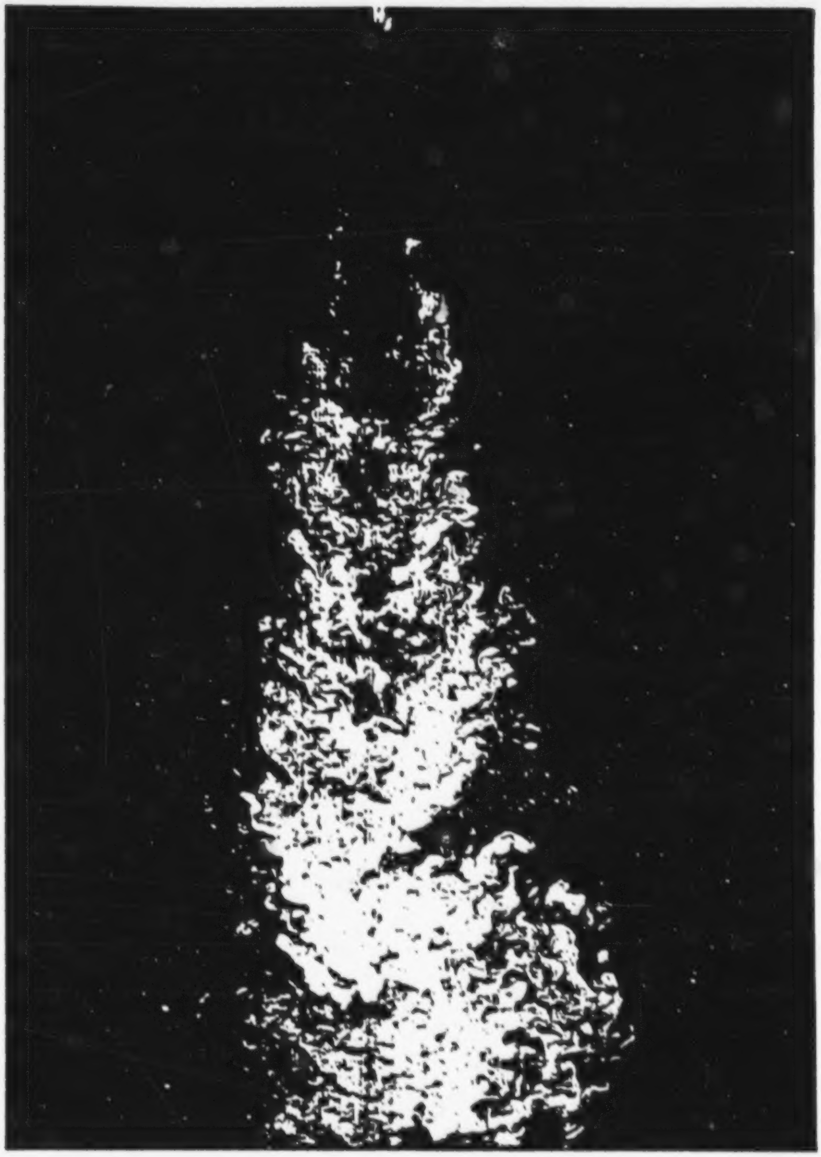

Figure 3. Chemical product concentration on the plane of symmetry of the jet, ϕ = 25:1, Re = 10,000.

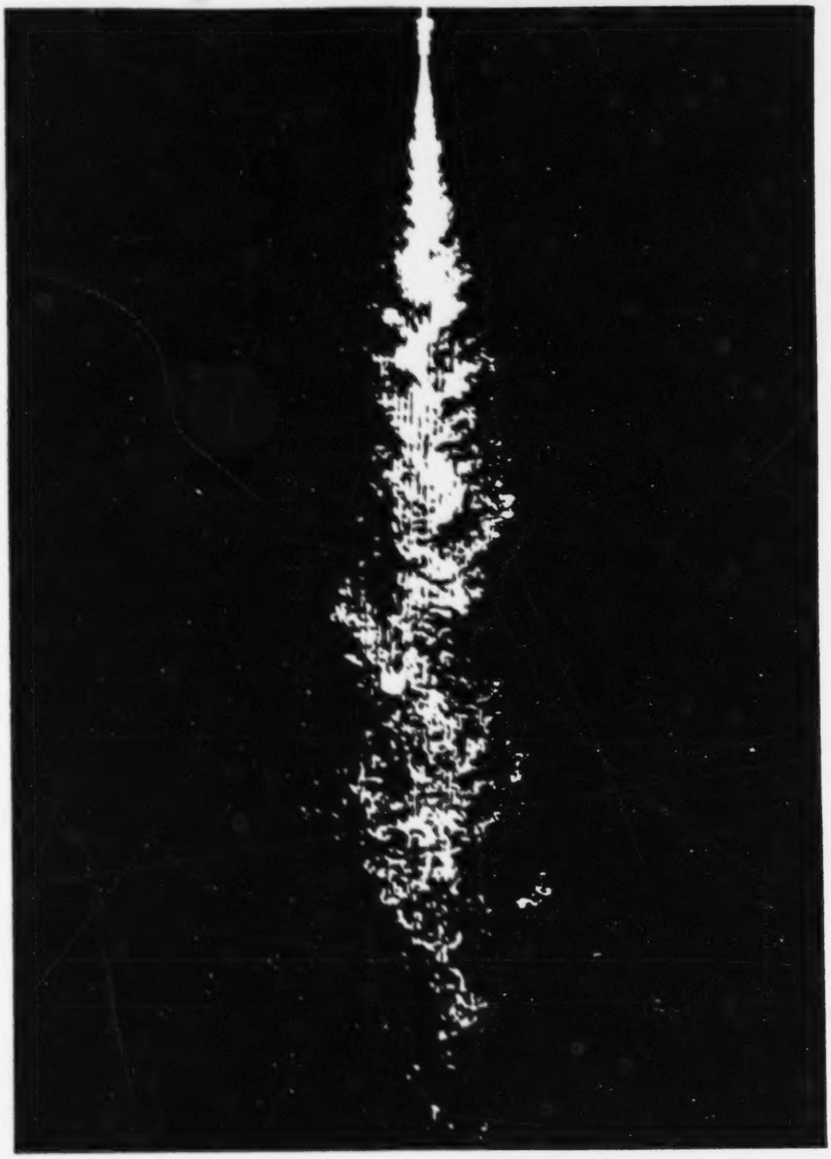

Figure 4. Unreacted jet fluid concentration on the plane of symmetry of the jet, equivalence ratio $\phi = 20:1$, Reynolds number Re = 10,000.

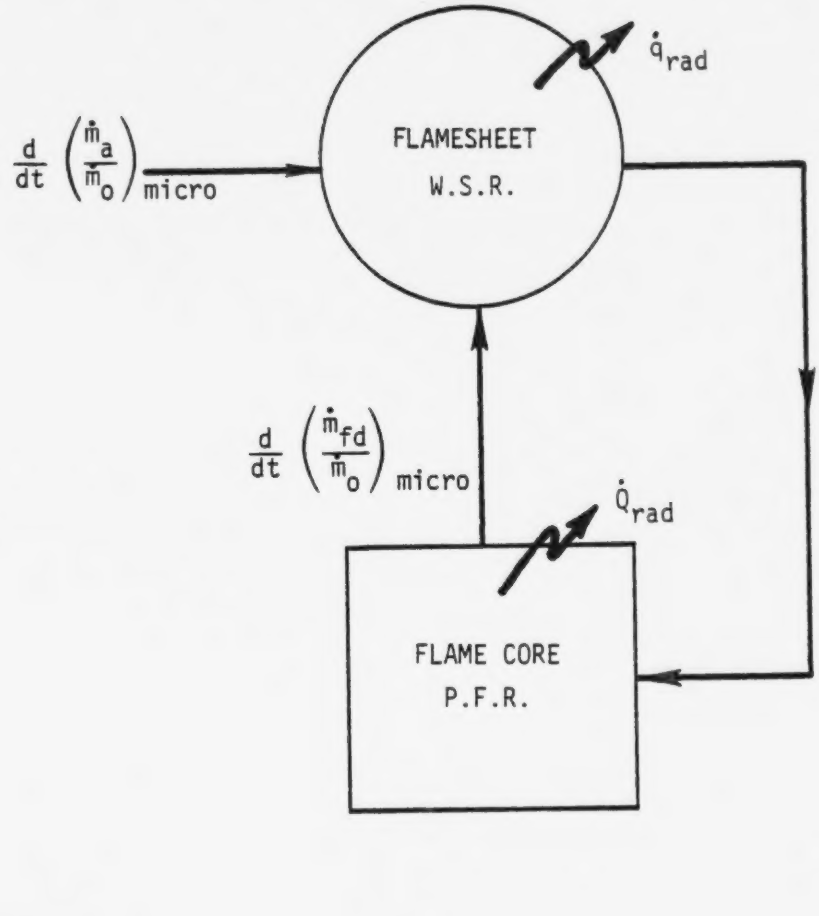
$\dot{q}_{rad}$
FLAMESHEET
W.S.R.
$\frac{d}{dt}\left(\frac{\dot{m}_a}{\dot{m}_o}\right)_{micro}$
$\frac{d}{dt}\left(\frac{\dot{m}_{fd}}{\dot{m}_o}\right)_{micro}$
$\dot{Q}_{rad}$
FLAME CORE
P.F.R.

Figure 5. Schematics of reactor model.

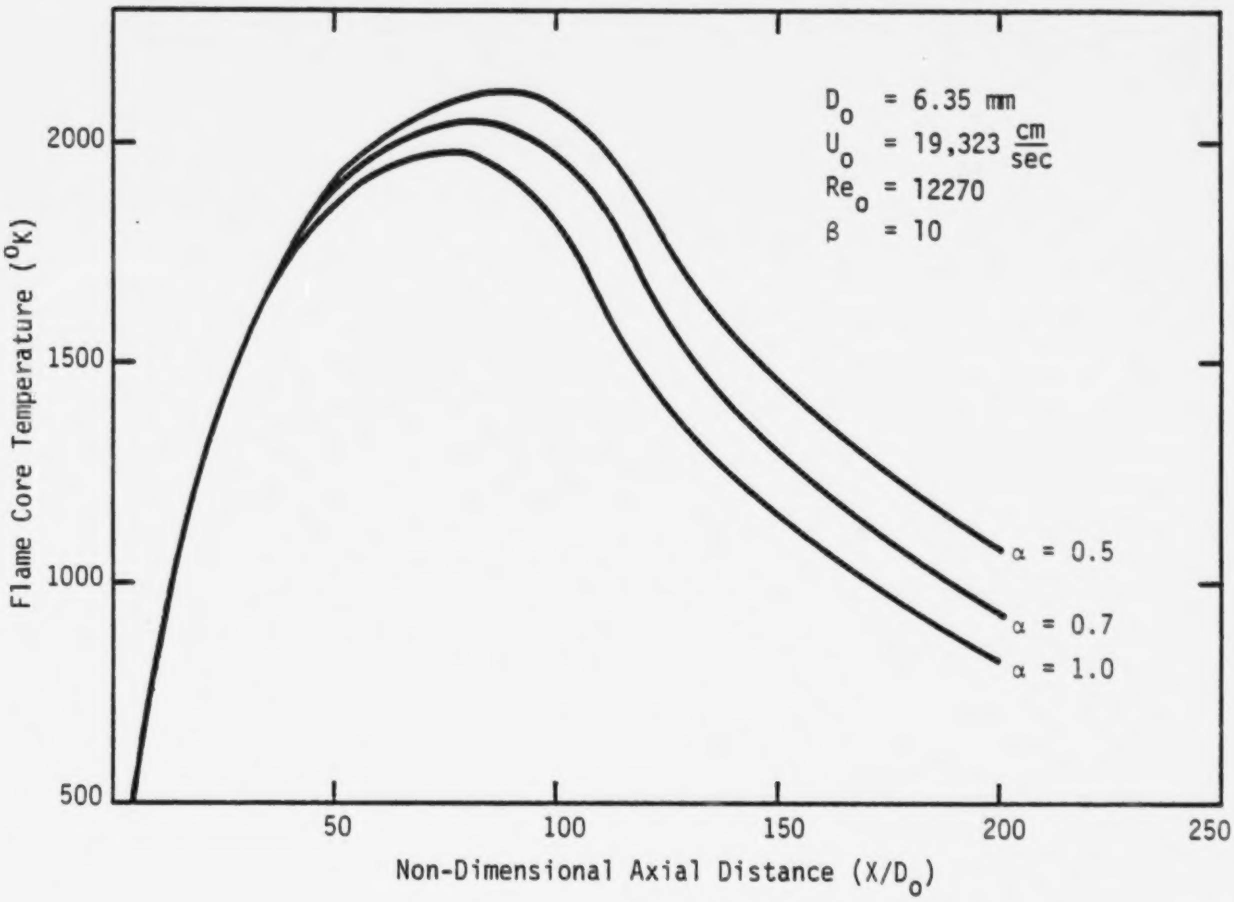

Figure 6. Effect of radiative heat transfer on flame core temperature history.

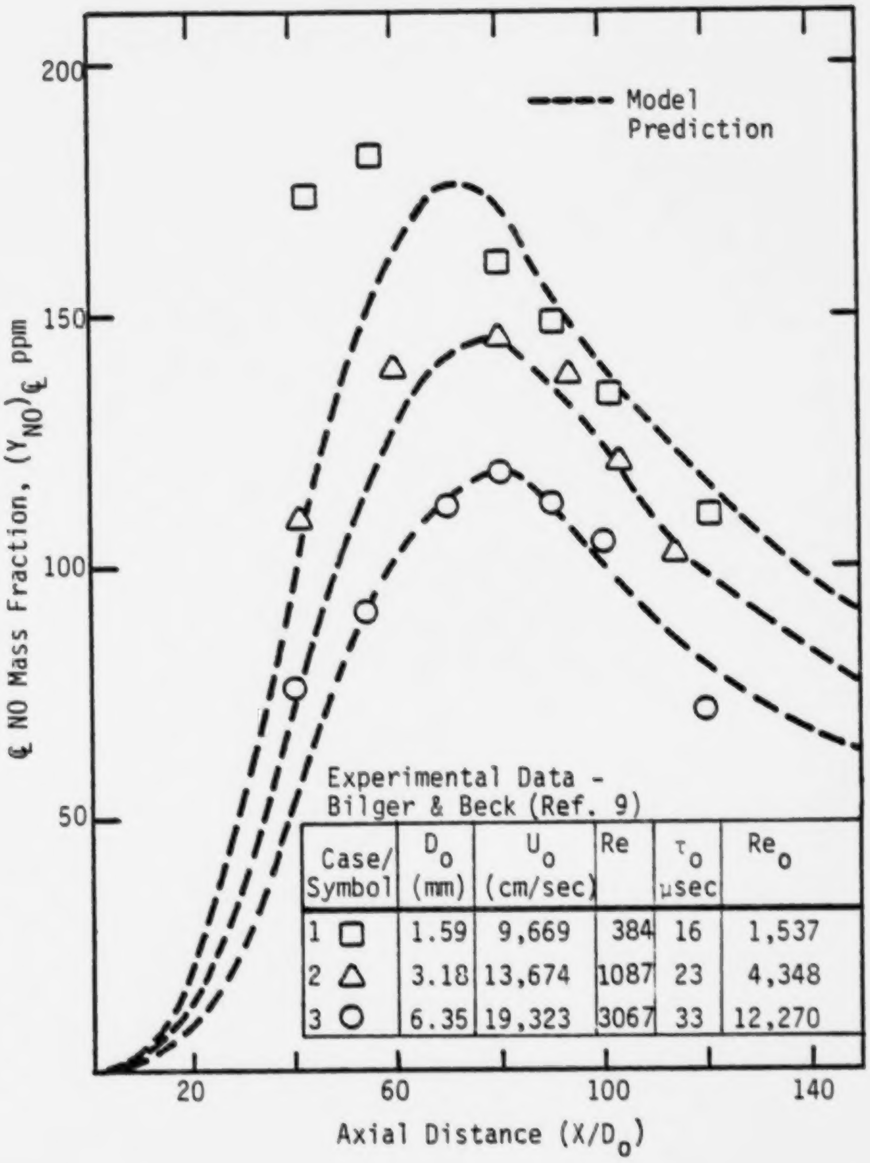

Experimental Data - Bilger & Beck (Ref. 9)

Case/ Symbol	D_o (mm)	U_o (cm/sec)	Re	τ_o μsec	Re_o
1 □	1.59	9,669	384	16	1,537
2 △	3.18	13,674	1087	23	4,348
3 ○	6.35	19,323	3067	33	12,270

Figure 7. Comparison of model calculated NO against measurements ($Fr = 6 \times 10^{-5}$) for H_2/air flames.

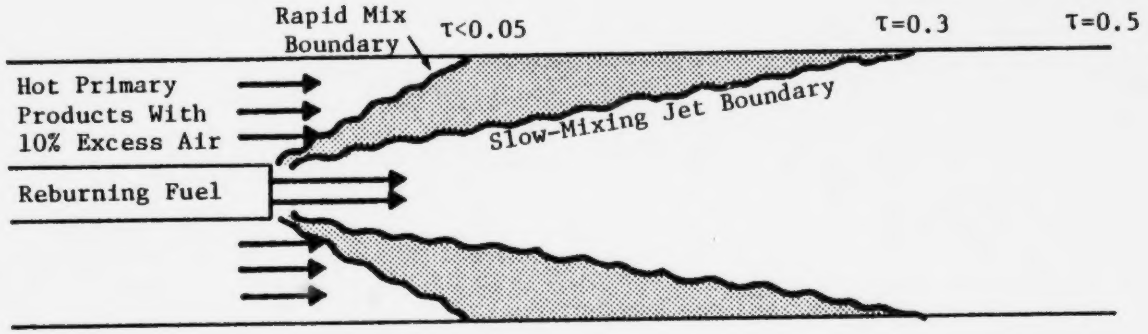
Rapid Mix
Boundary
τ<0.05
τ=0.3
τ=0.5
Hot Primary
Products With
10% Excess Air
Slow-Mixing Jet Boundary
Reburning Fuel

Figure 8. Numerical simulation of reburning stage.

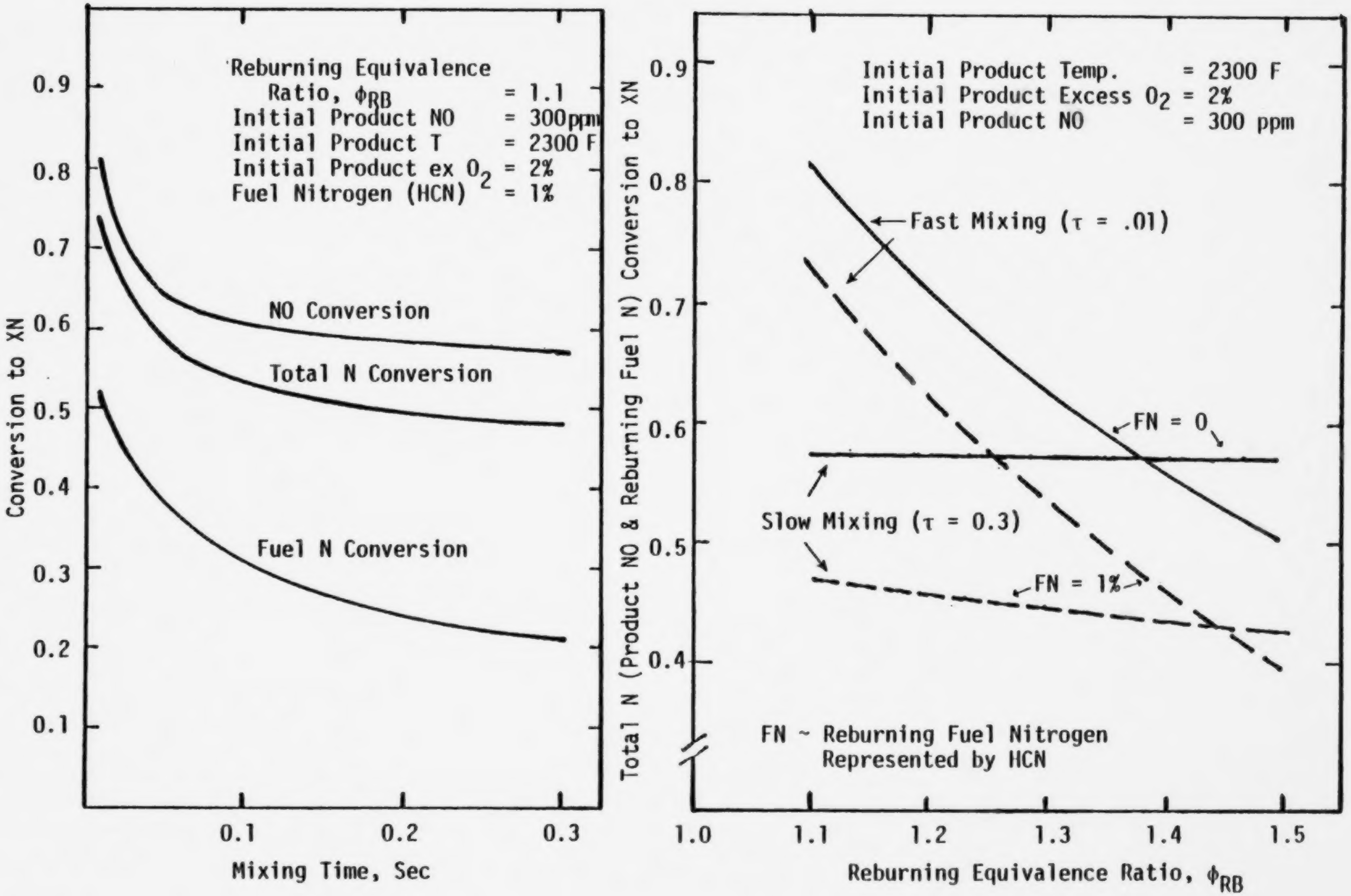

a.

b.

Figure 9. Influence of mixing rate on nitrogen conversion in reburning stage (NO reduction stage, not including burnout stage).

TABLE 1. COMPARISON OF PREDICTED AND MEASURED EMISSION INDICES FOR CH_4/AIR TURBULENT DIFFUSION FLAME

Flame No.	21	22	23	24
D_o (cm)	0.3	0.3	0.35	0.35
U_o (cm/sec)	2,070.	1,720.	1,780.	1,850.
Re_o	3,200.	2,630.	3,200.	3,340.
Fr	14,710.	10,000.	9,335.	10,000.
L_f/D_o	170.	157.	163.	171.
$(E)_{exp.} \times 10^3$	1.10	1.20	1.17	1.19
$(E)_{cal.} \times 10^3$	1.07	1.14	1.03	1.02

FORMATION AND CONTROL OF POLLUTANT EMISSIONS DURING STOKER-FIRED COAL COMBUSTION

By:

G. P. Starley, D. M. Slaughter, J. M. Munro,
F. W. Bradshaw, G. Silcox, and D. W. Pershing
Department of Chemical Engineering
University of Utah
Salt Lake City, Utah 84112

"Although the research described in this paper has been funded wholly or in part by the United States Environmental Protection Agency through cooperative agreement #809267 to the University of Utah, it has not been subjected to Agency review and therefore does not necessarily reflect the views of the Agency and no official endorsement should be inferred."

ABSTRACT

This paper describes the results of the study on the formation and control of nitrogen and sulfur oxides in coal-fired spreader-stoker systems. A 140,000 Btu/hr tower furnace was utilized to define the evolution and oxidation of fuel nitrogen and sulfur in the suspension phase. The influence of combustion parameters on the conversion of fuel sulfur and nitrogen during the fixed-bed phase of the combustion process was defined with a 300,000 Btu/hr over-feed furnace. Finally, a 750,000 Btu/hr model spreader-stoker furnace was used to study the coupling between the two combustion phases and evaluate the overall utility of control concepts.

The results indicate that NO emissions from spreader-stoker fired coal furnaces are due to relatively high conversions of fuel nitrogen evolved from particles less than 0.1 inches in the suspension phase, and low conversion of fuel nitrogen during the bed combustion. In the suspension phase, nitrogen is evolved at approximately the same rate as carbon is oxidized. Local oxygen availability is a primary control parameter for both phases of combustion. Minimum overall fuel nitrogen conversions of 6 percent were achieved in the pilot scale facility by controlling the stoichiometry of both combustion zones. NO_x emissions from coal-fired spreader stokers can be reduced by either removing the fines from the coal feed or controlling the stoichiometry throughout the furnace.

INTRODUCTION

In recent years considerable research has focused on pulverized coal burning; however, many current industrial coal units are stoker-fired and these systems have received only limited attention. Stoker-fired boilers are significant in terms of both coal consumption and contributions to national NO_x and SO_x emissions. Almost 20 percent of the coal consumed in the U. S. is burned in stoker systems. They are the single largest source of combustion generated particulate emissions and a major source of NO and SO_x emissions. (1)

The spreader stoker is the most common large mechanical stoker. In this system a multiblade, overthrow rotor projects large coal particles (80%> 8 mesh, max size = 1¼") onto a moving or vibrating grate. The smaller particles burn in suspension while the heavier pieces fall to the grate for combustion in a thin (2-6") bed. Coal heat release rates are approximately 750,000 $Btu/hr/ft^2$.

Recent pilot and field tests have demonstrated the potential of combustion modifications for NO control in stoker-fired boilers. Tests on a 25,000 pph steam spreader-stoker indicated that decreased overall excess air resulted in lower NO_x emissions (2) and SO_2 emissions were reduced when coal/limestone pellets were fired. Field results for large-scale industrial stokers have shown little effect of overfire-air percentage and an apparent increase in NO_x with increasing load. (3) Full scale testing on a modified spreader stoker boiler by Maloney and coworkers (4) has demonstrated the importance of flue gas recirculation for both NO_x and particulate control. Laboratory experiments in a 180mm pot furnace (batch operation) have suggested that the oxidation of volatile fuel nitrogen may be of major importance in stoker systems, particularly in the early portion of the burning. (5)

This paper summarizes an EPA-funded program to study the formation and control of SO_2 and NO in coal-fired spreader stokers. The approach was primarily experimental; three types of laboratory furnaces were utilized to investigate the suspension burning, the bed combustion, and the overall process. Exhaust and in-flame species and temperature measurements were made with bituminous coals to define the influence of combustion conditions on SO_2 and NO emissions.

EXPERIMENTAL

Model Spreader Stoker Furnace

The primary experimental facility used in this work was the 750,000 Btu/hr model spreader stoker furnace (MSF) shown in Fig. 1. This eight-section, refractory wall unit (6) had a one ft^2 dumping grate and the vertical dimensions were scaled approximately 1:1 with commercial practice. Coal was fed at 60 lb per hour onto a rotating, multi-vane spreader by a metering auger. The variable speed spreader, located 32 inches above the stainless-steel grate, distributed the coal uniformly across the bed. All sections contained multiple sampling ports, and overfire-air slots. All air streams were at ambient temperature.

Tower Furnace

The 70,000 Btu/hr tower furnace (Fig. 1b) was utilized to investigate suspension phase combustion. This refractory wall combustor (7) was 6 inches in inner diameter, 8½ ft long and contained provision for auxiliary heating (by firing natural gas in annular channels around the main chamber) to maintain constant wall temperature. Sized coal particles were fed into the furnace center through a stainless-steel water-cooled injector 32 inches above the bottom. A high-intensity gas burner, attached to the horizontal extension at the furnace bottom, produced hot combustion products which flowed vertically upward to simulate the combustion products leaving an actual stoker bed. Particles falling to the furnace bottom were collected in a water-quenched trap. Unburned particles reaching the flue were collected in a water-quenched, 200-mesh screen system.

Fixed Bed Furnace

The 300,000 Btu/hr fixed-bed furnace (Fig. 1c) was 11 inches by 15 inches inside, had a 0.75 ft^2 grate, and was used for detailed investigation of bed combustion. (8) The composite refractory walls contained multiple overfire-air slots, large observation windows, and in-flame probe ports. Coal was continuously metered onto the grate from above to simulate the bed-feeding process in a spreader stoker. Suspension phase burning of the fines was essentially eliminated by sizing the coal to ¼ inch by 1 inch. The ambient temperature combustion air was distribued between the three-section underfire-air plenum and two levels of overfire air-ports.

Analytical Measurements

Exhaust gas samples were withdrawn with a water-cooled stainless-steel probe and pumped to the continuous instrumentation which included a chemiluminescent NO analyzer, a paramagnetic O_2 analyzer, and an NDIR analyzer for CO and CO_2. In-flame HCN samples were withdrawn through a controlled-temperature (250°F) probe and analyzed with a HP 5840 gas chromatograph containing an NPD. NH_3 was sampled with an acid spray probe, collected in a series of bubblers, and analyzed with a gas sensing electrode. (9)

Fuels

Table 1 shows the ultimate and proximate analysis of each of the coals used in this study. These data were obtained by an independent laboratory.

SUSPENSION COMBUSTION

This section of the paper summarizes the tower furnace results on the importance of suspension phase particle combustion. The objectives of these studies were to define those particle sizes which experienced significant reaction in the overthrow phase and to establish the fate of the fuel nitrogen and sulfur in those particles.

Fate of Major Constituents

Figure 2 presents typical results from gas phase analysis for CO, CO_2, NO, NO_2 and SO_2 and from mass and composition of the solids collected at the furnace top and bottom. (H_2O and N_2 were estimated by difference.) The data shown are for the 1900°F thermal condition (wall temperature = 1900°F), the Indiana coal, the smallest 10 percent of a commercial stoker feed ($d < .063$ inches), and a natural gas firing rate equivalent to a bed-heat release rate of 670,000 $Btu/hr/ft^2$. (Commercial practice ranges from 500,000 to 750,000 $Btu/hr/ft^2$.)

Carbon. Figure 2A indicates that for the smallest particle size range, more than 50 percent of the inlet carbon was oxidized at all conditions. The data are reported in terms of mean free-stream oxygen, the average oxygen concentration in the furnace. (The range was approximately $\pm$ 1% O_2.) Increasing the mean free-stream oxygen from 2 to 10 percent increased the vertical velocity from 11 to 19 feet per second and decreased the material collected at the furnace bottom (the particles which would fall to the grate in a commercial system) because of increased entrainment. CO_2 formation increased with increasing oxygen due to both increasing entrainment and increasing oxygen partial pressure. Both effects must have been significant because the increase in CO_2 greatly exceeded the decrease in bottom carbon (Fig. 2A).

Hydrogen. Figure 2B shows similar data on the fate of hydrogen. The hydrogen content of the bottom solids decreased with increasing mean free-stream oxygen, paralleling the carbon behavior. The hydrogen content was slightly lower, indicating that some hydrogen is evolved from the particles which fall to the grate. The exhaust solids contained essentially no hydrogen, suggesting that the material which is carried over head in a commercial unit is primarily devolatilized char. It is, therefore, not surprising that this material often proves difficult to burn, even in a furnace equipped with a "fly-ash reinjection system."

Sulfur. The fate of the fuel sulfur is also shown in Fig. 2C. In general, the sulfur balance closure was excellent. The sulfur content of the bottom solids decreased with increasing mean free-stream oxygen, a direct result of increased entrainment due to the increased vertical velocity. The SO_2 formation remained surprisingly constant as the oxygen concentration was increased because the sulfur content of the exhaust solids increased.

Nitrogen. Figure 2D shows the fate of the Indiana coal nitrogen. Increasing the mean oxygen decreased the fraction of nitrogen reaching the bed and slightly increased that carried into the exhaust; both effects are primarily due to increased particle entrainment. NO formation decreased significantly at low mean-free-stream oxygen concentrations as expected from pulverized coal data. (10)

Influence of Process Variables

Experiments were conducted to establish the influence of mean free-stream oxygen concentration, particle size, and thermal environment on the fate of carbon, hydrogen, sulfur, and nitrogen in the suspension phase (Figs. 3-4). Reactor wall temperatures of 1900°F and 2100°F, and particle size ranges obtained by mechanically screening the raw coal were studied.

Carbon. Figure 3A summarizes the influence of the combustion parameters on the fraction of the feed carbon oxidized to CO_2 in the suspension phase. Increasing mean free-stream oxygen from 2 to 10 percent increased the carbon oxidized at all combustion conditions studied due to the five-fold increase in oxygen partial pressure and to the increased entrainment caused by the higher vertical velocity.

Particle size had a dramatic effect on carbon oxidation. At the nominal commercial operating conditions (6% O_2, 2100°F), approximately 80 percent of the coal particles less than .063 inches burned in the suspension phase, while less than 20 percent of the particles between .063 and .111 inches burned. Thus, the data shown in Figure 3A indicate that particles small enough to be entrained in the upward flow (less than .063 inches) oxidized almost completely; but large particles which fell directly to the grate ($d > .11$ inches) remained essentially unreacted.

Increasing the reactor temperature by approximately 200°F increased the combustion of the entrained particles due to both increased devolatilization rates and increased reaction rates. Little effect of bulk temperature was observed at low O_2 concentrations and large particle sizes because essentially no particles were entrained at this condition. Simple drag calculations, assuming spherical particles with constant density, indicated that at the 2 percent oxygen condition, particles greater than .025 inches would fall, while at the 10 percent oxygen condition, particles up to .035 inches would be entrained.

Hydrogen. Figure 3B shows that, in general, the influence of the combustion parameters on hydrogen oxidation is weaker than on carbon. Increasing the reactor temperature by 200°F slightly increased the hydrogen oxidation due to the increased volatile evolution rates. Increasing the mean particle size dramatically reduced the hydrogen oxidation because of reduced entrainment and changes in specific surface area; however, even with the large particles, hydrogen oxidation exceeded carbon oxidation at all conditions.

Sulfur. Figure 3C shows the influence of the combustion parameters on the oxidation of total sulfur. Again, there was a strong influence of particle size due to entrainment effects. With the smallest particles, increasing oxygen had little effect on sulfur oxidation; but with the large particles, increasing oxygen decreased sulfur oxidation, particularly at the high temperature, and this is believed to be related to the inhibition of sulfate decomposition. (11) Increasing temperature increased the sulfur evolution and oxidation even more than carbon oxidation (Fig. 3A).

Nitrogen. Figure 4A shows the fate of the nitrogen remaining in the solid phase relative to the solid phase carbon in the char (normalized with respect to the nitrogen-to-carbon ratio in the unburned coal). Particles which fell to the bottom had burned only slightly (the hydrogen content of the solid was still significant) and exhibited some nitrogen enrichment. Thus, the evolution of nitrogen slightly lagged the evolution and oxidation of the early hydrocarbon volatiles and this is in agreement with inert pyrolysis studies. (12, 13) However, the N/C ratio in the exhaust solids was less than that in the raw coal, demonstrating that the final nitrogen compounds reacted preferentially to the most refractory char species. Since the exhaust solids exhibited behavior opposite that of the bottom solids, and since their relative masses were approximately equal for the .063" particles, the data shown in Fig. 4A indicate that the overall nitrogen evolution rate was near that of carbon. The exhaust data also showed that decreasing particle size and increasing bulk gas temperature both increased fuel nitrogen evolution.

Figure 4B summarizes the effects of the combustion parameters on the percent of the evolved fuel nitrogen which was ultimately converted to NO. Conversions were relatively high (ca. 40%) and essentially independent of the mean-free-stream oxygen, except at very low O_2 levels. The smaller particles exhibited slightly higher fuel nitrogen conversions (Fig. 4B) and this agrees with pulverized coal results on much smaller particles. (14) Decreasing particle size is known to increase the volatile nitrogen evolution rate (Fig. 4) and believed to enhance the probability of O_2 availability for XN (e.g. NH_3, HCN, etc.) oxidation. (The importance of intraparticle XN reduction reactions is decreased as particle size decreases.) (15) Bulk gas temperature had relatively little effect on fuel nitrogen conversion (Fig. 4B).

The suspension phase results demonstrated that only particles less than 0.1 inches undergo significant reaction in the overthrow phase and that overall, fuel nitrogen is evolved at approximately the same rate as carbon is oxidized. The conversion of the evolved nitrogen is relatively high (ca. 40%) and depends primarily on local oxygen availability. Particle size and thermal environment effects are of second-order importance.

FIXED-BED COMBUSTION

The fixed-bed furnace was designed to provide a simulation of the fuel-bed burning regime in a coal-fired spreader stoker. In this system the coal fines were removed (by mechanical screening) to minimize suspension burning.

Figure 5 illustrates the overall influence of bed-region stoichiometry on exhaust emissions of sulfur oxides (SO_2) and nitrogen oxides (NO_x). The data represent emissions obtained for Utah coal (bituminous) firing at a nominal superficial burning rate of 322,000 Btu/hrft^2 and a constant overall stoichiometry of 1.39 ± 0.06. The overfire air was added at ambient temperature at 21-inches and 44-inches above the fuel-bed.

Figure 5A illustrates the effect of bed-region stoichiometry on exhaust SO_2 emissions. The dashed line refers to theoretical SO_2 emissions (.057 lbm $SO_2/10^6$ Btu) for the Utah coal based on complete conversion of the inherent fuel sulfur to SO_2. The data (solid circles) indicate that there was virtually no effect of bed-region stoichiometry on SO_2 emissions. As expected, high fuel sulfur conversion, averaging 89 percent, was obtained over the entire range of first-stage stoichiometries.

In Figure 5B, the effect of first-stage stoichiometry on exhaust NO_x emissions (in lbm $NO_2/10^6$ Btu) is illustrated. The data indicate that decreasing the bed-region stoichiometry, at a constant overall stoichiometry, resulted in decreased exhaust NO emissions. The highest NO emissions were measured under excess-air firing of the fuel-bed, in excess of 0.5 lbm $NO_2/10^6$ Btu (16.5 percent fuel nitrogen conversion to NO). Substantially lower exhaust emissions were produced under fuel-rich (staged) combustion conditions. The minimum NO emissions (0.2 lbm $NO_2/10^6$ Btu, 6.2 percent conversion) were achieved at a bed-region stoichiometry of 0.65. This stoichiometry appeared to be the optimum operating condition with respect to NO emissions for the Utah bituminous coal. Exhaust NO emissions increased appreciably as the furnace was further staged below the optimum stoichiometry. Chen et al. (16) noted a similar dependence of exhaust NO emissions on first-stage stoichiometry during pulverized coal firing.

Figure 6 illustrates the carbonaceous and nitrogenous species distributions entering the second-stage flame, as a function of first-stage stoichiometry. The measurements were made at 21-inches above the fuel-bed and the overfire-air was added at 35.5-inches and 44-inches. The overall stoichiometry was held constant at 1.38 ± 0.05.

Figure 6A illustrates the measured nitrogenous species distribution entering the second stage over a range of first-stage stoichiometries. The data have been reduced to unit stoichiometry for comparison on a normalized basis. The data indicate that under locally excess-air conditions, the total fixed nitrogen species, TFN (TFN = NO + NH_3 + HCN; hexagons) were predominantly composed of NO (circles) and very little NH_3 (triangles) and HCN (diamonds) was present. Detailed gas chromatographic analyses determined that HCN, NH_3, N_2 and NO were the only nitrogenous species present in the combustion gases in appreciable concentrations. As the bed-region stoichiometry was decreased, first-stage TFN concentrations decreased and reached a minimum of approximately 320 ppm at a stoichiometry of 0.90. At the TFN minimum, NH_3 and NO were both present in appreciable concentrations. Fenimore and Fraenkel (17) and Morley (18) demonstrated that in fuel-rich hydrocarbon flames, N_2 formation occurs most efficiently when both NH_3 and NO are present at appreciable levels.

Under fuel-rich conditions, TFN concentrations increased to levels in excess of 550 ppm, far above equilibrium predictions (approximately 10 ppm). The fixed nitrogen species were predominantly non-oxidized intermediates and HCN was the preferred species. The HCN increase, with decreasing bed-region stoichiometry, appeared to be directly related to the decay in NO. Haynes (19) demonstrated that HCN can be regenerated in fuel-rich hydrocarbon flames by the reaction of NO with hydrocarbon fragments. Below the optimum first-stage stoichiometry ($SR_B = 0.65$), the first-stage TFN concentrations increased steadily and exhaust NO emissions increased correspondingly. The increase in exhaust NO emissions under heavily staged conditions ($SR_B > 0.60$) can be attributed to higher concentrations of oxidizable nitrogenous intermediates entering the second-stage flame.

Figure 6B shows the carbonaceous species distribution entering the second stage, over a range of first-stage stoichiometries. Under excess-air burning conditions, oxygen was present in the combustion gases and CO_2 was the preferred carbonaceous species. Below stoichiometric burning, CO_2 concentrations decreased and CO concentrations increased with increasingly staged conditions. Material balance calculations written over the first stage indicated that the fuel carbon was not fully accounted for by the carbon oxides. Unaccounted carbon and hydrogen were attributed to hydrocarbons (CH_x) in the fuel-rich combustion gases. The hydrocarbon concentration increased steadily with decreasing first-stage stoichiometry. The rapid growth in HCN concentration entering the overfire-air region corresponded directly with the increase in hydrocarbon content of the first-stage gases.

For the Utah bituminous coal, second-stage burning occurred in an excess-air diffusion flame fueled by carbon monoxide and hydrocarbons. As first-stage stoichiometry decreased, and overall stoichiometry remained constant, the partial pressures of both oxidant (O_2) and oxidable species (CO, CH_x, NH_3 and HCN) increased. The fate of the nitrogenous intermediates in the second-stage flame is illustrated in Figure 7. The data are represented as the fraction of fixed nitrogen species converted to NO as a function of TFN concentration. The percent TFN conversion in the second stage was computed based on detailed species measurements at the exit of the first stage and at the furnace exhaust.

Overall, TFN conversion to NO appeared to be inversely proportional to concentration. As TFN concentration increased, under fuel-rich conditions, conversion decreased to a minimum of approximately 40 percent. Under excess-air conditions (open symbols) NO was the dominate species ($NO >> NH_3 + HCN$) and conversion (or NO retention) was high, in excess of 90 percent. Under fuel-rich conditions NH_3 and HCN were preferred ($NH_3 + HCN >> NO$) and oxidation of these species was inherently low.

Fenimore (20) and DeSoete (21) showed that HCN does not form or destroy NO directly, but reacts to form NH_3. Morley (18) demonstrated that the amine (NH_i) oxidation reaction to form NO occurs at approximately the same rate as the amine reduction reaction with NO to form N_2, at flame conditions. The only apparent route for nitrogenous species reactions is through HCN and NH_3 to form NO or N_2. Further, the NO recycle mechanism by reaction with hydrocarbon fragments to form HCN, effectively enhances the rate of NO reduction to N_2. In fact, the ultimate NO concentration is apparently a function of the rate of hydrocarbon burnout (19). The overall mechanism increases the rate of N_2 formation in the second-stage flame and ultimately results in a low fractional conversion of nitrogenous intermediates to NO.

A multi-variable linear regression was used to calculate exhaust NO emissions from concentrations of the intermediate nitrogenous species entering the second stage. The resulting correlation was:

$$NO_{EX} = 74 + 0.79\cdot SR_1\cdot(NO_1) + 0.10\cdot(NH_3) + 0.32\cdot(HCN)$$

and the overall correlation coefficient (r^2) was 0.9 based on 17 data sets. The intercept (A_0 = 74 ppm) in the regression equation is an estimate of the thermal NO formation in the second stage and is a reasonable approximation of thermal NO_x in hydrocarbon flames (50 ppm to 90 ppm). The second term shows the dependence of first-stage NO formation on local stoichiometry and is coupled to the hydrocarbon recycle mechanism. The final two terms predict the relative contribution of NH_3 and HCN to NO formation.

Figure 8 illustrates the NO exhaust emissions as a function of bed-region stoichiometry. The solid diamonds represent experimentally measured emissions and the open circles correspond to exhaust emissions predicted by the correlation. The correlation showed good agreement with the measured NO emissions over the entire range of the data.

MODEL SPREADER-STOKER STUDIES

System Validation

Experiments were conducted in the model spreader-stoker furnace to investigate the coupling between the bed and suspension zone combustion and to assess the overall influence of the stoichiometry distribution and overfire-air height on NO formation and control. Initial validation tests were conducted to compare the pilot scale furnace with emissions data from full scale units. In full scale spreader-stoker systems, typical air distribution profiles employ 80 to 85 percent of the air as underfire air. The remaining air, overfire air, is split between two levels of jets, typically at approximate heights of 1.5 feet and 6 feet above the grate. The effect of a change in the total air flow on a full scale furnace is illustrated in Fig. 9 (solid lines) from the work of Langsjoen et al. (22)

NO emissions data from the model spreader-stoker unit, operated at typical field conditions, are also shown in Fig. 9 (solid points). These tests were conducted with Utah coal at a firing rate of 470,000 Btu/hr. Overfire air represented 18 percent of the total air supplied to the furnace. The overfire air was introduced at 20 and 48 inches above the grate; the ratio of the air introduced at 48 inches to that at 20 inches was maintained constant at 1.15. The quantitative agreement between the pilot scale model spreader stoker emissions and the field testing data suggest that the pilot furnace appropriately simulates the combustion conditions which are of primary importance to NO formation.

Influence of Combustion Parameters

In more extensive tests, the furnace air distribution (stoichiometry and overfire-air height) was varied. Total furnace stoichiometry was held constant at 1.45; the coal feed rate was 40 lb/hr. (470,000 Btu/hr/ft^2). As in the fixed-bed studies, bed-region stoichiometry was found to be the principal parameter influencing NO emissions (Fig. 10).

As the bed-region air/fuel ratio was reduced the NO emissions decreased significantly. As the bed-zone stoichiometry was further reduced with the overfire air at 20" (below the spreader at 32"), the emissions ultimately began to increase again just as in the fixed-bed experiments (Fig. 5B) However, the optimum stoichiometry for the model spreader-stoker furnace (SR_{bed} = 0.8) was much leaner than for the fixed-bed furnace. This suggests that the presence of the overthrow phase shifted the TFN distribution, probably by enhancing the homogeneous and heterogeneous destruction of NO in the first, fuel-rich stage.

Figure 10 indicates the strong influence of overfire-air height on NO emissions during staged combustion. The height of overfire-air injection was varied from 7 to 72 inches above the grate; the level of coal injection (spreader) was at 32 inches. Injecting the overfire-air above the spreader enhances the probability that fuel N evolved from the small particles burning in the suspension phase will react to form N_2. In addition, increasing the overfire-air height increases the rich-zone residence time and allows TFN species leaving the fuel-bed to decay further toward their low equilibrium levels.

Importance of Coal Fines

As noted in the previous sections, the conversion of fuel nitrogen to NO in the suspension zone (ca. 40%) greatly exceeds the conversion in the bed region (ca. 10%). To evaluate the impact of suspension burning on NO formation in a system where the overthrow and bed phases are coupled, several series of experiments were conducted with fuel particle size distributions PSD-2 and PSD-3, which had been passed over 8 and 4 mesh screens, respectively, to reduce the fines content of the coal feed. These two feed size distributions, PSD-2 and PSD-3, represented 85 and 80 percent, respectively, of the normal feed distribution.

In the first series of experiments, the furnace was operated under conditions typical of full-scale units. Figure 11A shows the NO_x emissions from the MSF under field-operating conditions for the three different feed particle size distributions. The uppermost set of points represents a duplication of the data presented in Figure 9. By reducing the mass of coal which burns in the suspension phase, the NO emissions were reduced as much as 20%. In all cases the total burning rates were 470,000 Btu/hr.

In typical field-operating conditions, both the fuel bed and the suspension zone are under excess-air conditions (Figure 11A; hence, a separate series of experiments was conducted to show the effect of suspension-zone stoichiometry on NO formation with the coal feed most deficient in fines (PSD-3). Figure 11B shows the effect of bed-zone stoichiometry on NO emissions with overfire air height as a parameter. The dotted line indicates results obtained with the normal coal feed. In the fines removal mode, the NO emissions were reduced over those obtained with the typical coal size distribution except under cases where the bed zone was highly staged and the height of overfire air injection was above the spreader (> 32 inches). The effect of overfire air height is minimal when the fines are absent from the feed because suspension zone burning has been essentially eliminated. Further, in practical terms these data suggest that if a stoker operator is willing to operate with a fuel-rich bed and suspension zone, fines removal is not needed; however, under normal, excess-air operating conditions fines removal can produce approximately a 20% NO reduction.

CONCLUSIONS

This study indicates that NO emissions from spreader stoker fired coal furnaces are the result of relatively high conversions (25-45%) of the fuel nitrogen evolved from particles less than 0.1 inches in the suspension phase and low conversions (5 to 15%) of fuel nitrogen from the bed combustion. In the suspension phase, nitrogen is evolved at approximately the same rate as carbon is oxidized and the percentage conversion is relatively insensitive to reaction zone temperature and particle size. However, particle size dramatically influences the amount of fuel nitrogen evolved.

The initial sulfur distribution in the raw coal varies with particle size; naturally occurring fines are unusually high in sulfate sulfur. The evolution and oxidation of organic sulfur depends primarily on the rate of carbon evolution; however, the rate of sulfate sulfur decompostion is most strongly influenced by local oxygen concentration and temperature.

Local oxygen availability is the primary control parameter for both phases of the combustion. Substantial NO emission reductions were achieved when the fuel-bed was operated under sub-stoichiometric conditions (fuel-rich). NO emissions decreased further when the suspension zone stoichiometry was reduced below 1.0 by moving the overfire-air injection location above the spreader. Minimum fuel nitrogen conversions of 6 percent were achieved suggesting that staged combustion produces a positive synergism between the suspension phase and the bed combustion. The suspension zone provides sites for heterogeneous reduction of NO formed in the bed and radical concentrations necessary to accelerate the decay of TFN formed in the bed. In addition, the low oxygen partial pressure decreases the conversion of nitrogen evolved in the suspension zone.

Thus, two types of control technology appear to be viable. First, the coal feed could be screened to remove the fines (particles less than 0.1 inches). This would essentially eliminate the high conversion of nitrogen evolved in the suspension zone and would result in an overall emissions reduction of approximately 5 to 25 percent depending on the amount of fines normally present in the raw coal. In addition, it might result in a more permeable coal layer on the grate which would improve underbed air distribution. Alternatively, the primary overfire air injection port could be moved above the spreader and the suspension zone and bed-region could both be operated sub-stoichiometric. This could result in an emission reduction as large as 50 percent; however, before this concept can be applied commercially, the influence on other important combustion parameters (e.g. bed thickness, grate temperature, and ash characteristics) must be evaluated.

ACKNOWLEDGMENT

The authors gratefully acknowledge EPA support under Grants R-805899 and R-809267 and the assistance of G. B. Martin, D. C. Drehmel, C. Carrell, S. Manis, S. Greene, C. Pettersson, and D. Hendricks.

REFERENCES

1. Mason, H. B., and L. R. Waterland. Environmental Assessment of Stationary Source NO_x Combustion Modification Technologies. Proceedings of the Secondary Stationary Source Combustion Symposium. EPA-600/7-77-73a, NTIS, Springfield, Virginia, 1977.

2. Giammar, R. D., D. R. Hopper, P. R. Webb, and E. Radhakrishnan. Evaluation of Emissions and Control Technology for Industrial Stoker Boilers. Proceedings of the Third Stationary Source Combustion Symposium. EPA-600/7-79-050a, NTIS, Springfield, Virginia, 1979.

3. Galbrielson, J. E., and P. L. Langsjoen. Field Tests of Industrial Stoker-Fired Boilers for Emission Control. Proceedings of the Third Stationary Source Combustion Symposium. EPA-600/7-79-050a, NTIS, Springfield, Virginia, 1979.

4. Maloney, K. L. et al. Combustion Modifications for Coal-Fired Stoker Boilers. EPA/EPRI 1982 Joint Symposium on Stationary Combustion NO_x control, Dallas, Texas, November, 1982.

5. Haynes. B. S. and N. Y. Kirov. Comb. Flame, 23: 277, 1974.

6. Munro, J. M. Formation and Control of Pollutant Emissions in Spreader-Stoker Fired Furnaces. Ph.D. Dissertation, Department of Chemical Engineering, University of Utah, 1982.

7. Slaughter, D. M. Formation of Sulfur Oxides in Suspension Coal Combustion. M.S. Thesis, University of Utah, 1982.

8. Starley, G. P. Influence of Combustion Parameters in Nitrogen Oxide Formation in Fixed-Bed Combustion. M.S. Thesis, University of Utah, 1980.

9. Winter, R. M. Measurement of Nitrogenous Intermediates to Optimize a Staged-Combustion System. M.S. Thesis, University of Utah, 1981.

10. Pershing, D. W., and J. O. L. Wendt. Sixteenth Symposium (International) on Combustion. The Combustion Institute, 1977.

11. Slaughter, D. M., D. W. Pershing, D. C. Drehmel, and G. B. Martin. Parameters Influencing the Evolution and Oxidation of Sulfur in Suspension Phase Combustion. Nineteenth Symposium (International) on Combustion. The Combustion Institute, Pittsburgh, Pennsylvania, 1983.

12. Soloman, P. R. The Evolution of Pollutants during the Rapid Devolatilization of Coal. Report R76-952588-2, United Technologies Research Center, East Hartford, Connecticut, 1977.

13. Pohl, J. H., and A. F. Sarofim. Sixteenth Symposium (International) on Combustion. The Combustion Institute, 1977.

14. Pershing, D. W., M. P. Heap, and S. L. Chen. Pulverized Coal Combustion: Pollutant Formation and Control. A. F. Sarofim, editor. In press (1982).

15. Wendt, J. O. L., and O. E. Schulze. On the Fate of Fuel Nitrogen During Coal Char Combustion. AIChE J., 22: 102, 1976.

16. Chen, S. L., M. P. Heap, D. W. Pershing, and G. B. Martin. Influence of Coal Composition on the Fate of Volatile and Char Nitrogen During Combustion. Nineteenth Symposium (International) on Combustion. The Combustion Institute, Pittsburgh, Pennsylvania, 1983.

17. Fenimore, C. P., and H. A. Fraenkel. Formation and Interconversion of Fixed-Nitrogen Species in Laminar Diffusion Flames. Eighteenth Symposium (International) on Combustion. The Combustion Institute, Pittsburgh, Pennsylvania, 1981.

18. Morley, C. The Mechanism of NO Formation from Nitrogen Compounds in Hydrogen Flames Studied by Laser Fluorescence. Eighteenth Symposium (International) on Combustion. The Combustion Institute, Pittsburgh, Pennsylvania, 1981.

19. Haynes, B. S. Reactions of Ammonia and Nitric Oxide in the Burnt Gases of Fuel-Rich Hydrocarbon-Air Flames. Combust. and Flame. 28: 81, 1976.

20. Fenimore, C. P. Reactions of Fuel-Nitrogen in Rich Flame Gases. Combust. and Flame. 26: 249, 1976.

21. DeSoete, G. G. Overall Reaction Rates of NO and N_2 Formation from Fuel Nitrogen. Fifteenth Symposium (International) on Combustion, The Combustion Institute, Pittsburgh, Pennsylvania, 1975.

22. Langsjoen, P. L., J. O. Burlingame, and J. E. Gabrielson. Emissions and Efficiency Performance of Industrial Coal Stoker Fired Boilers. EPA -600/7-81-111a. NTIS, Springfield, Virginia, 1981.

Table 1.

Fuel Analysis

PROXIMATE ANALYSIS	UTAH	INDIANA	VIRGINIA
Moisture	6.20	2.96	4.86
Ash	9.20	14.15	13.48
Volatile Matter	37.62	33.45	27.28
Fixed Carbon	46.98	49.44	54.38
ULTIMATE ANALYSIS			
Moisture	6.20	2.96	4.86
Carbon	66.93	61.79	68.16
Hydrogen	4.65	4.16	4.26
Nitrogen	1.11	1.24	1.76
Sulfur	0.33	2.17	1.73
Osygen	11.58	13.53	5.75
Ash	9.20	14.15	13.48
ASTM Rank[1]	HVC Bituminous	HVC Bituminous	HVA Bituminous

[1] HV: high volatile

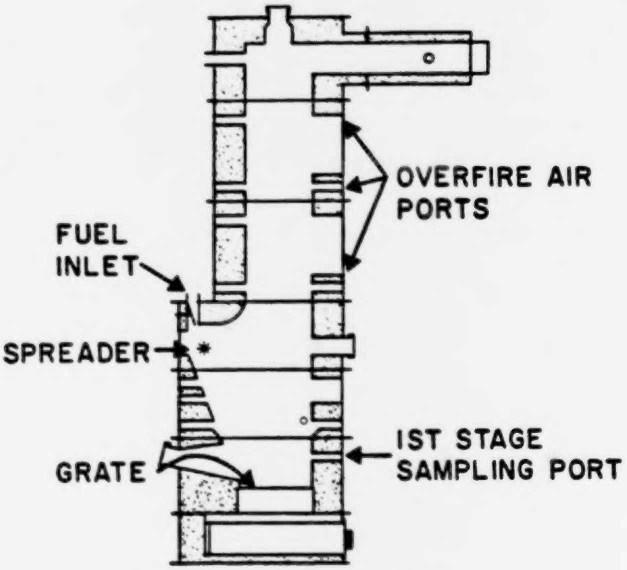
OVERFIRE AIR PORTS
FUEL INLET
SPREADER
GRATE
1ST STAGE SAMPLING PORT

A. MODEL STOKER FURNACE

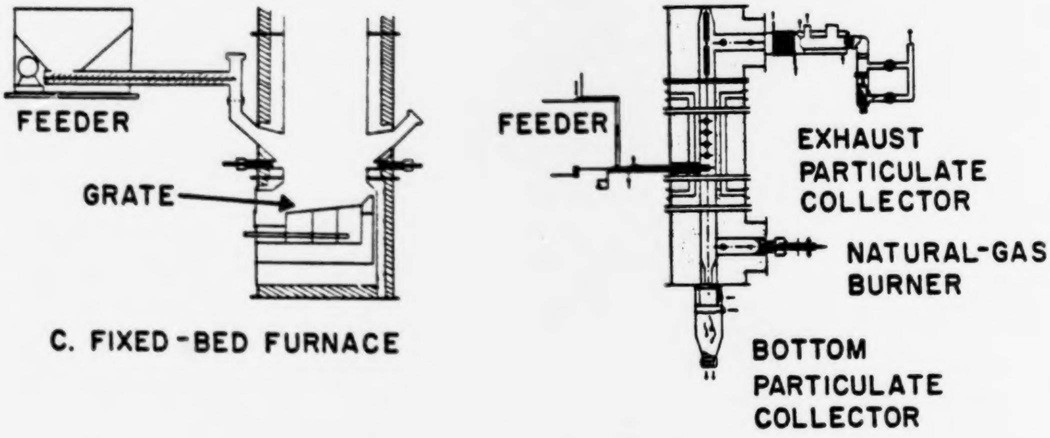
FEEDER
GRATE
FEEDER
EXHAUST PARTICULATE COLLECTOR
NATURAL-GAS BURNER
BOTTOM PARTICULATE COLLECTOR

C. FIXED-BED FURNACE

B. TOWER FURNACE

Figure 1. Experimental furnace facilities.

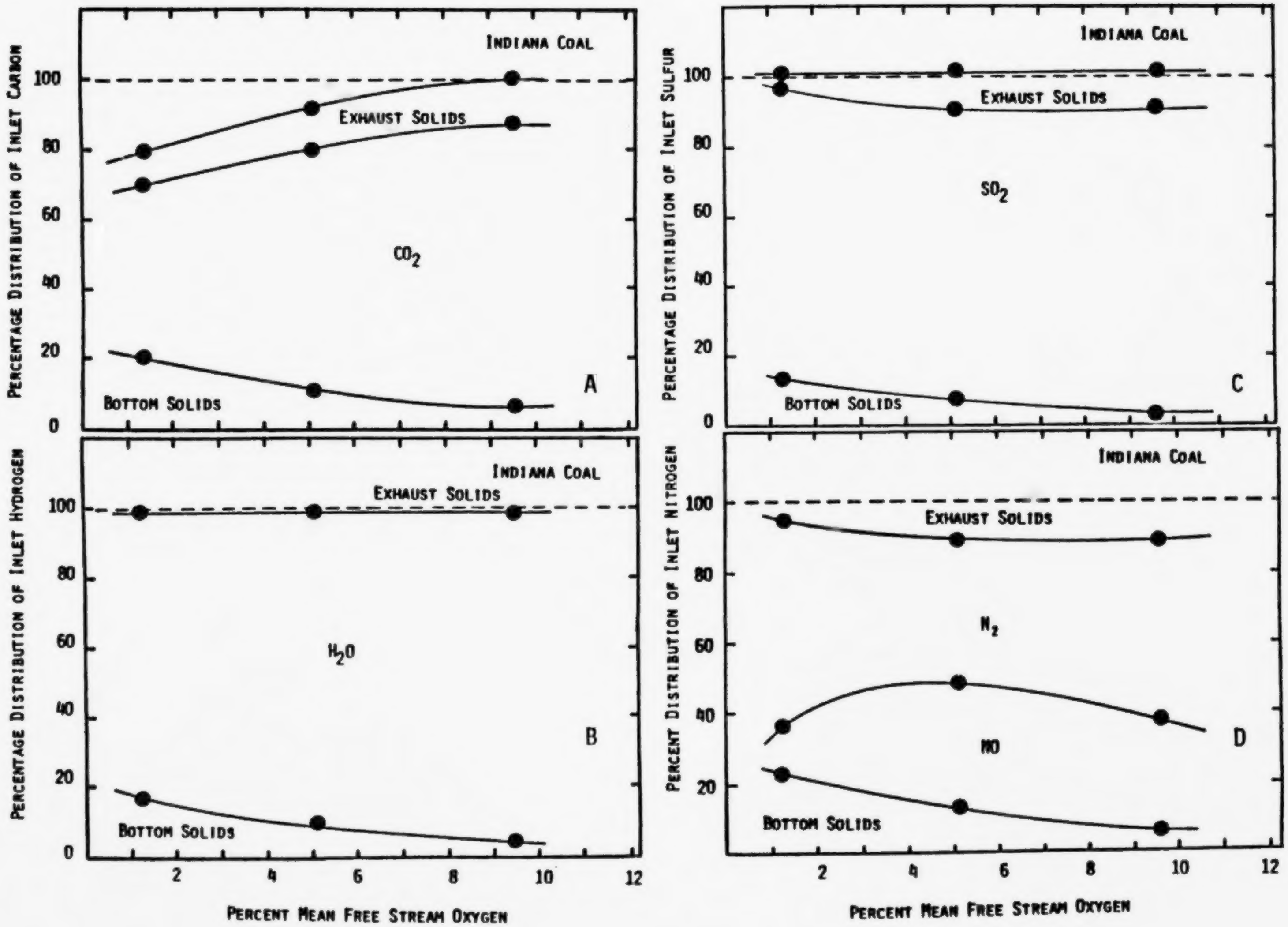

Figure 2. Fate of carbon, hydrogen, sulfur and nitrogen in the tower furnace for particles < .063 in. with 1900^{o}F thermal environment and 670,000 Btu/hr/ft^2.

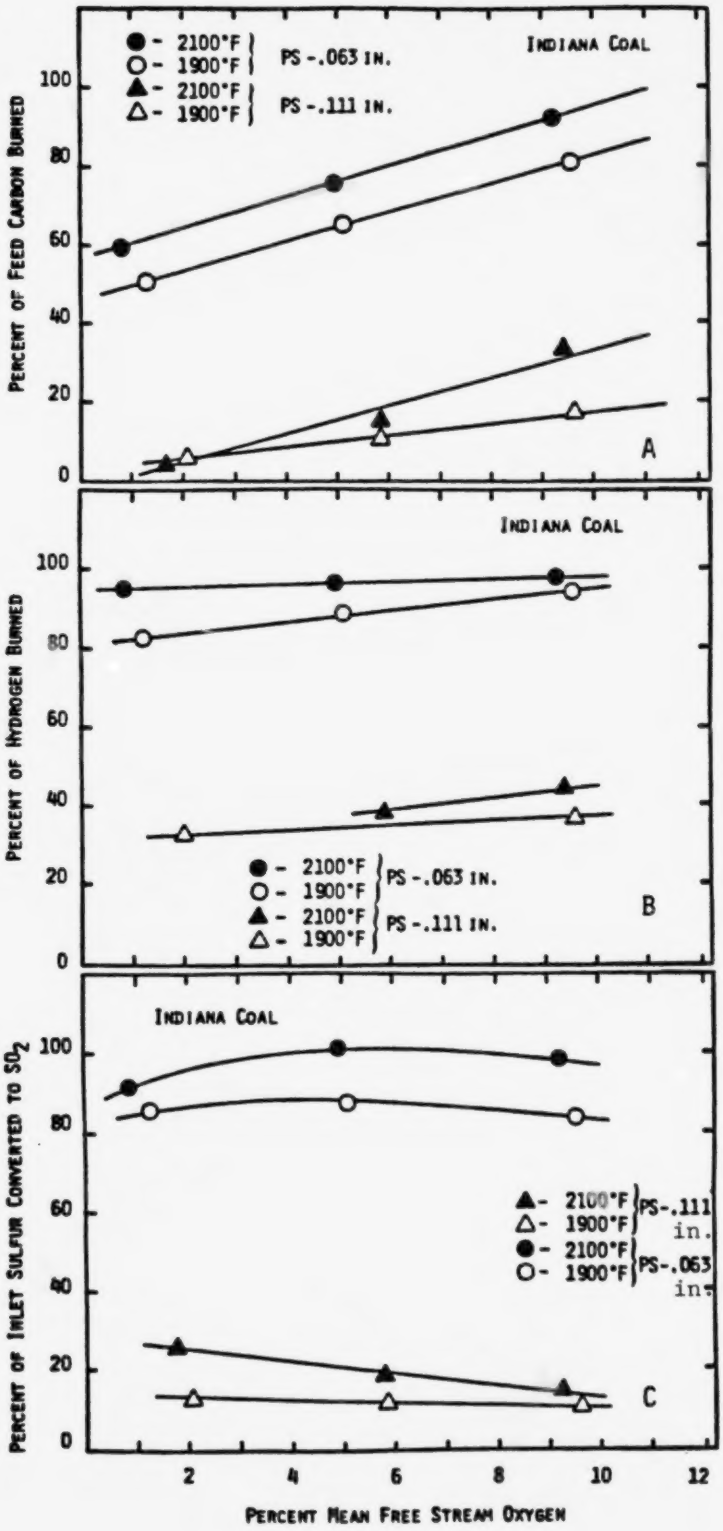

Figure 3. Influence of combustion parameters, thermal environment, oxygen partial pressure and coal particle size on carbon, hydrogen and sulfur oxidation.

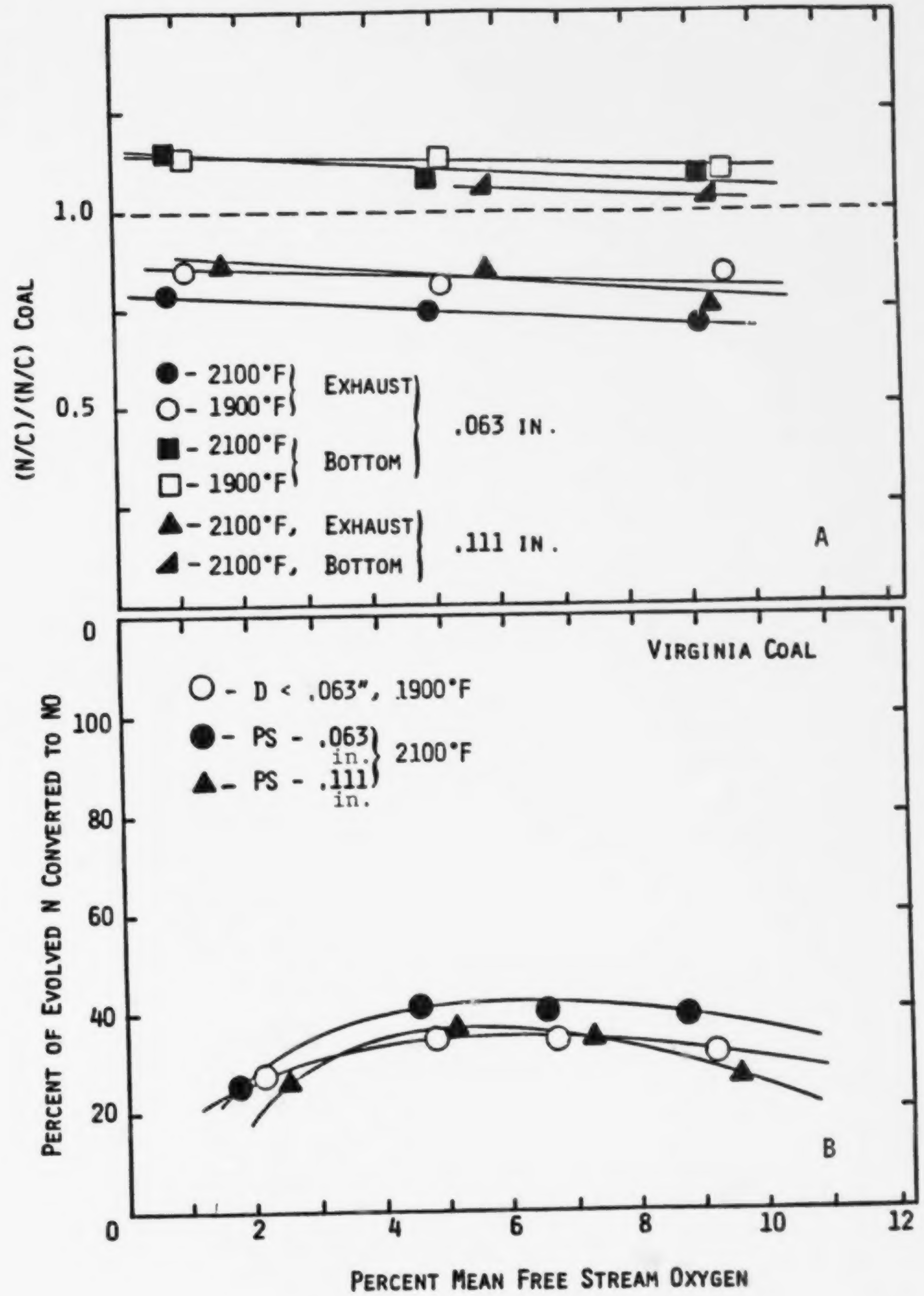

Figure 4. Influence of combustion parameters on fate of coal nitrogen.

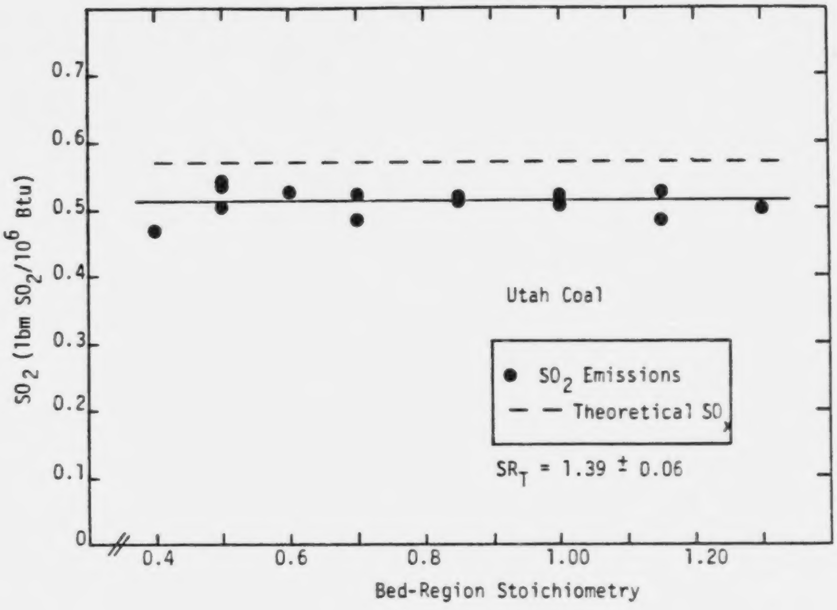

Figure 5a. Effect of bed stoichiometry on SO_2 emissions.

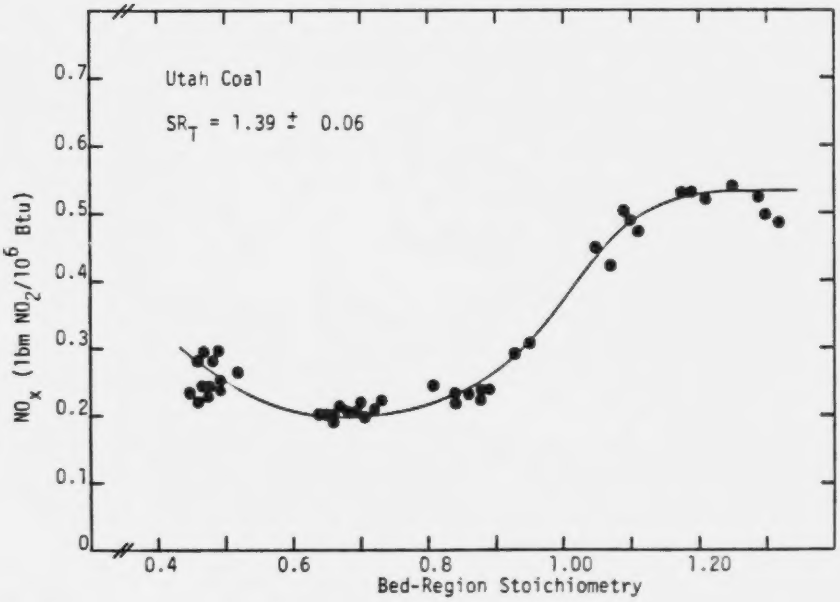

Figure 5b. Effect of bed stoichiometry on NO_x emissions.

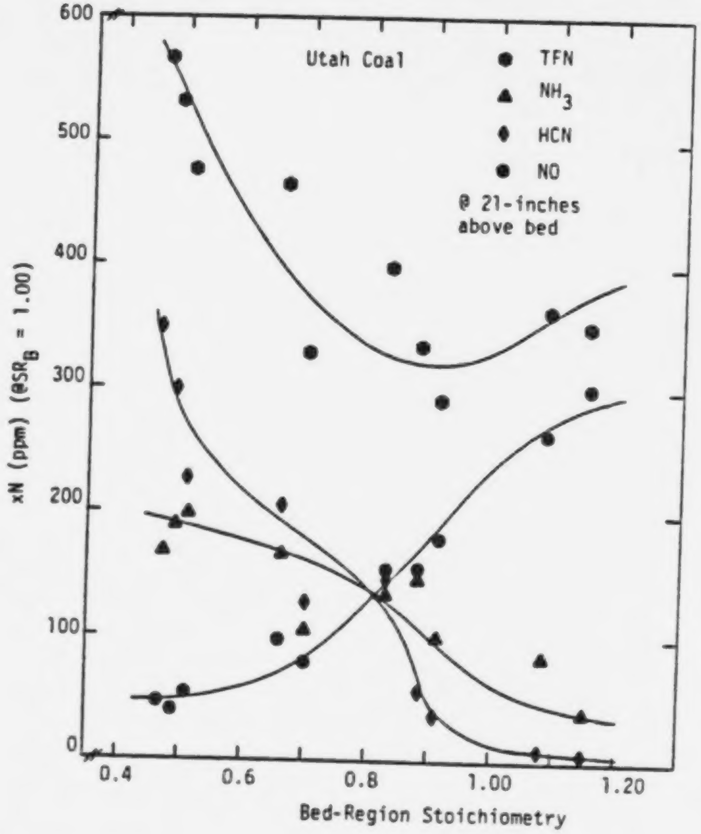

Figure 6a. Nitrogenous species at second stage.

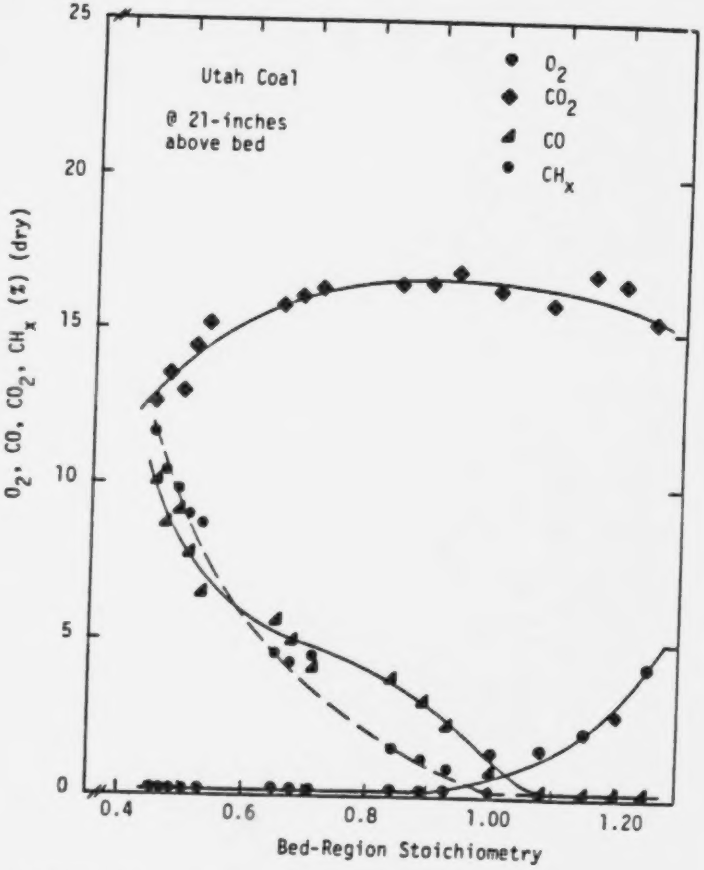

Figure 6b. Carbonaceous species at second stage.

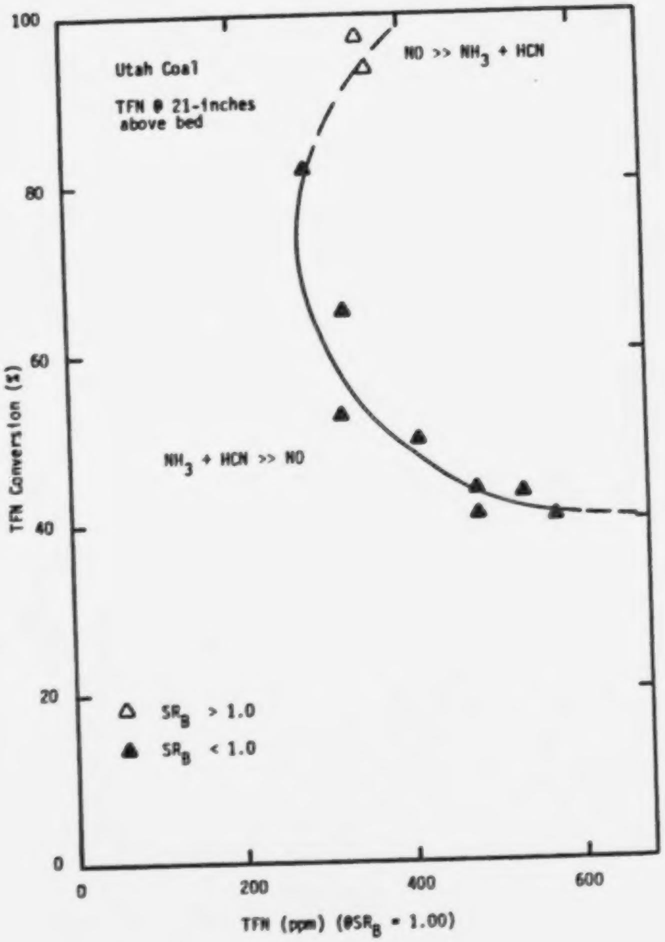

Figure 7. Conversion of fixed-nitrogenous species to exhaust NO.

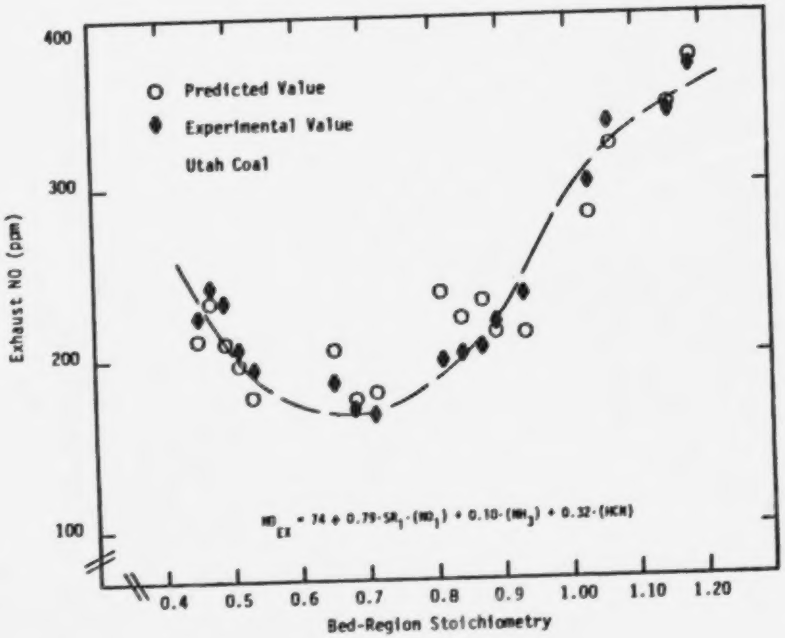

Figure 8. Comparison of measured and predicted exhaust NO emissions for Utah coal.

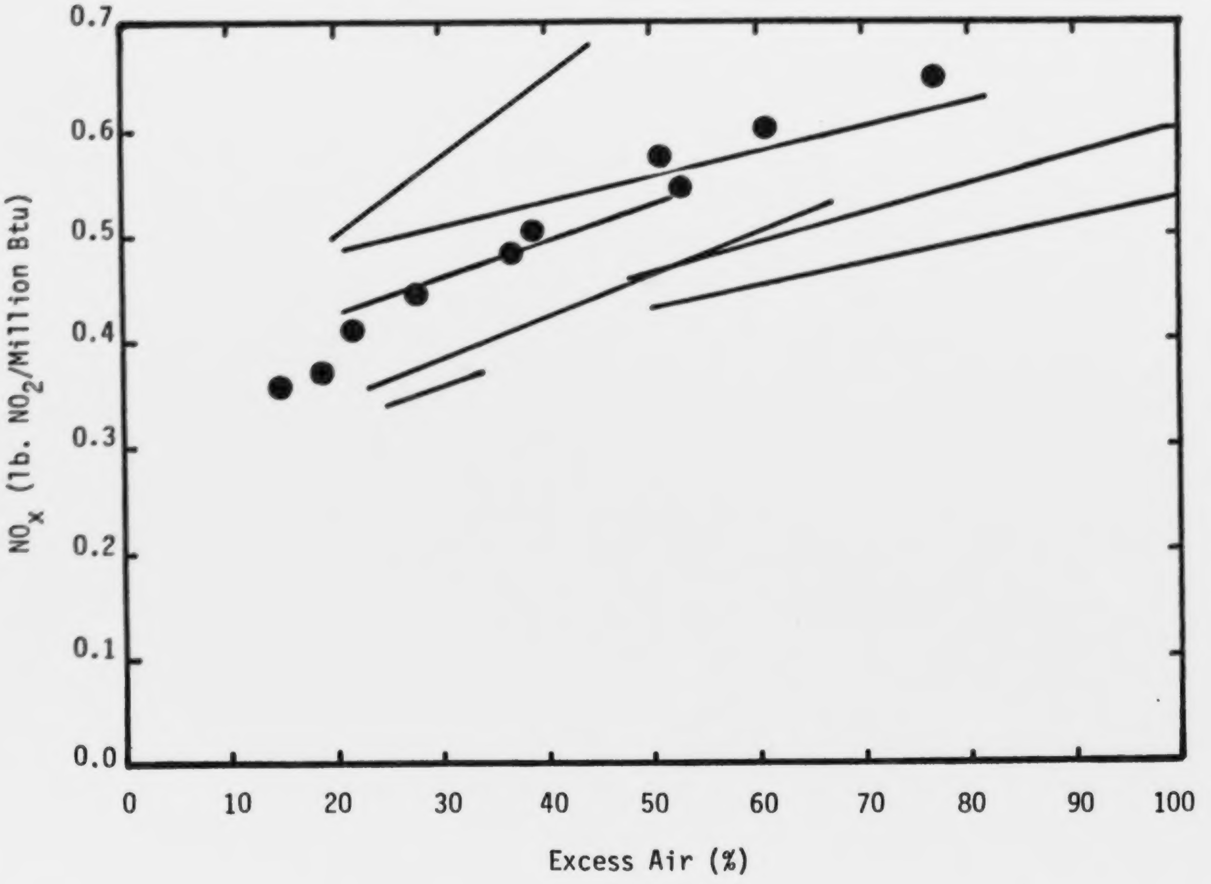

Figure 9. Comparison with field data (solid symbols MSF data, lines ref. 22).

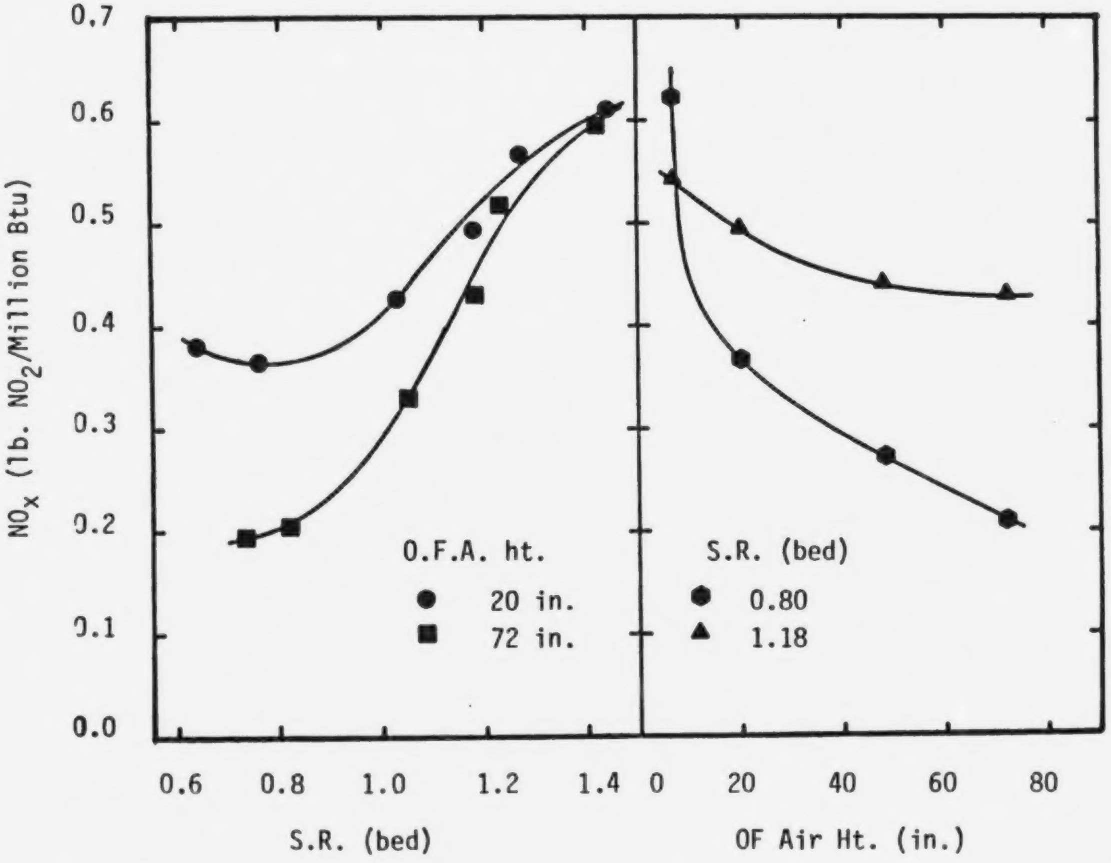

Figure 10. Influence of air distribution.

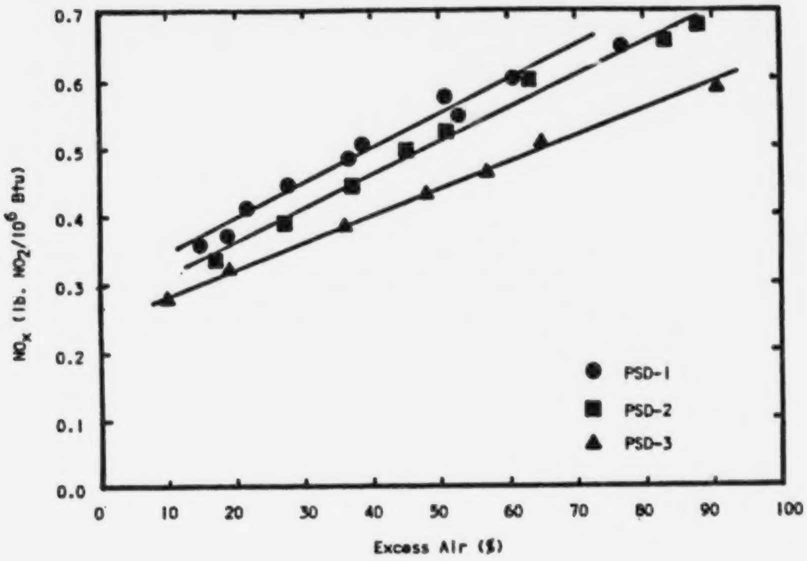

Figure 11a. Effect of particle size distribution on field comparison results.

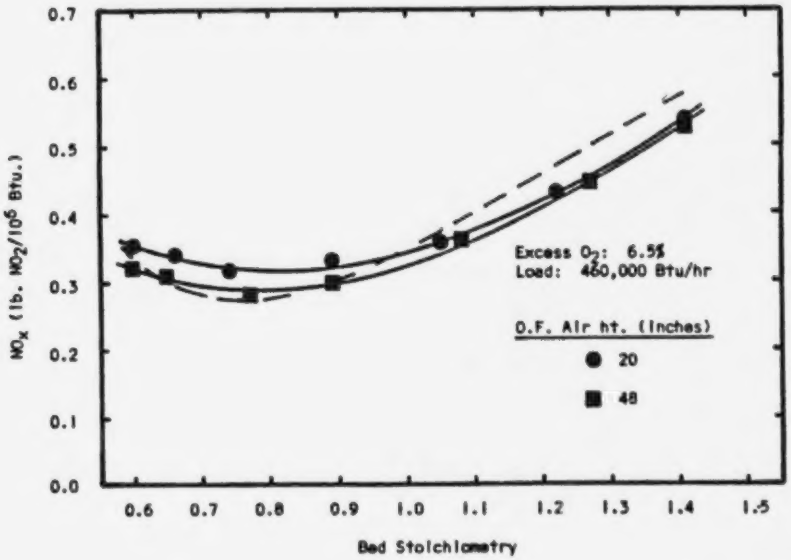

Figure 11b. Effect of bed stoichiometry with PSD-3.

(Dotted line indicates PSD-1 results)

SESSION IX

STATIONARY ENGINES AND INDUSTRIAL PROCESS SYSTEMS

Chairman, Robert E. Hall
EPA, IERL/RTP

EMULSION FUEL AND OXIDATION CATALYST TECHNOLOGY FOR STATIONARY DIESEL ENGINES

By:

J. H. Wasser
U.S. Environmental Protection Agency
Industrial Environmental Research Laboratory
Research Triangle Park, North Carolina 27711

ABSTRACT

This paper presents recent results from comprehensive emissions measurements made on the EPA, Industrial Environmental Research Laboratory-RTP diesel-engine/generator set. The diesel set was equipped with two emission control systems: an oxidation catalyst in the exhaust and a fuel-oil/water emulsification unit in the fuel supply line. NO_x reductions resulting from emulsion fuel use are quantified along with resultant increases in organic emissions. The effects of the exhaust oxidation catalyst on the organic emissions are documented, including results of mutagenesis and cytotoxicity assays. Catalyst and emulsion effects on SO_2/SO_3 emissions are also quantified. Basic conclusions based on these reported results are that emulsion fuel provides control of diesel NO_x emissions, but at the expense of increased organic emissions. The oxidation catalyst will control CO and light gaseous hydrocarbons, but does not adequately control complex organics emitted by the diesel.

INTRODUCTION

The Combustion Research Branch (CRB) of EPA's Industrial Environmental Research Laboratory, Research Triangle Park (IERL-RTP), North Carolina, sponsors an on-going contract and in-house program to investigate emissions from stationary reciprocating internal combustion engines. This paper will describe the results obtained during in-house tests in applying fuel-oil/water emulsion and oxidation catalyst technology to a stationary diesel engine. The purpose of this work was to obtain comprehensive emission measurements of the diesel exhaust. These emissions measurements included criteria pollutants and particulates/organics.

EXPERIMENTAL APPROACH

A series of experiments were designed to evaluate the emissions from the CRB diesel-generator set and the effect of oil/water emulsion fuel combined with an oxidation catalyst on the levels of these emissions. Table 1 outlines the experiments conducted. All experiments were scheduled by assignment of their order with random numbers. A practical water/fuel ratio was selected for each load level based on prior experiments which determined water/fuel versus NO_x levels.

EXPERIMENTAL SYSTEM COMPONENTS

The diesel engine used for this study is part of an electrical generator package. The engine is a Caterpillar Model D334, prechamber ignition, turbocharged and after-cooled, four stroke cycle, six cylinder diesel with 638 in.^{3} ($1.045 \times 10^{-2} m^3$) displacement rated at 165 kW electrical output for continuous service. Other pertinent data include:

Bore: 4.75 in. (120.65 mm)
Stroke: 6.00 in. (152.4 mm)
Compression Ratio: 17 to 1
Dry Weight: 2390 lb (1084.09 kg)
Standard Timing: 8° BTDC
Engine Speed: 1800 rpm (constant)

The catalytic reactor used in this study is an Engelhard Industries PTX-643D. This unit is a platinum metal catalyst on a monolith porous ceramic support with a honeycomb structure. The catalyst is enclosed in an Inconel band and a stainless steel outer housing.

Engine load is provided by an AVTRON Model K463 load bank connected to the diesel-generator set. This load bank provides load demands up to 225 kW in 5 kW increments.

The fuel used in the engine is a No. 2 diesel oil with an API gravity of 33.9°. The bound-nitrogen content of this fuel is 54 ppm, thus fuel nitrogen conversion to NO_x is not a major factor in the emission levels measured in this study. The sulfur content [0.24% (wt)] is sufficient to produce significant sulfate (SO_3, SO_4) emissions if SO_2 is oxidized in the engine or exhaust system. Other fuel properties were:

Carbon: 86.62% (wt)
Hydrogen: 13.15% (wt)
Ash: Trace (<0.01%)
HHV: 19,396 Btu/lb (45.07 MJ/kg)
Density: 0.8397 g/cm^3 @ 100°F (38°C)
Viscosity: 2.52 centipoise (2.52 mPa·s) @ 100°F (38°C)
Cetane Index: 43.5

The water for emulsion formation is deionized city water. Deionization is provided by a Continental Water Service anion and cation exchange resin system. Emulsion formation takes place in a mixer and gear pump unit located 2 m (6.5 ft) from the diesel engine fuel injection system.

SAMPLING AND ANALYTICAL SYSTEM

Instruments for determining the gaseous and particulate emissions from the diesel engine are listed in Table 2. In addition to these EPA-operated instruments, extensive analytical work was performed by contractors. Battelle Columbus Laboratories performed comprehensive analysis on selected diesel emission samples using liquid chromatography, infrared spectroscopy, and low resolution mass spectrometry (on the organic extract), and spark source mass spectrometry and atomic absorption (for inorganic analyses). Litton Bionetics performed bioassays on selected diesel emission samples including Ames Salmonella Assay for mutagenicity and CHO Clonal Assay for cytotoxicity.

EMISSION CHARACTERISTICS

Nitrogen Oxides

The experiments on this diesel engine indicate a baseline NO_x emission pattern with a 22.2 g/kg (450 ppm @ 15 percent O_2) peak at 40 kW load, and lower emissions (between 11.5 and 15 g/kg) at the other load levels studied. NO_x emissions for each of three control conditions (emulsion, catalyst, and emulsion + catalyst combined) are compared in Figure 1. The ratio of NO_x emissions for the catalyst runs indicates little effect on these emissions by the catalyst. A regression line through the data is close to the baseline. A water/fuel (W/F) ratio near the maximum that could be comfortably tolerated by the engine was selected for each load level studied. This W/F ratio varied:

Load, kW	W/F
0	0.39
40	0.31
80	0.49
120	0.60
160	0.27

Even with the variability in the W/F ratio, the NO_x reduction obtained at each load level was approximately 60 percent. The regression line through the data gave virtually no difference between the emulsion and the combined conditions: many of the data points were coincident. Evidently, the catalyst has no effect on NO_x emissions when emulsion fuel is used in the engine. A slight upward trend in the regression line with load is caused by the data at 160 kW where the W/F ratio was lower. This pattern of NO_x emission was expected based on prior tests. The NO_x emission levels are typical of what might be expected if a precombustion chamber diesel utilized water/fuel emulsion as a NO_x control method. The remainder of this paper will report the effects on other pollutant emissions that would result if this 60 percent NO_x control level were applied to this engine.

Carbon Monoxide

Experimental results indicated a CO baseline emission pattern with a 33.8 g/kg (735 ppm @ 15 percent O_2) peak at zero kW load, and rapidly decreasing emissions as load is added to the engine. This condition represents the lowest temperature regime in the engine, thus the CO oxidation is reduced at zero load. At half load (80 kW) and above, the baseline CO emission is nearly constant around 3 g/kg (70 ppm @ 15 percent O_2). The effect of the three control conditions on CO emissions is illustrated in Figure 2. Emulsion fuel at 80 kW and below increases CO emissions to greater than 45 g/kg (>1000 ppm @ 15 percent O_2), the limit of detectability. This condition is shown off-scale in the figure. At 120 and 160 kW, the increases in CO are still substantial but now measurable. Higher combustion temperatures at the higher load conditions provide for the better burnout of the CO. The effect of the oxidation catalyst is to reduce CO emissions nearly 90 percent at all loads above zero kW (where the exhaust temperature is too low for the catalyst to operate). When the catalyst is used with the emulsion fuel to combine NO_x and CO control, an average CO reduction of 55 percent is obtained. This "average," however, is the regression line through widely scattered data points, indicating that the control capability is highly variable. It is not clear from this limited data why this scatter occurs. Evidently the oxidation catalyst will counteract the adverse effect of emulsion fuel on CO emissions.

Total Gaseous Hydrocarbons

Experimental results indicate a total gaseous hydrocarbons (THC) baseline emission pattern similar to the CO pattern. There is a peak of 2.69 g/kg (37 ppm @ 15 percent O_2) at zero kW load, with emissions dropping rapidly with load to 0.21 g/kg (3 ppm @ 15 percent O_2) at full load. Again, this is caused by the low temperature engine regime at zero load as was the case with CO emission. The effect of the three control conditions on THC emissions is illustrated in Figure 3. Use of emulsion fuel, as for CO emissions, drastically increased the THC emissions at most load levels. The peak increases to 37.6 g/kg (520 ppm @ 15 percent O_2) at zero kW load, and the emissions remain above the baseline except at 160 kW. Data with the catalyst in operation indicate a reduction of 60 to 80 percent in THC emissions. Referring to Table 3, when the catalyst and emulsion fuel are both used, THC emissions are substantially reduced from the emulsion-only condition, but remain above baseline at half load (80 kW) and below. Thus, it appears that the catalyst does provide some countereffect to the emulsion on the hydrocarbon compounds that are detectable in a heated flame ionization analyzer. The heavier hydrocarbons emitted by the engine must also be considered.

Emission levels of hydrocarbons, as determined by the modified EPA Method 5, are listed in Table 4. The modified Method 5 train has an organic absorber (XAD-2) module added downstream of the filter. Inspection of this data essentially confirms the pattern of hydrocarbon emissions evident from the THC analyzer. The emulsion can produce large increases in both lighter (TCO) and heavier (GRAV) hydrocarbons, especially at less than full load operation of the diesel engine. The catalyst, in general, reduces hydrocarbon emissions affecting both lighter and heavier compounds. But the catalyst is able to overcome only part of the effect of the emulsion except at high load conditions.

Sulfur Oxides

Experimental results indicate that emissions of SO_2 are essentially constant over the load range of the machine for baseline operation. This is expected because SO_2 levels are usually fixed by the sulfur content of the fuel. The analytical instrument average was 4.72 g/kg (45 ppm @ 15 percent O_2), compared to a 4.77 g/kg value computed from the fuel sulfur content. The NO_x control methods, however, did affect SO_2 emissions. This effect involved conversion of some SO_2 to sulfate under some conditions. These results are illustrated in Figure 4. The emulsion fuel averaged about 3.4 percent conversion of SO_2 to sulfate, a relatively insignificant amount. The exception was at zero kW load where the high excess air condition gave a 21 percent conversion to sulfate. The oxidation catalyst, as may be expected, gave conversions up to 62 percent at full load. When the data for the emulsion plus catalyst are inspected, the result is essentially a combination of the two control methods taken individually even to the increase at zero kW load.

Particulates

Particulate emissions were measured using the Modified Method 5 sampling train. This method uses filtration at stack temperature to collect the particulate matter in the exhaust from the diesel engine. For baseline conditions (no NO_x control), the particulate level reached a maximum value of 119.5 mg/m^3 at zero kW load. There was a decline to 30 mg/m^3 at half load (80 kW), and the emissions then remained nearly constant to full load (160 kW). Effects of the control methods are illustrated in Figure 5. The results are difficult to interpret. Emulsion fuel increased particulates at zero kW load but gave reductions at most higher load conditions. (The emulsion run at 80 kW resulted in higher particulates and is also the high hydrocarbon run noted in Table 4. This may be an aberration that occurred on that run only and may not be representative of the emulsion effect.) The catalyst did not affect particulate at zero kW as would be expected since it is not up to operating temperature. At 40 kW, particulates were reduced, but for higher load levels, large increases in particulates occurred. This pattern was essentially repeated by the combined control condition. A similar pattern resulted from particulate mass determinations using the sulfate train filter (a less accurate measure than Method 5); thus the pattern may be real. Evidently, the catalyst gives rise to increased particulate emissions, and there appears to be an interaction between the catalyst and emulsion that further increases the emission. Future work will include in-depth analysis of the particulates to determine their composition.

Bioassay and Chemical Analyses

Bioassay and chemical analyses were limited to full load operation samples for baseline and catalyst runs by time constraints, except for polycyclic aromatic hydrocarbon (PAH) spot tests. The results of bioassay testing of three fractions of the diesel exhaust are given in Table 5. It is evident that both mutagenic (potentially carcinogenic) and toxic compounds are emitted by the diesel in baseline operation. The addition of the oxidation catalyst to the exhaust stream appears to increase the bioactivity of the organic compounds: both mutagenicity and toxicity were higher. The largest amount (20 times greater mass than any other organic containing part of the total sample) of organic was the organic module extract which contains all heavy organics not associated with particulates at stack temperature conditions. This fraction of the exhaust emissions was further fractionated to attempt identification of the compound types involved. The fraction bioassay data is presented in Table 6. Mutagens were contained in Fractions 3, 4, and 5. Chemical analyses indicated that these fractions contained nitrate and nitro-organic compounds. The analysts indicated that these compounds were commonly found in the diesel exhaust samples. All of the fractions tested appeared to be toxic. More detailed identification of the organic compounds present was not within the scope of this study.

The PAH spot test was applied to all of the runs made, but only the 80 kW emulsion run gave a positive response. Evidently this test was an abnormal condition; quite likely the amount of water added was greater than specified for the test because of a control malfunction. This condition indicates that there will be a stage in water addition where PAHs will begin to form, thus limiting NO_x control by water addition to the prechamber diesel engine.

At the time this paper was prepared, the possibility of nitro/nitrate organic mutagenic compounds being formed as an artifact in the sampling system was under further study.

CONCLUSIONS

Several conclusions can be drawn from the measurements.

- Emulsion fuel provides NO_x control in addition to the inherent control provided by the prechamber (staging) effect. There is also a reduction in particulate emissions.

- This NO_x/particulate control is achieved at the expense of increased CO, THC, TCO, and GRAV, especially at less than full load.

- An oxidation catalyst in the exhaust provides control of CO and hydrocarbons when used alone.

-When combined with emulsion fuel, the catalyst still provides CO control, but could only control hydrocarbons adequately at near full load operation.

-Additional side effects of the catalyst are creation of a sulfuric acid emission (important if S is present in the fuel) and increased particulate emission above half load on the machine.

-The oxidation catalyst appeared to increase particulate emissions at load levels above 40 kW, with or without emulsion fuel use.

-The oxidation catalyst appeared to increase the mutagenicity and toxicity of heavy organic compounds emitted, while reducing their amount.

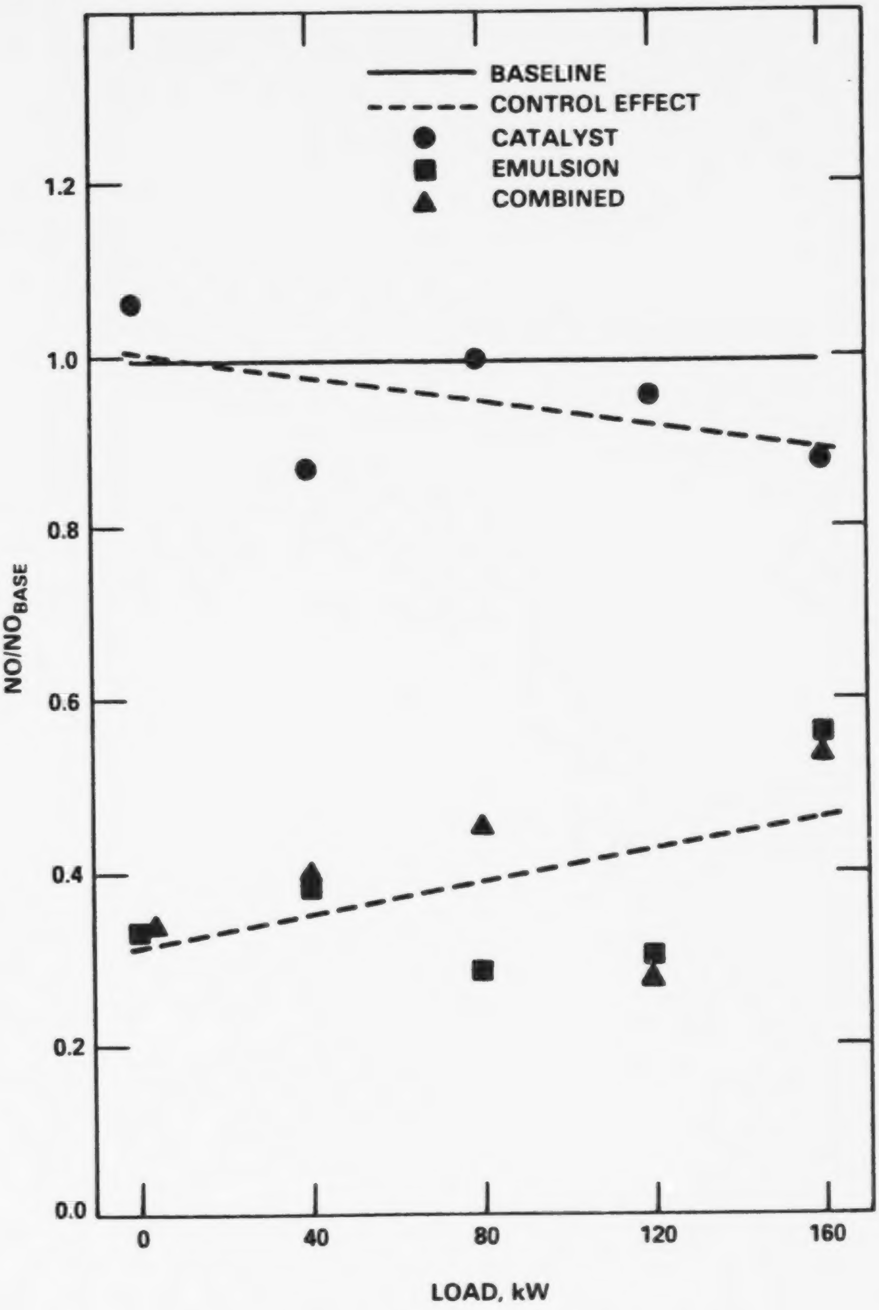

Figure 1. Effect of control on NO emissions.

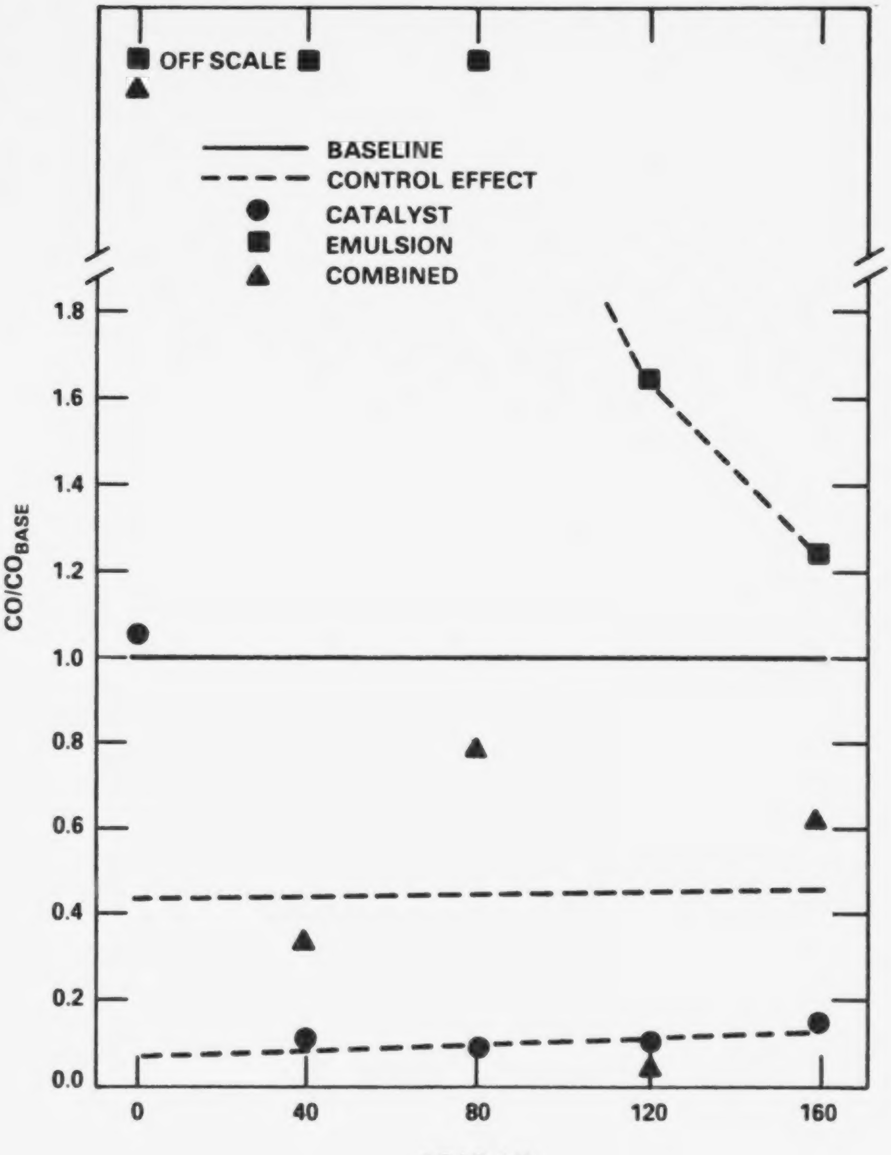

Figure 2. Effect of control on CO emissions.

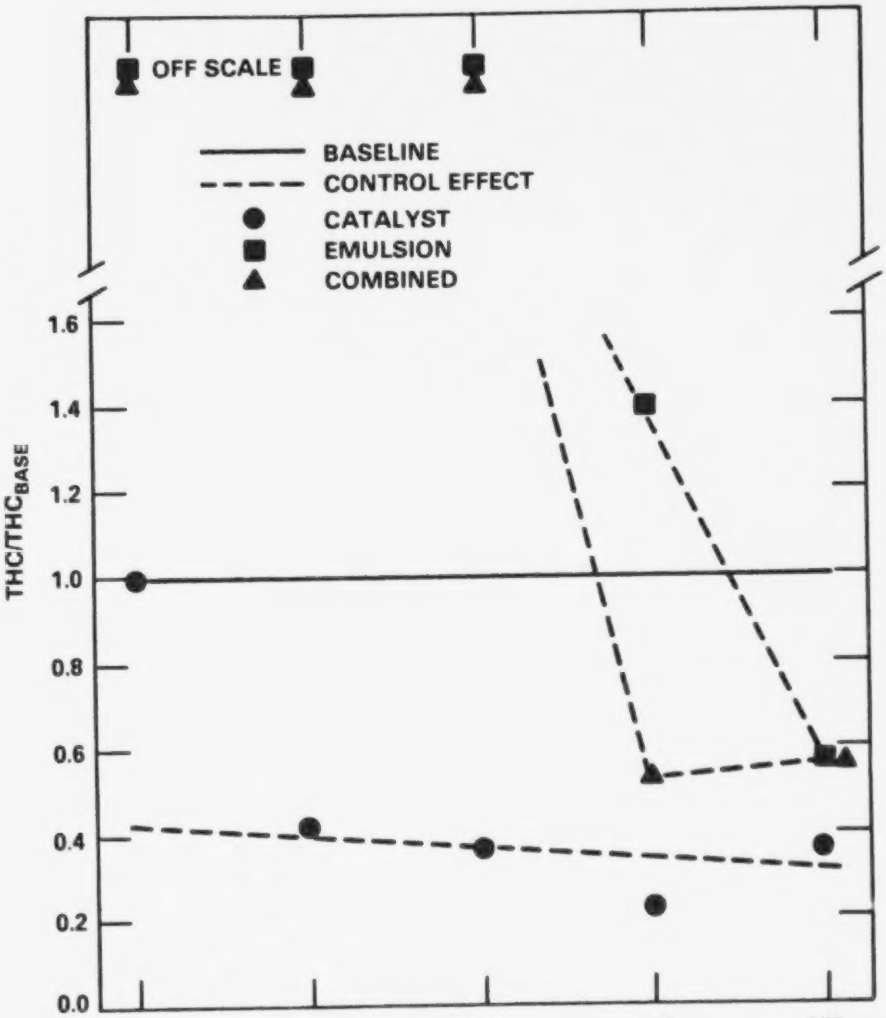

Figure 3. Effect of control on THC emissions.

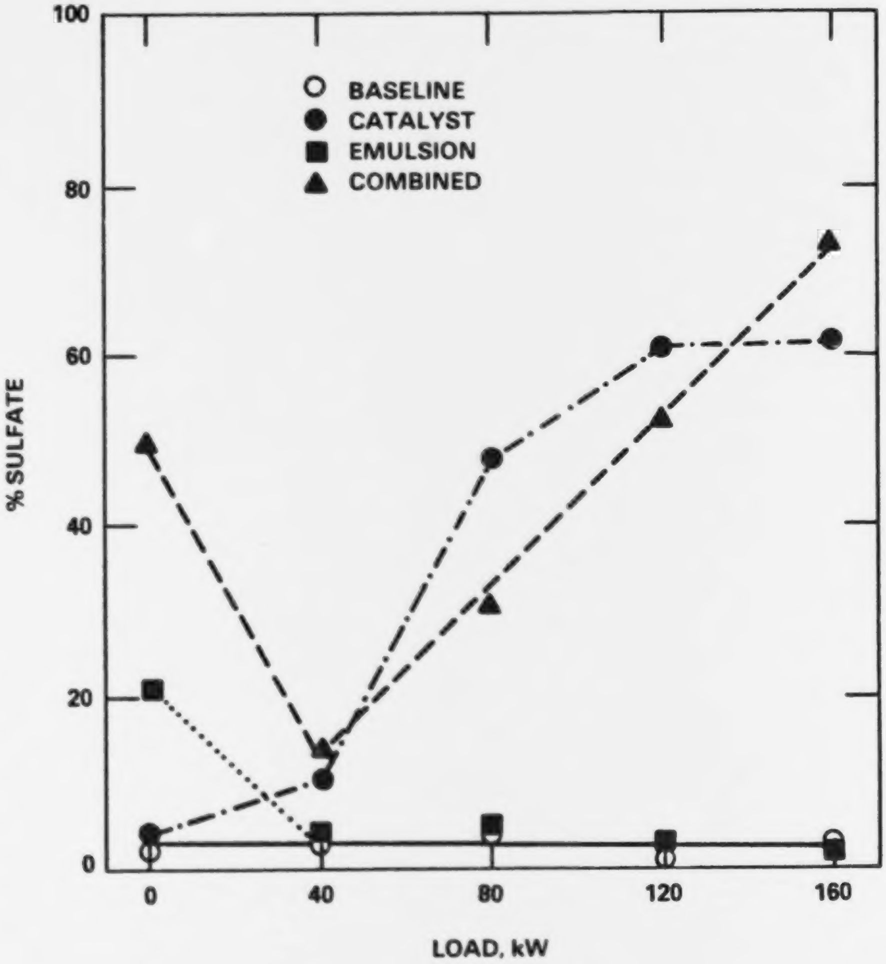

Figure 4. Conversion of SO_2 to sulfate.

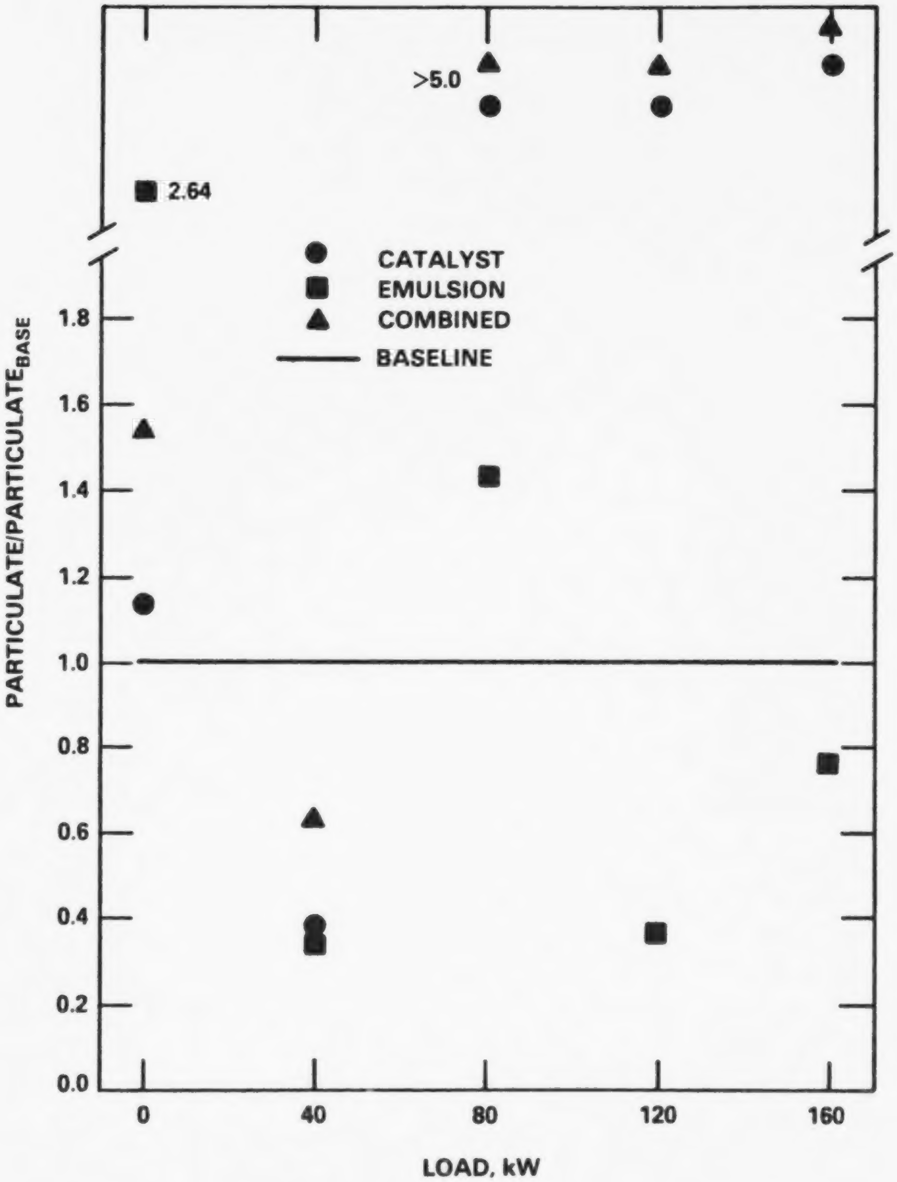

Figure 5. Effect of control on particulate emissions.

TABLE 1. EXPERIMENTAL PROGRAM

Experiment Set	Variables	Study Range
Baseline	Generator Load	Zero to 160 kW @ 40 kW intervals
Fuel Emulsion	Generator Load Water/Fuel Ratio	Zero to 160 kW @ 40 kW intervals One water/fuel ratio at each load
Catalyst	Generator Load	Zero to 160 kW @ 40 kW intervals
Catalyst + Fuel Emulsion	Generator Load Water/Fuel Ratio	Zero to 160 kW @ 40 kW intervals One water/fuel ratio at each load

TABLE 2. SAMPLING AND ANALYTICAL INSTRUMENTS

Flue Gas Constituent	Analyzer
O_2	Beckman Paramagnetic
CO_2	Beckman NDIR Model 865
CO	Beckman NDIR Model 865
Hydrocarbons	Scott Flame Ionization Model 415
NO_x	TECO Chemiluminescence
Particulates/Organics	RAC Staksampler + XAD-2 Module
Organic Extract	HP5840A Gas Chromatograph
SO_2	TECO Pulsed Fluorescent Model 40
SO_3/SO_4	Goksoyr-Ross Condensation Coil + Beckman Model 24 Spectrophotometer
Smoke (Opacity %)	Berkeley Model 107

TABLE 3. HYDROCARBON EMISSIONS
(total gaseous, g/kg fuel)

	0 kW	40 kW	80 kW	120 kW	160 kW
Emulsion	37.59	5.73	9.25	0.56	0.12
Combined	37.59	2.58	1.95	0.21	0.12
Baseline	2.69	1.56	0.56	0.40	0.21
Catalyst	2.70	0.60	0.22	0.09	0.08

TABLE 4. HYDROCARBON EMISSIONS (XAD-2 EXTRACT)

Load, kW	Control	TCO[a] (mg/m^3)	GRAV[b] (mg/m^3)
0	Baseline	22.1	17.6
0	Emulsion	541	431
0	Catalyst	24.4	8.4
0	Emulsion + Catalyst	368	232
40	Baseline	28.8	24.1
40	Emulsion	268	184
40	Catalyst	4.28	0
40	Emulsion + Catalyst	100	109
80	Baseline	13.0	4.43
80	Emulsion	2820	155
80	Catalyst	2.33	1.41
80	Emulsion + Catalyst	105	42.8
120	Baseline	8.03	4.03
120	Emulsion	13.5	0.27
120	Catalyst	1.11	0
120	Emulsion + Catalyst	5.48	0.8
160	Baseline	4.49	0
160	Emulsion	6.72	2.07
160	Catalyst	0.693	2.01
160	Emulsion + Catalyst	1.42	1.83

[a] TCO = Total Chromatographable Organics (lighter than C_{17}, bp 300°C)
[b] GRAV - Gravimetric (heavier than C_{17}, bp 300°C)

TABLE 5. BIOASSAY ANALYSES (FULL LOAD)

Sample Description	Organic Module Extract (gaseous heavy organics)	Particulate Filter Extract (<3 μm particles)	Large Particle Extract (>3 μm particles)
Ames[a]/ Baseline	Low Mutagenicity Toxic	Low Mutagenicity Not Toxic	N.D.[d]
Ames/ Catalyst	Moderate Mutagenicity Toxic	Moderate Mutagenicity Not Toxic	N.D.
CHO[b]/ Baseline	Moderate to High Toxicity	Not Toxic	N.D.
CHO/ Catalyst	High Toxicity	Not Toxic	N.D.
RAM[c]/ Baseline	N.D.	N.D.	Low Toxicity
RAM/ Catalyst	N.D.	N.D.	Moderate Toxicity

[a] Ames Salmonella Mutagenesis Assay
[b] Chinese Hamster Ovary Cytotoxicity Assay in Culture
[c] Rabbit Alveolar Macrophage Cytotoxicity Assay in Culture
[d] Not Determined

TABLE 6. ORGANIC MODULE EXTRACT FRACTIONS (CATALYST)

Fraction No.	% of Sample	Bioassay Result
1	13.2	Not Mutagenic/High Toxicity
2	0.8	Not Mutagenic/N.D.[a]
3	1.9	Moderate to High Mutagenicity/N.D.
4	11.0	Moderate Mutagenicity/High Toxicity
5	13.1	Moderate to High Mutagenicity/High Toxicity
6	60.0	Not Mutagenic/High Toxicity

[a] Toxicity Not Determined

EMISSION CONTROL METHODS FOR LARGE STATIONARY ENGINES: PART I COMBUSTION MODIFICATIONS FOR SPARK GAS ENGINES

By:

Robert P. Wilson, Jr.
Arthur D. Little, Inc.
Acorn Park
Cambridge, Massachusetts 02140

ABSTRACT

An experimental program was conducted on a 20-in. bore, single-cylinder spark-ignition engine in order to evaluate methods for emissions reduction in large stationary engines by combustion modification.

The test engine was a two-stroke, turbocharged, natural-gas-injected model operated at 130-psi bmep (brake mean effective pressure) and 330 rpm. The NO_x-reduction methods tested included charge refrigeration, multiple spark plugs, and torch ignition. Earlier tests had shown that there are three constraints on lean, low NO_x operation: (1) misfire, (2) increase in fuel consumption, and (3) turbocharger capacity limitation. Tests shown that a reduction in manifold air temperature substantially alleviated the turbocharger capacity constraint; however, the cooled air aggravated the misfire limit and increased combustion duration. Both torch ignition and an increased number of spark plugs extended the lean limit of engine operation, suppressing misfire and improving fuel consumption. The combination of multiple spark and charge refrigeration gave promising results.

This paper has been prepared under Contract No. 68-02-2664 under the sponsorship of the U. S. Environmental Protection Agency, covering work completed during the period March 1980 through August 1982.

1.0 INTRODUCTION

Large-bore stationary engines are a significant source of NO_x emissions in the United States. Covering a power range from 100 to 750 hp per cylinder, and a speed range from 300 to 1200 rpm, this engine class includes both diesel and spark ignition types. Most large-bore engines are turbocharged in order to reduce fuel consumption. Spark gas engines are primarily used in gas compressors for pipeline transmission and for recovery and gathering of natural gas; these engines account for an estimated 2% of the fuel usage and 11% of the NO_x emissions of stationary sources.(1)

Emissions control efforts for large-bore engines are primarily directed toward reducing NO_x, since the emissions of carbon-containing species (CO, HC, soot) are relatively low and the conventional engine fuels are essentially sulfur-free. The "uncontrolled" NO_x emission rate of these engines is about 4 lb/10^6 Btu, which is double that of automotive engines and is almost a factor of six greater than the coal-fired utility boiler (which is the stationary source of greatest concern) for a given amount of fuel. This remarkably high NO_x emission rate is caused by four factors:

- Compression preheating to about 1000°F, which increases the flame temperature;
- Low heat loss during combustion, which maintains high flame temperature;
- Air/fuel ratio in the 18-20 range, which maximizes NO_x; and
- Low rpm, which results in 10-20 msec residence time at high flame temperature.

In certain portions of the combustion chamber, the flame temperature is so high that the NO_x level reaches equilibrium (8,000-12,000 ppm) and then begins to decrease by the reverse of the Zeldovich mechanism as the gas cools by expansion.

The state-of-the-art in stationary spark gas engines in recent years has produced models with lower NO_x. Modest reductions in NO_x from uncontrolled levels have been achieved by retarded timing and fuel/air ratio adjustments, both of which generally carry a fuel consumption penalty. Prototype control technologies capable of more substantial NO_x reductions (e.g., torch ignition and catalyzed reduction of NO_x by ammonia) have been reported by several engine manufacturers (2,3), but the technology is still developmental. The engine experiments reported below were undertaken in an EPA-sponsored program aimed at defining potential options for reducing NO_x without incurring significant fuel consumption penalty or increases in CO, HC, or particulate emissions.

2.0 SCOPE OF EXPERIMENTAL SPARK-IGNITION RESEARCH

Table 1 presents the emission-control methods which have been investigated in the experimental research phase of the project, which is 90%

complete at this writing. The selection of these methods was based on the projected NO_x reduction, the projected added costs (per horsepower), and the relative feasibility. With the exception of catalyst methods, the projected cost of each method in Table 1 is less than 3% of the total cost of engine operation, including fuel, maintenance, and amortized capital costs. The catalyst methods cost approximately 15-20% of the total cost of engine operation.

The NO_x control methods which were tested for large-bore spark-ignition engines take advantage of three well established approaches for NO_x reduction:

- Reduced flame temperature,
- Leaner combustion, and
- Stratified combustion*.

The "reduced temperature" approaches simply shift the gas elements to a state where the NO_x production rate is much lower. The "leaner combustion" approaches force the combustion to begin and proceed at lower fuel/air ratio where the NO_x production rate is reduced. The "stratified combustion" approaches create lean and rich zones, thereby avoiding the critical "middle-range" of fuel/air ratios where NO_x production is at a maximum.

3.0 EXPERIMENTAL ARRANGEMENTS

The tests were conducted using a Cooper Model Z330 single-cylinder, two-stroke engine with 20-in. bore and 20-in. stroke dimensions, which produced 681-hp rated power at 130-psi brake mean effective pressure (bmep) and 330 rpm. Gas fuel was injected directly into the cylinder during the compression stroke, and the resulting mixture was ignited by two spark plugs nominally firing at 7 degrees crank angle before top dead center (btdc). Other instrumentation particulars have been presented earlier.(5)

4.0 SYNOPSIS OF PREVIOUS RESULTS--LEAN BURN LIMITS

A brief review of earlier results(4) from the research program is given in order to provide a framework for discussing the current data on multiple spark, charge refrigeration, and torch ignition. The NO_x emissions of the engine in its normal configuration were obtained for several spark timings and air/fuel ratios to establish a baseline or reference for further tests. All runs were at rated power and speed (130-psi bmep and 330 rpm). The results, shown in Figure 1, show that the air/fuel ratio affected NO_x markedly, reducing NO_x a factor of six (from 24 to 4 g/bhp-hr) as the mixture was leaned out from a fuel/air equivalence ratio of 0.80 to 0.62. The horizontal axis of Figure 1 is the fuel/air equivalence ratio, ϕ, which is a measure of richness of the mixture (for example, $\phi = 0.80$ means that the fuel/air ratio is 80% of the stoichiometric ratio). Retarded spark timing also reduced NO_x; for example, retarding the timing from 9 degrees to 5 degrees btdc produced a 27 to 34% NO_x change, depending on fuel/air ratio. This was equivalent to 7 to 8% NO_x reduction per degree of retard, which is consistent with other investigators.(6) The fuel/air equivalence ratio giving minimum fuel consumption was $\phi = 0.71$, and "production" Z330 engines are normally set up with that air rate for applications where NO_x is not a major consideration. At $\phi = 0.71$, the bsfc was 6650 Btu/bhp-hr and the NO_x emission level was about 14 g/bhp-hr.

---

*Here stratified combustion is used in a general sense, rather than in reference to the "PROCO" or any other specific design.

The steepness of the graph of NO_x vs fuel/air ratio, which is characteristic of all premixed combustion systems, suggests that the most fruitful approach for low NO_x is to lean out the mixture. However, several limits are encountered as the mixture is shifted to lower fuel/air ratio:

Misfire Limit: Positive reproducible ignition becomes more difficult to achieve with very lean mixtures. The flame may begin to propagate away from the spark plug, but falter or travel at low flame speed. The first sign of misfire is increased variation in peak cylinder pressure. Instrumentation on the Model Z330 single-cylinder engine automatically calculated the standard deviation in peak pressure (σ). Below $\sigma = 90$ psi, the engine exhibited satisfactory ignition. In the 90-120 psi range, some misfire was noticed but engine operation was marginally feasible. Above about 120-130 psi, misfire was considered definitely unacceptable. For the baseline engine, Figure 1 shows $\sigma = 120$ psi was reached at about $\phi = 0.65$. This is the fuel/air equivalence ratio at which misfire becomes unacceptable for the baseline engine.

Late or Incomplete Combustion: Flame propagation is slower for very lean mixtures. This leads to penalties in fuel consumption and formation of CO and HC emissions due to pockets of mixture which remain partially unburned. Notice in Figure 1 that the brake specific fuel consumption (BSFC) increases as the fuel/air equivalence ratio is extended below about $\phi = 0.65$.

Turbocharger Capacity Limit: In any shift to higher air/fuel ratio, in order to maintain power, the fuel flow cannot be reduced. Instead, the air pressure must be increased; but the ability of the engine to supply itself with high pressure air is limited. For a typical spark gas engine, turbocharger efficiency is limited to about 64%, which ultimately limits the fuel/air ratio. Turbocharger capacity limitations are more important for today's two-stroke engines than the four-stroke models.

The emphasis of the present experimental program was on finding a way to overcome the misfire limit. It was reasoned that improvements in turbocharger efficiency could be attempted once lean burning without fuel-consumption penalty or misfire were feasible.

Before testing specific NO_x controls, an attempt was made to find out if the baseline engine configuration was nearly optimum with respect to the choice of piston shape and the location of the gas valve and spark plugs. Manufacturers often vary these components to "tune" an engine for best fuel consumption and emissions. Three piston shapes were tested. The "Mexican hat" and the "flat top" (baseline) pistons gave essentially equivalent performance, except that the Mexican hat piston allowed slightly leaner operation without misfire. The "teepee" piston shape gave unfavorable fuel consumption. Variations in the location of the spark plug pairs and the gas valve made very little difference in NO_x or fuel consumption with proper timing adjustments. The baseline engine configuration with flat-top piston, center spark plugs, and center gas valve was used as the baseline for the remainder of the tests.

5.0 CHARGE REFRIGERATION

The formation of NO_x during the combustion process is acutely sensitive to the peak flame temperature, which is of course directly related to the compressed gas mixture temperature at the time of spark discharge. Accordingly, a series of tests were run to investigate the effects of reducing the temperature of the air in the intake manifold. In addition to the cooling effect, a second benefit expected from air refrigeration was the capability to obtain higher air/fuel ratios with a given turbocharger. Fifteen years ago, Helmich(7) explored charge refrigeration as a means of boosting the trapped air mass, raising engine efficiency by 5%, but NO_x was not measured. In the present test series, a 75-hp Freon refrigeration system was placed upstream of the manifold. The system was sized at about 10% of the engine output, and was capable of reducing the air temperature from 110°F (nominal value) to 35°F at full load engine operation. We observed some frost formation on the evaporator section. In practical refrigeration applications, the design must prevent ice buildup in the evaporator, which is virtually certain for air temperatures at 35°F or below (because the evaporator must operate at lower temperatures than the air). Calculations showed that the actual power requirements for refrigeration during the tests were only 10-30% of the 75 hp capacity of the system. Furthermore, the amount of exhaust-heat available after the turbocharger would be adequate to power the air refrigeration system for a multicylinder engine.

The results of this series of tests showed that NO_x was reduced 41% by a 75°F reduction in air temperature at fixed fuel/air ratio. As shown in Figure 2, the bsfc penalty associated with this NO_x reduction was about 2%. However, the extent of misfire was unacceptable at the maximum cooling condition (35°F air temperature). Figure 2 is based on data obtained by cooling the inlet air and reducing air manifold pressure to compensate for the increased density which would otherwise occur. Therefore, the NO_x reductions were not as great as when the air/fuel ratio was allowed to increase. As shown in Figure 3, the present data is in general agreement with previous investigators.(6,8,9) In some of the previous tests, which show relatively large NO_x reductions for a given air temperature reduction, it is is presumed that the air/fuel ratio may have been allowed to increase.

Near the lean limit of operation, the effect of cooled air was detrimental to engine behavior, as illustrated in Figure 4. The colder the air, the higher the fuel/air ratio at which misfire was observed (see the top family of curves in Figure 4). In other words, the engine had to be operated richer at reduced air temperature. For example, the engine had to be operated about 7% richer at 50°F air temperature than at 110°F. The potential NO_x reduction shown in Figure 2 could not be obtained near the lean limit, because the mixture had to be enriched to avoid misfire. Table 2, containing data extracted from Figure 3, shows how reduced air temperature caused an increase in the minimum acceptable fuel/air ratio. The right-hand column of Table 2 shows that the net effect on NO_x was not favorable. However, air cooling alleviated the turbocharger capacity limit to a certain extent. It is projected that reducing the air temperature to 50°F would enable an engine to run about 5% leaner with a given turbocharger. Based on Figure 1, this would be equivalent to a potential NO_x reduction of about 30%. If this hypothetical extention of the lean limit were to be achieved and combined with the observed NO_x reduction due to cooling (see Figure 2), the total potential reduction would be 50-60%. This potential NO_x reduction offered by reduced air temperature can only be achieved if misfire can be avoided and combustion duration shortened. Thus, test results indicate that charge refrigeration should be combined with ignition and combustion enhancement methods such as torch ignition or high energy spark.

This point is underscored by the heat release profiles in Figure 5. These profiles show that charge refrigeration:

- Extends ignition delay by 1-2 degrees,
- Lowers the peak rate of heat release, and
- Extends the combustion duration.

These are the same effects that a leaner mixture would produce.

6.0 MULTIPLE SPARK

In an attempt to extend the lean limit of satisfactory engine operation, the number of active ignition sites was increased from two to six in a series of tests. The additional spark plugs were intended to improve ignition and shorten the combustion duration of lean mixtures. For example, Kuroda et al.(10) reported that substitution of a multiple spark plug arrangement on an automotive engine reduced combustion duration by 20 degrees, allowing exhaust gas recirculation and a 60% NO_x reduction. Figure 6 illustrates the placement of the additional spark plugs in the present test series. The conventional engine had two spark plugs, each covering about a 5-in. radius sphere of flame travel. In principle, additional plugs should have increased the surface area of the flame front and shortened the required flame-travel distance.

The added ignition sites suppressed misfire, allowing very lean engine operation, as shown in Figure 7. Whereas the two-plug configuration was limited to $\phi = 0.65$ (NO_x = 7.0 g/bhp-hr) at the onset of misfire, the six-plug configuration was able to operate at $\phi = 0.62$ (NO_x = 4 g/bhp-hr) without misfire. Furthermore, the fuel consumption was not degraded, which implies that the added ignition enabled the leaner mixture to be burned in the same combustion time.

The ability of multiple spark plugs to shorten the combustion duration for lean mixtures was confirmed by heat release profiles derived from cylinder pressure traces. As shown in Figure 8, the maximum heat release rate with six spark plugs was 30% greater than with two plugs (compare the two curves at $\phi = 0.64$ and 0.65). Therefore, the flame speed and/or flame area must have been 30% greater with six plugs. The combustion duration was noticeably shorter (by about 8 degrees CA) with six plugs, and the back of the heat release "triangle" was steeper, indicating that combustion ceased more abruptly (as could be expected with multiple flame fronts). The legend in Figure 8 shows that both the bsfc and the cyclic irregularity (σ) were substantially improved by increasing the number of spark plugs. For the two runs under comparison, the NO_x increased from 5.9 to 9.8 g/bhp-hr, because the timing and fuel/air ratio were held fixed.

The feasibility of using multiple spark plugs to achieve very lean operation is also illustrated in Figure 8. Note that the six-plug heat release profile at $\phi = 0.60$ was nearly identical to the two-plug profile at 0.64, and that the NO_x was thereby reduced from 5.9 to 3.7 g/bhp-hr.

The primary remaining problem with the six-plug approach is that the standard turbocharger could not provide enough air to operate the engine at an air/fuel equivalence ratio as lean as $\phi = 0.62$. In the previous section it was reported that the turbocharger feasibility limit was relaxed by charge refrigeration. This suggested that the two methods would be complementary.

7.0 MULTIPLE SPARK IN COMBINATION WITH CHARGE REFRIGERATION

Additional tests were conducted with six spark plugs at 50°F air temperature to determine if the misfire problem experienced with refrigerated charge could be remedied by multiple spark plugs. The tests were conducted near the lean limit of engine operation. The results were favorable; at very lean conditions ($\phi = 0.64$), the multiple-spark/refrigeration combination reduced the index of misfire from $\phi = 160$ psi to $\phi = 129$ psi, which is just above the acceptable threshold. Moreover, this combination yielded the most favorable NO_x/bsfc performance in the test series (3.9 g/bhp-hr and 6724 Btu/bhp-hr).

8.0 TORCH IGNITION (PRELIMINARY RESULTS)

8.1 Objectives

One of the most promising means of extending the lean limit of engine operation is torch ignition. In this method, a burning jet issues from a small ignition cell which has been charged with a richer mixture than the main chamber. Torch ignition was in use as early as 1952 on the Fairbanks Morse opposed-piston 8-1/8 in. bore engine(11) and in recent years has been studied for both lean-burn automotive applications(12,13,14) and for stationary spark-gas engines.(2,3,15,16,17) The present series of tests were undertaken in order to systematically explore the effects of critical design parameters of torch ignition such as:

- Fuel/air ratio of the ignition cell,
- Throat size and geometry,

- Number, location, and direction of torches,
- Ignition cell volume, and
- Methods of charging the ignition cell with fuel.

These parameters were varied in order to better understand the mechanism by which torch ignition corrects the problems of misfire, late burning, and incomplete combustion, and thereby extend the lean limit of engine operation.

8.2 Ignition Cell and Fuel Injection Arrangements

Since the automotive experience with torch ignition had shown that localized NO_x production by the torch can be relatively high, the volume of the ignition cell was designed to be as small as possible. At the same time, the cell must be large enough to project a burning jet of adequate size, and also be large enough to accommodate the spark plug, gas injector and (in this case) pressure tap. Two 5.9 cu.-in. ignition cells were used in the present single cylinder engine tests; each cell was about 1.1% of the 550 cu.-in. clearance volume. As shown in Figure 9, each cell had a 13/32-in. opening positioned about 25% of the cylinder radius from the liner wall. The ignition cells could be rotated to provide various torch directions, and the caps could be exchanged to provide different orifice sizes and shapes. In the present tests only one orifice size was tested.

Fuel gas was metered separately into the ignition cells through poppet valves as shown in Figure 9. The fuel flow to the cells was approximately 3-4% of the total fuel gas per cycle. Fuel gas was delivered at about 10-20 psi above cylinder pressure for a 60° CA period at the end of the scavenging process, just before port closure. Fuel gas pressure at the cell was used to indirectly control torch fuel/air ratio, and this was adjusted to minimize bsfc. The volume of fuel gas injected (at actual density) exceeded the physical volume of the ignition cell, and part of the fuel presumably passed through the orifice into the main chamber (a portion of which may have been lost out the exhaust ports). Tests verified that the amount of fuel escaping with the scavenge air was kept to a minimum. During the compression stroke, air was added to the ignition cell.

All tests were made at full load (130 psi BMEP), two timings (3° and 6° BTDC), and several fuel/air equivalence ratios in the range of $\phi = 0.70$ to $\phi = 0.55$.

8.3 Extension of the Lean Limit

The use of torch ignition in place of ordinary spark plugs extended the limit of engine operation from $\phi = 0.66$ to $\phi = 0.58$-.60, which corresponds to a 12% increase in maximum feasible air/fuel ratio. As shown in Figure 10, the NO_x level of this particular engine was thereby reduced from about 8 g/bhp-hr to a range of 2.9-3.6 g/bhp-hr. There was no evidence of the onset of misfire at fuel/air mixtures as lean as $\phi = 0.56$, indicating very positive ignition cycle after cycle. The standard deviation of peak pressure dropped to the 40-60 psi range throughout the tests. Furthermore, the fuel consumption (BSFC) remained low at very lean mixture ratios with torch ignition, indicating that the effective burning rate did not diminish as the mixture was leaned out.

Two problem areas were in evidence at such lean engine operating conditions:

(1) Hydrocarbon emissions: As shown in Figure 10 and as has been reported by others(13,14,16), the emission level of unburned hydrocarbons increased to the 5-7 g/bhp-hr range at ϕ = 0.58-.60. This problem will be discussed below.

(2) Turbocharger feasibility: The measured exhaust gas energy content is apparently too low at ϕ = 0.58-.60 to allow current turbochargers to function properly.

8.4 Torch Location and Direction

The experimental cylinder head has four cavities for the ignition cells, spaced about 90° apart. When two ignition cells are installed, they can be located on the same or opposite sides of the cylinder, and the torch axes can be aligned to converge or to diverge. A series of runs were made to test the sensitivity of lean limit engine performance to various cell arrangements. As shown in Figure 11, three of the arrangements were superior in terms of the BSFC/NO_x tradeoff. These three, C, F, and E, had at least one torch directed toward the center of the cylinder.

Some design guidelines emerge from the data on Figure 11: the superiority of arrangement C over A suggests avoiding designs where the air swirl motion pushes the combustion jets away from the center of the chamber. The fact that H and B were relatively unfavorable suggests that two torches work better when converging toward each other.

8.5 Amount of Torch Fuel

The fraction of fuel partitioned to the two ignition cells was adjusted to the setting which gave minimum fuel consumption (presumably, best combustion). For the present ignition cell and orifice design, the fuel metered to the two cells (2.1% of clearance volume) ranged between 2.5 and 4.8%, depending on the timing, air/fuel ratio, and torch location. With a typical torch fuel fraction of 3.6%, the fuel/air ratio of the torch can be estimated at 3.6/2.1 = 1.7 times that of the main chamber (e.g., about ϕ = 1 for the torch, assuming ϕ = 0.6 in the main chamber). This estimate is corroborated by calculations of the partial pressure of fuel after the compression process. Larger ignition cells and/or smaller orifices could be expected to produce somewhat richer torches.

The most favorable torch arrangements (C and F) required the least torch fuel fractions. Conversely, torches giving poor performance required more fuel and therefore had relatively lean main chamber gases. It should be noted that with 96% of the fuel partitioned to the main chamber (98% of the volume), the main chamber fuel/air ratio is about 2% lower than the overall ratios given on the x-axis of Figure 10.

8.6 Unburned Hydrocarbons

Preliminary data show unburned hydrocarbons were in the 6 ± 1 g/bhp-hr range at the lean limit ($\phi = 0.58$-.60). This is 4 ± 1 g/bhp-hr higher than the baseline engine, and is apparently the cause of the 3% BSFC penalty (a loss of 4 g/bhp-hr of fuel at 50 Btu/g heating value represents a bsfc penalty of 200 Btu/hr-hr). The ignition characteristics are excellent at $\phi = 0.58$, as evidenced by the low values of σ, so that solutions to the hydrocarbon problem might allow us to explore engine operation below $\phi = 0.58$.

Increasing hydrocarbon emissions under lean burn conditions are not unique to torch ignition; this characteristic has been observed in numerous automotive engine test projects.(18,19) As the mixture in the main chamber becomes leaner, the flame speed is lowered and the last elements to be reached by the flame "front" may not completely burn. In addition, certain pockets of mixture are known to be leaner than average, and some may be below the flammability limit as the mixture is leaned out.

Approaches to reducing unburned hydrocarbons which are being tested include smaller ignition cell orifices and better mixing.

8.7 Comments on the Torch Ignition Mechanism

In order to elucidate the physics of the combustion jet, it is helpful to study the transient pressures inside the cell and in the main chamber (see Figure 12). Note first that there was no significant lag in pressure differential between the two chambers; this was expected because of the orifice size of this particular ignition cell. The spark ignition event was at 6 degrees BTDC, and the cell pressure began to rapidly increase about 3 degrees later. This ignition delay is consistent with a stoichiometric mixture and is much shorter than is observed for conventional lean-burn main chamber ignition.

The duration of the combustion jets was quite brief (4 degrees or 1.8 msec) and coincided with top dead center. Note that the maximum pressure in the cell was only about 50-60% higher than the main chamber pressure. This indicates the absence of choked flow; we had a subsonic rather than supersonic jet.

Examination of other pressure traces showed that the greater the torch fuel fraction, the higher the maximum cell pressure. This suggests that the mixture ratio of the cell contents was near stoichiometric.

9.0 SUMMARY

A preliminary test series on the single-cylinder 20-in. bore test engine established that significant NO_x reductions could not be obtained by rearrangement of the spark plug location, gas valve location, or piston shape. Attempts to create a stratified charge by modifying the gas valve also proved to be ineffective in reducing NO_x.

The most effective approach to NO_x reduction was to lean out the air/fuel ratio of the mixture. The baseline data on the Z330 single-cylinder engine established the potential for reducing NO_x from a level of 14 g/bhp-hr (normal operation) to below 4 g/bhp-hr by leaning out the mixture to a fuel/air equivalence ratio of about $\phi = 0.62$. However, three constraints prevent lean operation below a fuel/air equivalence ratio of about $\phi = 0.66$ (NO_x = 7 g/bhp-hr): (1) misfire, (2) increase in bsfc, and (3) turbocharger capacity limitation.

The performance of various test configurations at the lean limit are compared in Table 3 and Figure 13. Tests showed that a reduction in manifold air temperature substantially alleviated the turbocharger capacity constraint, and reduced the NO_x level at normal fuel/air ratio ($\phi = 0.69$) from 14 to 9 g/bhp-hr. However, for lean operation, the cooled air was detrimental to engine behavior, aggravating the misfire limit and increasing the combustion duration.

Increasing the number of ignition sites proved to be quite beneficial to lean-limit operation of the engine, suppressing misfire tendency and improving the specific fuel consumption. Operation at $\phi = 0.62$ was feasible with six spark plugs, and the combustion duration remained within acceptable limits. As shown in Table 3, the multiple spark approach would allow the NO_x level to be reduced to 4 g/bhp-hr if it were not for the turbocharger capacity constraint.

Torch ignition had the same type of effect on engine emissions as six spark plugs; however, suppression of misfire was more complete. Operation at $\phi = 0.58$-0.60 was feasible with torch ignition, and the bsfc was acceptable. NO_x levels below 3 g/bhp-hr were reached with satisfactory fuel consumption. However, suitable turbocharger technology is necessary to operate at this lean setting (260% air). Hydrocarbon emissions were excessive in the preliminary series of tests.

As illustrated in Figure 13, one of the most promising configurations in the present test series was the combination of multiple spark and charge refrigeration, which allowed lean operation within the turbocharger capacity, reduced NO_x to 3.9 g/bhp-hr, and increased bsfc by only 1%. The combination of torch ignition and charge cooling would also appear to be promising.

ACKNOWLEDGEMENTS

John H. Wasser, the EPA Technical Project Officer, provided guidance and contributed technical insights during these spark-ignition engine tests. I also wish to acknowledge several individuals at Cooper Energy Services (Paul Danyluk, Fred Schaub, and Mel Helmich) who have been responsible for the engine tests and the translation of NO_x-control concepts into practical engine hardware. Key contributions to this phase of the project have been made by several members of the project team at Arthur D. Little, including Phil Gott and John Mendillo. Finally, I wish to acknowledge the work of Maureen Donovan in the preparation of this manuscript.

REFERENCES

1. Waterland, L. R., Lim, K. J., Salvesen, K. G., Evans, R. M. Higginbotham, E. G., and Mason, H. B., "Environmental Assessment of Stationary Source NO_x Control Technologies: Second Annual Report," EPA-600/7-79-147 (NTIS No. PB 300469), June 1979.

2. Helmich, M. J., "Clean Burn Engine," AGA Transmission Conference, New Orleans, May 21-23, 1979.

3. Chrisman, B., "Exhaust Emissions: Regulations and Control Technology," 27th Annual Meeting of the Gas Compressor Institute, Liberal, KS, April 1980.

4. Wilson, R. P., Jr., "Single-Cylinder Tests of Emission Control Methods for Large-Bore Stationary Engines." In: Proceedings of the Joint Symposium on Stationary Combustion NO_x Control; Vol. IV, EPA-600/9-81-028d (NTIS No. PB81-236143), July 1981.

5. Wilson, R. P., Jr., Mendillo, J. V., Gott, P. G., Danyluk, P. R., Schaub, F. S., Wasser, J. H., "Single-Cylinder Tests of NO_x Control Methods for Spark Gas Engines," ASME Paper 82-DGP-27, 1982.

6. U.S. Environmental Protection Agency, "Stationary Internal Combustion Engines, Standards Support and Environmental Impact Statement: Volume 1. Proposed Standards of Performance," EPA-450/2-78-125a, July 1979.

7. Helmich, M. J., "Development of Combustion Air Refrigeration System Enabling Reliable Operation at 220 psi bmep for a Large 4-Cycle Spark-Ignition Gas Engine," ASME 66-DGEP-7, 1966.

8. McGowin, C. R., Schaub, F. S., and Hubbard, R. L., "Emissions Control of a Stationary Two-Stroke Spark-Gas Engine by Modification of Operating Conditions," AGA/IGT Proceedings, 2nd Conference on Natural Gas Research and Technology, Atlanta, GA, 1972.

9. Schaub, F. S., and Beightol, K. V., "NO_x Emission Reduction Methods for Large Bore Diesel and Natural Gas Engines," ASME Paper 71-WA/DGP-2, ASME Winter Annual Meeting, 1971.

10. Kuroda, H., Nakajima, Y., Sugihara, K., Takagi, Y., and Muranaka, S., "The Fast Burn with Heavy EGR, New Approach for Low NO_x and Improved Fuel Economy," SAE Paper 780006, February 1978.

11. Kasel, E., Personal Communication regarding the Colt Turbocharged Model 38DS-848 Spark Ignition Engine, October 27, 1978.

12. Gussak, L. A., "High Chemical Activity of Incomplete Combustion Products and a Method of Prechamber Torch Ignition for Avalanche Activation of Combustion in Internal Combustion Engines," SAE Paper 750890, 1975.

13. Wyczalek, F. A., Harned, J. L., Maksymiuk, and Blevins, J. R., "EFI Prechamber Torch Ignition of Lean Mixtures," SAE Paper 750351, 1975.

14. Oppenheim, A. K., Teichman, K., Hom, K., and Stewart, H. E., "Jet Ignition of an Ultra-Lean Mixture," SAE Paper 780637, 1978.

15. Danyluk, P. and Schaub, F. S., "Emission Reduction by Combustion Modification in Two Stroke Spark Ignited Gas Engines and by Catalytic Conversion," ASME Paper 81-DGP-7, 1981.

16. Serve, J. V., "NO_x Reduction on Large Bore Turbocharged SI Engines," ASME Paper 82-DGP-16, 1982.

17. Cummins, T. L., "Clean Burn Engines--A User Report," Compressor Short Course, Norman, OK, 1982.

18. Schwarz, H., "Ignition Systems for Lean Burn Engines," paper C95/79, p. 87, I.MECH.E Conference Publication 1979-9. Fuel Economy and Emissions of Lean Burn Engines, MECH.ENG. Publications, Ltd., London, 1979.

19. Peters, B.D., "Mass Burning Rates in a Spark Ignited Engine Operating in the Partial-Burn Regime," paper C92/79, p. 63, I.MECH.E Conference Publication 1979-9. Fuel Economy and Emissions of Lean Burn Engines, MECH.ENG. Publications, Ltd, London, 1979.

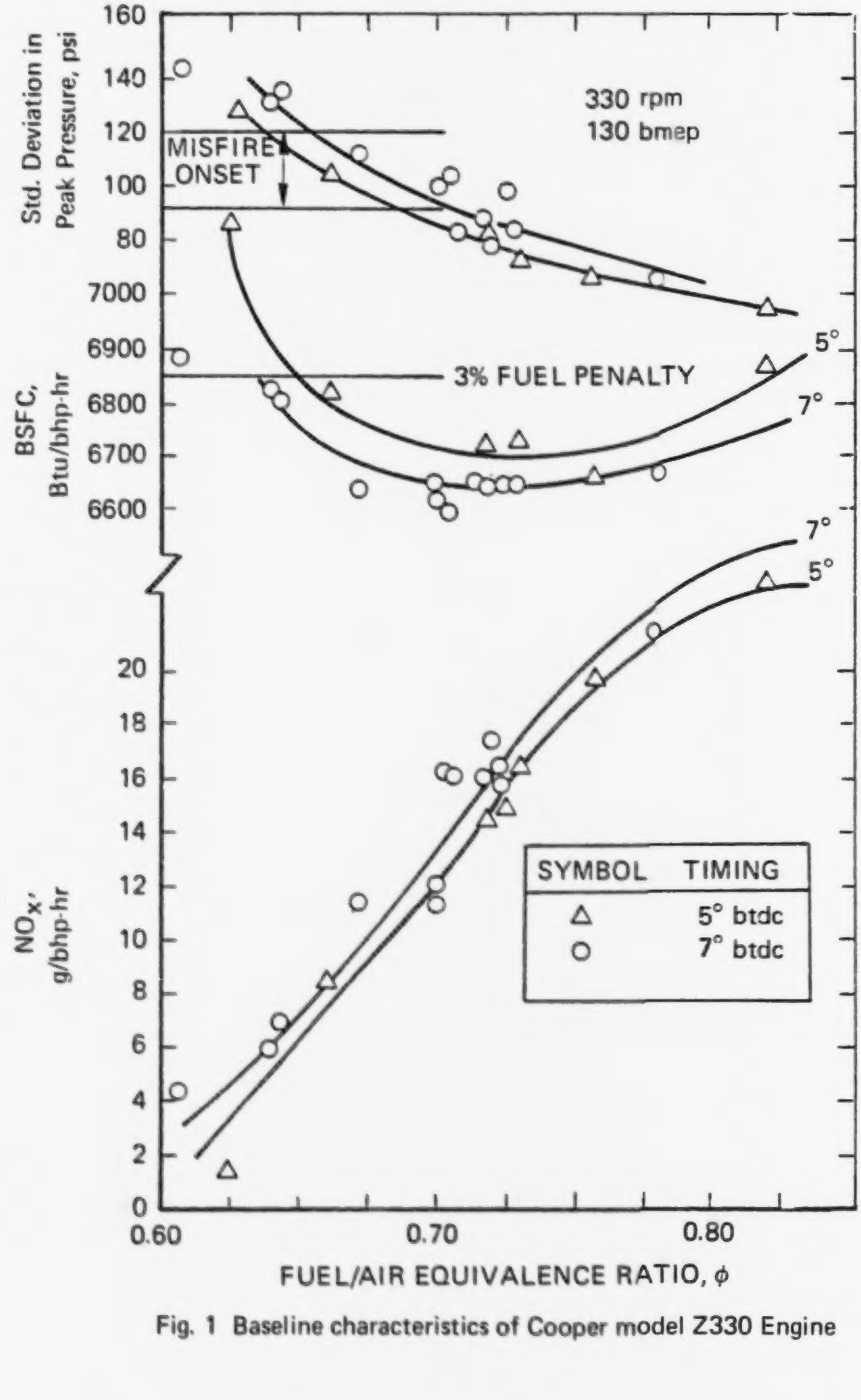

Fig. 1 Baseline characteristics of Cooper model Z330 Engine

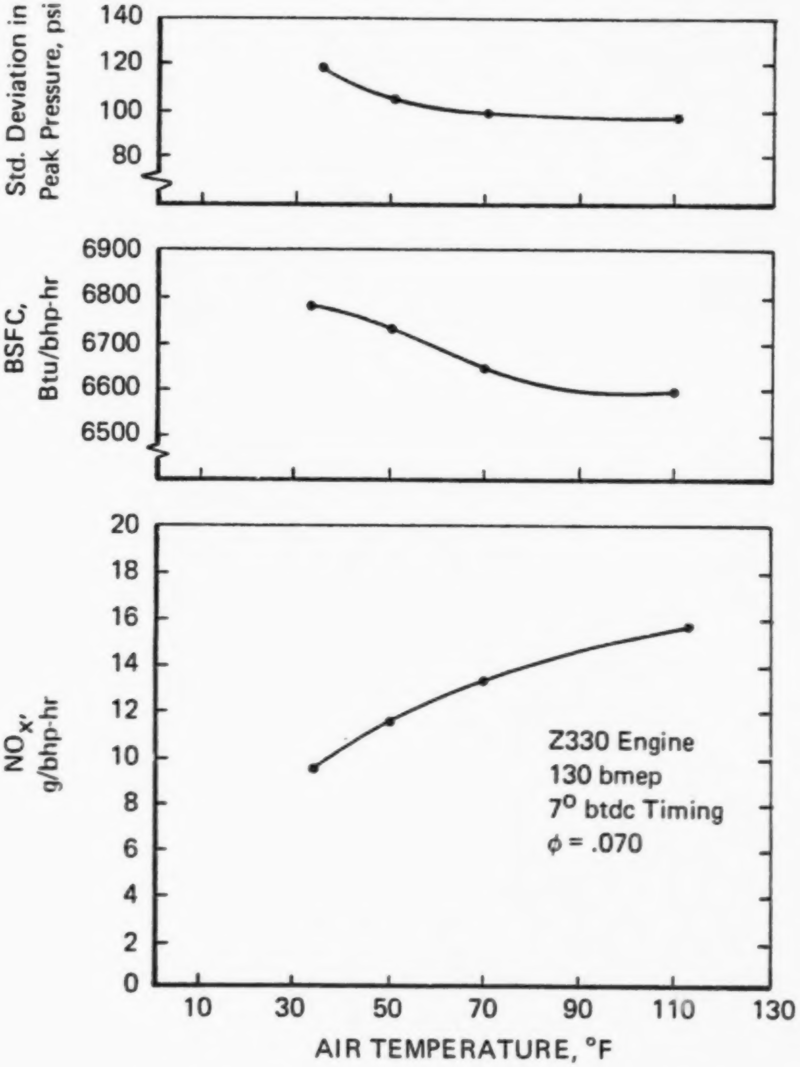

Fig. 2 Effect of air temperature (fixed air/fuel ratio)

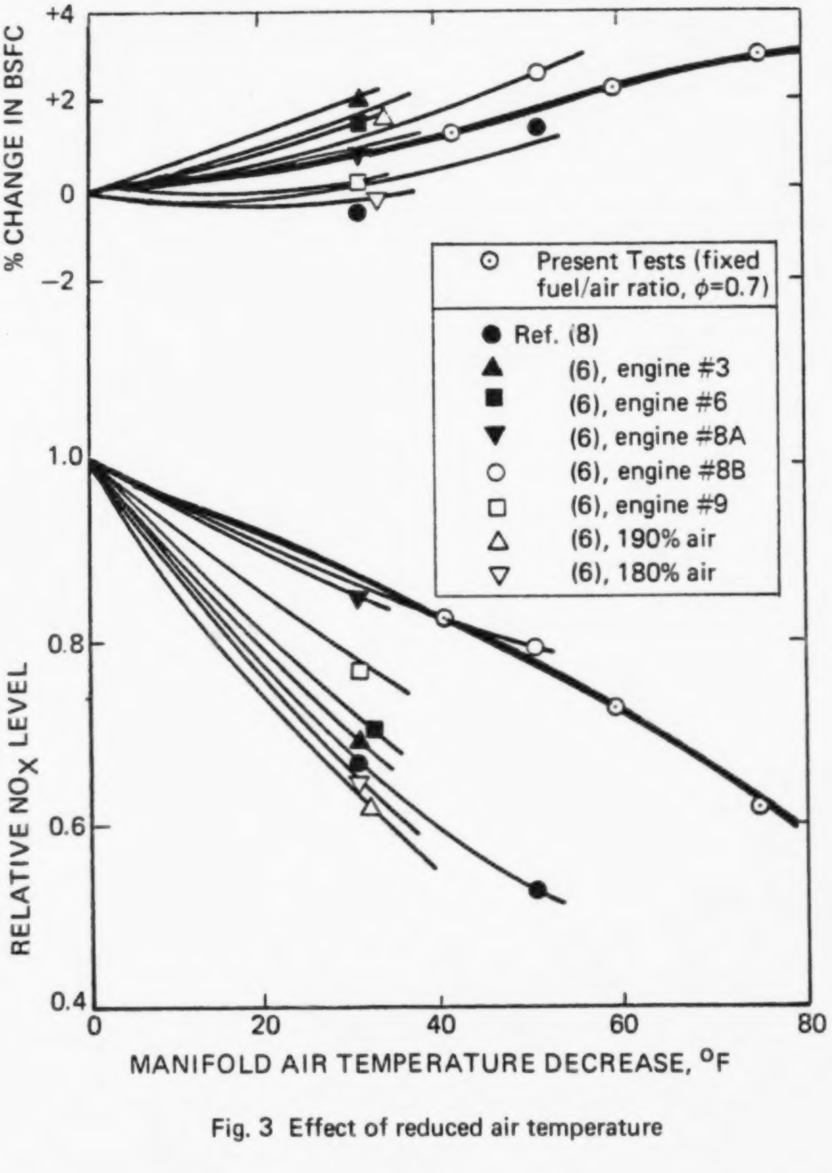

Fig. 3 Effect of reduced air temperature

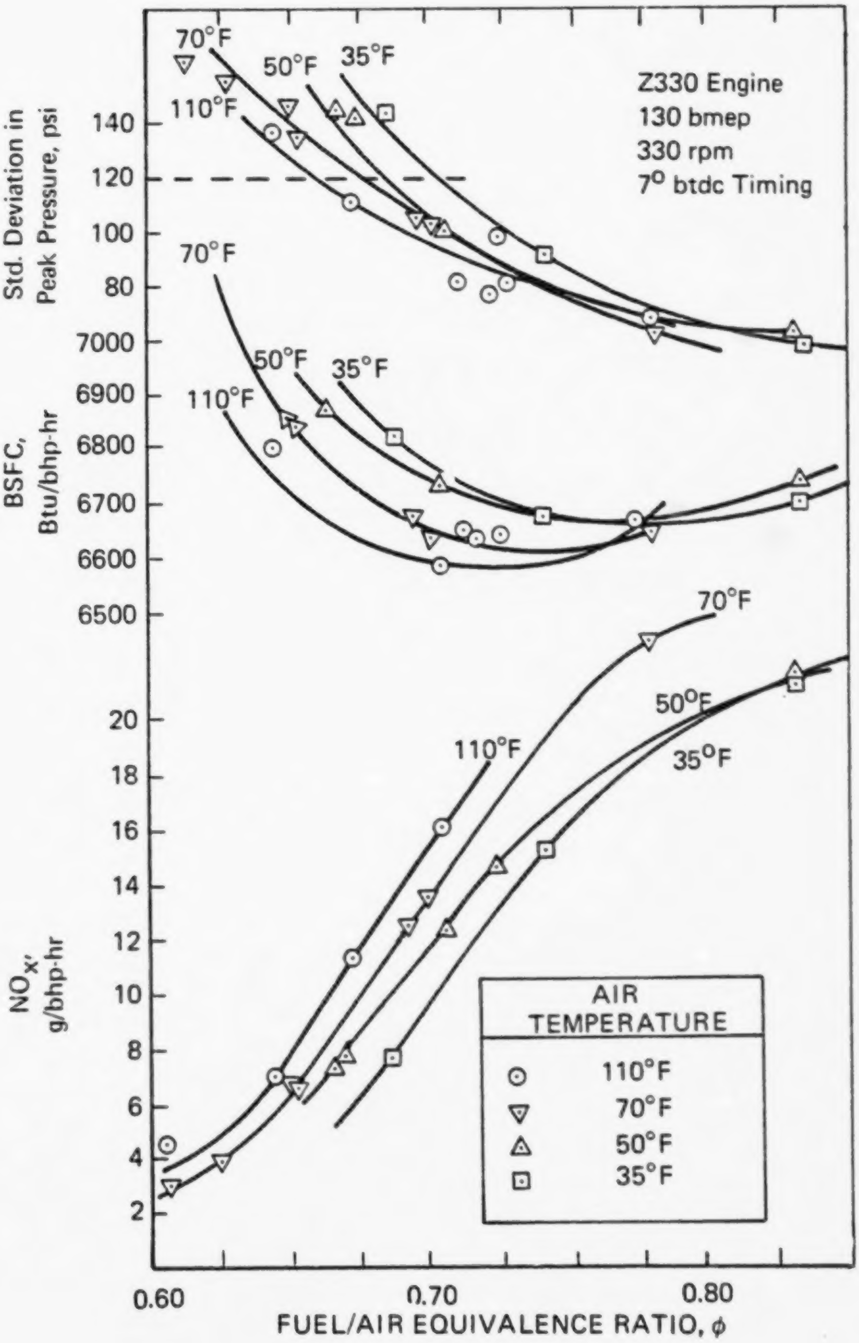

Fig. 4 Effect of charge refrigeration

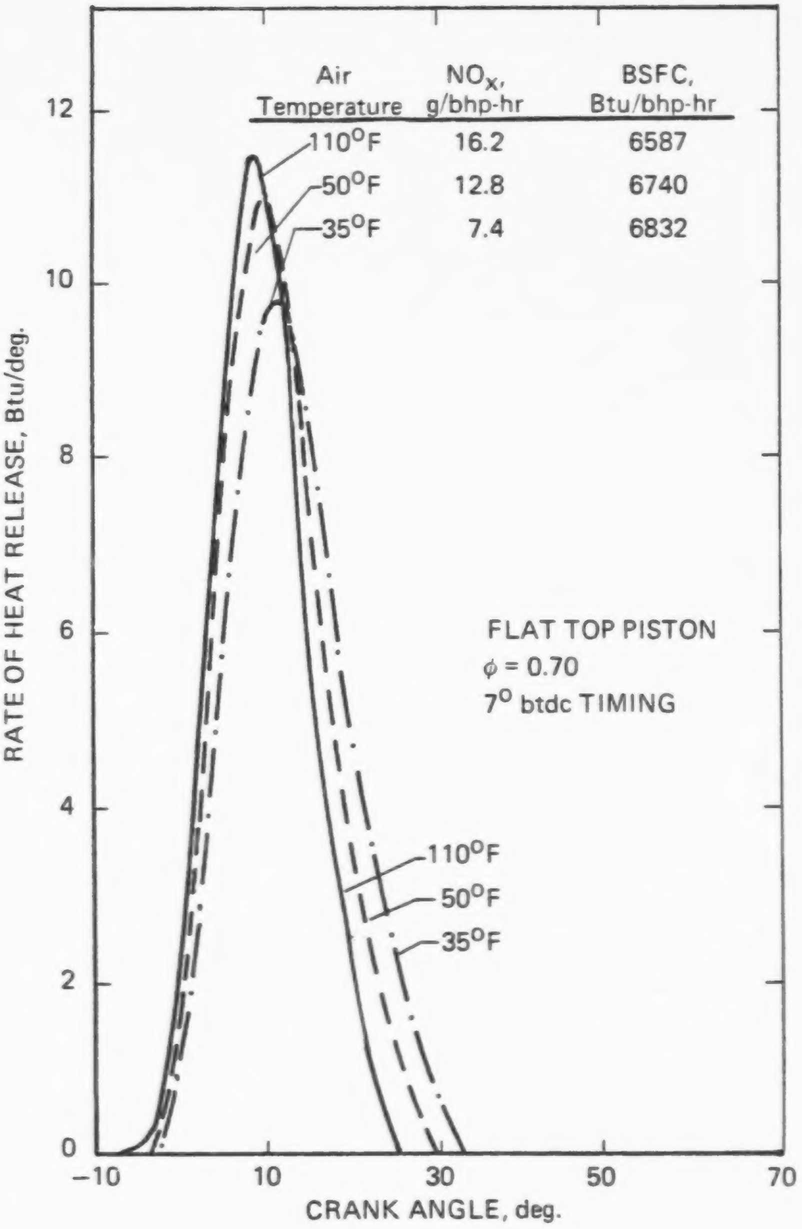

Fig. 5 Effect of air temperature on rate of heat release

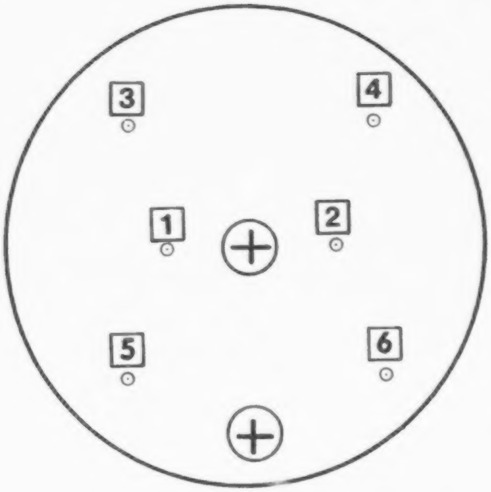

Fig. 6 Six-plug configuration

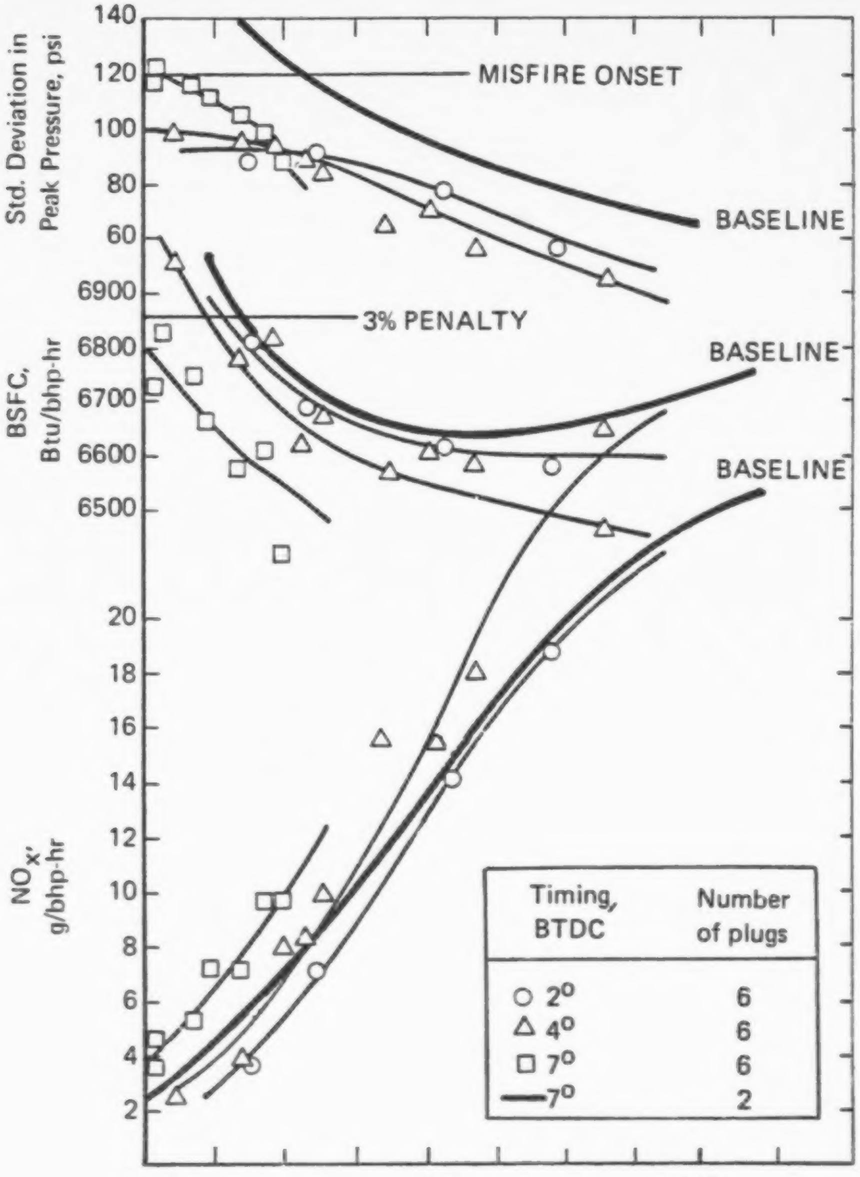

Fig. 7 Effect of multiple spark plugs

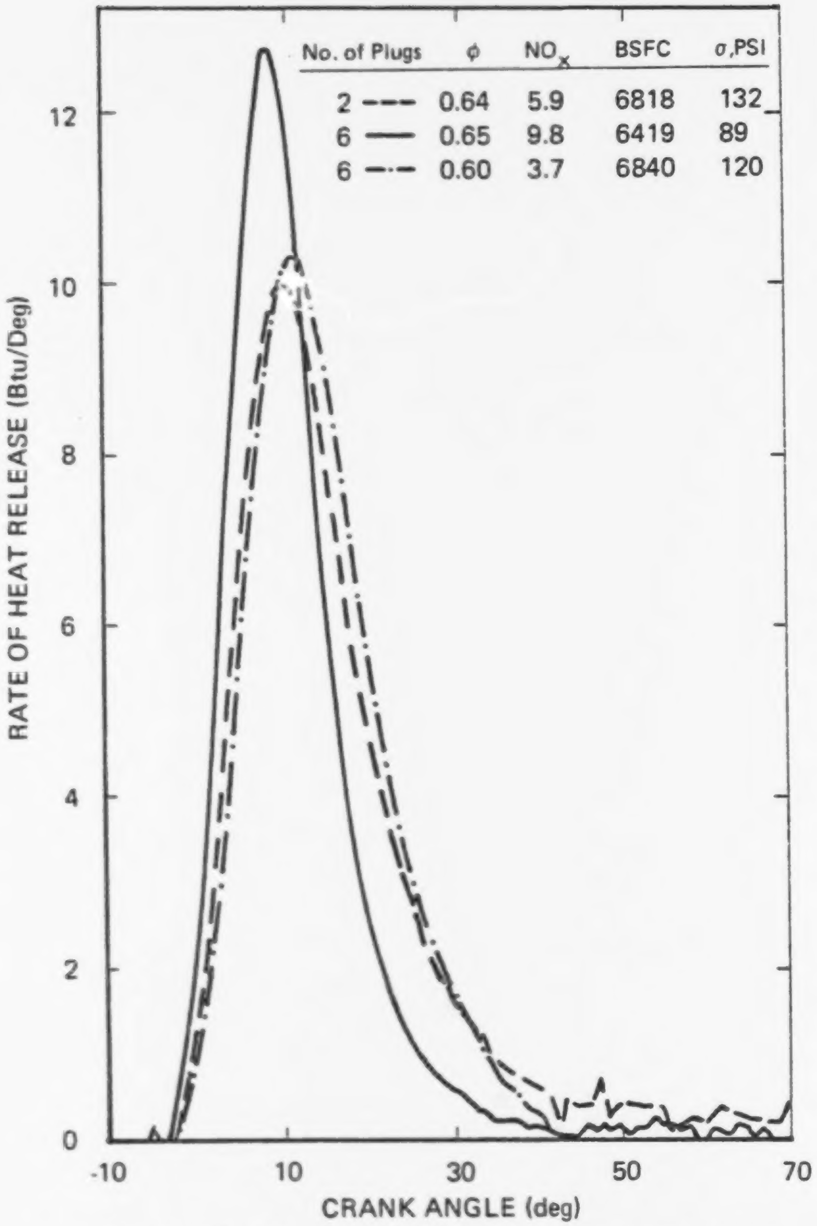

Fig. 8 Effect of multiple spark plugs on rate of heat release

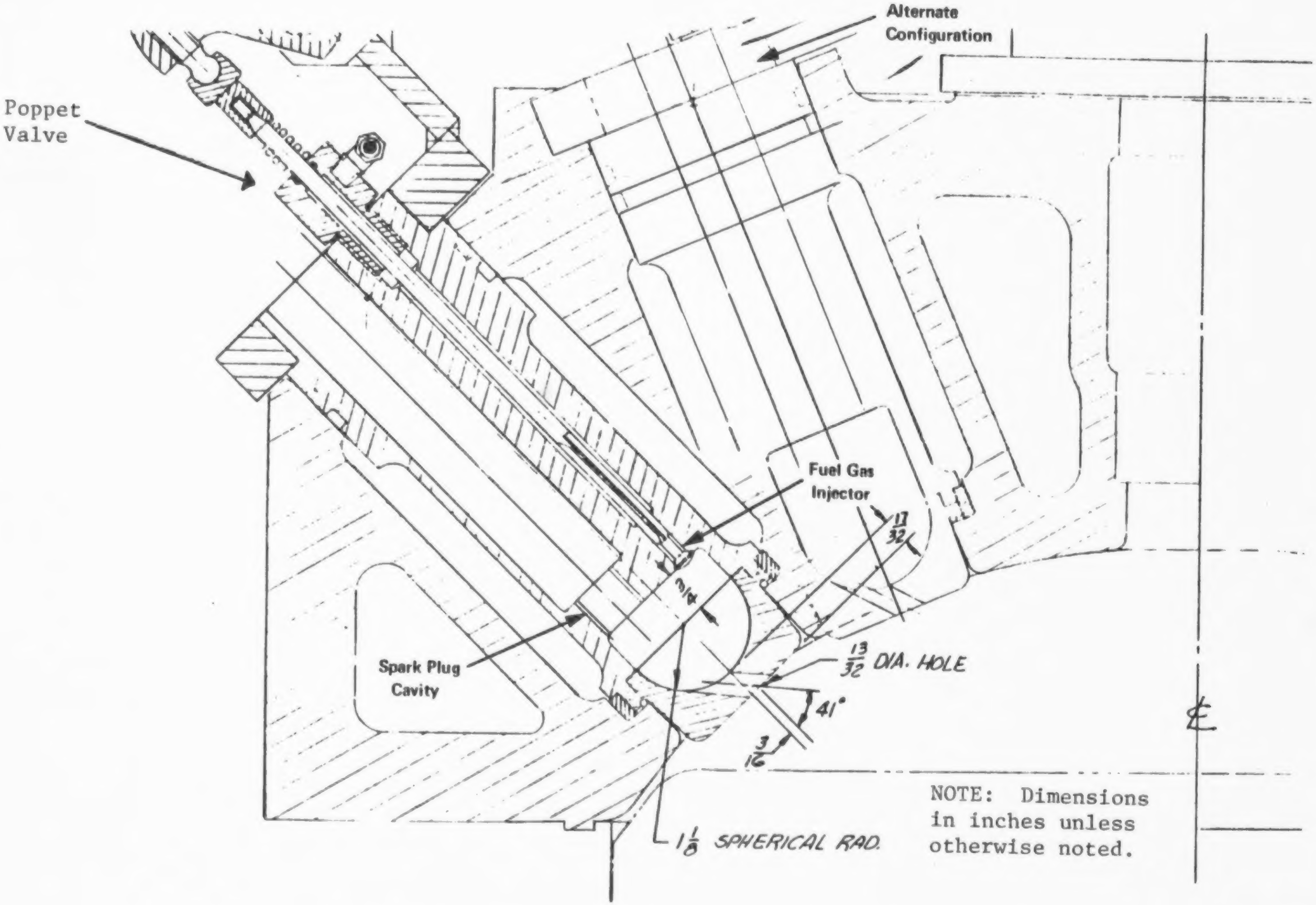
Poppet Valve
Alternate Configuration
Fuel Gas Injector
$\frac{17}{32}$
$\frac{3}{4}$
Spark Plug Cavity
$\frac{13}{32}$ DIA. HOLE
41°
$\frac{3}{16}$
$1\frac{1}{8}$ SPHERICAL RAD.
℄

NOTE: Dimensions in inches unless otherwise noted.

FIGURE 9 TORCH CELL WITH ORIFICE CONFIGURATION C-3

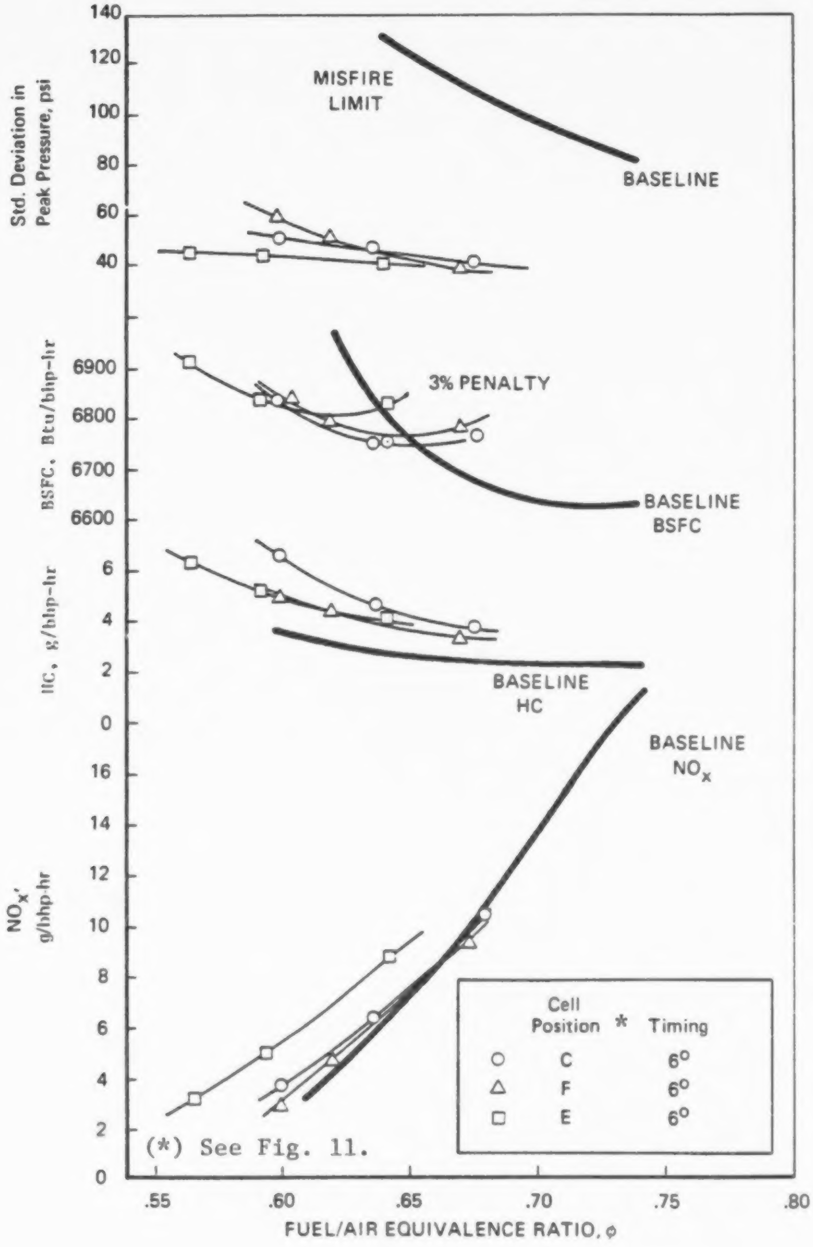

(*) See Fig. 11.

Figure 10 Effect of torch ignition

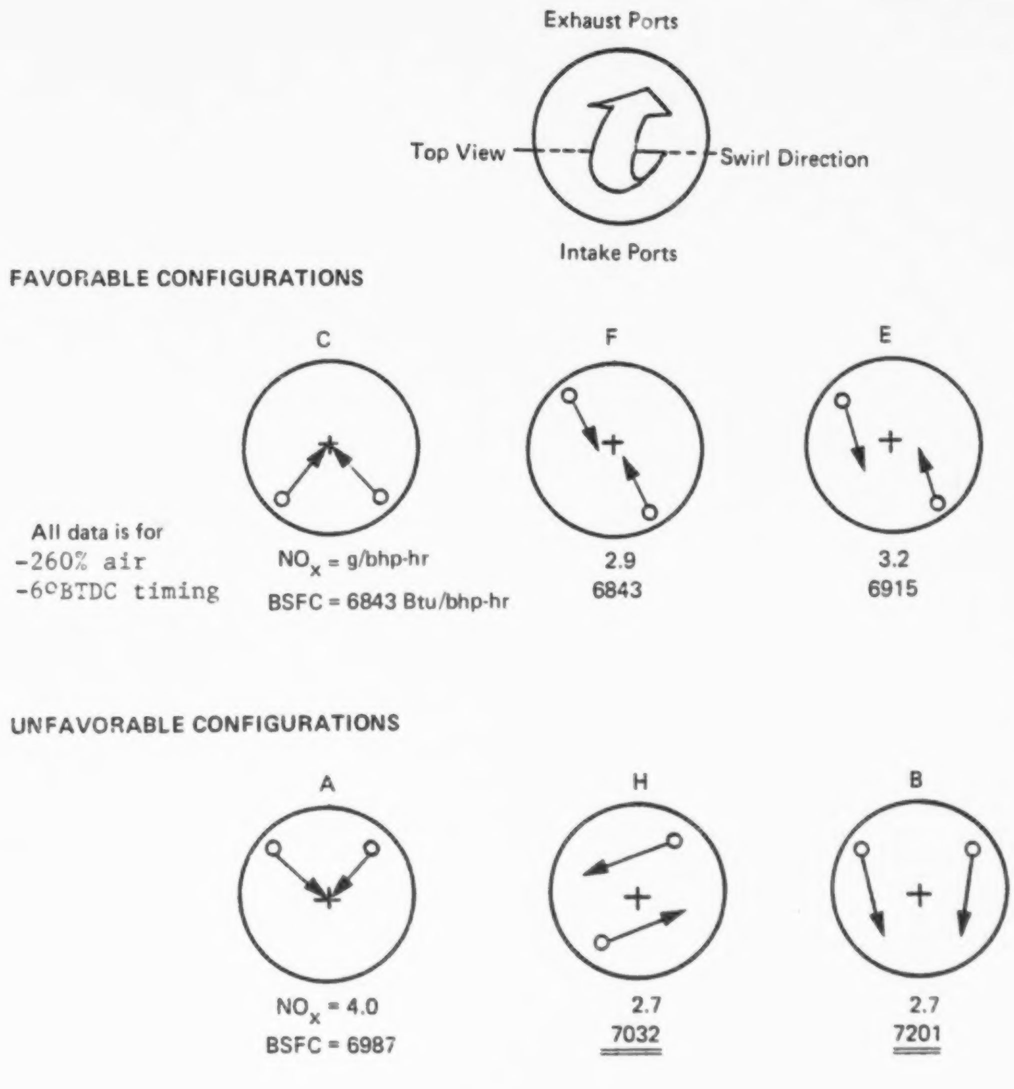
Exhaust Ports
Top View
Swirl Direction
Intake Ports
FAVORABLE CONFIGURATIONS
C
F
E
All data is for
-260% air
-6°BTDC timing
NOx = g/bhp-hr
BSFC = 6843 Btu/bhp-hr
2.9
6843
3.2
6915
UNFAVORABLE CONFIGURATIONS
A
H
B
NOx = 4.0
BSFC = 6987
2.7
7032
2.7
7201

Figure 11 Torch placement configurations

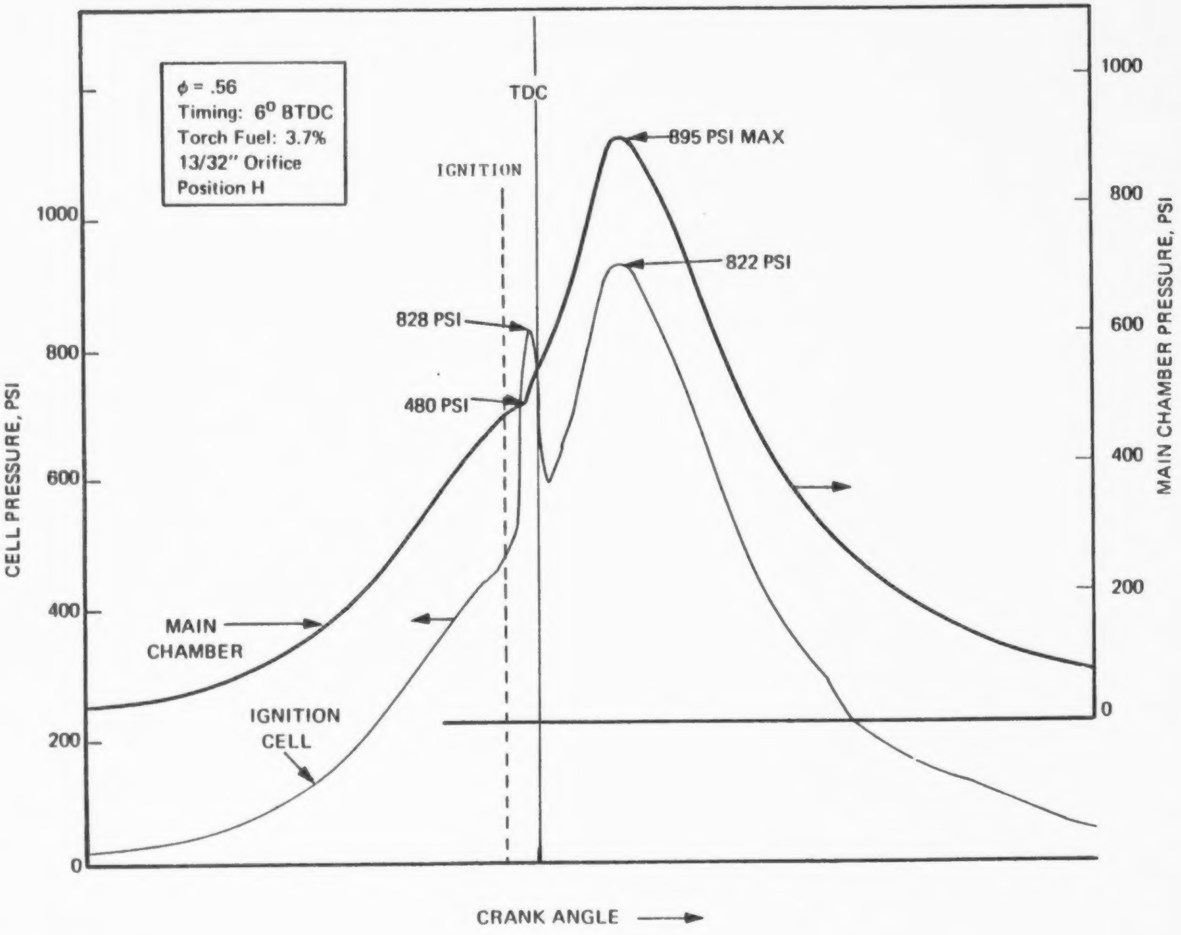

Fig. 12 Ignition cell pressure history

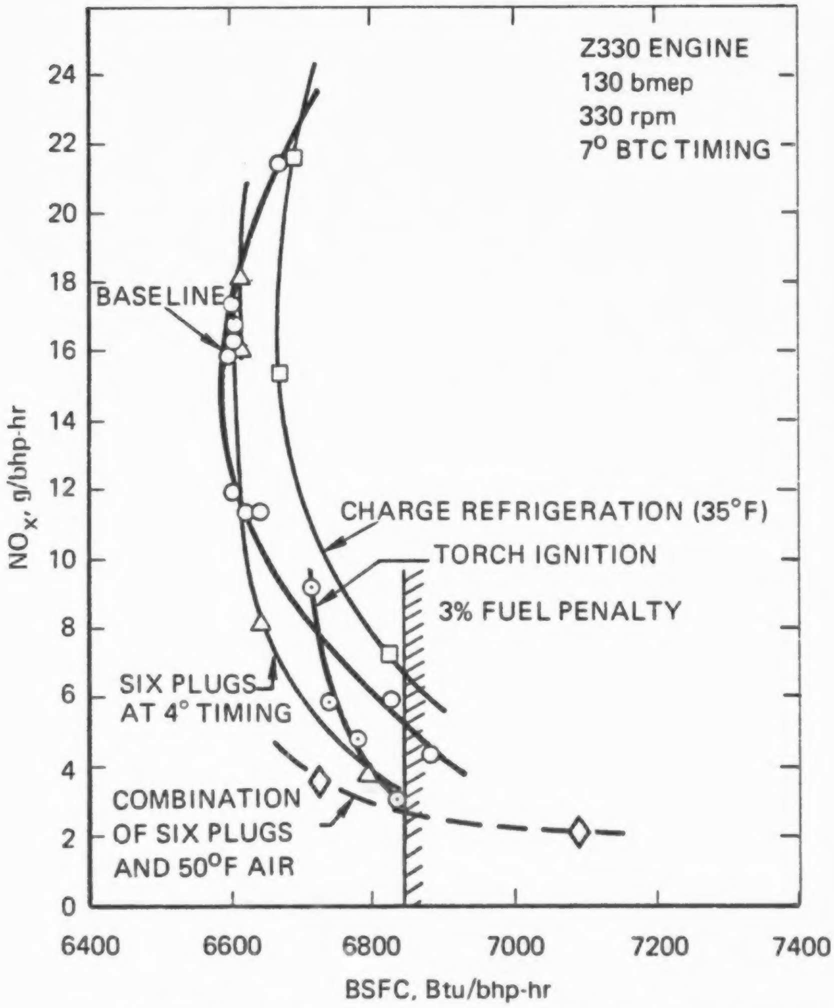

Fig. 13 Combined effect of charge refrigeration and multiple spark

TABLE 1. SPARK-GAS ENGINE MODIFICATIONS SELECTED FOR TESTING

Approach	Engine Modification	Present Results	Earlier Results(4)
Conventional "Tuning"	Spark Location		●
	Gas Valve Location		●
	Piston Shape		●
Lean Burn	Multiple Spark	●	
	Torch Ignition	●	
Stratified Charge	Modified Precombustion Mixing (Modified gas valves)		●
Lower flame temperature	Charge Refrigeration	●	

TABLE 2. EFFECT OF AIR TEMPERATURE ON AIR/FUEL RATIO TOLERABLE WITHOUT MISFIRE

Standard Deviation in Peak Pressure psi	Air Temp., °F	Fuel/Air Equivalence Ratio, ϕ	NO_x g/bhp-hr
100	110	0.667	12.5
	70	0.704	14.0
	50	0.714	13.5
	35	0.735	14.0
125	110	0.645	7.0
	70	0.670	9.5
	50	0.680	9.0
	35	0.700	9.2
140	110	0.625	5.5
	70	0.653	7.5
	50	0.671	7.5
	35	0.690	7.5

Note: All ϕ and NO_x values interpolated from actual test data.

TABLE 3. COMPARISON OF NO_x REDUCTION METHODS

Configuration	Lean Limit Characteristics			Selected Performance at Lean Limit	
	Fuel/Air Equivalence Ratio (ϕ)	Std. Deviation of Peak Pressure, psi	Comments	NO_x, g/bhp-hr	BSFC, Btu/bhp-hr
Baseline (normal operation)	0.69	90	Well above lean limit	13.0	6650
Lean Operation	0.65	120	Misfire limitation	7.0	6800
Modified Gas Valve	0.63	120	Smaller valves reduced misfire and improved bsfc	6.5	6680
Charge Refrigeration					
70°F	0.67	125	Misfire limit	9.5	6740
50°F	0.69	125	Misfire limit	9.0	6800
35°F	0.70	125	Misfire limit	9.2	6790
Multiple Spark (six plugs) with Retarded Timing	0.62	100	Eliminates misfire but turbocharger capacity limit remains	4.0	6800
Combination of Charge Refrigeration (50°F) and Multiple Spark	0.64	129	Just above tolerable misfire limit; no turbocharger limit	3.9	6720
Torch Ignition	0.59	40	Eliminates misfire, but turbocharger capacity limit and incomplete combustion remain.	2.9	6840

EMISSION CONTROL METHODS FOR LARGE STATIONARY ENGINES:
PART II COMBUSTION MODIFICATIONS FOR DIESEL ENGINES

By:

Robert P. Wilson, Jr.
Arthur D. Little, Inc.
20 Acorn Park
Cambridge, Massachusetts 02140

ABSTRACT

An experimental program was conducted on a four-stroke, turbocharged 11-inch bore diesel engine in order to evaluate methods for emission reduction. The tests reported herein covered water/fuel emulsion and exhaust gas recirculation (EGR). The principal finding was that NO_x could be reduced 45-50% at full load by application of either EGR (at 15% by volume) or water/fuel emulsion (at W/F = 50% by volume). The low-energy emulsor proved just as effective as the high-energy emulsor, and it was found that surfactants were unnecessary. Smoke was reduced substantially at moderate water levels. Tests of the EGR/emulsion combination showed that the increased smoke associated with EGR could be controlled by emulsion-firing.

This paper has been prepared under Contract No. 68-02-2664 under the sponsorship of the U.S. Environmental Protection Agency, and covers work completed during the period March 1980 through November 1981.

1.0 INTRODUCTION AND SCOPE OF TESTS

Stationary applications of medium-speed diesel engines, such as oil drilling and electric power generation, account for an estimated 1.3% of the fuel usage and 8% of the NO_x emissions of U.S. stationary sources. Although emission control efforts for large-bore diesel engines are primarily directed toward reducing NO_x, smoke and hydrocarbon emissions (especially polycyclic aromatics) are also of concern for diesels. Most diesel NO_x control methods reduce the intensity of combustion and therefore increase smoke and unburned hydrocarbon (UHC) emissions.

Modest reductions in NO_x from uncontrolled levels can be achieved by retarded timing, which generally carries a fuel consumption penalty and is limited by excessive exhaust temperatures. The engine experiments reported below were undertaken in an EPA-sponsored program aimed at exploring other diesel combustion modifications which show potential for reducing NO_x without incurring significant fuel consumption penalty (or increases in CO, HC, or particulate emissions).

Table 1 shows the diesel engine modifications that were tested in this program. These modifications were based on three guidelines for NO_x reduction: (a) to delay the start of combustion and modify the fuel spray so as to reduce the early burn rate, (b) to lower the flame temperature by the use of diluents such as EGR and water, and (c) to accelerate the later stage of burning to prevent extended combustion duration. The rationale for this approach is that the first fuel elements to burn are thought to be the most NO_x-productive, not only because they exist the longest at high temperature, but also because they experience compression heating when the rest of the mixture burns. Therefore, to reduce NO_x, attempts are made to delay the ignition of the early-burning elements (by injection retard) and reduce the flame temperatures by mixture alteration (exhaust gas recirculation (EGR)) or water injection. The ideal burning profile for minimizing NO_x would accelerate the burning rate during the later stages of combustion to compensate for reducing the rate of early burning, as pointed out by Murayama et al. (1). For detailed discussions, see Wilson (2) and Kau et al. (3).

2.0 EXPERIMENTAL TEST ARRANGEMENTS

NO_x reduction methods were tested on a four-stroke turbocharged single-cylinder engine, the Model PA-6 of S.E.M.T. design. This engine is representative of medium-speed diesel engines with regard to engine speed, compression ratio, injection system design, and combustion chamber design. Key characteristics of the engine are:

- Displacement: 1090 $in.^3$ (11 in. bore, 11.4 in. stroke).
- Compression ratio: 11.8/1.
- Rated power: 350 bhp @ 1000 rpm.
- Rated brake mean effective pressure (bmep): 270 psi at full load.

- Reference injection system: 20-mm plunger, 8 x 0.50-mm nozzle. (A larger plunger and nozzle are standard on production engines.)

- Piston shape: Mexican hat.

- Standard injection timing (mechanical): 23.5 degrees btdc (16 degrees btdc actual).

All testing was done utilizing a No. 2 diesel fuel of 84.6% carbon, 13.6% hydrogen, and cetane index of 59.5. Additional information on the emissions and cylinder pressure instrumentation is available (4).

3.0 SYNOPSIS OF PREVIOUS RESULTS

In order to place the new EGR and emulsion test results in perspective, a brief summary of prior results (5) is given below.

3.1 Baseline

During the first test series, engine performance and emissions characteristics were determined at two-thirds and full load, at rated (1000) rpm, and at several timings. At standard timing for best fuel consumption (23.5° btdc), NO_x was 10.4 g/bhp-hr and fuel consumption was 180 g/bhp-hr. The fuel consumption for this single-cylinder research engine was about 17% higher than for the multicylinder production engine. This was primarily due to additional friction losses, and secondarily due to the smaller injection pump and nozzle configuration selected for the baseline. Since the NO_x/bsfc characteristics are representative of large-bore diesel engines, the PA-6 seems to be appropriate as a test engine. Under baseline conditions, the smoke level was 0.5 Bosch number, and particulate mass was in the range of 40 to 60 mg/m^3.

The NO_x emissions and fuel consumption of the PA-6 are strongly influenced by the timing of the start of injection. The NO_x can be reduced 28% by retarding the (actual) start of injection from 18 to 10 degrees btdc (about 4% per degree). However, due to late burning, this is not a feasible NO_x control method; with 8 degrees retard, the exhaust temperature exceeds the 650°C limit for this engine and the fuel penalty is about 7% (about 0.8% per degree of retardation, on the average).

3.2 High Injection Rate

The objective of high injection rate was to deliver the fuel to the combustion chamber in less time, but with minimum disturbance to the spray characteristics and to the dynamic response of the high pressure fuel line. The basic PA-6 fuel system was modified to increase the injection rate by increasing the plunger diameter, shortening the effective stroke of the fuel pump, and exchanging the nozzle for one with larger orifices. Seven combinations of plungers and nozzles were tested, which would increase the rate up to 40% for an ideal incompressible fluid. The actual increase in rate was less; this fuel system had very "soft" characteristics and suffered from needle bounce and secondary injection.

High injection rate combined with retarded timing did not reduce NO_x without a fuel consumption penalty at full load. Secondary injection handicapped the performance of the high-rate fuel configurations by taxing the cycle efficiency (bsfc) with a portion of late-burning fuel.

At two-thirds load, NO_x was reduced by about 5% at fixed bsfc by using the 24-mm plunger (8 x 0.6 mm nozzle). However, this reduction became insignificant at retarded timing.

3.3 Pilot Injection

In interpreting the pilot injection effects, the extended duration of injection must be taken into account. The pilot fuel injection system was "softer," resulting in an increase in the duration of injection from 32 degrees to about 42 degrees. Furthermore, the modified fuel injection occurred in two stages (33° and 9° duration). The secondary injection of fuel had a pronounced effect on engine characteristics: bsfc increased about 5%, maximum cylinder pressure dropped about 7%, exhaust temperature increased 35°C, and smoke increased about 1 Bosch unit. The effect was comparable to retarded timing.

The pilot quantity was varied from 2 to 17% of the total fuel per cycle. In general, pilot quantities below 6% were most effective; larger pilot quantities degraded bsfc when combustion occurred prior to top dead center (minimum volume).

At full load, most runs with pilot injection did not improve the bsfc or NO_x characteristics. A few runs with 40 degrees advance and pilot quantity in the 1-4% range did reduce NO_x by 10-15%, but the trend was not consistent.

The use of a common injector for pilot and main charge presumably explains why the NO_x reductions with pilot injection were no greater than with retarded timing alone.

4.0 WATER/FUEL EMULSION

The water/fuel (W/F) emulsion system used on the PA-6 tests is shown in Figure 1. In this system, water and fuel flows were metered independently (by weigh scale) and mixed in a tee to provide any predetermined water/fuel ratio. Downstream of the tee, the mixture of water and fuel was emulsified on-line using one of two emulsors:

- Hydroshear--a low energy emulsor (pressure drop about 150 psi) consisting of a conical shear-producing cavity. The water/fuel mixture entered the cavity in a tangential direction, and was emulsified by fluid shear forces.

- Gaulin--a high energy emulsor (pressure drop about 2000 psi) which expanded the water/fuel mixture through a small orifice, producing an emulsion.

Both emulsors were as close to the injection pump as practical to minimize separation or "slugging" of the unstabilized emulsions before injection. Photomicrographs suggested that the Gaulin-produced emulsion contained water elements of about 1-3 micron size; whereas ,the Hydroshear water elements were several times larger. The fuel return line was piped into a tee at the emulsor inlet to re-emulsify the water/fuel mixture after every pass through the injection pump. In general, the emulsion recirculation rate through the emulsor was 3-10 times the engine consumption rate.

The emulsion test matrix included the following parameters:

- Type of emulsor (Hydroshear, Gaulin).
- Water/fuel ratio (7, 13, 27, and 45% by volume).
- Injection system capacity (20, 22, and 24-mm plungers with nozzles ranging from 8 x 0.50-mm to 9 x 0.60-mm).
- Timing (15 to 21.5 degrees btdc, mechanical).
- Load (two-thirds and full load).

This matrix was designed to investigate the practical limits of operation with emulsions.

The typical effect of substituting an emulsion for straight diesel fuel at constant timing and load is illustrated by Figure 2. This figure is for the Hydroshear emulsor at full load, but comparable results were observed for all variations of load, timing, and emulsor type. A 24-mm plunger was used here (instead of the 20-mm standard plunger) to allow adequate maximum fuel delivery at full load with at least 45% water in the fuel (by volume). Key conclusions drawn from Figure 2 are:

- At constant timing, NO_x was typically reduced 35-45% by emulsions of 50% water/fuel ratio by volume.
- At constant timing, bsfc apparently was reduced by 2.5-5.0% at 50% W/F ratio by volume.
- The low energy emulsor (Hydroshear) yielded comparable results to the high energy emulsor (Gaulin).

Bosch smoke index was decreased with increased water/fuel ratio.

Typical results from the present study are normalized and compared to the medium-speed engine data of other investigators in Figure 3. At low water/fuel ratios (e.g., up to 30%), the reductions in NO_x and bsfc are in very good agreement with data generated by Taylor(6), Bastenhof and Genot,(7) and Herrmann and Magnet(8) on large-bore diesels. At high water/fuel ratios (i.e., 50-60% W/F by volume), where there was no prior data on medium speed engines, the present study has demonstrated reductions of NO_x in excess of 60% at part load. The effectiveness of emulsions at such high water contents and at part load engine operation agrees with earlier data for high speed diesel engines.(9)

The combined effect of W/F emulsion and retarded timing on the NO_x versus bsfc tradeoff is quite favorable (see Figure 4, in which the two dependent variables are cross-plotted for various timings). By retarding timing about 2°CA and increasing the W/F ratio to approximately 50%, NO_x decreased by 40-50% without a fuel consumption penalty. Even more substantial NO_x reductions were observed at two-thirds load with the standard injection system (see Figure 5). Here NO_x was reduced by up to 60% without a fuel consumption penalty.

These results can be qualitatively explained, based on expected physical effects of the emulsion on the diesel combustion process:

(1) The added water vapor increases the specific heat of the products of combustion, lowering the flame temperature.

(2) The flame-zone oxygen is diluted with water vapor, curtailing the NO-formation reaction and lowering the flame temperature.

(3) Secondary atomization of the fuel may occur as a result of the differential vapor pressures.

The third mechanism is perhaps the most interesting, because of its potential to explain the increased burning rate and suppressed smoke formation that were observed. Data that supports the theory of improved atomization with emulsions is shown in Figure 6, which is a direct comparison of the heat release profiles generated from cylinder pressure data for various water/fuel ratios at identical load and timing. It shows that increasing W/F ratios increases ignition delay and maximum rate of heat release, and shortens the total combustion duration .

Water/fuel emulsions apparently increased the ignition delay, as illustrated in Figure 7. Ignition delay was increased approximately 2 degrees CA per 10% water added to the fuel, consistent with data reported by Cook and Law(10), Murayama et al.(11), and Greeves, Khan, and Onion(12). Possible mechanisms of increased ignition delay include: (a) reduced post-compression compression gas temperatures (due to latent heat loss), and (b) H_2O inhibition of autoignition kinetics (Dryer(13)).

Associated with the increased ignition delay period, the maximum rate of pressure rise also increased with water/fuel ratio. Typically, the rate of pressure rise increased 1.5 bar/°CA for every 10% water added to the fuel by volume. No audible knock or structural damage was noticed with as much as 60% water by volume. Peak cylinder pressures were nearly constant for all water contents.

Two injection pump seizures were observed; these seizures were attributed to metal particles originating from a damaged Hydroshear emulsor unit. Other pump seizures occurred during start-up or load change, presumably because operational procedures caused "slugging." For example, it was essential to run on pure No. 2 diesel fuel prior to engine shutdown in order to prevent pump seizure upon start-up. No pump seizures were observed during continuous steady-state operation. However, pump leakage increased by 50%, and some possible signs of cavitation erosion were observed on the plunger at the conclusion of a 50-hour run. No evidence of water was found in the engine lube oil during the testing. Long term tests of emulsions are recommended in view of the favorable NOx/bsfc effects observed in the present tests.

5.0 EXHAUST GAS RECIRCULATION

The exhaust gas recirculation (EGR) system used in the study is shown in Figure 8. A fraction of the exhaust gas was extracted from the turbocharger exit stream and was diverted to a water scrubber for particulate removal. The scrubber was a venturi water-impaction type operating at a pressure drop of 0.10-0.12 bar, with a specification of 92-97% particulate removal efficiency for 0.2-1.0 micron particles. The cleaned EGR gas was then cooled to standard inlet air temperature (about 60°C) and mixed with the inlet air stream. The fraction of EGR in the inlet mixture was calculated by measuring the concentration ratio of CO_2 in the EGR and inlet air streams. The concentration ratio of NO was also measured as a check. These two independent measurements agreed to within a fraction of 1 percent EGR.

Corrosion coupons, placed at key locations in the EGR, inlet, and exhaust systems, qualitatively measured the accumulation of soot and corrosion.

The effects of EGR at full load and constant timing are shown in Figures 9 and 10. (In the latter, the data is normalized to reference values obtained at zero EGR.) Key findings are:

- There is a "knee" in the bsfc vs. EGR curve at about 10-15% EGR, above which EGR becomes prohibitively costly in terms of fuel consumption.
- Typically, at the optimum value of 14-15% EGR (by volume) in the inlet mixture, NO_x was reduced by 45-55%.
- The side effects were marginally tolerable at this level of EGR (bsfc increased by 3-4% and the Bosch smoke index was below 2.5).

The NO_x reductions found in the present study are compared to data reported by previous investigators in Figure 11. In this figure, the oxygen concentration in the trapped volume just before injection is plotted along the axis rather than the EGR fraction, to permit comparison with theory.(14) The broken line represents calculated theoretical reductions in the rate of

NO formation based on the following assumptions about NO formation (see Wilson et al.(14)):

- The rate of formation of NO rises exponentially with temperature.
- The flame-zone temperature (the primary NO-formation region) is the adiabatic temperature, which is related to the oxygen mass fraction according to the droplet diffusion flame theory.

The net result of this theory is that the relative rate of NO formation in the diffusion flame is reduced by the lower available oxygen in an EGR mixture. As shown in Figure 11, the previously observed data and calculated theoretical NO_x reduction corroborate the present results.

As expected, EGR does improve the NO_x versus bsfc tradeoff with retarded timing, as shown in Figure 12. By retarding timing slightly (2 degrees CA) and adding 15% EGR, NO_x can be reduced from 10.8 to 5.2 g/bhp-hr with under 4% bsfc penalty.

Although EGR can be extremely effective in reducing NO_x at higher levels of EGR in the inlet mixture, practical limitations on the maximum feasible amount of EGR include: (a) smoke emissions, (b) fuel consumption penalty, (c) excessive turbine inlet temperatures (aggravated by late burning), (d) excessive scrubber requirements to prevent soot accumulation in the intercooler and turbocompressor, and (e) power requirements for the EGR system. On two occasions during the testing, inadequate water flow to the scrubber severely packed the intercooler within hours.

6.0 COMBINED EGR AND W/F

Results of the previous section indicate that EGR can be effective in reducing NO_x emissions but suffers from severe smoke and bsfc penalties at EGR concentrations above 15% in the inlet mixture. Recalling the benefits of water/fuel emulsion (namely, reduced NO_x, reduced bsfc, and reduced smoke), these two methods were combined in an attempt to cure the smoke and bsfc problems of EGR. Water spray in the intake manifold was also attempted as a remedial measure to the smoke and bsfc problems.

Figure 13 shows the effect of combined EGR and emulsion on the NO_x, bsfc, and smoke. In general, the combination was quite beneficial at part load but did not improve the bsfc/smoke/NOx relationship at full load. Typically, in previous tests with 20% EGR alone, NO_x was reduced to 1.7-3.2 g/bhp-hr with an 8% bsfc penalty and a 350% increase in smoke. This was the case at both two-thirds and full load. At two-thirds load, by combining a 44% W/F emulsion with 20% EGR, the same NO_x reduction (to 1.9 g/bhp-hr) was achieved with only 3% bsfc penalty and no smoke increase. However, at full load, 11% W/F emulsion did not reduce smoke at moderate EGR levels, so higher W/F ratios were not attempted. The engine was reduced to 93% load for a 50-hour endurance test with 18.5% EGR and 25% W/F emulsion. This test showed no obvious plugging or coating of intercooler or turbocompressor surfaces. For the duration of the test, NO_x remained at 2.5 g/bhp-hr and bsfc at about 187 g/bhp-hr.

Water spray was found to be half as effective as emulsion for a given amount of water, and entailed smoke and fuel consumption penalties. For example, a spray of 60% W/F ratio reduced NO_x only 25-35% with a 3.4% fuel penalty.

7.0 SUMMARY

The comparative effectiveness of six emission control methods is illustrated in Figure 14, which plots two dependent variables (NO_x and bsfc) for various levels of timing. Making the arbitrary premise that the maximum tolerable bsfc penalty to achieve NO_x control would be 4%, Table 2 summarizes the levels of NO_x which could be achieved based on the Model PA-6 engine tests.

The most effective NO_x-reduction approach for full-load engine operation was water/fuel emulsion, which produced a 58% NO_x reduction on the Model PA-6 engine when combined with retarded timing. Other significant findings with water/fuel emulsion were that: (a) a 50% NO_x reduction could be obtained with no fuel consumption penalty, (b) the low-energy emulsor proved just as effective as the high-energy emulsor, (c) surfactants were unnecessary for the on-line emulsifications system on No. 2 diesel fuel, (d) smoke was reduced substantially at moderate water levels, and (e) emulsion firing apparently increases burning rate and decreases combustion duration. Long term endurance tests with emulsions are needed to resolve questions of water compatibility with the fuel system. Any practical application of emulsions to diesel engines would require substantial fuel system optimization.

Exhaust gas recirculation (EGR) was nearly as effective as water/fuel emulsion, reducing NO_x by 51% at full load (within the 4% fuel penalty). The optimum amount of EGR was 14-15% by volume, above which smoke and fuel consumption were excessive. Apart from fuel consumption and smoke increases, other practical aspects of EGR include: (a) the scrubber (required to prevent soot accumulation in the intercooler) and (b) power requirements of the EGR system.

The combination of EGR and water/fuel emulsion was shown capable of NO_x reductions in excess of 75% at 66-93% load. Apparently, the emulsion cures the smoke and burn-time problems of EGR.

NO_x reductions were under 30% ,with either pilot injection or increased rate of injection results nearly matched by simple retarded timing. These results were attributed to limitations in the design of the modified experimental fuel system.

ACKNOWLEDGEMENTS

John H. Wasser, the EPA Technical Project Officer, has contributed substantially to the project, in part based on his experience derived from EPA in-house diesel engine tests. I also wish to acknowledge several individuals at the Fairbanks Morse Division of Colt Industries (Eugene Kasel, Dennis Bachelder and the late Charles Newton) and at Societe de-'Etudes de Machines Thermiques (S.E.M.T.; Alfred Genot and D. Bastenhof) who have been responsible for the engine tests and the translation of NO_x-control concepts into practical engine hardware. Key contributions to the diesel phase of the project have been made by several members of the project team at Arthur D. Little, Inc. including John Mendillo, Ken Menzies and Larry Richardson. Finally, I wish to acknowledge the work of Maureen Donovan in the preparation of this manuscript.

REFERENCES

1. Mur a yama, T., Miyamoto, N., Sasaki, S., and Kojima, N., "The Relation Between Nitric Oxide Formation and Combustion Process in Diesel Engines," 12th International Congress on Combustion Engines (CIMAC), Tokyo, 1977.

2. Wilson, R. P. Jr., "Emission-Control Concepts for Large-Bore Stationary Engines," EPA Contract No. 68-02-2664, Interim Report on Phase I and Phase II, in print.

3. Kau, C. J., Heap, M. I., Tyson, T. J., and Wilson, R. P., Jr., "Prediction of Nitric Oxide Formation in A Direct Injected Diesel Engine," 16th Symposium on Combustion, p. 337, Combustion Institute, 1976.

4. Wilson, R. P., Jr., Mendillo, J. V., Genot, A., Bachelder, D. L., and Wasser, J. H., "Single-Cylinder Tests of Emission Control Methods for Medium-Speed Diesel Engines," ASME Paper No. 82-DGP-28, Presented at the Energy-Sources Technology Conference & Exhibition, March 7-10, 1982.

5. Wilson, R. P., Jr., "Single-Cylinder Tests of Emission Control Methods for Large-Bore Stationary Engines. In: Proceedings of the Joint Symposium On Stationary Combustion NO_x Control: Vol. IV, EPA-600/9-81-028d (NTIS No. PB81-236143), July 1981.

6. Taylor, D. H., "Exhaust Emissions from Medium Speed Diesel Engines," ISME Conference, Tokyo, November 1978.

7. Bastenhof, D. and Genot, A., "Comment Reduire La Pollution due aux Gaz d'Echappement des Diesels de Forte Puissance," S.E.M.T. Report, January 1977.

8. Herrmann, R. and Magnet, J. L., "Reduction de la Pollution Atmospherique per les Gas d'Echappement des Moteurs Diesel," 12th International Congress on Combustion Engines (CIMAC), Tokyo, 1977.

9. Wasser, J. H., and Statnick, R. M., "Emission Characteristics of Small Stationary Diesel Engines," In Proceedings of the Second Stationary Source Combustion Symposium, Vol. V, EPA-600/7-77-073e (NTIS No. PB 274897), July 1977.

10. Cook, D. H., and Law, C. K., "A Preliminary Study on the Utilization of Water-in-Oil Emulsions in Diesel Engines," Combustion Science and Technology, 1978.

11. Murayama, T., Tsukahara, M., Morishina, Y., and Miyamoto, N., "Experimental Reduction of NO_x/-Smoke and BSFC in a Diesel Engine Using Uniquely-Produced Water (0-80%) to Fuel Emulsion," SAE Paper 780224, 1978.

12. Greeves, G., Khan, I. M., and Onion G., "Effects of Water Introduction on Diesel Engine Combustion and Emissions," 16th Symposium on Combustion, p. 321, Combustion Institute, 1976.

13. Dryer, F. L., "Water Addition to Practical Combustion Systems--Concepts and Applications," 16th Symposium on Combustion, p. 279, Combustion Institute, 1976.

14. Wilson, R. P., Jr., Muir, E. B., and Pellicciotti, F. A., "Emissions Study of a Single-Cylinder Diesel Engine," SAE Paper 740123, 1974.

15. Parker, R. F. and Walker, J. W., "Exhaust Emission Control in Medium Swirl Rate Direct Injection Diesel Engines," SAE Paper 720755, 1972.

16. Bascom, R. C., Broering, L. C., and Wulfhorst, D. E., "Design Factors That Affect Diesel Emissions," SAE Paper 710484-84, 1971.

17. Shahed, S. M., Chiu, W. S., and Yumlu, V. S., "A Preliminary Model for the Formation of Nitric Oxide in Direct Injection Diesel Engines and its Applications in Parametric Studies," SAE Paper 730083, 1973.

18. Marshall, W. F. and Fleming, R. D., "Diesel Emissions as Related to Engine Variables and Fuel Characteristics," SAE Paper 710836, 1971.

19. Walder, C. J., "Reduction of Emissions from Diesel Engines," SAE Paper 730214, 1973.

20. McConnell, G., "Oxides of Nitrogen in Diesel Engine Exhaust Gas: Their Formation and Control," Proc. Inst. Mech. Engrs. 178, 1963.

21. Pischinger, R. and Cartellieri, W., "Combustion System Parameters and Their Effect Upon Diesel Engine Exhaust Emissions," SAE Paper 720756, 1972.

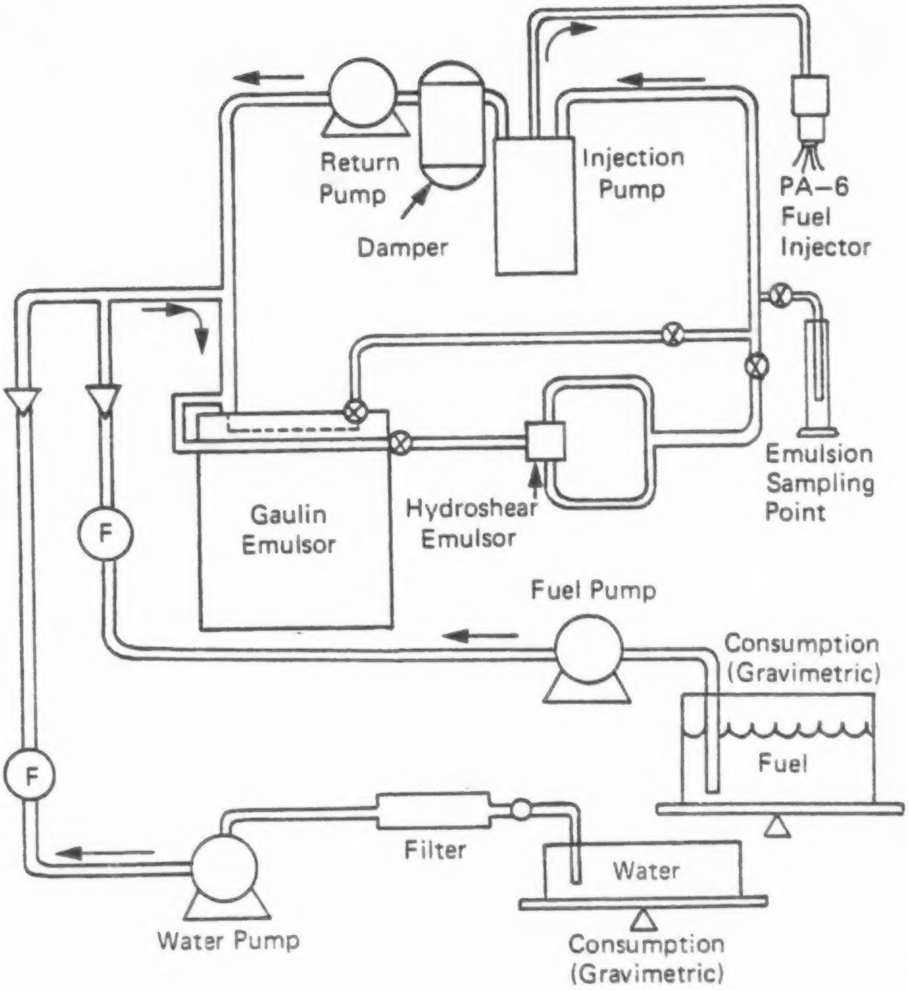
Return Pump
Damper
Injection Pump
PA-6 Fuel Injector
Emulsion Sampling Point
Gaulin Emulsor
Hydroshear Emulsor
F
Fuel Pump
Consumption (Gravimetric)
Fuel
F
Filter
Water
Water Pump
Consumption (Gravimetric)

Figure 1. Emulsifier arrangement

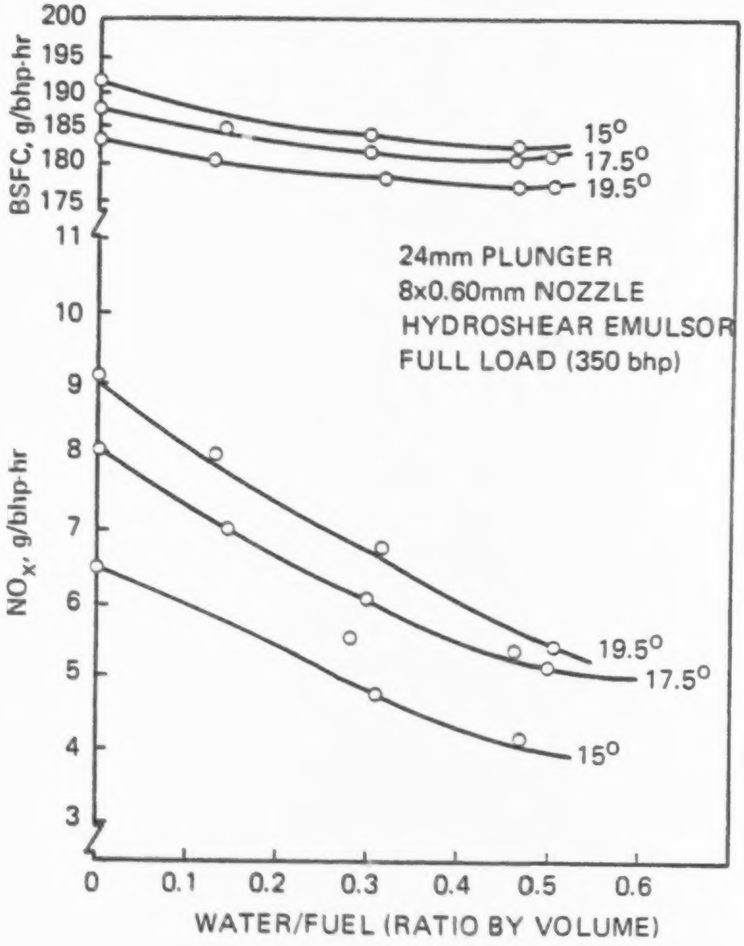

Figure 2. Effect of emulsion

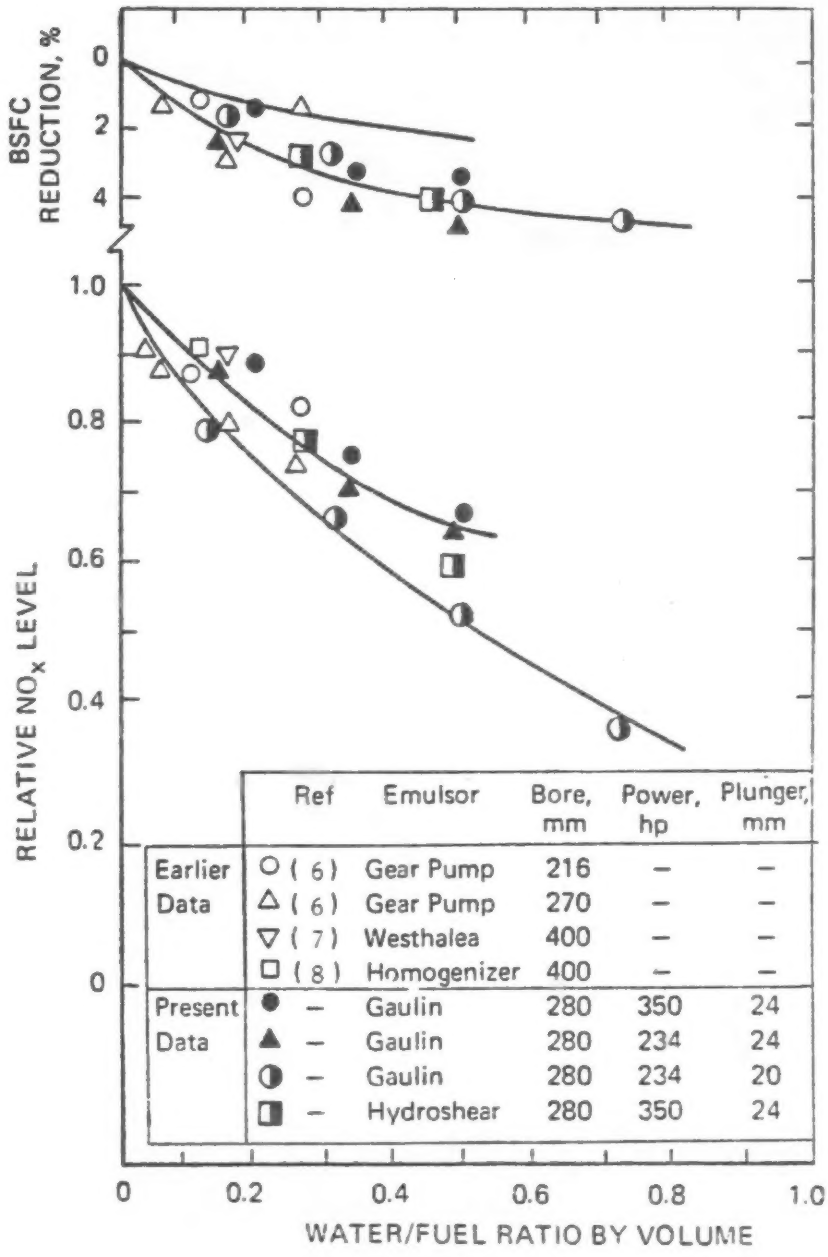

		Ref	Emulsor	Bore, mm	Power, hp	Plunger, mm
Earlier Data	○	(6)	Gear Pump	216	–	–
	△	(6)	Gear Pump	270	–	–
	▽	(7)	Westhalea	400	–	–
	□	(8)	Homogenizer	400	–	–
Present Data	●	–	Gaulin	280	350	24
	▲	–	Gaulin	280	234	24
	◑	–	Gaulin	280	234	20
	◨	–	Hydroshear	280	350	24

Figure 3. Effect of emulsions on medium-speed diesels (400-1000 rpm)

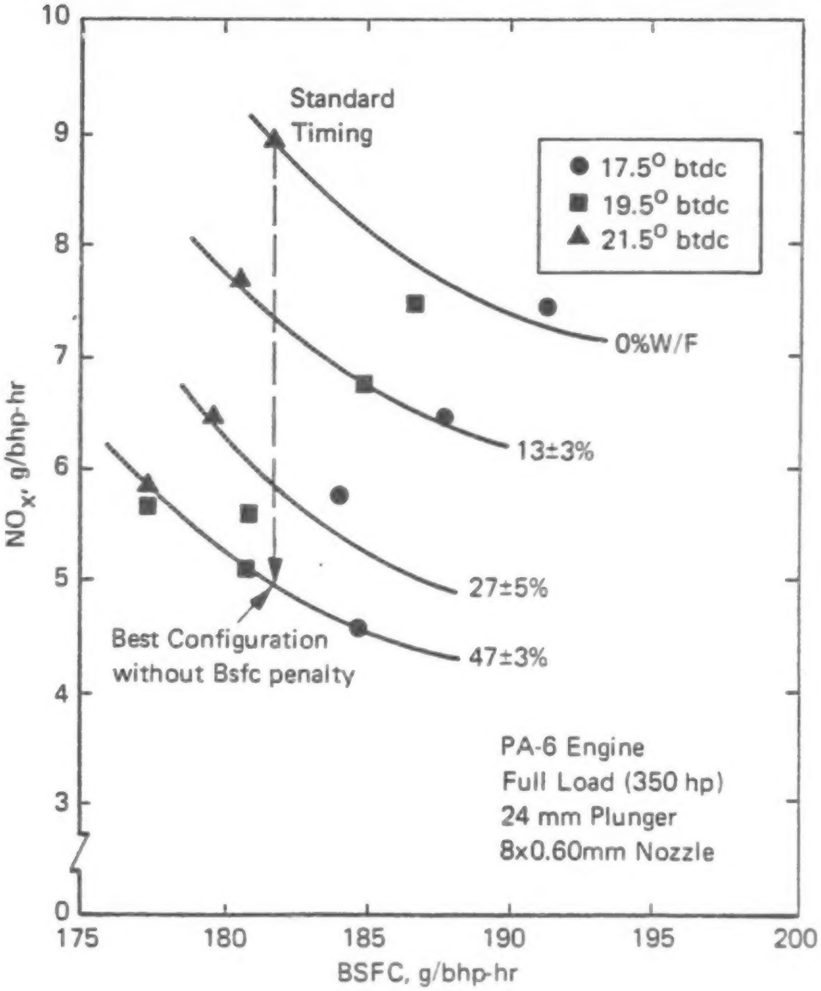

Figure 4. Effect of emulsion with variable timing (full load)

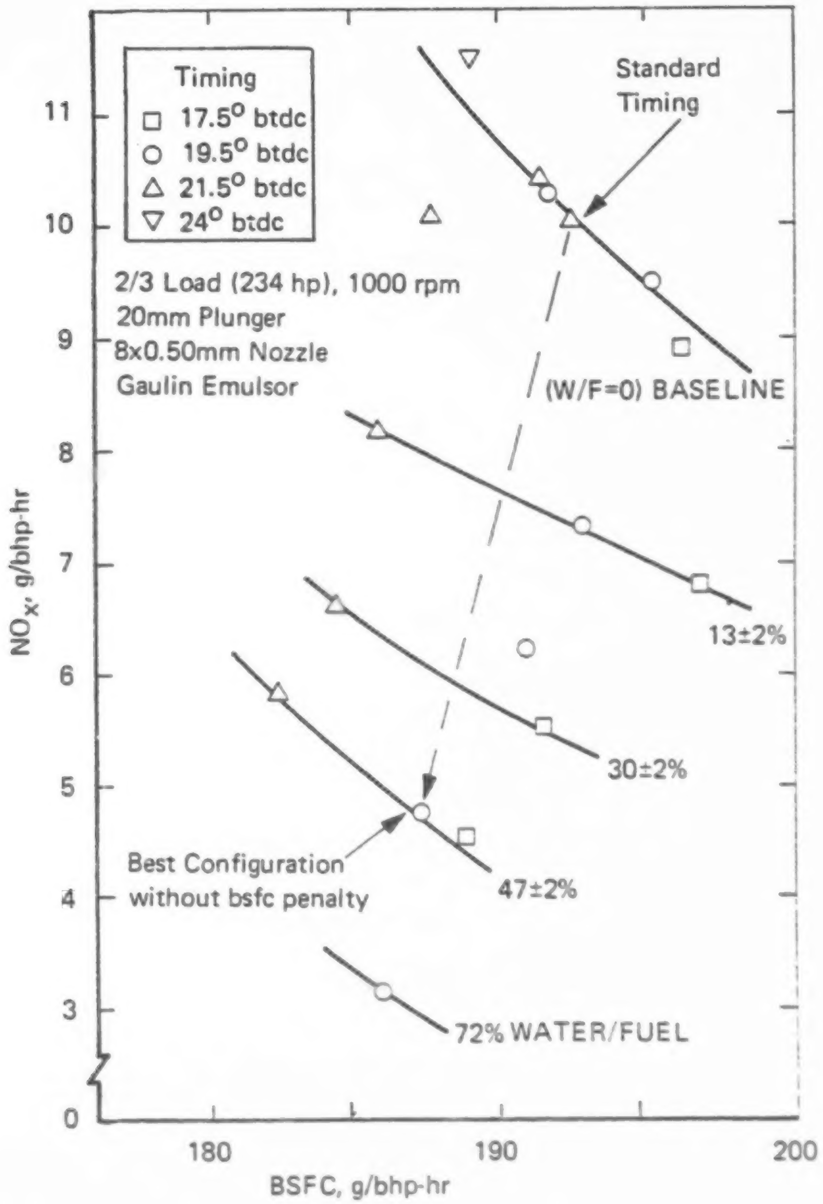

Figure 5. Effect of emulsion with variable timing (two-thirds load)

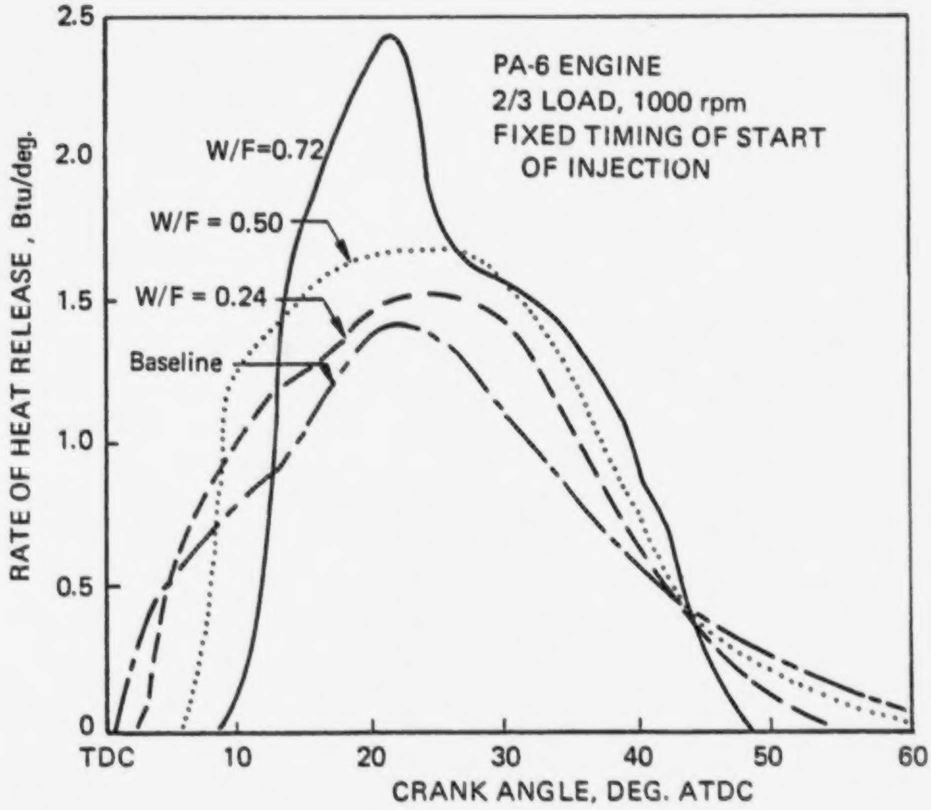

Figure 6. Effect of water/fuel ratio on rate of heat release

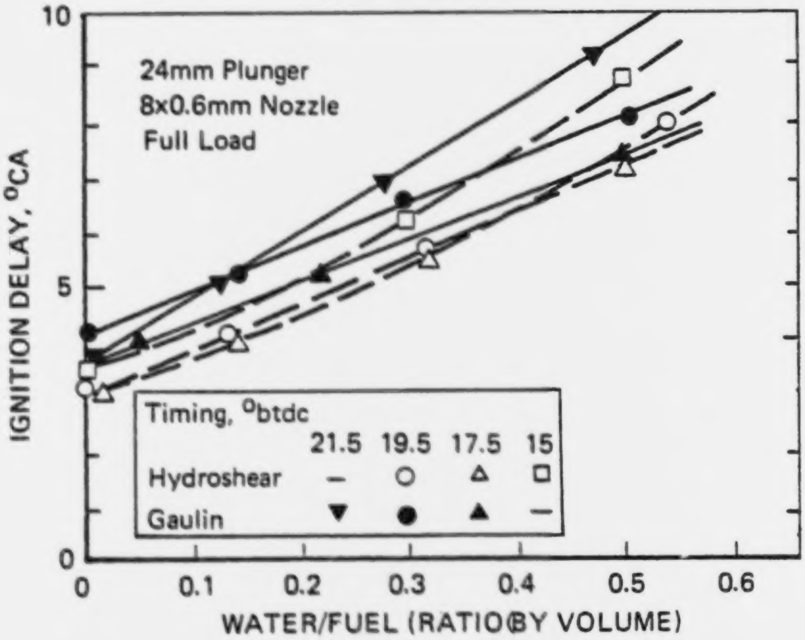

Figure 7. Effect of water/fuel ratio on ignition delay

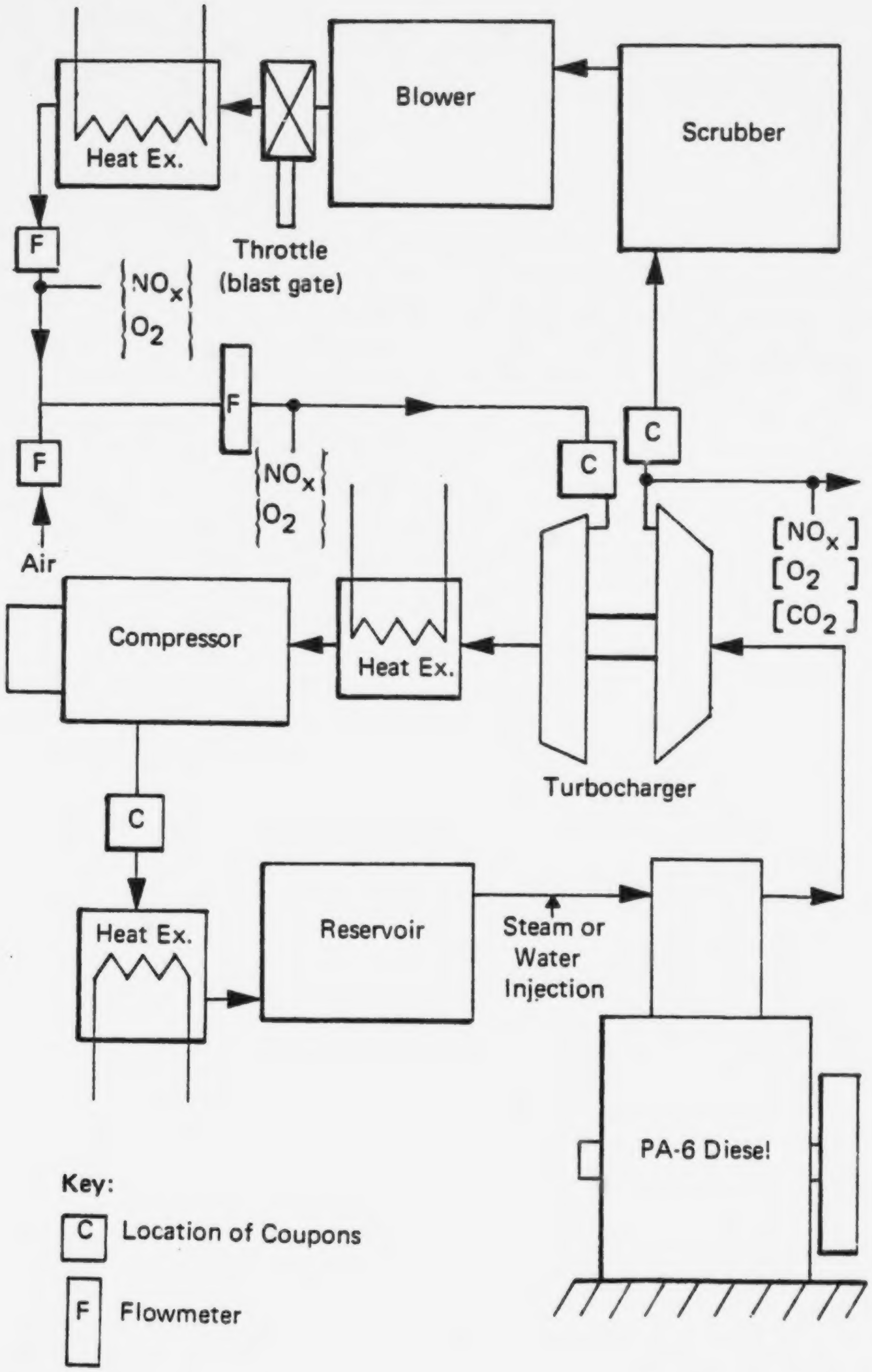
Heat Ex.
Blower
Scrubber
Throttle (blast gate)
F
NO_x
O_2
F
F
NO_x
O_2
C
C
Air
Compressor
Heat Ex.
Turbocharger
NO_x
O_2
CO_2
C
Heat Ex.
Reservoir
Steam or Water Injection
PA-6 Diesel
Key:
C Location of Coupons
F Flowmeter

Figure 8. EGR test setup

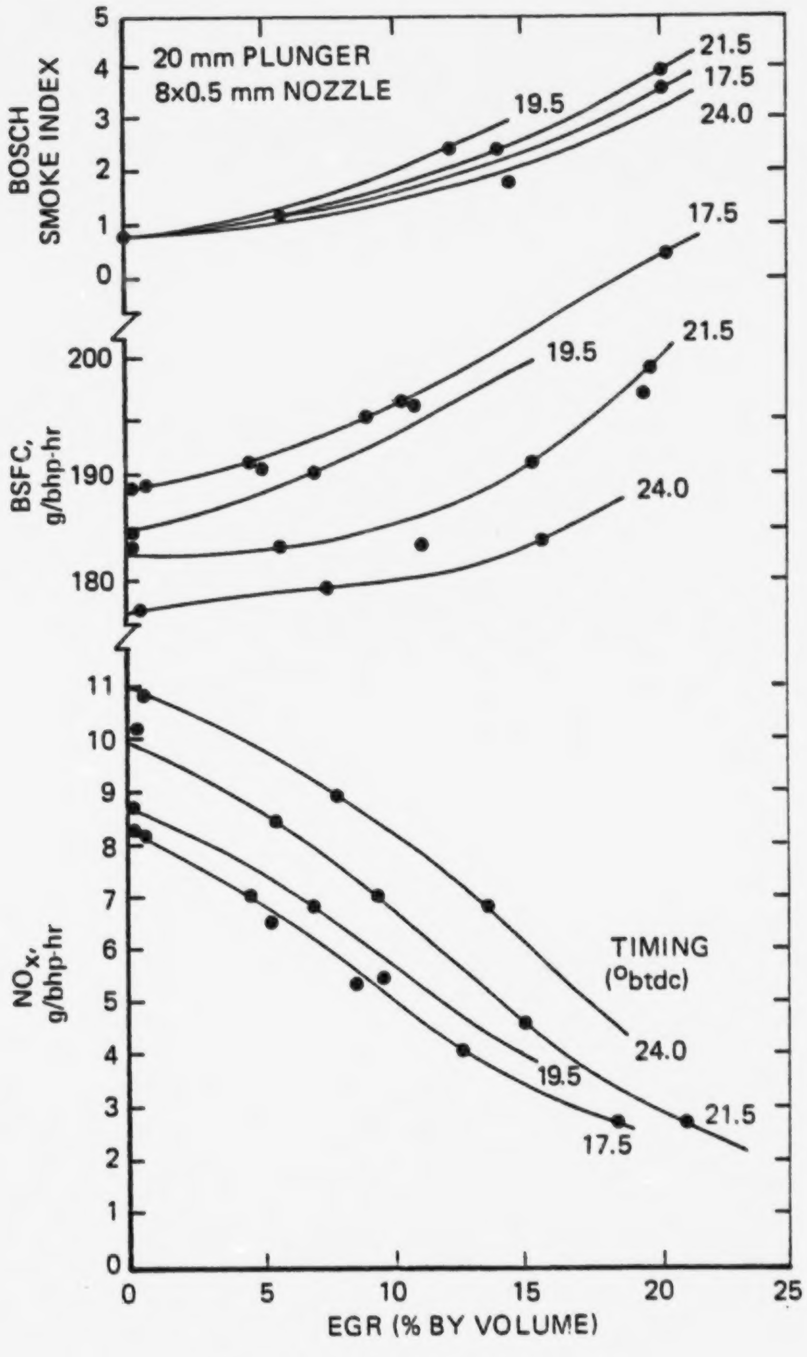

Figure 9. Effects of EGR at full load

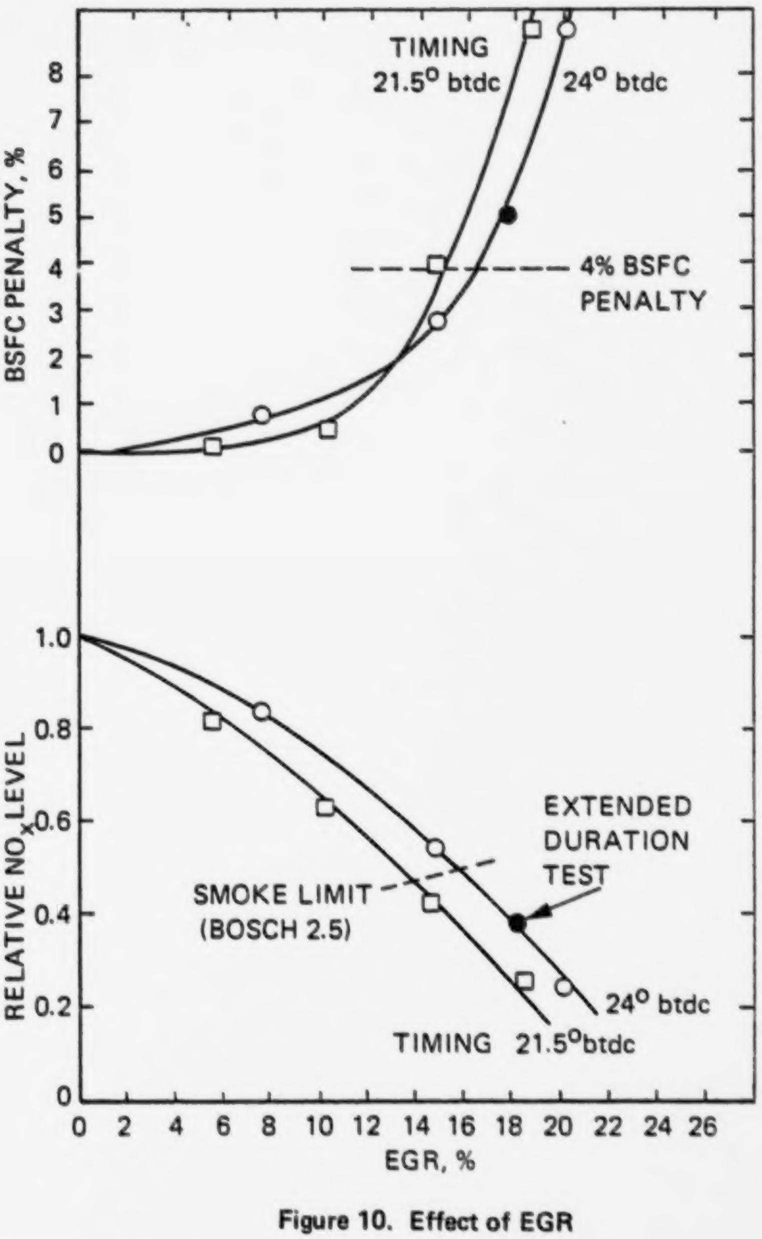

Figure 10. Effect of EGR

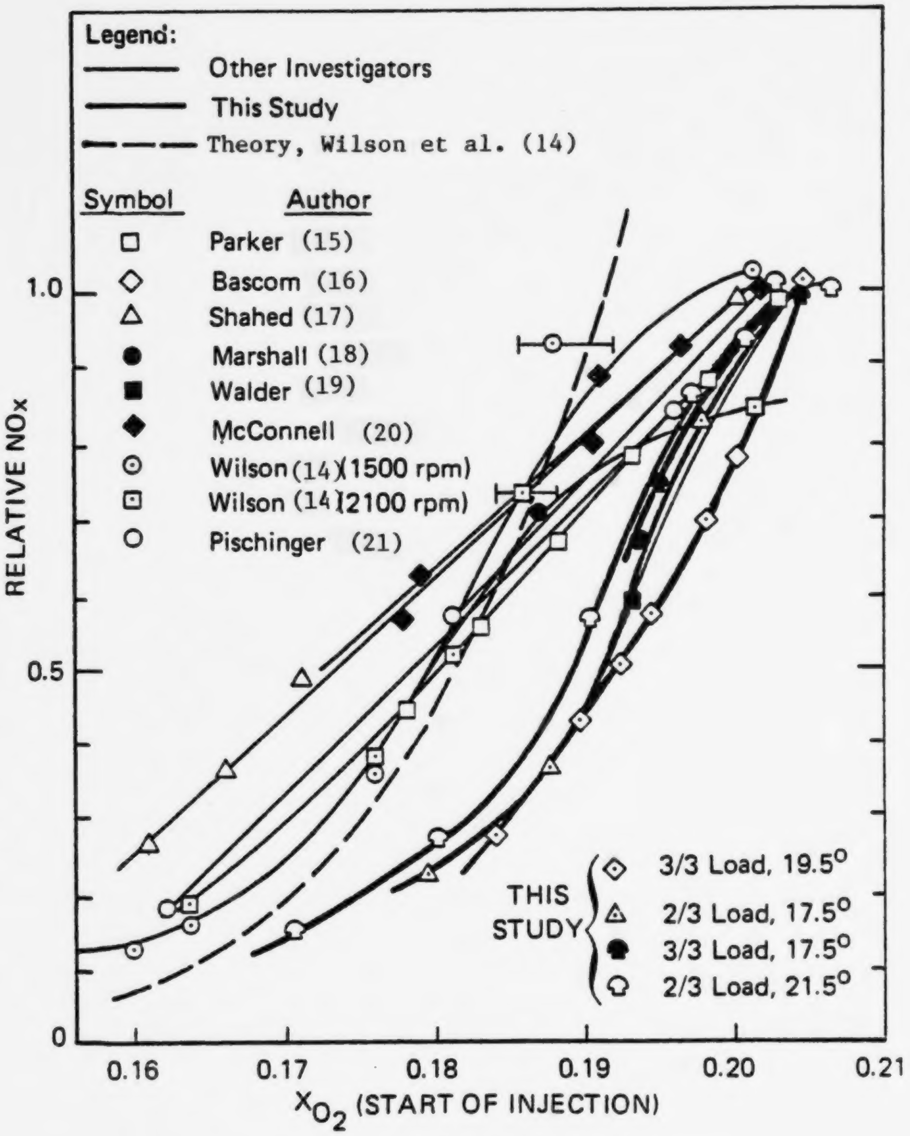

Figure 11. Effect of EGR (previous studies)

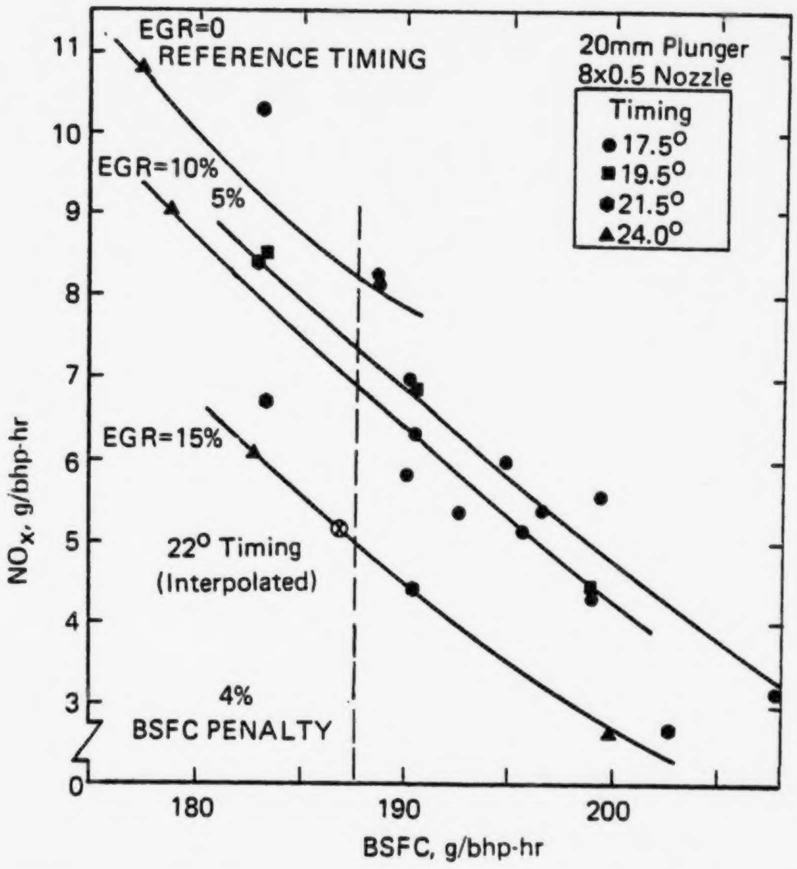

Figure 12. Effect of EGR on the NO_x/BSFC Tradeoff, with retarded timing

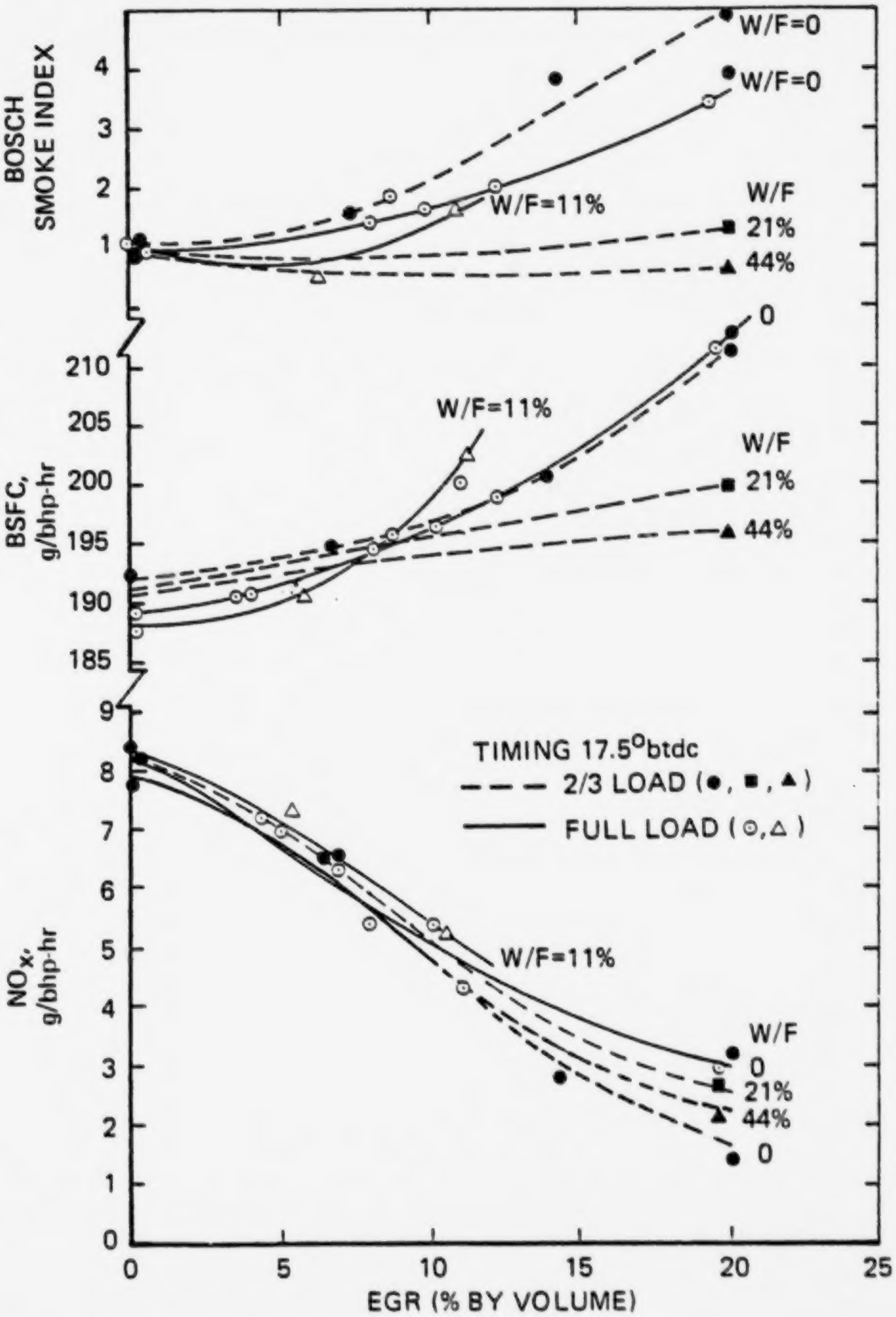

Figure 13. Combined EGR and emulsion

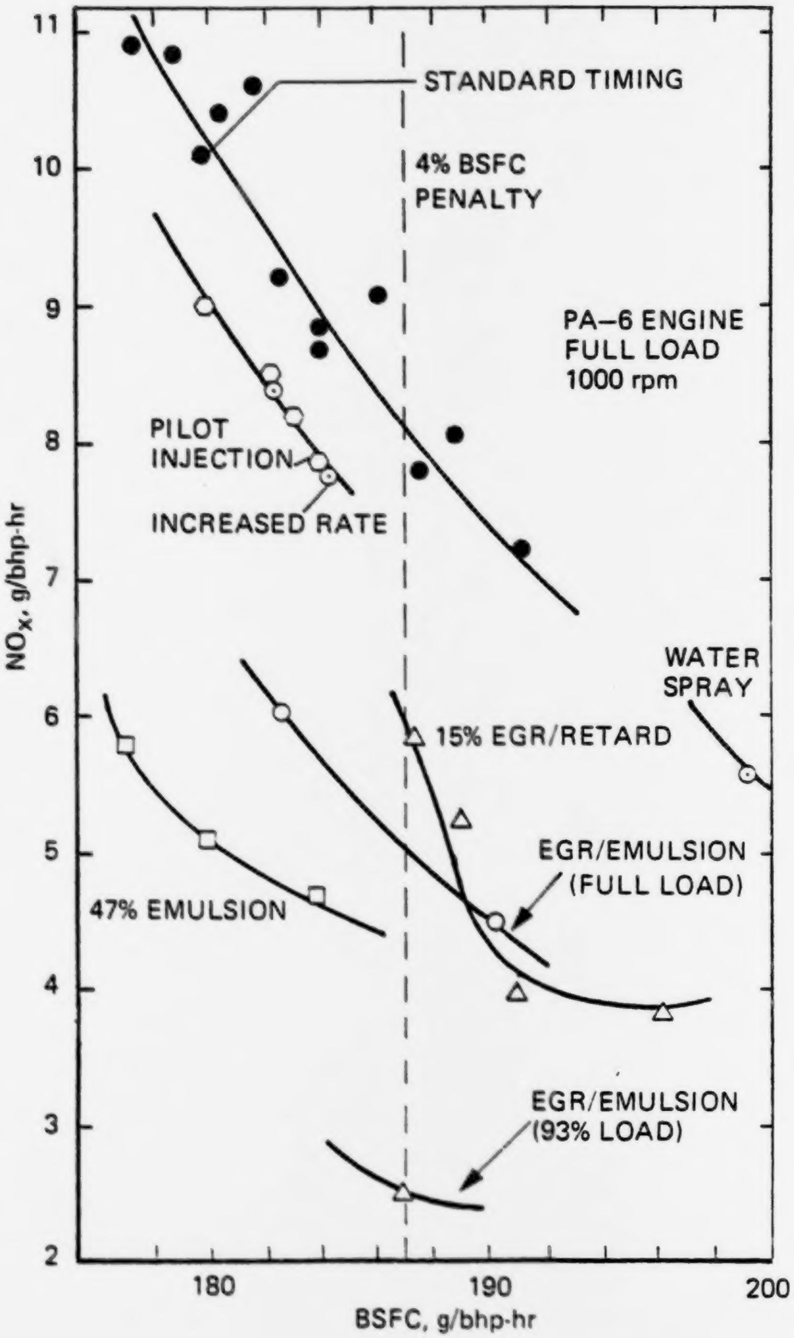

Figure 14. Comparison of NO_x-control methods

TABLE 1. DIESEL ENGINE MODIFICATIONS SELECTED FOR TESTING

Approach	Engine Modification	Present Results	Earlier Results
Delay start of burning and accelerate the end of burning	Increased fuel injection rate with retarded timing		●
	Pilot injection with retarded timing		●
Lower flame temperature by the use of diluents	Water/fuel emulsion	●	
	Exhaust gas recirculation	●	

TABLE 2. COMPARISON OF NO_x-CONTROL METHODS AT FIXED FUEL CONSUMPTION PENALTY (4%)

Configuration Tested	NO_x at Full Load, g/bhp-hr	NO_x Reduction
Baseline (23.5° btdc)	10.4	-
Retarded timing (17.5°btdc)	8.2	21%
Pilot injection	7.4	29%
Increased rate	7.4	29%
EGR(15%)/retard	5.1	51%
W/F emulsion(47%)/retard	4.4	58%
Combined 20% EGR and 25% W/F emulsion	2.5*	76%

*Data for 93% load

EMISSION CONTROL METHODS FOR LARGE STATIONARY ENGINES: PART III - CATALYTIC NO_x REDUCTION BY AMMONIA

By:

Robert P. Wilson, Jr.
Arthur D. Little, Inc.
20 Acorn Park
Cambridge, Massachusetts 02140

ABSTRACT

Catalyst tests on lean spark-gas and diesel engines showed that up to 97% NO_x reduction could be obtained with various base-metal catalysts, but only with a high degree of control over exhaust temperatures, ammonia injection rate, particulates, and space velocity. Continuous tests showed a slight drop in catalyst efficiency within 24 hours. Diesel particulate deposition on the catalyst enhanced performance in small amounts but was detrimental in larger quantities.

This paper has been prepared under Contract No. 68-02-2664 under the sponsorship of the U.S. Environmental Protection Agency, and covers work completed during the period September 1981 through July 1982.

1.0 BACKGROUND AND OBJECTIVES

In order to control NO_x emissions to very low levels, new methods are being developed whereby NO_x is reduced by passing exhaust gas over a noble or base metal oxide catalyst in the presence of ammonia. These advanced catalytic methods are relative costly ($50-150/HP or more) but are of considerable interest for certain California APCD's, Japan, and other locations where the ambient NO_x level is critical. For this reason, a number of studies have been undertaken in recent years to assess the feasibility of catalytic treatment of exhaust gases for boilers(1,2,3) and spark-gas engines.(4,5) The application of catalyzed ammonia treatment to stationary engines is not a simple matter of transferring the technology intact from boilers to engines. Several factors intervene: two-stroke gas engines and 4-stroke diesel engines operate at 10-15% exhaust O_2 levels (compared to 1-5% for boilers); engines operate at 600-900°F exhaust, compared to 400-600°F for boilers; engines have higher NO_x levels per Btu and thus require greater ammonia quantities; and engines are operated with frequent load adjustments and therefore may require more sophisticated ammonia control systems.

The purpose of the present catalyst test series was to evaluate the feasibility of catalytic ammonia treatment for a typical lean-running spark-gas engine and for a medium-speed diesel engine. The uncertainties and issues addressed were as follows:

- Effectiveness of catalyst/NH_3 for high-oxygen content exhaust gases typical of lean-running gas and diesel engines (10-15% O_2).
- Effectiveness of catalyst/NH_3 for normal exhaust manifold temperature, which ranges from 600 to 900°F, depending primarily on engine design, load, and timing.
- Influence of inlet NO_x level on effectiveness of the catalyst (for fixed space velocity and temperature).
- Comparative effectiveness of several catalysts in order to identify typical temperature "windows" of operation and to assess the range of performance of various catalysts.
- Determination of maximum adequate space velocity (i.e., minimum catalyst matrix volume).
- Assessment of changes in catalyst effectiveness over a continuous 100-hour test period.
- Ammonia injection and control, including discrimination at levels under 50 ppm at the outlet gases of the catalyst.
- Influence of diesel soot build-up on the effectiveness of the catalyst.

2.0 CONVERTER AND CONTROLS

A reaction chamber (capacity 50 SCFM) with suitable controls and instrumentation for exhaust gas flow rate, temperature, and ammonia flow rate was used in the tests. A chemiluminescent analyzer was used to measure NO_x upstream and downstream of the converter, and a dispersive infrared (DIR) analyzer also was used to measure NH_3 downstream.

A schematic diagram of the catalytic reactor is shown in Figure 1. A portion of the engine exhaust gas (up to 50 SCFM) was diverted to the reactor preheater. The preheater heat flux was controlled via a feedback-control loop from a thermocouple/temperature controller located at the reactor inlet. Reactor inlet gas temperature could be adjusted with this system to any setting between 400 and 1100°F with an accuracy of ± 5°F. Ammonia was injected and mixed with the exhaust gas just downstream of the preheater. Ammonia flow rate was measured with calibrated rotameter (flow rates were also verified with the DIR). The hot exhaust gases and NH_3 then entered the catalytic reaction chamber. Temperature, pressure, and gaseous emissions concentrations were measured upstream and downstream of the reactor. Ammonia concentration was measured downstream of the reactor with a modified differential infrared analyzer (as described in Section 4.0). After exiting the reactor, the exhaust gases were cooled and directed through a rotameter to obtain a total gas flow measurement.

3.0 CATALYST SAMPLES AND SPACE VELOCITY

We contacted major suppliers such as Engelhard, Dupont, Johnson-Matthey, Cyanamid, Met-Pro, and Shell-UOP to solicit catalyst samples compatible with the 6-in. pipe, 50 SCFM reaction chamber (See Figure 2). Smaller samples were accommodated by using the center portion of the reactor. The space velocity could be systematically varied. Four catalyst manufacturers delivered samples for testing, which are listed in Table 1 along with the catalyst type and sample geometry. Catalyst samples were secured and sealed at the annular edge area with "Fiberfax" ceramic packing materials and a ceramic adhesive.

Space velocity was varied from 10,000 hr^{-1} to 60,000 hr^{-1} by changing the exhaust gas flow rate. Superficial space velocity for each sample was calculated based on the bulk volume of the catalyst (regardless of void space or surface area) and the gas flow rate at standard conditions. Although not physically meaningful, this method of reporting space velocity has become industry practice because of its convenience.

4.0 AMMONIA SAMPLING AND ANALYSIS

One of the basic problems associated with catalytic exhaust treatment by ammonia injection is reliable accurate detection of ammonia, especially at levels below 100 ppm. At these levels, the conventional approach of using a chemiluminescent detector (with and without NH_3 conversion to NO) can be relatively inaccurate, because of the need to subtract two measurements of comparable magnitude.(6) Accordingly, a dispersive infrared (DIR) ammonia analyzer was designed and assembled specifically for this application.* Modifications to the infrared instrument included the following:

- High temperature lenses and lens mounts.
- High capacity sample cell heater (400 W).
- Water cooling of detector electronics.

These modifications were intended to allow gas sampling temperatures above 220°C, so as to prevent precipitate (e.g., ammonium nitrate) formation from the interaction of sample gas constituents. Without cell heating, the precipitation of ammonium sulfates, sulfides, nitrates, and nitrides at below 220°C would quickly cloud and etch the optical surfaces. Moreover, these precipitates would introduce errors by removing the species of interest (NH_3, NO_x) from the sample gas, converting them to a form unmeasurable by the detectors.

The lenses and mirror used in the Foxboro DIR analyzer were tested for durability in a filtered diesel engine exhaust gas stream at ADL. The silver bromide lenses and gold-plated aluminum mirror (the major optical components) were immersed in a diesel engine exhaust stream in the presence of 1000 ppm NH_3 and 600 ppm NO_x. No significant clouding of the lenses or mirror was detected at sample temperatures above 210°C. However, below 210°C, clouding caused by precipitation was severe.

In order to keep sample gas temperatures above 220°C between the catalytic reactor sample ports and the DIR NH_3 analyzer, a heated sampling system was designed and installed. During the tests, sample lines and filter assemblies were heated to maintain 230-250°C sample gas (or calibration gas) temperature at the entrance to the DIR analyzer. Inlet temperature was successfully controlled to within ± 5°F by the feedback loop shown in Figure 1.

The modified Foxboro DIR analyzer has proven to be accurate and reliable in detecting NH_3 in the 0-500 ppm range in the spark-ignition engine exhaust stream. The accuracy of detection was as low as ± 5 ppm under ideal conditions. This performance far exceeds the accuracy exhibited by the chemiluminescent detector used in the "difference" mode (± 50 ppm). The observed zero drift and span drift were about ± 10%/day and ± 2%/day, respectively. The minimum detectable NH_3 concentration was about 10 ppm.

In order to measure NH_3 using a chemiluminescent NO analyzer, it is necessary to convert the NH_3 to NO upstream of the analyzer. It has been reported that available converters, such as the device used in our tests (a stainless steel line held at 780°C), operate at efficiencies in the 70-80%

---

*The Foxboro Miran-II instrument (50-cm path length) was used for the basic components of this elevated temperature version.

range.(6,7) In the present tests, the efficiency of the converter was checked directly using the DIR NH_3 analyzer (which itself was calibrated with span gas). Figure 3 shows the comparison of the two measurement techniques. The significant conclusion which can be drawn from the data on this figure is that the "difference method" using an NH_3 converter in conjunction with a chemiluminescent analyzer gave readings which were consistently much lower than the calibrated DIR analyzer. Our confidence in the DIR analyzer was also reinforced by the readings obtained when the catalyst reactor was operated with a known concentration of excess NH_3. Below 100 ppm, the chemiluminescent technique gave readings which were about 50 ± 20% of the calibrated DIR readings. At higher levels of ammonia, we found that the chemiluminescent analyzer was indicating 20-80 ppm NH_3 when the actual level (DIR) was 100-250 ppm. Therefore, the need for ammonia measurement and control is perhaps more critical than the earlier literature on selective catalytic NO_x reduction would suggest.

5.0 CATALYST PERFORMANCE TESTS--SPARK-GAS ENGINE

5.1 Test Engine

Performance tests on four catalyst samples (see Table 1) were completed on an exhaust slipstream from a GMVH-6 spark-ignition engine at Cooper/Mt. Vernon, operating on natural gas. The engine was operated at 1350 hp, 330 rpm for most tests, with timing varied to give various NO_x levels. The exhaust concentrations of O_2, CO_2, CO and HC were 12.5%, 4.1%, 100 ppm, and 600 ppm, respectively. In the balance of this section, the catalysts will be identified with letters (A, B, C, D) since it is our intention to study the current state of performance rather than to focus on a comparison of specific manufacturer's samples.

5.2 Effect of Reactor Inlet Temperature

Figure 4 shows the effect of reactor inlet temperature on catalyst performance for samples A, B, C, and D with space velocity fixed at 10,000 hr^{-1} (this space velocity represented a favorable condition). These tests were run at constant NH_3/NO_x mole ratio (1.1:1), inlet concentration of NO_x (900 ppm), and O_2 level (12.5%). The basic result can be summarized as follows: for the base-metal catalyst samples (A, B, C), NO_x was reduced by 95-97% over a 100°F wide temperature window. For 90% reduction, the temperature window was about 200°F wide. With the present test arrangement, catalyst D could not be operated under conditions (temperature, SV) which were suitable for peak performance. Although maximum catalyst efficiency occurred within slightly different temperature windows for each catalyst, it can be seen from Figure 4 that engines operating with exhaust gas between 550 and 800°F would be well matched to at least one of these three catalysts without the need for any heating or cooling. Most lean-spark-gas engines operate in the 600-900°F range of exhaust gas temperature, subject of course to load and speed variations.

5.3 Effect of Space Velocity

The effect of space velocity (gas flow rate per unit volume of catalyst) is displayed in Figure 5. At optimum gas temperature, catalysts A, B, and C dropped from 95-97% to about 80-90% effectiveness when space velocity was increased from 10,000 to 30,000 hr^{-1}. At 60,000 hr^{-1}, these three catalysts operated with an effectiveness of about 65-75%. It should be pointed out that the space velocity (SV) as defined here gives only an approximate idea of the physical size of the catalyst required to treat a given exhaust gas flow rate. The average gas residence time could be obtained from 1/SV by making two corrections as follows:

- A factor of about x 0.4-0.5 to correct gas flow to actual conditions instead of standard conditions.
- A factor of about x 0.5-0.7 to correct from superficial catalyst volume to actual void space within the catalyst matrix. All the catalysts tested were monolithic.

In other words, the actual gas residence time was 20% to 33% of the value indicated by 1/SV in these experimental tests. Additional factors related to performance (such as effective catalyst surface area) were not available for catalyst A, B, C, or D.

5.4 Effect of Ammonia and Exhaust Gas Concentrations

The NO_x concentration of the gas entering the catalyst had little effect on the conversion efficiency, as long as the ammonia concentration was adjusted to equal (or exceed) the NO_x level. Figure 6 shows the typical effect of variations in inlet NO_x concentration on catalyst efficiency at constant space velocity and inlet temperature. In general, catalysts A, B, and C were found to exhibit uniform performance in the 800 to 1400 ppm NO_x range. Below the 800 ppm NO_x level, slight reductions in conversion efficiency were observed for catalysts A and B.

In addition, the HC and CO level of the exhaust gas had a slight effect on NO_x reduction, particularly at low NO_x levels. Presumably the CO and/or hydrocarbon species acted as chemical-reducing agents to some extent.

The overall conversion reaction between NO and NH_3 calls for equal molar quantities of each:

$$4NO + 4NH_3 + O_2 \rightarrow 4N_2 + 6\ H_2O$$

As would be expected based on this reaction, the extent of NO_x reduction decreased noticeably as NH_3 was reduced below the stoichiometric ratio of $NH_3/NO_x = 1.0$. Figure 7 shows the observed effect of mole ratio of NH_3/NO_x on catalyst performance. At ammonia levels above $NH_3/NO_x = 1.1$, further NO_x reduction was negligible and bypass ammonia (as detected by the DIR analyzer) increased linearly from the 20-50 ppm range to the several hundred ppm range.

Figure 8 shows the ratio of the measured NH_3 at the outlet of the reactor to the excess NH_3 (i.e., inlet NH_3 less the NO_x actually converted). Note that at higher temperatures (800-900°F), most of the excess ammonia was converted in the reactor (presumably to N_2 and H_2O). At lower temperatures (500-700°F), a large fraction of the excess ammonia survived the catalyst environment. Space velocity also had a distinct effect on NH_3 "breakthrough"; at 60,000 hr^{-1} the NH_3 breakthrough was about 1.5 to 2 times more than at 30,000 hr^{-1}. It is interesting to note, by comparing Figure 8 to Figure 4, that the NH_3 breakthrough is greatest at the temperature where the NO_x reduction is greatest. The significance of the data on ammonia breakthrough shown in Figure 8 is that ammonia controls appear to be an essential part of any exhaust gas treatment system of this type. One cannot rely on the catalyst to convert most of the excess ammonia to N_2 and H_2O except at relatively high temperatures.

5.5 Extended Duration Tests

Catalysts A and C were selected for extended tests (100-hour duration) in order to explore the possibility of near-term changes in catalyst performance and to better characterize the response of the catalyst to small fluctuations in temperature and ammonia level. Discrete measurements were made at hourly intervals for 8 hours out of each 24-hour period during continuous running. The catalysts were operated near the limits where earlier tests had shown that small changes in temperature, NH_3/NO_x ratio, and space velocity would have detectable effects. Parameter settings were as follows:

- Catalyst A: 20,000 hr^{-1}, 620°F, $NH_3/NO_x = 1.1$
- Catalyst C: 20,000 hr^{-1}, 775°F, $NH_3/NO_x = 1.1$

The expected NO_x reduction corresponding to these parameters (based on earlier tests) were about 90% and 85%, respectively, at the start of the tests.

The results are shown in Figure 9. Both catalysts exhibited about 5-10 percentage points drop in NO_x-reduction efficiency during the first 24 hours of operation. On two occasions, the inlet temperature was increased to 950°F in an attempt to "refresh" the catalyst by increasing the oxidation rate at the surface. This procedure seemed to have a temporary beneficial effect, increasing the catalyst efficiency by a few points.

The basic conclusion of these 100-hour runs is that steady-state catalyst performance is somewhat lower than the peak performance of a fresh catalyst (in this case about 5-10% lower). However, there were no substantial changes in catalyst effectiveness during the first 100 hours of operation.

The temperature window for optimum performance, however, did shift during the 100-hr run of each catalyst. Figure 10 shows that operation for extended duration reduced the catalyst effectiveness at lower temperatures, but appeared to have little effect on the high temperature performance.

5.6 Comparison with Prior Reported Results

Other investigations of catalyzed reduction of NO_x by ammonia in spark-ignition engine exhaust have reported catalyst performance figures which are comparable to the present results. As shown in Table 2, for four base-metal catalysts tested on engines, reported peak efficiencies have been 98, 95, 97, and 95% compared to the 97% observed for three base metal catalysts in the present work. Temperature windows were also quite consistent with the present results.

6.0 CATALYST PERFORMANCE TESTS--DIESEL ENGINE

Previous studies of catalytic reduction of NO_x by ammonia have been conducted exclusively on spark-ignition engines, in part because of the significance of the stationary spark-gas engine in California, where many of the early applications were prompted. In the present study, exploratory catalyst tests were undertaken on a typical 4-stroke diesel engine, in order to determine the effectiveness and practical considerations of applying the ammonia injection technique for this class of engine. The primary difference between spark-ignition and diesel engine exhaust gases is the presence of particulate soot in the latter type of exhaust. In addition, the exhaust gas in the present 4-stroke diesel tests was characterized by higher exhaust temperature (900°F) and lower O_2 (10%) than the 2-stroke spark-gas engine described above in Section 5.0. Test engine parameters were as follows:

- Superior Model 40GDXS 6 cylinder
- No 2 diesel fuel
- Full load 710 hp
- 900 rpm
- 88% excess air (approx. 10% O_2); i.e., total air equal to 188% of stoichiometric air
- bmep 152 psi

Catalyst A (base metal) was selected and the identical catalyst and reactor which had been used earlier in the spark-gas engine tests was used in this test series. The catalyst operating conditions and sampling protocol were the same as used in the spark-gas tests (see Figure 1) except for one important difference: the chemiluminescent method was used for NH_3 in place of the dispersive infrared NH_3 analyzer, which developed leaks and exhibited drift, presumably because of fine-particulate deposits on the optical components of the cell. The mirror, windows, and seals were replaced, but some leakage remained and significant zero drift resumed within hours of operation on diesel exhaust.

The chemiluminescent method for NH_3, as carried out at Superior using a Beckman 955 analyzer, appeared to give NH_3 readings which were 30-50% higher than the excess NH_3 entering the reactor, in contrast to the opposite results in the spark gas tests (see Figure 3). For example, with 600 ppm NO_x converted and 830 ppm NH_3 supplied to the reactor, indicated NH_3 emissions by the chemiluminescent method were generally in the 300-400 ppm range.

NO_x conversion efficiencies for Catalyst A peaked at about 98%, which is comparable to the peak efficiency observed for Catalyst A in the spark-engine tests. However, as shown in Figure 11, there was an interesting difference in performance: the gas temperature for peak performance shifted from 620°F to 750°F, and the temperature window for 90% conversion was extended from 700°F to 850°F. This temperature shift phenomenon has been observed in limited diesel tests by one catalyst manufacturer,(9) and is attributed to the coating of diesel soot which builds up on the catalyst. Apparently, accumulated soot in small amounts can enhance catalyst surface activity, presumably due to chemical transformations involving the carbon, base metal oxide, and alumina substrate.

However, large deposits of soot inhibit species diffusion and impair catalyst performance, as illustrated in Figure 12, which shows NO_x conversion during an 85-hour run conducted to study near-term degradation. Note that the NO_x reduction dropped from about 90% to 80% in the first few hours of testing, and then decreased steadily thereafter to a level of about 70% after 85 hours. The pressure drop across the catalyst increased steadily from 0.4 to 1.1 in. H_2O during this period, indicating buildup of soot. Photographs of the catalyst surface after testing (Figure 13) confirmed that substantial soot buildup had occurred.

7.0 SUMMARY OF FINDINGS--CATALYST TESTS

Based on the test results described above, we can conclude the following:

(1) Under ideal conditions (adequate space velocity and judicious control of exhaust temperature, NH_3 level, and particulates), 97% NO_x reduction could be obtained with three different base metal catalysts.

(2) NO_x reduction of diesel engine exhaust was comparable to that observed in spark-gas engine exhaust. In fact, accumulated soot in small amounts enhanced the performance of the catalyst at higher temperatures.

(3) Space velocity exhibited a threshold of 20,000-30,000 hr^{-1} for good performance, depending on catalyst.

(4) NH_3/NO_x ratio should be controlled between 1.0 and 1.1 for optimum results; higher values can result in NH_3 emissions of several hundred ppm whereas values at 0.9 or below leave the NO_x reduction incomplete.

(5) Extended continuous runs on two catalysts and two engines suggest that realistic expectations for long term

catalyst performance may lie in the 75-85% range. A drop in NO_x reduction efficiency of 5-10% was seen within 24-hours for all tests.

(6) Diesel soot must be reduced to very low levels in order for diesel exhaust to be treated by catalyzed ammonia reduction. Otherwise, substantial soot layers accumulate and impair catalyst performance.

(7) The chemiluminescent method for NH_3 measurement may significantly underestimate ammonia concentrations because of the inefficiency of the converter. Uncertainty is inherently large because of the need to differentiate between two measurements of comparable magnitude.

(8) A specially designed dispersive infrared analyzer for NH_3 was assembled and used to measure NH_3 levels in the 10-500 ppm range for spark-gas engines. The optical path must be protected against ammonium nitrate deposits (which form below 220°C) and diesel soot deposits. This analyzer offers promise as a means to prevent excessive NH_3 emissions by feedback control.

ACKNOWLEDGEMENTS

John H. Wasser, the EPA Technical Project Officer, recognized the catalyst work as a logical adjunct to combustion-modification tests and substantially assisted during the catalyst project. John Bedrossian and Greg Demattia of Foxboro Analytical were instrumental in the development of a novel ammonia analyzer. I also wish to acknowledge several individuals at Cooper Energy Services (Paul Danyluk, Fred Schaub, Claude Miller, and Marold Lavy) who have been responsible for the engine tests. Key contributions to the catalyst phase of the project have been made by several members of the project team at Arthur D. Little, including: John Mendillo, Jim Aronson, Doug Shooter, and Ken Menzies. Finally, I wish to acknowledge the work of Maureen Donovan in the preparation of this manuscript.

REFERENCES

1. EPRI Contract with Kawasaki Heavy Industries on Selective Catalytic Reduction, EPRI Journal, Vol. 4, p25, 1979.
2. Faucett,H.L., Maxwell,J.D., and Burnett,T.A., Technical Assessment of NO_x Removal Processes for Utility Application, EPA-600/7-77-127 (NTIS No. PB 276637), November 1977.
3. Burnett,T.A., and Faucett,H.L., Impact of Ammonia Utilization of NO_x Flue Gas Treatment Processes, EPA-600/7-79-011 (NTIS No. PB 300596), January 1979.
4. Danyluk, P. and Schaub, F. S., "Emission Reduction by Combustion Modification in Two Stroke Spark Ignited Gas Engines and by Catalytic Conversion," ASME Paper 81-DGP-7, 1981.
5. Dupaski, R. and Padar, F., "NO_x Reduction on Large Bore SI Engines Using Catalytic Converters," ASME Paper, 1982.
6. Myatt, B. M. (GCA Corporation), Private Communication, July 1982.
7. Chehaske, J. T., Engineering Sciences, Private Communication, October 18, 1982.
8. Chehaske, J. T., "Survey and Analysis of Flue Gas Treatment Methods --Selective Catalytic Reduction of Nitrogen Oxides Using Ammonia and Manual Controls," Preliminary Draft Report to AGA Pipeline Research Committee, September 1982.
9. Fournier, L. B., E.I. DuPont De Nemours and Co. (Inc.), Private Communication, October 15, 1982.

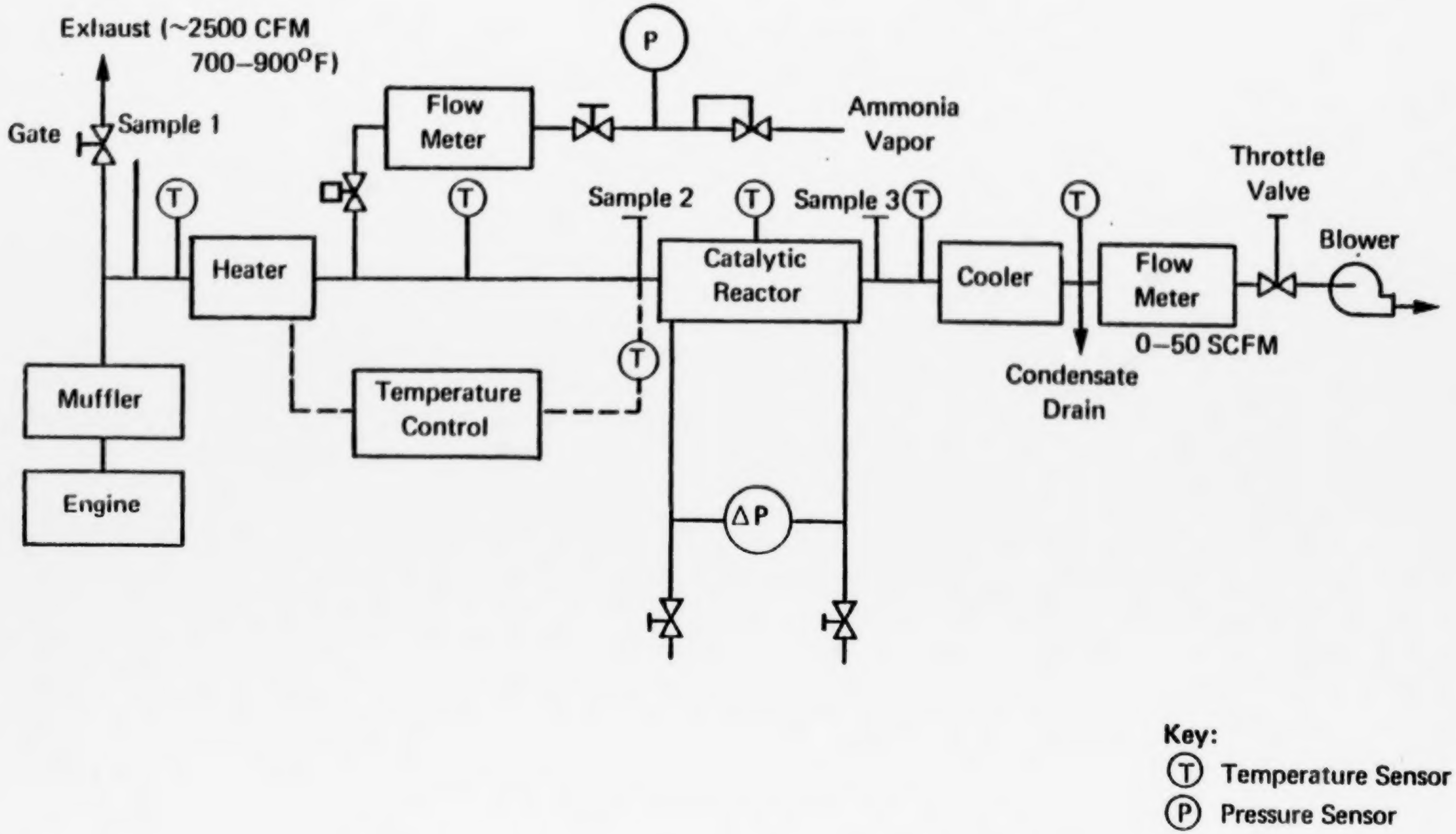
Exhaust (~2500 CFM
700–900°F)
Gate
Sample 1
Flow Meter
P
Ammonia Vapor
Throttle Valve
Blower
T
Heater
Sample 2
T
Sample 3
Catalytic Reactor
Cooler
Flow Meter
0–50 SCFM
Condensate Drain
Muffler
Engine
Temperature Control
ΔP
Key:
T Temperature Sensor
P Pressure Sensor

Figure 1. Schematic of catalytic reactor test rig.

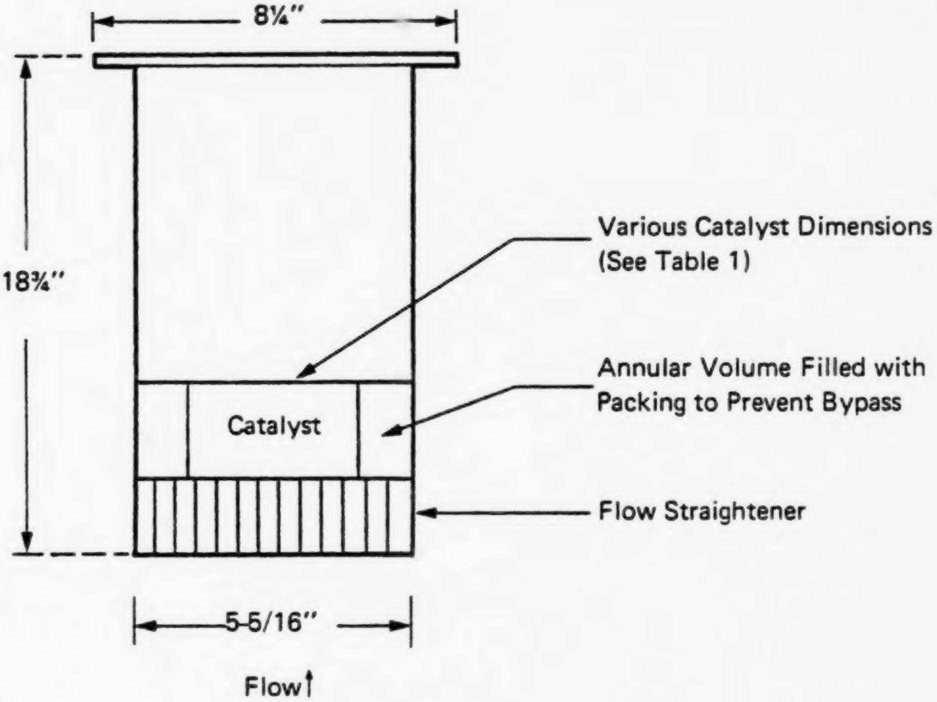
8¼"
18¾"
Various Catalyst Dimensions (See Table 1)
Catalyst
Annular Volume Filled with Packing to Prevent Bypass
Flow Straightener
5-5/16"
Flow↑

Figure 2. Catalyst "Can" geometry.

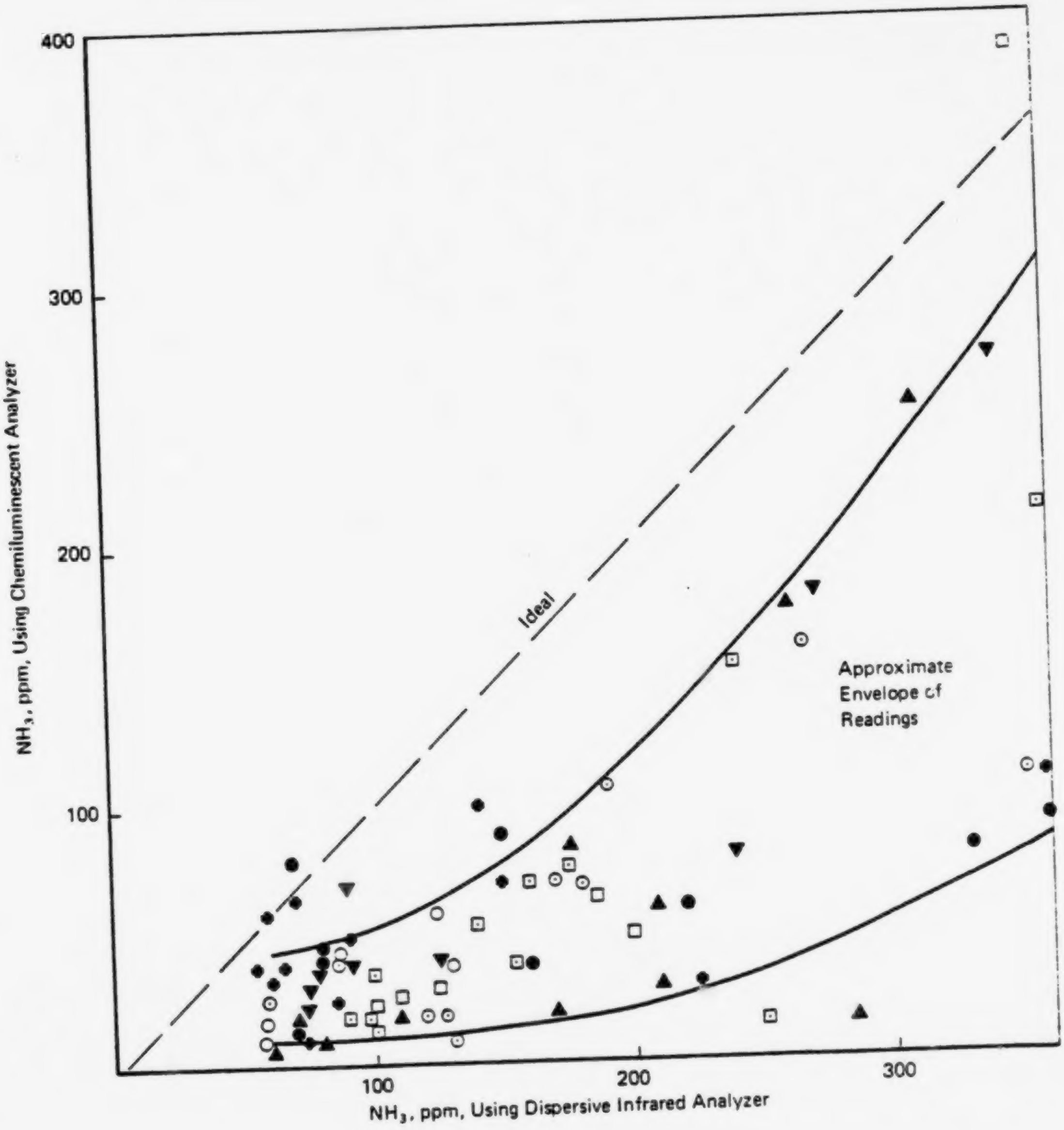

Figure 3. Comparison of two ammonia measurement techniques.

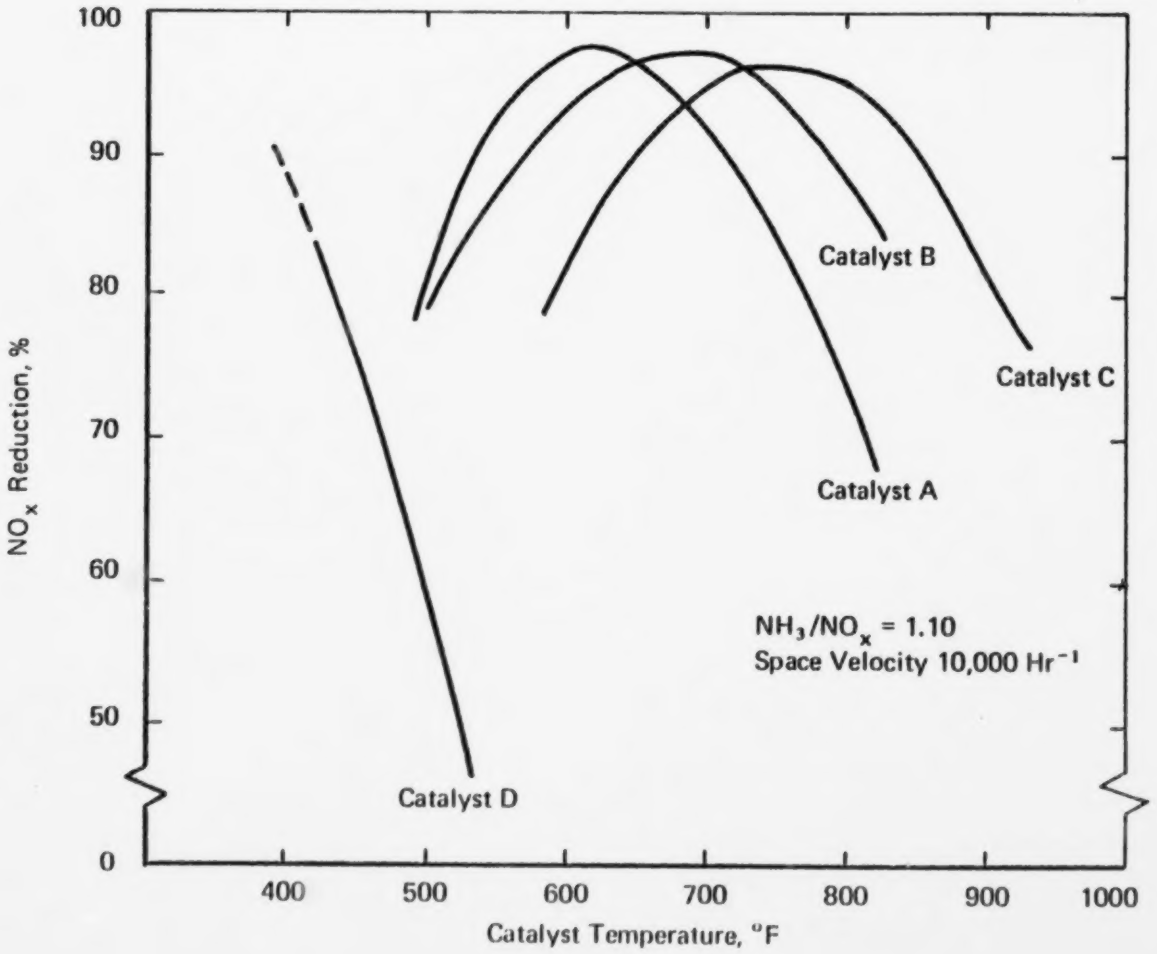

Figure 4. Performance of four catalysts.

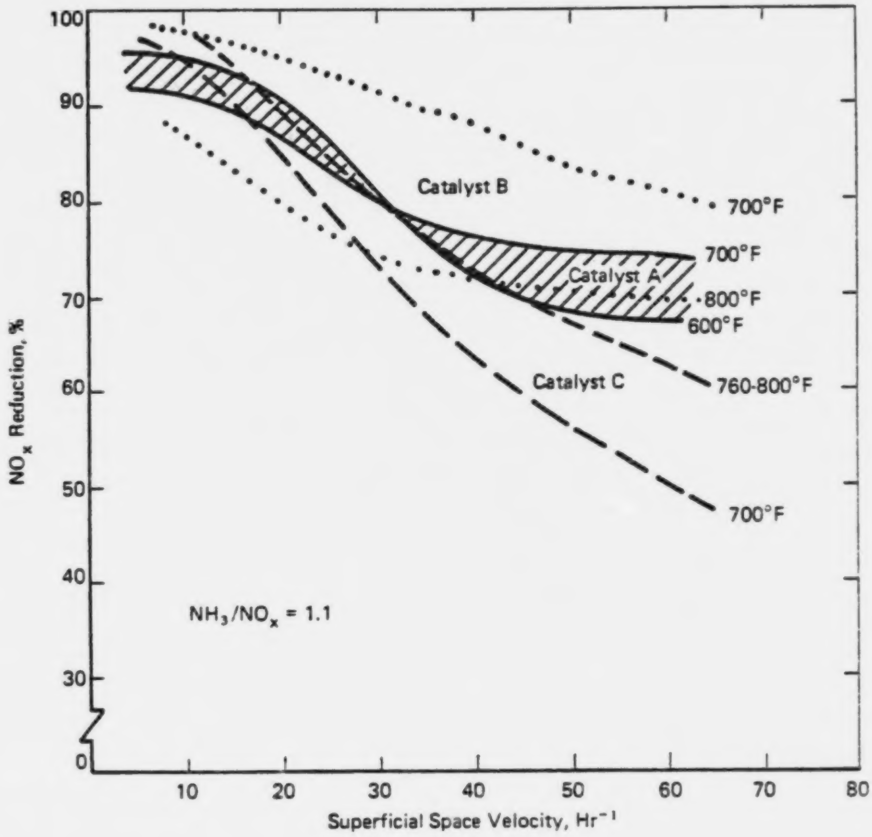

Figure 5. Effect of space velocity.

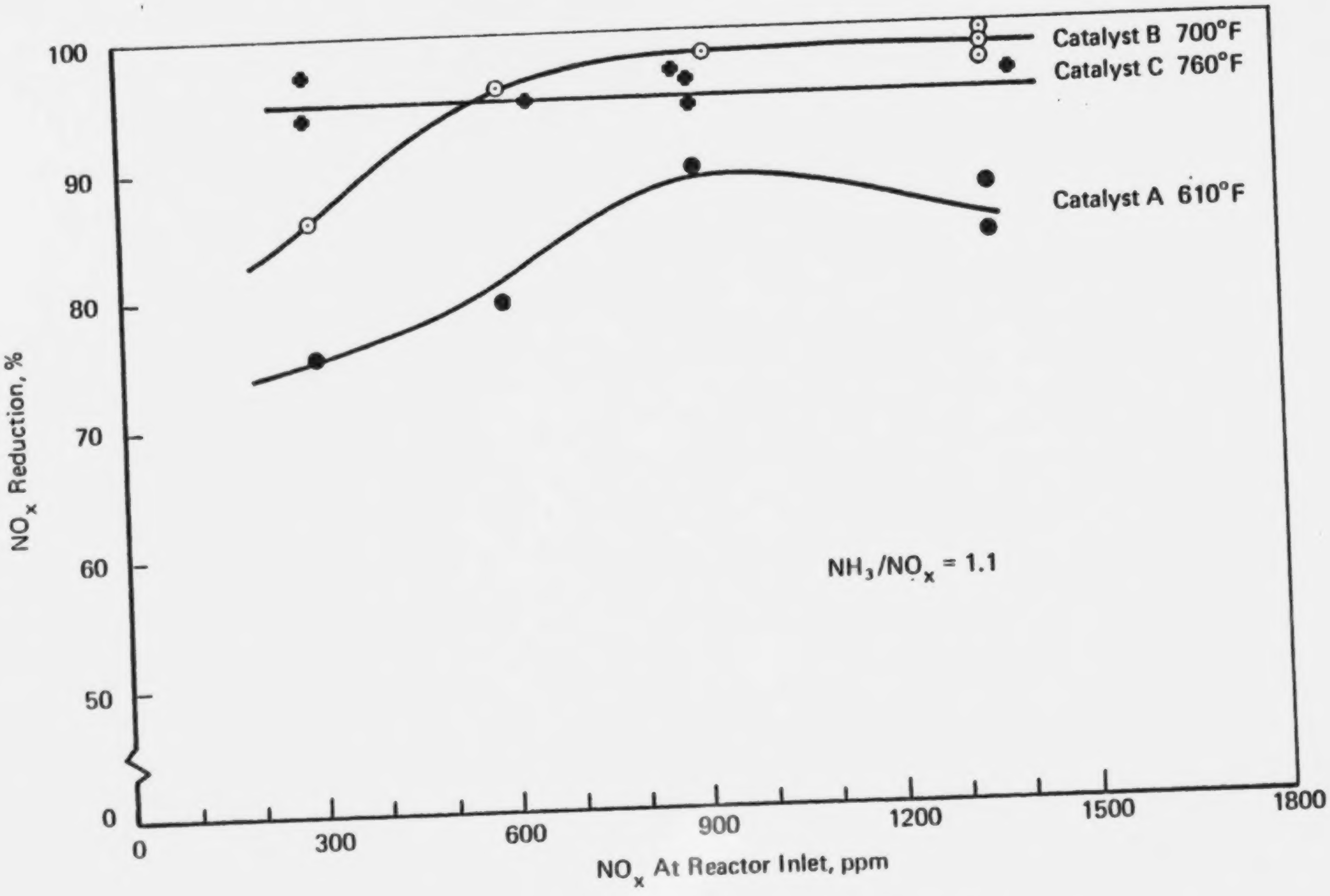

Figure 6. Effect of inlet NO$_x$ concentration on catalyst effectiveness.

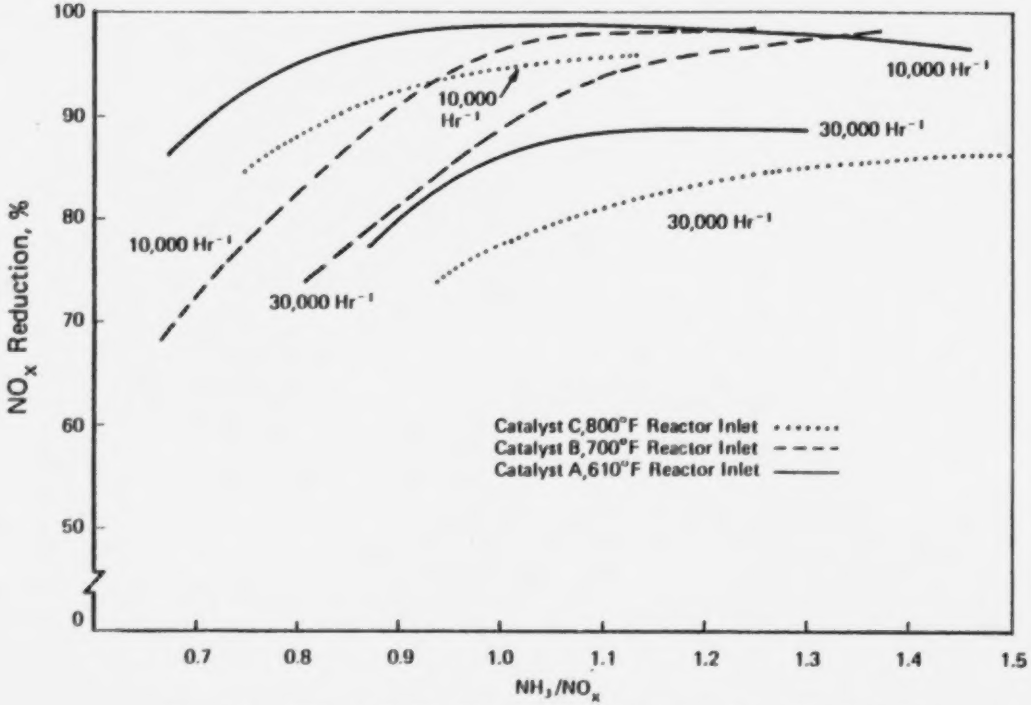

Figure 7. Effect of NH$_3$/NO$_x$ mole ratio on catalyst effectiveness.

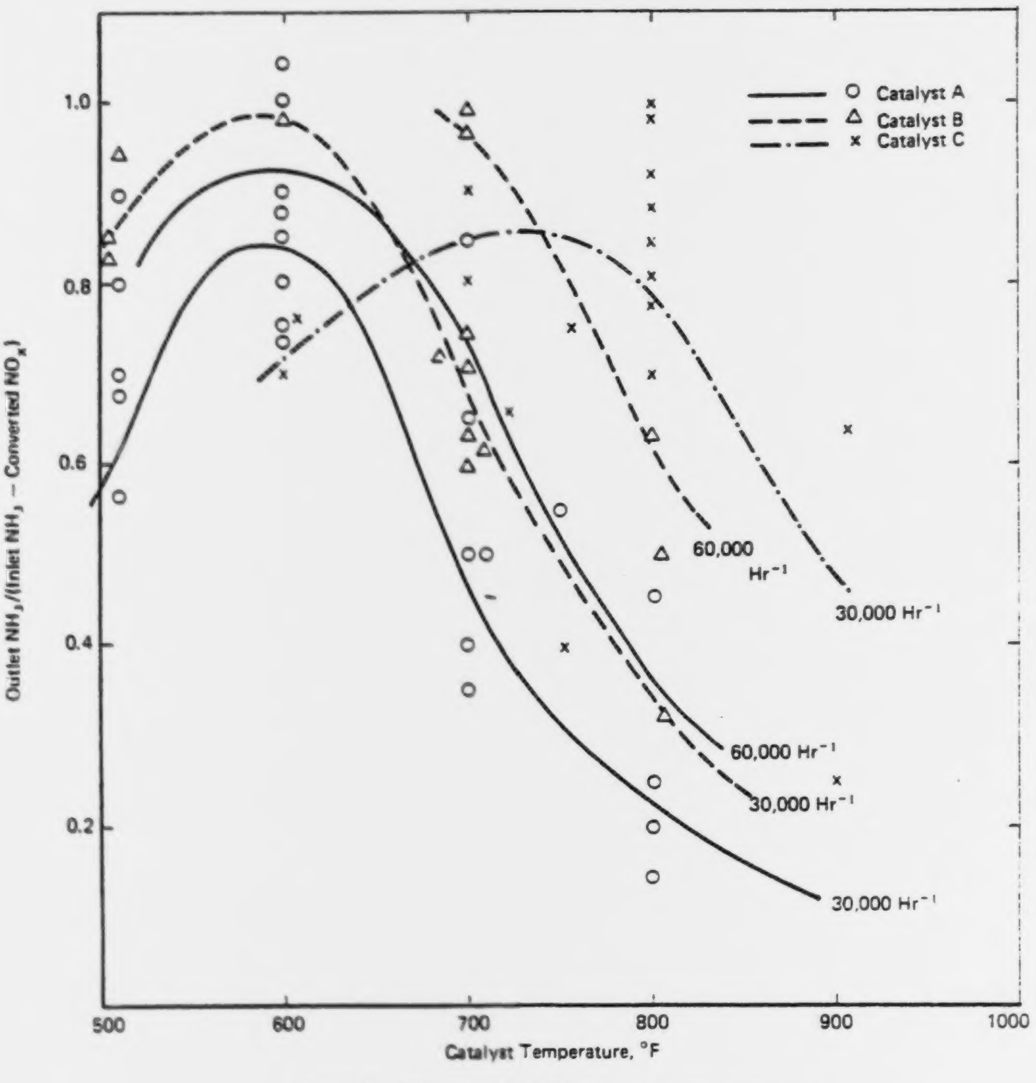

Figure 8. Effect of catalyst on excess ammonia.

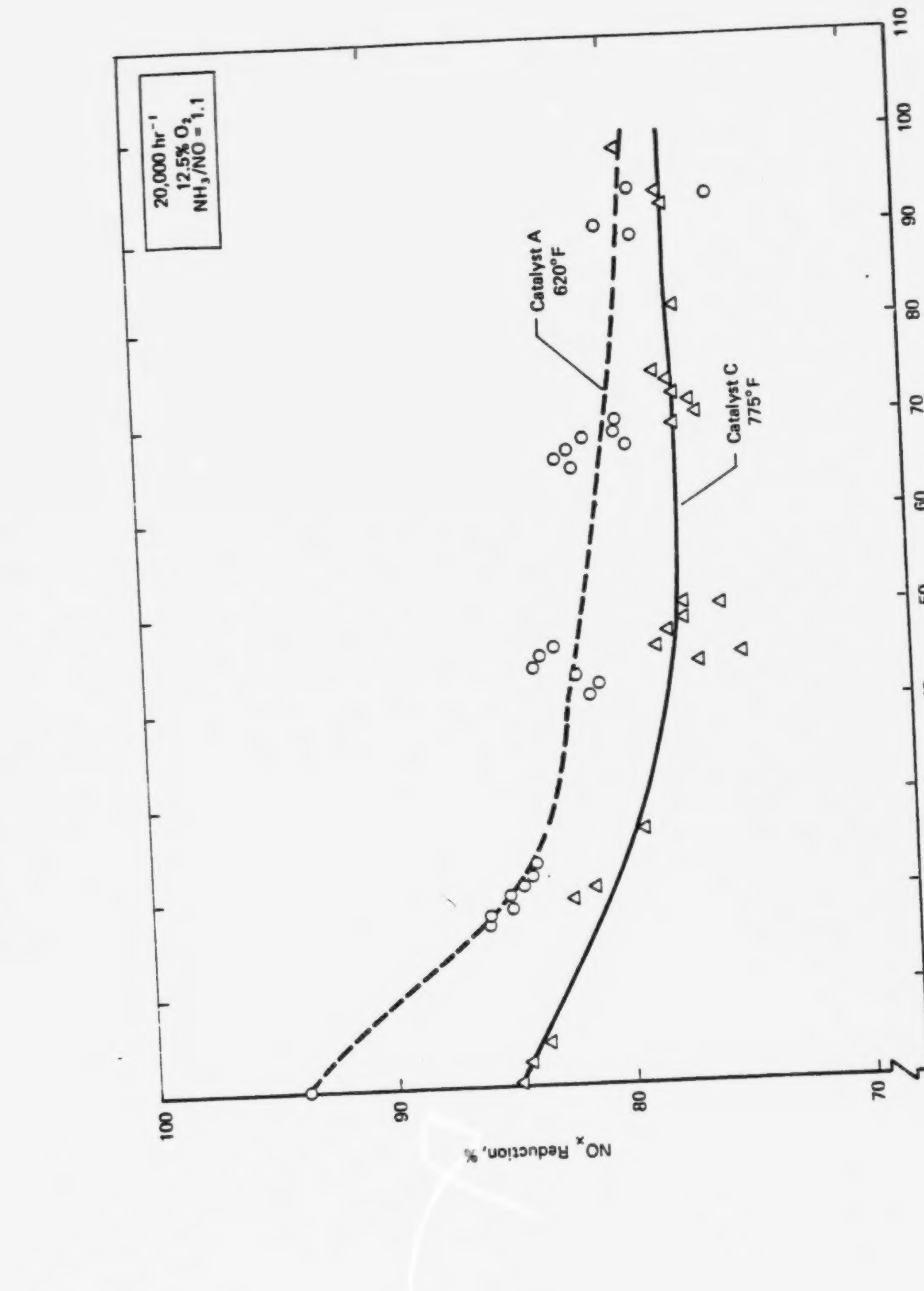

Figure 9. Extended duration tests.

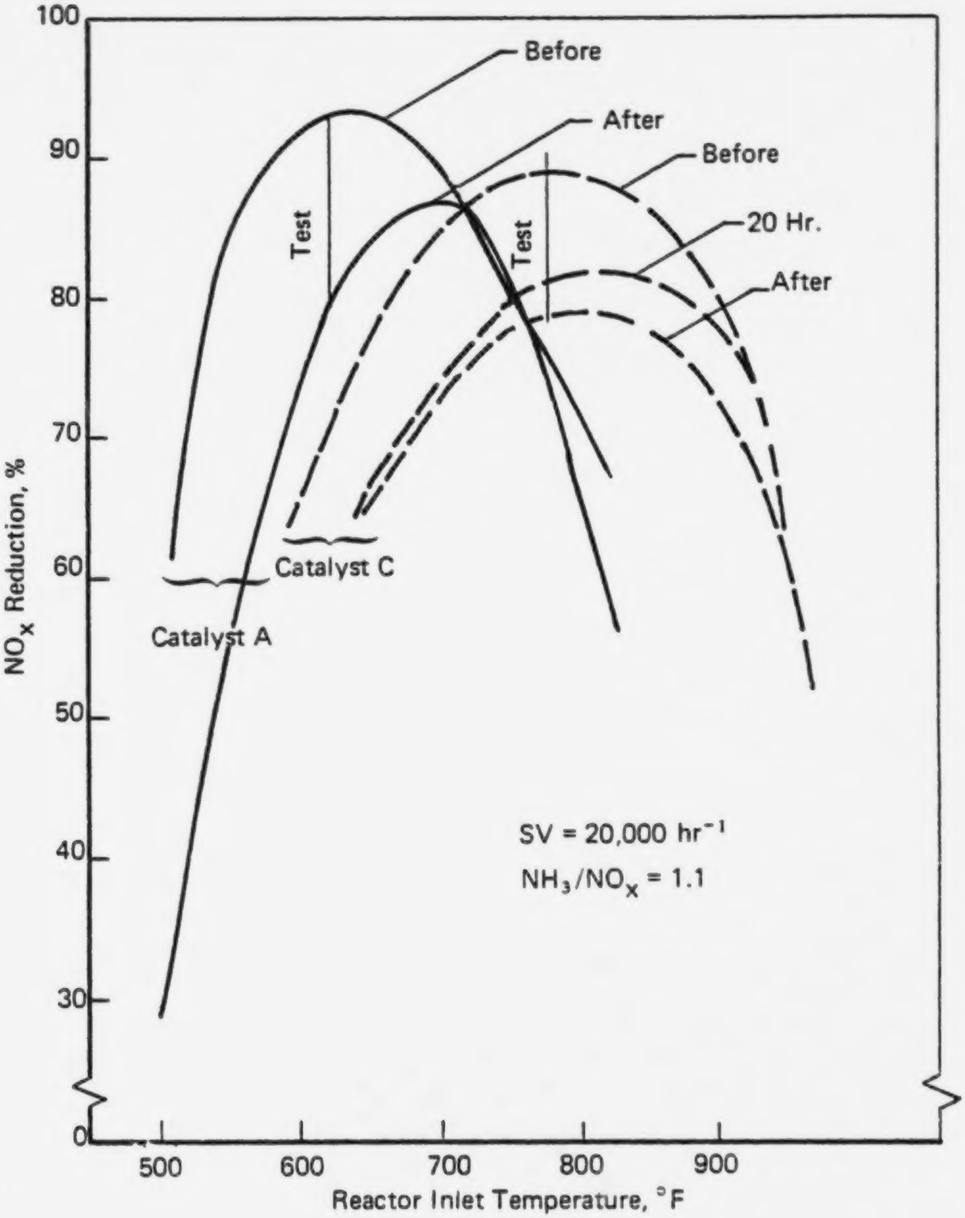

Figure 10. Catalyst Effectiveness Before and After 100-Hr-Run

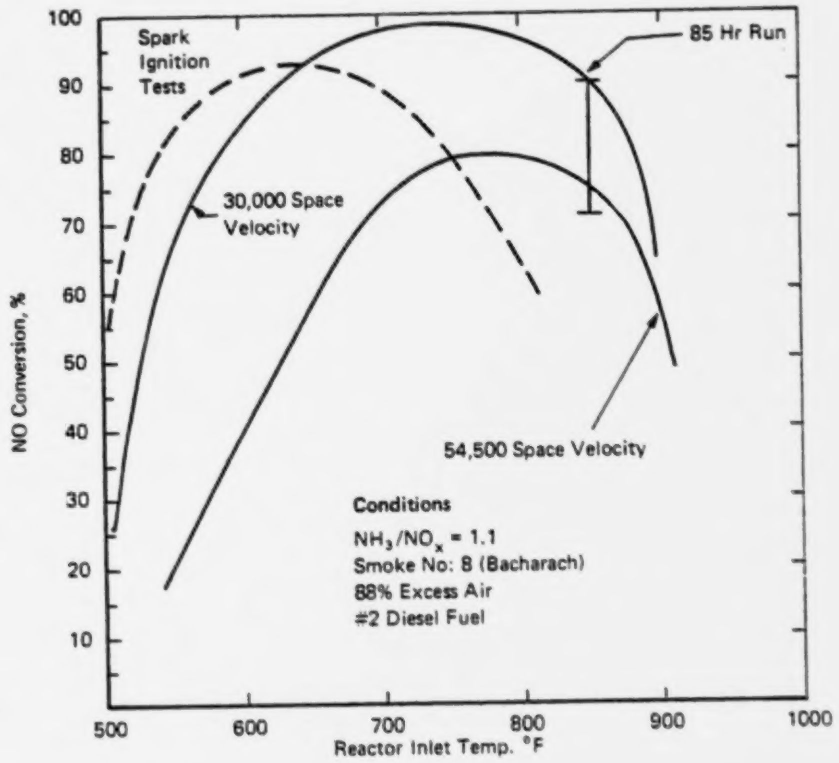

Figure 11. Performance of catalyst A on diesel exhaust.

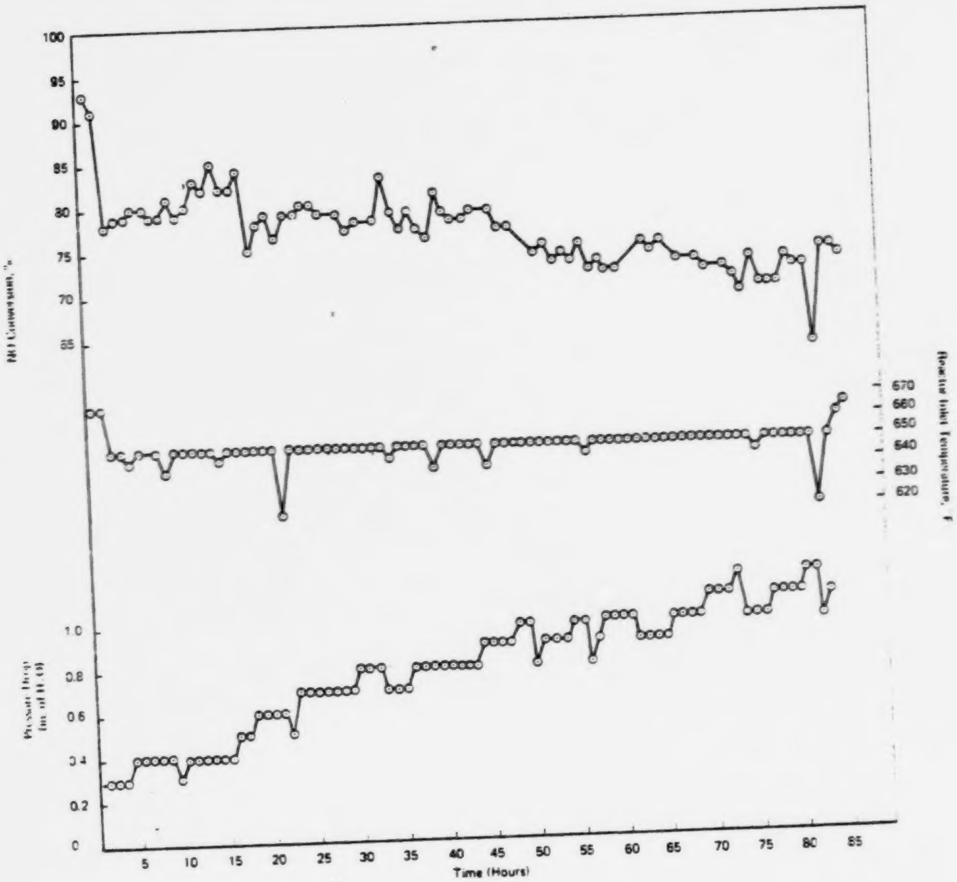

Figure 12. Performance of Catalyst A during 85-Hr. run.

Conditions

Gas temperature: 650 °F
Soot loading: #8 Bacharach
Duration of test: 85 hr

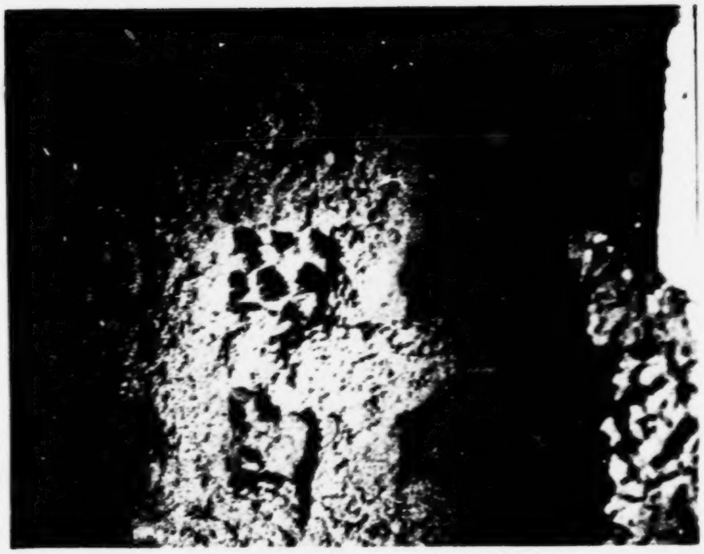

(a) Upstream face

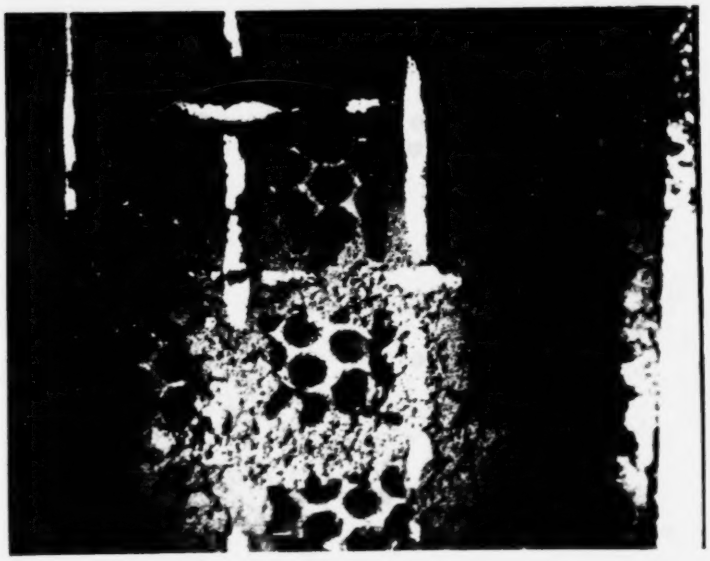

(b) Downstream face

Figure 13. Diesel soot accumulation on catalyst.

TABLE 1. CATALYST CONFIGURATIONS
(All Monolithic Substrate)

Manufacturer	Catalyst Type	Geometry (dia. x length)	Gross Volume (ft^3)	Superficial Space Velocity (hr^{-1}) at 1200 scfh
DuPont	Base Metal	4.5" x 4"	.0368	32,600
		3" x 5"	.0204	58,700
Engelhard	Base Metal	3" x 6"	.0245	49,000
Johnson Matthey	Base Metal	4.2" x 3"	.0240	49,600
Met-Pro	Noble Metal	5" x 4"	.0454	26,400

TABLE 2. COMPARISON OF PRESENT RESULTS WITH SELECTED CATALYST TESTS

Exhaust Gas Source	O_2 Level	Catalyst(s)	Arrangement	SV (hr^{-1})	Peak Efficiency at Temperature	Temperature Window (90%)	Ref.
Superior 8GTL Natural Gas Engine (10" bore)	6-8%	A (Base)	SS	20,000 to 25,000	98% @ 600°F	450 to 660°F	5
		B (Base)	SS		95% @ 550°F	500 to 630°F	
		C (Noble)	FF	"	72% @ 480°F	NA	
		D (Noble)	SS	"	75% @ 440°F	NA	
Cooper Bessemer Spark-Gas Engine	12%	Base Metal	SS	920 SCFH	97% @ 680°F	510-740°F	4
1850 HP Spark Gas Engine (2 cycle, turbocharged)	12.4-13.7%	Base Metal	FF	5400 to 8700	95% @ 770°F	Testing Limited to 700-800°F	8
GMVH-6 1350 HP Spark Gas Engine	12-13%	A (Base)	SS	10,000 hr^{-1}	97% @ 610°F	530-700°F	Present Results
		B (Base)		"	97% @ 690°F	570-790°F	
		C (Base)		"	97% @ 750°F	650-850°F	
		D (Noble)		"	(85% @ 420°F)*	NA	

*Peak not reached

SS = sidestream;
FF = full flow

APPLICATION OF COMBUSTION MODIFICATION TECHNOLOGY FOR NO_x CONTROL TO PROCESS HEATERS

By:

Robert J. Tidona
KVB, Inc.
18006 Skypark Boulevard
Irvine, California 92714

DISCLAIMER

"The research described in this article has been funded wholly or in part by the United States Environmental Protection Agency through contracts 68-02-2144 and 68-02-2645 to KVB, Inc. Although it has been subjected to the Agency's required peer and policy review, it does not necessarily reflect the views of the Agency and no official endorsement should be inferred."

ABSTRACT

A full-scale natural draft refinery process heater rated at 16.1 MW thermal input was modified to incorporate a staged combustion air injection system. The heater was tested for thirty days firing refinery gas at constant load with the staged air system in continuous operation. Up to fifty percent of the total combustion air to the heater was supplied by means of the staged air system. The staged air was injected by means of lances inserted through the heater floor. A combination of lowered excess air and staged combustion air was applied for about 15 days resulting in mean NO emissions of 18.5 ng/J, a 71 percent reduction from the baseline NO emissions of 64 ng/J. The remainder of the test was conducted at normal operating excess air levels with staged combustion air. NO emissions averaged 25.5 ng/J, 60 percent below baseline. At normal stack O_2, operation of the staged air system did not require additional plant personnel or attention. No changes in heat flux distribution within the furnace were observed. Post-test examination of the hardware showed no discernible deterioration of the staged air system.

Tests of ten process heaters equipped with low-NO_x burners resulted in NO_x levels 32 to 77 percent below average emission factors for standard burners depending on heater type and fuel. Heaters tested under this task included four natural draft and six mechanical draft units firing gas distillate and residual oils. Four of the mechanical draft units had preheated combustion air.

An extended duration test of a 5.3 MW thermal input natural draft process heater equipped with low-NO_x burners resulted in mean NO emissions of 44 ng/J. Heater operation with the low-NO_x burners presented no reliability or functional problems during the test. The average stack O_2 concentration was 5.8 percent by volume, dry basis. Daily average CO emissions were generally below 25 ppm, dry at 3 percent O_2, and never exceeded 90 ppm.

INTRODUCTION

Field tests of refinery process heaters which have been modified to incorporate NO_x-reducing combustion techniques have been made and the effectiveness of these techniques in lowering NO_x emissions assessed. The combustion modification technology tested on the heaters included low-NO_x burners, staged combustion air lances, and lowered excess air. Excess air variations were also performed in combination with each of the other two modification techniques.

At previous symposia KVB has reported the results of combustion modification testing of a naturally drafted subscale process heater (Ref. 1) and a full-scale vertical cylindrical natural draft crude heater (Ref. 2). This report summarizes the results of a 30-day continuous emission monitor test on that same full-scale heater equipped with staged combustion air lances firing refinery gas as well as updated cost information pertaining to the staged air system. In addition, emissions measured during field tests on ten process heaters equipped with commercially available low-NO_x burners are reported. The results of a 30-day test on one process heater equipped with low-NO_x burners are also included.

Objective and Scope

The objective of this program was to investigate advanced combustion modification concepts requiring relatively minor hardware modifications that could be used by operators and/or manufacturers of selected industrial process equipment to reduce emissions and to improve thermal efficiency. The study was to be performed for equipment in which the modifications would be most widely applicable and of the most significance in mitigating the impact of stationary source emissions on the environment. Another objective was to assess the feasibility of these modifications to the extent that they could be readily adopted by the fuel burning equipment manufacturers.

PROCESS HEATER TEST SITES AND EMISSIONS SAMPLING SYSTEM

Process Heater With Staged Combustion Air Lances

The test unit was a natural draft, vertical cylindrical crude oil heater which supplies a charge to a crude oil distillation column. The unit had a maximum firing rate capability of 16.1 MW (55 x 10^6 Btu/h) and a maximum throughput of 108 m^3/h (16,250 bbl/day). It was fired by six John Zink DBA-22 burners* which could burn gas or oil or both fuels simultaneously and were rated at a maximum firing rate of 2.68 MW (9.14 x 10^6 Btu/h) each. This unit has been described in Reference 2.

---

*Mention of trade names does not constitute approval by the U.S. Environmental Protection Agency.

The staged combustion air system used at this site is shown in Figure 1. This application of staged combustion utilized air lances in the firebox to supply air to the flame zone a given distance above the base of the flame. The system consisted of 24 vertical 316 L stainless steel pipes 3.18 cm (1-1/4 in.) in diameter arranged four per burner, 90 deg. apart. The staged air lances were mounted on a 91 cm (36 in.) diameter circle so that they were 10.2 (4 in.) radially outward from the outside of the burner tile. A 45-deg. elbow was placed on each pipe to provide better mixing across the flame. A fan supplied air to the lances through a manifold and flexible tubing. The lances could be varied in height up to 1.2 m (4 ft) from the base of the burners. Extensions for the lances allowed staging heights up to 2.4 m (8 ft) for oil firing tests.

Process Heaters Equipped With Low-NO_x Burners

The process heaters tested under this task included four natural draft and six mechanical draft units firing gas, distillate oil, or residual oil. Four of the mechanically drafted units had preheated combustion air. A summary of test heater characteristics is provided in Table 1. All of the test heaters were located in the state of California.

The unit on which the 30-day continuous emission monitoring test was conducted was a 62.9 m^3/h (9500 bbl/day) natural draft unit firing natural gas. It was a vertical cylindrical crude heater with three John Zink LNC-16 low-NO_x burners. Maximum heat input rate was approximately 5.3 MW (18×10^6 Btu/h). A detailed description of the unit may be found in Reference 3.

Emissions Sampling Instrumentation

Monitoring of the required gaseous and particulate emissions for all of the short-term tests and for the 30-day test of the staged air lances was performed with an EPA-furnished mobile laboratory. The laboratory's monitoring capabilities are presented in Table 2. A detailed description of the mobile emissions laboratory has been presented in Reference 4. Continuous gaseous emissions analyzers provided the capability for measurement of O_2, CO_2, CO, SO_2, NO, NO_x, and HC (as methane) in the flue gas. The O_2, CO_2, and CO concentrations were measured on a dry basis. SO_2, HC, and NO_2 measurements were made through a heat-traced sample line and were determined on a wet basis. NO could be sampled either wet or dry.

For the 30-day test of the low-NO_x burner-equipped process heater, a portable continuous emission monitor described in Reference 3 was used to measure O_2, CO_2, CO, and NO extracted with an unheated sample line. Both the portable monitor and the mobile laboratory instrumentation were certified in accordance with Performance Specification 2 (PS2) and 3 (PS3), 40 CFR 60. These establish minimum performance specifications that the NO monitoring system must meet in terms of accuracy, calibration error, 2- and 24-hour zero drifts, 2- and 24-hour calibration drifts, response time, and operational period.

DISCUSSION OF RESULTS

Extended Duration Test of the Staged Air System

Gaseous emissions data were measured continuously and recorded on an automatic data logger, strip chart recorders and a magnetic tape recorder. Fifteen-minute averages of NO, O_2, CO and CO_2 emissions were recorded on tape. Strip chart records were used to verify the data logger tapes and to fill in any gaps in the data from the automatic data logger. Daily tabulations of the emissions and unit operating data were provided by a technician on-site. A daily log was also kept with comments relative to unit operation and monitor operation. The emissions and unit operating data were tabulated in a format for input to a computer program for data analysis. A preliminary screening of the data was performed prior to input to the computer program.

After the preliminary screening, the data were input to the computer and a listing of 15-minute averages was compiled. These data were then used to compile 24-hour averages for the entire test period. A summary of the 24-hour averages compiled from the 15-minute averages for the 30-day test period is presented in Table 3.

After conducting baseline tests to measure the gaseous emissions without staged combustion air, the staged air system was activated and the stack oxygen was lowered to approximately 2 percent. The heater was then operated in this mode steadily for 15 days. After approximately 15 days, a change in the crude charge required an increase in firing rate. Since there are no automatic controls on the heater, the increase in fuel flow resulted in a deficiency in oxygen and high CO values. The operators responded by opening the stack damper resulting in large values of stack oxygen. Efforts were made to reduce the stack O_2 to the previous 2 percent level. Due to the changing conditions and lack of automatic controls, it was decided to operate the remainder of the test at about 4 percent stack oxygen. The highest 24-hour average CO emission rate was 71 ng/J (216 ppm at 3 percent O_2, dry). Peak values of CO were approximately 1300 ppm. Both O_2 and CO_2 were measured to provide redundant measurements for dilution calculations.

The NO emission rate as a function of days from the start of testing is presented in Figure 2.* The peak occurred during the upset condition when stack O_2 was increased. Even under the high O_2 condition, with the staged air system operating, the NO emission rate was much lower than the baseline level. The NO emission rate as a function of stack O_2 is shown in Figure 3. A linear regression analysis of these data showed a good correlation ($r^2 = 0.85$).

---

*Tests conducted on 12 refinery process heaters (various fuels singly or in combination) have shown that, on average, NO_2 represented 2.8 percent of NO_x (ranging from 0.5 to 4.4 percent). This low value justified neglecting the measurement of NO_2 during the extended duration test.

The NO emission rate data were then divided into two groups corresponding to 2 percent excess oxygen and 4 percent excess oxygen. Graphical analyses of the NO emission rates showed the data to be log-normally distributed. Figure 4 presents a log-probability curve of NO emission rate for the nominal 2 percent stack O_2 condition. The mean NO concentration for the 2 percent O_2 setting is 18.5 ng/J (0.04 lb/10^6 Btu). The nominal 4 percent O_2 condition is shown in Figure 5. The mean value of NO emission rate for these data is 25.5 ng/J (0.06 lb/10^6 Btu) with 99 percent of the values less than 30 ng/J (0.07 lb/10^6 Btu). The results of the 30-day test are summarized in Table 4. The overall NO_x reduction is based on the average NO emissions over the entire 30 days of the continuous monitor test.

Cost Effectiveness of Staged Combustion Air and Lowered Excess Air Applied to Natural Draft Process Heaters

The cost effectiveness of combustion modifications applied to three heater sizes is shown in Table 5. The values for lowered excess air and for staged combustion air plus lowered excess air on the largest heater are negative indicating a savings in combination with a NO_x reduction. This is a desirable situation; however, one must realize that a modification which saves money yet produces only a small NO_x reduction will have a large negative cost effectiveness ratio. This may not be the most desirable modification if the level of NO_x reduction is lower than is necessary to achieve compliance with regulations or to offset future emissions from plant expansions. The cost effectiveness values for staged combustion air are valid for gas firing and for firing a 50-50 mixture of No. 6 oil and gas.

The cost and cost effectiveness of staged combustion is compared with that of other commercially available modifications in Table 6 for a 29.3 MW (100 x 10^6 Btu/h) natural draft process heater. The values for low-NO_x burners and for selective non-catalytic reductions are developed from Reference 5. The values for cost effectiveness from Reference 5 have been adjusted to include state and federal taxes and a capital annualization factor of 0.2773. Fuel penalties were already included where efficiencies were reduced by modifications discussed in Reference 5; however, no credit was taken in Reference 5 for fuel savings where efficiencies increased due to a modification. Thus, the usual fuel savings due to installation of low-NO_x burners (since they often operate at lower excess air than standard burners) are not accounted for in Table 6. Note also that the column "Annual Operating Costs (Savings)" does not include taxes or insurance; however these items are accounted for in the cost effectiveness column.

From Table 6, it is observed that for a natual draft heater firing gas fuel both the percent NO_x reduction and the cost effectiveness of staged combustion compare favorably to other commercially available combustion modification techniques. Lowered excess air is certainly the most desirable modification from a financial standpoint; however it offers the least NO_x reduction capability. For oil-fired heaters, however, the NO_x reduction capability of lowered excess air may approach both low-NO_x burners and staged combustion lances (applied at normal O_2).

NO Emissions from Ten Refinery Heaters With Low-NO_x Burners

Figure 6 shows NO emissions as a function of stack oxygen for the ten process heaters tested. These data show that for all cases, lowering the oxygen resulted in lower NO emissions. The gas-fired heaters had lower NO emissions than did the distillate-oil-fired heater, and the residual-oil-fired heaters had the highest NO emissions. The gas-fired heaters with combustion air preheat had higher NO emissions than gas-fired heaters with ambient combustion air. The points at which significant CO emission or visible smoke occurred are marked in the figure as "CO limits."

Gas-fired heaters with ambient combustion air produced NO emissions in the 40-50 ng/J (80-100 ppm at 3 percent O_2, dry*) range in the "as found" condition. By lowering the stack oxygen to a CO limit or to the minimum acceptable operating condition as determined by the plant, NO emissions were reduced to approximately 25 ng/J (50 ppm). Heaters with preheated combustion air produced "as found" NO emissions in the 58 to 76 ng/J (115 to 150 ppm) range. Lowering stack oxygen resulted in NO reduction to a 25-43 ng/J (50-85 ppm) range.

"As found" NO emissions from a natural draft distillate-oil-fired process heater were 92-117 ng/J (168-212 ppm) and were reduced to approximately 58 ng/J (105 ppm) by lowering excess air to the single burner.

Emissions in the "as found" condition were considerably higher for the three units firing residual oil. All were natural draft units and two of them were found to be emitting 207-281 ng/J (370-500 ppm) of NO. The unit at Site 5 fired 15 to 20 percent refinery gas simultaneously with the residual oil. This unit was found to be emitting 194-205 ng/J (350-370 ppm) of NO and was the only unit firing residual oil which showed a significant tendency toward reduced emissions when excess air levels were lowered. At reduced excess air settings this unit produced about 166 ng/J (300 ppm) of NO.

Table 7 is a summary of gaseous emissions and efficiency for each site tested in the present study. A comparison of emissions at as found conditions and at optimum low-NO_x conditions (i.e., lowest NO emission without adverse effects on flame stability or unit efficiency) is made in this table. At most sites significant reductions in NO emission below as found levels could be achieved along with small increases or, at worst, no change, in efficiency. With respect to flame stability, product flows and temperatures, and emissions of CO, unit operations at the optimum low-NO_x conditions were generally unchanged from the as found conditions.

A summary of NO emissions from the heater configurations studied in this program over the tested range of operating variables is given in Table 8. The values reported in parentheses are ppm corrected to 3 percent O_2, dry. (NO_2 emissions were not included in this table due to lack of data at some sites. The data available from Sites 6-10, however, show that the NO_2 emissions averaged only 3.6 percent of the total NO_x emissions.)

---

*All emission concentrations given as ppm are corrected to 3% O_2, dry basis.

In Reference 6 past NO_x emissions data on refinery process heaters firing oil and gas were summarized. These data are presented in Table 9. Unfortunately, the paucity of baseline data from oil-fired process heaters with standard burners renders comparisons with the present low-NO_x burner data difficult. Mechanically drafted heaters with low-NO_x burners firing gas, however, appear to have significantly lower NO_x emissions relative to the standard burners. Examination of Tables 8 and 9 reveals that low-NO_x burners produced NO_x emissions (neglecting NO_2) which were 32 to 77 percent less than the average emission factor for all standard burners on mechanical draft, gas-fired heaters. The variations in NO_x emissions from low-NO_x burners were due to operating differences among units such as excess air level and air register settings. It is important to note that there is no NO_x data available on any of the units tested in this program for operation with standard burners. Thus, a direct comparison of NO_x emissions with and without low-NO_x burners cannot be made for any particular heater. Because of a lack of availability no naturally drafted gas-firing low-NO_x burners were tested during the present program; hence, a comparison with their standard counterparts cannot be made at this time.

Extended Duration Test of a Refinery Heater With Low-NO_x Burners

Gaseous emissions were obtained in a manner similar to that used during the extended duration test of the process heater equipped with staged combustion air lances. A summary of the 24-hour average emissions compiled from the 15-minute averages for the 30-day test period is presented in Table 10.

During the test period, the heater load or charge rate varied from a low value of 42.5 m^3/h (6411 bbl/day) to a maximum of 57.2 m^3/h (8638 bbl/day). This corresponds to a variation from 67 percent to 90 percent of rated capacity. Fuel flow measurements were unavailable. The heat input rates were estimated from the fuel and stack gas analyses.

Figure 7 shows daily average stack oxygen concentration as a function of time from the start of testing. During the first nine days of the endurance test the heater operated at an average of 3.8 percent O_2 (3.1 to 4.7 percent O_2). After nine days of testing the heater had to be shut down for maintenance. The peak O_2 value occurred when the heater was brought back on line after being down for 13 days. The stack O_2 was then lowered to about 6.8 percent by the operators. The operators were then requested to further lower the stack O_2. The heater then operated for seven days at an average O_2 of 5.0 percent before an upset was caused by a faulty charge compressor. This caused large fluctuations in load which forced the operators to increase O_2 to an average of 7.8 percent to prevent smoking from occurring during load surges. The O_2 was then subsequently lowered to 6.4 percent for the remainder of the test period. The heater had no O_2 measurement system (either permanently installed or portable) and only a manual damper control, so upsets in firing rate (or load) resulted in fairly large fluctuations in stack O_2 concentration due to over-compensation by the operators. For this reason the operators preferred maintaining a fairly high O_2 concentration (>5.0 percent). The corresponding daily NO average emissions are shown in Figure 8. CO emissions were always less than 100 ppm.

The stack O_2 concentration was found to be strongly influenced by the heater load or firing rate. Without active stack damper controls, the oxygen concentration tended toward high values as the heater firing rate diminishes. Data collected also showed that the NO emissions were not a strong function of O_2 concentration in this heater. It should be noted that gradual load changes accomplished over a period of hours could occur with only minor variations in stack O_2. However, rapid changes in throughput (such as those caused by the charge compressor problems) could drastically alter the flue gas composition.

The daily average NO emission rate was plotted on logarithmic-probability paper as shown in Figure 9. These data resulted in a staight line which indicates the data are best represented by a log-normal distribution. Examination of this figure shows the mean NO value to be 44 ng/J (0.10 lb/10^6 Btu). The geometric dispersion, which is analogous to a standard deviation in a normal distribution, is 1.07. The figure shows that 99 percent of the values are less than 50 ng/J (0.116 lb/10^6 Btu).

CONCLUSIONS

The work reported herein has satisfied all of the program objectives. The effectiveness of advanced combustion modifications in reducing NO_x emissions has been investigated during field testing of industrial process heaters. The retrofit of the staged combustion air system required only minor hardware modifications for its installation. No adverse heater operational effects were noted. The retrofit of low-NO_x burners to an existing heater will require some amount of rework of the burner front. The amount of rework will depend primarily on the difference in diameter between the existing burners and their corresponding low-NO_x replacements.

The staged combustion air system applicability does not appear to have any significant limitations. The system can be designed to circumvent potential mechanical interferences on the burner front. In addition, the number of lances, their diameter, length, and placement can be tailored to match most physical requirements. The retrofit of low-NO_x burners could be limited on the basis of their flame shape. Heaters with either a narrow width or short height may not be suitable retrofit candidates as flame impingement on the tubes may occur.

The combustion modifications employed on the petroleum process heater proved to be an effective NO_x control technique. Staged combustion air resulted in a 60 percent reduction in NO emission rate with the unit operating at 4 percent stack oxygen and a 71 percent reduction with the oxygen lowered to 2 percent. Operation of the heater with the above combustion modifications in effect for 30 days did not require any additional operating personnel or attention. No changes in temperature distribution within the furnace were observed. Post-text examination of the hardware showed no discernible deterioration of the staged air system. At baseline stack O_2 of 4 percent, the mean NO emission level was 25.5 ng/J (0.06 lb/10^6 Btu). At 2 percent O_2, the mean NO emission level was 18.5 ng/J (0.04 lb/10^6 Btu).

The cost of these NO_x reduction techniques appears to be competitive with other means of NO_x control applied to process heaters. The effectiveness of low-NO_x burners depends upon operating techniques, especially excess air level and air register settings. By making changes in excess air and air register settings, NO_x emissions were reduced at every site with improved overall heater performance.

Gas-fired heaters equipped with commercially available low-NO_x burners and operating with ambient combustion air produced NO_x emissions in the 40-50 ng/J (80-100 ppm at 3 percent O_2, dry) range in the "as found" condition. At the minimum acceptable excess air condition as determined by the plant, NO_x emissions were reduced to approximately 25 ng/J (50 ppm). Heaters with preheated combustion air produced "as found" NO_x emissions in the 58 to 76 ng/J (115 to 150 ppm) range. Lowering excess air resulted in NO_x reduction to a 25-43 ng/J (50-85 ppm) range.

"As found" NO emissions from a low-NO_x-burner-equipped natural draft distillate-oil-fired process heater were 92-117 ng/J (168-212 ppm) and were reduced to approximately 58 ng/J (105 ppm) by lowering excess air to the single burner.

Emissions in the "as found" condition for two of the three natural draft units firing residual oil with low-NO_x burners installed were 207-281 ng/J (370-500 ppm) of NO. The third unit fired 15 to 20 percent refinery gas simultaneously with the residual oil. This unit was found to be emitting 194-205 ng/J (350-370 ppm) of NO and was the only unit firing residual oil which showed a significant tendency toward reduced emissions when excess air levels were lowered. At reduced excess air settings this unit produced about 166 ng/J (300 ppm) of NO.

An extended duration test of a natural draft process heater with low-NO_x burners resulted in a mean NO value of 44 ng/J (0.10 lb/10^6 Btu) with the heater load fluctuating from 42.5 to 57.2 m^3/h (6411 to 8638 bbl/day). From previous field tests the average NO_x emissions from various types of natural draft process heaters with standard burners were 61 ng/J (0.14 lb/10^6 Btu). Heater operation with the low-NO_x burners presented no reliability or functional problems during the 30-day test.

REFERENCES

1. Hunter, S. C. et al. Application of Advanced Combustion Modifications to Industrial Process Equipment - Process Heater Subscale Tests. In: Proceedings of the Third Stationary Source Combustion Symposium, Vol. III, EPA-600/7-79-050c, February 1979.

2. Tidona, R. J. et al. Emission Reduction by Combustion Modification for Petroleum Process Heaters. In: Proceedings of the Joint Symposium on Stationary Combustion NO_x Control, Vol. IV, EPA-600/9-81-028d, July 1981.

3. Carter, W. A. and R. J. Tidona. Thirty-Day Field Test of a Refinery Process Heater Equipped with Low-NO_x Burners, EPA-600/7-83-010, February 1983.

4. Tidona, R. J. et al. Emissions from Refinery Process Heaters Equipped With Low-NO_x Burners. EPA-600/7-81-169, October 1981.

5. South Coast Air Quality Management District and Stationary Source Control Division, Air Resources Board, Joint Staff Report, SS-81-016. Public Meeting to Consider a Suggested Control Measure for the Control of Emissions of Oxides of Nitrogen from Boilers and Process Heaters in Refineries, October 1981.

6. Hunter, S. C. and S. S. Cherry. NO_x Emissions from Petroleum Industry Operations. API Publication No. 4311, American Petroleum Institute, Washington, D.C., October 1979.

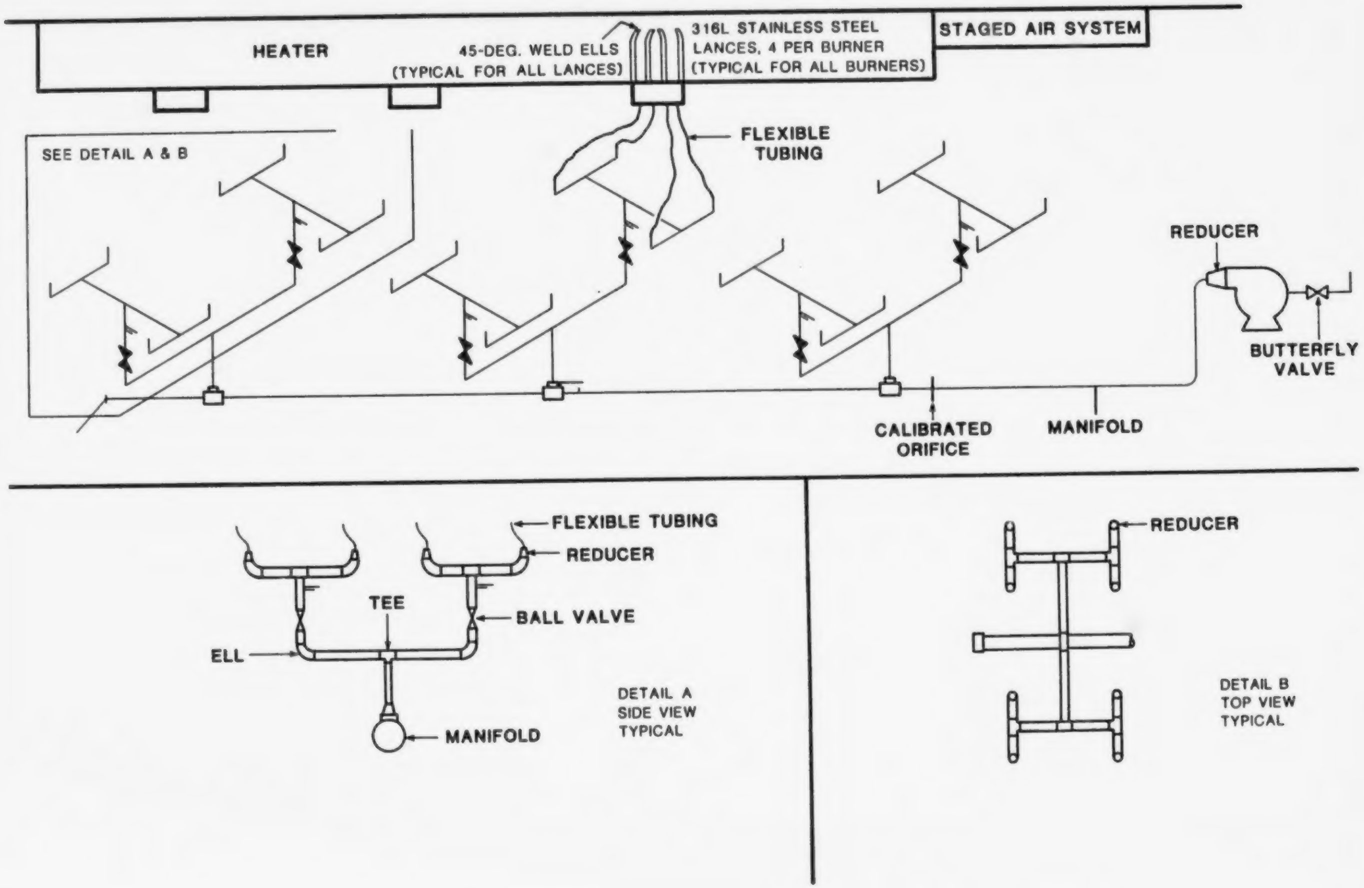
HEATER
45-DEG. WELD ELLS
(TYPICAL FOR ALL LANCES)
316L STAINLESS STEEL
LANCES, 4 PER BURNER
(TYPICAL FOR ALL BURNERS)
STAGED AIR SYSTEM
SEE DETAIL A & B
FLEXIBLE TUBING
REDUCER
BUTTERFLY VALVE
CALIBRATED ORIFICE
MANIFOLD
FLEXIBLE TUBING
REDUCER
TEE
BALL VALVE
ELL
MANIFOLD
DETAIL A
SIDE VIEW
TYPICAL
REDUCER
DETAIL B
TOP VIEW
TYPICAL

Figure 1. Flow schematic of staged combustion air system for a natural draft process heater.

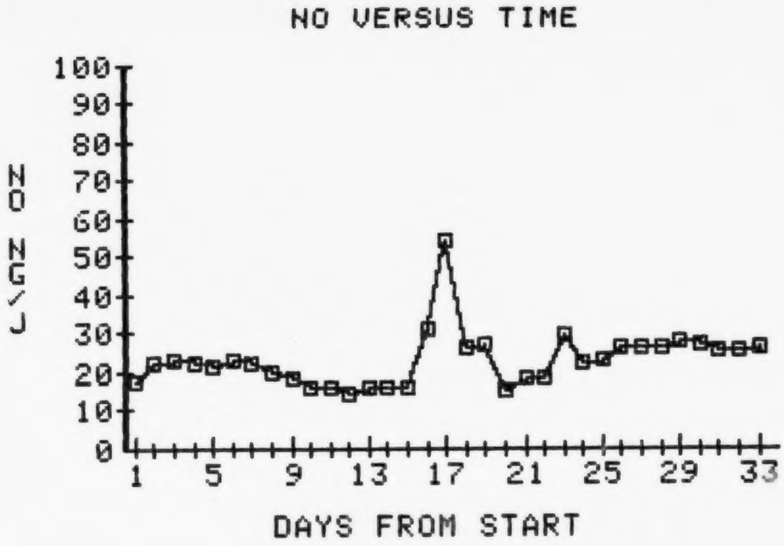

Figure 2. NO emissions during a 30-day test of a process heater with staged combustion air lances.

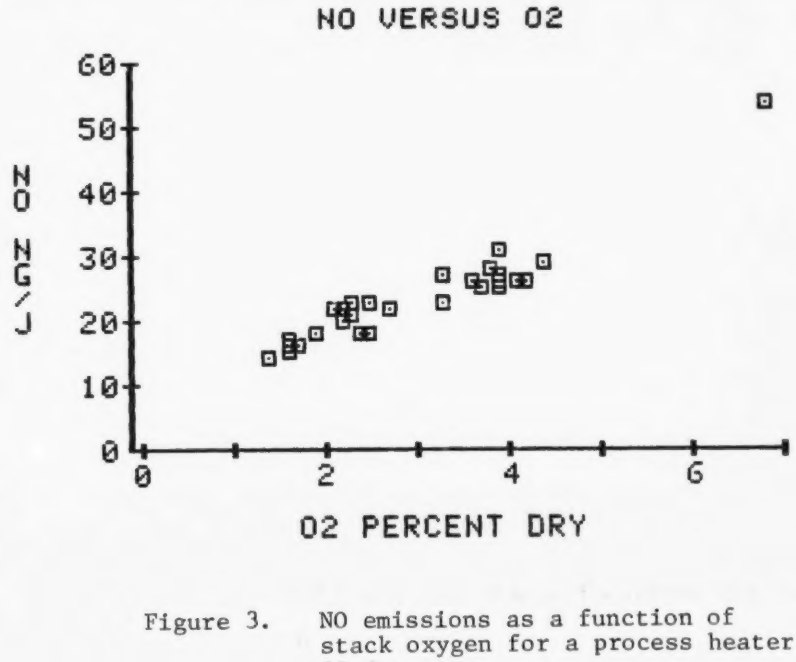

Figure 3. NO emissions as a function of stack oxygen for a process heater 30-day test.

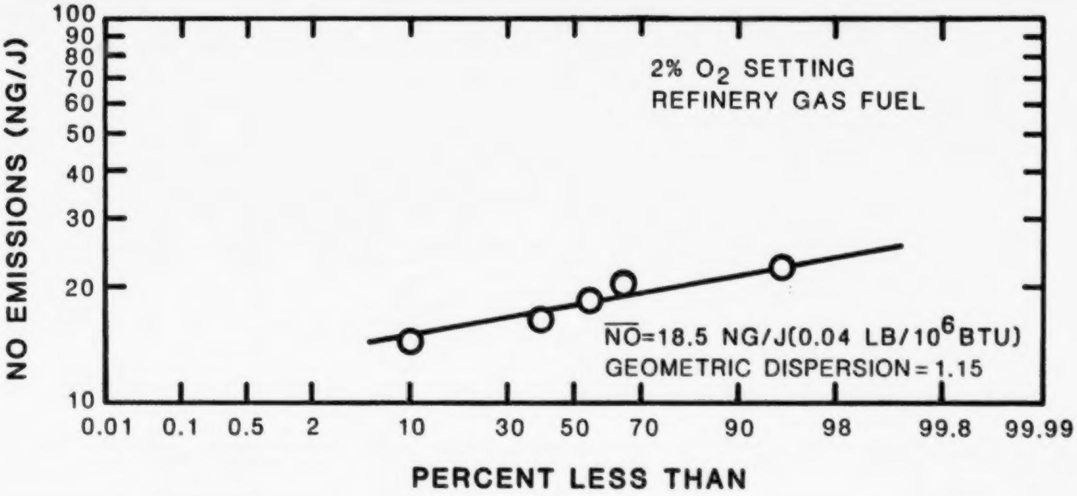

Figure 4. Log-probability curve of NO emissions for a petroleum process heater at reduced excess air setting.

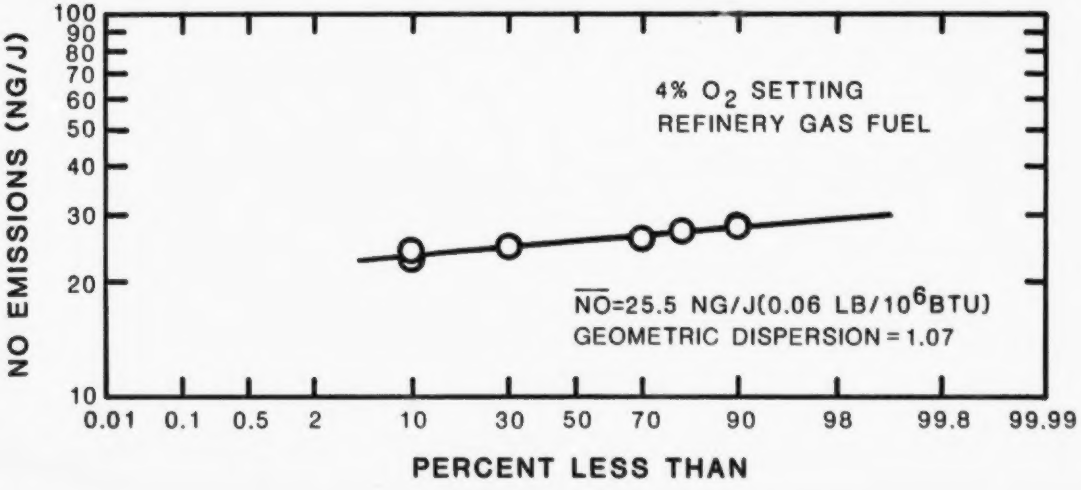

Figure 5. Log-probability curve of NO emissions for a petroleum process heater at normal operating excess air.

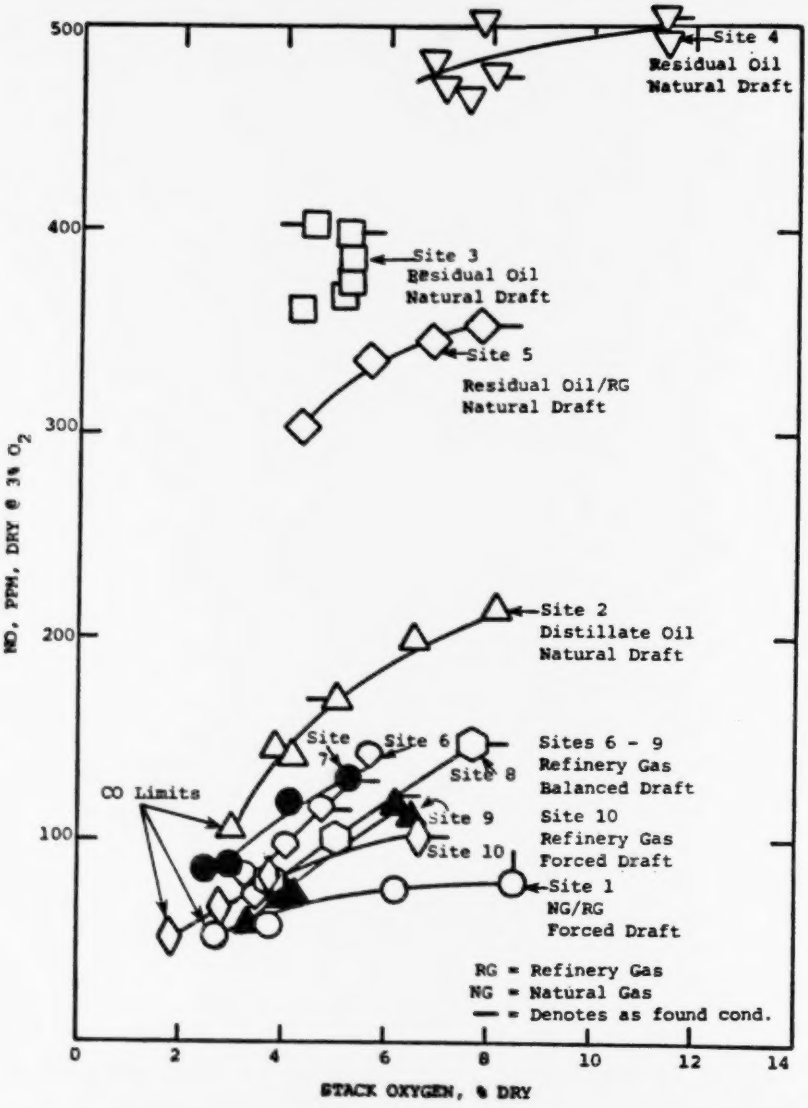

Figure 6. NO emissions as a function of stack oxygen for low-NO_x burners in process heaters.

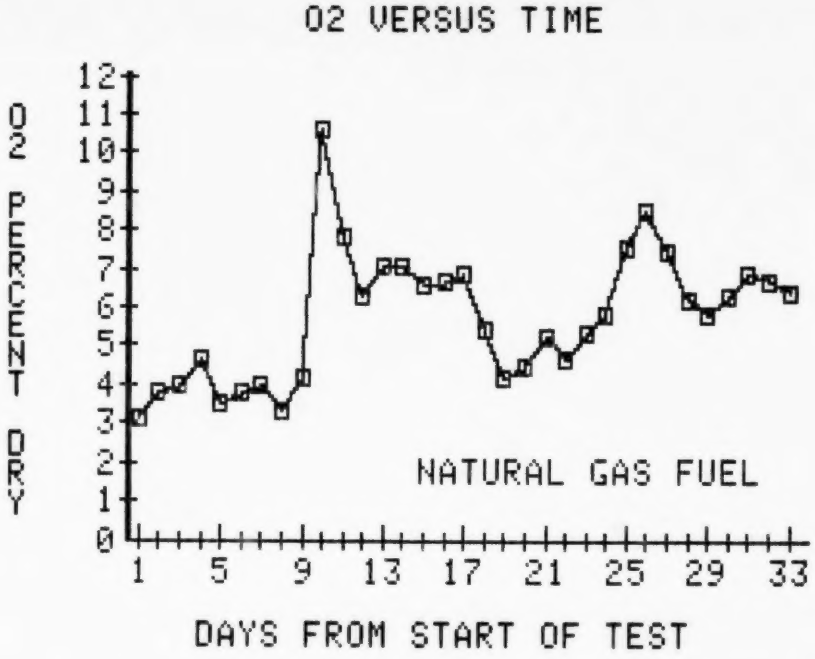

Figure 7. Daily average O_2 concentration as a function of time for a process heater with low-NO_x burners.

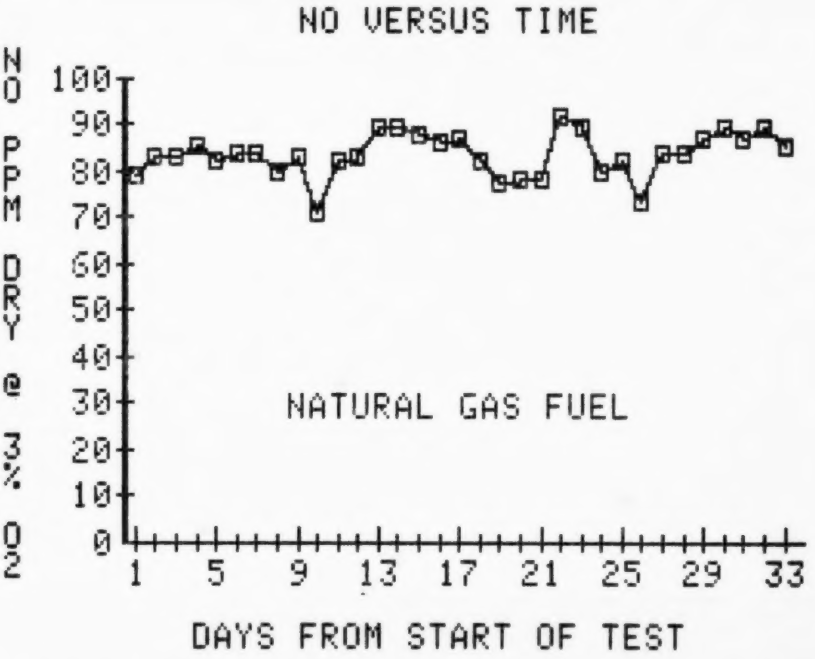

Figure 8. Daily average NO concentration as a function of time for a process heater with low-NO_x burners.

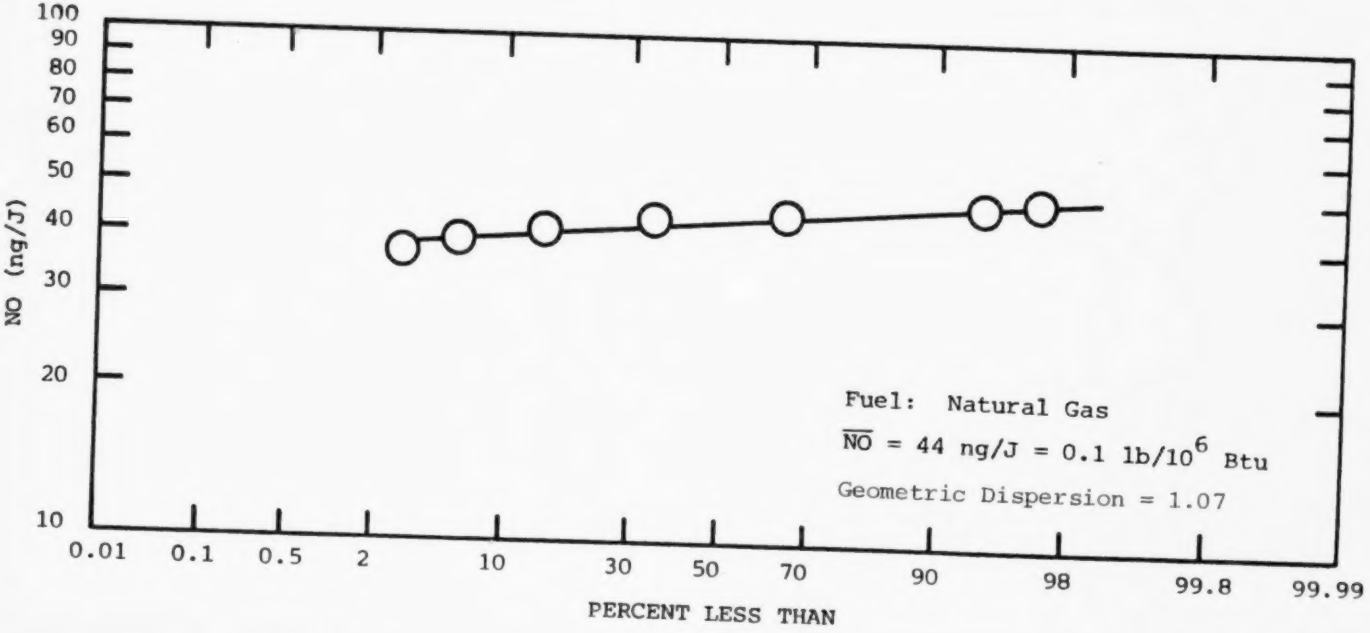

Figure 9. Log-probability plot of NO emission rate - process heater with low-NO_x burners

TABLE 1. HEATER TEST SITES - LOW-NO_x BURNERS

Site No.	Heat Input Rate		No. of Burners	Fuel(s) Tested	Heater Configuration	Burner Type
	MW	10^6 Btu/hr				
1	6.4	22	3	Ref. and Nat. Gas	Ambient, Forced Draft	John Zink LNC-PC-16
2	4.7	16	1	Lo-S Resid. Oil	Natural Draft	John Zink LNC-16
3	11.7	40	12	#6 Oil	Natural Draft	John Zink LNC-12
4	6.7	22.9	3	#6 Oil	Natural Draft	John Zink LNC-16
5	11.7	40	10	#6 Oil and Ref. Gas	Natural Draft	John Zink LNC-PC-10
6	9.7	33	8	Ref. Gas	Preheat, Bal. Draft	CEA Low-NO_x*
7	14.4	49	8	Ref. Gas	Preheat, Bal. Draft	CEA Low-NO_x*
8	8.8	30	8	Ref. Gas	Preheat, Bal. Draft	CEA Low-NO_x*
9	6.4	32	8	Ref. Gas	Preheat, Bal. Draft	CEA Low-NO_x*
10	8.8	30	1	Ref. Gas	Ambient, Forced Draft	CEA Low-NO_x*

*Combustion Equipment Associates (CEA) - model number not available.

TABLE 2. EMISSION MEASUREMENT INSTRUMENTATION

Species	Manufacturer	Measurement Method	Model No.
Hydrocarbon	Beckman Instruments	Flame Ionization	402
Carbon Monoxide	Beckman Instruments	IR Spectrometer	865
Oxygen	Teledyne	Polarographic	326A
Carbon Dioxide	Beckman Instruments	IR Spectrometer	864
Nitrogen Oxides	Thermo Electron Co.	Chemiluminescent	10A
Particulates	Joy Manufacturing Co.	EPA Method 5 Train	EPA
Sulfur Dioxide	DuPont Instruments	UV Spectrometer	400

TABLE 3. SUMMARY OF 24-HOUR AVERAGE GASEOUS EMISSIONS DATA

PETROLEUM PROCESS HEATER, STAGED COMBUSTION AIR, REFINERY GAS FUEL
24 HOUR DATA
DRY STACK GAS CONCENTRATION

DATE	LOAD bbl/day*	O2 VOL% MEAS	CO2 VOL% MEAS	CO PPMV MEAS	NO PPMV MEAS	CO PPMV 3%O2	NO PPMV 3%O2	CO NG/J	NO NG/J
5/ 1/81	10717.0	1.6	12.3	8	35	7	32	2	17
5/ 2/81	10717.0	2.1	12.0	11	43	10	40	3	22
5/ 3/81	10717.0	2.3	11.9	11	45	10	43	3	23
5/ 4/81	10717.0	2.2	11.9	13	44	12	42	4	22
5/ 5/81	10717.0	2.3	11.9	28	42	26	40	8	21
5/ 6/81	10717.0	2.5	11.7	9	44	8	42	2	23
5/ 7/81	10717.0	2.7	11.6	28	43	27	42	9	22
5/ 8/81	10717.0	2.2	11.9	6	39	5	37	1	20
5/ 9/81	10717.0	1.9	11.8	13	36	12	33	4	18
5/10/81	10717.0	1.6	12.3	13	32	12	29	3	16
5/11/81	11178.7	1.6	12.3	43	32	39	29	13	16
5/12/81	10717.0	1.4	12.4	9	30	8	27	2	14
5/13/81	10717.0	1.7	12.2	5	32	4	29	1	16
5/14/81	10717.0	1.6	12.2	12	33	11	30	3	16
5/15/81	10717.0	1.6	12.1	12	32	11	29	3	16
5/16/81	10717.0	3.9	10.5	70	55	73	57	24	31
5/17/81	10717.0	6.8	8.9	7	79	8	100	2	54
5/18/81	10717.0	3.6	10.8	209	48	216	49	71	26
5/19/81	10717.0	3.3	10.8	95	49	96	49	31	27
5/20/81	10717.0	1.6	11.9	55	31	51	28	16	15
5/21/81	10717.0	2.4	11.7	11	36	10	34	3	18
5/22/81	10717.0	2.5	11.7	48	36	46	34	15	18
5/23/81	10717.0	4.4	10.5	20	50	21	54	7	29
5/24/81	10717.0	2.1	12.0	20	43	19	41	6	22
5/25/81	10717.0	3.3	11.3	98	43	99	43	32	23
5/26/81	10717.0	4.2	10.7	7	45	7	48	2	26
5/27/81	10717.0	4.2	10.6	8	45	8	48	2	26
5/28/81	10717.0	4.1	10.4	5	46	5	49	1	26
5/29/81	10717.0	3.8	10.8	10	51	10	53	3	28
5/30/81	10717.0	3.9	10.8	13	49	13	51	4	27
5/31/81	10717.0	3.9	10.8	12	45	12	47	4	25
6/ 1/81	10717.0	3.7	10.8	8	45	8	46	2	25
6/ 2/81	10717.0	3.9	10.6	6	46	6	48	2	26

*barrels/day (bbl/day • 6.624 • 10^{-3} = m^3/h)

TABLE 4. 30-DAY TEST RESULTS FOR A PROCESS HEATER WITH STAGED COMBUSTION AIR LANCES

Baseline NO_x (ng/J)	NO_x Reduction @ 4% O_2 (%)	NO_x Reduction @ 2% O_2 (%)	NO_x Reduction Overall (%)
64	60 (25.5 ng/J)	71 (18.5 ng/J)	64 (22.9 ng/J)

TABLE 5. COST EFFECTIVENESS IN \$/Mg (\$/lb) OF NO_x REDUCTION FOR COMBUSTION MODIFICATIONS APPLIED TO THREE NATURAL DRAFT PROCESS HEATER SIZES

	Heater Size		
Modification	16.1 MW	29.3 MW	147 MW
Staged Combustion Air at 4% O_2	2636 (1.20)	2362 (1.07)	1934 (0.88)
Staged Combustion Air + Lowered Excess Air	1089 (0.50)	700 (0.32)	-40 (-0.02)
Lowered Excess Air Firing Gas	-5843 (-2.66)	-6853 (-3.12)	-4813 (-2.19)
Lowered Excess Air Firing Oil and Gas	-1459 (-0.66)	-1712 (-0.78)	-2189 (-1.00)

TABLE 6. COST AND COST EFFECTIVENESS OF VARIOUS CONTROL TECHNOLOGIES APPLIED TO A 29.3 MW NATURAL DRAFT PROCESS HEATER

Type of Control	Approximate Percent NO_x Reduction	Installed Capital Cost $/MW	Annual Operating Costs (Savings) $/Year	Average Cost Effectiveness $/Mg	$/lb
Lowered Excess Air (gas fuel)	15	2,035	58,821	<0	<0
Low-NO_x Burners	35	2,915	--	2,599	1.18
Selective Noncatalytic Reduction	50	4,266	46,089	5,176	2.35
Staged Combustion Air, Normal O_2 (gas fuel)	60	2,529	30,508	2,362	1.07
Staged Combustion Air, Low O_2 (gas fuel)	71	4,563	(30,722)	700	0.32

TABLE 7. OPTIMUM LOW-NO_x AND AS-FOUND GASEOUS EMISSIONS AND EFFICIENCIES AT TEN HEATERS EQUIPPED WITH LOW-NO_x BURNERS

		As Found					Optimum Low-NO_x					
Site	Heater[†] Config.	NO (ng/J)	NO (ppm)	O_2 (%)	CO (ppm)*	Htr. Eff. (%)	NO (ng/J)	NO (ppm)	O_2 (%)	CO (ppm)*	Htr. Eff. (%)	% NO Reduction
1	121	39.0	77	6.2	0	79.9	24.0	48	3.0	20	83.0	38.5
2	211	92.4	168	5.1	11	64.0	80.4	145	4.0	11	64.0	13.0
3	311	222.0	396	5.2	11	63.4	203.0	361	4.3	11	64.5	8.5
4	311	268.0	477	8.1	0	67.9	264.0	471	7.1	0	68.6	1.5
5	411	194.0	352	7.7	11	---	167.0	303	4.4	22	---	13.9
6	132	57.9	114	4.8	11	69.8	38.1	75	3.5	11	71.3	34.2
7	132	65.8	130	5.3	11	68.0	35.4	70	2.3	33	68.5	46.2
8	132	74.9	148	7.7	14	65.4	41.0	81	3.8	15	69.2	45.3
9	132	60.2	119	8.4	0	66.4	32.9	65	3.3	10	68.8	45.3
10	121	51.6	102	6.7	13	73.1	32.9	65	2.8	10	74.4	36.2

*Dry, corrected to 3% O_2.

†Heater configuration designations as follows:

1st Digit	2nd Digit	3rd Digit
Fuel burned	Draft type	Air temp.
1 = gas	1 = natural	1 = ambient
2 = dist. oil	2 = forced	2 = preheated (approximately 544 K, 520°F)
3 = residual oil	3 = balanced	
4 = combined oil & gas		

TABLE 8. NO EMISSIONS FROM PROCESS HEATERS WITH LOW-NO_x BURNERS

Unit Type	Fuel Type			
	Gas (Ref. or NG)	Distillate Oil	Residual Oil + Gas	Residual Oil
Natural Draft	-	58-117 $\frac{ng}{J}$ (105-212 ppm)	167-202 $\frac{ng}{J}$[1] (303-366 ppm)	207-284 $\frac{ng}{J}$ (369-506 ppm)
Forced Draft, Ambient Air	26-52 $\frac{ng}{J}$ (51-102 ppm)	-	-	-
Balanced Draft, Air Preheat	25-75 $\frac{ng}{J}$ (50-148 ppm)	-	-	-

[1] Ratio of heat input from oil to heat input from gas <83/17

TABLE 9. MEAN NO_x EMISSIONS FROM PROCESS HEATERS WITH STANDARD BURNERS

Unit Type	Fuel Type			
	Gas (Ref. or NG)	Distillate Oil	Residual Oil + Gas	Residual Oil
Natural	60.6 $\frac{ng}{J}$ (25 tests)	-	-	-
Mechanical	111 $\frac{ng}{J}$ (6 tests)	-	89.6 $\frac{ng}{J}$[1] (5 tests)	138 $\frac{ng}{J}$ (3 tests)
Not Reported (Bay Area A.P.C.D.)	70.0 $\frac{ng}{J}$ (64 tests)	-	-	-
Not Reported (AP-42)	95 $\frac{ng}{J}$ (8 tests)	198 $\frac{ng}{J}$ (4 tests) - oil - firing only; type unspecified		

[1] Ratio of heat input from oil to heat input from gas <60/40

TABLE 10. SUMMARY OF DAILY AVERAGE GASEOUS EMISSIONS

PETROLEUM PROCESS HEATER, LOW NOX BURNERS
24 HOUR DATA
DRY STACK GAS CONCENTRATION

DATE	LOAD bbl/day*	O2 VOL% MEAS	CO2 VOL% MEAS	CO PPMV MEAS	NO PPMV MEAS	CO PPMV 3%O2	NO PPMV 3%O2	CO NG/J	NO NG/J
7/31/81	7920.0	3.1	10.2	11	79	11	79	3	43
8/ 1/81	7920.0	3.8	9.5	7	80	7	83	2	45
8/ 2/81	7920.0	4.0	9.3	8	79	8	83	2	45
8/ 3/81	7920.0	4.7	9.1	7	77	7	85	2	46
8/ 4/81	7755.0	3.5	9.5	7	80	7	82	2	44
8/ 5/81	8580.0	3.8	9.4	8	81	8	88	2	46
8/ 6/81	8580.0	4.0	9.2	6	80	6	84	2	45
8/ 7/81	8580.0	3.3	10.0	6	79	6	80	2	43
8/ 8/81	8580.0	4.2	9.3	5	78	5	83	1	45
8/21/81	6550.0	10.6	5.1	48	41	83	71	27	38
8/22/81	6550.0	7.8	7.1	6	60	8	82	2	44
8/23/81	6700.0	6.3	7.9	6	68	7	83	2	45
8/24/81	7150.0	7.1	7.5	8	69	10	89	3	48
8/25/81	7150.0	7.1	8.0	11	69	14	89	4	48
8/26/81	6811.4	6.6	8.1	5	71	6	88	2	48
8/27/81	6524.8	6.7	8.1	5	69	6	86	2	47
8/28/81	7531.5	6.9	7.9	7	68	8	87	2	47
8/29/81	8638.2	5.4	8.9	6	71	6	82	2	44
8/30/81	8290.0	4.2	9.6	22	72	23	77	7	41
8/31/81	8290.0	4.5	9.3	13	72	14	78	4	42
9/ 1/81	8025.5	5.2	8.7	7	69	7	78	2	42
9/ 2/81	8500.0	4.7	9.6	49	84	53	92	17	50
9/ 3/81	7546.8	5.3	10.4	6	78	6	89	2	48
9/10/81	6990.5	5.8	9.0	18	68	21	80	7	43
9/11/81	7000.0	7.5	7.9	21	62	28	82	9	44
9/12/81	7000.0	8.5	7.3	30	51	43	73	14	39
9/14/81	7000.0	7.4	7.9	12	64	15	84	5	46
9/15/81	7000.0	6.2	8.8	15	69	18	84	6	45
9/16/81	7000.0	5.8	9.0	16	74	19	87	6	47
9/17/81	6892.3	6.3	8.8	15	73	18	89	6	48
9/18/81	6849.5	6.9	7.7	12	68	15	87	5	47
9/19/81	6935.3	6.7	8.6	16	71	20	89	6	48
9/20/81	7000.0	6.8	8.7	17	69	20	85	6	46

*barrels/day (bbl/day • 6.624 • 10^{-3} = m^3/h)

NO_x GENERATION, EMISSION AND CONTROL FROM CEMENT KILNS IN THE UNITED STATES

By:

Mallory S. May
Gifford-Hill & Company, Inc.
Department of Environmental Affairs
8435 Stemmons Freeway
Dallas, Texas 75247

ABSTRACT

During the past 10 years, considerable knowledge of NO_x generation, emission and control has been obtained from research of the combustion of fossil-fuels and from combustion in utility boilers and industrial processes. Although many have tried, this data cannot be extrapolated to the portland cement manufacturing process. Recent regulatory and process-control interest in the generation and emission of NO_x in the cement manufacturing process has stimulated the acquisition of information and the development of research pertaining to this matter within the cement industry.

In this paper, the existing data from the U.S. cement manufacturing industry has been reviewed. From this data it may be concluded that coal-fired conventional systems emit less NO_x; NO_x emissions from preheater/precalciner systems vary with the system. Coal increases NO_x emissions in some NSP systems. Final conclusions about NSP systems must await further study of raw materials and operational contributions to NO_x generation.

I. DESCRIPTION OF THE PORTLAND CEMENT MANUFACTURING PROCESS

Most of the hydraulic cement in the United States is portland cement. Portland cement, a cementous, crystalline compound composed of metallic oxides, is produced by a pyroprocess in a rotary kiln from raw materials, e.g., limestone, shale, clay and sand, containing calcium carbonate and aluminum, iron and silicon oxides. This manufacturing process may be conveniently divided into five stages correlated with location and temperature of the materials in the rotary kiln.

(1) Evaporation of uncombined water from raw materials occurs as material temperature increases to 212°F.

(2) As the material temperature increases from 212°F to approximately 800°F, dehydration and precalcination occur.

(3) Between 800°F and 1650°F, carbon dioxide is liberated from the carbonates.

(4) Following calcination, sintering of the oxides occurs at temperatures up to 2750°F in the burning zone of the rotary kiln.

(5) Cement clinker is produced, following sintering, as the temperature of the material decreases from 2750°F to 2500°F.

Figure 1 is a typical drawing of a rotary kiln. The raw-material mix enters the kiln at the elevated end; the burner is at the opposite end. The raw materials are changed into cementous oxides of metals by a counter-current, heat-exchange process. The materials are continuously and slowly moved to the lower end by the rotary movement of the kiln. The fuel burned in the kiln is natural gas, oil and coal. Many cement plants have converted to coal since 1974; recently, alternate fuels such as waste solvents, chipped rubber, shredded municipal garbage and coke have been used.

There are basically three variations to the cement manufacturing process, i.e., wet, dry and dry preheater/precalciner processes. These processes are essentially identical relative to the manufacture of cement from raw materials. However, the type of process does change the equipment design, the method of operation and the consumption of fuel. Fuel combustion is different between wet and dry processes and the preheater/precalciner process. In the former, all fuel combustion occurs in the kiln. In the latter, some fuel combustion occurs in a precalcining or calcining vessel before the materials enter the kiln (Figure 1). Generally speaking, the length of the rotary kiln (Figure 1) and the consumption of fuel decrease as the manufacturing process changes from wet to dry to preheater/precalciner equipment for the same mix design of raw materials. However, the relationship is not linear, but it may generally be said that BTU/ton significantly decreases as plant configuration changes from wet to dry to preheater/precalciner for obvious reasons.

II. GENERATION OF NO_x IN THE CEMENT MANUFACTURING PROCESS

Oxides of nitrogen (NO_x) are generated during fuel combustion by oxidation of chemically bound nitrogen in the fuel and by thermal fixation of nitrogen in the combustion air. Also, as the flame temperature increases, the amount of thermally generated NO_x increases; the amount of NO_x generated from fuel increases as the quantity of nitrogen in the fuel increases. In the cement manufacturing process there are two combustion zones in which NO_x may be generated, i.e., the burning zone of the kiln and the burning zone of a precalcining vessel (Figure 1). Also, in the cement manufacturing process, the type of fuel burned will affect the quantity and type of NO_x generated. Natural gas combustion with a high flame temperature and low fuel nitrogen may generate a different quantity of NO_x than oil or coal which have higher fuel nitrogen but lower flame temperatures.

The fuels vary in the cement manufacturing process. Generally, natural gas is used only in the kiln, while coal and oil are used in the kiln and precalcining vessel. Therefore, the generation and emission of NO_x is related to the type of fuel burned to the extent that fuel affects the flame temperature and contains chemically bound nitrogen.

III. EMISSIONS OF NO_x FROM THE CEMENT MANUFACTURING PROCESS

Until the mid-1970's, NO_x emissions from rotary kilns had received little attention in the United States, except for some plants that correlated NO_x emission with burning-zone conditions to control the quality of the product. Hence, there has been only a limited amount of data collected until recently; essentially all of this data has come from grab samples. Only in the past 18 months have continuous monitoring programs begun. It will probably be late 1984 before significant amounts of this data will be available. However, during the past eight years enough grab samples have been collected and analyzed to suggest some relationships between fuel, processes, temperatures and NO_x generation.

In Table I, a comparison of NO_x emissions from two dry-process kilns with different fuels is shown in terms of pounds of NO_x per ton of clinker produced. NO_x emissions declined from both Kiln A and Kiln B as fuels changed from gas to oil to coal. On the other hand, in both Figures 2 and 3, NO_x emissions in pounds per ton of clinker increased when fuel was changed from oil to coal.

Table II represents data of coal-fired wet and preheater/precalciner processes. The wet process emissions are comparable with other similar data. The preheater/precalciner data are contradictory. One is extremely low; the other is comparable to some oil data. The data in Table III support the inconsistency of the data in Table II. Coal-fired preheater/precalciner data varies.

Finally, Figures 2 and 3 provide clear-cut comparisons of oil and coal fuels in a preheater/precalciner process.

From this data three observations appear to be clear. Changes in fuel from gas to oil to coal in a dry process result in a decrease in NO_x emissions. Secondly, the NO_x emissions of coal-fired preheater/precalciner processes vary, probably related to the configuration of the process. Finally, coal-fired preheater/precalciner has greater NO_x emissions than the same system fired with oil.

IV. CONTROL OF NO_x FROM THE CEMENT MANUFACTURING PROCESS

Presently, there is data to support only two types of reduction of NO_x in the cement industry. First, for conventional wet and dry-process kilns, NO_x emissions are reduced by fuel conversion with coal producing the least amount of NO_x. With new construction, the data is not yet clear. Some preheater/precalciner systems have low emissions; others have high emissions.

There is not a single type of preheater/precalciner system used in the cement industry. There are at least ten different systems. Each system appears to have unique emissions properties. However, it does appear that for a single system, oil in the calciner produces less NO_x than coal (Figures 2 and 3). The NO_x emissions from the preheater/precalciner appear to be related to their design. Some have very low emissions and others have emissions in a mid-range of some conventional or wet processes. At the present time there is insufficient data to choose a NSP system to minimize NO_x emissions.

V. CONCLUSIONS

Coal-fired conventional systems emit less NO_x (Table I). NO_x emissions from preheater/precalciner systems vary with the system (Table III). Coal increases NO_x emissions in some NSP systems (Figures 2 and 3).

As an explanation for these observations, the following hypotheses are proposed:

- In the case of the reduced NO_x emissions associated with coal-fired, conventional systems, the reduction was probably due to change in flame temperature. Since NO_x generation is directly related to temperature, the lower temperature of a coal flame produces less NO_x than the higher temperature gas flame. However, it is important to remember that this hypothesis assumes that all other process conditions are similar, e.g., raw materials, equipment configuration and burning conditions.
- There are at least ten different equipment configurations of preheater/precalciner systems. The variations of NO_x emissions from these systems are affected by their design, especially the precalcining part of the process. However, a clear-cut conclusion regarding NO_x emissions from various preheater/precalciner systems will not be made easily

since nitrogen in the raw materials may affect NO_x emissions and it is unlikely that two different NSP systems will be constructed at the same site.

- Where NO_x emissions increased with conversion of oil to coal in the calciner of a NSP system, the source of the increase is fuel nitrogen.

VI. FORECAST

California Portland Cement Company and Gifford-Hill & Company, Inc. have initiated research programs to gather data pertaining to NO_x emissions from conventional and NSP processes. Other companies are continuously monitoring their NSP systems. The Portland Cement Association is investigating the contribution of nitrogen in the raw materials to the NO_x emissions and KVB, as reported at this symposium, is investigating the parameters which affect NOx generation from a rotary cement kiln. Within three to four years, much more information about NO_x emissions in the U.S. cement industry will be available.

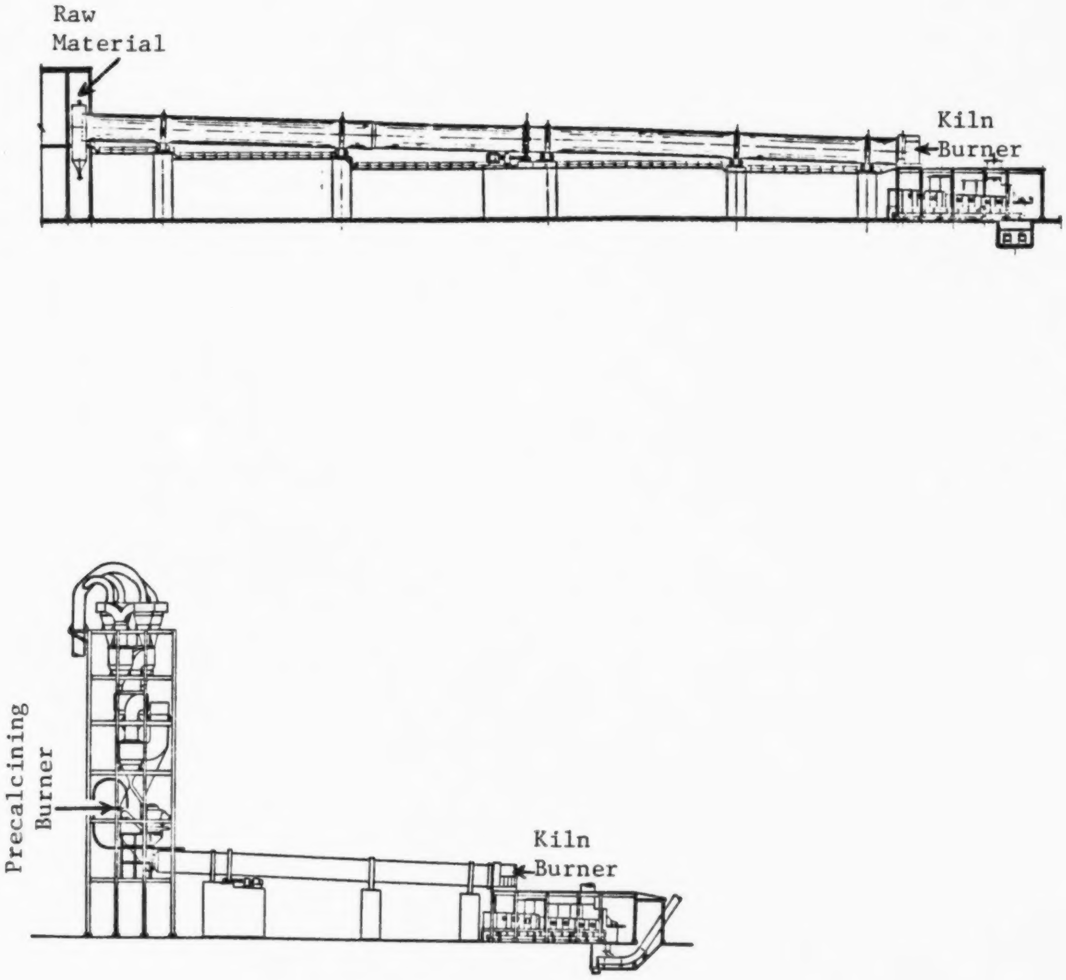
Raw Material
Kiln Burner
Precalcining Burner
Kiln Burner

Figure 1

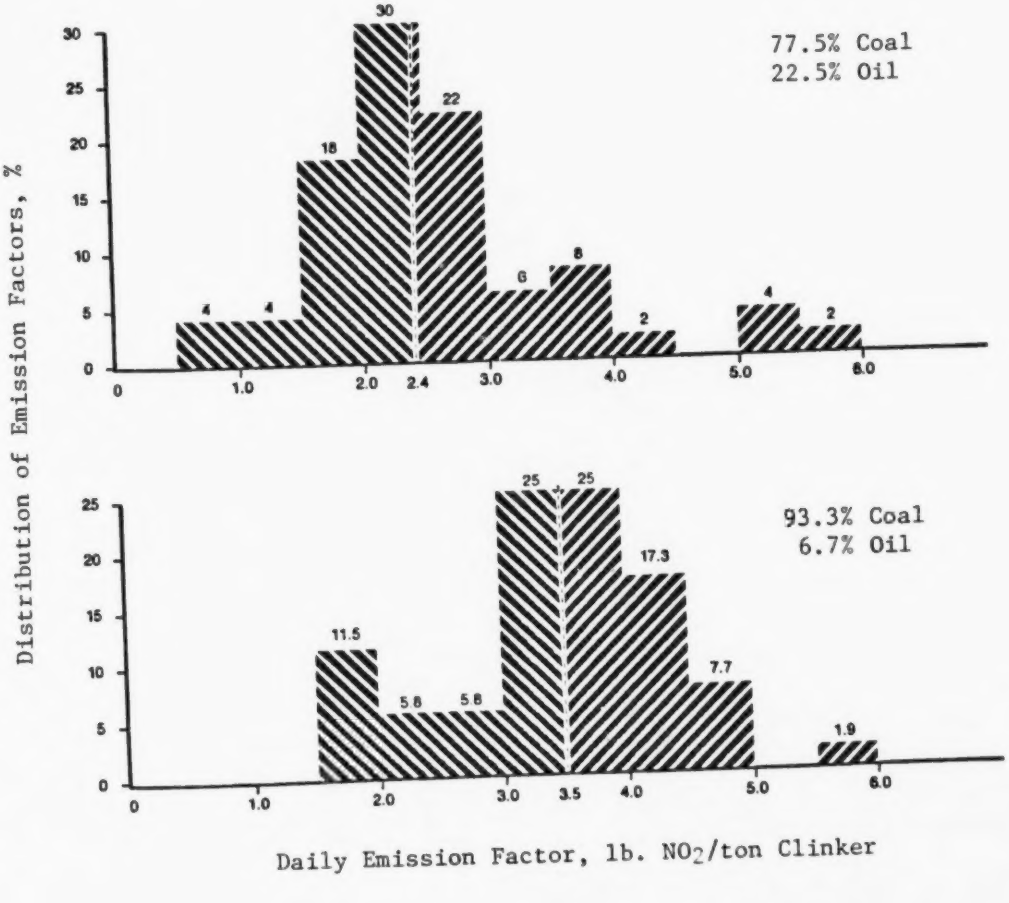

Figure 2. Comparison of NO_x emissions from two fifty-day periods using various combinations of oil and coal fuel.

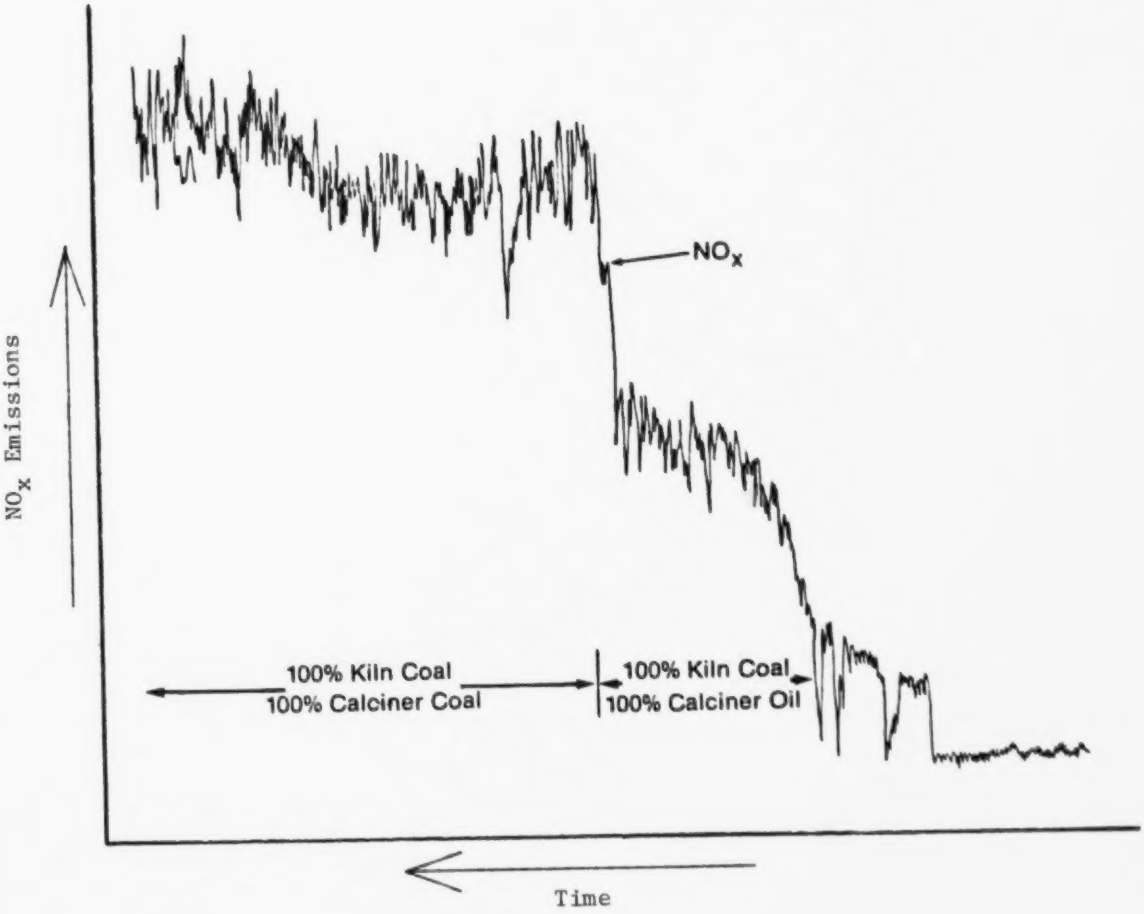

Figure 3. Comparison of NO$_x$ emissions from a NSP System using coal as kiln fuel and oil and coal for fuel in calciner.

TABLE I. COMPARISON OF NO_x EMISSIONS FROM TWO KILNS BURNING DIFFERENT FUELS

	Gas (lb/ton)	Oil (lb/ton)	Coal (lb/ton)
Kiln A	19.32[1]	9.2[1]	4.8[2]
Kiln B	14.00[1]	9.0[1]	5.6[2]

[1] KVB 1975

[2] ARB 1981

TABLE II. COMPARISON OF WET PROCESS WITH PREHEATER/PRECALCINER (NSP) WITH COAL AS FUEL

	lb/ton
Wet Kiln A	2.9 [1]
Wet Kiln B	4.8 [2]
NSP C	7.1 [3]
NSP D	1.4 [4]

Data By:

1 STW Testing, Inc.

2 Enviro-Test, Inc.

3 KVB, Inc.

4 Bay Area Air Quality Management District

TABLE III. NO_x MEASUREMENTS FOR COAL-FIRED PRECALCINER SYSTEMS

System	lb NO_x/ton clinker
A	2.73
B	4.32
C	4.1
D	3.60
E	2.37 - 5.26
F	2.84 - 3.79
G	3.79
H	3.60
I	4.08
J	4.98
K	7.5
L	3.97

APPLICATION OF COMBUSTION MODIFICATION TECHNOLOGY FOR NO_x CONTROL TO CEMENT KILNS

By:

Wallace Carter and R. C. Benson
KVB, Inc.
18006 Skypark Boulevard
Irvine, California 92714

DISCLAIMER

"The research described in this article has been funded wholly or in part by the United States Environmental Protection Agency through contracts 68-02-2144 and 68-02-2645 to KVB, Inc. Although it has been subjected to the Agency's required peer and policy review, it does not necessarily reflect the views of the Agency and no official endorsement should be inferred."

ABSTRACT

Field tests were conducted on a subscale rotary cement kiln to evaluate the effect of various combustion modifications on gaseous emissions. This work, sponsored by the U.S. Environmental Protection Agency, was conducted in a research kiln donated by Gifford-Hill, a major cement manufacturing company. The kiln is rated at 68 kg (150 lb) clinker per hour.

A coal burner was designed and fabricated for use in the kiln. The burner allowed for variation in primary air velocity and swirl. A secondary air heater was incorporated to vary the combustion air temperature.

The effect of flue gas recirculation, vitiated primary air, primary/secondary air ratio, burner tip velocity and secondary air temperature on NO_x emissions were evaluated. An optimum operating condition for minimizing NO_x emissions was defined. A discussion of these results is presented.

INTRODUCTION

KVB has previously reported on subscale and full-scale cement kiln combustion modification tests (Refs. 1 and 2). The EPA-sponsored tests evaluated the effects on NO_x emission of several types of modifications including air preheat, fuel injection velocity and oxygen content of the primary combustion air stream. Tests in a combustion tunnel, simulating kiln conditions, showed that dilution of the primary air stream with an inert gas, altered fuel injection velocity and reduced combustion air preheat were the most effective techniques tested for lowering the NO_x emission level.

The present paper summarizes the results of a test program conducted with a subscale rotary cement kiln firing natural gas and pulverized coal. The kiln was modified to incorporate flue gas recirculation and combustion air preheat. A coal burner was fabricated and installed in the kiln. The flue gas recirculation system was designed to inject flue gas into the secondary combustion air stream or into a tertiary air stream in the burner.

The objective of this program was to investigate advanced combustion modification concepts requiring relatively minor hardware modifications that could be used by operators and/or manufacturers of rotary cement kilns to reduce oxides of nitrogen emissions. The ultimate objective is to demonstrate the feasibility of these modifications to the extent that they could be readily adopted by cement manufacturers.

The initial phase of testing was conducted with natural gas fuel to define kiln operation over a range of operating variables such as excess air, primary to secondary air ratio and combustion air preheat. Once the performance of the kiln was documented with natural gas fuel, a change to coal firing was implemented. Kiln NO_x emissions were evaluated as a function of combustion air temperature, primary air velocity, primary to secondary air ratio, flue gas recirculation rate and primary (carrier) air oxygen content.

TEST FACILITY AND EMISSIONS SAMPLING

Test Unit Description

The test facility for the subscale rotary kiln tests is located at a major California cement plant. The kiln, pictured in Figure 1, is 8.2 m (27 feet) long and 0.38 m (15 inches) inside diameter. The kiln produced clinker at an average rate of approximately 45 kg (100 pounds) per hour. Maximum clinker output was about 68 kg (150 pounds) per hour. The refractory brick lining is 0.15 m (6 inches) thick near the burner and 0.08 m (3 inches) thick for the remainder of the kiln length. The rotary kiln's speed is adjustable, but was operated at 2 rpm for these tests.

The host cement company completely refurbished the kiln, the raw feed system and the peripheral equipment. In addition to the modifications to the kiln and equipment, the host company provided training for KVB personnel and laboratory facilities and assistance. The company also provided an optical pyrometer for measuring the flame zone temperature.

The kiln had no provision for heating combustion air. In order to more closely simulate actual operating conditions, a combustion air preheater was fabricated. A metallic recuperator was installed on a combustion chamber which was fired by a separate natural gas burner. Combustion air temperature was then varied by regulating the firing rate of the auxiliary burner.

The kiln was originally designed for gas firing. A burner for firing pulverized coal and/or natural gas was designed, fabricated, and installed by KVB. The nominal burner parameters used in the design were specified by Gifford-Hill and were representative of full-scale applications. A schematic of the burner is shown in Figure 2. There were a total of three combustion air streams associated with the subscale burner and kiln system. These streams, and their temperatures were:

- Primary

  Coal fuel - used for conveyance of coal from pulverizer to burner, preheated to 361-367 K (190-200°F).

  Natural gas fuel - ambient temperature, 294-319 K (70-115°F).

- Secondary

  Main source of combustion air for both coal and natural gas fuels. Entered kiln through firing hood (not through burner) as in full-scale practice. For coal fuel preheated to 811-906 K (1000-1170°F). For natural gas fuel testing was conducted with secondary air temperature ranging from ambient (294-319 K, 70-115°F) to 922 K (1200°F).

- Tertiary

  Ambient temperature (294-319 K, 70-115°F) for coal fuel only. Passed through natural gas circuit in burner. Used only for very few tests as it caused an increase in NO emissions.

The design of the burner was intended for varying burner parameters, including primary air velocity, insertion depth, and primary air/tertiary air distribution. Primary air velocity variation could be conducted by inserting a spacer over the center tube. The insertion depth of the fuel and burner air into the kiln could also be varied. The burner air could be proportioned between the inner annulus primary air stream and the outer annulus tertiary air stream. The burner was fed pulverized coal from a vibrated volumetric screw feeder. The screw speed is continuously variable over a 10 to 1 range.

A flue gas recirculation system was installed by KVB. Flue gas was extracted from the kiln exit and ducted to the kiln hood. The flue gas flow rate was measured with a sharp-edged orifice. Figure 3 shows a flow schematic of the modified kiln system.

Emission Measurements and Instrumentation

All gaseous emission measurements were made at the feed end of the kiln as shown in Figure 3. An uncooled probe with a sintered metal filter was used to obtain the exhaust gas sample. All gaseous emission measurements, whether in units of ppm or percent, are on a volume basis in keeping with common practice.

The emission measurements were made with instrumentation mounted in a mobile laboratory. All the instruments require sample conditioning equipment contained in this trailer owned by EPA-IERL and operated by KVB on EPA contracts. The gaseous species measurements are made with analyzers in the mobile laboratory. Additional portable analyzers are carried to sample ports for spot measurements. Weighings and titrations for free lime analysis of clinker samples were conducted in the rear of the mobile laboratory. The trailer also includes work areas for meetings and day-to-day review of the test plan.

The analytical instrumentation system consists of five analyzers and associated equipment for simultaneously measuring the composition of the flue gas. The analyzers, recorders, valves, controls, and manifolding are shock mounted to a panel in the trailer. The flue gas constituents measured by analyzers are oxides of nitrogen (NO, NO_x), carbon monoxide (CO), carbon dioxide (CO_2), oxygen (O_2), and sulfur dioxide (SO_2). In addition, a gas chromatograph is installed for measuring hydrocarbons (HC). The following table lists the instruments used for measuring each gaseous constituent.

EMISSION MEASUREMENT INSTRUMENTATION

Species	Manufacturer	Measurement Method	Model No.
Hydrocarbon	Carle Instruments	Gas Chromatograph	1197SX
Carbon Monoxide	Beckman Instruments	IR Spectrometer	865
Oxygen	Teledyne	Polarographic	326A
Carbon Dioxide	Beckman Instruments	IR Spectrometer	864
Nitrogen Oxides	Thermo Electron Co.	Chemiluminescent	10A
Sulfur Dioxide	DuPont Instruments	UV Spectrometer	400

Kiln Operation

Raw feed was delivered to the test site in a bulk feed trailer. The raw feed was then pelletized using a rotating disc pelletizer and transferred into the kiln feed hopper. The raw feed pellets were fed into the kiln using a vibrator and small bucket conveyor.

On cold startup, the kiln was heated slowly with natural gas firing, without introducing the raw feed. After the feed was introduced, the firing rate was increased to further raise the temperature until an acceptable clinker was produced. Secondary and primary air flows and temperatures were adjusted during kiln heatup to predetermined levels and allowed to stabilize. After the required temperatures and flow rates were achieved and stabilized, the switch to coal firing was made. As the coal feed rate was increased, the natural gas flow was diminished to maintain a constant kiln temperature. An engineer had the responsibility of setting and maintaining all combustion related controls.

The coal burned was taken from the host company coal pile and pulverized. The coal was pulverized to a fineness of 20 percent residue on 200 mesh, packaged in 23 kg (50 lb) bags and delivered in drums to the test site. Samples of the coal were taken and submitted to an independent laboratory for analysis.

Test Results With Natural Gas

The initial testing on the kiln was conducted with the burner firing natural gas. The effect of kiln excess air, combustion air preheat, primary to secondary air ratio and flue gas recirculation rate on NO* emissions was evaluated. Table 1 is a summary of the results of these tests. Each is discussed separately in the following paragraphs:

- Kiln Excess Air

  The effect of kiln excess air on the NO emission level was evaluated for ambient combustion air and for combustion air heated to 811 K (1000°F). The data shown in Figure 4 show this effect. As these data indicate, the NO emission level is very sensitive to the kiln oxygen level but is more sensitive at higher combustion air temperature. A linear regression analysis of the data showed good correlation and the slope was 48 ppm per % O_2 for ambient combustion air and 99 ppm per % O_2 for combustion air preheated to 811 K (1000°F).

---

*Previous tests conducted on full-scale kilns (Ref. 2) have shown that the NO_2/NO_x ratio was 4 percent on the average (ranging from 3 percent to 6 percent). This was the justification for not measuring NO_2 during this program.

- Combustion Air Preheat

  The effect of combustion air preheat on NO emissions was shown in Figure 5 for three levels of primary air flow. These data show that for all the conditions tested, the NO emission level is substantially higher with elevated combustion air preheat. At 20 percent primary air, the NO emission level is more than doubled at a combustion air temperature of 811 K (1000°F), relative to ambient combustion air.

- Primary/Secondary Air Ratio

  With the KVB burner, shown in Figure 2, a portion of the total combustion air is injected through a central annulus which includes a swirl vane at the tip. This primary air is unheated for natural gas operation. A series of tests was conducted in which the amount of primary air was varied while the overall combustion air was held constant. The data shown in Figure 6 indicates that the NO levels are significantly higher when the primary air flow represents approximately 20 percent of the total air flow. At levels below approximately 20 percent, the flame intensity (mixing) is less, resulting in relatively lower NO. At 20 percent primary air flow, the flame is well mixed, resulting in relatively high NO emissions. At the higher levels of primary air (33 percent of the total), the degree of mixing is high due to the high primary air velocity, but this is overshadowed by a larger amount of relatively cold air being introduced into the flame zone as primary air.

- Flue Gas Recirculation

  The flue gas recirculation system described in an earlier paragraph was evaluated in a series of tests designed to show the effect of recirculation rate on NO emissions. Secondary combustion air temperature was held constant at approximately 906 K (1170°F) while the recirculated flue gas was varied. The recirculated flue gas temperature varied but averaged approximately 394 K (250°F). The recirculated flue gas was injected directly into the secondary air stream at the kiln hood. The flue gas injected into the secondary air had a pronounced effect on NO emissions. First, the bulk temperature of the secondary air is reduced due to the lower FGR temperature, and secondly, the overall combustion air oxygen content in the flame zone is reduced due to vitiation by the recirculated flue gas.

The effect of recirculation rate on NO emissions is shown in Figure 7 for the rotary kiln firing natural gas. These data show that the recirculation of flue gas into the combustion air can be very effective when firing natural gas. An NO reduction of approximately 70 percent was achieved with flue gas recirculation. This reduction is consistent with NO reduction in other types of combustion devices when firing natural gas.

Test Results With Pulverized Coal

Testing with pulverized coal began following the natural gas tests. After some initial problems obtaining a steady coal flow were corrected, a parametric test program was initiated. Parameters to be evaluated included excess air, secondary combustion air preheat, primary air velocity, primary to secondary air ratio, flue gas recirculation rate and primary air dilution. The effect of each of these combustion modifications on NO emissions is discussed in the following paragraphs. The results of the coal-fired parametric tests are summarized in Table 2. Table 3 presents the results of the coal analysis. The coal is classified as a high volatile "C" bituminous.

- Kiln Excess Air

  The effect of kiln excess air variation on NO emissions is shown in Figure 8 for a secondary combustion air temperature of 867 K (1100°F). This figure shows, as did the gas-fired data, that the NO emission level is strongly dependent upon the operating O_2 level. At 867 K (1100°F) combustion air temperature, a decrease in kiln exit O_2 of one percent results in a decrease in NO emissions of approximately 63 ppm. The other levels of air preheat exhibit similar trends although the absolute NO levels are higher with increasing combustion air temperatures.

  A linear regression analysis was performed on the data for each level of air preheat. The correlation coefficient (r^2), calculated for each condition, showed that a linear curve fit gives an excellent representation of the data. The solid lines through the data represent the calculated linear curve. Also shown on this figure are the slopes and correlation coefficients. Data at other combustion air temperatures displayed similar trends.

- Combustion Air Preheat

  The effect of secondary combustion air temperature on NO emissions was evaluated from approximately 811 K to 894 K (1000°F to 1150°F). Combustion air temperatures lower than approximately 783 K (950°F) tended to result in poor combustion of the coal (high CO, smoke levels). The data for the kiln operating at 3.5 percent O_2 are shown in Figure 9 as a function of secondary air temperature. The curve shows that the NO increased slightly as secondary combustion air temperature increased. The slope of the curve is increasing with increasing temperature within the range of temperatures tested. The curve indicates that NO emissions are much more sensitive to combustion air temperature at temperatures greater than 894 K (1150°F). At the conditions shown in this figure (i.e., 3.5 percent O_2 and 27 percent primary air flow), reducing the combustion air temperature from 906 K to 839 K (1170°F to 1050°F) resulted in a reduction in NO of 10.7 percent (from 840 ppm to 750 ppm). This modification, however, results in reduced thermal efficiency.

- Primary Air Velocity

Figure 10 shows the effect of primary air velocity on NO emissions for a typical kiln exit oxygen concentration (3.5 percent O_2). Primary air velocity was varied by decreasing the air flow rate from the baseline condition. The primary air burner area was kept constant for this series of tests. This method of varying the primary air velocity also produced variations in the primary/total air ratio. Figure 10 also shows the primary/total air ratios for this series of tests. As noted, this ratio varied by only a modest amount.

The results show that NO emissions at low primary air velocity (10.8 m/s) (2128 fpm) are reduced by approximately 30 percent from the baseline condition (14.7 m/s) (2890 fpm). The penalty for low primary air velocity is poor mixing in the flame zone and increased carbon monoxide emissions (Figure 11). As expected, combustion was not as complete with the longer, larger flame and lengthened burning zone effected by lowered primary air velocity.

Another series of primary air velocity variation tests was attempted. This test series was based on a constant air flow rate and variable primary air burner area. A spacer was located about the burner's inner annulus to constrict the coal/primary air flow area and increase the mixture velocity. The extended flame length with this velocity increase was unsatisfactory for the subscale kiln operation and resulted in an unstable flame.

- Primary/Secondary Air Ratio

The effect of the primary to secondary air ratio on NO emissions is shown in Figure 12 for a constant kiln operating O_2 level of 3.5 percent. These tests were conducted by maintaining the primary air flow and velocity constant while reducing the secondary air flow. Only small changes in secondary air flow were necessary in order to achieve the range in the primary/secondary air ratio; thus, the overall O_2 was relatively unaffected. These data show that a peak value of NO emission is encountered at approximately 23 percent primary air. As the percentage of primary air is reduced, NO emission decreases due to poorer flame zone mixing resulting from lower injection velocity. At primary air levels greater than about 23 percent, the effect of the relatively cold primary air overshadows the increased mixing effect.

- Flue Gas Recirculation

  Flue gas recirculation (FGR) as a combustion modification was evaluated with the kiln firing pulverized coal. Tests were conducted at several recirculation rates, with the flue gas being injected into the secondary air stream at the kiln hood. The primary and secondary air flows were both kept constant with the primary flow representing 27.2 percent of the total air flow. The results of a series of FGR tests is shown in Figure 13 for the kiln operating at 5.4 percent O_2 and with secondary air temperature of 889 K (1140°F). A higher O_2 was required for the FGR tests in order to maintain flame and kiln stability. At lower O_2 a ring of partially reacted feed would form inside the kiln which would interfere with the flow of feed and combustion products through the kiln. Injection of the flue gas showed little effect on NO emissions even at relatively high recirculation rates. This is in sharp contrast with natural gas firing where FGR was the most effective combustion modification.

- Vitiated Primary Air

  During laboratory tests at KVB, the effect of primary air oxygen content on NO emissions was found to be quite significant. One of the major objectives of this test program was to determine the effect of primary air oxygen content on NO emissions under real process conditions. The primary air circuit of the test facility was plumbed so that an inert gas could be injected into the air stream upstream of the orifice which measured the flow in the circuit. Downstream of the measurement orifice, a sample port was installed for measuring the oxygen content of the primary air. A portable oxygen analyzer was used for measuring the O_2 content just prior to entering the burner.

  A series of tests were conducted during which gaseous nitrogen was injected into the primary air stream to lower the O_2 concentration. The effect of the primary air oxygen content on NO emissions is shown in Figure 14 for the kiln operating at an overall O_2 level of 4 percent. These data show a strong influence on NO emissions as a function of primary air oxygen content. These results substantiate the findings and conclusions of the KVB laboratory study reported in Reference 1.

CONCLUSIONS

The work reported herein has satisfied all of the program objectives. The effectiveness of advanced combustion modifications in reducing NO emissions has been investigated during field testing on a subscale gas- and coal-fired cement kiln. The retrofit of these combustion modifications has been accomplished with a minimum amount of kiln hardware changes. The flexibility in the burner design was a key to most of the investigations undertaken.

The implementation of these combustion modifications on a full-scale kiln will be site-specific. For example, the relative proximity of a source of flue gas products to the burner will probably govern the use of these products to partially (or totally) replace primary air for coal conveyance.

The following specific conclusions may be drawn from the field testing and the analyses performed on the data:

- The subscale tests corroborated laboratory combustion tunnel test results.
- Combustion modifications can be effective in reducing NO emissions from rotary cement kiln.
- NO emissions are very sensitive to the O_2 level.
- Primary air vitiation was the most effective combustion modification for NO reduction.
- Flue gas recirculation into the secondary combustion air is more effective with gas firing than with coal firing.

REFERENCES

1. Tidona, R. J. et al., "Evaluation of Combustion Variable Effects on NO_x Emissions from Mineral Kilns," EPA Contract No. 68-02-2645 (IERL-RTP-1462), May 1983.

2. Hunter, S. C. et al., "Application of Combustion Modifications to Industrial Combustion Equipment," EPA-600/7-79-015a, January 1979.

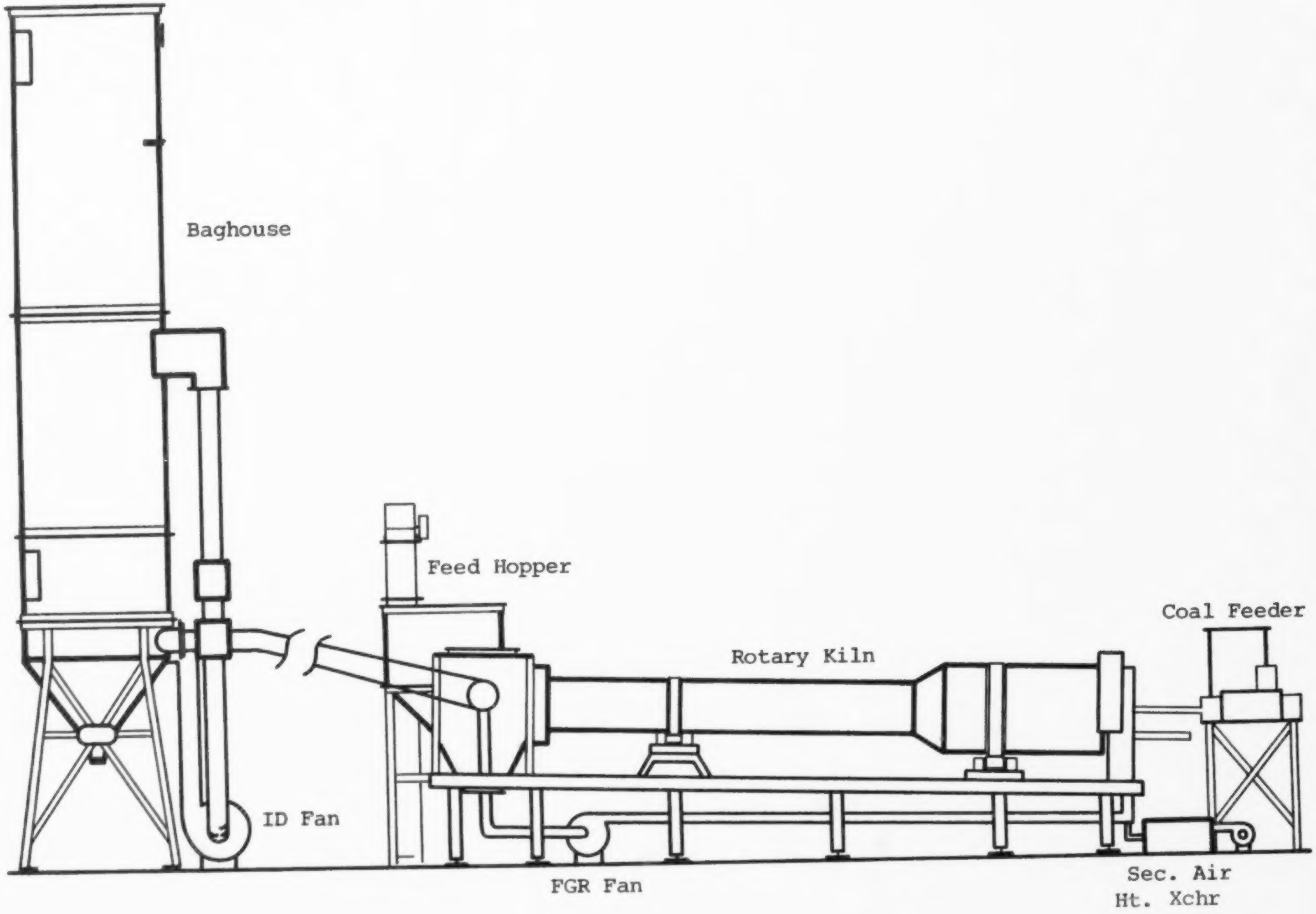
Baghouse
Feed Hopper
Coal Feeder
Rotary Kiln
ID Fan
FGR Fan
Sec. Air
Ht. Xchr

Figure 1. **Arrangement of Kiln System Components**

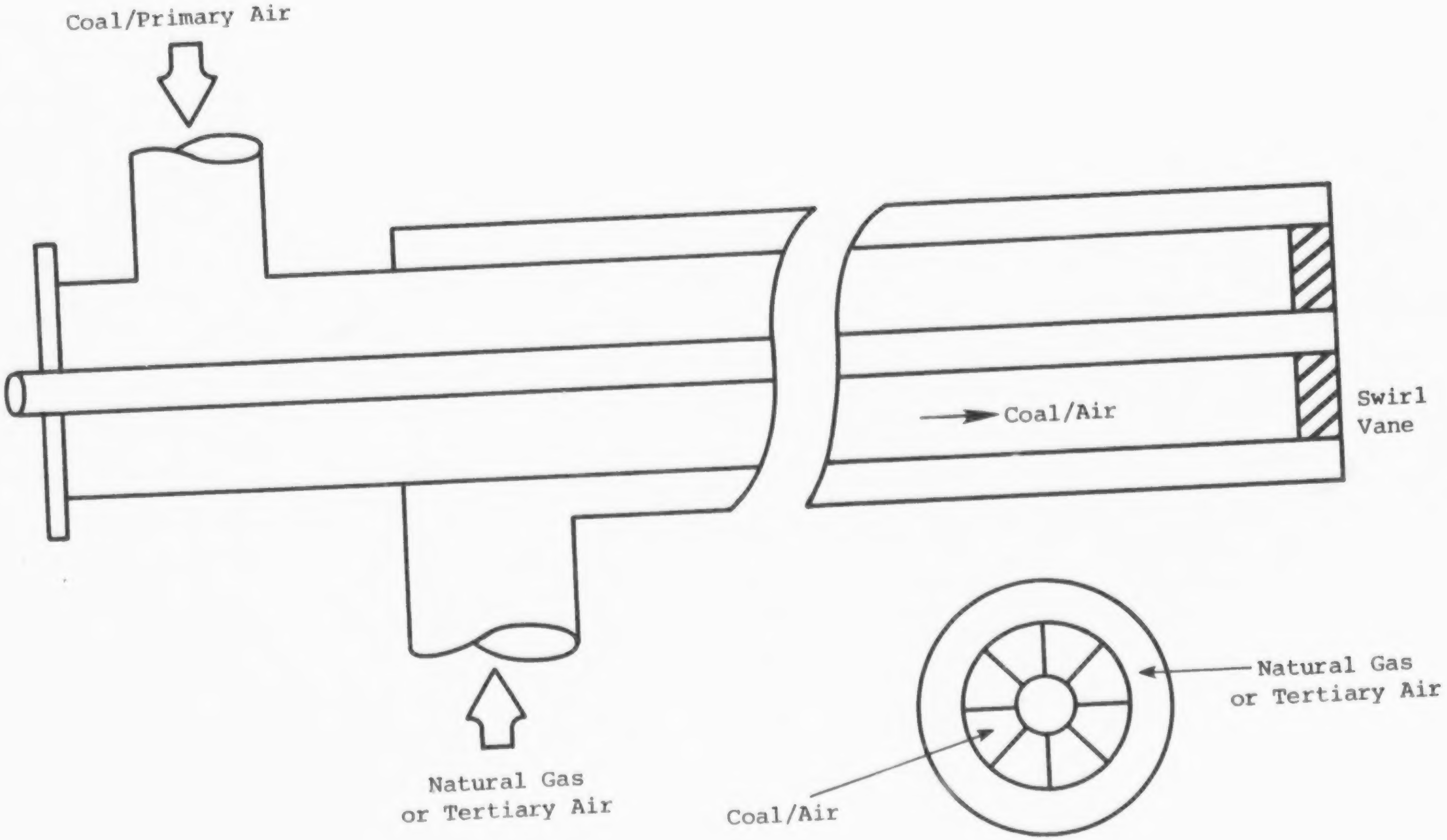

Coal/Primary Air
Coal/Air
Swirl Vane
Natural Gas or Tertiary Air
Coal/Air
Natural Gas or Tertiary Air

Figure 2. Schematic of Pulverized Coal Burner

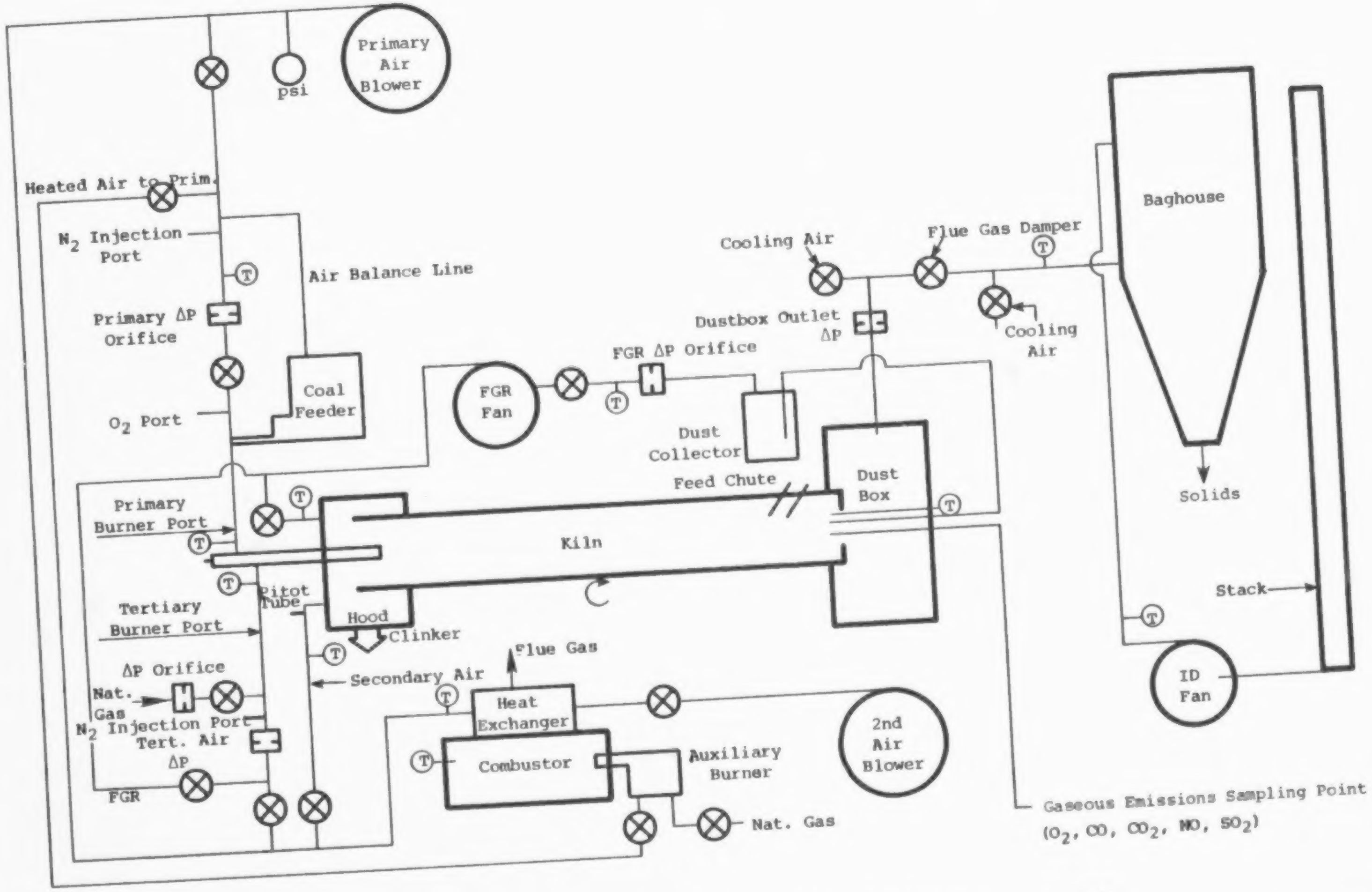
Primary Air Blower
psi
Heated Air to Prim.
N_2 Injection Port
Air Balance Line
Primary ΔP Orifice
Coal Feeder
O_2 Port
FGR Fan
FGR ΔP Orifice
Dust Collector
Cooling Air
Flue Gas Damper
Dustbox Outlet ΔP
Cooling Air
Baghouse
Solids
Stack
ID Fan
Feed Chute
Dust Box
Kiln
Primary Burner Port
Pitot Tube
Hood
Clinker
Tertiary Burner Port
ΔP Orifice
Nat. Gas
N_2 Injection Port
Tert. Air ΔP
FGR
Secondary Air
Flue Gas
Heat Exchanger
Combustor
Auxiliary Burner
Nat. Gas
2nd Air Blower
Gaseous Emissions Sampling Point
(O_2, CO, CO_2, NO, SO_2)
T

Figure 3. Schematic of Test Facility Subscale Cement Kiln

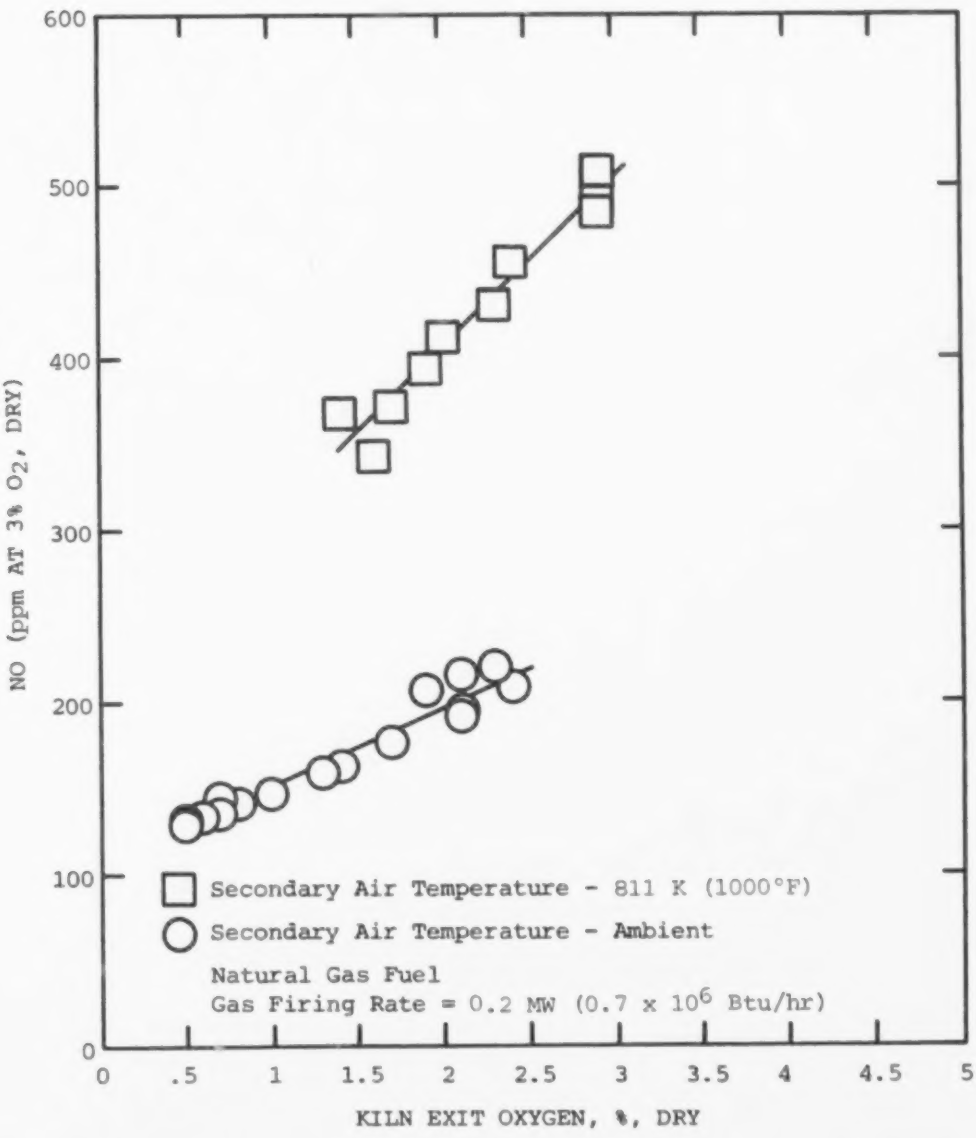

Figure 4. **The Effect of Kiln Exit Oxygen on** NO Emissions

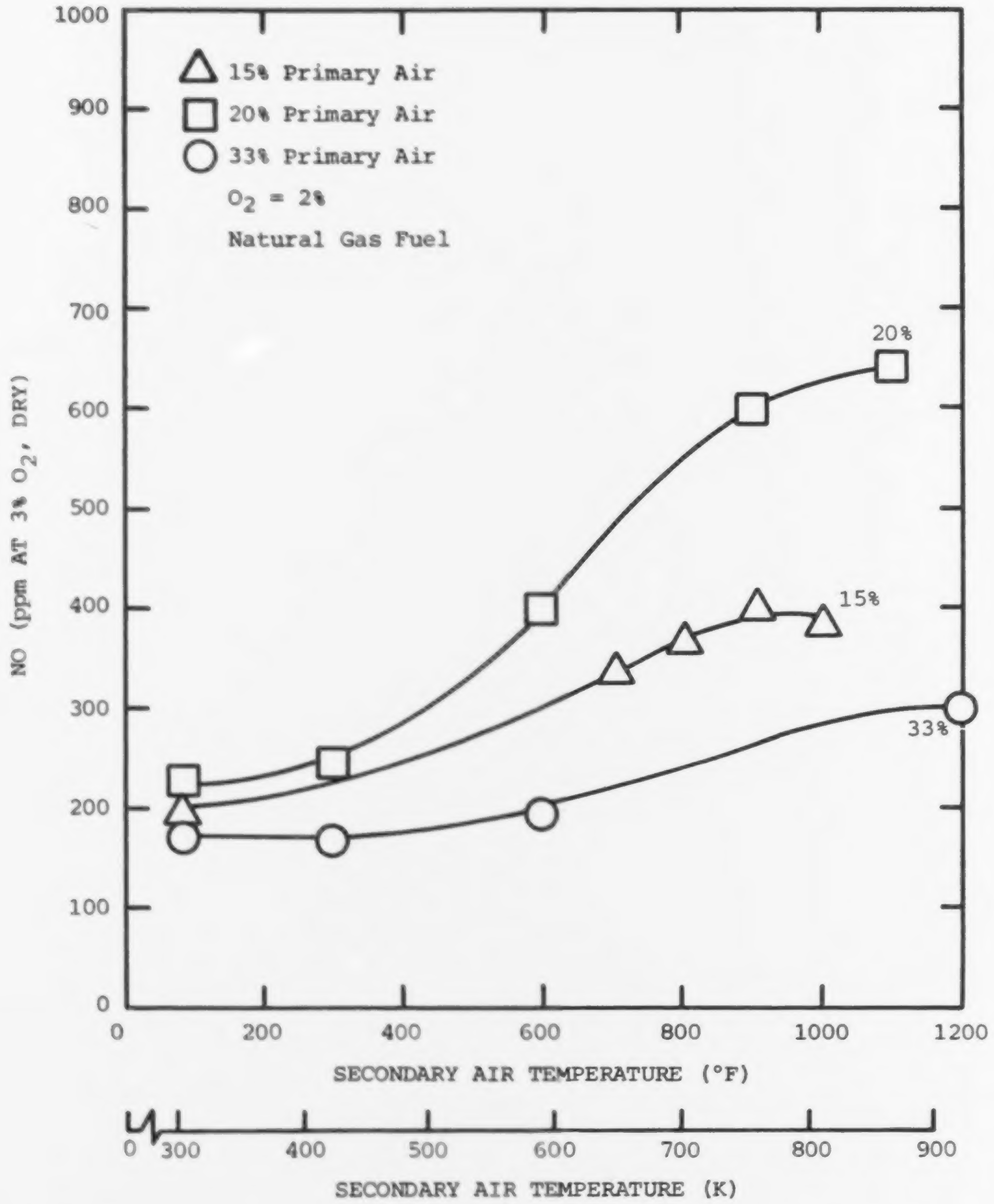

Figure 5. The Effect of Secondary Air Temperature on NO Emissions

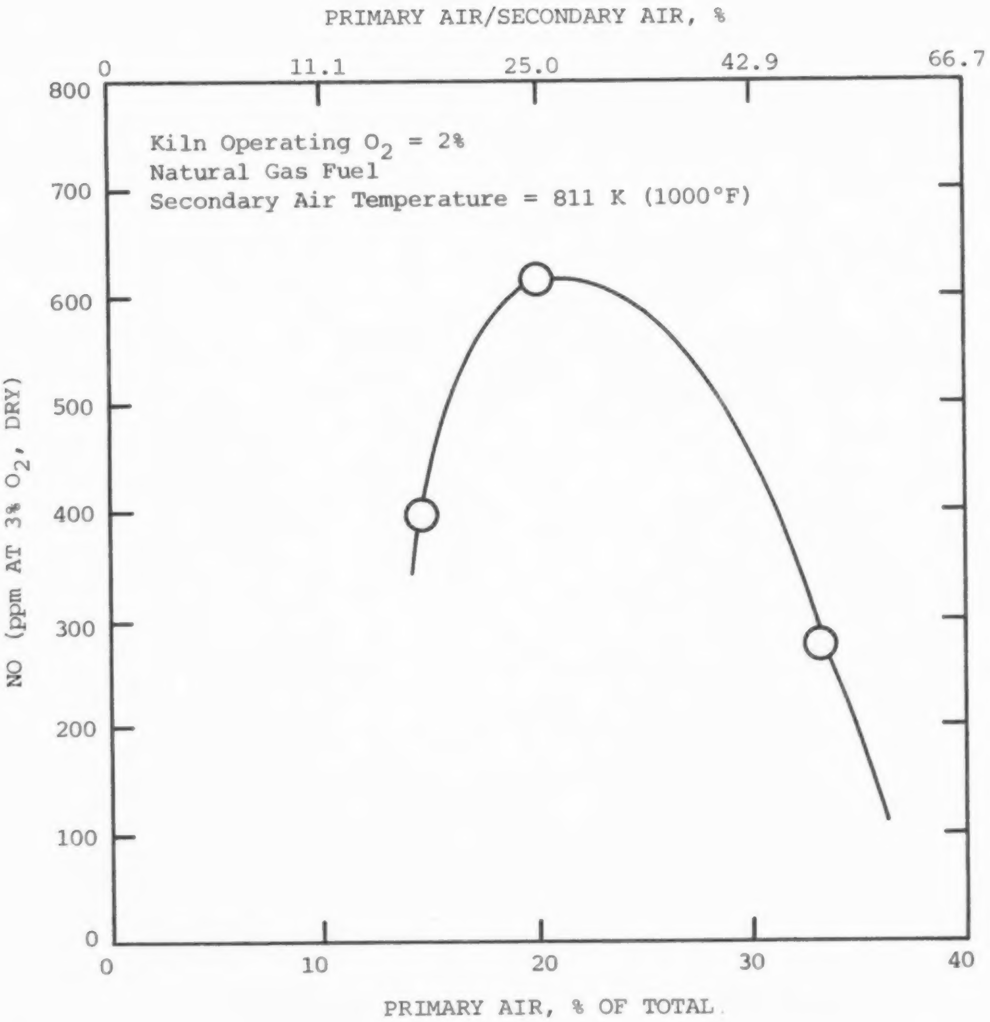

Figure 6. The Effect of Primary to Secondary Air Ratio on NO Emissions for Natural Gas Combustion

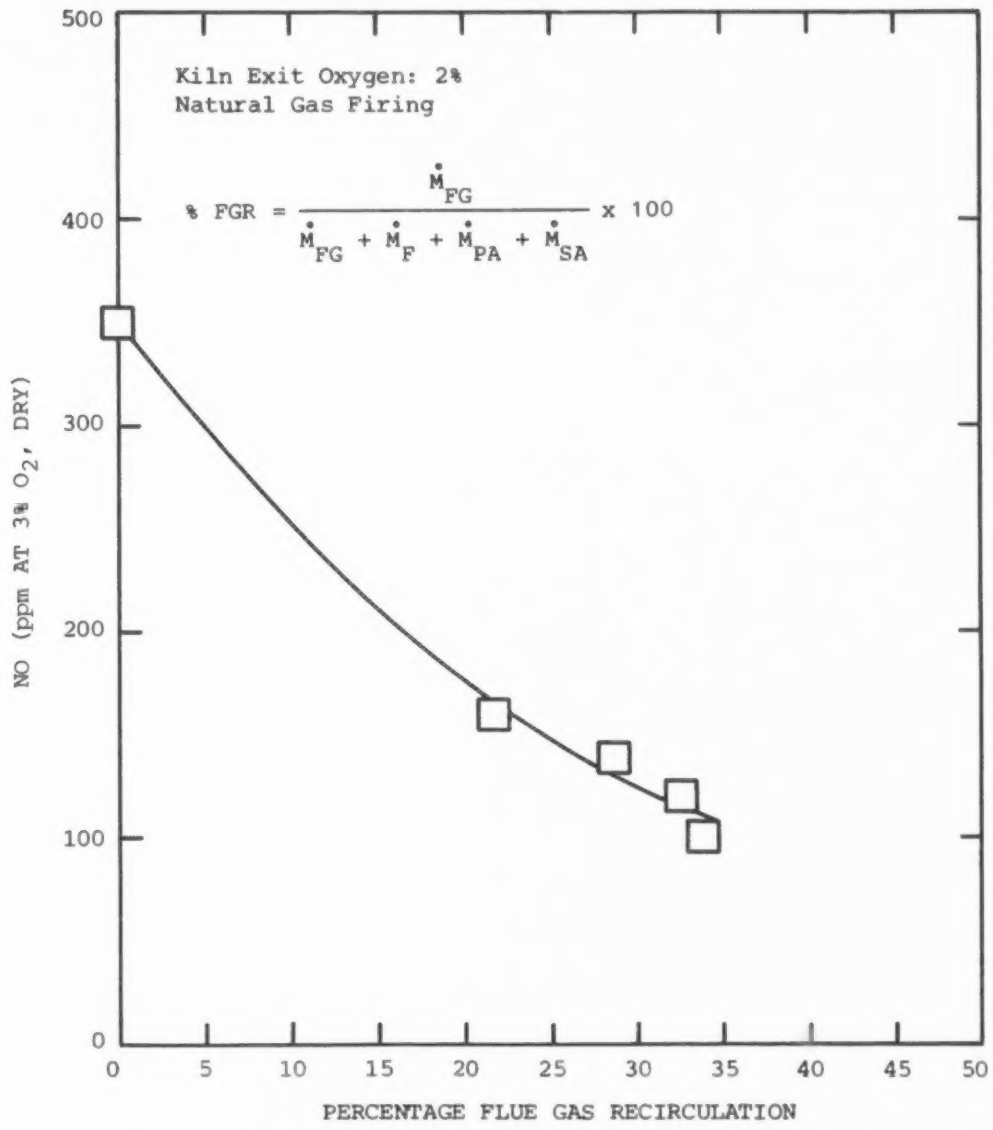

Figure 7. **The Effect of Flue Gas Recirculation on** NO Emissions

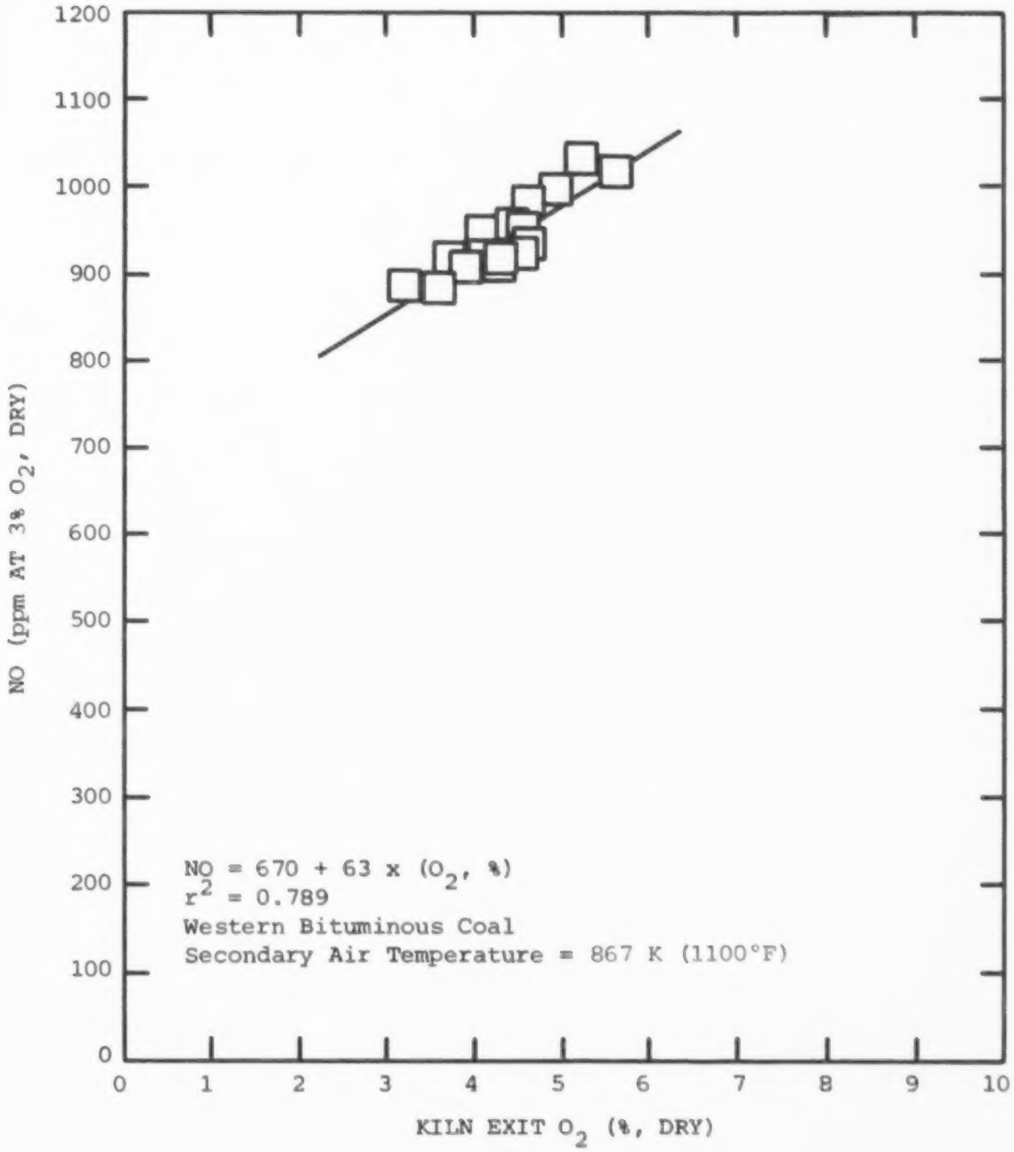

Figure 8. **The Effect of Kiln Excess Oxygen on NO Emissions**

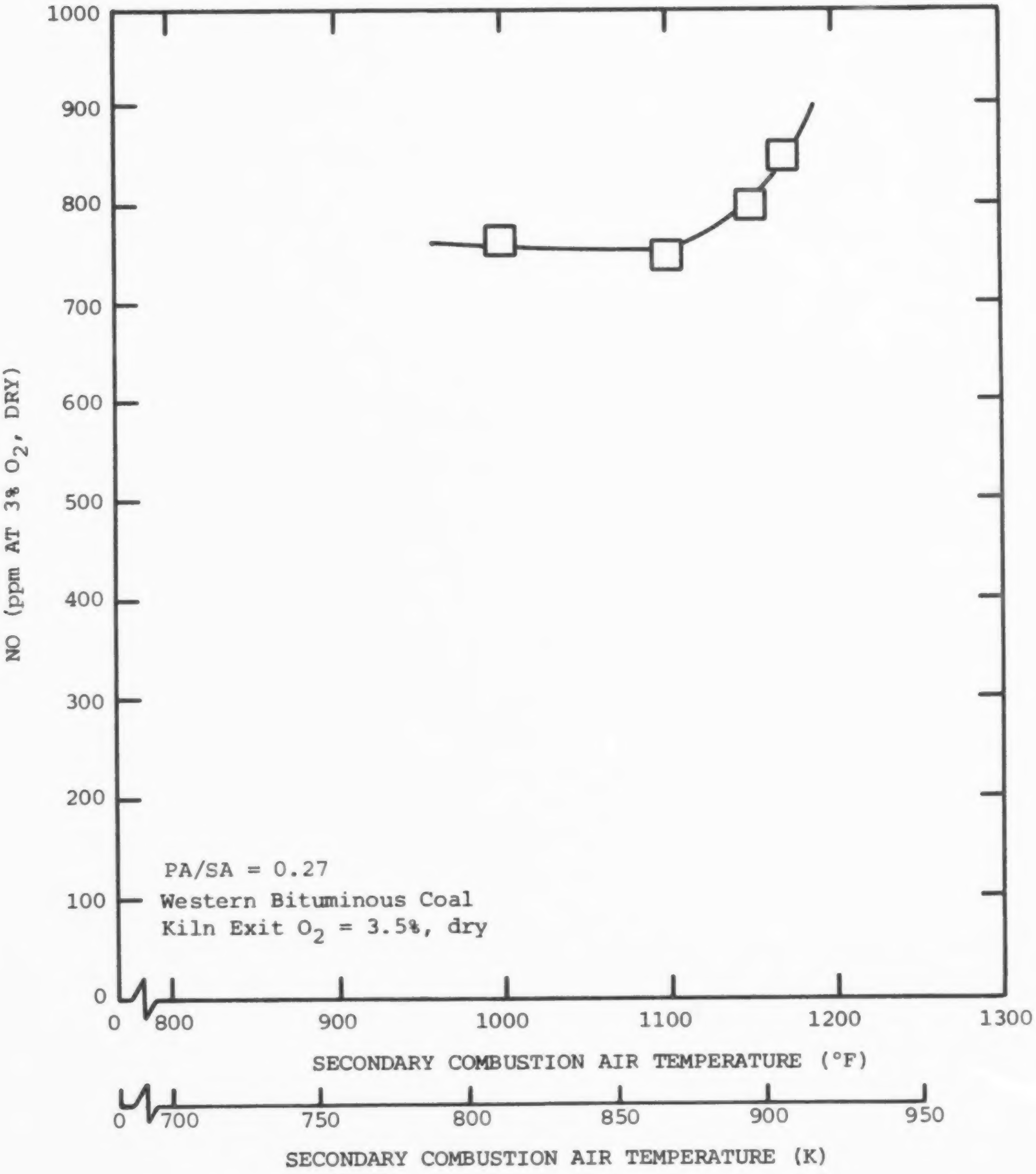

Figure 9. **The Effect of Secondary Combustion Air Temperature on** NO Emissions

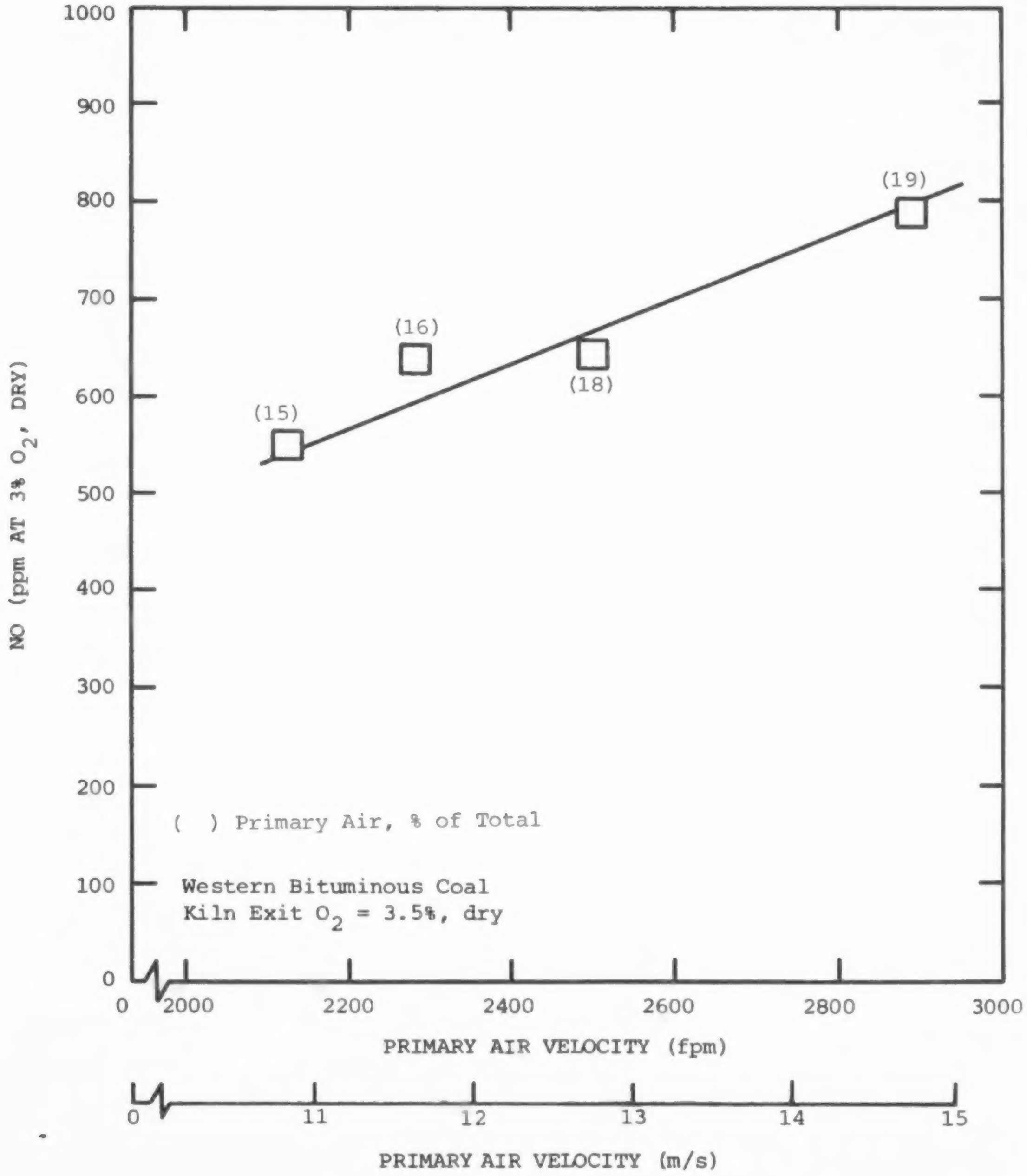

Figure 10. **The Effect of Primary Air Velocity on** NO Emissions

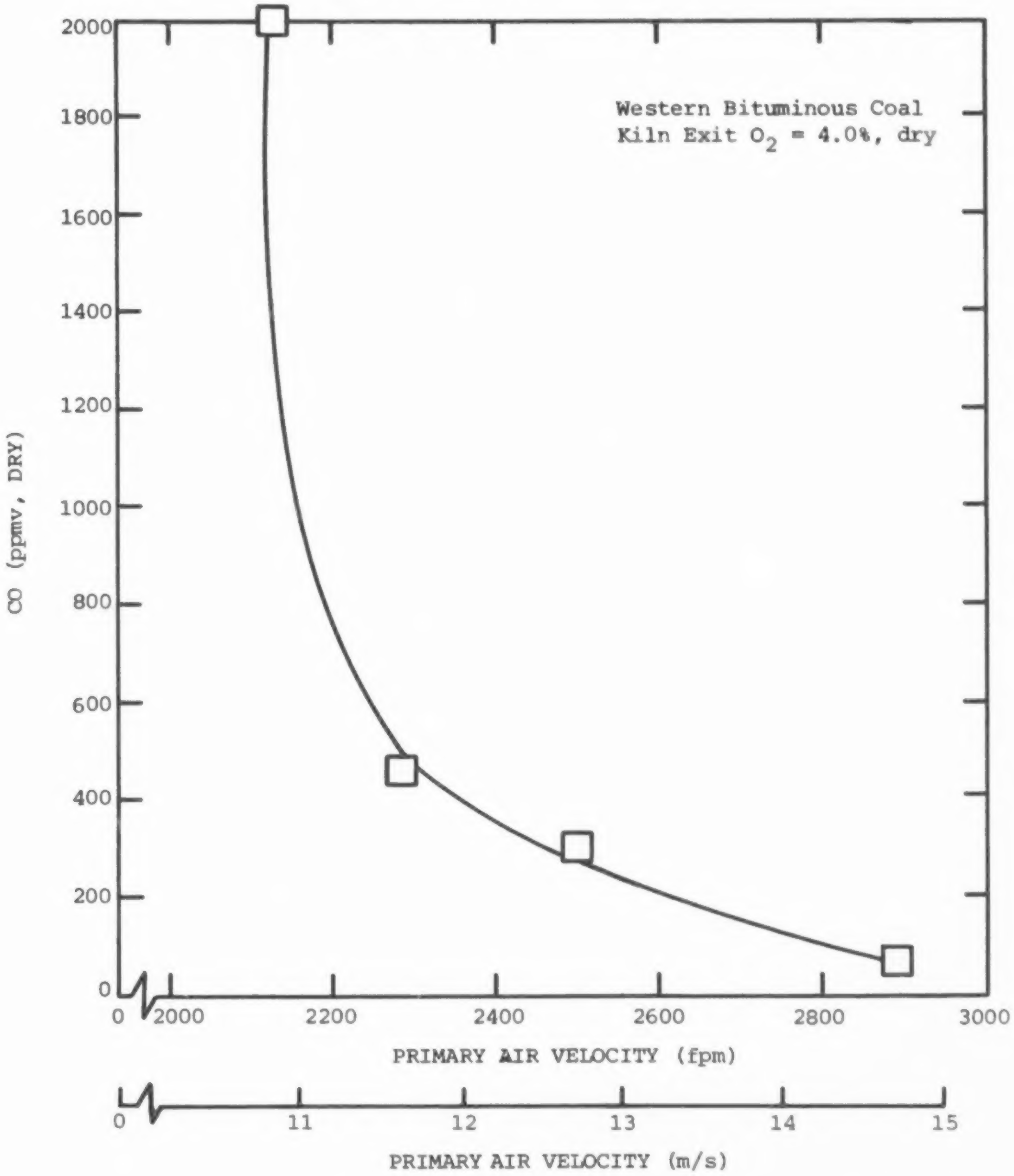

Figure 11. The Effect of Primary Air Velocity on CO Emissions

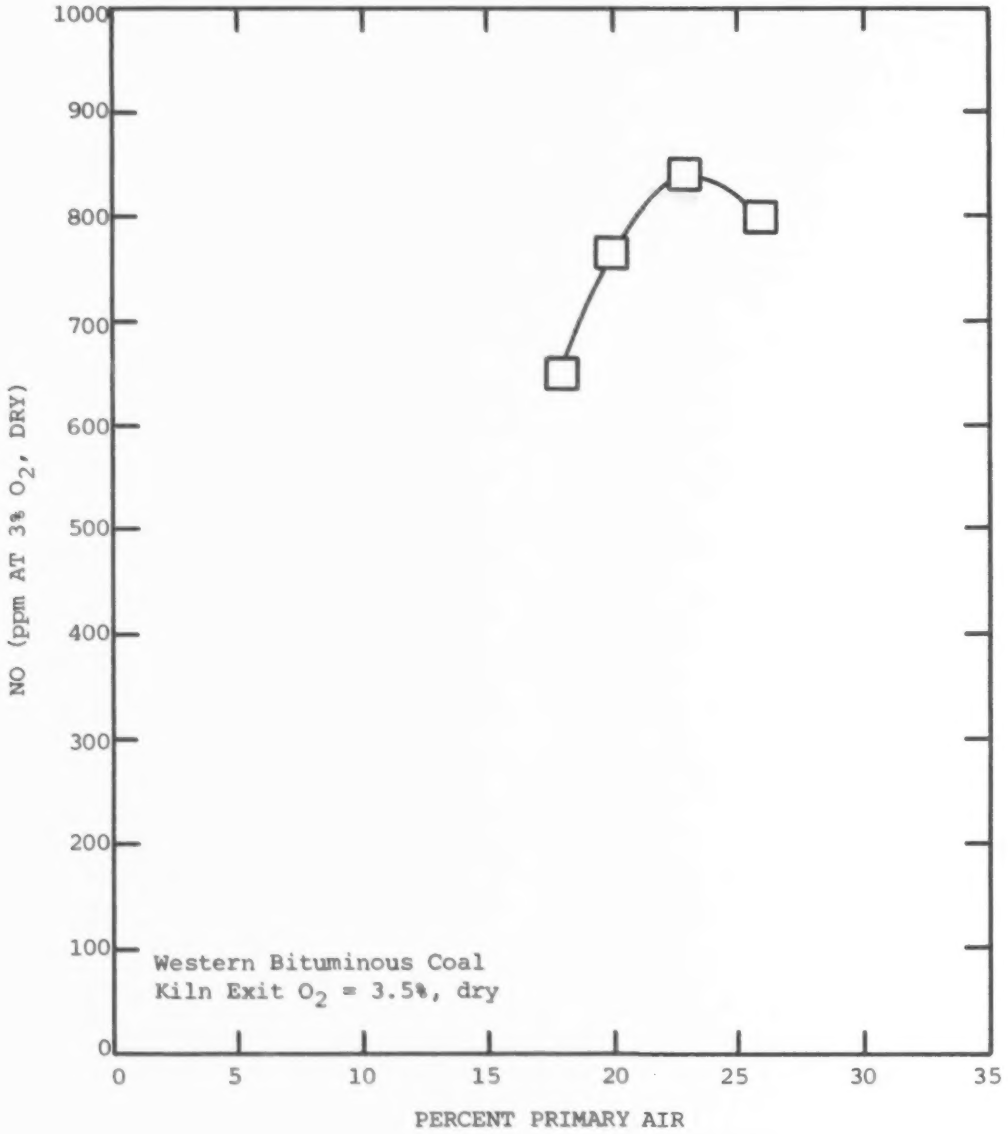

Figure 12. The Effect of Coal Primary Air/Secondary Air Ratio on NO Emissions

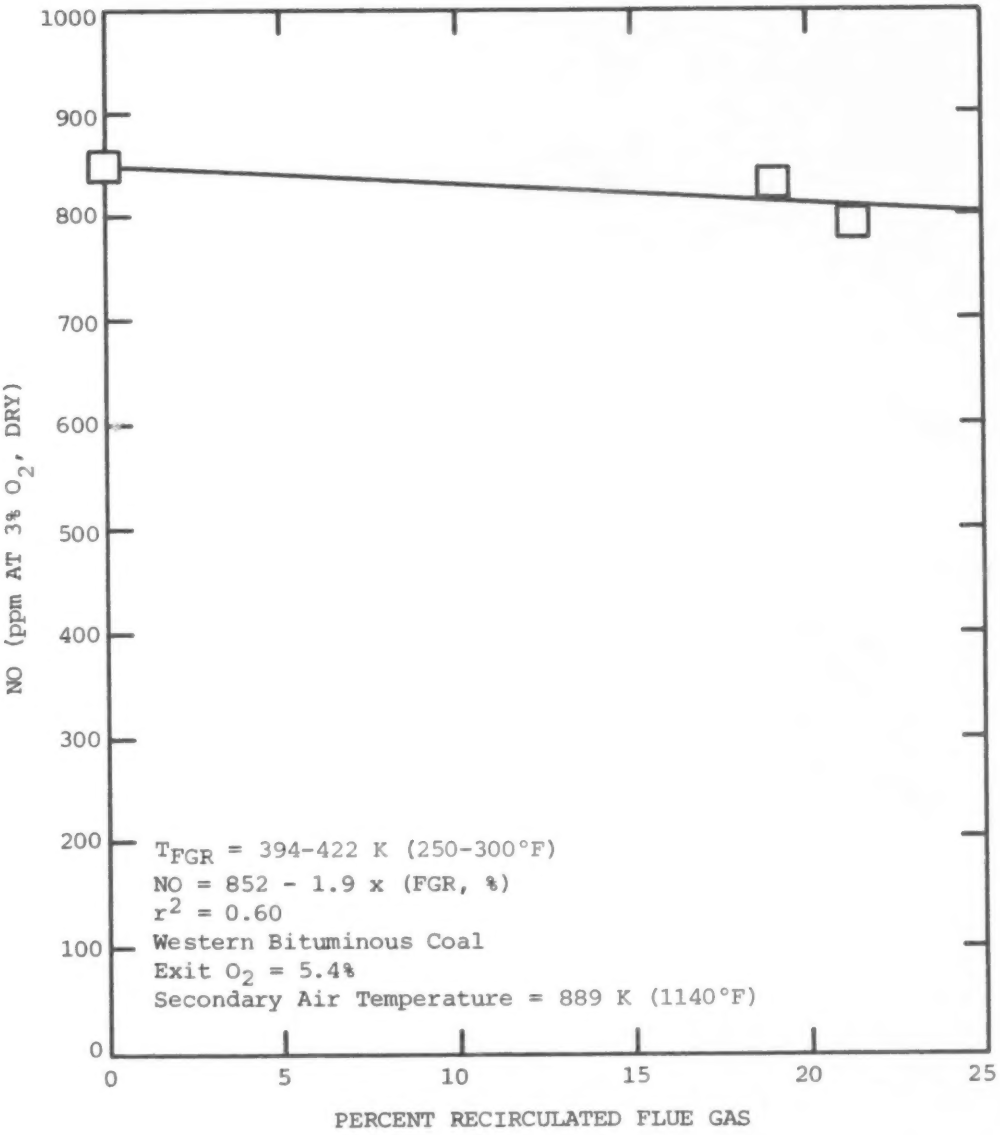

Figure 13. **The Effect of Flue Gas Recirculation Rate on NO Emissions for a Subscale Cement Kiln**

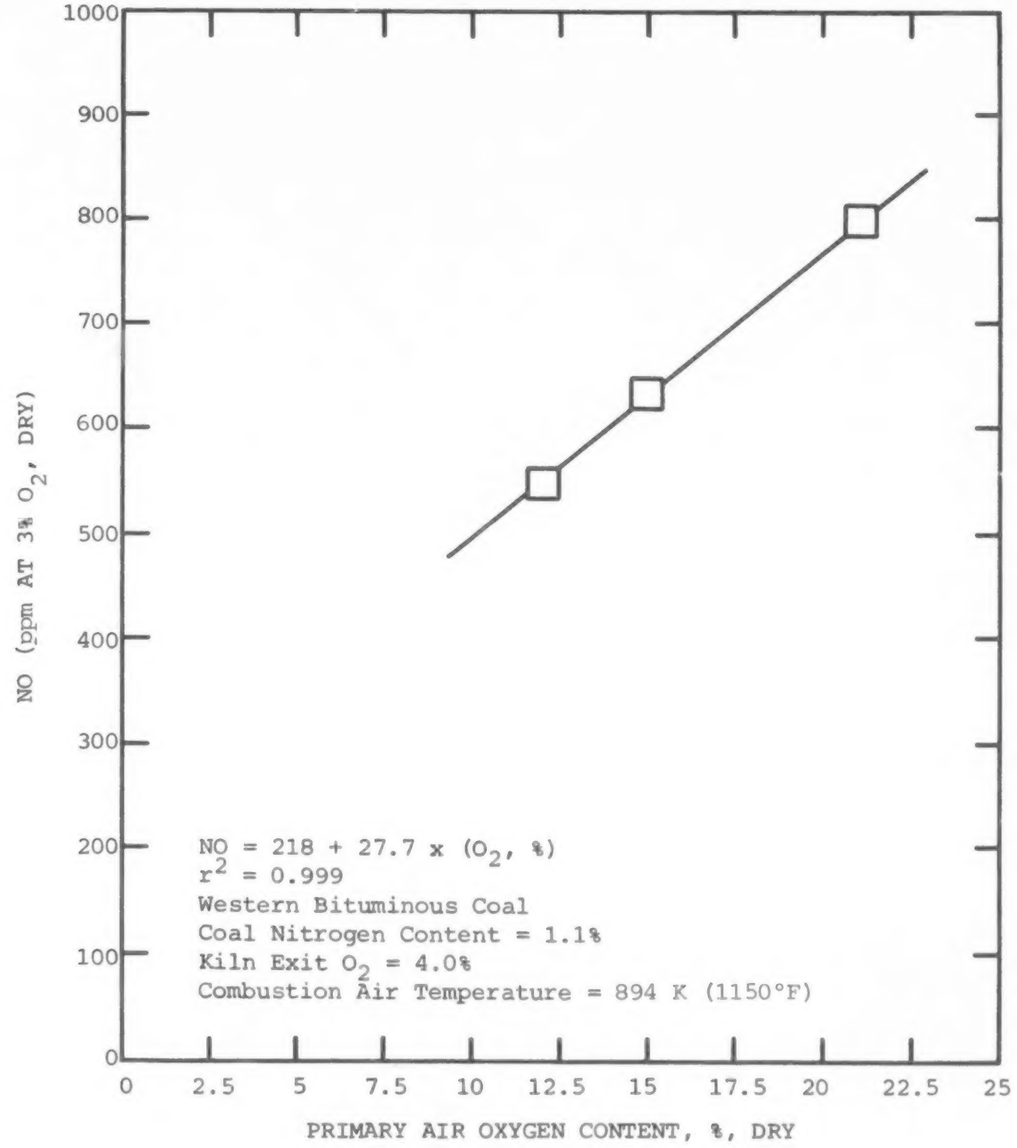

Figure 14. The Effect of Primary Air Oxygen Content on NO Emissions

TABLE 1. NATURAL GAS FIRING - SUBSCALE CEMENT KILN

Test Series		SA Temp. °F	SA Temp. K	% Primary Air	% FGR	Fuel Firing Rate MW (x 10^6 Btu/hr)	Kiln Exit O_2 (%, dry)	NO (ppmv, @ 3% O_2, dry)	CO_2 (%, dry)	Maximum % NO Reduction from Baseline
PA/SA Variation (20/80)	Baseline	1100	867	19.1	0	0.21 (0.70)	2.0	640	11.2	64.4
		900	756	↓		↓	↓	600	↓	
		600	589					400		
		300	422					243		
		Amb.						228		
PA/SA Variation (33/67)	Baseline	1200	922	33.0	0	0.21 (0.70)	2.0	300	11.5	43.3
		600	589	↓		↓	↓	194	↓	
		300	422					180		
		Amb.						170		
SA Temp. Variation	Baseline	1000	811	14.6	0	0.19 (0.64)	2.0	404	14.2	47.5
		900	756	↓		↓	↓	419	↓	
		800	700					364		
		700	644					350		
		Amb.						212		
FGR	Baseline	1168	904	28.0	0	0.19 (0.64)	2.0	340	15.8	70.6
		↓		↓	21.6	↓	↓	163	↓	
					28.6			135		
					32.6			110		
					33.8			100		

NOTE: All CO data for the nominal O_2's listed are less than 200 ppmv.

PA: Primary Air

SA: Secondary Air

TA: Tertiary Air

FGR: Flue Gas Recirculation

TABLE 2. COAL FIRING - SUBSCALE CEMENT KILN

Test Series		SA Temp. K	SA Temp. °F	PA Velocity m/s	PA Velocity fpm	% PA	% TA	PA or TA Vitiation, % O_2	% FGR	Avg. O_2 (%, dry)	Avg. NO (ppmv Corrected to 3% O_2)	Avg. CO_2 (% vol., dry)	Maximum NO Reduction from Baseline %
SA Temp. Variation	Baseline	906	1170	16.7	3285	27.2	0	0	0	3.5	840	15.8	10.7
		894	1150	16.7	3285	27.2	0	0	0	3.5	800	15.8	
		867	1100		↓	↓	↓	↓	↓	↓	750	↓	
		811	1000								765		
PA Velocity Variation	Baseline	894	1150	14.7	2890	19	0	0	0	3.5	790	16.4	30.4
			↓	12.7	2500	18	↓	↓	↓	↓	643	↓	
				11.6	2285	16					637		
				10.8	2128	15					550		
PA/SA Variation	Baseline	906	1170	15.2	3000	18	0	0	0	3.5	650	16.3	14.9
		906	1170	15.2	3000	20	0	0	0	3.5	764	↓	
			↓		↓	23	↓	↓	↓	↓	840		
						26					800		
FGR	Baseline	889	1140	17.4	3420	27.2	0	0	0	5.4	850	14.5	5.4
			↓		↓	↓	↓	↓	19.0	↓	837	↓	
									21.3		804		
PA Vitiation (2880 fpm)	Baseline	894	1150	14.6	2880	20	0	21	0	3.0	711	14.5	6.8
			↓		↓	↓	↓	18	↓	↓	700	↓	
								15			663		
PA Vitiation (2500 fpm)	Baseline	893	1147	12.7	2500	20.8	0	21	0	4.0	800	17.6	37.5
			↓		↓	↓	↓	15	↓	↓	635	↓	
								12			500		

NOTES: All [SO_2] less than 150 ppmv.

All CO data for the average O_2's listed are less than 1000 ppmv (exception: 10.8 m/s [2128 fpm] primary air velocity test)

PA: Primary Air
SA: Secondary Air
TA: Tertiary Air
FGR: Flue Gas Recycle

TABLE 3. COAL FUEL ANALYSIS

Sample Taken 8-4-82

Proximate Analysis			Ultimate Analysis		
	As Rec'd	Dry Basis		As Rec'd	Dry Basis
% Moisture	7.34	XXXXX	% Moisture	7.34	XXXXX
% Ash	11.73	12.66	% Carbon	62.35	67.29
% Volatile	34.95	37.72	% Hydrogen	4.14	4.47
% Fixed Carbon	45.98	49.62	% Nitrogen	1.11	1.20
	100.00	100.00	% Chlorine	0.04	0.04
			% Sulfur	0.49	0.53
Btu/lb	10,740	11,591	% Ash	11.73	12.66
(kJ/kg)	(24,981)	(26,961)			
% Sulfur	0.49	0.53	% Oxygen (diff)	12.80	13.81
				100.00	100.00

DEVELOPMENT OF A LOW NO_x BURNER FOR ENHANCED OIL RECOVERY

By:

G. England, M. Heap, Y. Kwan
R. Payne, D. Pershing
Energy and Environmental Research Corporation
18 Mason
Irvine, California 92714

"Although the research described in this article has been funded wholly or in part by the United States Environmental Protection Agency through contract numbers 68-02-3125 and 68-02-3692 to Energy and Environmental Research Corporation, it has not been subjected to the Agency's required peer and policy review and therefore does not necessarily reflect the views of the Agency and no official endorsement should be inferred."

ABSTRACT

Data derived at laboratory and pilot-scale has been used to develop a low NO_x burner which is capable of operating with high nitrogen liquid fuels such as crude oils and synthetic fuels. Emissions of NO_x can be minimized by application of a staged combustion process in which the first stage is thermally isolated and provides long residence time under high temperature, optimally fuel-rich conditions. The design criteria for this process were developed in a previous study which was carried out in a 70,000 Btu/hr refractory tunnel furnace, and from these criteria two pilot-scale prototype burners have been developed and tested at 2×10^6 Btu/hr and 12×10^6 Btu/hr. The paper describes the results of the development tests and compares results of all three scales of experiment. Firing a heavy fuel oil containing 0.6 percent bound nitrogen, test results indicate that NO_x emissions of below 85 ppm (at 3 percent O_2) are possible while carbon monoxide and smoke are within acceptable limits. Translation of the design requirements to practical burner designs, and additional requirements for initial fuel/air contacting and second-stage air addition are presented and discussed. Data obtained over a scale range of 30:1 shows that residence time and temperature in the first stage are the single most important scaling parameters for this low NO_x burner design and aerodynamic effects are second order. A current EPA program to translate the bench-scale and pilot-scale experience into a 60×10^6 Btu/hr burner design which can be retrofitted to existing thermally-enhanced oil recovery (TEOR) steam generators is discussed.

1.0 INTRODUCTION

Nitrogen oxide emissions from stationary combustors can be reduced by combustion modification techniques which involve staging the heat release process. However, optimization of these techniques to control NO_x emissions from liquid fuel-fired combustors has proved difficult because of the limited knowledge of the controlling phenomena and the problems associated with the scaling of combustion systems. This paper describes the development and testing of a low NO_x liquid fuel-fired combustor whose design was based upon fundamental information generated in bench-scale reactors. These criteria are currently being applied in the design and construction of a 60 x 10^6 Btu/hr (17.5 Mw) low NO_x burner for field demonstration on a steam generator for thermally enhanced oil recovery (TEOR).

Many studies have been carried out to determine the mechanism of NO formation in flames both from molecular nitrogen (thermal NO) and from nitrogen contained in the fuel (fuel NO). Field test data(1) and laboratory studies(2,3) have established the importance of fuel NO to the total emission of nitrogen oxides from residual fuel oil flames. Thermal NO formation is strongly dependent upon temperature and its formation can be reduced by decreasing flame temperatures by techniques such as the addition of cooled combustion products to the combustion air (flue gas recirculation). However, since the majority of NO formed in residual fuel oil flames is fuel NO and its formation is not strongly dependent upon temperature, flue gas recirculation is not an effective NO_x control technique(4). Fuel NO formation is very sensitive to reactant stoichiometry. Fuel-rich conditions promote the formation of molecular nitrogen from fixed nitrogen species ($NO + NH_3 + HCN = TFN$) which are formed as the liquid fuel decomposes. Consequently, staged combustion, which involves the formation of a fuel-rich zone either by delaying fuel air mixing or by dividing the combustion air supply into two and injecting one portion downstream from the burner is the most effective NO_x control technique for residual fuels(5).

In a previous study(3) the parameters controlling the effectiveness of staged combustion for a wide range of liquid fuels containing bound nitrogen were defined in a series of bench-scale studies which were carried out in a refractory tunnel furnace. Exhaust NO levels from a staged combustion system are dependent upon:

1. First-Stage Processing. TFN is minimized if the residence time of the fuel-rich reactants is maximized at high temperatures and at an optimum stoichiometry which is temperature dependent.

2. Mixedness. Since stoichiometry must be controlled it is important that the reactants are well mixed.

3. Second-Stage Processing. Exhaust NO levels are the sum of thermal NO formation and conversion (or retention) of TFN species to NO during heat release in the second stage and the second stage must be designed to minimize these effects.

4. Fuel Properties. The rate of evolution of nitrogen species from the liquid fuel droplets has an impact because it dictates the time available for N_2 formation in the first zone. This can be overcome by minimizing droplet size.

The goal of the investigation reported in this paper was to use this information to construct a combustor which would have NO_x emissions less than 100 ppm (corrected to 0% O_2) and have acceptable emission levels for CO and smoke when firing fuels containing greater than 0.5% nitrogen.

The bench-scale tests indicated that TFN concentration is minimized most effectively by increasing the temperature of the fuel-rich zone. The combination of high first-stage temperature, optimum stoichiometry and long first-stage residence time resulted in exhaust NO_x levels below 100 ppm irrespective of the nitrogen content of the liquid fuel. To translate this information into a full-scale burner (c.a. 60 x 10^6 Btu/hr) requires information on how the controlling parameters scale. This paper describes results from experimental studies performed to achieve this understanding. The approach used was to obtain experimental data with 2 x 10^6 Btu/hr (0.6 MW) and 10 x 10^6 Btu/hr (3 MW) prototype combustors, and thereby confirm the appropriate criteria for the design and fabrication of the full-scale combustor.

2.0 TEST EQUIPMENT

Two prototype low NO_x burners shown in Figure 1, were constructed with nominal design firing rates of 2 x 10^6 Btu/hr (0.6 MW) (small pilot-scale or SP) and 10 x 10^6 Btu/hr (3 MW) (intermediate pilot-scale or IP). Each of the two test burners contains three major elements:

1. an air/fuel injection system,
2. a fuel-rich holdup zone, and
3. a secondary air injection section.

The primary zone is constructed from high temperature refractories and insulation to minimize heat loss through the walls and permit near-adiabatic conditions in the primary zone. Fuel and primary air are injected at the entry of a divergent which forms the initial section of the fuel-rich holdup zone. The residence time in the fuel-rich zone calculated at a first-stage stoichiometric ratio of 0.7 is approximately 0.50 sec. for the SP burner and 0.42 sec. for the IP burner. The primary products are directed through a convergent section which serves to minimize radiative heat loss, ensure complete mixing of the primary products, and minimize backmixing of secondary air into the primary zone. Secondary air is injected parallel to the burner axis annularly around the primary exit.

A number of different commercial atomizers were used in the two combustors. Most of the data was however, obtained with an ultrasonic, air-assist atomizer and an internal mixing steam-assist atomizer. At the 2 x 10^6 Btu/hr (0.6 MW) scale, the ultrasonic atomizer produced droplets with a narrow size distribution about a mean diameter of 20 μm, and the internal mixing atomizer produced droplets with a much broader size distribution about a mean diameter of 40 μm(3). At larger scales the ultrasonic atomizer has been found to produce droplets with a mean size greater than 120 μm(8).

The combustor tests were conducted in two different combustors:

- Firetube Simulator (FS). The combustion chamber is 10.5 feet (3.2 m) long with an internal diameter of 23.5 inches (0.6 m). The chamber is composed of calorimetric sections cooled by heat transfer fluid and has a nominal wall temperature of 450°F (230°C). Only the SP burner was tested in this facility.

- Small Watertube Simulator (SWS). The furnace is 17 feet (5.2 m) in length and 6 feet (1.8 m) inside diameter, is externally spray-cooled, and has a partial refractory lining. The total heat extraction is controlled by varying the percentage of internal surface which is covered by refractory. Both the SP and IP burners were tested in this facility.

The fuel and air flow to both furnaces were monitored continuously. The equipment used to measure exhaust gas concentrations and TFN levels in the first stage have been described in detail elsewhere(3).

3.0 FIRST STAGE PARAMETERS

Stoichiometry

Figure 2 shows the influence of the first-stage stoichiometric ratio (SR_1) on exhaust emissions from the bench-scale studies carried out in the tunnel furnace and the prototype tests with different residual oils containing approximately 0.6 percent nitrogen. The curves are generally lower but similar in shape to those obtained in other staged combustion studies. As SR_1 decreased, NO_x emissions decreased rapidly until a minimum was reached and then increased. Smoke and CO emissions from the SP burner were low for $SR_1 > 0.7$, but under more fuel-rich conditions emissions increased sharply. CO was less than 100 ppm and smoke number was generally less than 5 at the point where the minimum NO_x level occurred. CO and smoke emissions from the IP burner were also low for SR_1 greater than the point where minimum NO_x occurred; however, the sharp increase in emissions below this point was less severe . Differences in second-stage thermal environment between the 2 x 10^6 Btu/hr (0.6 MW) firetube simulator and the 10 x 10^6 Btu/hr (3 MW) small watertube simulator may contribute to the observed difference in burnout of CO and smoke. Comparison of the three sets of results indicates that concept scale-up shifted the optimum SR_1 from 0.8 to 0.7 in going from 70,000 Btu/hr (0.02 MW) to 2 x 10^6 Btu/hr (0.6 MW), and to 0.56 in going to 8 x 10^6 Btu/hr (2.5 MW). This shift can be attributed to reduced heat losses and therefore higher temperatures, and to changes in fuel-air mixing characteristics, associated with the increase in scale.

In the SP burner tests, TFN (NO, HCN, NH_3) species concentrations were measured at the exit of the fuel-rich zone to define the influence of scale on the fuel-rich processing. These data (Figure 3) show that the increased reactor temperature in the small pilot-scale prototype resulted in a reduction of minimum TFN level and a shift of the optimum stoichiometric ratio from 0.8 to 0.7. Equilibrium calculations (free energy minimization) confirmed that the optimum SR_1 should move more fuel-rich with increased temperature; however, the TFN concentrations shown in Figure 3 are greatly (circa 10^2) in excess of equilibrium values. Hence, even with a first-stage exit temperature of 2950°F (1620°C) ($SR_1 = 0.7$) and a first-stage residence time of 500 msec., kinetic limiatations are significant. Decreasing SR_1 reduced first-stage NO, but below approximately $SR_1 = 0.8$, significant amounts of NH_3 were formed. Thus, as in the bench-scale studies, there exists a minimum in the exhaust NO_x because of a competition between decreased first-stage NO and increased oxidizable nitrogen species. Other than shifting the optimum SR_1, concept scale-up did little to alter this competition or the TFN species distribution.

Time/Temperature History

The residence time in the fuel-rich zone required to achieve the desired TFN concentration is an important practical design parameter. Figure 4 summarizes minimum exhaust NO_x and TFN data for the tunnel furnace and the prototype burners firing in both the firetube simulator and the small watertube simulator as a function of the first-stage residence time. At both bench and small pilot scales, increasing the first-stage residence time significantly decreased exhaust NO_x because of an associated decrease in TFN. (Increasing first-stage residence time allows HCN, NH_3 and NO to decay further toward equilibrium values.) Both the exhaust NO_x and the TFN from the SP burner were lower than from the tunnel furnace because of the increased rich-zone temperature associated with the increase in scale.

Variations in first-stage residence time were achieved in the SP burner/firetube simulator tests by altering the firing rate, and in the SP burner/watertube simulator tests by changing the reactor length at a fixed firing rate. A strong correlation between the two sets of experiments suggests that the controlling processes are dominated by kinetic effects (time and temperature) and not by aerodynamics and that the principle influence of firing rate is on residence time. Clearly, increasing firing rate also increases first-stage temperature, but this effect is small because even at 2×10^6 Btu/hr (0.6 MW), the prototype heat losses were low. First-stage exit temperatures measured at SR_1 of 0.7 were 2950°F (1620°C) compared to adiabatic flame temperature of 3180°F (1750°C).

Since the time/temperature history of the fuel-rich zone was believed to be the primary scaling parameter, one-dimensional kinetic calculations were conducted to quantify this influence. The model used(9,10) assumed a 2 msec. well-stirred reaction-ignition zone followed by a variable-length plug-flow reactor. The fuel was CH_4 containing one weight percent N as HCN. Preliminary runs showed that the initial fuel nitrogen speciation input to the first stage had little effect on the ultimate TFN level. Rich-zone temperature was assumed to decay linearly from 2925°F (1600°C) to a specified temperature over 660 msec. Figure 5 summarizes results obtained with the kinetic model. Under fuel-rich conditions, the rate of TFN decay slows dramatically when the gas temperature drops below approximately 2600°F (1425°C). The dotted line on this figure shows the residence time at which the various temperature ramps have decayed to 2600°F. Thus, increasing first-stage residence time is only beneficial if the heat extraction rate is low enough to keep the local gas temperature above 2600°F. Further, even if the fuel-rich temperature is maintained at a high level (e.g., 2925°F case on Figure 5a), the rate of NO decay decreases precipitously when the NH_3 concentration falls to zero indicating that TFN speciation is important in the first-stage processing. These calculations support the concept that reactions of the form:

$$NO + NH_i \rightarrow N_2$$

are controlling the fuel-rich TFN reduction and that it is essential to have both high temperature (>2600°F), and a proper TFN species distribution to achieve very low exhaust NO_x. The calculations also indicate the need for a long residence time in the primary zone but that this requirement decreases with increasing first-stage temperatures for a fixed TFN level.

Fuel/Air Contacting

The influence of fuel/air contacting parameters early in the fuel-rich zone (e.g., nozzle design, atomization pressure, atomizing fluid, and air swirl) on prototype performance was investigated. Steam and air atomization both produced satisfactory results when the atomization pressure was high enough to provide adequate atomization. With long first-stage residence times (>600 msec), fuel injector parameters had little effect on minimum NO_x; however, both poor mixing and poor atomization (mean droplet diameter >100 microns) resulted in unacceptably high smoke in the small prototype.

As first-stage residence time was decreased, the importance of the fuel injection system design became more apparent. Figure 6 compares data obtained with a premixed burner to that obtained with the standard axial fuel nozzle arrangement. Both were fired in the SP burner mounted on the watertube simulator. The premixer was based on a high-swirl gas-turbine design(6) which utilized ultrasonic atomization. In the short first-stage residence time configuration (350 msec at $SR_1 = 0.7$), the premixer slightly reduced the exhaust NO emissions, and broadened the SR_1 for minimum emissions. A similar conclusion was reached by comparing data for a propane/NH_3 fuel (which represents a limit of instant fuel vaporization) to the California residual oil with the standard fuel nozzle. Thus, unless the first-stage residence time is extremely short (>200 msec), the characteristic time for fuel vaporization and mixing is small relative to the rich-zone residence time and hence atomizer design has a much greater effect on smoke formation than on minimum NO.

At the 10×10^6 Btu/hr (3 MW) prototype scale comparable investigations were carried out with a range of different atomizers, and with a high swirl premixed and conventional air register designs. Minimum NO_x emissions were found to be relatively insensitive to parameters affecting spray quality (e.g., atomizer type and operation), but were more sensitive to those factors controlling spray penetration (e.g., spray angle) and distribution (e.g., primary air velocity). While results are difficult to quantify, it was generally found that through the matching of atomizer and air register characteristics, those conditions which tended to provide for rapid initial mixing and uniform distribution of the fuel produced the best overall results.

4.0 SECOND-STAGE PARAMETERS

Temperature

All the TFN which exists in the first stage does not result in NO in the combustion products of the second stage. Thus, it is important to design the second-stage air injection system to minimize NO formation from TFN species. In addition, thermal NO formation must be minimized which requires that second-stage flame temperatures must be maintained below some critical threshold. Heat extraction between the fuel-rich zone and the secondary air injection system allows some control over temperature in the second-stage. Figure 7 presents SP burner/SWS results obtained when water-cooling tubes were placed around the periphery of the second-stage throat. This cooling removed approximately 6 percent of the heat input, and decreased the minimum exhaust NO_x by approximately 20 ppm. Exactly analogous results were achieved when 40 percent flue gas recycle was introduced with the second-stage air ($\Delta NO = 18$ ppm). In both tests there was a minor impact on smoke emissions; thus, it appears that at the optimum operating conditions, second-stage thermal NO formation accounts for approximately 20 percent of the total exhaust NO emissions. Use of interstage cooling may become more important in subsequent scale-up if air preheat is added and/or rich-zone heat loss is reduced further.

TFN Conversion

Variation in the temperature of the reactants exiting the first stage can affect exhaust NO levels because of a change in TFN distribution and/or reduced conversion rates in the second stage. Generally TFN conversion is high when NO is the dominant TFN species and when significant amounts of hydrocarbon are not carried into the second-stage flame. As TFN concentration increases below SR_1= 0.8, TFN conversion decreases due to increasing amounts of HCN and NH_3. The general conversion decrease is the result of a competition between N_2 formation reactions which are second-order in XN and the first-order NO formation reactions. Folsom, et al,(7) have shown that in a simple diffusion flame the conversion of HCN and NH_3 to NO and the retention of NO are affected by the hydrocarbon content of the fuel. NH_3 conversion is low when hydrocarbons are absent, and hydrocarbons are necessary for the reduction of NO or HCN to N_2. Thus, staged combustion requires the minimization of TFN as well as the production of an optimum TFN/fuel mixture for burnout.

Mixing

The method of secondary air injection can potentially impact exhaust NO_x levels, and different modes of injection have been examined in both prototype burner systems. The standard annular (parallel) air injection system provided a relatively slow mixing rate and tended to result in long diffusion-type flames. In the small prototype burner, rapid mixing was obtained by injecting the second-stage air radially through a water-cooled boom inserted along the firetube axis from the rear. NO_x emissions remained essentially constant when the ratio of air between the axial and radial injectors was varied; however, smoke emissions were substantially decreased as secondary air was transferred from the parallel injector to the radial injector. Similar results were obtained in both prototype burners when swirl vanes were added to the annular second-stage air injection system, suggesting a relative insensitivity of NO_x emissions to changes in mixing while providing some measure of control over flame shape. In larger practical scale burner systems, however, mechanical considerations may well preclude the use of narrow annular passages for secondary air injection. To overcome this limitation the potential use of discrete secondary air injection ports has been investigated in the intermediate prototype burner. Typical data are presented in Figure 8, and show that with axial injection there is no difference in minimum NO_x between the annulus and discrete ports; with radial injection to induce rapid mixing an increase of some 25 ppm NO_x was observed. This configuration produced short intense flames and, although the level of smoke emission was generally low, the range of operation over which low smoke could be maintained was extended. The reason for this apparent increased sensitivity to mixing at the larger scale is not immediately apparent from the data, but is believed to be due to increased formation of thermal NO_x in local high intensity combustion zones close to the air jets.

Figure 9 shows the effect of overall excess oxygen on NO_x emissions from the IP burner firing at 8 x 10^6 Btu/hr (SR_1 = 0.56) and at 12 x 10^6 Btu/hr (SR_1 = 0.62). NO_x increased by approximately 12 ppm at 8 x 10^6 Btu/hr and by 15 ppm at 13 x 10^6 Btu/hr (3.6 MW) in varying excess oxygen from 0.5 to 5.0 percent. This again points to the importance of the first-stage parameters in determining final emissions. Bacharach smoke number ranged from 1 to 4 and CO emissions less than 50 ppm (except at 13 x 10^6 Btu/hr and 0.3 percent excess O_2) for the data shown in Figure 9.

5.0 SCALING AND APPLICATION OF THE LOW NO_x CONCEPT

The results of the experimental work carried out on the bench and prototype combustors has provided an understanding of the controlling mechanisms of NO_x formation and control in staged liquid fuel combustion. The data suggests that application of these concepts can be achieved in a staged burner which consists of three major components with the following characteristics:

- Fuel Injection System
  - High quality atomization to produce a small mean droplet size
  - Rapidly mixed fuel and air
  - Minimal heat extraction to maximize fuel vaporization rate.
- First-Stage Fuel-Rich Zone
  - Stoichiometric ratio approximately 0.7 or lower to minimize TFN concentration.
  - Residence time in excess of 400 msec to allow sufficient TFN decay.
  - Control of heat loss to produce a first-stage exit temperature in excess of 2600°F (1425°C).
- Second-Stage Air Injection
  - Partial quenching to minimize thermal NO formation in the second stage.
  - Refractory choke to prevent backmixing and reduce heat loss.
  - Intermediate second-stage mixing to reduce smoke formation without affecting minimum NO_x.

The key elements in these design characteristics are the requirements for a high-temperature, optimally fuel-rich, primary combustion zone with a long residence time. A number of the remaining parameters are scale-dependent, and must be optimized at the burner scale under consideration. The mean droplet size produced by a given atomizer design, for example, does not remain constant with scale, but tends to increase as size increases.(8) While small droplets are more favorable, combustion conditions are such that droplet size alone does not have a large impact on minimum NO_x. Rather, increased droplet size leads to greater sensitivity to those parameters which control fuel air mixing and spray penetration. For practical concepts, optimum results are obtained by selecting and matching fuel spray angles and air register designs to provide for uniform distribution and rapid mixing.

Similarly, the overall burner performance has been shown to be more sensitive to the mode of secondary combustion air injection at larger burner scales. Rapid mixing is required to suppress smoke formation, but may impact minimum NO_x preformance. In practical applications a major additional concern is the shape of the second stage flame, and its interaction with its heat transfer surroundings, which can be strongly influenced by mixing. Final designs of secondary air injection will therefore represent a compromise between NO_x emissions, flame shape and smoke.

The impact of fuel type on the ability of such burners to achieve low NO_x emissions is also of importance. The influence of fuel-nitrogen content on the performance of the small-scale low NO_x prototype burner was established by conducting tests with a distillate oil, residual oils, a coal-liquid and propane/

NH_3. Data obtained in these tests are shown in Figure 10 which indicates that with the SP burner minimum NO emissions are only weakly dependent upon total fuel nitrogen content. Figure 10 also summarizes data obtained in the small-scale tunnel furnace, and in the larger 10 x 10^6 Btu/hr (3 MW) prototype. Concept scale-up reduced the dependence on fuel-nitrogen; this is probably because of the increased fuel-rich temperature. Thus this low NO_x concept should be capable of producing NO_x emissions less than 100 ppm at 0% O_2 (85 ppm at 3% O_2) even when firing the high nitrogen crude oils typical, for example, of the Kern County oil fields.

A program under EPA sponsorship is currently underway to demonstrate a burner based on these criteria in a 50 x 10^6 Btu/hr oil field steam generator (commonly referred to as "steamers") in the Kern County area of California. These units typically operate on lease crudes varying in nitrogen content from 0.6 to 0.8 percent, and under constant load for extended periods of time. Local regulations for the emission of NO_x, SO_x and particulates are very stringent in Kern County and maximum total NO_x emission levels of 0.14 lb/MMBtu (125 ppm at 0% O_2) are currently under consideration. Such low levels have traditionally been difficult to achieve with high nitrogen fuels through combustion modification while maintaining practical flame conditions within the steamer.

Figure 11 illustrates two current concepts of how a low NO_x burner based upon the above design principles may be incorporated into an existing steamer. The two designs shown are for; a regenerative system in which the refractory chamber is designed to provide for primary air preheat; and a simpler design employing a multi-layer refractory construction to minimize heat loss. Both concepts employ commercially available primary burner components and secondary air injection through discrete, inclined ports. Current plans are concentrating on the insulated design concept, and the program will provide for a preliminary evaluation of this burner in an experimental test furnace, prior to complete retrofit and final development in a field-operating steamer. The program will conclude with a 30-day field demonstration scheduled for early 1983.

ACKNOWLEDGMENTS

This work was supported by the U.S. Environmental Protection Agency Combustion Research Branch under Contracts 68-02-3125 and 68-02-3692, and W. S. Lanier, the EPA Project Officer.

REFERENCES

(1) Cato, G. A., L. J. Muzio, and R. E. Hall. "Influence of Combustion Modifications on Pollutant Emissions from Industrial Boilers", Proceedings of the Stationary Source Combustion Symposium, EPA 600/2-76-1526, Springfield, VA (1976).

(2) Pershing, D. W., J. E. Cichanowicz, G. C. England, M. P. Heap, and G. B. Martin, "The Influence of Fuel Composition and Flame Temperature on the Formation of Thermal and Fuel NO_x in Residual Oil Flames", Seventeenth Symposium (International) on Combustion, The Combustion Institute, Pittsburgh, PA (1979).

(3) England, G. C., M. P. Heap, D. W. Pershing, and R. K. Nihart, "Mechanisms of NO_x Formation and Control: Alternative and Petroleum-Derived Liquid Fuels", Eighteenth Symposium (International) on Combustion, The Combustion Institute (1981).

(4) Heap, M. P., et al., "Control of Pollutant Emissions from Oil-Fired Package Boilers", Proceedings of the Stationary Source Combustion Symposium, EPA 600/2-76-1526, NTIS, Springfield, VA (1976).

(5) Beer, J. M, M. T. Jaques, W. Farmayan, and B. R. Taylor, "Fuel Nitrogen Conversion in Staged Combustion of a High Petroleum Fuel", Eighteenth Symposium (International) on Combustion, The Combustion Institute, Pittsburgh, PA (1981).

(6) Pierce, R., M., S. A. Mosier, C. E. Smith, and B. S. Hinten, "Advanced Combustion Systems for Stationary Gas Turbine Engines: Volume II. Bench-Scale Evaluation", Final Report, EPA 600/7-80-0176, NTIS, Springfield, VA (1980).

(7) Folsom, B. A., C. W. Courtney, and M. P. Heap, "The Effects of LBG Composition and Combustor Characteristics on Fuel NO_x Formation", Transactions of the ASME, Vol. 102; No.2; April (1980).

(8) England, G. C., Unpublished data.

(9) Kramlich, J. C., W. R. Seeker, T. L. Corley, M. P. Heap, and T. J. Tyson, "Elementary Gas-Phase Mechanism Development", Draft Final Report, Vol. 1, EPA Contract 68-02-2631 (1981).

(10) Kau, C. J., and T. J. Tyson, "Numerical Model for Two-Phase One-Dimensional Flow Reactor", Unpublished Internal Report, Energy and Environmental Research Corporation, Irvine, CA (March, 1981).

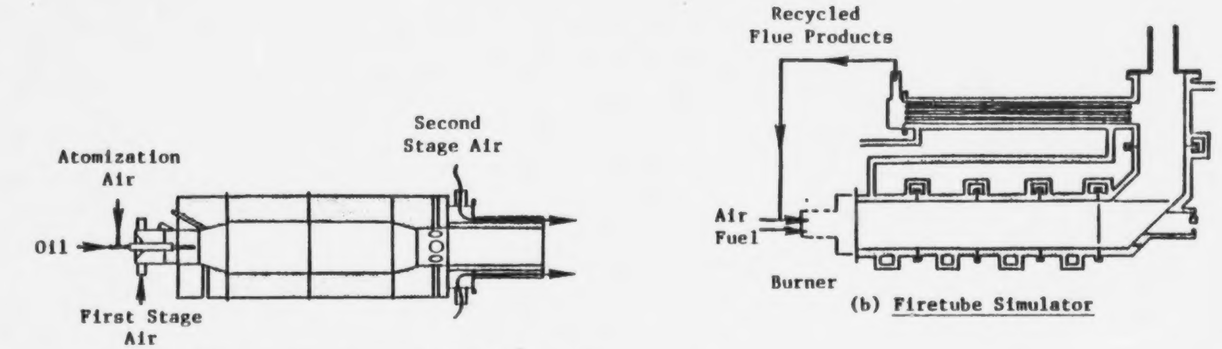
Atomization
Air
Oil
First Stage
Air
Second
Stage Air
Recycled
Flue Products
Air
Fuel
Burner

(a) Small Prototype Burner (2×10^6 Btu/hr)

(b) Firetube Simulator

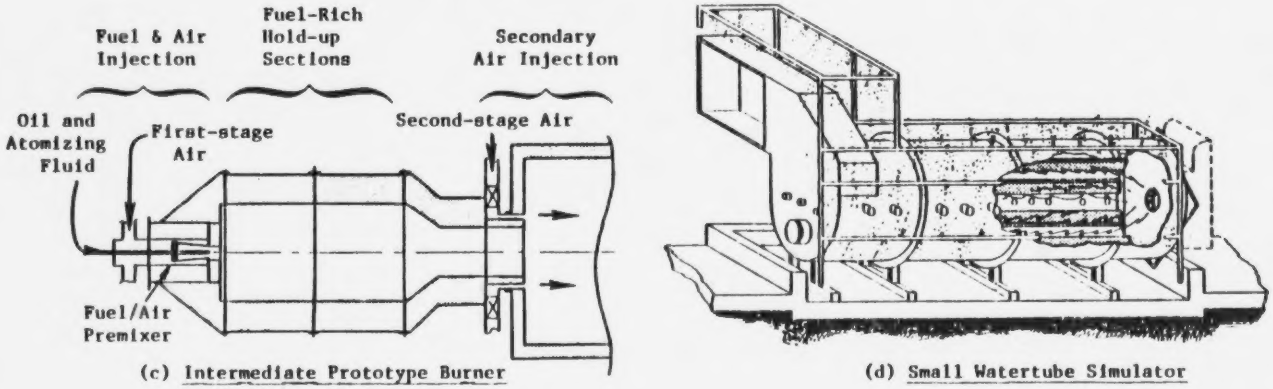
Fuel & Air
Injection
Fuel-Rich
Hold-up
Sections
Secondary
Air Injection
Oil and
Atomizing
Fluid
First-stage
Air
Second-stage Air
Fuel/Air
Premixer

(c) Intermediate Prototype Burner (10×10^6 Btu/hr)

(d) Small Watertube Simulator

Figure 1. Prototype burners and experimental test furnaces.

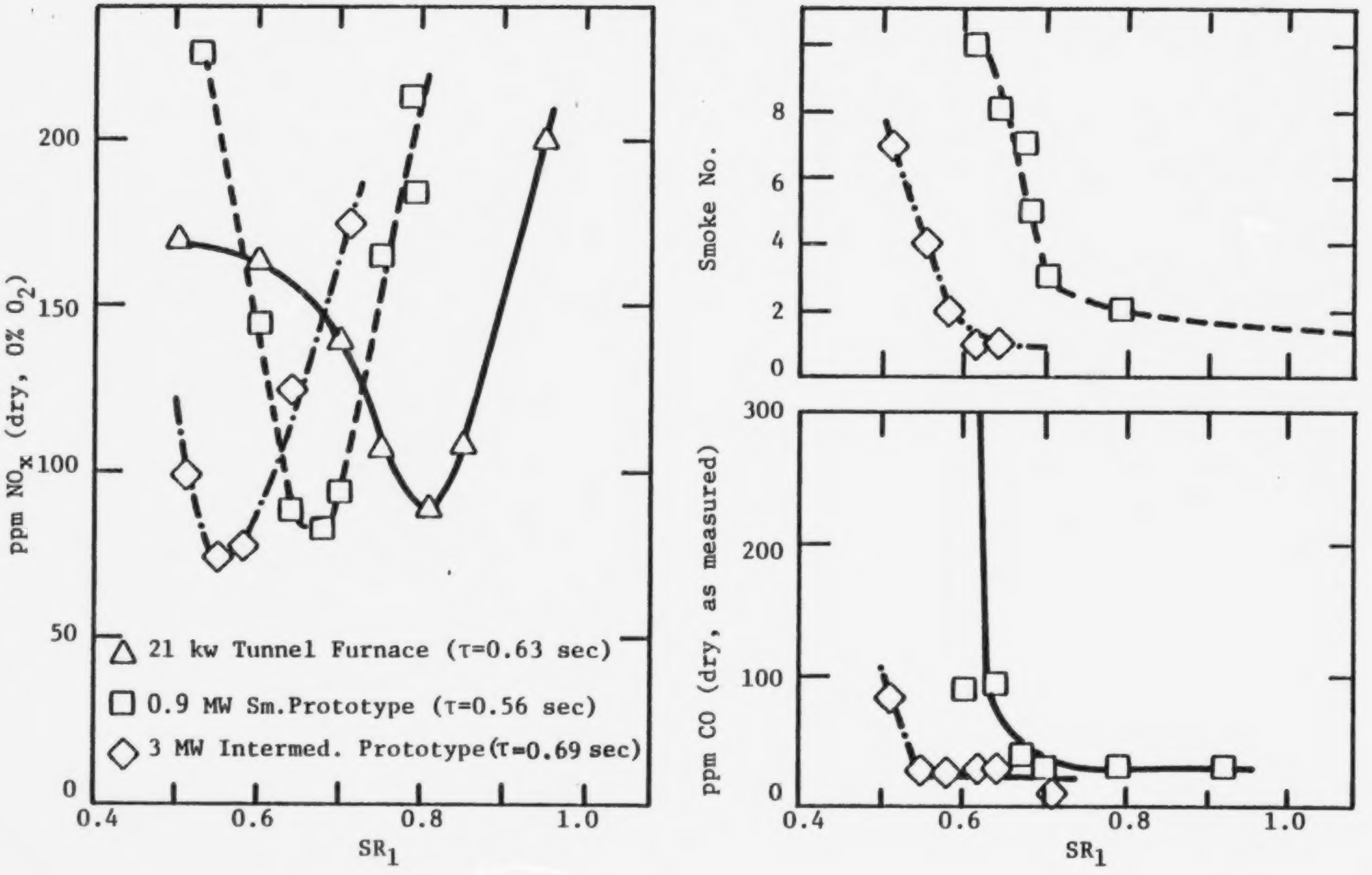

Figure 2. Influence of first-stage stoichiometry on NO_x, CO and smoke emissions (bench-scale and pilot-scale, California residual fuel oil).

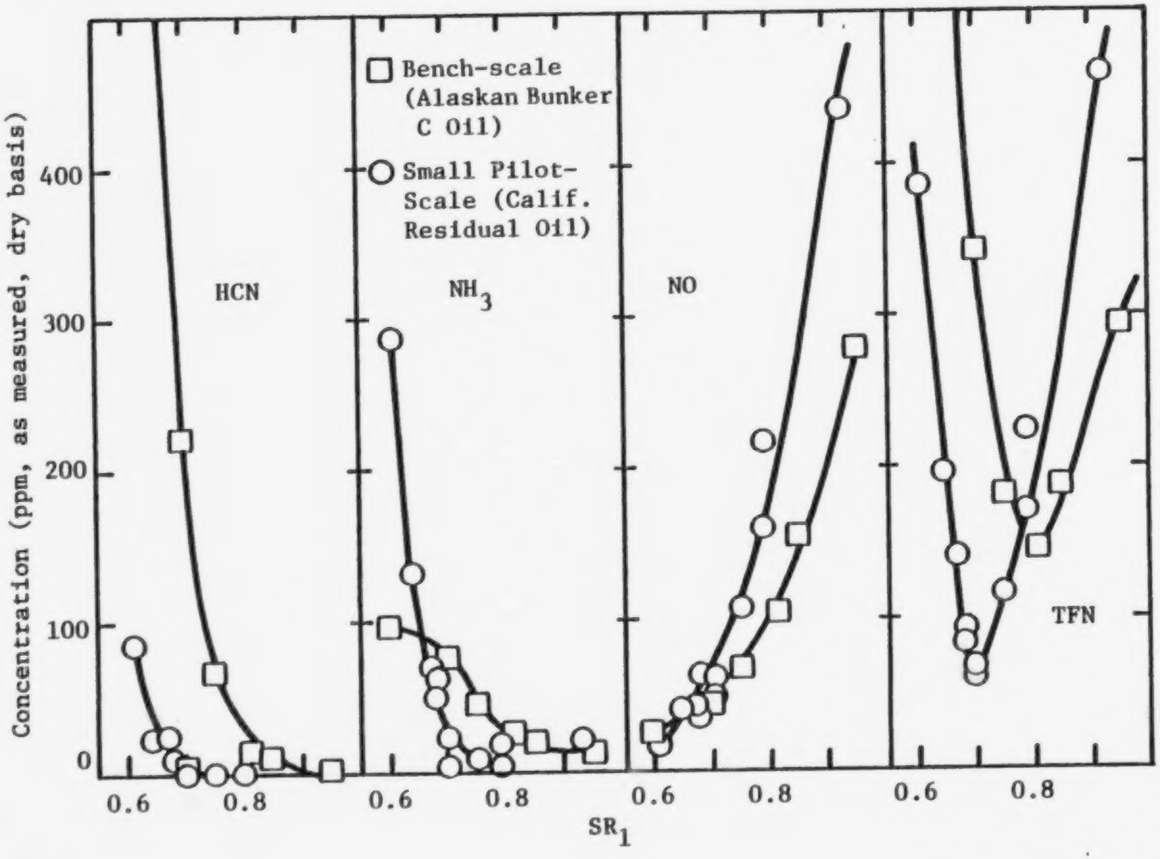

Figure 3. Influence of scale on first-stage exit total fixed nitrogen (TFN) species.

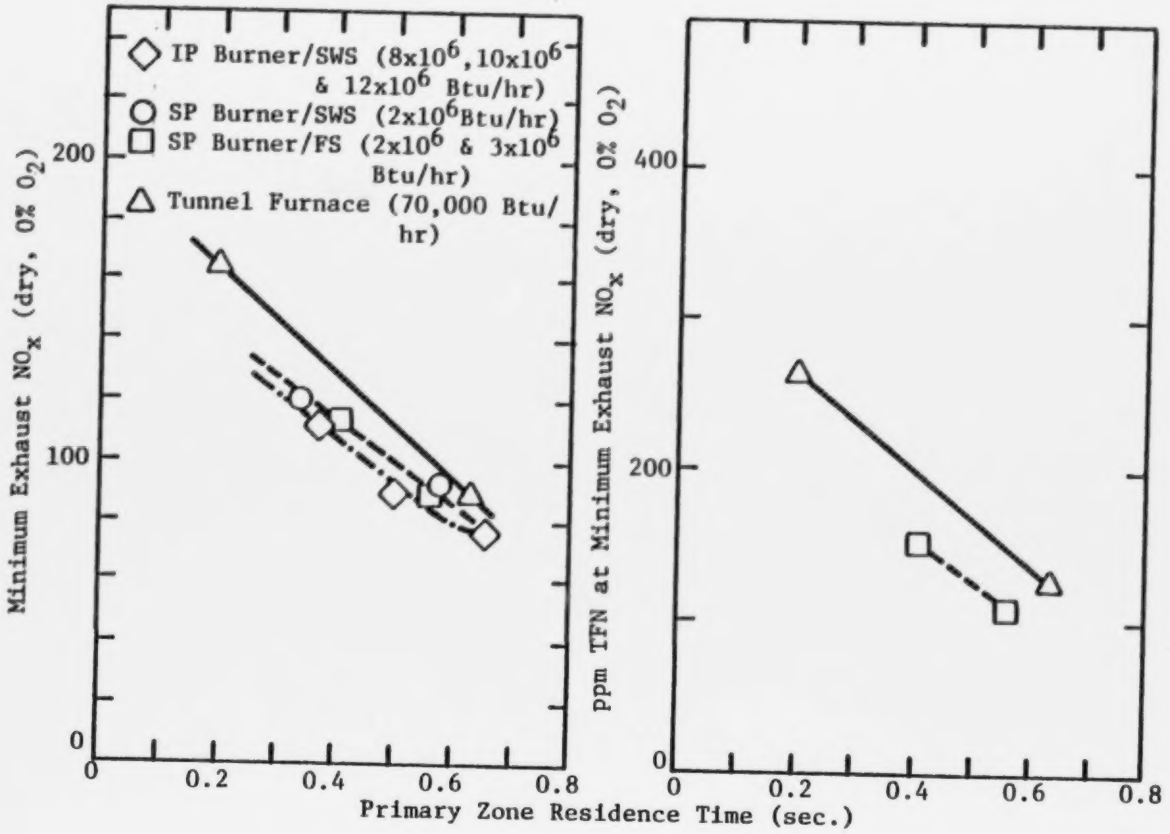

Figure 4. Second-stage NO_x production and first-stage TFN decay for bench-scale and pilot-scale.

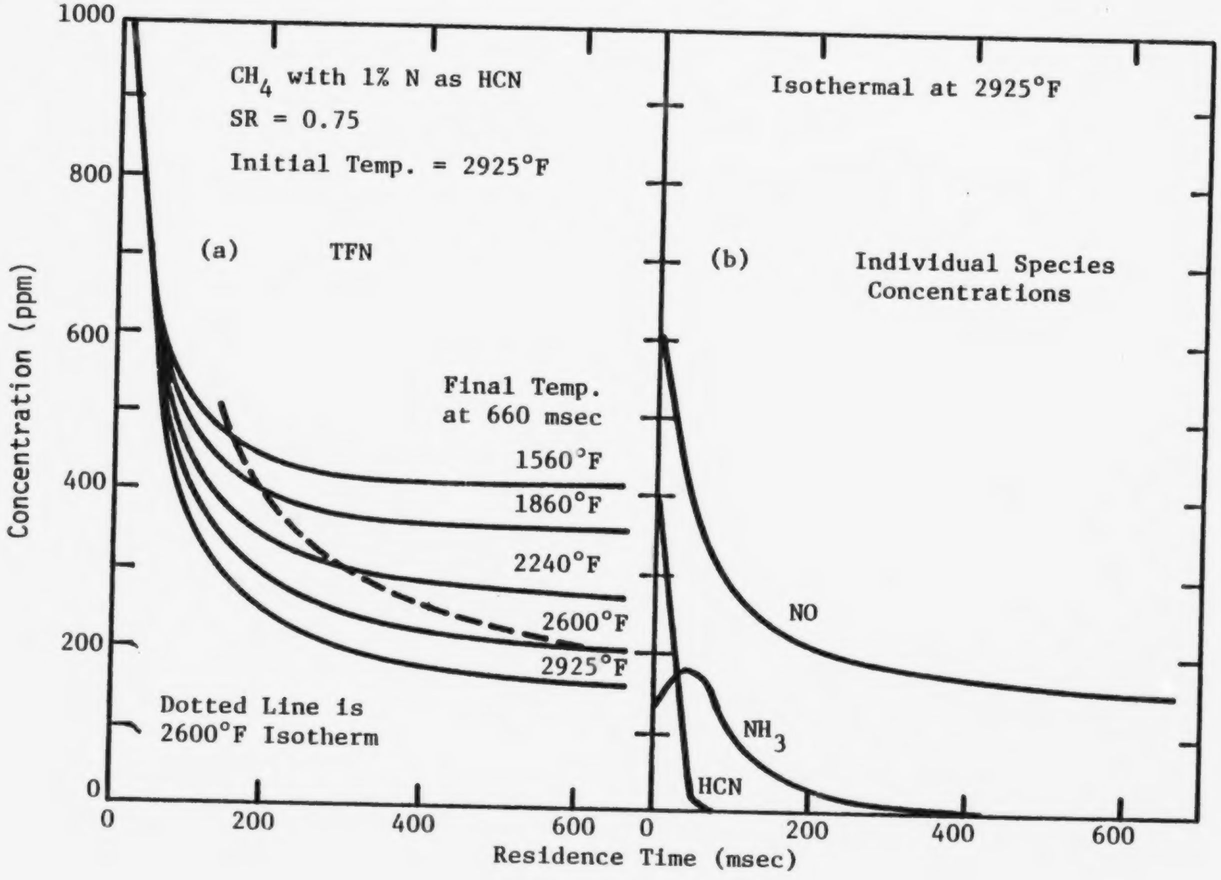

Figure 5. Calculation of (a) total fixed nitrogen decay and (b) decay of individual fixed nitrogen species.

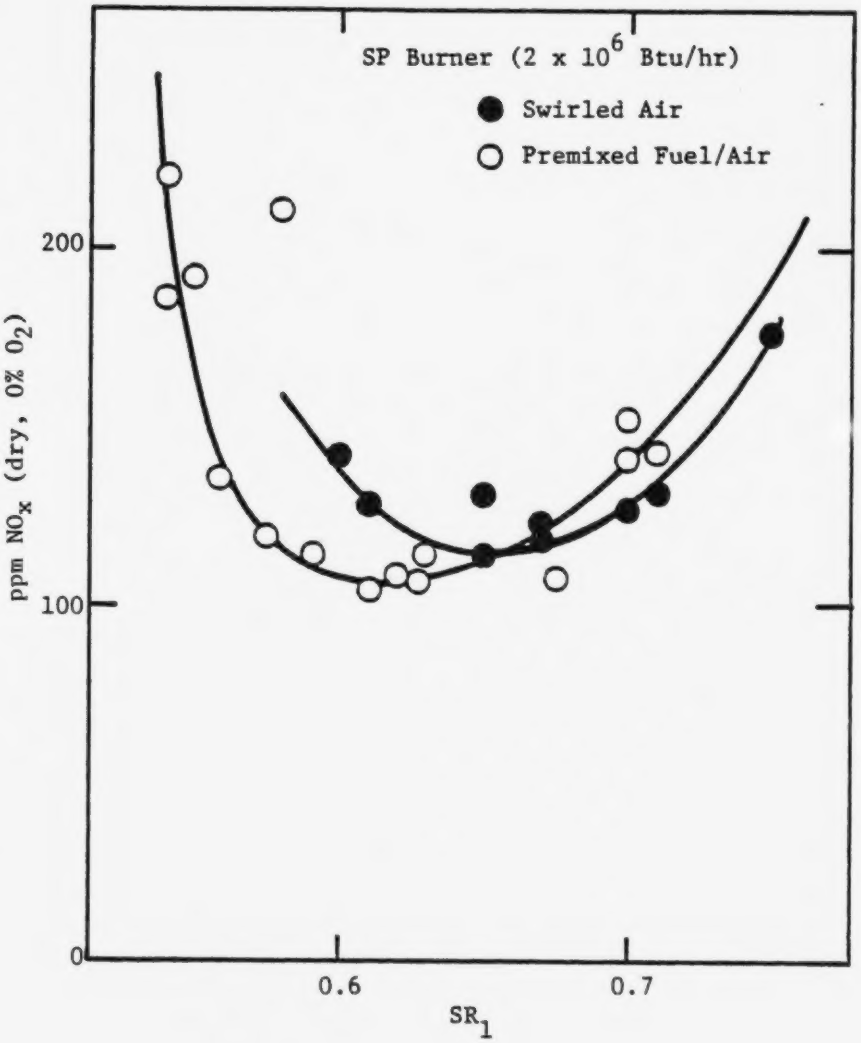

Figure 6. Pilot-scale second-stage NO_x emissions for premixed and non-premixed first-stage reactants (2×10^6 Btu/hr; California residual oil; 350 msec first-stage residence time at $SR_1 = 0.7$).

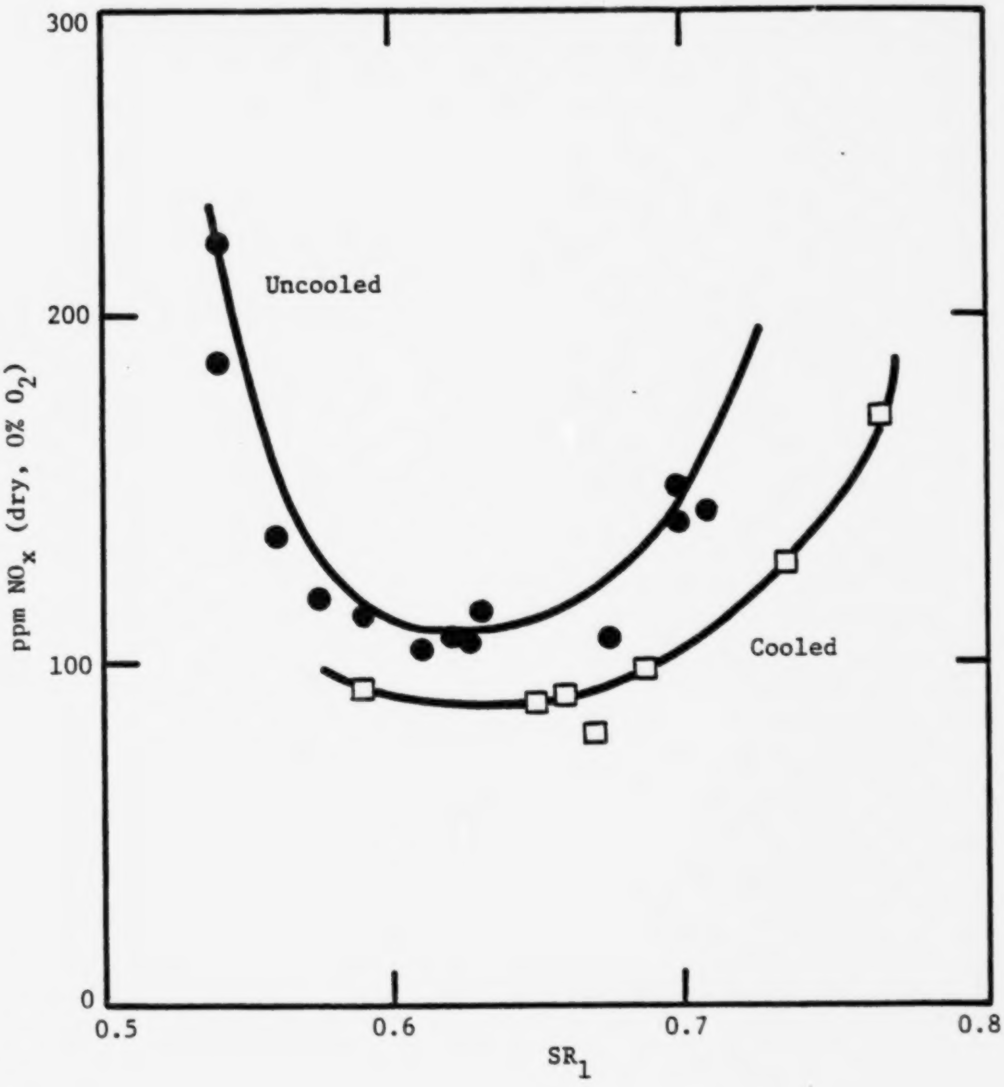

Figure 7. Pilot-scale second-stage NO_x emissions with and without inter-stage heat extraction (2 x 10^6 Btu/hr; 120,000 Btu/hr inter-stage heat removal in cooled case).

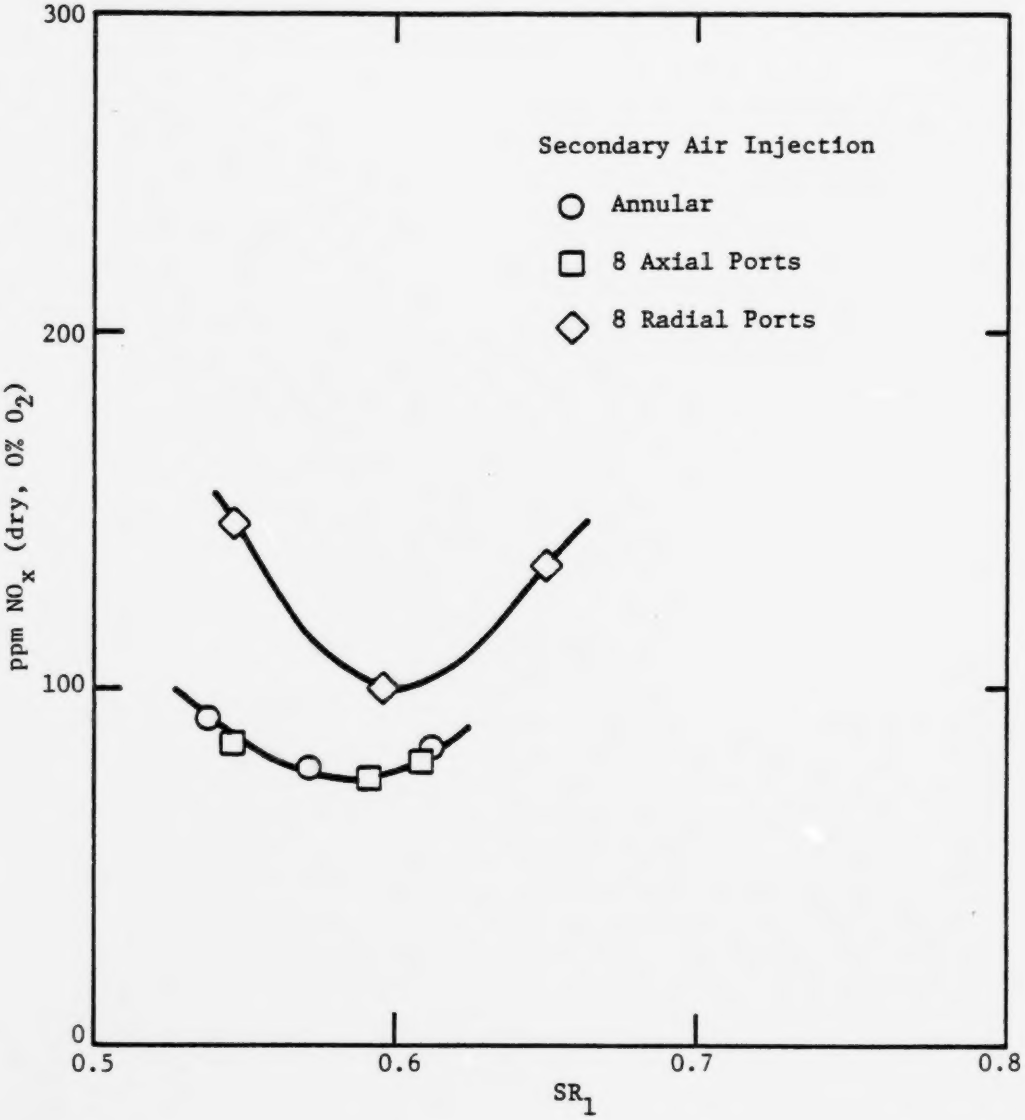

Figure 8. Effect of secondary air injection mode - 8 x 10^6 Btu/hr (2.4 MW) prototype burner.

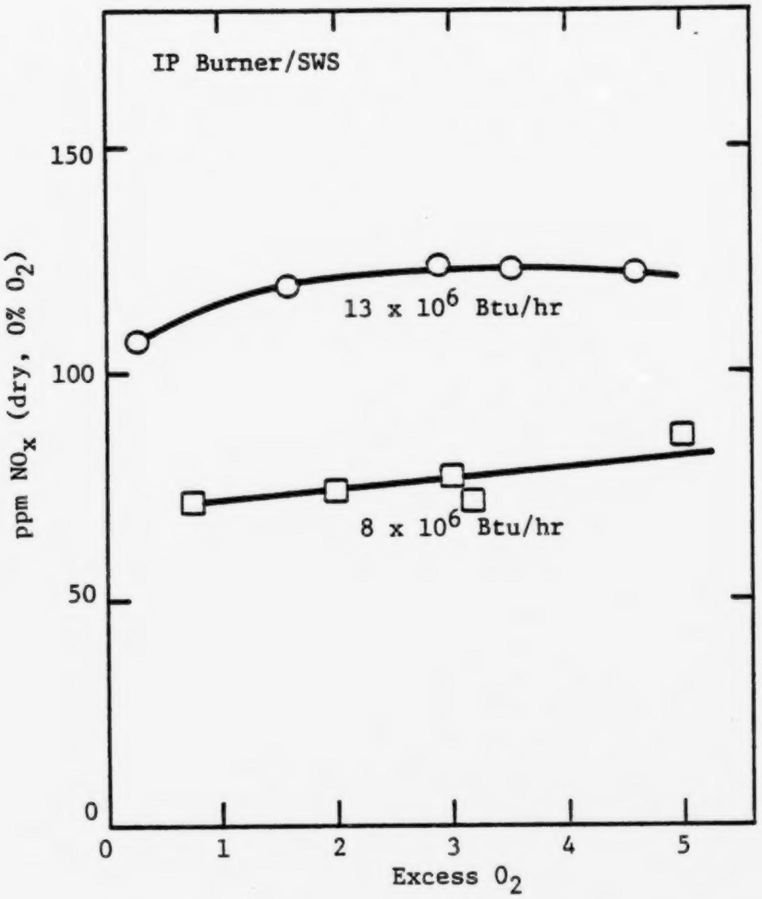

Figure 9. Influence of excess air on second-stage NO_x - IP burner.

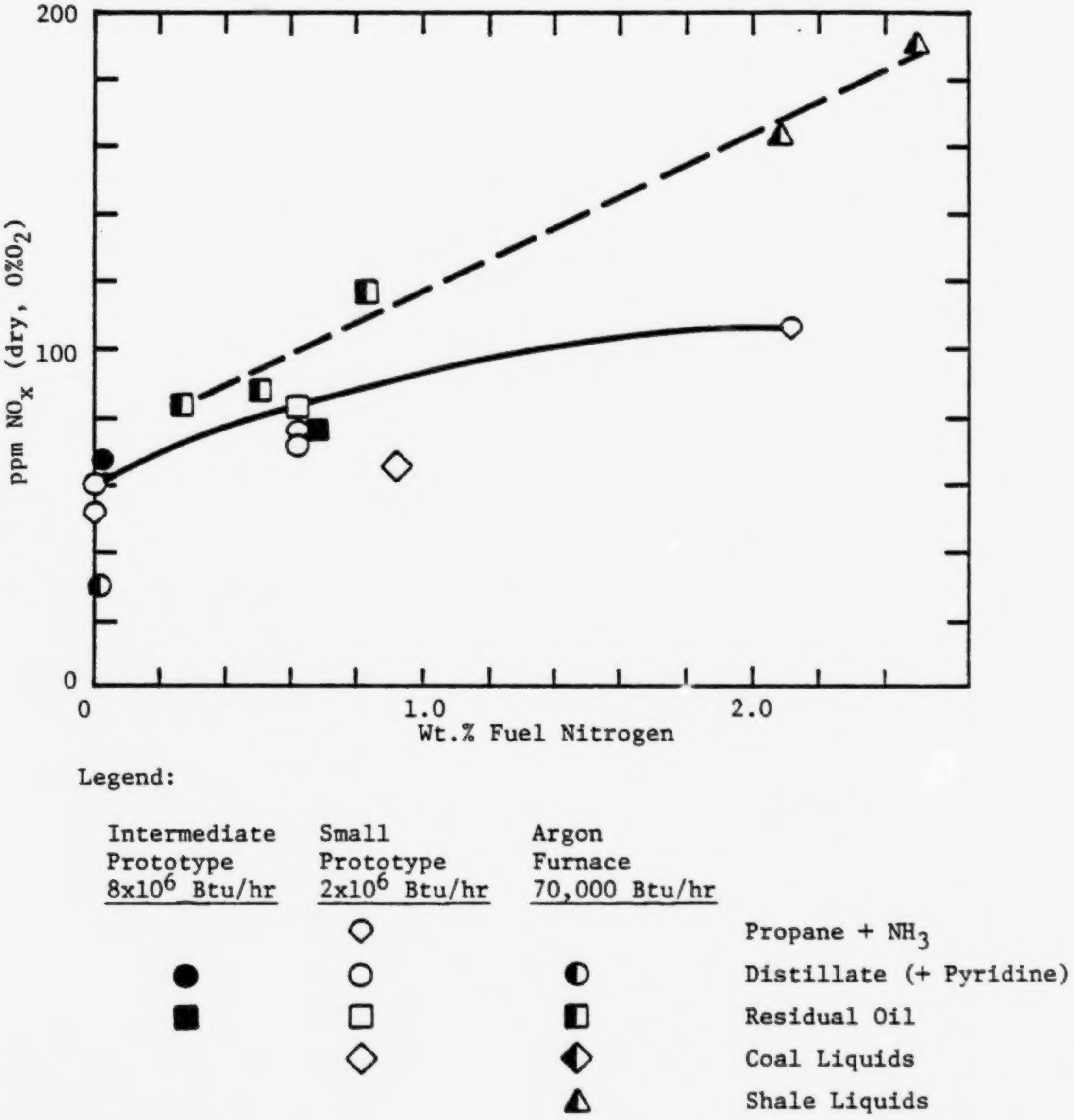

Figure 10. Influence of fuel nitrogen on second-stage NO$_x$-bench-scale and pilot-scale data.

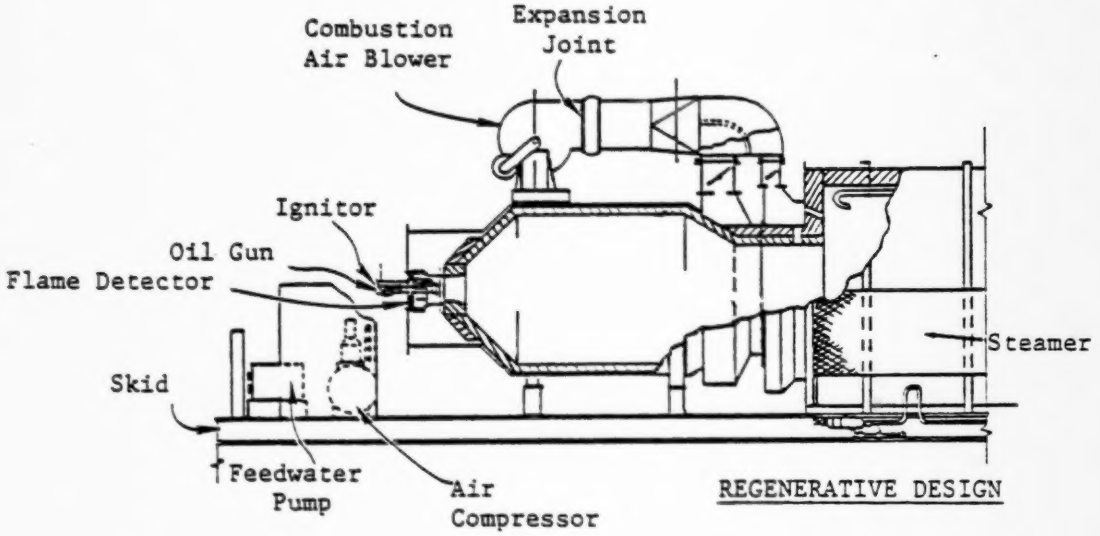
Combustion Air Blower
Expansion Joint
Ignitor
Oil Gun
Flame Detector
Steamer
Skid
Feedwater Pump
Air Compressor

REGENERATIVE DESIGN

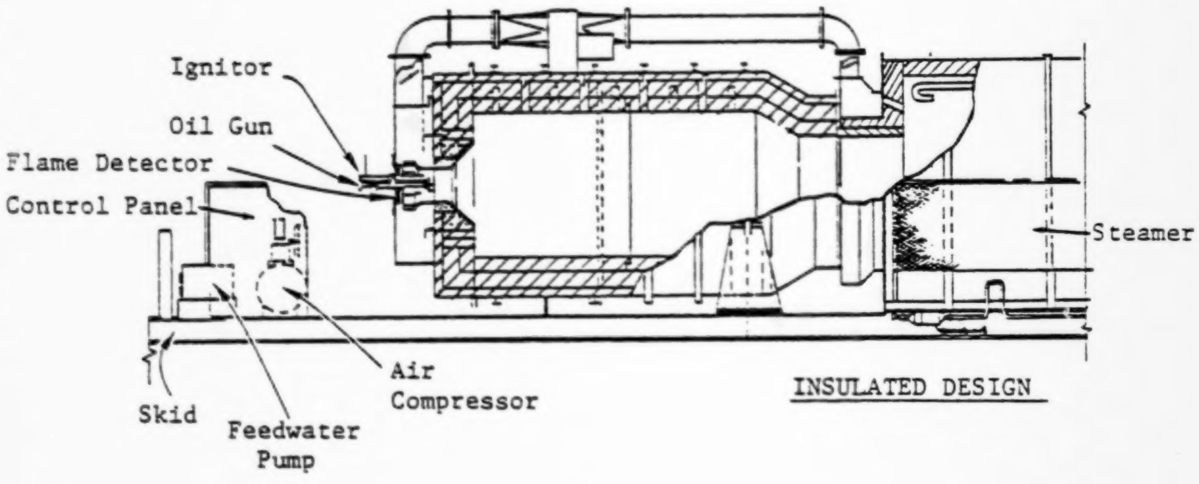
Ignitor
Oil Gun
Flame Detector
Control Panel
Steamer
Air Compressor
Skid
Feedwater Pump

INSULATED DESIGN

Figure 11. Conceptual burner designs for TEOR steam generators.

ENVIRONMENTAL ASSESSMENT OF INDUSTRIAL PROCESS COMBUSTION EQUIPMENT MODIFIED FOR LOW-NO_x OPERATION

By:

C. Castaldini, R. DeRosier, L. R. Waterland, and H. B. Mason
Acurex Corporation
Energy & Environmental Division
555 Clyde Avenue, P.O. Box 7555
Mountain View, California 94039

"The research described in this paper has been funded wholly or in part by the United States Environmental Protection Agency through contract 68-02-3188 to Acurex Corporation. It has been subjected to Agency review; however, it does not necessarily reflect the views of the Agency, and no official endorsement should be inferred."

ABSTRACT

Under the Combustion Modification Environmental Assessment (CMEA) program, comprehensive field tests of an oil refinery crude heater and an enhanced oil recovery (EOR) steam generator were performed. In these tests, flue gas emissions of NO_x, SO_2, SO_3, CO, CO_2, O_2, and particulate were measured. In addition, concentrations of inorganic elements; total volatile, semivolatile, and nonvolatile organics; and speciation for 58 organic priority pollutants including several polynuclear aromatic compounds were measured in the flue gas. Selected bioassay testing was also performed.

The refinery crude heater was equipped with staged air lances for NO_x control. Tests were performed under baseline (uncontrolled) operation and with NO_x emissions reduced 33 percent by introducing 44 percent of the combustion air through the staged air lances. The EOR steam generator was equipped with a Mitsubishi Heavy Industries (MHI) low-NO_x "PM" burner. Tests of this unit and a sister unit equipped with a conventional crude oil burner were performed.

This paper presents summary results of these tests, highlighting effects of control application on emissions and performance. The general conclusion is that the combustion modifications tested are of environmental benefit and cause few adverse performance effects.

INTRODUCTION

Industrial process combustion equipment has come under increased scrutiny in recent years from an emissions control perspective in recognition of its contribution to local air quality. In particular, refinery related NO_x emission sources provide a significant part of the air pollution problem in Southern California.

NO_x emissions from such processes can be reduced by combustion modification. In light of the continued development and use of combustion modifications and concerns that these modifications may have other effects on species concentrations in the exhaust streams, comprehensive tests were conducted on two industrial process combustors. Tests of an oil refinery crude heater were performed under baseline (uncontrolled) and NO_x controlled operation. Tests were also performed on an enhanced oil recovery (EOR) steam generator equipped with an MHI low-NO_x "PM" burner, with limited comparison testing of an identical EOR steamer equipped with a conventional burner. These tests were part of a 14-site test program conducted under the Combustion Modification Environmental Assessment (CMEA) program (EPA contract No. 68-02-3188) for the Combustion Research Branch of EPA's Industrial Environmental Research Laboratory, Research Triangle Park. This paper summarizes results from these tests.

MEASUREMENT METHODS

The sampling and analysis protocols used for the tests conformed to a modified and extended EPA Level 1 protocol for the flue gases (1). Flue gas sampling was done at the stack in both tests. Grab samples were also taken of fuel. Flue gas measurements performed included:

- Continuous monitoring for NO_x, CO, CO_2, and O_2
- Source assessment sampling system (SASS) train sampling
- EPA Method 5 sampling for solid particulate (condensable particulate also for the crude heater)
- Sulfur emissions measured by controlled condensation (crude heater) or EPA Method 8 (EOR steamer)
- Grab sampling for onsite gas chromatographic analysis of volatile organics with boiling points in the C_1 to C_6 range

The SASS train, shown schematically in figure 1, collects several kinds of samples for subsequent laboratory analysis. Particulate is collected on a heated filter at 230°C (450°F). Organics are collected in an organic sorbent module packed with a porous polymer resin (XAD-2) and held at 60°C (140°F). Volatile inorganic elements (Hg, As, and Sb) which have not condensed on collected particulate or in the organic sorbent module are trapped in the impingers.

The analysis protocol for SASS train samples and grab samples of fuel included:

- Fuel proximate and ultimate analysis
- Analyzing particulate, XAD-2 resin, impinger solutions, and fuel oil for 70 elements using spark source mass spectrometry (SSMS), and for mercury, arsenic and antimony using atomic absorption spectrometry (AAS) techniques
- Analyzing methylene chloride extracts of particulate and XAD-2 resin for total organic content in two boiling point ranges: semivolatile organics with boiling points between 100° and 300°C (nominally C_7 to C_{16} organics) by total chromatographable organic

(TCO) analysis and nonvolatile organics with boiling points greater than 300°C (nominally C_{16+} organics) by gravimetry

- Obtaining infrared (IR) spectra of the gravimetric residue of all extract samples
- Analyzing all extract samples for 58 semivolatile organic priority pollutants, including 16 polycyclic organic matter (POM) species by gas chromatography/mass spectrometry (GC/MS) according to EPA Method 625

XAD-2 extracts were subjected to bioassay testing to obtain a measure of the potential environmental effects posed by source discharges. Bioassay tests which measured potential health effects included the Ames mutagenicity assay, and the clonal toxicity assay using Chinese hamster ovary cells (CHO) (2).

CRUDE HEATER TESTS

Two tests were performed on a natural draft, crude-oil process heater rated at a maximum firing rate of 16 MW (55 million Btu/hr) heat input. The heater was fired by six John Zink DBA-22 natural draft burners, which are combination oil/gas burners with a 3:1 turndown ratio. Testing was performed with the unit firing approximately a 64/36 (heat input basis) refinery gas/oil mixture. All six burners were firing reabsorber gas from the plant; only four were cofired with oil. The other two burners had plugged oil guns which could not be cleaned in time for the tests.

Two tests were conducted on this unit. The first was a baseline test of the unit as it is normally operated. The second configuration tested included the addition of a system of variable height air lances arranged in a group of four per burner to introduce secondary air (up to one-half of the stoichiometric combustion air) for NO_x emissions reduction. The remainder of the combustion air in the low-NO_x configuration was delivered through secondary air registers located at the base of the heater. Air flow through the heater was controlled by a damper located above the convection section.

Unit Operation

Table 1 summarizes the heater operating conditions for both tests. No significant changes in unit operation occurred as a result of the staged combustion. Table 2 presents analyses of the fuel samples from both tests. The oil composition showed little change. Slight variations in fuel gas composition resulted in a slightly lower heating value gas for the low-NO_x test.

Flue Gas Emissions

Table 3 summarizes gaseous and particulate emissions measured during the baseline and staged combustion tests. Continuous monitors measured O_2, CO_2, CO, NO, and SO_2 emissions. Excess O_2 varied equally during each test, from about 3.1 to 4.3 percent. This variation in O_2 was probably caused by small changes in fuel flows and refinery gas composition occurring during each test. Lower average O_2 levels for the low-NO_x test is attributed to better control of air flow with forced combustion air through staged air lances. As noted in the table, NO was reduced 31 percent from 172 to 118 ppm (at 3 percent O_2, dry) from the baseline to the staged combustion tests. Previous tests on this unit had achieved a 64 percent NO reduction with 100 percent refinery gas firing (3). CO levels were essentially unchanged as were sulfur oxide (SO_2 and SO_3) emissions.

Particulate, as measured by both EPA Method 5 and the SASS train, apparently decreased in the low-NO_x tests. The only available test location for these two sampling trains was not ideal in that the upstream proximity of the draft damper caused a nonuniform flue gas velocity profile. The difference between the SASS and Method 5 particulate emission results may be attributed to the flow disturbance caused by the upstream damper.

Trace Element Emissions

The concentrations of 73 trace elements were determined in samples of the fuel and flue gas. Table 4 presents total flue gas concentrations (sum of the SASS train collected samples) for the most significant of these elements. Most significant (as used here) refers to elements emitted at levels of potential environmental concern. As a measure of possible concern, the emissions concentrations of the elements were compared to corresponding occupational exposure guidelines. The occupational exposure guidelines used were threshold limit values (TLV's) established by the American Conference of Governmental Industrial Hygienists (ACGIH) (4) or permissible exposure limits established by the Occupational Safety and Health Administration (OSHA) (5). These comparisons are performed only to rank species with respect to possible environmental effects; no conclusions regarding absolute hazard are made, nor are warranted.

The elements listed in table 4 are those which had flue gas concentrations exceeding one tenth of the occupational exposure guidelines. Only seven elements (Cr, K, Na, P, Ni, Cu, and Fe) exceeded this criterion. It is worth noting that none of these exceeded occupational exposure guidelines.

Organic Emissions

Table 5 summarizes measured organic emissions for both tests by organic boiling point range: volatile organics with boiling points less than 100°C (nominally C_1 to C_6), semivolatile organics with boiling points in the 100° to 300°C range (nominally C_7 to C_{16}), and nonvolatile organics with boiling points greater than 300°C (nominally greater than C_{16}). In both tests, the volatile organic fraction dominated the organic emissions. The baseline test showed volatile organics comprising 16.3 of the total 17.1 mg/dscm detected, while the low-NO_x test indicated that volatile organics comprised 2.8 of the total 3.4 mg/dscm detected. Both volatile and semivolatile organic emissions decreased in the low-NO_x test. Apparently the addition of forced draft air through the staging lances to this natural draft unit increased combustion efficiency. Nonvolatile organic emissions were unchanged between tests. In addition, all organics were in the vapor phase at SASS train particulate collection temperature as evidenced by the less than detectable result for the filter particulate.

GC/MS analyses of sorbent module extract from the SASS train were performed to detect and quantify specific POM and other organic priority pollutant species. Table 6 summarizes the results of these analyses. Duplicate analyses of the low-NO_x XAD-2 extract were performed to assess the precision of the analyses. Of the 58 species analyzed for, only those noted in table 6 were detected. In general, emissions of these species were lower in the low-NO_x test than the baseline. The general decrease in these species emissions is consistent with the decrease in total organic emissions noted in table 5.

Bioassay Testing

Both mutagenicity and cytotoxicity tests were performed on XAD-2 extracts from both tests. The toxicity of the extracts did not change between the two tests, being moderate in both cases. Mutagenicity was moderate in the baseline test and high in the low-NO_x test. This result is consistent with results from other combustion source tests. Sorbent module extracts are of consistently moderate to high mutagenicity and toxicity.

EOR STEAMER TESTS

Tests were also performed on an EOR steamer equipped with an MHI low-NO_x "PM" burner. Limited testing was also performed on an identical unit equipped with a conventional North American crude-oil-fired burner.

The MHI-PM burner, illustrated schematically in figure 2, uses a split flame arrangement, whereby an inner air-deficient diffusion flame is separated from an outer air-rich premix flame by a blanket of recirculated flue gas. This arrangement produces NO_x levels significantly lower than those from conventional burners. A certain amount of staged air (OFA), typically 10 percent, is injected about half way down the length of the cylindrical furnace through three sets of three ports each located at approximately 4, 8, and 12 o'clock. This OFA ensures that sufficient excess air and mixing is achieved prior to the combustion gas leaving the furnace.

Unit Operation

The test program performed included performance mapping in which the flue gas emissions were monitored while varying the MHI-PM burner operating parameters. The purpose was to evaluate the performance and sensitivity of emission levels to burner operating conditions. The following parameters were varied:

- Overall excess combustion air
- Staged combustion air (OFA) flowrate
- Flue gas recirculation (FGR) flowrate
- Diffusion air flowrate
- Premix air flowrate

Following these performance tests, a set of operating conditions was selected for comprehensive emission testing using the SASS train and other aspects of the sampling protocol noted above. This test was conducted at 9.5 percent FGR, 10 percent OFA, approximately 54 percent premix air, and

36 percent diffusion air. The fuel fired in all tests was Kern County crude oil, which typically has the composition presented in table 7.

Fuel Gas Emissions

Table 8 presents burner test conditions and emission levels measured at the furnace outlet and stack downstream of the economizer section for the performance evaluation tests. As noted, NO_x emissions from the unit varied almost two-fold with changes in the parameter varied. Certain conditions resulted in NO_x emissions at the stack below 100 ppm (3 percent O_2, dry); but these were, in general, accompanied by high CO emission and high smoke spot. Conditions which resulted in NO_x in the 110 ppm range with moderate CO are also noted.

Figures 3 and 4 illustrate the dependence of NO_x and CO at the stack on flue gas O_2. Both MHI and conventional burner test data are shown. Figure 3 shows that the NO_x emissions from the MHI burner were 45 to 65 percent lower than from a conventional burner at a given flue gas O_2. Figure 4 shows that CO emissions from the MHI burner increased steeply at flue gas O_2 below 2.5 to 3.0 percent. This contrasts with conventional burner behavior where CO emissions were still low at flue gas O_2 down to 2.5 percent. The higher CO levels from the MHI burner, which were accompanied by high smoke spot (see table 8), are attributed to flame impingement which was observed at the 4 and 8 o'clock positions at virtually all burner settings. Higher CO levels are attributed to increased flame impingement and excessively low diffusion zone stoichiometries during low O_2 and high OFA tests.

The effect of OFA flowrate on both CO and NO_x levels is illustrated in figure 5. CO levels decrease sharply at OFA rates below 10 percent. At 3 percent OFA, CO levels are nearly those of the conventional burner (see figure 4). NO_x emissions at minimum OFA, however, are not significantly higher than those at high OFA rates.

The effect of FGR on NO_x and CO emissions is shown in figure 6. FGR had a greater effect at a higher O_2 and lower OFA levels (4 percent and 8 percent OFA) than it did at lower O_2 and higher OFA levels (O_2 of 2.6 percent and 19 percent OFA). CO responded in an opposite manner. This can be explained in part by the greater mixing occurring at higher burner stoichiometries combined with lower FGR rates. This mixing tended to partly cancel the low-NO_x properties of the split flame. Conversely, the higher FGR rates combined with lower burner stoichiometry, while keeping the flames separate, will tend to cause greater impingement of the premix flame, which increases the CO levels.

Organic Emissions

Table 9 summarizes measured organic emissions from the MHI burner-equipped steamer by organic boiling point range. The organic emissions are dominated by the volatile (C_1 to C_6) fraction, which is composed primarily of compounds in the C_3 and C_4 boiling range. No semivolatile organics were detected. However, nonvolatile organics (nominally C_{16+}) were found in the particulate, though not in the sorbent module. This confirms the high smoke emissions for the tests, and suggests soot formation was occurring.

Table 10 summarizes the POM and other organic priority pollutant species identified by GC/MS analysis. Also noted in the table are levels of other organic species identified and quantitated in the GC/MS sample analyses. Duplicate analyses of the XAD-2 extract were performed to assess the precision of procedure. These results are presented in table 10 with the total being the sum of the particulate analysis and the average of the two XAD-2 runs. Of the POM's, only naphthalene, phenanthrene, and pyrene were found, and these only in the particulate. The other species detected are generally oxygenated aromatics and fused ring aromatics.

NITROUS OXIDE EMISSIONS

In addition to the sampling and analysis protocol noted in the preceding tests, determination of nitrous oxide emissions was also performed. Flue gas grab samples were collected in stainless-steel cylinders and subsequently analyzed for N_2O using a gas chromatography/electron capture detector (GC/ECD) technique adapted from studies measuring N_2O emanation from soils (6,7,8).

Samples were taken during each test of the refinery heater and during the MHI burner testing. N_2O emissions from the refinery heater were 59 ppm for baseline operations and 33 ppm (both at 3 percent O_2, dry) for low-NO_x operation. Associated NO emissions during these tests were 172 and 118 ppm (3 percent O_2, dry), respectively. For the EOR steamer N_2O emissions of 17 ppm at NO emissions of 112 ppm were measured. Sampling for N_2O has been performed in other field tests under the CMEA project and reported elsewhere (9,10). Results of all these tests are shown as a plot of N_2O versus NO emissions in figure 7.

It appears from figure 7 that N_2O emissions are roughly proportional to a unit's NO emissions. The data, taken from a range of combustion sources, suggest that N_2O emissions total are generally 20 to 25 percent of NO_x emissions.

SUMMARY

Comprehensive emissions testing was performed on a refinery crude heater and an enhanced oil recovery steamer equipped with an MHI-PM low-NO_x burner. The crude heater was tested with and without air lances to stage the combustion process. The EOR steamer was tested under a variety of burner parameter settings. A comprehensive test was performed for one low-NO_x combination of parameter settings.

Results from the refinery heater test include:

- NO_x emissions were reduced 31 percent from 172 to 118 ppm (at 3 percent O_2, dry) using the staged air lances
- CO emissions were unchanged though particulate emissions decreased
- Chromium, potassium, sodium, phosphorous, nickel, copper, and iron represent the trace elements emitted at levels of greatest potential concern

- Organic emissions are dominated by the volatile category. Total organic emissions decreased in the low-NO_x test, suggesting better combustion efficiency with forced air addition

Results from the EOR steamer tests include:

- NO_x emission reductions of 45 to 65 percent achieved by the MHI-PM burner
- CO emissions sharply increased as flue gas O_2 decreases below 2.5 to 3.0 percent for MHI-PM burner; for a conventional burner CO emissions are moderate at flue gas O_2 down to 2.5 percent
- Flue gas recirculation and OFA rates significantly affect CO and NO_x emissions for the MHI-PM burner. The effect of FGR depends on overall O_2 and OFA levels.
- Organic emissions are dominated by the volatile category. Nonvolatile organics in the particulate suggest soot formation under the conditions tested.

The data from both tests, when combined with other CMEA analyses, suggest that N_2O emissions are roughly proportional to NO emissions, totalling 20 to 25 percent of these emissions.

ACKNOWLEDGMENTS

This work is supported by EPA under contract 68-02-3188. Robert E. Hall is the EPA Project Officer. The assistance of the Acurex field test crew, supervised by B. C. DaRos, is gratefully acknowledged. The authors also wish to recognize the support and cooperation of the host site personnel who enabled these tests to be performed by allowing access to their facilities and accommodating the demands of time and material imposed by field tests of this type.

REFERENCES

1. Lentzen, D. E., et al. IERL-RTP Procedures Manual: Level 1 Environmental Assessment (Second Edition). EPA-600/7-78-201, (NTIS PB 293 795), U.S. EPA Industrial Environmental Research Laboratory, Research Triangle Park, North Carolina, October 1978.

2. Brusick, D. J., et al. IERL-RTP Procedures Manual: Level 1 Environmental Assessment, Biological Tests. EPA-60018-81-024 (NTIS PB 228966). U.S. EPA, Industrial Environmental Research Laboratory, Research Triangle Park, North Carolina, October 1981.

3. Hunter, S. C. and W. A. Carter. Control of NO_x Emissions From Petroleum Process Heaters Using Staged Air Lances. Presented at the Air Pollution Control Association Meeting, Palm Springs, California, October 13-16, 1981.

4. American Conference of Governmental Industrial Hygienists. Threshold Limit Values for Chemical Substances and Physical Agents in the Work Environment With Intended Changes for 1982. Cincinnati, Ohio, 1982.

5. OSHA Safety and Health Standards. 29 CFR 1910, Subpart Z.

6. Seiler, W. and R. Conrad. Field Measurement of Natural and Fertilizer-Induced N_2O Release Rates from Soils. J. APCA 31(7): 767-772, 1981.

7. Banna, S. M. and M. C. Branch. Gas Chromatographic Determination of Nitrogenous Species in Combustion Products. Combustion Science and Technology, 24:15-22, 1980.

8. Conrad, R. and W. Seiler. Field Measurement of the Loss of Fertilizer Nitrogen into the Atmosphere as Nitrous Oxide. Atmospheric Environment 14:555-558, 1980.

9. Waterland, L., et al. Environmental Assessment of Industrial Boilers Firing Coal/Liquid Mixtures or Wood. Presented at the 1982 Joint Symposium on Stationary Combustion NO_x Control, Dallas, November 1982.

10. Acurex Corporation. Unpublished Data. Mountain View, California, 1982.

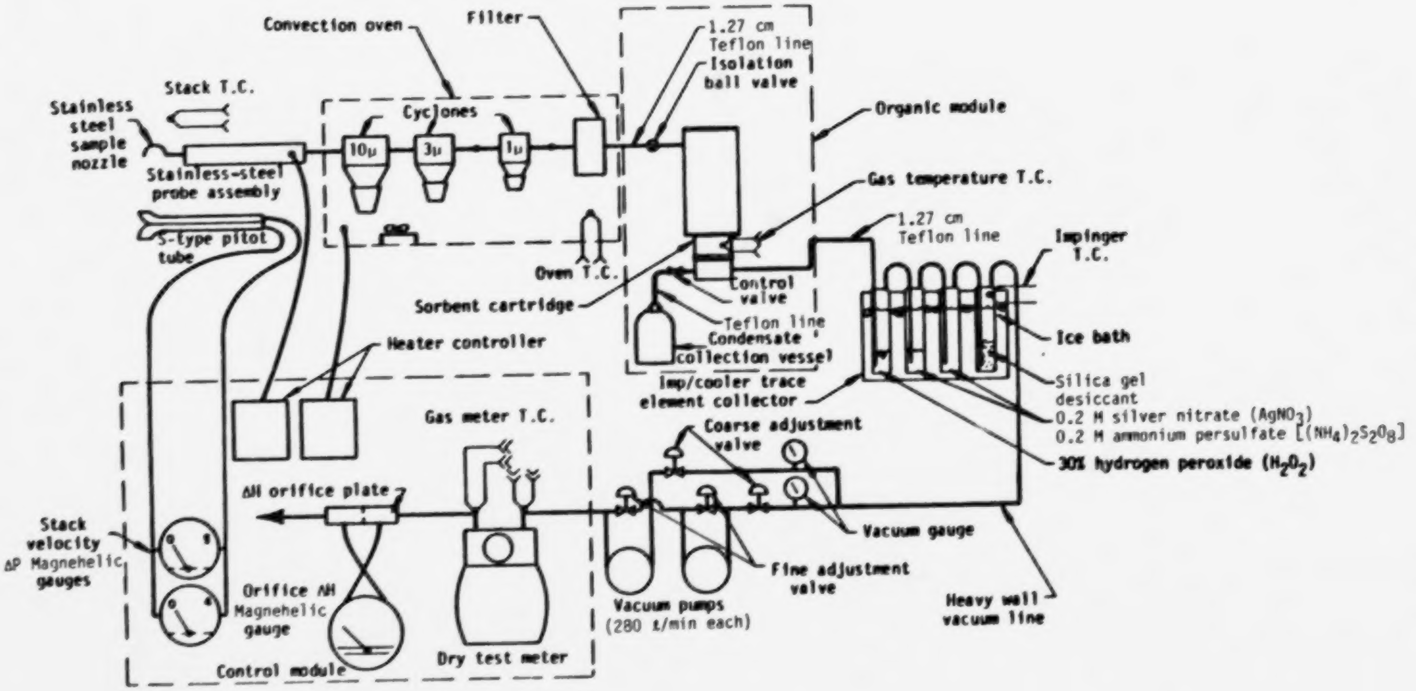
Stainless steel sample nozzle
Stack T.C.
Stainless-steel probe assembly
S-type pitot tube
Convection oven
Cyclones
10μ
3μ
1μ
Filter
Oven T.C.
1.27 cm Teflon line
Isolation ball valve
Organic module
Gas temperature T.C.
Sorbent cartridge
Control valve
Teflon line
Condensate collection vessel
1.27 cm Teflon line
Imp/cooler trace element collector
Impinger T.C.
Ice bath
Silica gel desiccant
0.2 M silver nitrate (AgNO3)
0.2 M ammonium persulfate [(NH4)2S2O8]
30% hydrogen peroxide (H2O2)
Heater controller
Gas meter T.C.
Coarse adjustment valve
Vacuum gauge
Fine adjustment valve
Heavy wall vacuum line
Vacuum pumps (280 ℓ/min each)
ΔH orifice plate
Stack velocity ΔP Magnehelic gauges
Orifice ΔH Magnehelic gauge
Control module
Dry test meter

Figure 1. Schematic of SASS train.

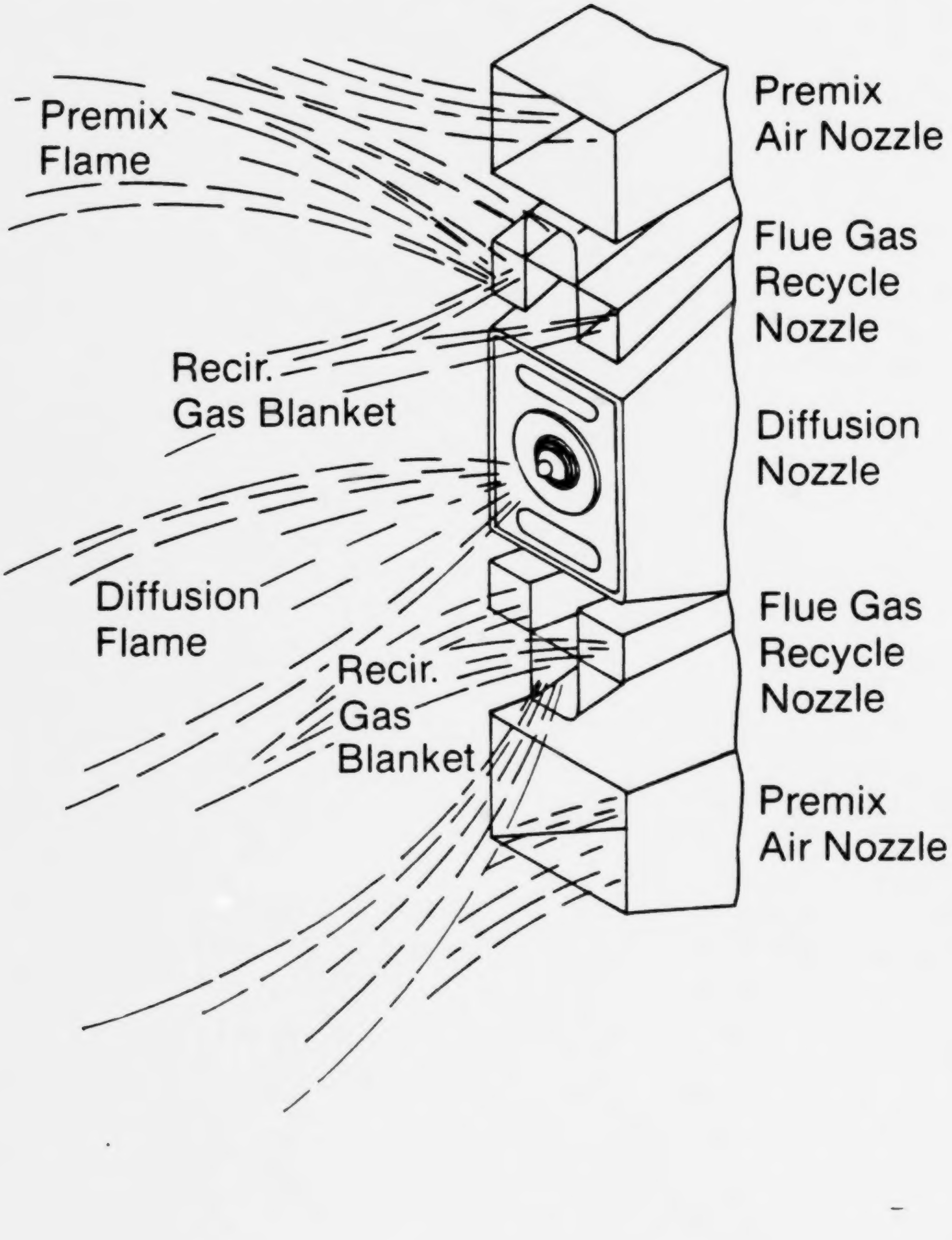
Premix Flame
Premix Air Nozzle
Flue Gas Recycle Nozzle
Recir. Gas Blanket
Diffusion Nozzle
Diffusion Flame
Recir. Gas Blanket
Flue Gas Recycle Nozzle
Premix Air Nozzle

Figure 2. MHI-PM burner.

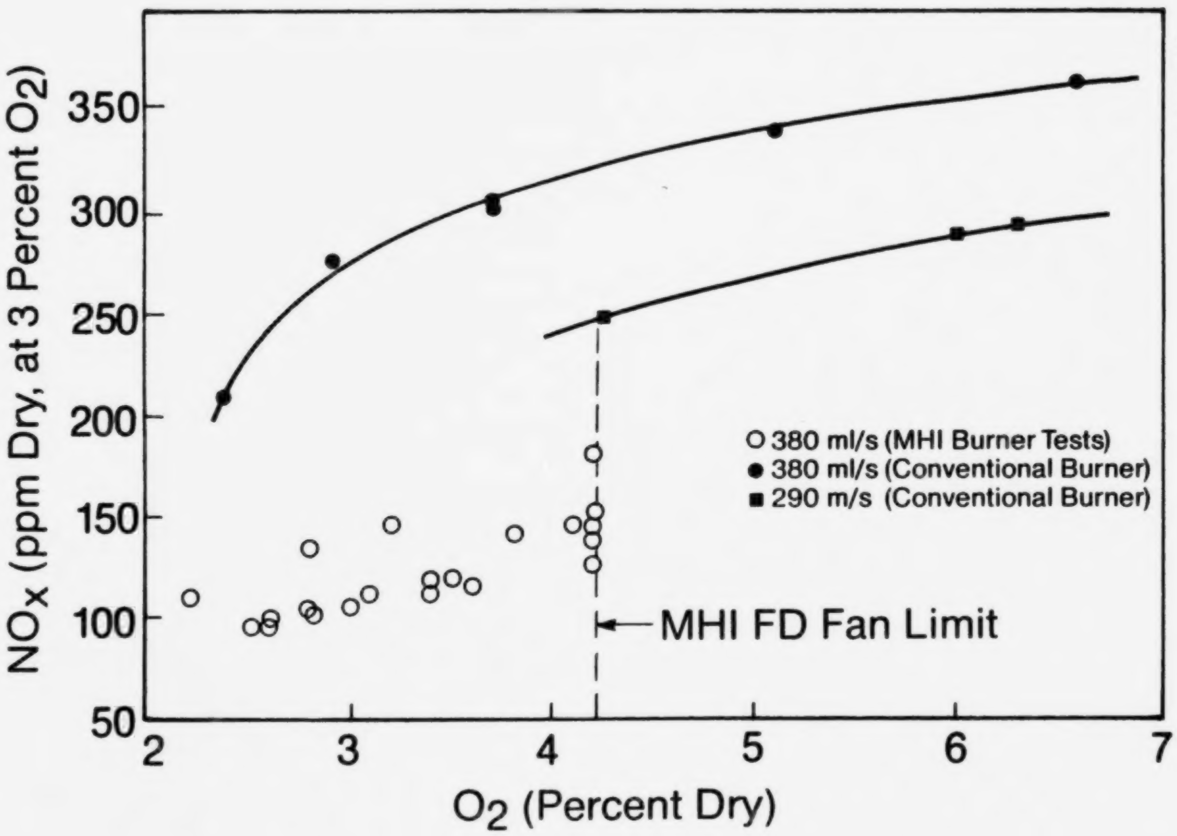

A87709

Figure 3. CO versus O_2 at stack (EOR steamer).

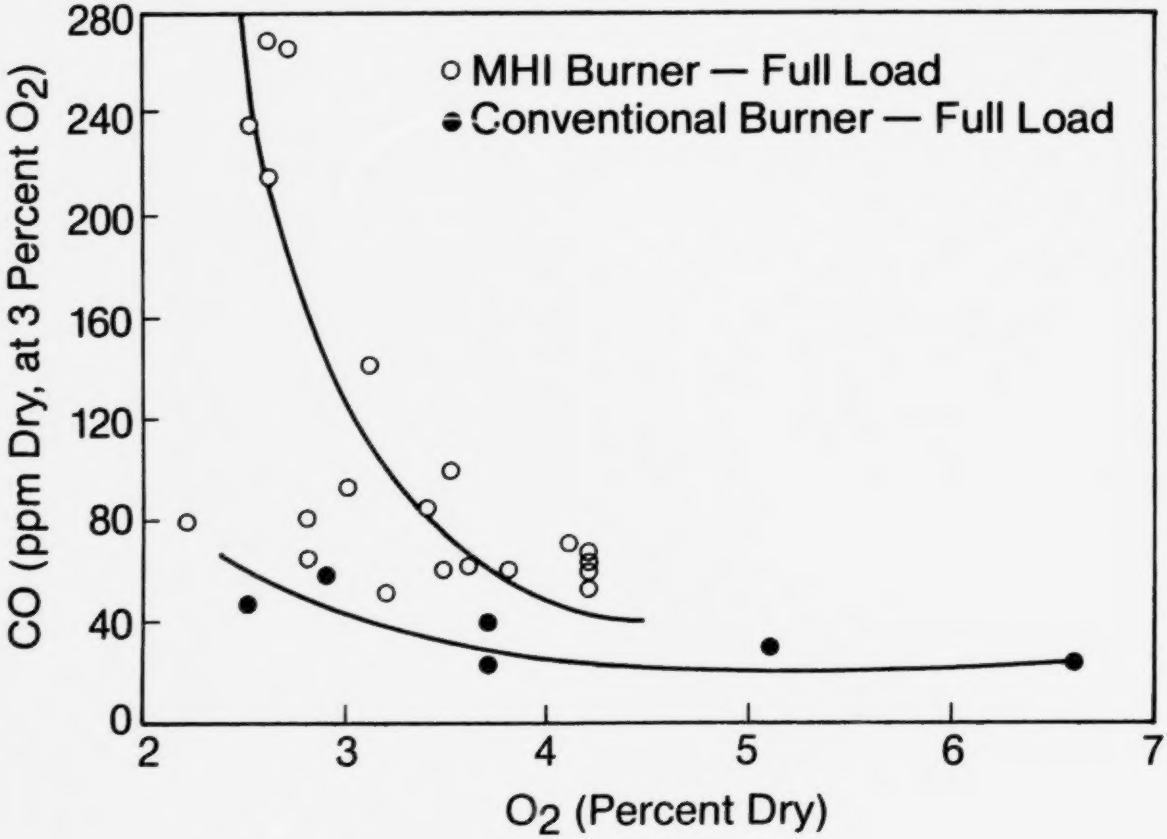

A21708

Figure 4. NO_x versus O_2 at stack (EOR steamer).

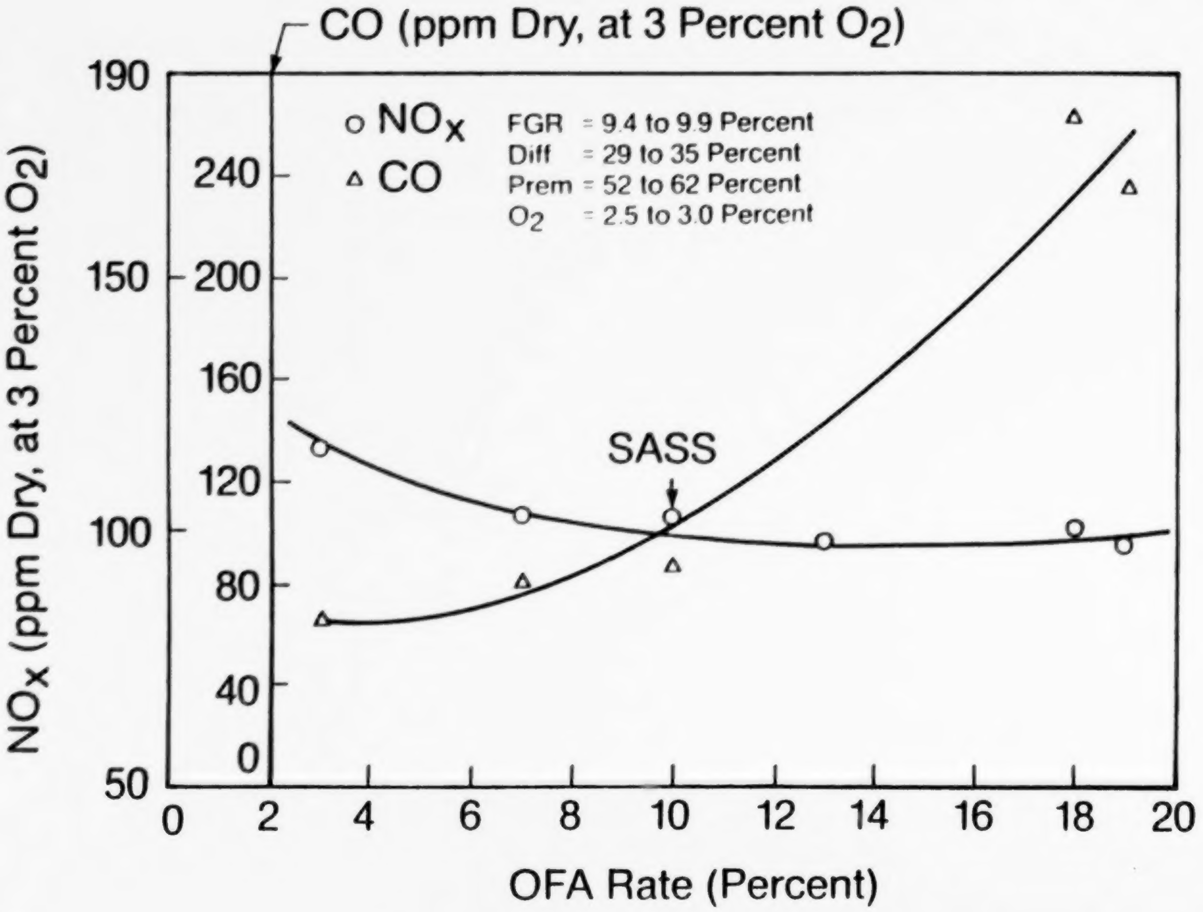

Figure 5. NO_x, CO versus OFA rate (EOR steamer).

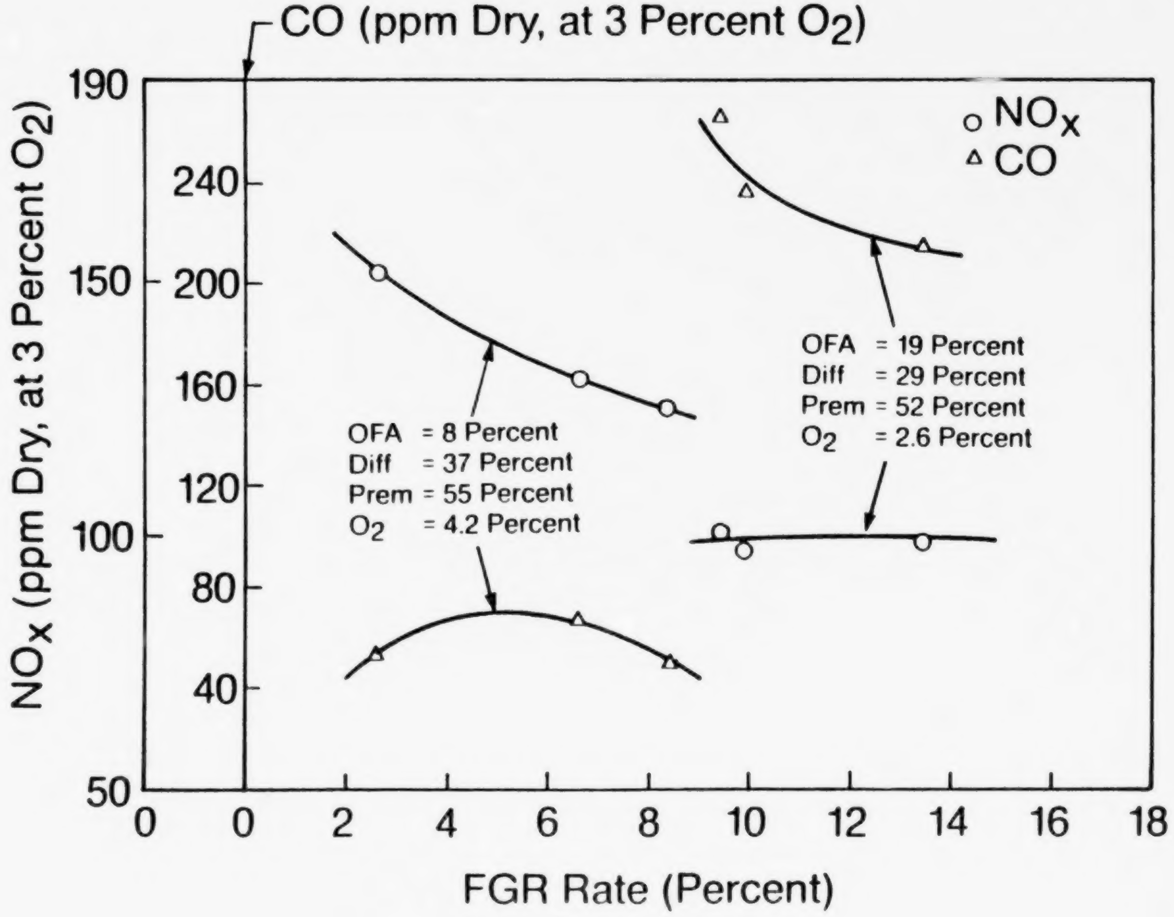

Figure 6. NO_x, CO versus FGR rate (EOR steamer).

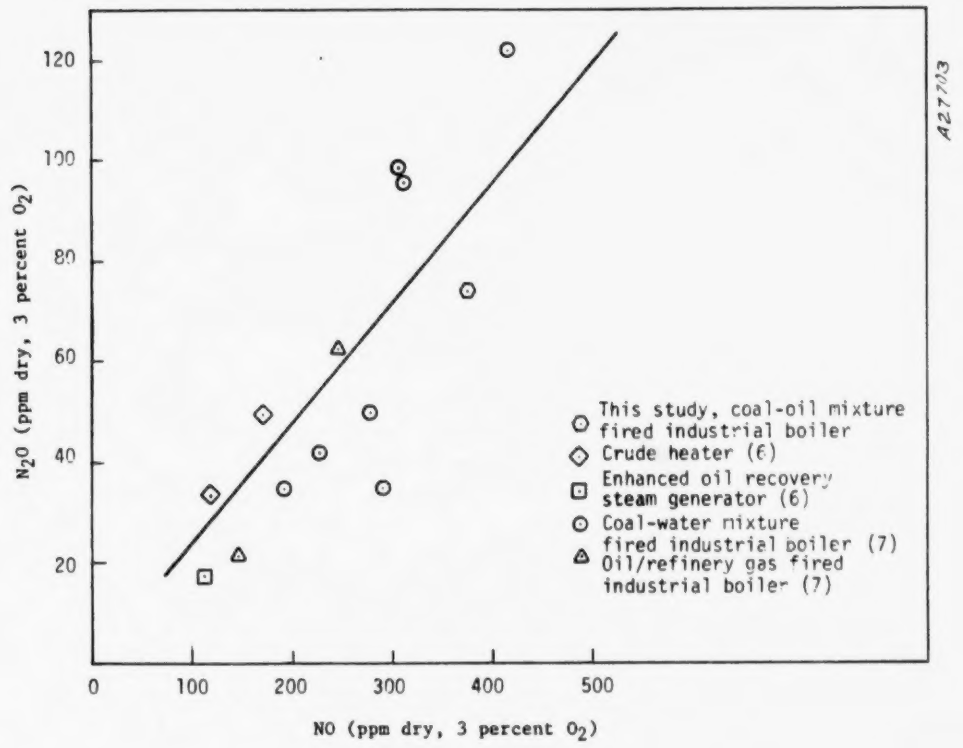

Figure 7. N_2O emission from combustion sources as a function of NO emissions.

TABLE 1. CRUDE HEATER OPERATING CONDITIONS

	Baseline		Low NO_x	
Process rate, l/s (bbl/day)	21.5	(11,640)	21.5	(11,640)
Reabsorber gas, m^3/min (scfm)	7.1	(251)	7.1	(251)
Heat input, MW (million Btu/hr)	8.35	(28.5)	8.13	(27.7)
Fuel oil, kg/min (lb/min)	6.59	(14.5)	6.55	(14.4)
Heat input, MW (million Btu/hr)	4.77	(16.3)	4.75	(16.2)
Temperatures, °C (°F)				
Crude in	196	(384)	196	(384)
Crude out (east)	338	(641)	339	(642)
Crude out (west)	336	(637)	339	(642)
Tube 13, pass A	403	(758)	405	(761)
Tube 13, pass B	407	(764)	395	(743)
Tube 15, pass A	391	(735)	387	(728)
Tube 15, pass B	373	(704)	373	(704)
Tube 20, pass A	397	(746)	395	(743)
Tube 20, pass B	411	(772)	395	(743)
Tube 25, pass A	411	(771)	406	(762)
Tube 25, pass B	416	(780)	408	(766)
Pressures, kPa (psig)				
Crude in (east)	960	(140)	960	(140)
Crude in (west)	896	(130)	896	(130)
Crude out	227	(33)	234	(34)
Burner -- oil[a]	324	(47)	324	(47)
Burner -- steam[a]	537	(78)	537	(78)
Burner -- gas[b]	30	(4.4)	30	(4.3)
Gas pressure to heater	234	(34)	241	(35)

[a] Average of four burners using oil

[b] Average of all six burners

TABLE 2. FUEL ANALYSES: CRUDE HEATER TESTS

	Baseline	Low NO_x
Fuel gas (percent by volume)		
Hydrogen	8.7	9.3
Nitrogen	1.1	0.8
Carbon monoxide	0.4	0.5
Methane	22.7	24.5
Ethane	16.7	16.5
Ethylene	3.8	4.0
Propane	29.2	28.5
Propylene	3.3	3.6
Isobutane	11.1	9.5
n-butane	1.7	1.3
Total butenes	0.5	0.7
Isopentane	0.2	0.2
n-pentane	0.1	0.1
C_6 plus	0.5	0.5
Higher heating value, MJ/m^3 (Btu/ft^3)	70.56 (1,892)	68.71 (1,843)
Oil (percent by weight)		
Carbon	87.37	86.66
Hydrogen	10.47	10.98
Oxygen (by difference)	0.39	0.61
Nitrogen	0.83	0.85
Sulfur	0.94	0.90
Higher heating value, MJ/kg (Btu/lb)	43.44 (18,720)	43.54 (18,760)

TABLE 3. FLUE GAS EMISSIONS: CRUDE HEATER TESTS

	Baseline		Low NO_x	
As Measured	Range	Average	Range	Average
O_2, percent (dry)	3.3 to 4.3	4.0	3.1 to 4.2	3.3
CO_2, percent (dry)	10.5 to 13.6	12.1	11.3 to 12.4	11.7
CO, ppm (dry)	0 to 10	3.8	0 to 10	3.4
NO, ppm (dry)	152 to 174	162	108 to 125	116
SO_2, ppm				
Continuous monitor (wet)	120 to 170	151	125 to 170	148
Controlled condensation (dry)	—[a]	97	—	115
SO_3				
Controlled condensation, ppm (dry)	—	2.4	—	1.8
Moisture, percent	—	15.9	—	16.5

	Baseline			Low NO_x		
Corrected	ppm[b]	ng/J	lb/10^6 Btu	ppm[b]	ng/J	lb/10^6 Btu
CO	4.0	1.19	0.0028	3.5	0.99	0.0023
NO (as NO_2)	172	83	0.19	118	56	0.13
SO_2						
Continuous monitor	190	128	0.30	180	118	0.27
Controlled condensation	103	69	0.16	117	77	0.18
SO_3						
Controlled condensation	2.5	2.1	0.0049	1.8	1.5	0.0035
	mg/dscm			mg/dscm		
Particulate — Method 5:						
Solid	31.1	8.35	0.019	20.0	5.0	0.012
Condensable	9.4	2.52	0.0059	3.2	0.80	0.0019
Total	40.5	10.9	0.025	23.2	5.8	0.014
Particulate — SASS	8.7	2.34	0.0054	8.1	2.0	0.0046

[a] Extractive sample

[b] At 3 percent O_2, dry

TABLE 4. TRACE ELEMENT EMISSIONS: CRUDE HEATER TESTS

Element	Concentration (μg/dscm)		
	Baseline	Low NO_x	Occupational Exposure Guideline[a]
Chromium, Cr	4.2	28	50
Potassium, K	110	1,100	2,000
Sodium, Na	910	640	2,000
Phosphorus, P	0.012	33	100
Nickel, Ni	>30	29	100
Copper, Cu	7.4	52	200
Iron, Fe	28	190	1,000

[a] Threshold Limit Value (4)

TABLE 5. TOTAL ORGANIC EMISSIONS: CRUDE HEATER TESTS

Organic Category	Baseline (mg/dscm)	Low NO_x (mg/dscm)
Volatile organics analyzed in the field by gas chromatography		
C_1	0	0
C_2	3.6	2.8
C_3	4.8	0
C_4	6.4	0
C_5	1.5	0
C_6	0	0
Total C_1-C_6	16.3	2.8
Semivolatile organics analyzed by TCO		
Filter	--	--
XAD-2	0.36	0.06
Organic module condensate	<0.001	0.02
Total C_7-C_{16}	0.36	0.08
Nonvolatile organics analyzed by gravimetry		
Filter	<0.2	<0.3
XAD-2	0.4	0.3
Organic module condensate	<0.1	0.2
Total C_{16+}	0.4	0.5
Total organics	17.1	3.4

TABLE 6. ORGANIC PRIORITY POLLUTANT EMISSIONS: CRUDE HEATER TESTS

Species	Baseline (μg/dscm)	Low NO_x (μg/dscm) Run 1	Run 2	Average
Phenol	1.0	0.20	0.55	0.4
Naphthalene	<0.04	0.40	0.78	0.6
1,2-dichlorobenzene	0.1	<0.04	<0.04	<0.04
1,3-dichlorobenzene	0.08	<0.04	<0.04	<0.04
1,4-dichlorobenzene	0.04	0.04	0.08	0.06
Nitrobenzene	0.2	0.04	0.08	0.06
2-nitrophenol	<0.2	0.43	0.39	0.41
1,2-diphenylhydrazine (as azobenzene)	1.4	<0.04	0.04	0.04
Phenanthrene	1.2	0.10	0.20	0.15
2,6-dinitrotoluene	<0.04	0.10	<0.04	0.07
Other polynuclears	<0.04	<0.04	<0.04	<0.04

TABLE 7. FUEL ANALYSIS: EOR STEAMER TESTS

	Percent by Weight
Carbon	86.61
Hydrogen	10.93
Nitrogen	0.83
Sulfur	1.16
Ash	0.03
O_2	0.44
Higher heating value,	
MJ/kg	42.33
(Btu/lb)	(18,238)

TABLE 8. MHI BURNER PERFORMANCE RESULTS

					Fuel Rate		Total Air[b]		Stack						Furnace Outlet				
Test No.	FGR (%)	OFA (%)	Premix[a] (%)	Diffusion[a] (%)	(1/s)	(Barrels/ Day)	(scm/s)	(scfm)	O_2 (%)	CO_2 (%)	CO (ppm[c])	NO_x (ppm[c])	THC (ppm[c])	Smoke	O_2 (%)	CO (ppm[c])	CO_2 (%)	NO_x (ppm[c])	SO_2 (ppm[c])
1	8.9	19	48	33	0.383	380	5.17	10,950	3.5	13.4	99	119	3.2	>10	4.3	70	12.9	124	597
2	9.4	18	52	30	0.385	209	4.92	10,430	2.7	13.9	266	102	4.4	10	3.3	80	13.9	113	594
3	13.4	19	52	29	0.381	207	4.80	10,170	2.6	13.9	215	99	3.2	9.5	3.1	80	13.9	108	582
4	9.9	19	53	29	0.390	212	4.94	10,460	2.5	14.0	236	95	5.3	10	3.1	73	14.0	109	592
5	9.9	13	52	35	0.379	206	4.78	10,120	2.6	14.0	269	97	3.9	8	3.0	76	13.9	105	576
6	9.4	15	51	34	0.377	205	5.01	10,610	3.4	13.9	60	119	2.2	6	4.0	59	13.0	126	573
7	8.8	15	51	34	0.388	211	5.27	11,160	3.8	13.3	60	140	1.4	3.5	4.4	44	12.9	140	581
8	9.1	11	56	33	0.386	210	4.96	10,510	3.2	13.2	51	145	1.1	3.5	3.3	45	13.9	144	568
9	9.8	9	57	34	0.386	210	4.72	10,000	2.2	14.6	79	110	1.0	8	2.3	58	14.5	112	585
10	9.3	8	57	35	0.388	211	4.72	10,000	3.1	13.3	141	111	4.5	10	2.2	104	14.7	102	616
11	8.8	8	57	35	0.386	210	4.92	10,430	4.1	12.5	70	145	8.5	6	3.2	54	13.8	126	595
12	8.2	8	58	34	0.396	215	5.31	11,250	4.2	12.5	64	180	8.6	3.5	4.2	46	12.9	174	570
13	8.4	8	55	37	0.388	211	5.32	11,270	4.2	12.4	51	126	1.8	4	4.6	55	12.5	125	587
14	8.8	8	55	37	0.390	212	5.07	10,750	3.4	13.0	85	111	1.1	8	3.6	67	13.5	114	573
15	6.6	8	55	37	0.390	212	5.35	11,350	4.2	12.3	66	131	1.4	6	4.5	58	12.7	131	572
16	2.6	8	55	37	0.390	212	5.42	11,480	4.2	12.3	54	152	1.1	2.5	4.6	53	12.6	149	582
17	8.4	7	59	34	0.405	220	5.41	11,450	4.2	12.6	60	143	1.4	4	4.1	50	13.1	144	556
18	9.1	6	58	36	0.377	205	4.83	10,230	3.6	12.9	62	116	0.5	6	3.3	64	13.8	113	558
19	9.8	7	58	35	0.386	210	4.72	9,990	2.8	13.5	80	106	0	8	2.3	87	14.5	98	574
20	9.8	3	62	35	0.388	211	4.78	10,140	2.8	13.6	64	133	0	6	2.5	55	14.5	126	583
21 (SASS)	9.5	10	54	36	0.386	210	4.79	10,150	3.0	13.3	93	106	0	8	2.5	68	14.5	108	586

[a] Premix and diffusion nozzles combustion air flows were not measured. Values shown here were estimated based on blower discharge pressure and static pressure readings in the windbox for diffusion and premix zones.

[b] Based on furnace outlet O_2 level and typical fuel analysis (C = 86.61, H = 10.93, N = 0.83, S = 1.16, O = 0.44, Ash = 0.03)

[c] Dry at 3 percent O_2

TABLE 9. TOTAL ORGANIC EMISSIONS: EOR STEAMER TESTS

Organic Category	mg/dscm	ng/J
Volatile organics analyzed in the field by gas chromatography		
C_1	0.2	0.7
C_2	0	0
C_3	8.4	29.8
C_4	2.2	7.8
C_5	0	0
C_6	0	0
Total C_1-C_6	10.8	38.3
Semivolatile organics analyzed by TCO		
Filter	--	
XAD-2	<0.004	<0.014
Total C_7-C_{16}	<0.004	<0.014
Nonvolatile organics analyzed by gravimetry		
Filter	0.3	1.1
XAD-2	<0.1	<0.35
Total C_{16+}	0.3	1.1
Total organics	11.1	39.4

TABLE 10. COMPOUNDS DETECTED IN THE GC/MS ANALYSES OF EOR STEAMER SAMPLES (μg/dscm)

Species	Filter	XAD-2 Run 1	XAD-2 Run 2	Total[a]
Phenol	0.22	0.96	1.4	1.4
Naphthalene	0.19	<0.04	<0.04	0.19
Phenanthrene	0.30	<0.04	<0.04	0.30
Pyrene	0.11	<0.04	<0.04	0.11
Benzothiazole	3.2	--	--	3.2
Fluoren-9-one	20	--	--	20
Ethylcarbazole	13	--	--	13
Terphenyl	5.2	--	--	5.2
Benzofurandione	--	0.37	0.52	0.44
Benzoic acid	--	35	33	34
Dichlorodibenzosulfone	--	0.48	0.55	0.52
Ethyl benzoate	--	0.37	0.44	0.40

[a] Based on the sum of filter and average of run 1 and run 2 XAD-2 analysis results

SESSION X

SMALL INDUSTRIAL, COMMERCIAL, AND RESIDENTIAL SYSTEMS

Chairman, Michael C. Osborne
EPA, IERL/RTP

COMBUSTION MODIFICATIONS FOR COAL-FIRED STOKER BOILERS

By:

K. L. Maloney
KVB, Inc.
18006 Skypark Boulevard
Irvine, California 92714

ABSTRACT

The objective of this EPA-sponsored program (Ref. 1) was to examine potential combustion modification processes for stoker-fired boilers that would reduce stack opacity and emissions of NO_x, SO_x, and particulates without adversely affecting boiler efficiency or steaming capacity. KVB had developed a laboratory-scale proprietary combustion modification system that not only met these objectives, but with an associated increase in boiler efficiency and performance. Full-scale field test evaluations of this patented process were conducted for EPA to evaluate its performance. The invention uses recirculated flue gas mixed with the combustion air both above and below the grate. Replacing a portion of the combustion air with recirculated flue gas allows the stoker to operate at lower overall excess air without fuel bed clinker formation. The recirculated flue gas provides the required fuel bed cooling that would normally be provided by larger amounts of excess air. The recirculated flue gas also provides the flow dynamics that larger amounts of excess air normally provide in order to fulfill the mixing requirements of fuel bed combustion. Flue gas recirculation is provided to the overfire air to reduce the amount of oxygen that is put into the furnace above the fuel bed. This, in combination with enlarged overfire air ports, improves over bed mixing of volatile fuel components and the excess oxygen in the furnace to complete burnout of the carbon in the fuel.

INTRODUCTION

Stoker boilers suffer from poor operating efficiency and inadequate air emission control to be attractive in today's market. They are however relatively inexpensive to purchase and can operate on inexpensive fuel. The work presented in this paper shows how the stoker boiler can have its fuel efficiency improved and the emission of particulate matter, nitrogen oxides (NO_x), and sulfur oxides (SO_x) reduced.

These combustion modifications should make the stoker boiler the coal-fired combustion system of choice for the industrial client.

KVB has applied for and received a U.S. patent (No. 4,335,660) (Ref. 2) covering the Stoker Gas Recirculation* systems that are discussed in this paper.

DISCUSSION

The Concept

The fundamental problem hampering boiler efficiency in stoker-fired systems is that of inadequate mixing of the fuel and air. Attempts have been made to improve this mixing by the use of overfire air and different grate designs,but the problem remained.

Simply stated, "the fuel and air do not have adequate time to mix properly within the bed dimensions." The fuel bed has the requirement that a certain mass flow of combustion air (gas) be supplied in order to cool the fuel bed so that the ash in the bed does not fuse into what is called a clinker (slag).

The requirements of mixing and cooling can be supplied if a portion of the flue gas is returned and mixed with the fresh combustion air. The replacement of some of the combustion air with flue gas allows a reduction in the excess air required for satisfactory combustion. This reduction in required excess air results in lower stack gas heat (enthalphy) losses thus improving boiler efficiency. The recirculation acts to improve the macro mixing by reducing the concentration of oxygen in the combustion air. In fact the oxygen concentration can be lowered almost to the flammability point (13 percent O_2) before combustion stability problems are encountered.

The moisture in the flue gas improves the reactivity of the carbon in the coal via the water/gas reaction thus improving carbon utilization in the boiler. This reaction is endothermic and as such removes additional heat from the fuel bed.

In the process of returning flue gas to the combustion air several other benefits are realized. If the flue gas is taken from the hopper section of a mechanical dust collector (cyclone) a significant improvement in the collection efficiency is realized. The particulate in the flue gas recycle stream is efficiently filtered by the grate and the fuel bed so that furnace exit dust loadings are not increased. Particulate emission reductions of 50 percent have been achieved with the use of SGR.

---

*Reg. Trademark of KVB

The SGR also acts as a vitiated (direct contact) air preheater. The increase in the combustion air temperature does not adversely affect the grates since the fuel bed actually operates at a lower measured temperature than without SGR.

The lower fuel bed temperatures allow for the capture of sulfur in the ash when calcium is naturally present or when lime or limestone is added to powdered coal and pelletized. Solid calcium/sulfur compounds are stable at the lower fuel bed temperatures at which SGR operates. Laboratory results with a coal/lime pellet of 1.3 to 1 calcium-to-sulfur molar ratio demonstrated 50 percent sulfur retention with the use of SGR.

Reduced stack gas flows that occur because of the lower excess air requirements for combustion mean that smaller ducts, flues, and dust collection equipment may be used. The lower flue gas flows mean that less gas has to be processed by a scrubber, ESP, or baghouse.

In existing equipment the retrofit of an SGR system might allow increased steaming capacity if the old boiler was limited by fan speed (I.D. or F.D.), opacity, particulates, or furnace pressure. This is because of the reduction of the gas flow requirements which takes some of the burden off the fans and the reduction in the particulate loading in the flue gas that goes to the stack. Reduced opacity is also achieved by the modifications to the overfire air system discussed below.

The Application

To apply Stoker Gas Recirculation, a series of flues are connected into the boiler system along with a gas recirculation fan. Figure 1 contains a cutaway of the boiler with a line drawing of the SGR system. Flue gas is extracted at a point downstream of the boiler firebox after it has been cooled in the boiler bank and economizer (heat trap). The flue gas flows through the fan and is injected into the stoker undergrate air duct downstream of the combustion air (forced draft) fan. At the point of injection of the recirculated flue gas into the air stream, proper mixing of the two streams is achieved by a distribution nozzle system.

Equipment and controls for stoker gas recirculation are installed in parallel with the existing stoker system. Therefore, there is no interference with operation of the stoker or boiler if gas recirculation is not utilized.

A flow control damper on the discharge of the SGR fan is positioned by a local drive unit receiving a control signal from a controller mounted on the boiler system control panel. The boiler operator can remotely operate this damper by "hand" or "automatic." In the automatic mode the SGR combustion control signal follows the forced draft flow controller and can be biased to set the ratio of SGR to air. On manual the operator can set the percent SGR desired.

Stoker Gas Recirculation will allow operation at reduced combustion air flow but the boiler operator must make adjustments. To adjust the relative air flow effectively, there must be a consistent means of measuring or detecting combustion air flow and boiler steaming rate. Continuously measuring excess oxygen content of the flue gas is a way to properly set the amount of gas recirculation. Alternately, the percent SGR can be read on the flow controls and then related to the boiler efficiency by graph.

Overfire Air Modifications

The goal of the modifications to the overfire air system is to increase the mixing of the fuel volatiles from the bed with the unused oxygen in the combustion air passing through the fuel bed. Figure 2 contains a line drawing of the SGR overfire air system and the main SGR system.

The overfire air provides mixing in the regions that it covers. However the coverage of the above bed region is usually inadequate when the jet penetration is poor. To improve the jet penetration and increase the momentum (mass) of gas admitted as overfire air,the diameter of each overfire air jet in the test boiler was increased from 3/4-inch to 2 inches. The area of the overfire air jets nozzles increased by more than a factor of 7. The new system then had the potential to introduce significantly more air (gas) into the furnace above the fuel bed. If this gas remained all air there would have been more oxygen in the overfire air than required, thus flue gas recirculation was mixed with the overfire air to reduce the excess oxygen introduced above the fuel bed.

Increasing the overfire air jet nozzle diameter reduced the opacity significantly at all boiler loads without increasing the overall excess oxygen. The overfire jets could be seen to penetrate further into the furnace than before the modification.

A further step to improve the overfire air coverage was made by the installation of sidewall overfire air jets. Four jets on each sidewall were located midway between the front and back of the furnace one foot above the grate. These jets were supplied from the same manifolds that supplied the front and back jets. The sidewall jets significantly reduced the opacity further.

Although the boiler could be run with 100 percent SGR in the overfire air, it was determined that 50 percent SGR was a more easily controlled mixture and that opacity readings were reduced below 15 percent at all loads and that the excess oxygen in the furnace was not increased above that desired for efficient operation.

TEST RESULTS

The test results discussed below were obtained on a 100,000 pph spreader-stoker boiler firing Western Kentucky coal.

Efficiency Improvements

Figure 3 contains a plot of the excess oxygen in the flue gas (excess air is shown on right ordinate) as a function of boiler steaming rate before and after SGR modification.

Before the modification the boiler was limited by high opacity at 80,000 pph steaming rate. At this level the boiler operated at 8 percent excess O_2. At lower loads the excess O_2 was 10 percent or higher.

After the SGR system was installed the excess O_2 was lowered at all loads, as shown by the curve labeled "after modification." The reduction in stack gas excess oxygen concentration shown by these curves represents a significant improvement in boiler efficiency. Table 1 contains a calculation of the fuel efficiency improvement that resulted only from the reduction in the stack gas heat loss. The heat loss factors were taken from Figure 4 for the bituminous coal composition given in the caption. The fuel savings were shown to be 6.67 percent for the conditions shown in Table 1. This represents an annual fuel savings of $147,400 based on 40,000 tons of coal per year and $55/ton coal.

Figure 5 contains the excess oxygen record over a 44-hour period for two identical boilers where one boiler was modified with SGR and the other unit was unmodified. The coal used during this test was of very poor quality. It was coal that had been in storage for many years and consisted of a large amount of fine coal. The unmodified unit had a difficult time maintaining clinker-free operation,while the unit with SGR-installed operated smoothly between 4 and 5 percent excess O_2.

Emission Reductions

Figure 6 contains the test results for opacity plotted as a function of boiler load both with and without the SGR system. These opacity data were taken before the overfire air system had been modified and before the sidewall overfire air modifications had been installed. These additional modifications combined to reduce the opacity even further than shown in Figure 6.

The "before" data shown in Figure 6 indicate that the boiler had a fairly narrow operating window within the opacity regulation of 40 percent. The boiler exceeded this 40 percent limit at 40,000 pph and again at 80,000 ppm steam.

After the SGR system was installed the opacity was below the 40 percent regulation at all steaming loads. In fact the maximum steaming rate was extended to 120,000 pph, thus providing the owner with a 40,000 pph increase in the available capacity of the boiler.

The reduction in excess air required to fire the boiler resulted in a reduction of the NO_x emission. Figure 7 contains the NO_x emission data plotted as a function of excess oxygen in the flue gas. Emissions approaching 100 ppm were measured at the lowest excess oxygen levels. The NO_x data taken with the SGR modification in place fell below the unmodified data. It is speculated that this is the result of a degree of "natural staging" that takes place when low fuel bed stoichiometries are achieved. Further work is underway to exploit these low fuel bed stoichiometries in a staged firing configuration to achieve even lower NO_x emissions from stoker boilers.

Significant particulate emission reductions were measured in back-to-back tests over a forty-hour test period each with and without the use of the SGR system. The average of five Method 5 particulate tests at two boiler loads are given in Table 2. At 60,000 pph with a 30 percent flue gas recirculation rate the average stack particulate emission rate was 0.145 lb/10^6 Btu heat input. This represented a 42 percent reduction over the unmodified average emission rate. At 80,000 pph with a 20 percent flue gas recirculation rate the average stack particulate emission rate was 0.1992 lb/10^6 Btu heat input which represented a 33 percent reduction from the unmodified emission rate.

Recent design changes to incorporate "hopper evacuation" from the cyclone dust collector into the SGR process promise to reduce even further the particulate emission rate.

The potential for SO_x emission control exists with the use of a limestone coal pellet and SGR. In laboratory tests on a 20-lb per hour coal stoker firing a coal/limestone pellet, 50 percent reduction in the SO_2 emission was measured with the use of SGR. The SGR allows the fuel bed to operate at the lower temperatures necessary to "trap" the sulfur as a solid sulfide or sulfate and be disposed of with the ash.

CONCLUSIONS

Combustion modifications to coal-fired stoker boilers have been implemented and tested on a 100,000 pph spreader stoker. The most promising modification is the use of flue gas recirculation into the main combustion air and the overfire air to control fuel bed clinker formation. This in turn allowed lower excess air combustion and resulted in boiler efficiency improvement thus saving fuel. The SGR process also reduces stack emissions of particulate, NO_x, and opacity as well as having the potential to reduce SO_x emission when used in conjunction with a limestone coal/pellet fuel.

ACKNOWLEDGMENTS

The author would like to thank the U.S. EPA for the funds for the demonstration program, and John H. Wasser, the EPA program manager, for his guidance, support, and understanding of the research program.

Special thanks are also in order to the University of Wisconsin at Madison for their participation as a host test site for the demonstration.

REFERENCES

1. EPA Contract 68-02-3166. Application and Assessment of Combustion Modification Concepts for Full-Scale Coal-Fired Boiler Systems. August 1978.

2. U.S. Patent No. 4,335,660 issued to K. L. Maloney, Ph.D. and N. Bayard de Volo assigned to KVB, Inc.

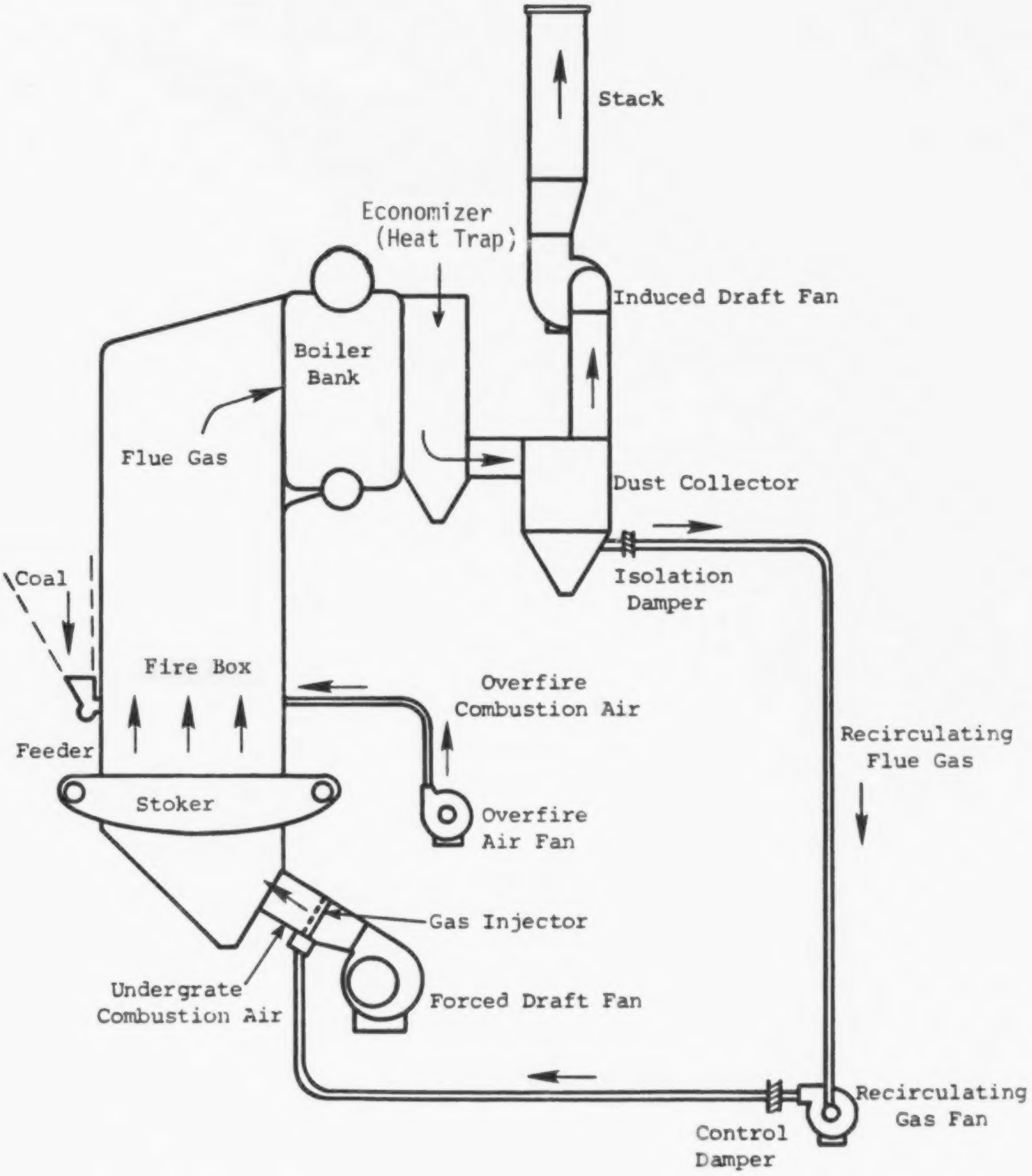
Stack
Economizer
(Heat Trap)
Induced Draft Fan
Boiler
Bank
Flue Gas
Dust Collector
Coal
Isolation
Damper
Fire Box
Overfire
Combustion Air
Feeder
Recirculating
Flue Gas
Stoker
Overfire
Air Fan
Gas Injector
Undergrate
Combustion Air
Forced Draft Fan
Control
Damper
Recirculating
Gas Fan

Figure 1. Schematic Diagram of Stoker Gas Recirculation

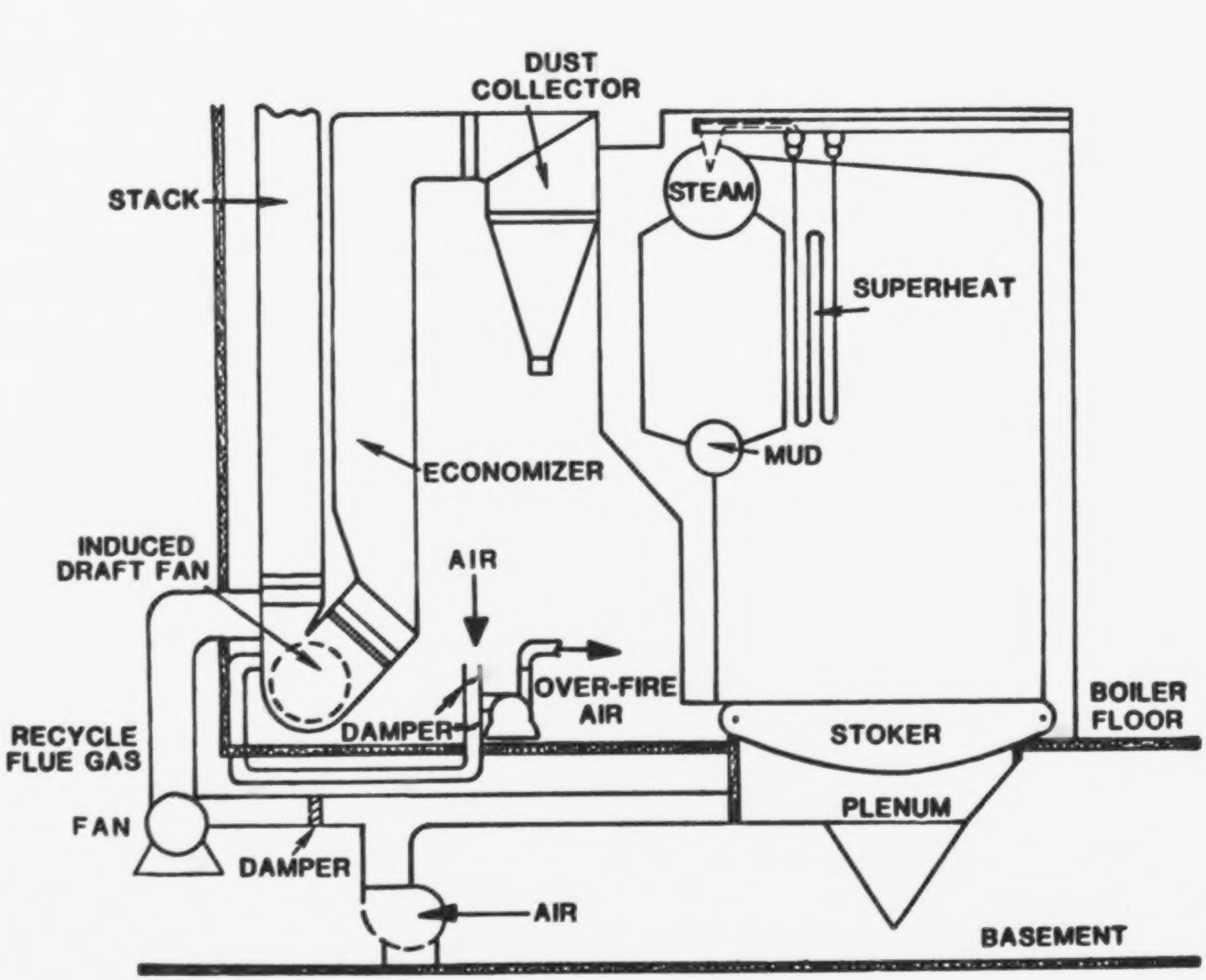
DUST
COLLECTOR
STACK
STEAM
SUPERHEAT
MUD
ECONOMIZER
INDUCED
DRAFT FAN
AIR
OVER-FIRE
AIR
DAMPER
BOILER
FLOOR
STOKER
RECYCLE
FLUE GAS
PLENUM
FAN
DAMPER
AIR
BASEMENT

Figure 2. Stoker Gas Recirculation System

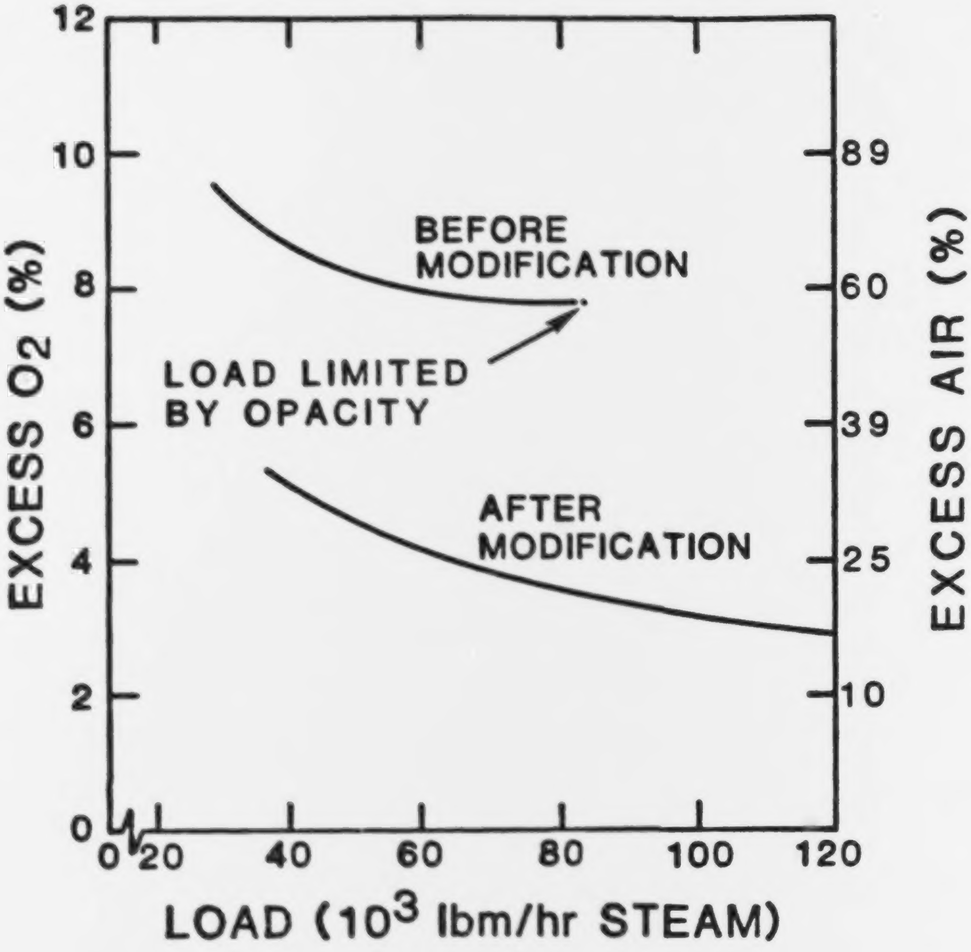

Figure 3. SGR Effects on Excess O_2

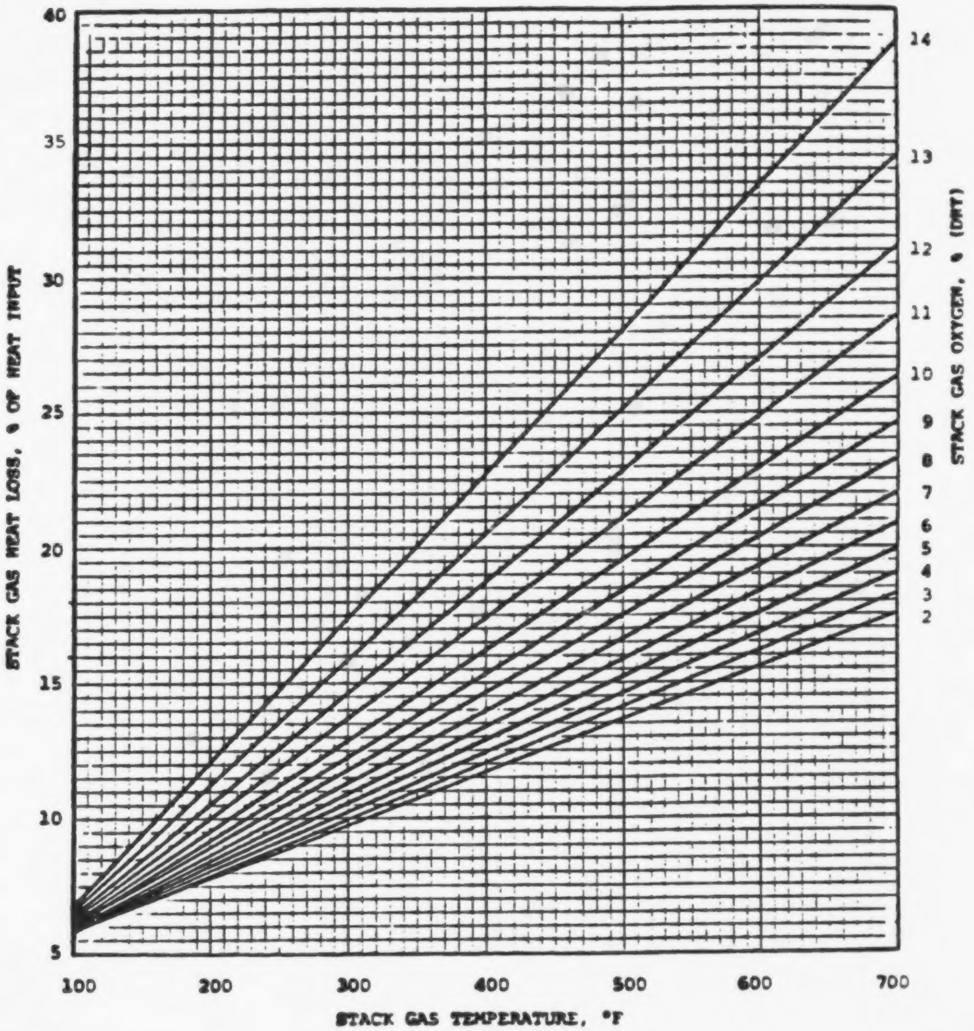

Figure 4. Stack gas heat loss as a function of stack gas temperature and stack gas oxygen for a typical bituminous coal. (Coal composition by weight: H_2O - 5 percent; C - 73 percent; H - 5 percent; N - 1.4 percent; S - 1.5 percent; O - 7.1 percent; ash - 7 percent; 13,000 Btu/lb; ambient air temperature - 80°F.)

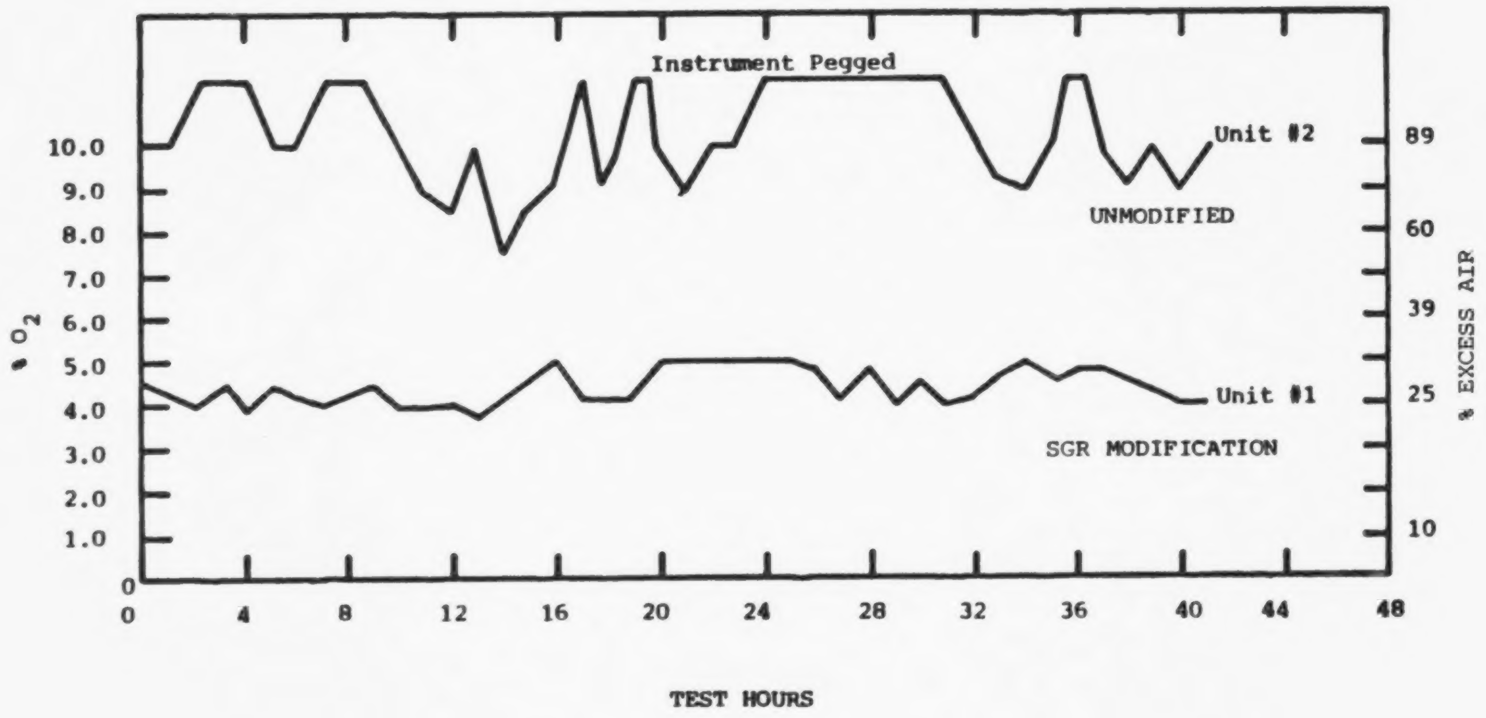

BOILERS ARE EXACTLY ALIKE BURNING THE SAME POOR QUALITY
(STRIKE) COAL

Figure 5. Continuous Test: %O_2 vs. Time (Unit #1 and 2)

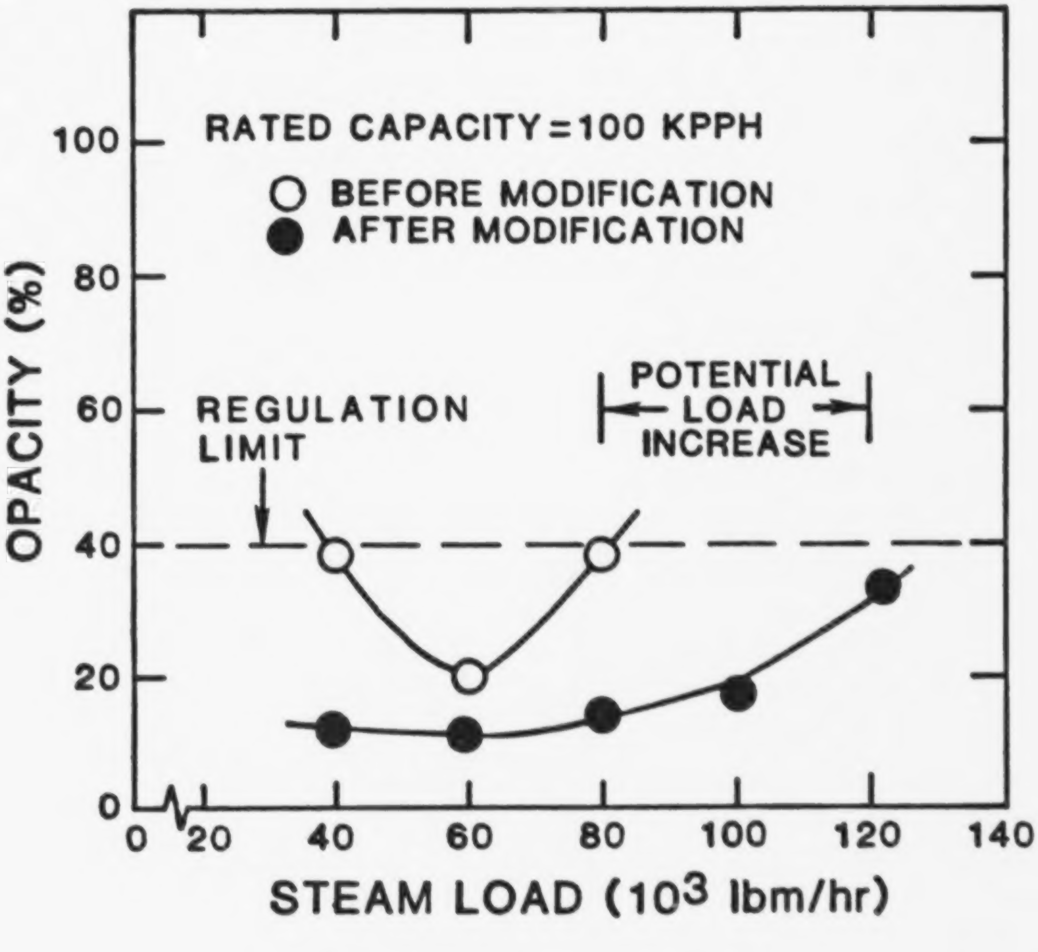

Figure 6. Effects of Opacity

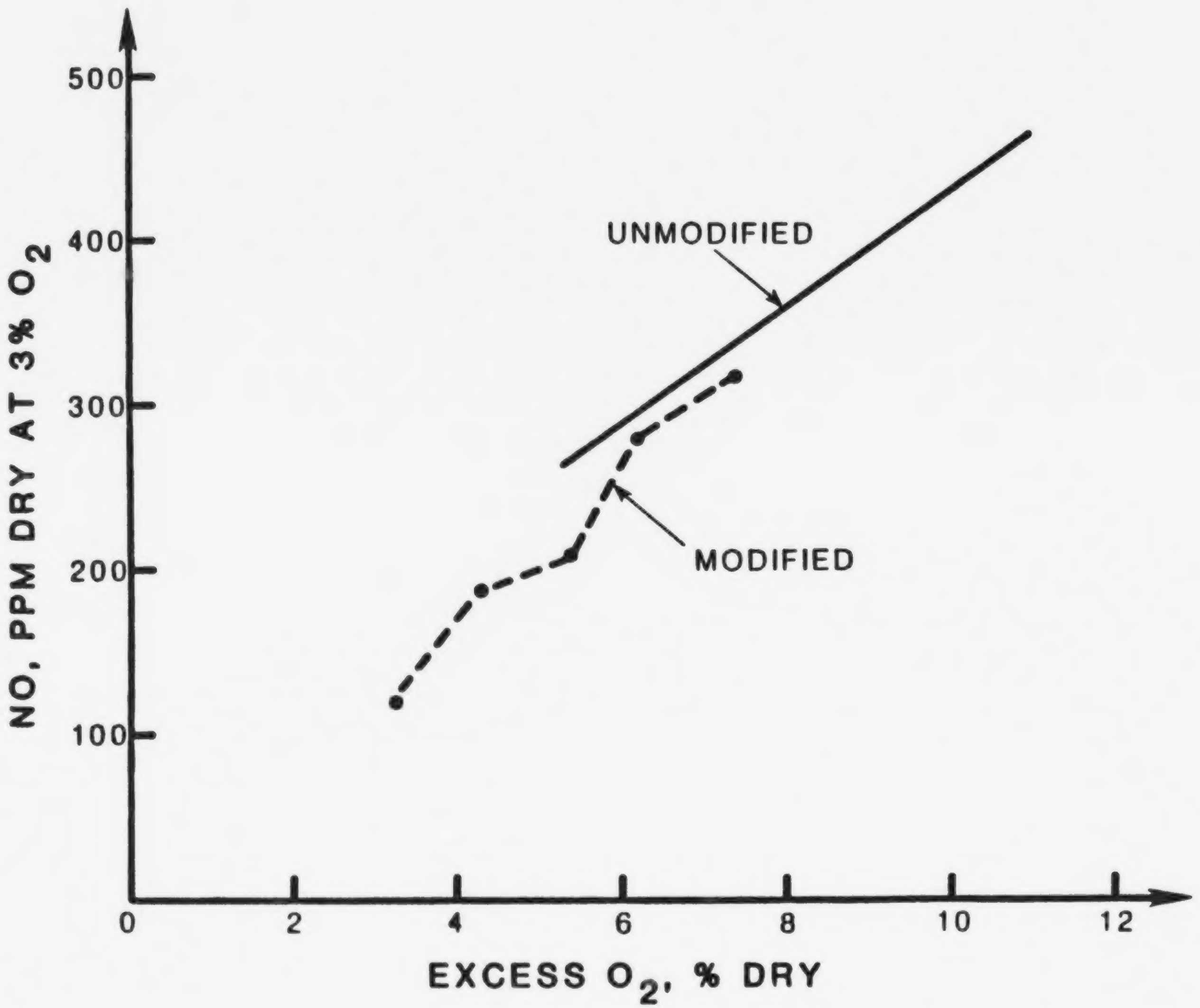

Figure 7. NO Emissions vs. Excess O_2

TABLE 1. SGR EFFICIENCY IMPROVEMENT

Before SGR Modification

	Stack			
Load	Excess O_2, %	Coal Use Factor	Temp., °F	% of Heat Input (A)
High	8	1/3	500	17.5
Medium	10	1/3	500	19.5
Low	12	1/3	500	22.8
				$\frac{59.8}{3} = 19.933$

After SGR Modification

	Stack			
Load	Excess O_2, %	Coal Use Factor	Temp., °F	% of Heat Input (B)
High	3	1/3	500	14.0
Medium	4	1/3	500	14.6
Low	5	1/3	500	15.2
				$\frac{43.8}{3} = 14.6$

$$\text{Fuel Savings} = \frac{(H^L A - H^L B) \times 100}{\text{Boiler Effic.}} = \frac{(5.333) \times 100}{0.80} = 6.667\%$$

TABLE 2. SGR PARTICULATE EMISSION REDUCTION

LOAD,pph	SGR, %	STACK PARTICULATE, LB/10^6BTU*	REDUCTION
60K	30	0.145	42%
80K	20	0.1992	33%

*DOWNSTREAM OF A MULTICYCLONE DUST COLLECTOR AVERAGE OF FIVE TESTS PERFORMED OVER A FORTY HOUR PERIOD

ADVANCED DEVELOPMENT OF A COAL/LIMESTONE FUEL PELLET FOR INDUSTRIAL BOILERS

By:

Bruce W. Rising, H. Nick Conkle,
and Robert D. Giammar
Battelle, Columbus Laboratories
505 King Avenue
Columbus, Ohio 43201

ABSTRACT

Research efforts on U.S. EPA Contract Nos. 68-02-2627 and 68-02-3189 have demonstrated that the limestone/coal fuel pellet has the potential for providing a means for burning high sulfur coals in an environmentally and economically acceptable manner. Furthermore, these pellets may provide an acceptable method of burning halogen-containing compounds. The pellets may also provide certain benefits when burned in fluidized-bed combustors. The continuation of the current project focuses on these aspects.

The overall technical objective of this program is to evaluate the feasibility of a coal/limestone fuel pellet as a SO_2 control for industrial boilers. The primary focus will be on application to stoker (fixed-bed) boilers, but fluidized-bed boilers will also be considered. A secondary objective is to determine the extent of halogen capture when halogen-containing wastes are incorporated into the limestone/coal fuel pellets.

The program consists of the following seven tasks, namely:

Task 1. Pellet Formula Optimization
Task 2. Calcium/Sulfur Reaction Chemistry
Task 3. Pellet Process Development
Task 4. Experimental Evaluation
Task 5. Pellet Fuel Production Run
Task 6. Alternate Pellet Applications
Task 7. Data Analysis/Report

INTRODUCTION

Research efforts on EPA Contract Nos. 68-02-2627 and 68-02-3189 have demonstrated that the limestone/coal fuel pellet has the potential for providing a means for burning high sulfur coals in an environmentally and economically acceptable manner. Furthermore, these pellets may provide an acceptable method of burning halogen-containing compounds. The pellets may also provide certain benefits when burned in fluidized-bed combustors. The continuation of the current project focuses on these aspects. Because this project has recently restarted, this paper outlines the major tasks to be undertaken.

TECHNICAL OBJECTIVE

The overall technical objective of this program is to evaluate the feasibility of a coal/limestone fuel pellet as a SO_2 control for industrial boilers. The primary focus is on application to stoker (fixed-bed) boilers, but fluidized-bed boilers will also be considered. A secondary objective is to determine the extent of halogen capture when halogen-containing wastes are incorporated into the limestone/coal fuel pellets.

APPROACH

The proposed program consists of the following seven tasks, namely:

Task 1. Pellet Formula Optimization
Task 2. Calcium/Sulfur Reaction Chemistry
Task 3. Pellet Process Development
Task 4. Experimental Evaluation
Task 5. Pellet Fuel Production Run
Task 6. Alternate Pellet Applications
Task 7. Data Analysis/Report

These seven specific tasks are discussed below.

Task 1. Pellet Formula Optimization

Pellets with satisfactory mechanical strength characteristics have been produced for one specific type of coal (high sulfur, mid-western bituminous) using a formulation developed on 68-02-2627. This formulation has not been used with other types of coals so the universality of it is unknown. Also, it is conjectured that the amount and mineral constituents of the ash and the form of the sulfur (inorganic vs organic) may be important in specifying the optimum formulation for a given coal.

Further refinement of the formulation is needed to identify a binder or process to provide complete weatherproofing of the pellets. The pellet formulation used in the past provided some degree of weather resistance but not of sufficient degree to allow for unprotective storage.

Additionally, a number of formulation variables were investigated in detail, but some were limited to a narrow range and merit additional consideration.

Accordingly, using the data generated on 68-02-2627 as a baseline, an expanded range of variables will be investigated. Pellet formulation variables to be investigated include:

- Limestone reactivity
- Binder type and amount
- Ca/S molar ratio
- Coal type
    - Eastern
    - Western
    - Lignite
    - Beneficiated
- Sulfur form (organic/inorganic)
- Coal and limestone particle size
- Pellet size.

The influence of process variables on pellet quality also will be considered.

The objective of this task is to develop a refined pellet formulation(s) that can be applied to a variety of coals.

Task 2. Calcium/Sulfur Reaction Chemistry

The objective of this task is to identify the specific mechanism involved in the calcium/sulfur chemistry associated with the pellet. The model developed on 68-02-2627 will be reviewed and updated as appropriate. Since the development of the model, there has been additional research into the calcium/sulfur reactions that may be pertinent to pellet combustion chemistry. Micro-Raman and infrared techniques will be utilized to identify the reaction species.

Task 3. Pellet Process Development

Pellets have been produced using available process technology. Only limited efforts were made to identify the best available technology and also to optimize the equipment operating variables. The application of the process or production technology was provided by others without research and development capabilities and, as a consequence, was found to be inadequate for large-scale continuous production. Accordingly, the objective of this task is to identify the best available technology that has the potential to produce acceptable pellets continuously on a large scale.

The scope of activities within this task include:

- In-depth review of agglomerating technology used in relevant materials processing industries
- Interactions with equipment manufacturers to identify key operating parameters and correlate these with product quality. We will also enlist the support of these manufacturers to refine their equipment.
- Limited laboratory experiments to determine the relationship between equipment operating parameters (pressure, temperature, and material residence time) on pellet quality
- Identification of drying procedures
- Experimental determination of mechanical strength characteristics.

Task 4. Experimental Evaluation

Pellet formulations will be evaluated in a laboratory size fixed-bed reactor to evaluate the combustion performance and emission characteristics of the improved pellets. Sulfur capture, carbon burnout, and reactivity of these pellets will be determined.

The more promising formulations will be evaluated in a limited number of experiments in Battelle's 25,000 lb steam/hr steam plant spreader-stoker boiler. These experiments will include measurement of environmental emissions and combustion performance, and will assess the physical characteristics of the pellets as they move through the entire coal storage and handling system.

Task 5. Pellet Fuel Production Run

Based upon the results of Tasks 1-4, an optimized pellet formulation will be used to prepare approximately 20 tons of fuel pellets for utilization in a low NO_x, modified, stoker boiler under construction for another EPA contract.

Task 6. Alternate Pellet Application

The limestone/coal pellet has the potential of being a viable industrial boiler fuel not only in stokers but possibly in fluidized-bed combustors. In addition, the limestone in the pellet may react and retain in the ash the halogen component of a waste material and, thus, offer a means of burning those materials.

A limited number of experiments will be performed in a conventional atmospheric fluidized bed to determine if burning pellets in a fluidized bed will increase calcium utilization and allow the fluidized bed to be operated at elevated temperatures. In addition, a limited number of experiments will be performed to determine the extent of halogen capture when certain waste materials are incorporated into a limestone/coal fuel pellet. The effect of the calcium/halogen ratio on capture will be investigated.

Task 7. Data Analysis/Report

A comprehensive assessment of the pollution control and coal utilization potential of the limestone/coal fuel pellet will be prepared. This assessment will address the aspects critical to the coal and boiler industry and indicate areas where further development is needed to commercialize the pellet. These critical areas include:

- Pollution control potential
- Stoker boiler operation performance
- Pellet fuel production
- Pellet fuel utilization economics
- Environment impact.

LOW-NO_X FIBER BURNER APPLICATION TO GAS-FIRED FIRETUBE BOILERS

By:

J. P. Kesselring and Wayne V. Krill
Alzeta Corporation
440 Clyde Avenue
Mountain View, California 94043

"Although the research described in this article has been funded wholly or in part by the United States Environmental Protection Agency through contract 68-02-3122 to Acurex Corporation, it has not been subjected to the Agency's required peer and policy review and therefore does not necessarily reflect the views of the Agency and no official endorsement should be inferred."

ABSTRACT

Low-NO_x fiber burners have been developed and tested in natural-gas-fired firetube boilers. The fiber burner is a matrix of ceramic fibers vacuum-formed into the appropriate burner configuration. In operation, premixed natural gas and air pass through the fiber layer and are ignited, burning only on the outer surface. The surface radiates energy flamelessly to the firetube wall, controlling the combustion temperature to a level at which significant thermal NO_x formation does not occur. Subscale characterization tests of the fiber burner show emissions of approximately 15 ppmv NO_x, 20 ppmv CO, and 1 ppmv HC when operating with 15 percent excess air. A full-size (1,055 MJ/hr heat input) fiber burner was retrofit into a 245-kW (25-hp) York-Shipley firetube boiler under EPA contract 68-02-3122 to perform laboratory demonstration testing. The burner fits within the first pass of the firetube boiler and occupies approximately the same volume as the conventional flame. Testing over a wide range of boiler load conditions and excess air levels has verified NO_x emission levels below 20 ppmv as well as increased boiler efficiency. The ability to over-fire the boiler by up to 20 percent with the fiber burner was also demonstrated. Burner durability was verified in a 1,000-hr test, providing the basis for further demonstration in field boilers.

INTRODUCTION

There are approximately 125,000 gas-fired firetube boilers in the 633- to 3,165-MJ/hr (0.6- to 3-million Btu/hr) firing range in the United States, and an additional 3,000 new units are sold annually. These boilers produce about 150 ppmv NO_x, making gas-fired firetube boilers the 26th largest NO_x source in the United States, accounting for 1 percent of the total NO_x produced. In addition, firetube boilers are usually located in population centers where their effect on air quality is greater than the inventory percentage would indicate. In the interest of improving air quality, the United States Environmental Protection Agency (EPA) has funded the development of low-NO_x burners for retrofit into existing boiler designs.

Under EPA Contract 68-02-3122, an approach was laid out that would culminate in the demonstration of a retrofit burner in a commercial-size firetube boiler. First, a burner concept was selected that met the needs of firetube boiler manufacturers. The feasibility of this concept was then tested, suitable burner materials identified, subscale testing performed, and finally, the retrofit burner demonstrated in laboratory testing.

After considering several low-NO_x burner concepts, the fiber burner was chosen for further development. Because of the burner's relative simplicity, few changes to the conventional boiler system were required to operate it with the fiber burner. In comparison, the other concepts considered included staged combustion and flue gas recirculation, which introduce hardware and cost complexities.

The fiber burner system concept selected for the firetube boiler retrofit is shown in Figure 1. Premixed natural gas fuel and air enter the burner system, pass through holes in the burner centerbody to enter a flow annulus, and then pass through the fiber layer itself. Combustion is initiated by a pilot (not shown) on the outside of the fiber layer. The entire burner assembly fits within the firetube combustion chamber and radiates directly to the combustion chamber wall.

THE FIBER BURNER

The fiber burner consists of a layer of ceramic fibers vacuum-formed onto a screen of the desired shape. The close-packed fibers form a porous matrix through which premixed natural gas and air pass prior to being ignited by some source (pilot, IID, etc.) downstream of the outer surface of the burner. Following ignition, the flame is quickly absorbed by the surface and combustion occurs with the outer surface radiating flamelessly and uniformly.

Fiber burners operate best at surface velocities below the mixture flame speed. Both the low thermal conductivity of the fibers and the cooling flow of reactants tend to insulate the inside of the burner from the combustion zone, thereby preventing flashback and stabilizing combustion on the burner surface. Because of the high radiant energy transfer from the fiber surface, the combustion temperature is controlled to levels between 1,200 and 1,367K (1,700° and 2,000°F), which correspondingly controls thermal NO_x formation.

The fiber burner operates at a heat release rate per unit area of burner surface of 252 kW/m^2 (80,000 $Btu/hr-ft^2$). The burner is sized based on this operating condition, but can be turned up to achieve 378 kW/m^2 (120,000 $Btu/hr-ft^2$) or down to obtain 189 kW/m^2 (60,000 $Btu/hr-ft^2$). Operation outside of these limits results in increased emissions of CO and NO_x. Typical emission trends for operation with natural gas fuel at 252 kW/m^2

are shown in Figure 2. Note that NO_x, CO, and HC are all less than 25 ppmv (on an air-free basis) at excess air levels between 15 and 55 percent.

FIRETUBE BOILER RETROFIT

Following extended subscale tests to confirm the operating and durability characteristics of the fiber burner, the retrofit of a fiber burner in a firetube boiler was initiated. The boiler selected for testing was a York-Shipley 245-kW (25-hp) firetube boiler, which was purchased and installed in the Acurex combustion laboratory. The boiler has three passes, produces steam at low pressure, operates on either gas or light oil, and has an energy output at full load of 886 MJ/hr (840,000 Btu/hr).

The as-received boiler was tested on natural gas over a range of stoichiometries at four load conditions and a range of excess air levels from 15 to 70 percent. The four load conditions were 50, 65, 80, and 100 percent of full load. NO_x emissions ranged from 50 to 70 ppmv, depending on load condition and excess air level. Additional data are discussed in the next section in comparison to the fiber burner performance data.

Minimal retrofit hardware was required to adapt the fiber burner to the York-Shipley boiler. The fiber burner had a maximum pressure drop of 373 Pa (1.5 in. w.g.) and used the existing blower. The front burner flange with refractory ring was replaced, and port holes were added for thermocouples and igniter.

A 1,055 MJ/hr fiber burner was prepared and installed in the firetube boiler. Figure 3 shows the burner prior to its installation in the boiler. In operation, combustion air is premixed with natural gas injected into four ports upstream of the burner. The reactants enter the burner, pass through the fiber layer, and are ignited with a standing pilot. Internally, a center body reduces the cross-sectional flow area to minimize the premixed gas volume and maintain the gas and air mixture at a high velocity. A perforated metal cylinder supports the fiber burner.

After installation was complete, testing on natural gas fuel over conditions similar to those used for the conventional burner was accomplished.

LABORATORY DEMONSTRATION TESTING

NO_x emissions as a function of excess air levels for various boiler loads are shown in Figure 4. The NO_x emissions for the fiber burner followed the expected trends of Figure 2, increasing with temperature, such as when load increases or excess air decreases. A reduction of approximately 50 ppmv is noted for the fiber burner when compared to the conventional burner. Not shown on Figure 4 are the data taken for the fiber burner operating at 120 percent load, which showed a NO_x level of 20 ppmv at 10 percent excess air.

Figure 5 shows CO emissions as a function of excess air at 100 percent load for the two burners. As noted in the figure, the knee in the CO-excess air curve occurs at 10 percent excess air for the fiber burner and at 30 percent for the conventional burner. Thus, the nominal operating points for the two burners are 10 and 30 percent excess air, respectively. The fiber burner CO emissions of approximately 25 ppmv at 10 percent excess air are comparable to those achieved with the conventional burner.

Unburned hydrocarbon emissions for two boiler loads are plotted in Figure 6. As noted, both the fiber and conventional burners have UHC emissions less than 30 ppmv at their nominal operating points.

Boiler efficiency was calculated according to ASME Power Test Code 4.1 Heat Loss Method. Figure 7 shows the comparative efficiencies of the boiler with both the conventional and fiber burners at their nominal operating conditions. Due to its ability to operate at 10 percent excess air without producing high CO emissions, use of the fiber burner results in a boiler efficiency increase of approximately 2 percent. In addition, because the as-received boiler was designed to operate with 30 percent excess air, the fiber burner can be overfired by 20 percent with a high boiler efficiency. The ability to operate at higher than rated capacity with good efficiency and emissions should be of interest to commercial boiler users.

The laboratory demonstration was completed with a 1,000-hr durability test of the burner. The boiler was run for a total of 1,020 hr and had 14 on/off cycles. Most of the testing was done at conditions of 100 percent load and 15 percent excess air. As shown in Figure 8, NO_x and CO emissions remained steady throughout the test at 13 and 29 ppmv corrected to 0 percent excess air. Boiler efficiency was constant at just over 82 percent. The unburned hydrocarbons, however, slowly increased throughout the test. HC were initially 23 ppmv, and rose to 166 ppmv at 1,020 hr. This increase in hydrocarbons was traced to an imperfect seal at the burner mounting collar which was repaired at 1,020 hr. The final UHC emissions were then 10 ppm as shown in Figure 8. Future burner designs would eliminate the connection at the burner collar to avoid leakage problems.

SUMMARY AND CONCLUSIONS

A comparison of the fiber burner and the conventional burner used in a 245-kW York-Shipley firetube boiler shows the performance listed in Table 1.

The 77 percent reduction in NO_x emissions using the fiber burner was accompanied by a 2-percent increase in boiler efficiency. This successful laboratory demonstration of the fiber burner applied to firetube boilers and the 1,000-hr durability test have verified the low-NO_x, high efficiency operation of the burner over an extended period of time, and make field testing of the system the next logical step.

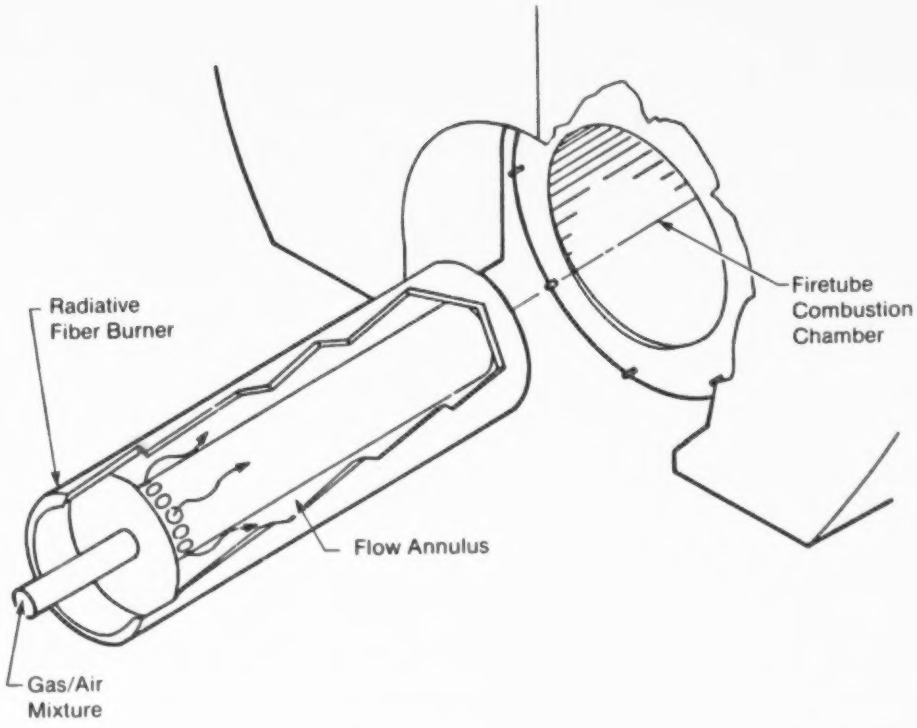
Radiative
Fiber Burner
Firetube
Combustion
Chamber
Flow Annulus
Gas/Air
Mixture

Figure 1. Fiber burner system concept.

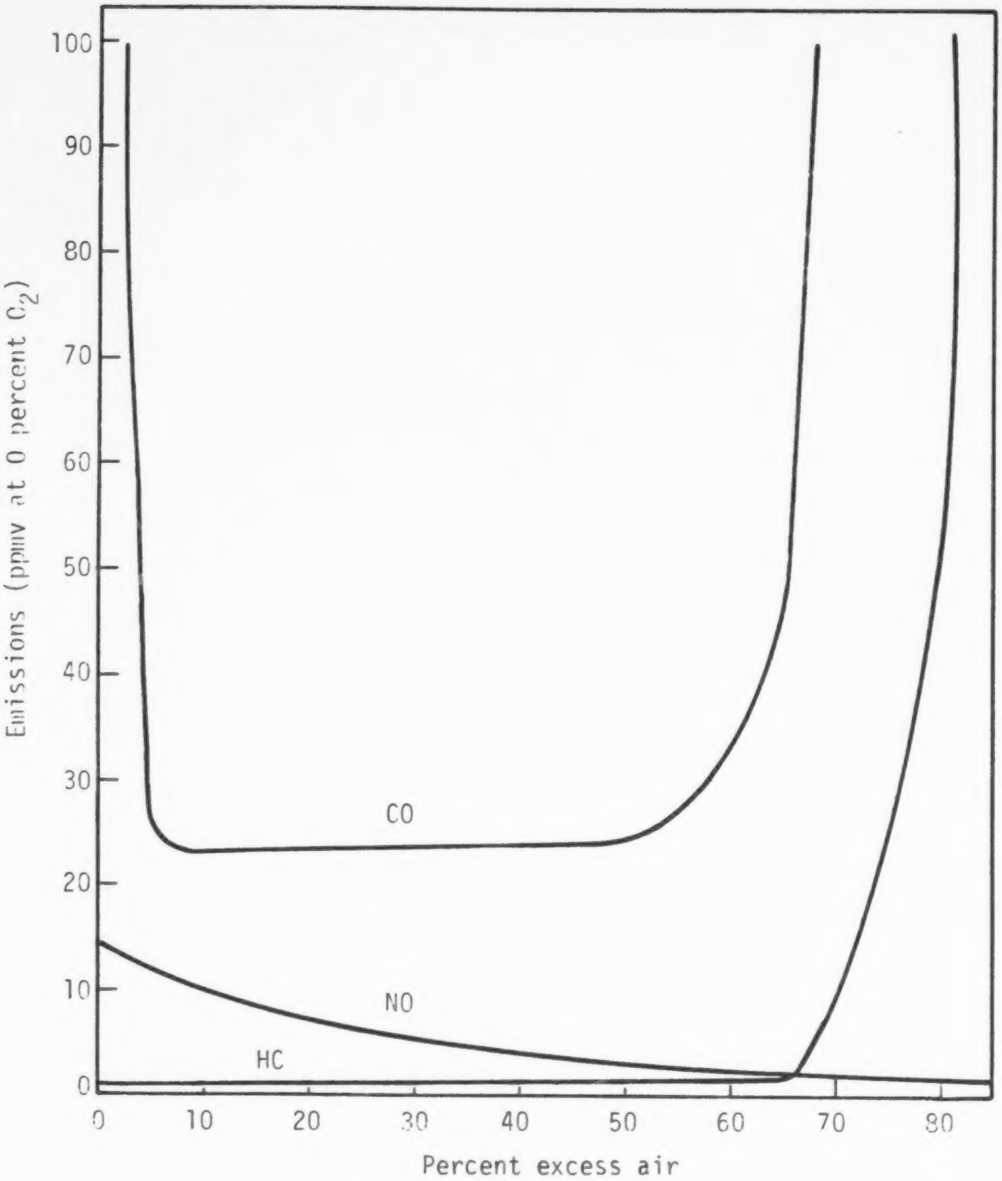

Figure 2. Fiber burner emission trends on natural gas fuel.

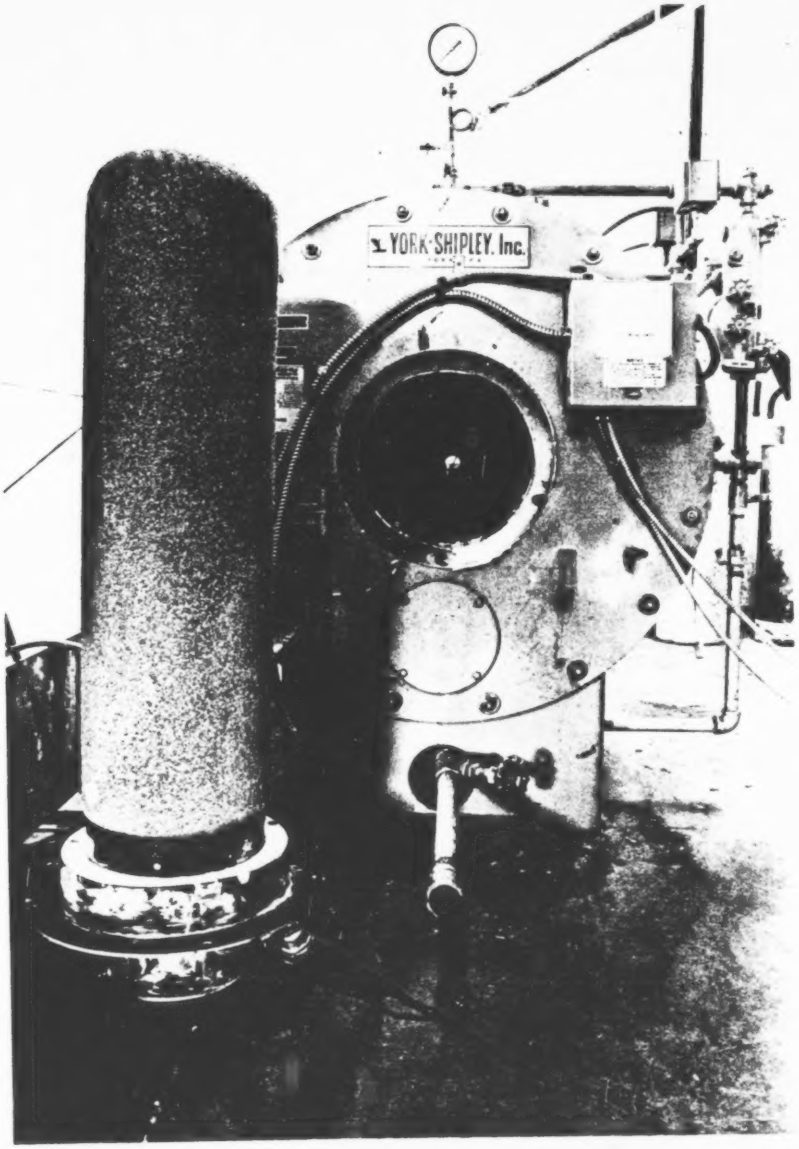
YORK-SHIPLEY, Inc.

Figure 3. Firetube boiler with Alzeta fiber burner.

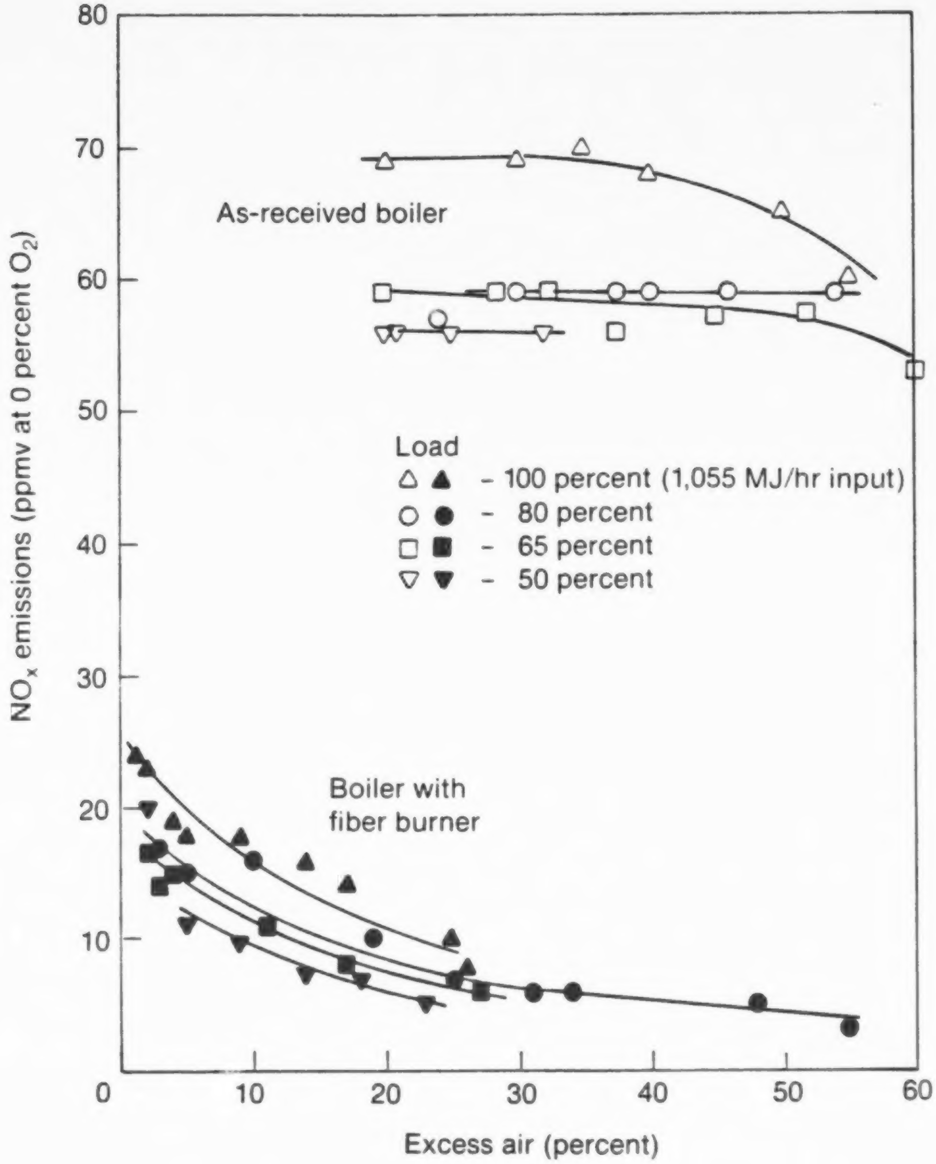

Figure 4. Firetube boiler NO$_x$ emissions at various boiler loads; natural gas fuel.

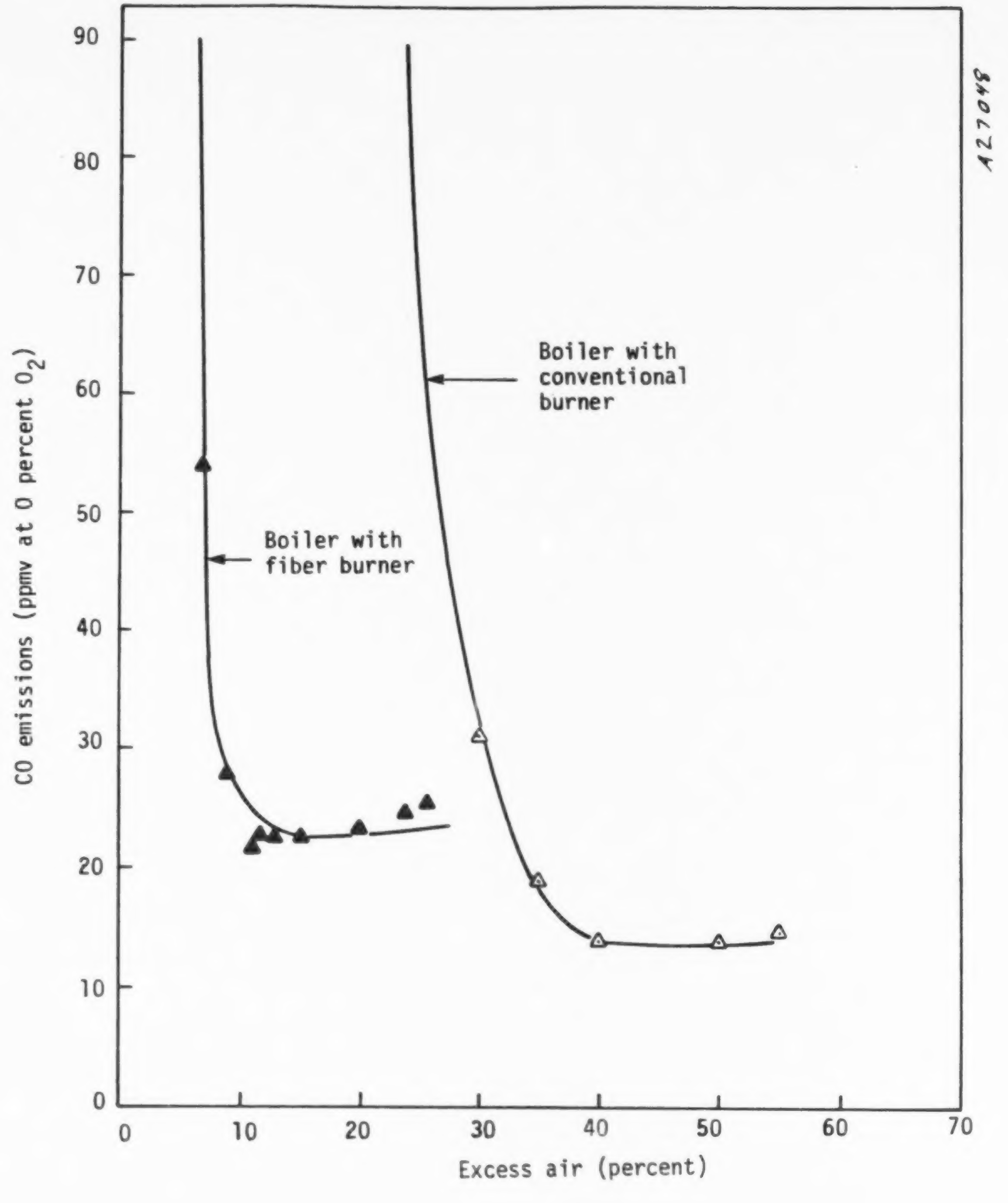

Figure 5. Firetube boiler CO emissions at 100 percent boiler load; natural gas fuel.

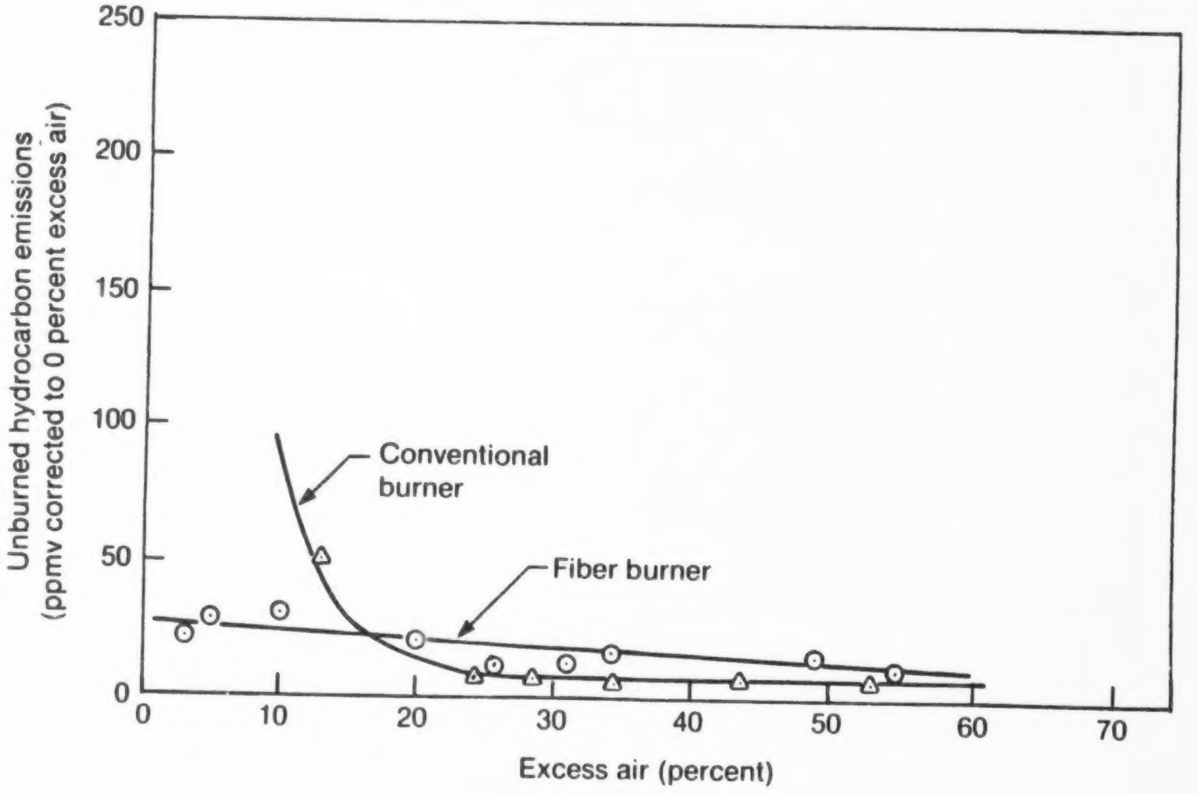

Figure 6. Firetube boiler UHC emissions at 80 and 100 percent boiler load; natural gas fuel.

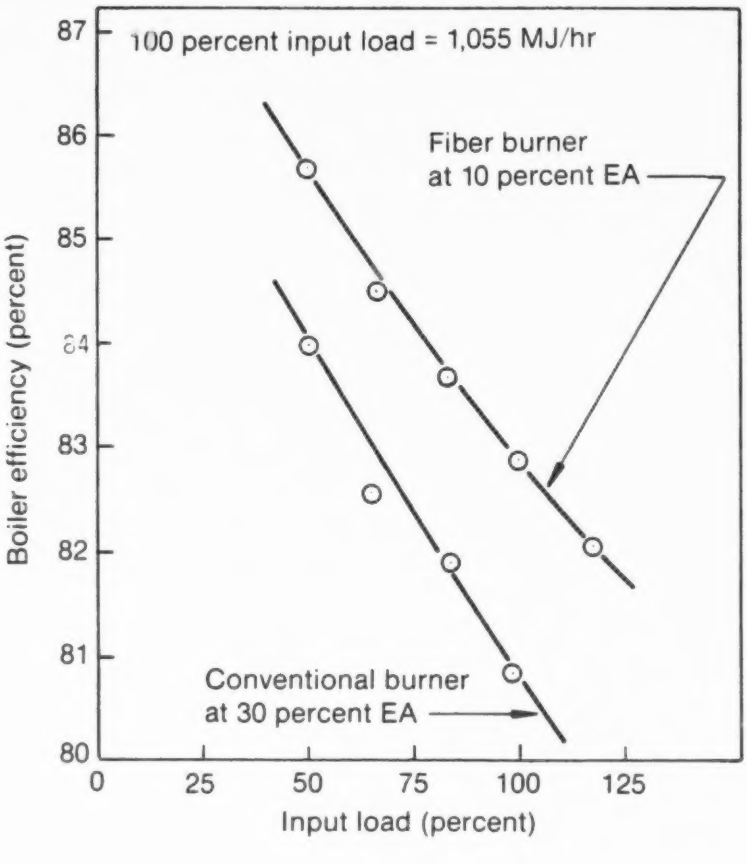

Figure 7. Firetube boiler efficiency at nominal operating conditions.

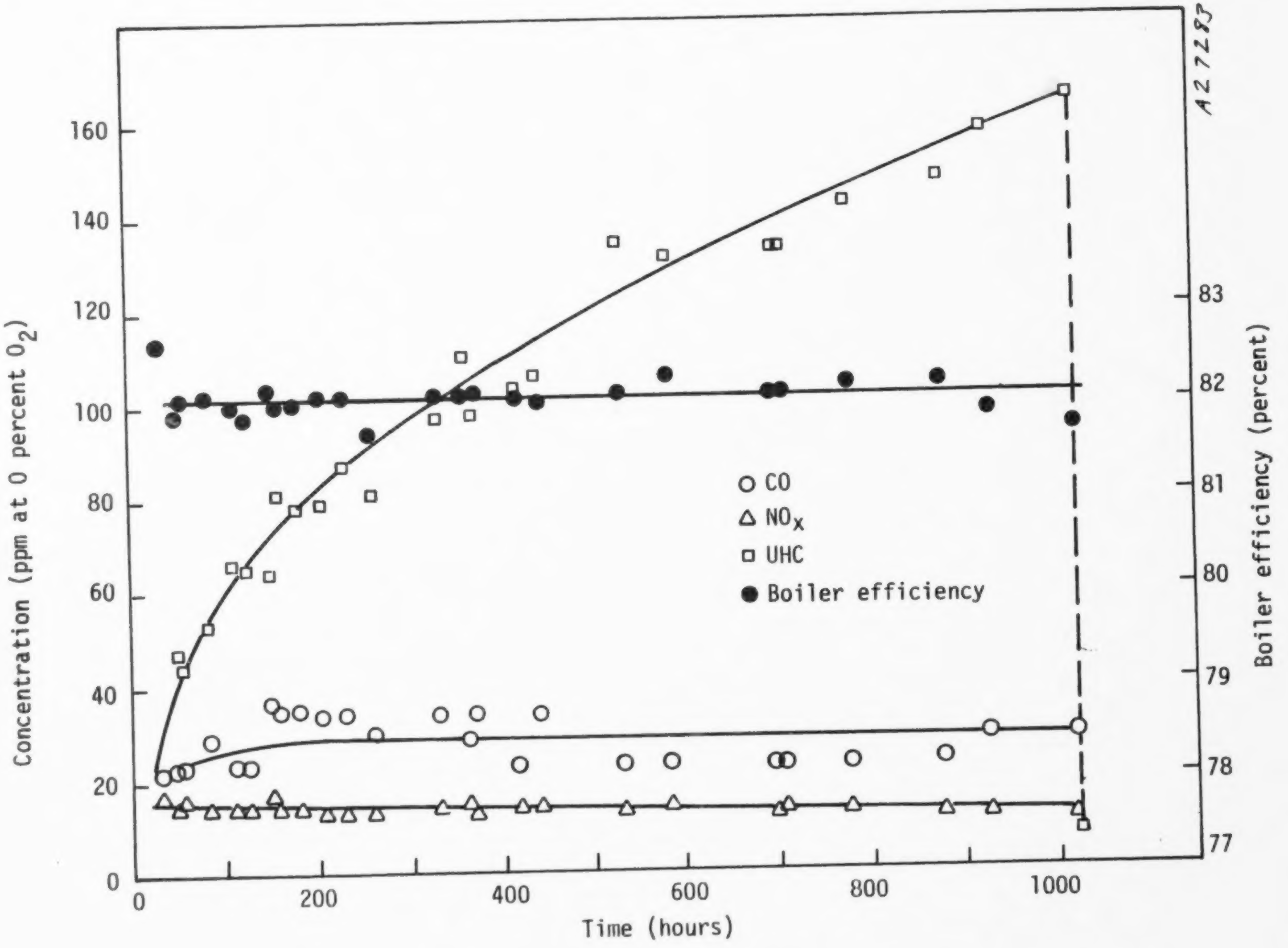

Figure 8. Fiber burner 1,000-hr durability test results.

TABLE 1. COMPARISON OF BURNER PERFORMANCE

Burner Type	Nominal Operating Point	Full Load Emissions[a] (ppmv)			Full Load Efficiency (percent)	Overfire Capability
		NO_x	CO	HC		
Fiber burner	10% EA	16	25	22	82.6	Yes
Conventional burner	30% EA	69	31	10	80.9	No

[a] At nominal operating point

ENVIRONMENTAL ASSESSMENT OF INDUSTRIAL BOILERS FIRING COAL-LIQUID MIXTURES AND WOOD

By:

L. R. Waterland, C. Castaldini, H. B. Mason, and R. DeRosier
Acurex Corporation
Energy & Environmental Division
485 Clyde Avenue
Mountain View, California 94042

"The research described in this article has been funded wholly or in part by the United States Environmental Protection Agency through contract 68-02-3188 to Acurex Corporation. It has been subjected to the Agency's required peer and policy review; however, it does not necessarily reflect the views of the Agency, and no official endorsement should be inferred."

ABSTRACT

In the past 2 years under the Combustion Modification Environmental Assessment (CMEA) program, comprehensive field tests of five small industrial boilers firing alternate fuels were performed. In these tests, flue gas emissions of NO_x, SO_2, SO_3, CO, CO_2, O_2, and particulate were measured. In addition, concentrations of inorganic elements; total volatile, semivolatile, and nonvolatile organics; and speciation for 58 organic priority pollutants including several polynuclear aromatic compounds were determined in all source effluent streams (flue gas, bottom ash, collector ash, etc.). Bioassay testing of selected streams was also performed.

The boilers tested had steam raising capacities in the 1.2 to 3.8 kg/s (10,000 to 30,000 lb/hr) range. Two were fired with a coal-oil-water mixture, one with a coal-oil mixture, and two with wood waste. The units fired with a coal-oil-water mixture were tested both with and without an additive for SO_2 capture. One unit used limestone addition; the other used soda ash. One wood-fired unit was tested firing two fuels: dry wood waste, and green wood waste.

This paper presents summary results of these tests, highlighting the effects of the use of these alternate fuels on emissions and performance.

INTRODUCTION

Industrial boiler fuels other than those traditionally burned in these units (coal, oil, and natural gas) are receiving increased attention as possible means of reducing industrial sector energy costs and reliance on uncertain energy supplies. Two classes of these, often referred to as alternate fuels, are coal-liquid mixtures (coal-oil, coal-water, and coal-oil-water mixtures) and wood.

Recent tests have sought to demonstrate the feasibility of firing various coal-liquid mixtures and resolve operational problems associated with the use of these fuels in industrial boilers. In addition, wood is seeing increasing use as an industrial boiler fuel in industries with access to dependable wood or waste wood supplies.

The projected increased use of these nontraditional boiler fuels, combined with the relative lack of emission data on units firing them, has raised questions concerning the potential environmental effects associated with their combustion. To address these questions and to establish a data base on the emission profiles from industrial boilers firing these nontraditional fuels, comprehensive field tests were performed on three coal-liquid-fuel-fired boilers and two wood-waste-fired boilers. These tests were part of a 14-site test program performed under the Combustion Modification Environmental Assessment (CMEA) program (EPA Contract No. 68-02-3188) for the Combustion Research Branch of EPA's Industrial Environmental Research Laboratory — Research Triangle Park, North Carolina. This paper summarizes results from these tests.

MEASUREMENT METHODS

The sampling and analysis protocols used in the tests conformed to a modified and extended EPA Level 1 protocol for the boiler flue gases and any discharged ash streams (1). In general, flue gas sampling was done at the boiler outlet. Grab samples were also generally taken of fuel and ash stream discharges (e.g., bottom ash and/or particle control device hopper ash).

Flue gas measurements usually performed included:

- Continuous monitors for NO_x, CO, CO_2, and O_2
- Source Assessment Sampling System (SASS) train sampling
- EPA Method 5 sampling for solid and condensible particulate emissions
- Modified Controlled Condensation System sampling for SO_2 and vapor phase SO_3
- Grab sampling for onsite gas chromatographic analyses of volatile organics with boiling points in the C_1 to C_6 range

The SASS train, shown schematically in figure 1, collects several kinds of samples for subsequent laboratory analysis. Particulate is collected in four size ranges (nominally >10 μm, 3 to 10 μm, 1 to 3 μm, and <1 μm) in heated cyclones and a filter at 230°C (450°F). Organics are collected in an organic sorbent module packed with porous polymer resin (XAD-2) and held at 60°C (140°F). Volatile inorganic elements (Hg, As, and Sb) which have not condensed on collected particulate or in the organic sorbent module are trapped in the impingers.

The general analysis protocol samples included:

- Fuel ultimate analysis
- Analyzing particulate, XAD-2 resin, impinger solutions, fuel, and ash stream samples for 70 elements using spark source mass spectrometry (SSMS) and for mercury, arsenic, and antimony using atomic absorption spectrometry (AAS) techniques
- Analyzing methylene chloride extracts of particulate, XAD-2 resin, and any ash stream samples for total organic content in two boiling point ranges: semivolatile organics with boiling points between 100° and 300°C (nominally C_7 to C_{16} organics) by total chromatographable organics (TCO) analyses, and nonvolatile organics with boiling points greater than 300°C (nominally C_{16+} organics) by gravimetry
- Obtaining infrared (IR) spectra of the gravimetric residue of all extract samples
- Analyzing all extract samples for the 58 semivolatile organic priority pollutants, including 16 polycyclic organic matter (POM) species, by gas chromatography/mass spectrometry according to EPA Method 625

If sufficient quantities were available, selected samples were subjected to bioassay testing to obtain a more direct measure of the potential environmental effects posed by source discharges. Bioassay tests which measure potential adverse health effects included the Ames mutagenicity assay, the clonal toxicity assay using Chinese hamster ovary (CHO) cells, the cytotoxicity assay using rabbit alveolar macrophage (RAM), and the whole animal toxicity (WAT) assay in rodents (2). Bioassay tests which measure potential adverse ecological effects included toxicity assays using a freshwater alga (Selenastrum capricornutum), a freshwater invertebrate (Daphnia magna), and a freshwater fish (fathead minnow — Pimephales promelas) (2).

COAL-LIQUID MIXTURE TESTS

Three industrial boilers fired with a coal-liquid mixture were tested. Two of these, site 1 and site 2, were fired with a coal-oil-water mixture (COW). The third boiler, site 3, was fired with a coal-oil mixture (COM). Design specifications for the three units tested are given in table 1.

Tests of the two COW-fired boilers were performed both with and without the addition of an additive aimed at reducing SO_2 emissions. The additive used at site 1 was limestone. Soda ash was tested at site 2. Bulk fuel compositions for each of the tests are given in table 2. As noted, the coal-liquid mixtures tested contained between 40 and 50 percent coal by weight. The COW fired at site 1 was prepared using beneficiated coal, aimed at reducing its ash content, and a mixture of No. 6 residual and No. 2

distillate oil. Only residual oil was used in preparing the coal-liquid mixtures at the other two sites.

Table 3 gives the ultimate fuel analyses for the mixtures burned during the emission testing. As noted, addition of the SO_2 control additive for the COW tests increased overall fuel ash content and decreased its heating value.

Boiler Operation

Table 4 summarizes the boiler operating parameters during the tests performed. As noted, for the tests at site 1, boiler steam load was about 75 percent of rated capacity. Excessive coke accumulation in the combustion chamber prevented operation at higher loads. In addition, some problems were experienced in maintaining a constant COW flowrate, and some fuel feed system components did not give satisfactory performance. The burner tip showed wear after 6 hr of use and needed to be replaced before each test. Plugging of the fuel feed strainer and the burner itself also occurred.

Evidence of furnace slagging and/or tube fouling was noted in the tests at site 2 in the form of steadily increasing stack temperature over the duration of a test. Stack temperatures noted in table 4 were averaged over each test's duration. Figure 2 shows the increase in stack temperature over the period of each test. As noted in the figure, stack temperature increased from about 140° to 160°C (280° to 320°F) over the 6-hr duration of the COW test. Stack temperature at the beginning of the subsequent COW with soda ash test started at about the same as that at the end of the COW test, and increased at a much more rapid rate until it exceeded 200°C (350°F) after 3 hr. This more rapid increase is attributed to a faster rate of tube fouling with the soda ash additive present. As a consequence of this rapid fouling the test of COW with soda ash additive had to be terminated after 3.5 hr.

No problems with boiler operation during the COM tests at site 3 were encountered. Significant rates of ash accumulation in the furnace and convective passes had been experienced in previous tests in this unit. However, such problems were not noted in these tests.

Flue Gas Emissions

Table 5 summarizes the flue gas compositions for each of the tests. As shown, average CO emissions for all the tests were acceptably low (<100 ppm) except for the COW with soda ash test in the firetube unit at site 2. Average emissions of CO in this test were almost 500 ppm. Evidently, with the addition of the soda ash additive, sufficient flame quenching occurred to lead to these higher CO emissions.

Emissions of NO were comparable for all the tests, falling in the 200 to 330 ng/J range. NO emissions decreased about 15 percent with the addition of the limestone additive in the COW tests at site 1 and 10 percent with the soda ash additive at site 2. This too may have been due to lower combustion temperatures attendant to injection of the inert additives.

The most surprising aspect of the data noted in table 5 is the effect on SO_2 emission of the additives, injected with the aim of reducing these emissions. The limestone sorbent at site 1 was totally ineffective in reducing SO_2 or SO_3 emissions (independent determination of SO_2 and SO_3 using EPA Method 8 gave comparable results to the controlled condensation method results cited in table 5).

However, addition of the soda ash sorbent apparently reduced SO_2 emissions over 98 percent (again, independent measurement of SO_2 emissions using a continuous monitor gave results comparable to the controlled condensation method results noted in table 5). Sulfur mass balance closure for the two soda ash additive tests was comparable, with most of the fuel inlet sulfur accounted for as SO_2 emissions without soda ash addition, and as sulfur in the particulate and boiler deposits with soda ash addition. The effectiveness of the soda ash sorbent could be due to the fact that it was mixed directly with the COW fuel, becoming dissolved in the aqueous phase of the mixture. This could lead to good contact between sorbent and vapor phase SO_2/SO_3 upon firing.

Table 6 shows the particulate size distributions measured by the SASS train at the boiler outlet for each of the tests. The size distributions for all tests, except the COW with soda ash test, are very similar: >10 μm accounting for the greatest fraction and <1 μm accounting for the smallest fraction. Indeed, the addition of limestone to the COW burned at site 1 had virtually no effect on the emitted particle size distribution. However, the addition of soda ash to the COW burned at site 2 caused a dramatic shift in particle size distribution to the submicron sizes. This would be expected if the soda ash were dissolved in the aqueous phase of the COW fuel.

Nitrous Oxide Emissions

In addition to the sampling and analysis protocol previously noted, testing at the COM-fired unit at site 3 included determination of nitrous oxide emissions (N_2O). Flue gas grab samples were collected in stainless-steel cylinders and subsequently analyzed for N_2O using a gas chromatography/electron capture detector (GC/ECD) technique adapted from studies measuring N_2O emanation from soils (3,4,5).

Two separate samples taken during the tests at site 3 gave N_2O emissions of 73 and 74.5 ppm (dry, 3 percent O_2), respectively. This result is almost 20 percent of the measured NO emissions from the boiler as noted in table 5. Sampling for N_2O has been performed in other field tests under the CMEA project (6, 7). Results of all these, shown as a a plot of N_2O versus NO emissions, are given in figure 3.

It appears from the data in figure 3 that N_2O emissions are roughly proportional to a unit's NO emissions. The data, taken from a range of combustion sources, suggest that N_2O emissions are generally about 20 to 25 percent of NO emissions.

Trace Element Emissions

As noted above, the concentrations of 73 trace elements were determined in samples collected in the tests of the boilers fired with coal-liquid mixtures. Total flue gas concentrations (the sum of levels in all samples collected by SASS train) for the 15 most significant of these are noted in table 7. Most significant here is taken to mean emitted at levels of possible environmental concern. As a measure of possible concern, the emission concentrations of the elements were compared to corresponding occupational exposure guidelines. The occupational exposure guidelines used were Threshold Limit Values (TLV's) established by the American Conference of Governmental Industrial Hygienists (ACGIH) (8) or permissible exposure limits established by the Occupational Safety and Health Administration (OSHA)(9). These comparisons are performed only to rank species with respect to possible environmental effects; no conclusions regarding absolute hazard are made, nor are warranted.

Table 7 lists those elements which had flue gas emission concentrations greater than an occupational exposure guideline from any of the sources tested, listed in order of the magnitude by which their emissions exceed the respective guideline. Of the 15 element emissions noted in the table, 10 of them (As, Cr, Ni, P, Li, Pb, V, Fe, Be, and Ba) were emitted at levels exceeding respective occupational exposure guidelines from all three boilers and all five tests performed. In addition, emission levels of the elements noted in table 7 were generally of comparable levels (usually within a factor of 2 or 3) for all the tests.

Of course, the trace element concentrations noted in table 7 correspond to samples taken at the boiler outlet. Emissions of particulate-bound elements would be decreased, perhaps by an order of magnitude, downstream of a particulate control device.

Organic Emissions

Table 8 summarizes measured organic emissions for each of the tests, by organic boiling point range: volatile organics with boiling points less than 100°C (nominally C_1 to C_6), semivolatile organics with boiling points in the 100° to 300°C range (nominally C_7 to C_{16}), and nonvolatile organics with boiling points greater than 300°C (nominally C_{16+}). Total organic species emissions from the two COW-fired units were comparable in the 10 mg/dscm range. In addition, total organic emissions increased for both these units with addition of sulfur sorbent additive.

Organic emissions from the boiler at site 1 were relatively evenly distributed by boiling point range, and increases with limestone addition occurred in all ranges. Flue gas particulate accounted for negligible amounts of emitted organics.

In contrast, emissions of semivolatile organics were negligible from the unit at site 2. Furthermore, the increase in emissions with soda ash addition is entirely attributable to an increase in particulate organic content from negligible amounts to 4 mg/dscm. This increase suggests soot formation and is consistent with the much higher CO levels noted for this test.

Organic emissions from the COM-fired boiler at site 3 were low, and almost exclusively nonvolatile organics.

Table 9 shows results of the analyses for the semivolatile organic priority pollutants, including several POM species, for each test. Of the species sought, only those noted in table 9 were detected. As shown in table 9, emissions of POM's and phenols were highest (though still quite low, generally near the detection limit of the protocol) from the unit at site 1. Naphthalene and phenanthrene were present in the greatest amounts. Only two species were detected in the samples from site 2; none were found in the samples from site 3. In addition, emissions of essentially all the species found in the site 1 samples increased with limestone addition. This increase and indeed the relative levels of these species found in all the tests, parallels the total organic emission levels noted in table 8.

Bioassay Testing

Table 10 presents results of the bioassay testing performed on samples collected in the tests of the coal-liquid-fired boilers. Both mutagenicity and cytotoxicity bioassay tests were performed on XAD-2 extracts and SASS particulate. Results in the table are consistent among tests: XAD-2 extracts were consistently of moderate to high mutagenicity and moderate or lower toxicity. Flue gas particulate was of nondetectable mutagenicity and low toxicity. This suggests that potentially hazardous flue gas species are in the vapor phase, at least at the temperature at which the particulates are collected in the SASS train (230°C).

WOOD-FIRED TESTS

Two wood-fired industrial boilers were also tested. The first of these (site 4) was a coal-fired underfeed stoker watertube unit converted to burn sawmill residue (hogged fuel and sawdust). The second boiler tested was a horizontal return tube (HRT) firetube unit originally designed to burn woodwaste. This boiler design is very popular in the forest products industry in the southeastern United States. Design data for each of the boilers tested are given in table 11. The data noted for the site 4 unit reflect its original design specifications for burning bituminous coal. After modification of this boiler for wood firing, steam capacity decreased to 3.2 kg/s (25,000 lb/hr), with decreased superheated steam temperature and pressure.

The site 4 unit collected flue gas particulate with a multicyclone mechanical collector. The site 5 unit also had a multicyclone control device; however, flyash reinjection was used on this boiler. Flue gas testing was performed downstream of these control devices.

Two tests were conducted at site 4: one in which kiln-dried mill residue was burned (dry wood), the other in which green mill residue (green wood) was burned. Dry mill residue was fired during testing at site 5. Ultimate analyses of each of the fuels fired are given in table 12. A range of composition, heating value, and moisture content is noted.

Boiler Operation

Table 13 summarizes the boiler operating parameter settings during the tests performed. As noted, the unit at site 4 was tested at between 35 (dry wood) and 50 (green wood) percent of capacity. The steam flows noted in table 13 are calculated from heat loss boiler efficiency and heat input data since plant personnel acknowledged that steam flows noted on the boiler room console were unreliable. The site 5 unit was tested at about 70 percent of capacity.

The most interesting aspect of the data noted in table 13 is the high excess air level at which each unit was operating. As a consequence, dry gas heat losses from the boilers were quite significant leading to very low boiler efficiencies, also noted in table 13. The efficiency of the site 5 unit was slightly higher due to the lower moisture content in the fuel fired.

Flue Gas Emissions

Table 14 summarizes the flue gas composition for each of the tests performed. High flue gas O_2 levels, consistent with the high excess air operation, are noted. The CO emissions from each of the boilers are also very high, in the several thousand ppm range to the 1 percent level (dry at 3 percent O_2 basis). CO emissions of these levels are generally considered undesirable from an operational standpoint for two reasons: corresponding combustibles losses limit boiler efficiency, and emissions at these levels (several thousand ppm) can represent an explosion hazard. Clearly these units were operating at such high excess air levels that flame quenching with attendant incomplete combustion was occurring. Figure 4 shows a plot of 15-min averages of NO and CO emissions versus flue gas O_2 over the duration of the two tests at site 4. The figure shows that the variation of NO and CO emissions is essentially continuous over the two tests. CO emissions are less than 1,000 ppm at flue gas O_2 less than 12 percent, but increase rapidly with increasing O_2 to over 1.5 percent at flue gas O_2 over 17 percent.

NO emissions remain relatively constant (about 200 ppm) with O_2 between 12 and 16 percent, then decrease as flue gas O_2 increases above 16 percent. This NO and CO versus O_2 behavior is consistent with flame quenching at the high O_2 levels.

Similar qualitative conclusions are drawn from the site 5 data, though absolute NO and CO levels at a given flue gas O_2 are different. NO emissions from this unit were higher than those from the site 4 unit, most likely in part due to the higher fuel nitrogen content and in part due to the lower excess air levels (less flame quenching) at which the unit was operating.

SO_2 and SO_3 emissions were measured in these tests, but were found to be negligible, consistent with the low fuel sulfur contents.

Table 15 shows the emitted particle size distribution for each of the tests. The distribution of particles in the four size ranges was relatively even for the site 4 dry wood test. A shift to larger sizes occurred with green wood firing. Most (weight basis) of the particulate emitted from the site 5 unit was in the submicron range. This might be expected from a unit which reinjected particulate collected in a cyclone collector.

Trace Element Emissions

Similar to the table 7 listing of trace element emissions from the boilers firing a coal-liquid mixture, table 16 lists those trace elements emitted from the wood-fired boiler tests at levels greater than 10 percent of their respective occupational exposure guideline. The table shows that all 11 elements noted were emitted in all three tests at levels greater than 10 percent of their occupational exposure guideline. In addition, the emission levels of the elements listed were generally comparable (within a factor of 3 or so) from test to test.

Organic Emissions

Table 17 summarizes measured organic emissions for each of the tests by organic boiling point range. As shown in the table, most of the organics emitted in each test were in the volatile range (boiling point less than 100°C). The nonvolatile range (boiling point greater than 300°C) accounted for the next greatest fraction. The relative emission levels from test to test of all the other organic categories measured parallel the relative CO emissions noted in table 14.

Flue gas particulate-bound organics were negligible at site 4; some nonvolatile species were found on the particulate from site 5.

Table 18 summarizes the organic content of the mechanical collector hopper ash from site 4. Most of the flyash organic was in the nonvolatile category. Ash organic content was essentially the same (about 700 mg/kg) for both dry and green wood combustion.

Table 19 lists the results of the analyses for the semivolatile organic priority pollutants in flue gas samples for each of the wood-fired boiler tests. The table also presents results from simultaneous tests of these units by the North Carolina Department of Natural Resources and Community Development (DNR). The North Carolina DNR performed independent tests of these units (concurrent with this study's tests) specifically aimed at quantitating POM species emissions from the boilers (10). The DNR tests employed a modified EPA Method 5 sampling train, with sorbent extract analysis by capillary column gas chromatography/flame ionization detector. Their results are presented here for comparison and validation.

As noted in the table, with a few exceptions (notably naphthalene and phenanthrene), the emission results are remarkably comparable. Naphthalene and phenanthrene appear to be emitted at greatest levels. Again, relative emission levels of the species noted in the table generally parallel relative CO and total organic emissions as noted in tables 14 and 17.

Bioassay Testing

Table 20 summarizes results of the health effects bioassay testing of flue gas samples (particulate and XAD-2 extract) and ash streams from the wood-fired boilers. Table 21 presents a corresponding summary of results of the bioassay testing of the ash stream discharges for ecological effects. Again results noted in the tables are relatively consistent among the tests. Further, the general conclusion drawn from bioassay testing of samples from the coal-liquid-fired boilers (see table 10) are confirmed in tables 20 and 21.

The XAD-2 extracts were consistently of moderate to high mutagenicity and toxicity. No other samples assayed had detectable mutagenicity.

Two particle size fractions were assayed for the green wood test at site 4. Interestingly, the fine particulate was of moderate cytotoxicity; whereas, the coarse particulate was of nondetectable to low toxicity. Ash streams (mechanical collector hopper ash and bottom ash) were also of nondetectable to low toxicity. Again, results suggest that potentially hazardous components in boiler discharges are still in the vapor phase at stack and/or particulate collection temperature.

SUMMARY

Comprehensive emissions testing was performed on two coal-oil-water mixture, one coal-oil mixture, and two wood-fired industrial boilers. The two COW-fired boilers were tested with and without additive injection aimed at reducing SO_2 emissions. One wood-fired boiler was tested burning both kiln-dried sawmill residue (dry wood) and green mill residue (green wood).

Results from the coal-liquid mixture boiler tests suggest:

- Limestone addition was ineffective in reducing SO_2 emissions
- Soda ash dissolved in the fuel mixture was very effective in reducing SO_2 emissions (greater than 98 percent SO_2 removal); however, severe fouling problems were encountered
- Additives can decrease combustion efficiency leading to increased CO and organic emissions, and soot formation, accompanied by a slight decrease in NO_x emissions

- N_2O emissions from such combustion devices appear to total about 20 to 25 percent of NO_x emissions

- Arsenic, chromium, nickel, phosphorous, lithium, lead, and vanadium represent the trace elements emitted at levels of greater potential concern than others

- Naphthalene and phenanthrene are the major, often the only, polycyclic organic matter compounds emitted

- Most of the potentially hazardous species in the flue gas are in vapor phase at stack and/or particulate collection temperatures as evidenced by the fact that organic sorbent extract was consistently of moderate to high mutagenicity and toxicity in bioassay tests, while stack particulate was of consistently nondetectable mutagenicity and nondetectable to low toxicity

Results from the wood-fired boiler tests suggest:

- Such units, under as-found operation, may be operating at very low efficiency due to very high excess air settings. Such operation gives high (up to over 1 percent) CO and high organic emissions. Under such operation, CO and organic species emissions increase with increasing excess air.

- Flyash reinjection shifts particulate emissions to finer size ranges

- Nickel and phosphorous represent the trace elements emitted at levels of greater potential concern

- Under high excess air operation volatile organics (boiling points <100°C) account for the greatest fraction of organic species emissions

- Naphthalene is the POM species emitted in greatest quantity (µg/dscm) by far. Emission levels of phenanthrene and pyrene appear to be the next highest

- Potentially hazardous flue gas species also appear to be largely in the vapor phase at stack and/or particulate collection temperatures, and to partition to fine particulate as evidenced by bioassay testing. Organic sorbent extracts are of consistently moderate to high mutagenicity and toxicity. Fine (<3 µm) particulate was of moderate toxicity while coarse (>3 µm) or composite particulate was of nondetectable to low toxicity. Ash streams (mechanical collector hopper ash and bottom ash) were of nondetectable to low toxicity.

ACKNOWLEDGMENTS

This work is supported by EPA under Contract 68-02-3188. Robert E. Hall is the EPA Project Officer. The assistance of various Acurex field test crews, all supervised by B. C. DaRos, is gratefully acknowledged. The authors also wish to recognize the great support and cooperation of all the host site personnel, too numerous to mention here, who kindly supplied access to test facilities and accepted the inconveniences associated with field tests of the type performed. Their support was critical to the success of the program.

REFERENCES

1. Lentzen, D. E., et al. IERL-RTP Procedures Manual: Level 1 Environmental Assessment (Second Edition). EPA-600/7-78-201 (NTIS PB 293795), U.S. EPA, Industrial Environmental Research Laboratory, Research Triangle Park, North Carolina, October 1978.

2. Brusick, D. J., and R. R. Young. IERL-RTP Procedures Manual: Level 1 Environmental Assessment, Biological Tests. EPA-600/8-81-024 (NTIS PB 228966), U.S. EPA, Industrial Environmental Research Laboratory, Research Triangle Park, North Carolina, October 1981.

3. Seiler, W., and R. Conrad. Field Measurement of Natural and Fertilizer-Included N_2O Release Rates from Soils. J. APCA, 31(7):767-772, 1981.

4. Conrad, R., and W. Seiler. Field Measurement of the Loss of Fertilizer Nitrogen into the Atmosphere as Nitrous Oxide. Atmospheric Environment, 14:555-558, 1980.

5. Banna, S. M., and M. C. Branch. Gas Chromatographic Determination of Nitrogenous Species in Combustion Products. Combustion Science and Technology, 24:15-22, 1980.

6. Castaldini, C., et al. Environmental Assessment of Industrial Process Combustion Equipment Modified for Low-NO_x Operation. Presented at the 1982 Joint Symposium on Stationary Combustion NO_x Control, Dallas, November 1982.

7. Acurex Corporation. Unpublished data. Mountain View, California, 1982.

8. American Conference of Governmental Industrial Hygienists. Threshold Limit Values for Chemical Substances and Physical Agents in the Work Environment with Intended Changes for 1982. Cincinnati, Ohio, 1982.

9. OSHA Safety and Health Standards. 29 CFR 1910, Subpart Z.

10. Wainwright, P. B., et al. A POM Emissions Study for Wood-Fired Boilers. North Carolina Department of Natural Resources and Community Development, Raleigh, North Carolina, 1982.

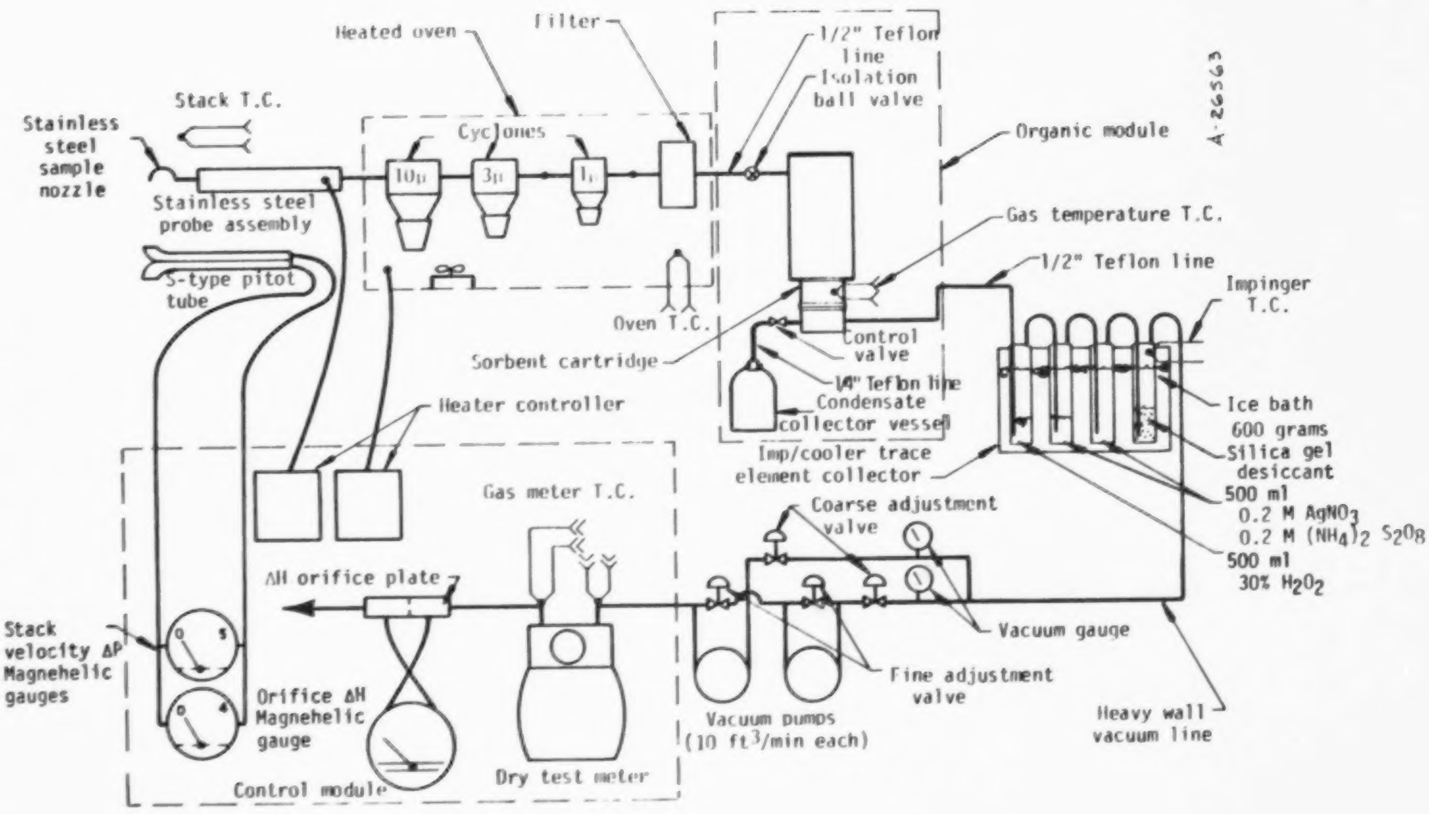
Stainless steel sample nozzle
Stack T.C.
Stainless steel probe assembly
S-type pitot tube
Heated oven
Cyclones
10μ
3μ
1μ
Filter
Oven T.C.
1/2" Teflon line
Isolation ball valve
Organic module
A-26563
Gas temperature T.C.
Sorbent cartridge
Control valve
1/4" Teflon line
Condensate collector vessel
Imp/cooler trace element collector
1/2" Teflon line
Impinger T.C.
Ice bath
600 grams Silica gel desiccant
500 ml 0.2 M AgNO3 0.2 M (NH4)2 S2O8
500 ml 30% H2O2
Heater controller
Gas meter T.C.
Coarse adjustment valve
Vacuum gauge
Fine adjustment valve
Heavy wall vacuum line
Vacuum pumps (10 ft3/min each)
ΔH orifice plate
Dry test meter
Stack velocity ΔP Magnehelic gauges
Orifice ΔH Magnehelic gauge
Control module

Figure 1. Schematic of SASS train.

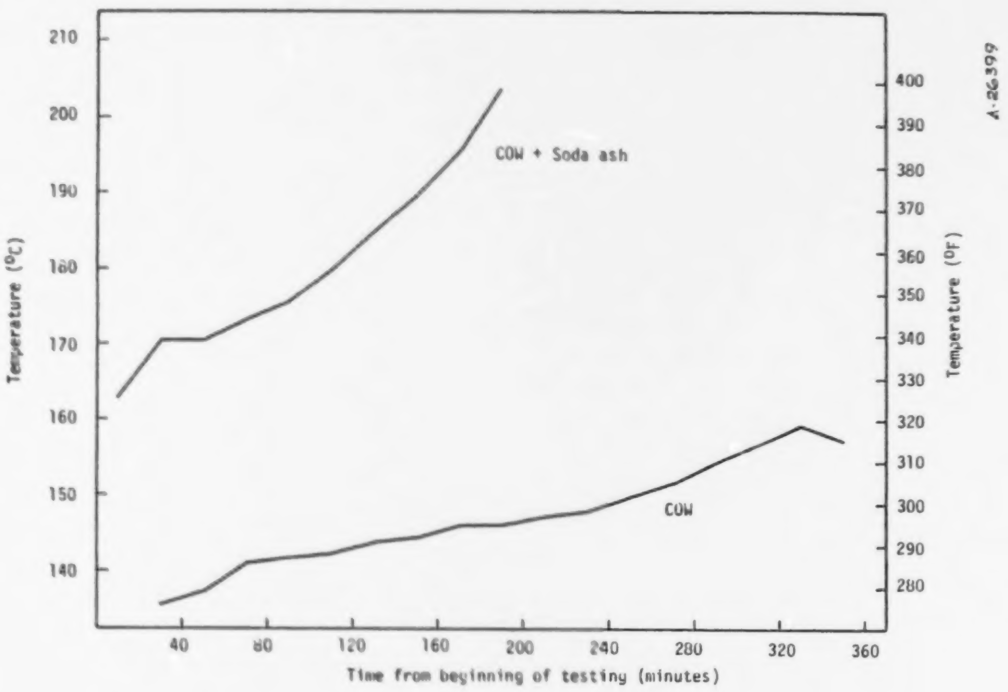

Figure 2. Stack gas temperatures: Site 2 COW tests.

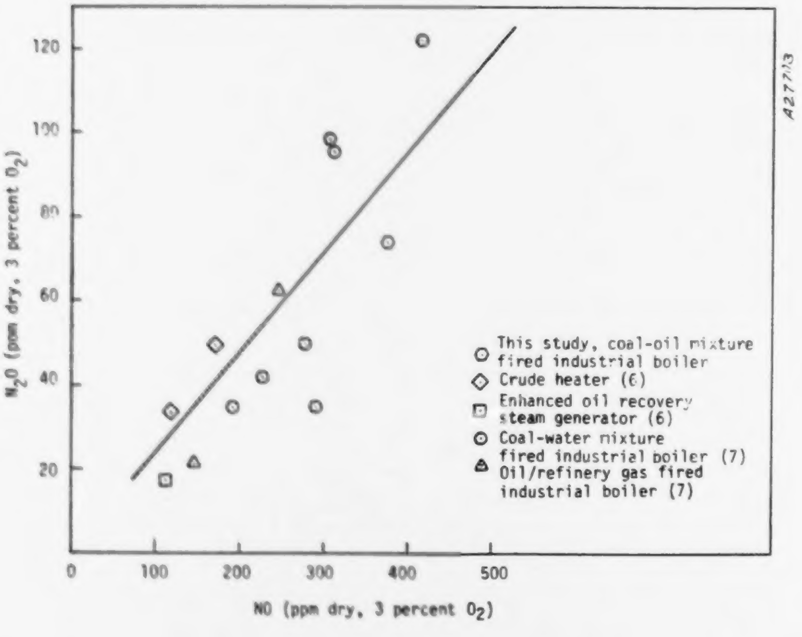

Figure 3. N_2O emissions from combustion sources as a function of NO emissions.

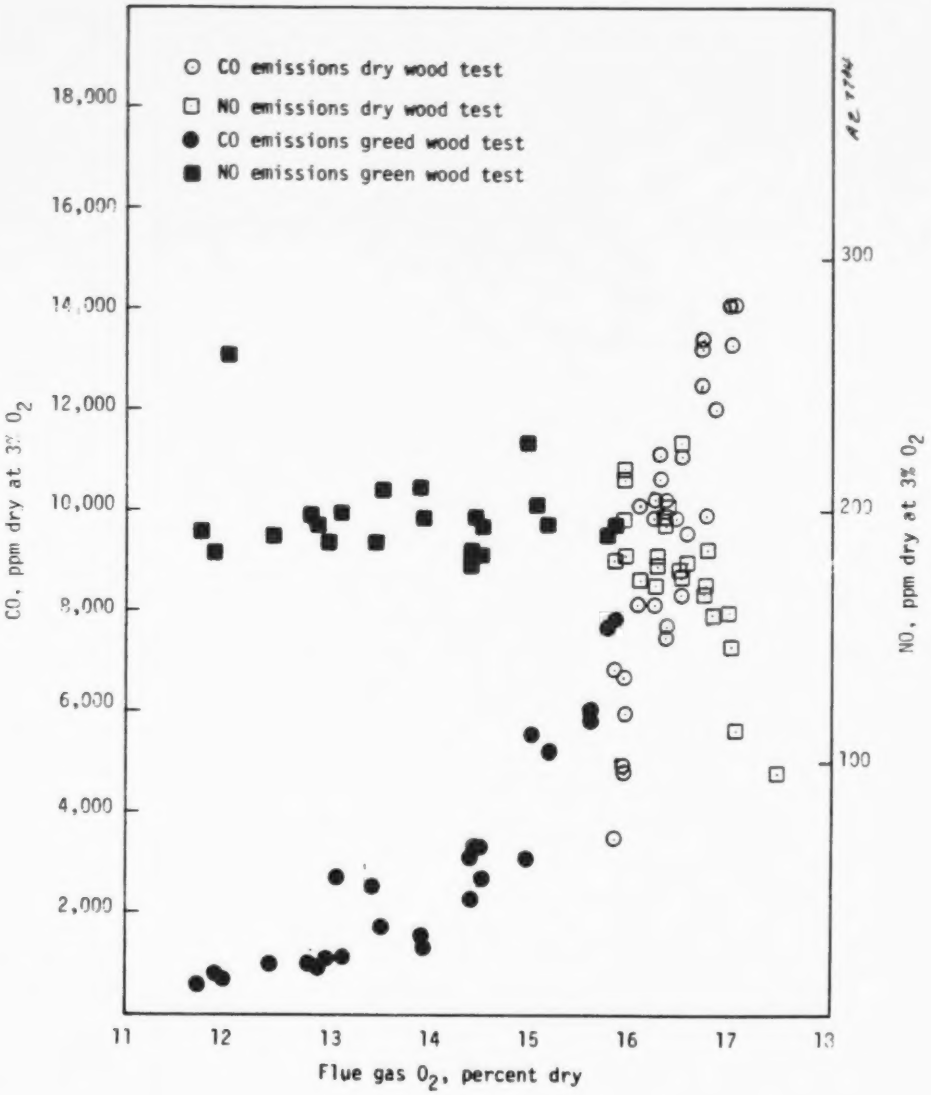

Figure 4. CO and NO versus O_2 for the site 4 tests.

TABLE 1. BOILER DESIGN DATA: COAL-LIQUID FUEL TESTS

	Site 1 (COW)	Site 2 (COW)	Site 3 (COM)
Manufacturer	York-Shipley	Cleaver Brooks	Nebraska Boiler
Design	Firetube	Firetube	D-type watertube
Steam flow, kg/s (lb/hr)	1.14 (9,000)	1.52 (12,000)	3.03 (24,000)
Steam temperature, °C (°F)	185 (365)	185 (365)	190 (375)
Steam pressure, MPa (psig)	1.03 (150)	1.03 (150)	1.2 (175)

TABLE 2. BULK FUEL COMPOSITION: COAL-LIQUID FUEL TESTS

	Site 1		Site 2		Site 3
Bulk Composition (percent by weight)	COW	COW and Limestone	COW	COW and Soda Ash	COM
Coal	50[a]	38[a]	42	38.6	41.5
Oil	30[b]	25[b]	42	39.2	58.5
Water	20	15	16	14.5	—
Additive	—	22	—	7.7	—

[a] Beneficiated coal

[b] Oil for this site is mixture of No. 6 (75 percent by weight) and No. 2 (25 percent by weight)

TABLE 3. FUEL ULTIMATE ANALYSES: COAL-LIQUID FUEL TESTS

Ultimate Analysis (percent by weight, dry basis except as noted)	Site 1		Site 2		Site 3
	COW	COW and Limestone	COW	COW and Soda Ash	COM
Carbon, C	80.7	63.1	78.0	71.8	80.5
Hydrogen, H	7.1	5.5	8.6	7.8	8.1
Nitrogen, N	0.5	0.5	0.8	0.7	0.9
Sulfur, S	5.2	3.5	1.9	1.9	1.5
Oxygen, O[a]	0.7	0.5	6.7	4.6	3.3
Ash	5.8	26.9	4.0	13.2	5.7
Moisture[b]	19.6	18.0	15.6	15.5	1.2
Higher heating value,[b] MJ/kg (Btu/lb)	29.91 (12,870)	23.41 (10,070)	31.41 (13,490)	26.95 (11,580)	37.74 (16,240)

[a] By difference
[b] As fired

TABLE 4. BOILER OPERATING CONDITIONS: COAL-LIQUID FUEL TESTS

Parameter	Site 1		Site 2		Site 3
	COW	COW and Limestone	COW	COW and Soda Ash	COM
Heat input, MW (10^6 Btu/hr)	2.87 (9.8)	2.95 (10.1)	3.78 (12.9)	3.22 (11.0)	8.30 (28.4)
Steam flow, kg/s (lb/hr)	0.84 (6,700)	0.83 (6,600)	[b]	[b]	3.03 (24,000)
Excess air, percent	41	49	17	14	15
Stack temperature, °C (°F)	218 (425)	210 (410)	146[a] (295)	181[a] (357)	268 (515)

[a] Average over test
[b] Unit produced hot water, about 19 l/s (300 gal/min) at about 120°C (250°F) during tests performed

TABLE 5. FLUE GAS EMISSIONS: COAL-LIQUID FUEL TESTS

	Site 1		Site 2		Site 3
Species	COW	COW and Limestone	COW	COW and Soda Ash	COM
O_2, percent dry	6.1	6.5	3.3	3.2	3.0
CO_2, percent dry	12.6	12.2	13.6	13.0	13.8
CO, ppm dry at 3 percent O_2	86	76	25	426	38
(ng/J)	(30)	(27)	(11)	(195)	(15)
NO_x, ppm dry at 3 percent O_2	454	392	477	427	376
(ng/J as NO_2)	(271)	(220)	(332)	(330)	(252)
SO_2, ppm dry at 3 percent O_2	2,680	3,070	1,090	14	749
(ng/J)	(2,110)	(2,540)	(1,060)	(14)	(698)
SO_3, ppm dry at 3 percent O_2	13	41	0.60	0	7.6
(ng/J)	(13)	(42)	(0.74)	0	(8.9)
Particulate, mg/dscm	3,910	4,520	1,970[a]	3,720[a]	1,380
(ng/J)	(1,470)	(1,700)	(722)	(1,460)	(484)

[a] Particulate as measured by SASS instead of Method 5. Method 5 not performed for COW test; for COW and soda ash test, Method 5 result was the same as SASS: 3,720 μg/dscm (1,460 ng/J).

TABLE 6. FLUE GAS PARTICLE SIZE DISTRIBUTION: COAL-LIQUID FUEL TESTS

	Site 1		Site 2		Site 3
Percent by Weight in Size Range (μm)	COW	COW and Limestone	COW	COW and Soda Ash	COM
>10	46	48	42	27	55
3 to 10	39	39	29	1	31
1 to 3	10	9	24	3	12
<1	5	4	5	69	2

TABLE 7. TRACE ELEMENT EMISSIONS: COAL-LIQUID FUEL TESTS

	Site 1		Site 2		Site 3	
Element	COW (μg/dscm)	COW and Limestone (μg/dscm)	COW (μg/dscm)	COW and Soda Ash (μg/dscm)	COM (μg/dscm)	Occupational Exposure Guideline[a] (μg/m^3)
Arsenic, As	3,300	4,500	160	89	29	10[b]
Phosphorous, P	3,400	4,600	2,000	850	3,600	100
Chromium, Cr	1,300	1,200	1,100	400	1,700	50
Nickel, Ni	690	1,500	1,000	650	1,200	100
Lithium, Li	86	29	110	33	300	22
Lead, Pb	1,300	1,300	780	930	560	150
Copper, Cu	1,300	1,800	130	140	300	200
Vanadium, V	3,400	4,400	920	680	1,300	500
Iron, Fe	4,300	5,600	2,700	5,300	4,800	1,000
Beryllium, Be	12	9.1	12	2.6	13	2.0
Titanium, Ti	7,300	4,600	2,000	1,700	36,000	6,000
Cobalt, Co	84	87	29	9.7	280	50
Barium, Ba	2,600	2,000	1,200	1,100	1,200	500
Potassium, K	2,900	4,800	1,500	1,200	3,600	2,000
Antimony, Sb	52	110	5.5	0.34	6.2	50

[a] Threshold Limit Value (8) unless noted
[b] OSHA permissible exposure limit (9)

TABLE 8. TOTAL ORGANIC EMISSIONS: COAL-LIQUID FUEL TESTS

	Site 1		Site 2		Site 3
Organic Category	COW (mg/dscm)	COW and Limestone (mg/dscm)	COW (mg/dscm)	COW and Soda Ash (mg/dscm)	COM (mg/dscm)
Volatile organics (C_1 to C_6)	7	19	3.8	4.1	0.06
Semivolatile organics (C_7 to C_{16})	1.0	6.7	<0.04	<0.02	<0.05
Nonvolatile organics (C_{16}+)					
Particulate	<1	<1	<0.3	4.0	<0.6
Sorbent module	4.1	6.8	2.9	5.0	0.3
Total	4.1	6.8	2.9	9.0	0.3
Total	12	33	6.7	13.1	0.36

TABLE 9. POLYCYCLIC ORGANIC MATTER (POM) EMISSIONS: COAL-LIQUID FUEL TESTS

	Site 1		Site 2		Site 3
Species	COW (μg/dscm)	COW and Limestone (μg/dscm)	COW (μg/dscm)	COW and Soda Ash (μg/dscm)	COM (μg/dscm)
Acenaphthene	0.8	3.0	<0.05	<0.2	<0.05
Acenaphthylene	<0.1	2.0	<0.05	<0.2	<0.05
Anthracene	0.2	1.0	<0.05	<0.2	<0.05
Benz(a)anthracene	0.1	<0.1	<0.05	<0.2	<0.05
Chrysene	0.2	0.6	<0.05	<0.2	<0.05
Fluoranthene	0.3	0.6	0.05	<0.2	<0.05
Fluorene	2.0	7.0	<0.05	<0.2	<0.05
Naphthalene	41	110	<0.05	<0.2	<0.05
Phenanthrene	4.9	17	0.1	0.7	<0.05
Pyrene	0.2	0.6	<0.05	<0.2	<0.05
Phenol	2.8	12	<0.05	<0.2	<0.05
2,4-Xylenol	<0.1	4.0	<0.05	<0.2	<0.05

TABLE 10. BIOASSAY RESULTS: COAL-LIQUID FUEL TESTS

	Bioassay[a]		
Test/Sample	Ames Mutagenicity	CHO Cytotoxicity	RAM Cytotoxicity
Site 1			
XAD-2 extract			
COW	M	M	—
COW and limestone	M	M/L	—
SASS Particulate			
COW	ND	—	L
COW and limestone	ND	—	L
Site 2			
XAD-2 extract			
COW	H/M	M	—
COW and soda ash	H	≤M	—
Site 3			
XAD-2 extract	H	≤M	—
SASS particulate	ND	—	L

[a]H: High mutagenicity/toxicity
M: Medium mutagenicity/toxicity
L: Low mutagenicity/toxicity
ND: Nondetectable mutagenicity/toxicity
--: Assay not performed

TABLE 11. BOILER DESIGN DATA: WOOD FUEL TESTS

	Site 4[a]	Site 5
Manufacturer	Wickes	McBurney
Design	Stoker Watertube	HRT Firetube
Steam flow, kg/s	6.3	2.5
(lb/hr)	(50,000)	(20,000)
Steam temperature, °C	338	185
(°F)	(640)	(365)
Steam pressure, MPa	1.7	1.0
(psig)	(250)	(150)
Particulate control	Multicyclone	Multicyclone, total flyash reinjection

[a]Original coal-fired stoker design specification

TABLE 12. FUEL ULTIMATE ANALYSES: WOOD FUEL TESTS

Ultimate Analysis (percent by weight as fired)	Site 4		
	Dry Wood	Green Wood	Site 5
Carbon, C	45.27	35.07	44.91
Hydrogen, H	5.44	3.60	5.42
Nitrogen, N	0.12	1.10	0.17
Sulfur, S	0.04	0.02	0.04
Oxygen, O[a]	37.78	26.06	43.33
Ash	0.33	1.29	0.47
Moisture	11.02	33.85	5.66
Higher heating value, MJ/kg (Btu/lb)	17.9 (7,720)	13.3 (5,740)	18.9 (8,140)

[a] By difference

TABLE 13. BOILER OPERATING CONDITIONS: WOOD FUEL TESTS

Parameter[a]	Site 4		
	Dry Wood	Green Wood	Site 5
Heat input, MW (10^6 Btu/hr)	5.1[b] (17.5)	7.3[b] (24.8)	10.3[b] (35.1)
Steam flow, kg/s (lb/hr)	1.1[c] (8,400)	1.6[c] (13,000)	1.7 (13,600)
Excess air, percent	387	213	165
Stack temperature, °C (°F)	227 (440)	224 (435)	343 (650)
Boiler efficiency,[d] percent	55.3	61.3	69.4

[a] Average over test
[b] Calculated from stack gas flow and O_2
[c] Calculated from efficiency and heat input
[d] Heat loss method

TABLE 14. FLUE GAS EMISSIONS: WOOD FUEL TESTS

Species[a]	Site 4		
	Dry Wood	Green Wood	Site 5
O_2, percent dry	16.4	13.9	13.1
CO, ppm dry at 3 percent O_2 (ng/J)	9,810 (3,690)	2810 (1,080)	63 to 9,200[b] (18 to 2,670)
NO, ppm dry at 3 percent O_2 (ng/J as NO_2)	175 (108)	194 (123)	305 (146)
Particulate, mg/dscm (ng/J)	180 (220)	330 (270)	180 (100)

[a] Average over test
[b] Excessive variation precluded average

TABLE 15. FLUE GAS PARTICLE SIZE DISTRIBUTION: WOOD FUEL TESTS

Percent by Weight in Size Range (μm)	Site 4		
	Dry Wood	Green Wood	Site 5
>10	30	47	23
3 to 10	23	29	16
1 to 3	15	8	10
<1	32	16	51

TABLE 16. TRACE ELEMENT EMISSIONS: WOOD FUEL TESTS

Element	Site 4 Dry Wood (μg/dscm)	 Green Wood (μg/dscm)	Site 5 (μg/dscm)	Occupational Exposure Guideline[a] ($\mu g/m^3$)
Silver, Ag	790	14	1.9	10
Nickel, Ni	120	290	190	100
Phosphorous, P	160	280	120	100
Barium, Ba	160	330	190	500
Potassium, K	300	1,300	400	2,000
Iron, Fe	190	470	140	1,000
Sodium, Na	720	370	730	2,000
Chromium, Cr	8.2	17	15	50
Lead, Pb	5.2	18	45	150
Copper, Cu	11	59	32	200
Cobalt, Co	5.6	0.79	11	50

[a] TLV (8)

TABLE 17. TOTAL ORGANIC EMISSIONS: WOOD FUEL TESTS

Organic Category	Site 4 Dry Wood (mg/dscm)	Site 4 Green Wood (mg/dscm)	Site 5 (mg/dscm)
Volatile organics[a] (C_1 to C_6)	84	43	5.0
Semivolatile organics (C_7 to C_{16})	6.2	0.71	<0.01
Nonvolatile organics (C_{16}+)			
Particulate	<0.3	<0.3	0.4
Sorbent module	9.5	1.4	0.3
Total	9.5	1.4	0.7
Total	100	45	5.7

[a] Average over test

TABLE 18. TOTAL ORGANIC CONTENT OF ASH STREAM SAMPLES

Organic Category	Site 4 Mechanical Collector Hopper Ash Dry Wood (mg/kg)	Site 4 Mechanical Collector Hopper Ash Green Wood (mg/kg)
Semivolatile organics (C_7 to C_{16})	20	20
Nonvolatile organics (C_{16}+)	700	650
Total	720	670

TABLE 19. POLYCYCLIC ORGANIC MATTER (POM) EMISSIONS: WOOD FUEL TESTS

	Site 4 (μg/dscm)						Site 5 (μg/dscm)		
	Dry Wood			Green Wood					
	DNR[a]			DNR[a]			DNR[a]		
Species	Run 1	Run 2	This Study	Run 1	Run 2	This Study	Run 1	Run 2	This Study
Acenaphthalene	NA[b]	NA	0.5	NA	NA	—	NA	NA	—
Acenaphthene	NA	NA	—	NA	NA	0.1	NA	NA	—
Acenaphthylene	NA	NA	—	NA	NA	5.2	NA	NA	0.3
Anthracene	—[c]	—	—	0.52	—	0.20	—	—	—
Benzo(a)anthracene	0.15	—	—	0.12	0.65	—	—	—	—
Benzofluoranthenes	0.29	—	0.10	—	—	—	—	—	—
Benzo(a)pyrene	<0.21	—	—	0.10	—	—	—	—	—
Chrysene	—	—	—	0.20	—	0.04	—	—	—
Fluoranthene	—	—	—	—	0.53	0.30	—	—	0.08
Fluorene	—	—	0.65	—	—	—	—	—	—
Indeno(1,2,3,-cd)pyrene	—	—	—	0.51	—	—	—	—	—
3-Methylcholanthrene	—	—	—	0.17	—	—	—	—	—
Naphthalene	51.7	63.9	4.5	21.9	44.8	—	6.34	0.85	3.3
Phenathrene	—	—	7.0	—	—	2.0	—	—	0.30
Pyrene	—	—	0.30	3.7	4.8	0.20	—	0.30	0.20
Phenol	NA	NA	4.7	NA	NA	0.96	NA	NA	0.38
Detection limit	0.05	0.45	0.05	0.02	0.16	0.04	0.12	0.08	0.04

[a] (10)
[b] NA: Species not analyzed
[c] —: Concentration below detection limit

TABLE 20. HEALTH EFFECTS BIOASSAY RESULTS: WOOD FUEL TESTS

	Bioassay[a]			
Test/Sample	Ames Mutagenicity	CHO Cytotoxicity	RAM Cytotoxicity	Whole Animal Toxicity
Site 4 Dry Wood				
XAD-2 extract	H/M	H	—	—
SASS particulate	ND	—	—	—
Mechanical collector hopper ash	ND	—	L/ND	ND
Site 4 Green Wood				
XAD-2 extract	H	H	—	—
<3 μm particulate	ND	—	M	—
>3 μm particulate	ND	—	L/ND	—
Mechanical collector hopper ash	ND	—	ND	ND
Site 5				
XAD-2 extract	H	M	—	—
SASS particulate	ND	—	L	—
Bottom ash	ND	—	L/ND	ND

[a]H: High mutagenicity/toxicity
M: Moderate mutagenicity/toxicity
L: Low mutagenicity/toxicity
ND: Nondetectable mutagenicity/toxicity
—: Assay not performed

TABLE 21. ECOLOGICAL EFFECTS BIOASSAY RESULTS: WOOD FUEL TESTS

	Bioassay[a]		
Test/Sample	Freshwater Alga	Freshwater Invertebrate	Freshwater Fish
Site 4 Dry Wood			
Mechanical collector hopper ash	L	L/ND	ND
Site 4 Wet Wood			
Mechanical collector hopper ash	L	L/ND	—
Site 5 Bottom ash	L	L/ND	ND

[a]L: Low toxicity
ND: Nondetectable toxicity
—: Assay not performed

EMISSION CHARACTERIZATION FOR A RESIDENTIAL FLUIDIZED-BED WOOD-CHIP BURNER

By:

Robert S. Truesdale
Research Triangle Institute
P. O. Box 12194
Research Triangle Park, North Carolina 27709

ABSTRACT

NO_x and hydrocarbon emissions from residential wood and coal stoves, and from industrial wood-fired boilers, are compared with those from a novel residential wood-chip-fired heating system. Combustion conditions and fuel properties influencing NO_x and hydrocarbon emissions are identified. The most important factors influencing NO_x emission levels are fuel nitrogen content, temperature, and combustion efficiency. Hydrocarbon emissions are affected by temperature and combustion efficiency.

INTRODUCTION

The use of wood stoves for residential heating has become increasingly popular in recent years. Wood stoves have been installed at the rate of one million per year since 1977,[1] and the trend is expected to continue because of the rising cost of oil and gas, and the increased awareness of the need to find an alternative to these nonrenewable fuels. In some areas where heating with wood is prevalent, increase in residential wood combustion has been associated with a significant decline in air quality.[2-6] In general, emissions from wood stoves and other residential heating sources are not controlled by regulation.[7]

The species of emissions from the combustion of solid fuels for residential space heating that are of primary concern are particulates, volatile hydrocarbons, and carbon monoxide--products of incomplete combustion.* On an equivalent heating value basis (e.g., per Btu input), wood combustion emissions are generally higher from residential sources than from other combustion units (such as industrial boilers) because of the relatively low combustion efficiency of most residential units, and typical operating conditions which are conducive to incomplete combustion.[8] In addition, industrial combustion units are often equipped with pollution control equipment, such as multiple cyclones, for particulate emission reduction.[9]

---

*NO_x emissions from residential solid-fuel-fired heaters are of lesser concern, but in areas with high densities of fireplaces or wood stoves, the NO_x emissions from these sources could significantly increase the total NO_x levels for an area.

Formation of nitrogen oxides (NO_x) is dependent upon fuel nitrogen content, the amount of air introduced into the combustor, combustion temperature, and type of combustion equipment.[8] Total NO_x emissions from residential combustion of wood are substantially lower than total emissions from residential heating units fueled with oil and gas,[8] reflecting the greater use of the more conventional fuels and greater NO_x emissions per Btu.

The purpose of this study was to measure NO_x and hydrocarbon emissions from a residential wood-chip furnace system, and to compare these emissions with those from a residential wood stove, a residential coal stove, and industrial wood-fired boilers.

EQUIPMENT AND MATERIALS

Figure 1 shows schematically the key features of the tested residential heating system, which utilized a fluidized-bed combustor. The system consists of five basic components:

1. A wood feed conveyor.
2. A fluidized-bed furnace with a 14-inch* diameter sand bed with an expanded bed height of 7 inches, a gas/water heat exchanger, and a forced draft fan.
3. A fabric filter using a 5-inch diameter, inside-out flow, shaker-cleaned filter bag, a removable ash container, and an induced-draft fan.
4. A water heater to supply hot water to the residence. The water is heated by both a gas-fired and a wrap-around heat exchanger using the hot water output of the fluidized-bed furnace. Valves are provided to bypass the hot water heat exchanger.
5. An auxiliary heater for supplying space heat to the residence when the wood system is not operating. The auxiliary heater incorporates a circulating water pump. Valves are provided to include or bypass the fludized-bed heat exchanger.

The advantage of this system is that by using small pieces of wood (i.e., wood chips) the flow rate of wood can be controlled. The system also permits control of excess air in the combustion process, resulting in both maximum recovery of the wood heating value and reduced emissions.

---

*To convert to centimeters, here and elsewhere in this paper, multiply inches by 2.54.

In addition to the fludized-bed mode, the furance was also modified for combustion in a cyclone mode. During the fluidized-bed mode, wood was fed through a tube in the center of the furnace vessel and dropped onto the particles of the fluid sand bed, where combustion took place. In the cyclone mode, the fluidized-bed was removed and replaced with a cyclone burner; wood was fed through a forced-draft fan and blown into the cyclone burner where it was combusted. The fuel that was used in these tests was chipped pine; the chips were approximately 1/4 to 1/2 inch in length.

For the wood stove tests, the stove used was a free-standing, air-jacketed design with a simple open firebox. Originally designed as a fireplace insert, this type of stove is being installed in increasing numbers of new residences. Dry oak wood, split and round, was used as the fuel. Tests were also conducted using bituminous coal as the stove fuel. During the wood stove tests, emission sampling was limited to a steady-state period, defined by stove heat output calculated from air temperatures at the air jacket outlets. Steady-state sampling was chosen because the purpose of this study was to compare emissions from a residential heating unit from different fuels, and start-up and shutdown conditions were deemed too variable for reproducible testing from fuel to fuel. It should be noted that by ignoring the start-up period, emission factors are lower than if this period was included in the sampling period. Steady-state conditions were maintained by adjusting drafts as necessary and charging fuel as necessary when heat output dropped.

A modified Method 5 sampling system[10] was used to sample organic and particulate emissions during each test. These samples were extracted per the standard EPA procedure and analyzed for total organics using gas chromatography. This sampling and analysis was carried out according to EPA's trial protocol for wood stove emission testing.[10] In addition, continuous analysis of NO_x was performed during each test by using a photoluminescent detector. Detailed discussions of these sampling and analytical techniques may be found elsewhere.[10,11,12]

For all tests, the devices were allowed to reach steady-state operating conditions, as defined by the heat output calculated from air jacket blower outlet temperatures during the test, prior to sampling. Duplicate tests were conducted for each type of equipment and fuel (wood stove--wood and coal; fluidized-bed and cyclone--wood chips). Two tests were also conducted in the fluidized-bed mode with bag filters for filtration of particulate in place. In the following discussion, emission factors and rates for each fuel represent the average of the two duplicate tests, except where indicated otherwise.

RESULTS

In general, the residential wood-chip furnace that was tested in this study was successful in reaching the goals of higher efficiency and lower emissions than the conventional wood-fired heating devices. Table 1 is a listing of important operating parameters for the units tested.

TABLE 1. OPERATING PARAMETERS

	Bed/firebox temperature (°C)	Stack temp. (°C)	Flue gas flow rate (scm/hr)	Fuel consumption (kg/hr)
Wood-chip furnace				
Fluidized-bed	861	76	52.0	3.84
Cyclone	953	86	44.9	3.66
Wood stove	526	267	56.6	4.25
Coal stove	531	312	49.5	1.50

NO_x Emissions

Figure 2 is a comparison of average NO_x emission factors from six fluidized-bed tests, two cyclone tests, two wood stove tests with oak logs, two wood stove tests with bituminous coal, and those typical from industrial boilers.[13] NO_x emission factors for the fluidized-bed and for the cyclone tests are both fairly low, with the cyclone test having slightly higher NO_x emissions, on the average, than the fluidized-bed test.

Examination of Figure 2 shows that NO_x emission factors from the fluidized-bed furnace and the cyclone are slightly higher than those measured in a conventional woodstove and are within the range reported for industrial wood boilers (0.1-1.2 g/kg).[13,14] Because the wood combustors represented in this table vary greatly in their firebox temperatures (526°-1100°C) and probably excess air percentages, it appears that for wood combustion in general the predominant factor influencing NO_x within the range reported above being influenced by the degree of thermal NO_x formation.

Bituminous coal was also combusted in the wood stove, and resulting emissions were measured. Examination of Figure 2 shows that NO_x emissions were significantly higher per unit weight of fuel in the coal stove test than they were in any of the residential wood-fired heating appliance tests. On an energy content basis, coal is still higher in NO_x emissions than any of the wood-fired units, although by not as great a margin (131.7 μg/kJ for coal stove vs. 92.3 μg/kJ for cyclone furnace). The higher NO_x levels for coal were primarily due to the amount of fuel nitrogen in the coal versus that in wood. The coal used in these tests had a nitrogen content of 0.93 percent, versus a nitrogen content of 0.45 percent for the oak logs tested in the wood stove.

Hydrocarbon Emissions

Examination of Figure 3 shows that hydrocarbon emission levels from a coal stove are comparable to those from a wood stove but are much higher than those from industrial boilers. The wood-chip combustion unit was effective in reducing total hydrocarbon emissions over those from wood or coal combustion in a wood stove. With respect to hydrocarbon emission factors, the cyclone-firing mode was much more efficient, in reducing total hydrocarbon emissions, than the fluidized-bed combustion mode (Figure 3). This is probably due to more efficient air/fuel mixing in the cyclone mode than in the fluidized-bed mode. During fluidized-bed combustion, wood chips were dropped onto the surface of the fluidized-bed where combustion apparently took place. This combustion was not complete, as evidenced by the runs with filter bags during which the particulate collected in the bags was observed to have considerable amounts of partially combusted wood in the form of carbon particles. Injection of the wood chips into the fluidized bed, rather than on top of the bed, might result in lower hydrocarbon emissions. This modification should be investigated with further tests.

It may be seen in Figure 3 that both the fluidized-bed combustion mode and the cyclone combustion mode of the wood-chip furnace were extremely effective in reducing total hydrocarbon emission levels below those measured from conventional wood stoves. The fluidized-bed tests achieved hydrocarbon emission factors very similar to those of industrial wood-fired boilers. The cyclone tests showed even more efficient reduction of hydrocarbon emissions, with emission factors being only a fraction of those measured in the industrial wood-fired boilers. This is consistent with the slightly higher NO$_x$ levels measured during the cyclone tests in comparison to the fluidized-bed and wood stove tests.

Figure 4 is a representation of benz(a)pyrene (BaP) emission factors from the various devices tested in this study and an average emission factor for seven small industrial wood boilers.[14] The three entries in this figure for the fluidized-bed combustor represent three different sampling modes: (1) at the flue gas outlet with no filter bag in place (fluidized-bed), (2) at the flue gas outlet with a fabric filtration bag in place prior to the sampling point (fluidized-bed w/bag), and (3) in the furnace iteself about 6 inches above the fluidized-bed (fluidized-bed above bed). BaP emissions from the fluidized-bed without the fabric filter are considerably higher than those measured from a conventional wood stove fired with wood or coal, in spite of lower total hydrocarbon emissions for the fluidized-bed unit. This implies that a larger fraction of the total hydrocarbons evolved during the fluidized-bed combustion of wood chips are being converted to polycyclic aromatic hydrocarbons (PAH). Thus, lower total hydrocarbon emissions do not necessarily result in lower PAH emissions for a solid fueled heating device. BaP emission factors for the tests with the probe just above the fluidized-bed were considerably lower than those samppled at the flue gas outlet, in spite of the same operating conditions, with emission factors similar to those for the conventional wood stoves. This suggests that PAH compounds are being formed above the sampling point, either in the upper regions of the furnace or in the water tube heat exchanger surrounding the furnace.

A fabric filter particulate control device was extremely effective in reducing particulate emissions from the fluidized-bed, with emissions being reduced from 2.5 g/kg without the bag to 0.04 g/kg with the bag. Accompanying this reduction in particulate was a reduction in the heavier PAH compounds, as evidenced by BaP emission factors in Figure 4. Two explanations are presented to account for this reduction. First, and probably most important, as the flue gas cooled in the water tube heat exchanger, heavier organic compounds such as BaP condensed from the flue gas stream and were adsorbed by the flue gas particulate. Removal of this particulate from the flue gas would thus reduce BaP emissions as well. Second, much of the particulate collected in the bag was a carbon char from partially combusted wood particles. It is possible that this charcoal material may act as a filter adsorbent, adsorbing heavier PAH compounds still in the vapor phase at the filter bag.

BaP emissions were below the level of detection (<0.003 mg/g) for the cyclone burner tested. This is below the BaP levels measured in the industrial wood boilers (Figure 4). Thus cyclone firing was very effective in reducing total hydrocarbon emissions and PAH emissions.

CONCLUSIONS

- Both the fludized-bed combustion mode and the cyclone-fired combustion mode of the residential wood-chip furnace were successful in reducing total hydrocarbon emissions when compared to a conventional wood stove. This was primarily due to increased combustion efficiency in the wood-chip furnaces over that of a wood stove, achieved with only a minor increase in NO_x emissions. Of the two wood-chip furnace configurations, the cyclone was significantly more successful in suppressing hydrocarbon emissons, with only a slight increase over those from the fluidized-bed.

- NO_x emissions from the two wood-chip combustor configurations were comparable to those from a wood stove. NO_x eissions from the combustion of coal in a wood stove were significantly higher, due to increased fuel nitrogen content.

- Benz(a)pyrene and total hydrocarbon emissions for the cyclone-fired combustion tests were significantly lower than emission factors for BaP from conventional wood stoves. However, BaP emission factors for the fluidized-bed combustion tests were higher than from residential wood stoves burning wood or coal. Lower total hydrocarbon emission factors for fluidized-bed combustion tests, as compared to those for wood stoves, imply that a larger fraction of the total hydrocarbons from fluidized-bed combustors are being converted to PAH compounds.

- The baghouse installed on this fluidized-bed combustion unit proved extremely effective in reducing total suspended particulate emissions from the combustion unit. In addition, collection of partially burned carbonaceous wood particles in the baghouse resulted in significantly lower emission factors for heavier PAHs, such as BaP, during the fluidized-bed combustion tests.

- Hydrocarbon emission sampling just above the bed for the fluidized-bed combustion mode indicates that most of the significant formation of BaP is occurring above the bed at the inlet of the water tube heat exchanger or in the water tube heat exchanger itself.

This work was supported under EPA Contract No. 68-02-3170-70.

REFERENCES

1. Trefil, J. Sawing Away at OPEC. Science 80, Vol. 1, No. 5, 1980. pp. 16-18.

2. Cooper, J.A., and J.G. Watson. Portland Aerosol Characterization Study. Oregon Department of Environmental Quality, 1979.

3. Sanborn, Cedric R., Richard L. Poirot, Gregory A. Heil, and Michael A. Blanchet. Preliminary Analysis of the Ambient Impacts of Residential Woodburning in Waterbury, Vermont. In: Proceedings of the Wood Heating Seminar, February 21-24, 1981, New Orleans, LA. Wood Heating Alliance, 1981. pp. 231-241.

4. Imhoff, Robert E., and Justice A. Manning, William M. Cook, and Timothy L. Hayes. Preliminary Report on a Study of the Ambient Impact of Residential Wood Combustion in Petersville, Alabama. In: Residential Solid Fuels--Impacts and Solutions. John A. Cooper and Dorothy Maleck, eds. Oregon Graduate Center, 1982. pp. 520-538.

5. Carlson, James H. Residential Wood Combustion in Missoula, Montana: An Overview of Its Air Pollution Contributions, Health Effects, and Proposed Regulatory Solutions. In: Residential Solid Fuels--Impacts and Solutions. John A. Cooper and Dorothy Maleck, eds. Oregon Graduate Center, 1982. pp. 539-550.

6. DeCesar, Richard T. The Quantitative Impact of Residential Wood Combustion and Other Vegetative Burning Sources on the Air Quality in Medford, Oregon. In: Residential Solid Fuels--Impacts and Solutions. John A. Cooper and Dorothy Maleck, eds. Oregon Graduate Center, 1982. pp. 551-565.

7. United States Department of Energy. Health Effects of Residential Wood Combustion: Survey of Knowledge and Research. DOE/EV-0114, September 1980.

8. DeAngelis, D.G., D.S. Ruffin, J.A. Peters, and R.B. Reznik. Source Assessment: Residential Combustion of Wood. Prepared by Monsanto Research Corporation for EPA, EPA-600/2-80-042b (NTIS No. PB81-136160). March 1980.

9. Milliken, John O. Airborne Emissions from Wood Combustion. Presented at the Wood Energy Institute, Wood Heating Seminar IV, Portland, Oregon, March 22-24, 1979.

10. Cooke, M., and J.M. Allen. Draft Report on Trial Protocol for Sampling and Analysis of Emissions from Residential Wood Combustion. Prepared for Industrial Environmental Research Laboratory Environmental Protection Agency, Contract No. 68-02-2686. 1981.

11. Gangwal, S.K., and D. G. Nichols. Chemical Characterization of Tar From Fixed-Bed Gasification of Eastern and Western Coals. Proceedings of the 20th Hanford Life Sciences Symposium, Richland, Wash., October 1980.

12. Gangwal, S.K., et al. Pollutants from Synthetic Fuels Production: Sampling and Analysis Methods for Coal Gasification. EPA-600/7-79-201 (NTIS No. PB80-104656). August 1979.

13. Nunn, A.B. NO_x Emission Factors for Wood-Fired Boilers. EPA-600/7-79-219 (NTIS No. PB80-102288). September 1979.

14. Wainwright, P.B., M.Y. Aldridge, and R.S. Truesdale. A POM Emissions Study for Industrial Wood-Fired Boilers. North Carolina Department of Natural Resources and Community Development. April 1982.

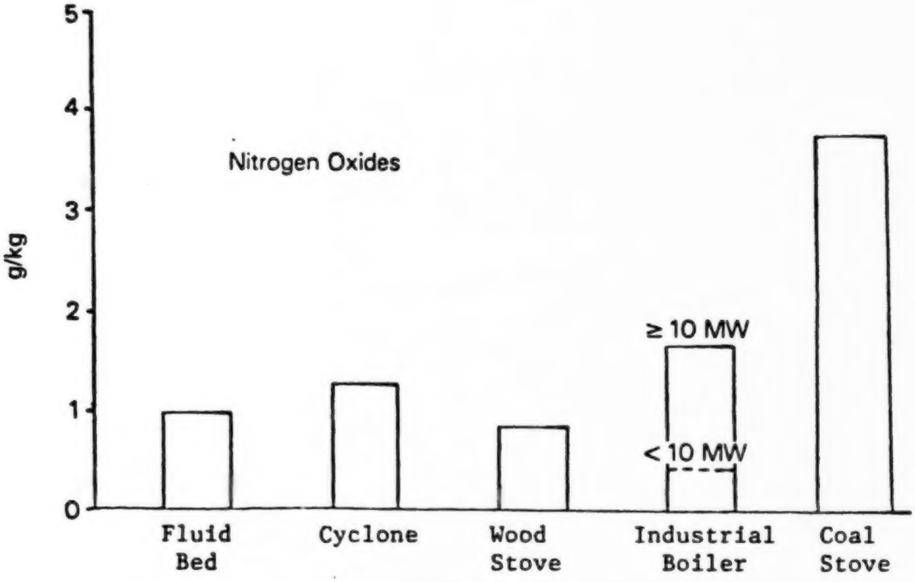

Figure 2. Comparison of NO_x emission factors, g/kg.

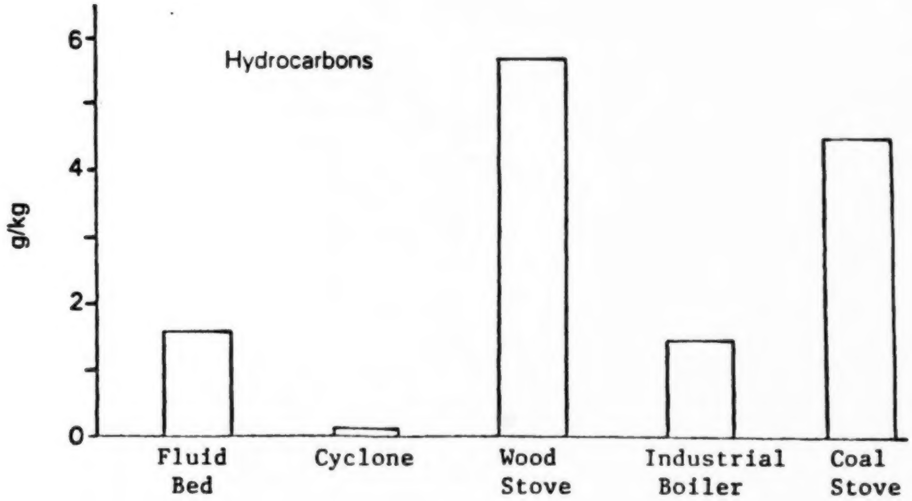

Figure 3. Comparison of total hydrocarbon emission factors, g/kg.

TYPING GUIDE SHEET

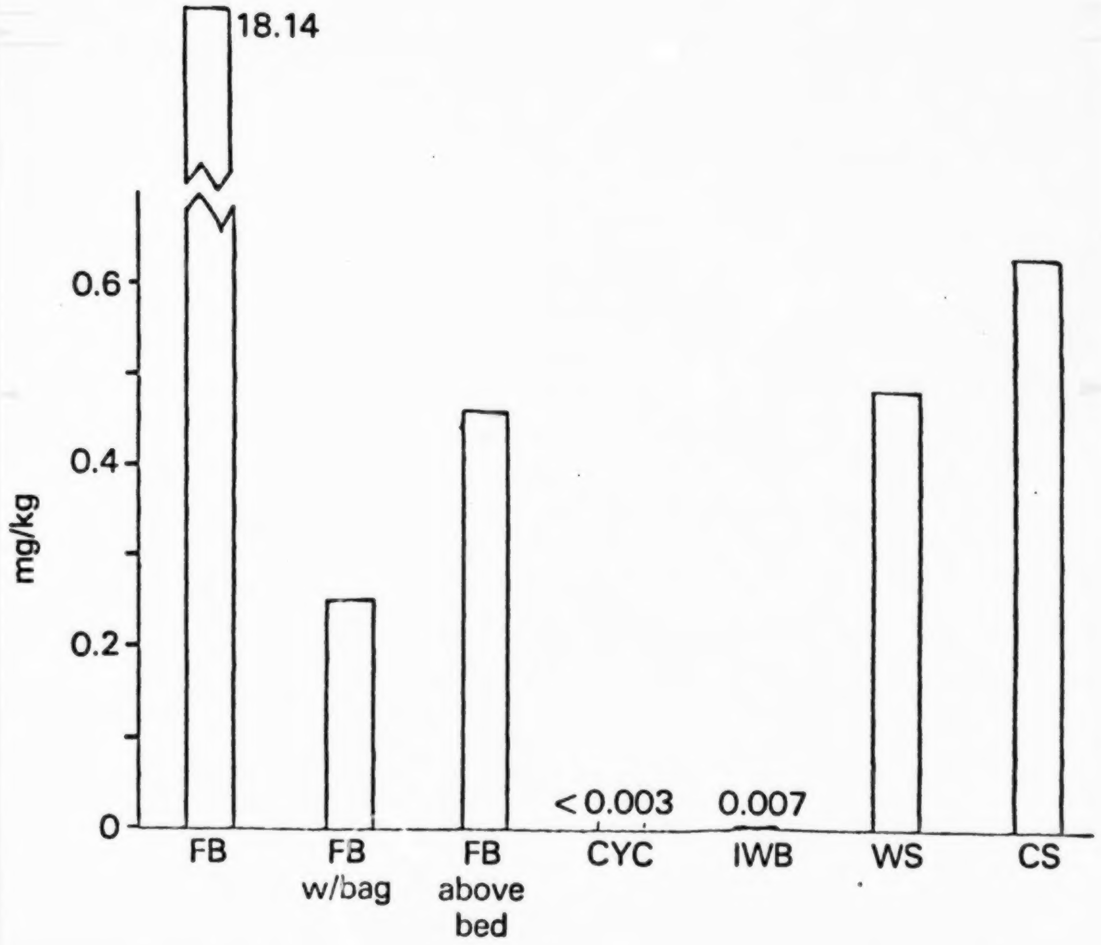

Figure 4. Benz(a)pyrene emission factors (mg/kg fuel). (FB = fluid bed, IWB = industrial wood boiler, WS = wood stove, CS = coal stove).

PAGE NUMBER
EPA-287 (Cin.)
(4-76)

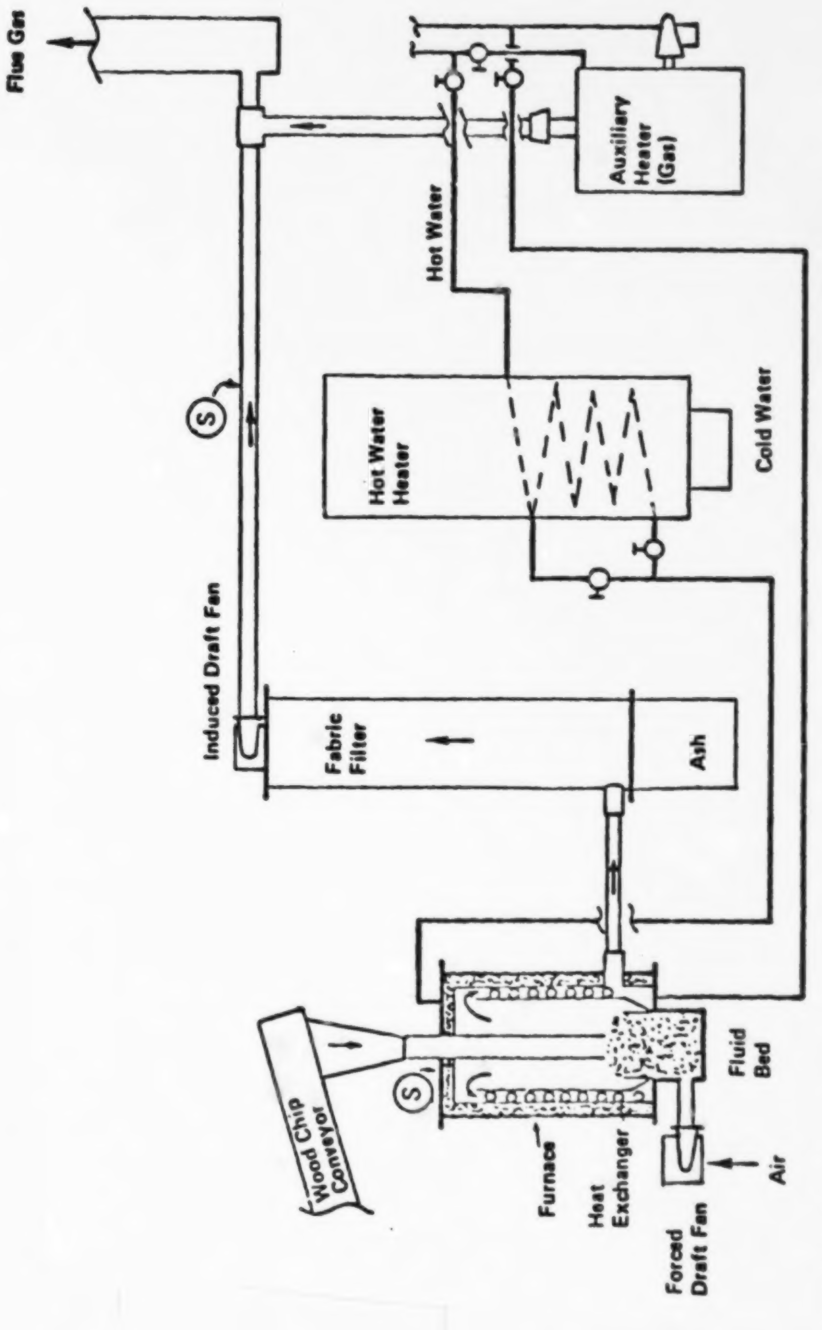
Flue Gas
Hot Water
Auxiliary Heater (Gas)
S
Hot Water Heater
Cold Water
Induced Draft Fan
Fabric Filter
Ash
Wood Chip Conveyor
S
Furnace
Heat Exchanger
Forced Draft Fan
Fluid Bed
Air

Note: S indicates sampling points.

Figure 1. Fluidized-bed residential heating system schematic.

COMBUSTION MODIFICATION TO REDUCE WOOD STOVE EMISSIONS

by

John M. Allen and
William H. Piispanen
Battelle, Columbus Laboratories
505 King Avenue
Columbus, Ohio 43201

"The research described in this article has been funded wholly or in part by the United States Environmental Protection Agency through Contract 68-02-3169 to Battelle, Columbus Laboratories. It has been subjected to the Agency's required peer and policy review; however, it does not necessarily reflect the views of the Agency, and no official endorsement should be inferred."

ABSTRACT

A recent laboratory program has characterized the organic emissions from residential wood stoves. Both CO and hydrocarbons were found to be effectively reduced by a catalytic afterburner. However the NO_x emissions were found to be increased appreciably. The afterburner was not supplied with auxiliary fuel because large amounts of CO and unburned hydrocarbons are normally emitted from the primary burning of the wood. Heated secondary air was supplied to the inlet of the afterburner; this is necessary to avoid quenching even though sufficient residual oxygen is normally present. An appreciable increase in NO_x concentration in the flue gas was observed as it passed through the catalyst unit. When the activated catalyst unit was replaced with a similar ceramic structure without the active coating, a reduction in NO_x was observed. The NO_x was predominantly NO in both situations. Wood is generally a low nitrogen fuel (0.1 percent), but nitrogen conversion to NO_x seems to be high in the catalytic afterburner, resulting in NO_x emissions between 100 and 170 ppm corrected to zero excess air.

INTRODUCTION

Previous studies of wood stoves have identified the several interrelated causes of undesired emissions from these residential appliances. The effectiveness of homogeneous secondary combustion in reducing emissions has been recognized and demonstrated (Ref. 1), yet the initiation and maintenance of this all-gas reaction is very difficult and seldom obtained at low burning rates (Ref. 2). The recent market introduction of catalytic afterburners in wood stoves shows promise of greatly increasing the occurrence and effectiveness of secondary combustion, resulting in reduced stove emissions of CO and hydrocarbons and improved overall thermal efficiency.

In previous studies of stove emissions it became evident that different techniques of flue gas sampling and subsequent sample analysis were being utilized by different experimentalists. This has provided confusion because their results were not always directly comparable. Consequently a protocol for sampling and analysis was proposed which should permit more valid comparisons (Ref. 3).

A brief experimental study currently in progress and being reported in this paper serves two purposes: to characterize the emissions from a catalytic wood stove focusing primarily on organic emissions, and to demonstrate the applicability of the proposed sampling and analysis protocol. In the progress of the study some surprising NO_x observations were made which will be discussed.

DESCRIPTION OF TEST METHODS

The study is being conducted at the Battelle Combustion Laboratory, which provides real time monitoring and data acquisition of various combustion parameters from wood heating appliances. A Webster Oak stove was installed in the facility and, after installing the catalyst unit, the stove was operated for 100 hours burning split white oak and pine. During these burns, the operation of the stove was observed in order to obtain reliable burning at low rates.

Description of Equipment and Sampling Methods

The Webster Oak stove contains a lower primary combustion chamber for the burning wood fuel, and a ribbed upper chamber for heat recovery from the combustion products before they leave the stove. The catalytic combustor device is located in the gas passage between the lower primary chamber and the upper secondary chamber. This upper chamber thus provides both an additional volume for completion of secondary combustion and effective recovery of heat released by any catalytically induced secondary combustion. Aspirated thermocouples and rake-type sample probes were installed in the stove to sample simultaneously the combustion gas entering the catalyst (primary) and the combustion gas leaving the stove (secondary). Thermocouples were also mounted to allow monitoring of (1) the secondary air temperature inside the air duct located within the combustion chamber, (2) several stove metal temperatures, (3) stack wall temperature, (4) dilution tunnel temperature, and (5) ambient air temperature. Also the viewing window over the catalyst was replaced with a fitting which permitted vertical traversing of the catalyst to measure gas temperatures within the catalyst. During the preliminary burns, the point of maximum temperature was determined between the catalyst substrate walls, and the thermocouple was then locked at that point.

The test facility is designed to provide continuous sampling and monitoring of various stove parameters as illustrated in Figure 1. The data collection and processing system is limited to collecting single point data and, due to the limitation of data storage, most of the tests were designed for 110 scans at 2-minute intervals (total time, 220 minutes).

Not shown in the test facility schematic drawing, is the NO/NO_x system used for this program. To measure both NO and NO_x in the primary and secondary combustion zone emissions would have required a total of four instruments and a total sample pressure greater than currently available. As an alternative, a timer box was designed for this program which cycled the NO and NO_x modes of the Beckman 955 chemiluminescent analyzer at 5-minute intervals. The Beckman instrument includes switching solenoids which are activated by the timer. The instrument signal output was wired through the switch to allow either NO or NO_x monitoring. Data were recorded on a dual pen recorder which allowed tracking both the NO/NO_x modes. Since NO_x and NO were being sampled, a heated line was used throughout. Since this heated line also supplied samples to the THC analyzers, a control valve was installed at the instrument sample inlet to control sample flow/pressure at the span values.

The test program included a total of six test burns. During five of the six tests, a sample for volatile gas analyses was taken at a point near the gas exit to the chimney by drawing a sample into a preevacuated glass bulb. Also, during the monitoring, flue gas samples were taken continuously from the stack at a point 30 inches up from the flue entrance into the insulated stack. This sample collection used an extractive sampler similar to an EPA Method 5 train but with the addition of a packed column of XAD-2 following the first impinger. The samples taken by these techniques are being thoroughly characterized as to organic species present as the principal objective of the test program.

Test Procedures

Tests were conducted by first starting a fire in the appliance using the split oak. During this time the sampling equipment was set up and leak checked, monitoring instruments were zeroed and spanned, and the data acquisition program was initiated by entering the instrument IDs, monitoring ranges, wood type and moisture, barometric pressure, scan interval, test duration, start time, weight and type of wood charge, and test title. Also, sample pump and line heaters were turned on to allow conditioning of systems.

After the initial charge had burned to glowing coals the bed was raked flat and the weight monitor was zeroed. A preweighed charge of wood was placed in the combustion chamber at exactly 1 minute prior to data acquisition with the primary air full open. All analyzers were then checked to ensure that flow rates and line pressures were at the span values and also that sample transport temperatures were within limits (400°F ± 25°F).

Upon initiation of data acquisition the continuous sampler was started. The stove operator monitored the catalyst temperature using a digital readout, and when the catalyst temperature reached 800°F the primary air supply was adjusted to a predetermined open set point. This time delay was normally less than 5 minutes. At no time through the duration of the burn was the air readjusted or fuel added to the stove. Data acquisition and extractive sampling continued until the predetermined run termination time was reached.

Post-Test Procedures

Following the testing operations, the extractive sampling system was removed from the stack and all openings were capped with clean foil. The system was then transported to the laboratory for recovery according to the wood stove sampling protocol. The analyzers were all purged with N_2 gas and then post-test zero and span checks were made to determine instrument drift or malfunction during testing.

Data Reduction

The results of the data acquisition were transferred to a data storage tape following the conclusion of each test. For the NO/NO_x data, strip charts were marked for identification. The data were later transferred to a graphics data tape during which time tabular columns of stored data were hard copied. The tabular columns were averaged to provide average parameters for each test. The graphics data were processed into hard copy graphics using a Tektronix Plot 50 package. Data from NO/NO_x strip charts were entered into the laboratory notebook and then transferred by hand into the Tektronix Plot 50 system. As a result, tests 2 through 6 produced the following data: (1) a package of instantaneous printouts of real-time and engineering data as collected by the operator, (2) tabular columns of selected real and calculated data over the total test duration, (3) graphic representations of 12 operating parameters as a function of time, and (4) selected parametric plot representations.

DESCRIPTION OF TEST RESULTS

The test program was designed to include six tests of the stove. Of these tests, five were conducted with the catalyst and one test, Number 6, was run with a ceramic substrate without the coating of catalytic material. Tests were designed for medium to low burn rates and run as close to reproducible conditions as possible except Test 3 which was conducted with a lower supply rate of the primary air. All tests used four pieces of wood.

The average operational data for tests Number 2 through 6 are included in Table 1.

Before looking at the test results, a brief review of how wood burns in a stove is appropriate. Early in a test burn the moisture and organic pyrolysis products are evolved leaving a char residue as the outer portion of the wood. During the middle portion of a burn, more pyrolysis products are evolved. Slow burning takes place, with the pyrolysis products passing through the char layer, and interior moisture often passing through the char layer simultaneously. Late in a test burn the residual fuel is all char; therefore, the hydrocarbon emissions are very low and surface burning takes place. The organic emissions, which are partially burned pyrolysis products, are generally much more concentrated during the early portion of the test burn.

Catalyst Performance

With a combustion catalyst in the stove the catalyst heats up very quickly and, as it reaches about 500°F, the catalytic action is effective and secondary combustion is started. Even when the gas temperature entering the catalyst goes below this 500°F, the catalyst will still be effective and maintain ignition with at least partial burning of the organics and combustible material passing through it. Figures 2a and 2b show a typical test with peak temperatures of the gas leaving the burning wood at about 600°F as they enter the catalyst. This temperature falls off throughout the remainder of the burn reaching a temperature just above 350°F at the end of the test burn. This we refer to as the primary gas flow, and it is mixed with heated secondary air as it enters the catalyst. Figure 3 shows the temperature as measured by the thermocouple imbedded within the catalyst. These temperatures are higher after heated air has been added to the primary combustion products, they have been well mixed, and secondary combustion has taken place. This temperature, you will note, goes much higher and stays high throughout about two thirds of the test period.

Figure 4 shows the effects of the catalyst on the total hydrocarbon (THC) emissions as indicated by flame ionization detector instrumentation. Emissions here are shown as pounds of total hydrocarbons per thousand pounds of wood burned. Therefore, the hydrocarbon emissions going into the catalyst (on the upper curve) and the hydrocarbon emissions leaving the stove (on the lower curve) are normalized on the same basis. The indicated reduction in hydrocarbon emissions was approximately 70 percent throughout the first half of the test burn (∿1.3 hours). At that time the temperature of the catalyst began to fall rapidly, with progressively less effective reduction in emissions. After 1.7 hours as the remaining fuel became essentially charred, the burning rate became lower, and the combustion products became more diluted with excess air. With fewer hydrocarbons entering the catalyst, its temperature fell rapidly and it became less effective in reducing emissions. The average reduction in hydrocarbons for the entire test burn was approximately 50 percent. These data clearly show the advantages of the catalytic unit in reducing organic emissions during the major portion of a test burn.

TABLE 1. OPERATING CONDITIONS FOR STOVE TESTS

Test No.	Weight of Wood Fired (lb)	Average Burn Rate (lb/hr)	Average Catalyst Temp.(°F)	Average Stack Temp.(°F)	Condition
2	10.0	3.5	941	364	High air
3	9.4	2.4	775	343	Low air
4	10.4	2.6	919	376	Med air
5	10.4	2.3	898	349	Med air
6	10.2	2.1	676	318	Uncoated catalyst

Effects on NO_x Emissions

Figure 5 shows the NO_x concentration in the flue gas for the same test. It falls off during the test in the same manner as the hydrocarbon emissions fall. Figure 6 shows the emissions of NO during the same test and, as you can see, they are very similar indicating that there was negligible NO_2 emitted from this stove. Figure 7 shows the concentration of NO_x entering the catalytic unit during the same test. This is also shown in parts per million in the gases entering the catalyst. Considering a large amount of secondary air was also admitted into the catalyst, these data have been corrected to zero oxygen content in both cases. The data are then presented in Figure 8. The surprising observation is that the gases leaving the stove are appreciably higher in nitrogen oxides than the gases entering the catalyst unit, and this difference is maintained throughout the test burn.

Non-Catalyzed Substrate

The catalyst in the stove was then replaced by an identical ceramic substrate that had not been treated by the addition of the catalyst surfaces. The temperature history of this uncatalyzed substrate is similar, except the early temperatures were a little lower and the temperature dropped to a lower value late in the test run. Figure 9 shows the differences quite dramatically, the upper curve being obtained with the activated catalyst, the lower curve being obtained with the dummy catalyst. Figure 10 shows the NO_x emissions both entering the catalyst substrate and leaving the stove. As with the activated catalyst, the emissions are appreciably higher leaving the stove than they are entering the catalyst. These data have again been normalized to zero oxygen content so they can be more directly compared. The NO_x leaving the stove throughout this test was approximately twice the NO_x entering the catalyst.

We are continuing our study of these data including a thorough characterization of the organics, and their combustion within the catalytic unit. Although not excessive compared to some sources, the NO_x emissions from this wood stove are appreciable. It appears from these tests that the ceramic substrate itself causes roughly doubling of the NO_x, and when the substrate is catalyzed the increase is more than doubled. Since this effect is unrelated to the fuel nitrogen content, it is believed that the NO formation is from atmospheric nitrogen through a free radical chain mechanism. The fact that almost all of the NO_x is NO is not surprising. Apparently, the higher catalyst substrate temperatures are sufficient to convert N_2 to NO. At temperatures greater than 1350°F the formation of NO would be quite likely ($K_p = 8.7 \times 10^{-5}$ at 1350°F). It is also possible that higher energy levels may occur at the molecular sites thus increasing NO formation, even with the uncoated surfaces.

REFERENCES

1. Control of Emissions from Residential Wood Burning by Combustion Modification, EPA-600/7-81/091 (NTIS PB81-217655), John M. Allen and W. Marcus Cooke, May 1981.

2. Techniques for Achieving More Complete Combustion in Wood Stoves, Proceedings "Residential Wood and Coal Combustion", 1982, Specialty Conference, Air Pollution Control Association, John M. Allen and William H. Piispanen.

3. Method for Sampling and Analysis of Organic Emissions from Residential Wood Combustion, American Chemical Society National Meeting, September 1982, W. Marcus Cooke, et al.

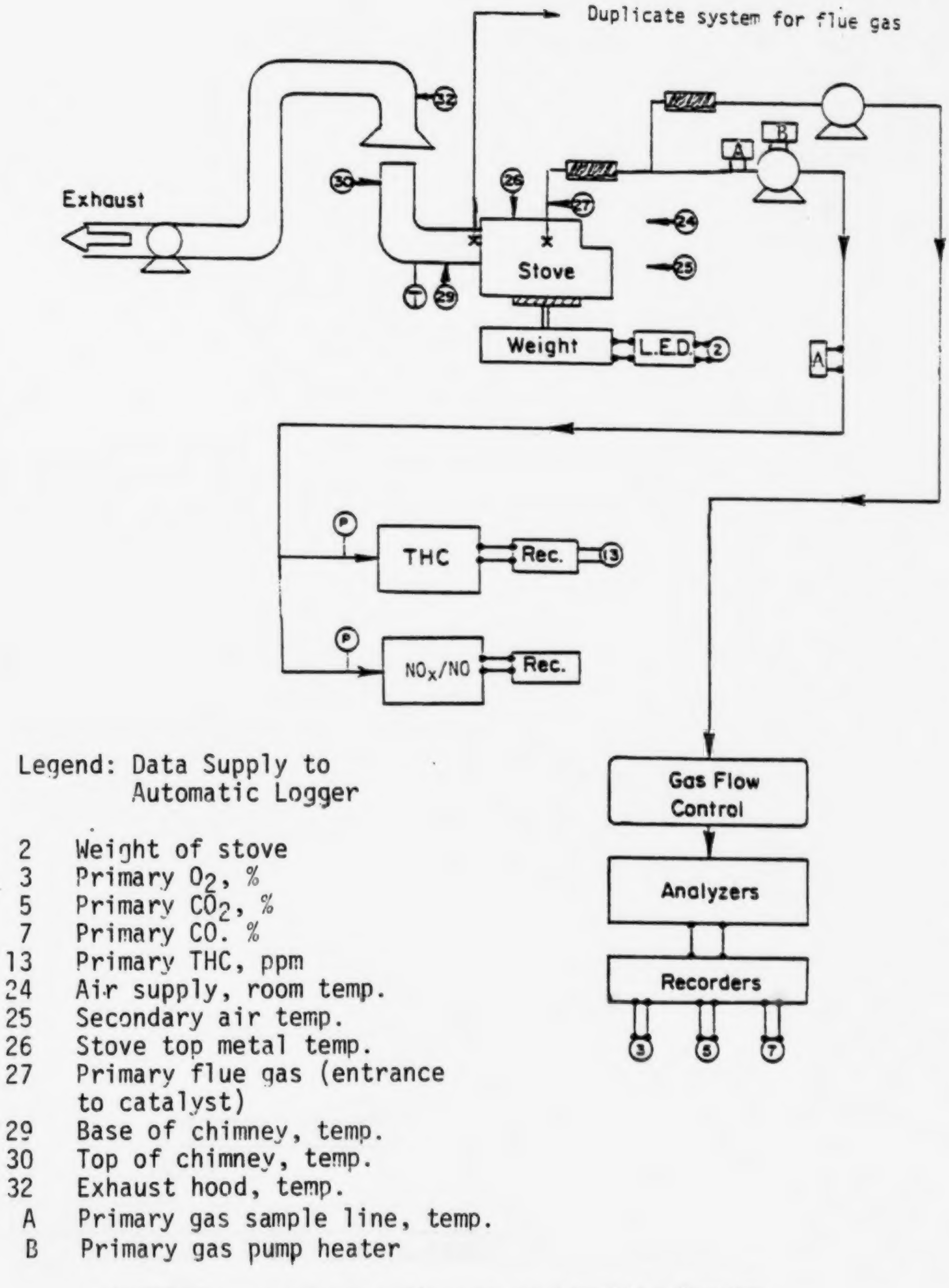
Duplicate system for flue gas
Exhaust
32
30
26
27
24
25
Stove
T
29
Weight
L.E.D.
2
B
A
A
P
THC
Rec.
13
P
NO_x/NO
Rec.
Gas Flow Control
Analyzers
Recorders
3
5
7

Legend: Data Supply to Automatic Logger

2	Weight of stove
3	Primary O_2, %
5	Primary CO_2, %
7	Primary CO. %
13	Primary THC, ppm
24	Air supply, room temp.
25	Secondary air temp.
26	Stove top metal temp.
27	Primary flue gas (entrance to catalyst)
29	Base of chimney, temp.
30	Top of chimney, temp.
32	Exhaust hood, temp.
A	Primary gas sample line, temp.
B	Primary gas pump heater

FIGURE 1. Schematic Diagram of Sampling System

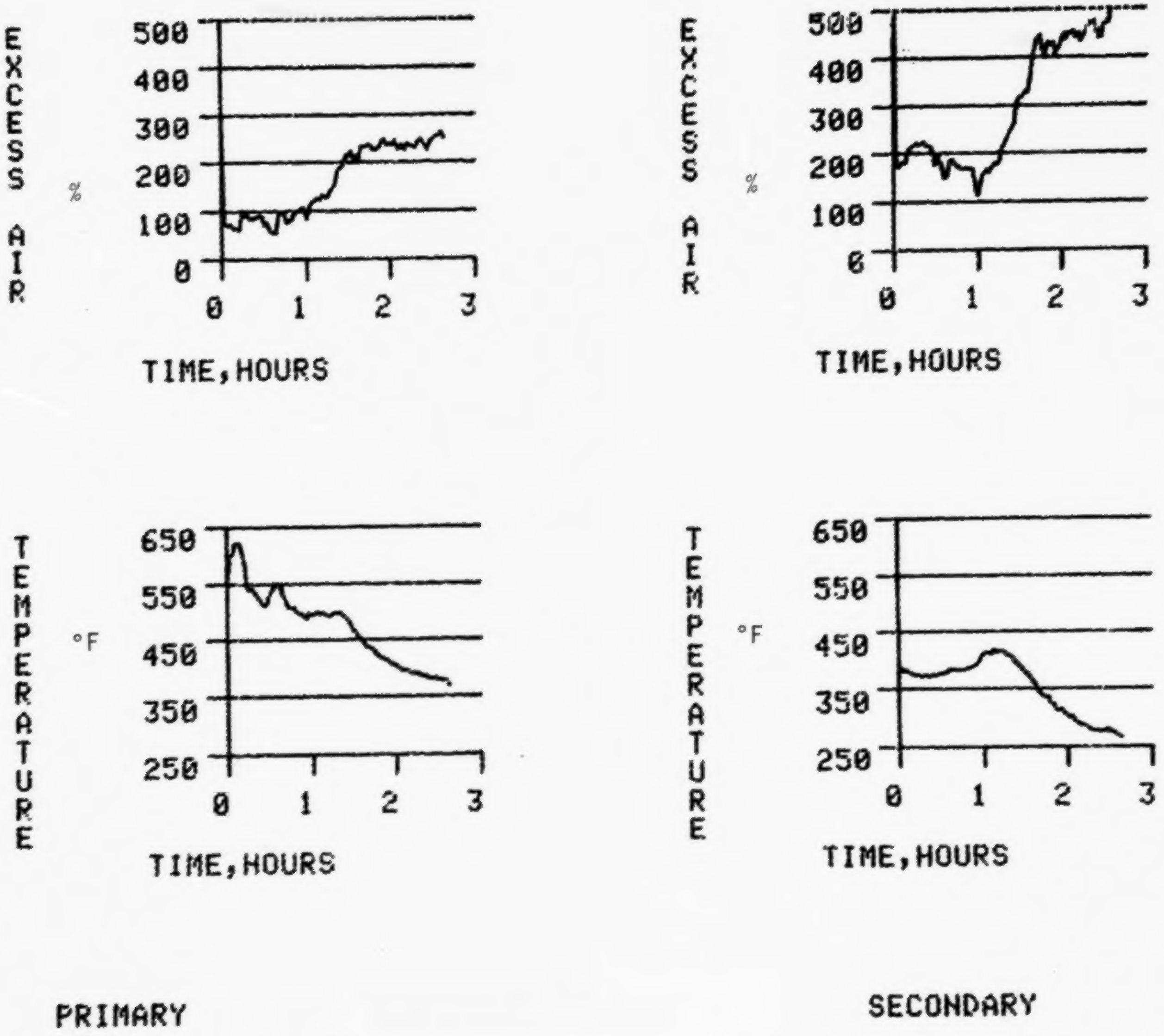

Figure 2a. Excess Air and Gas Temperatures, Active Catalyst Run. No. 5.

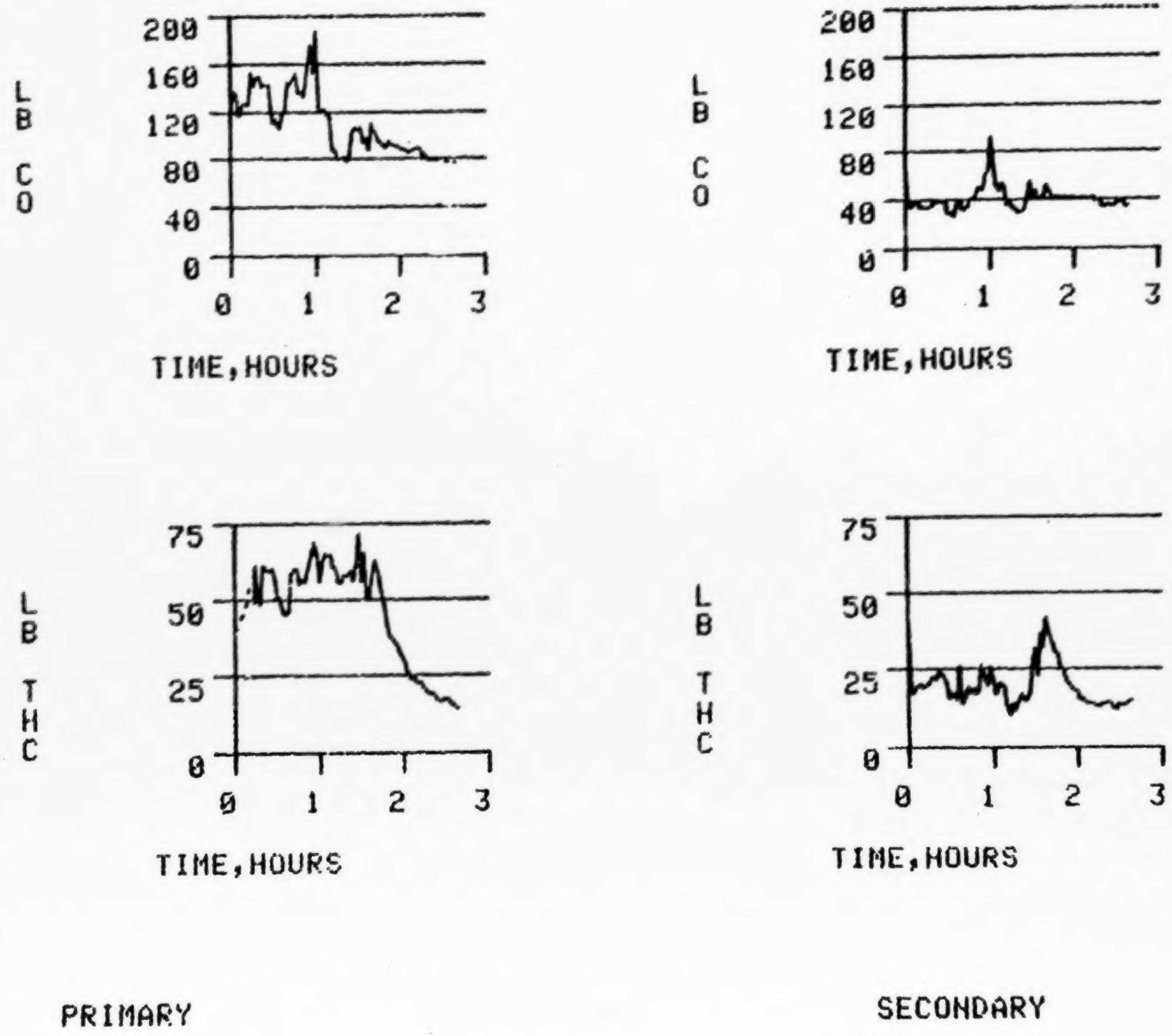

Figure 2b. Emission Factors, Active Catalyst Run No. 5 (lb emitted per lb wood burned).

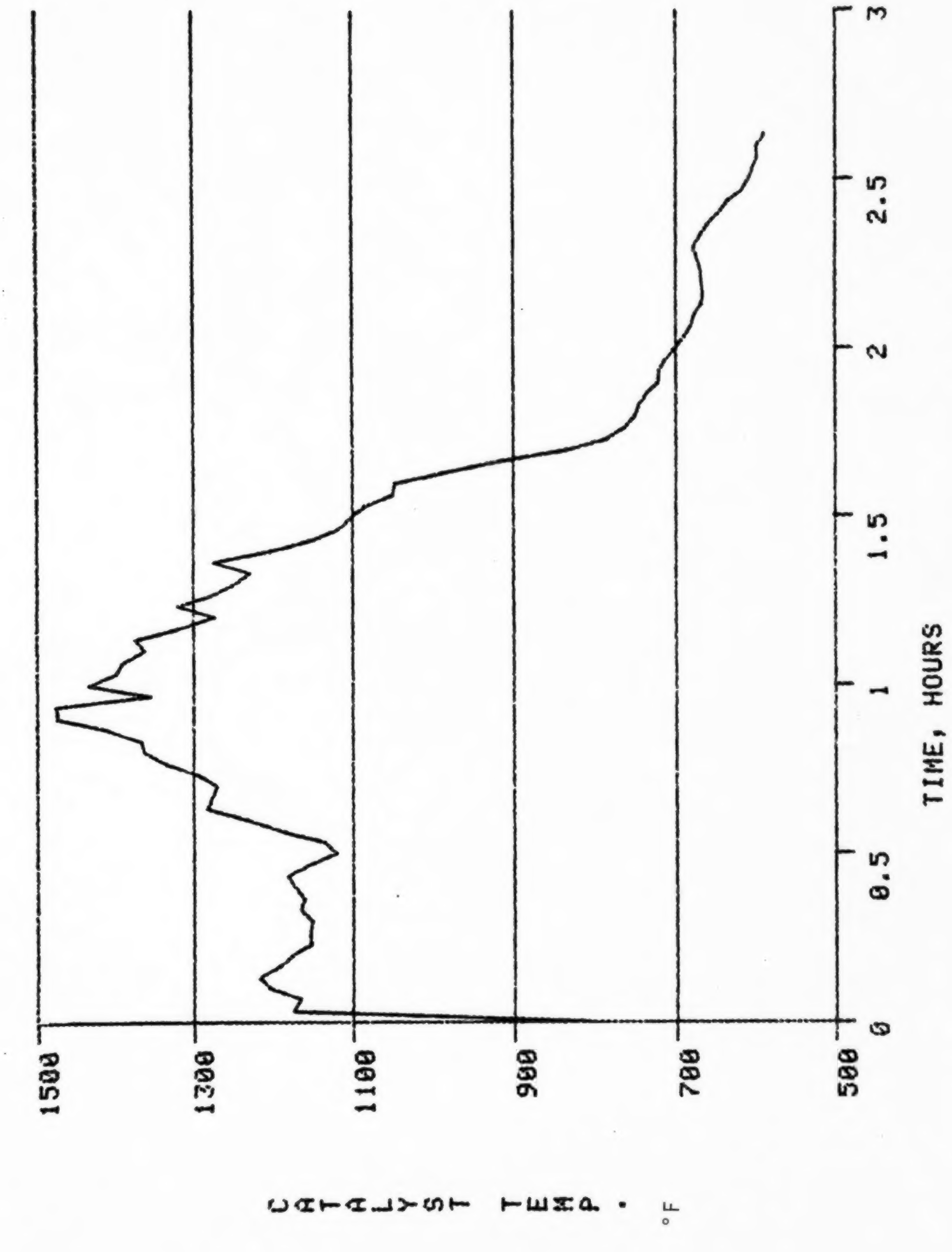

Figure 3. Temperature Within Active Catalyst (Run No. 5).

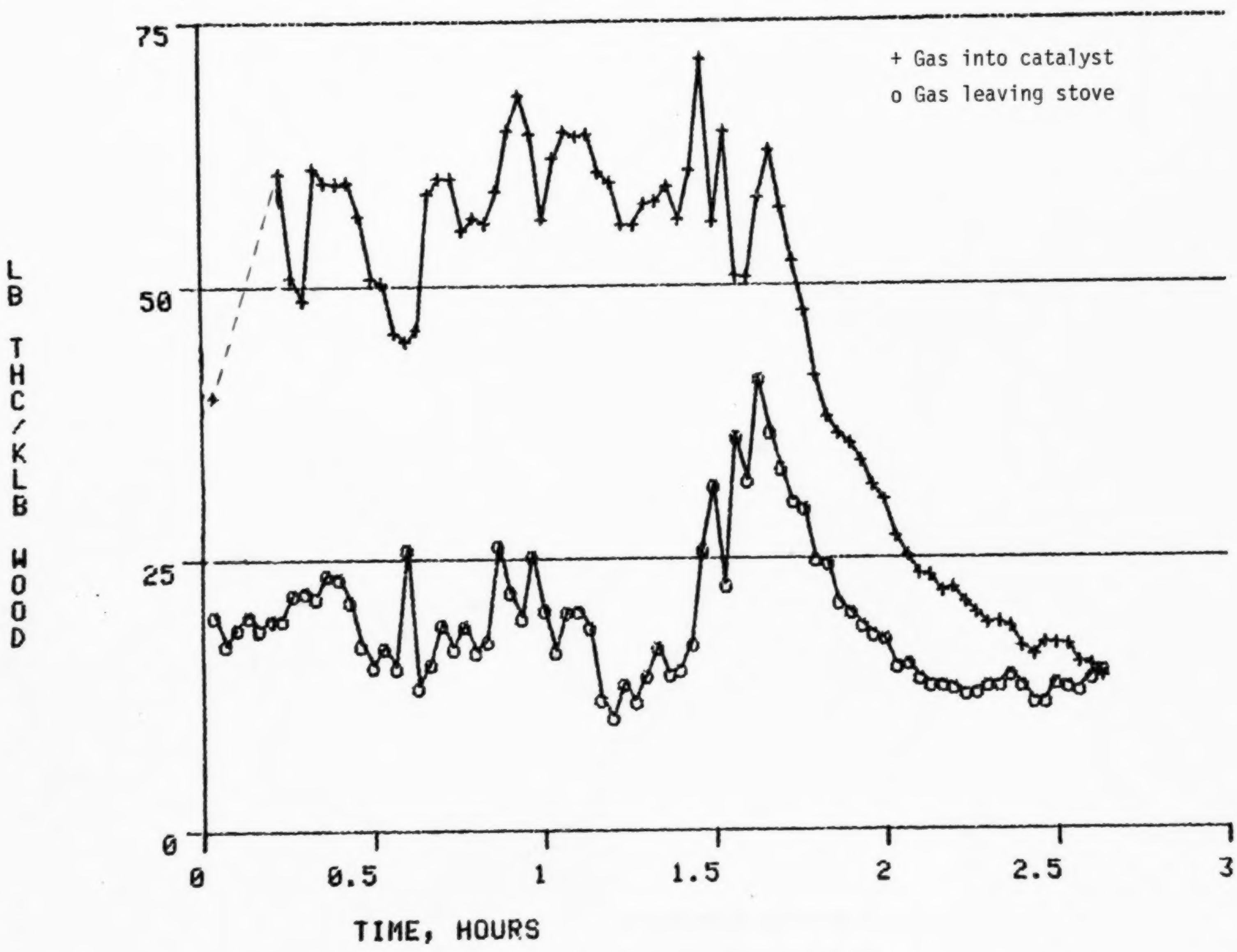

Figure 4. Hydrocarbon Emission Factors, Active Catalyst Run No. 5.

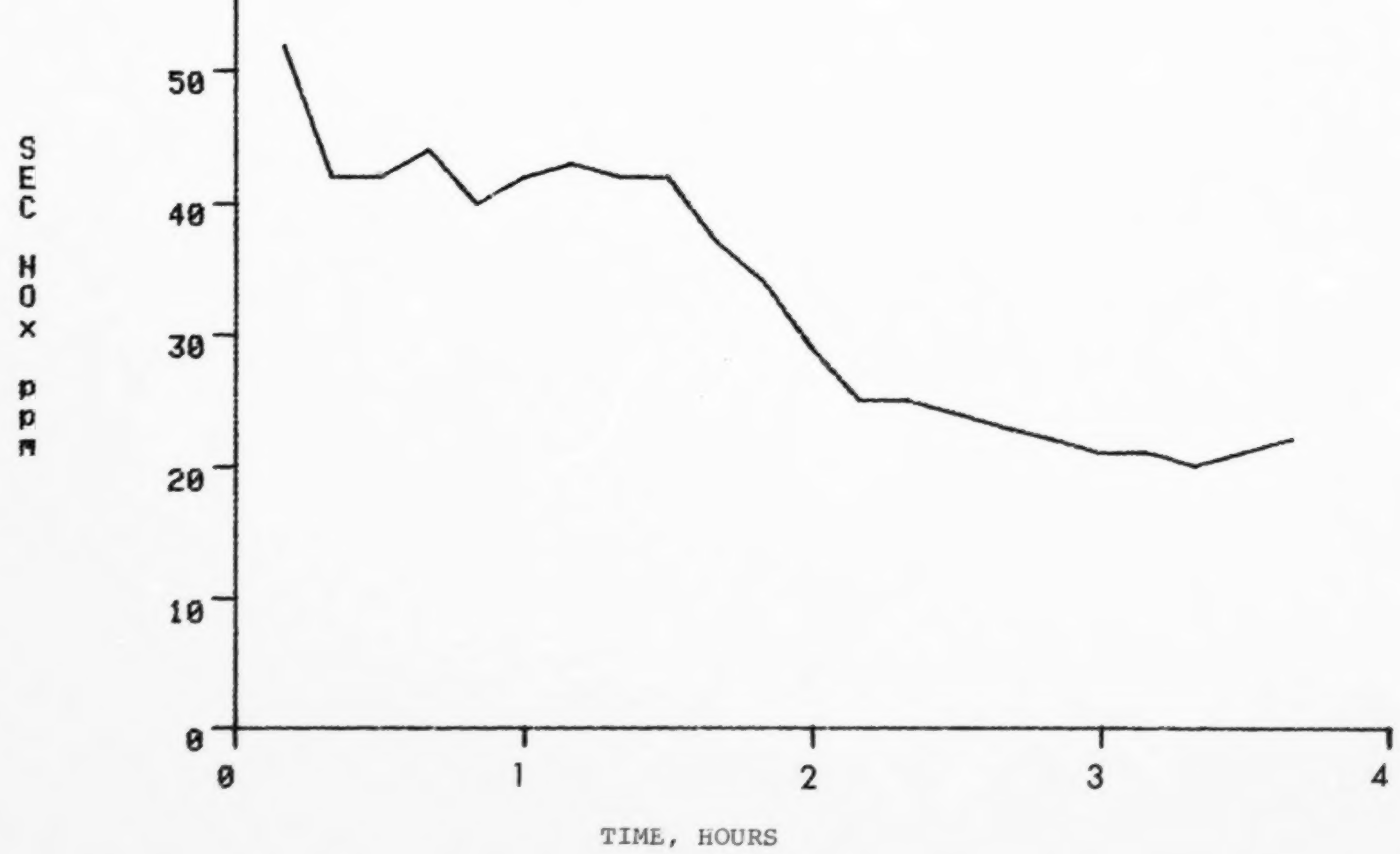

FIGURE 5. NO_x Concentration Leaving Stove, Active Catalyst Run No. 5.

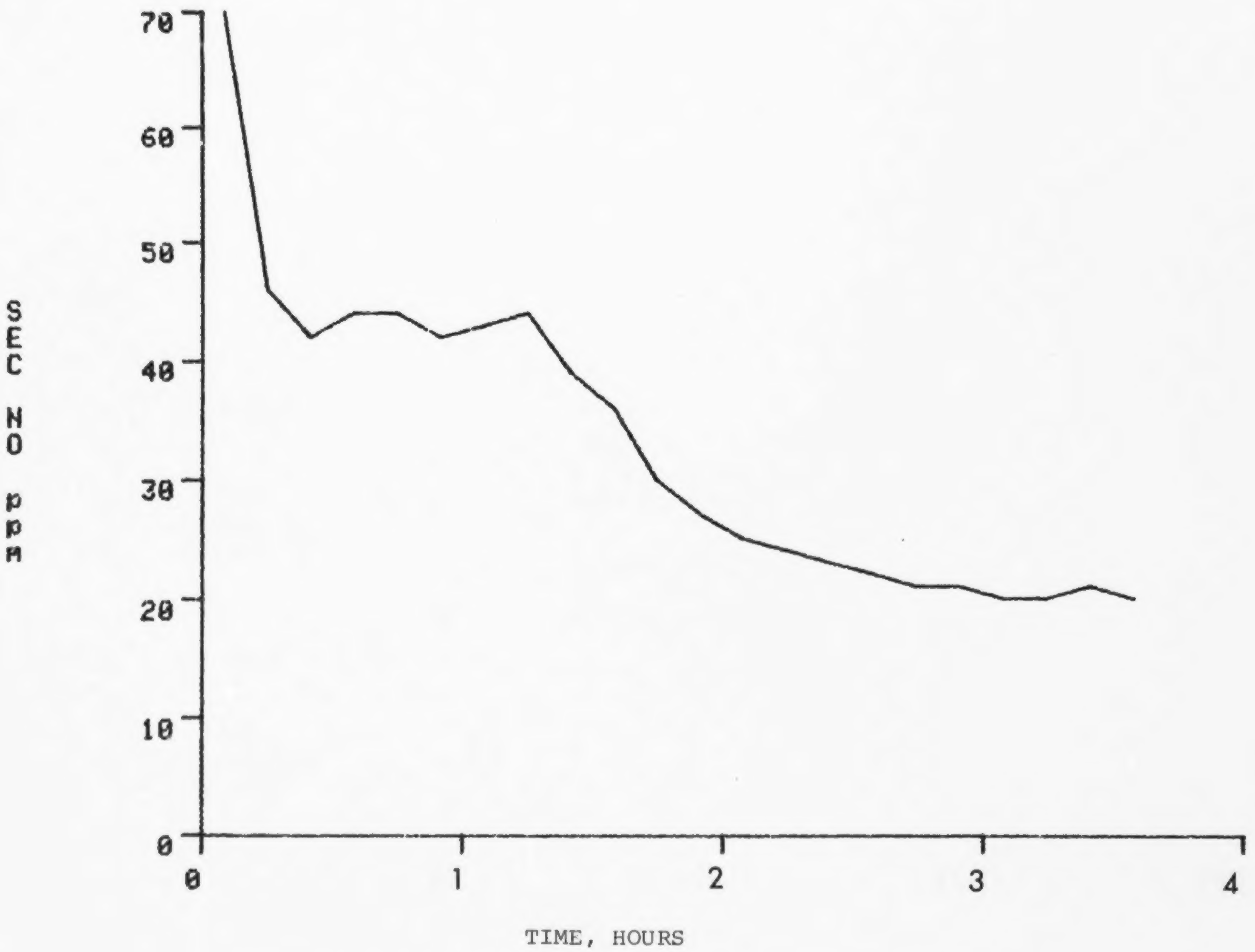

Figure 6. NO Concentration Leaving Stove, Active Catalyst Run No. 5.

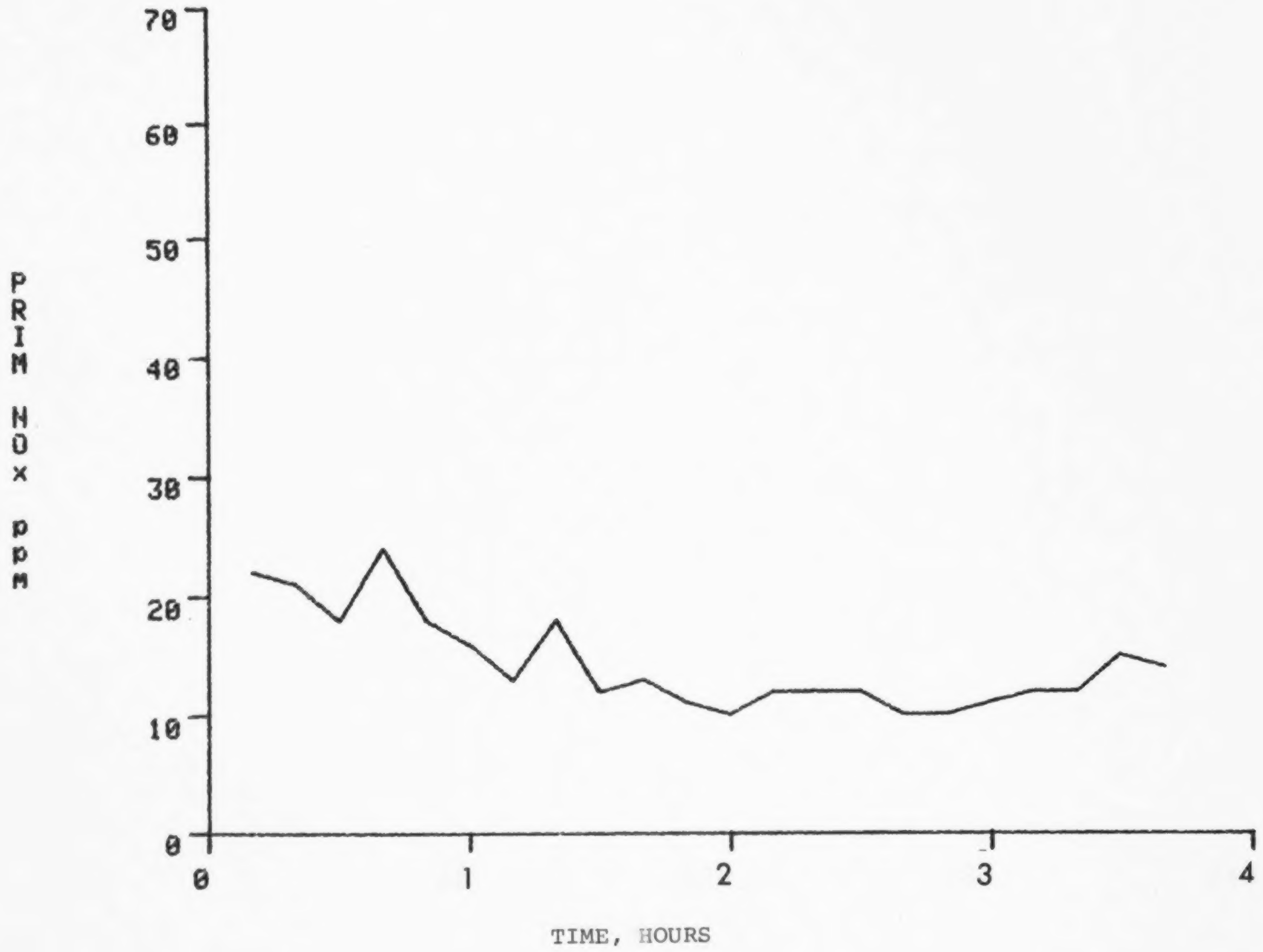

Figure 7. NO_x Concentration Entering Catalyst, Active Catalyst Run No. 5.

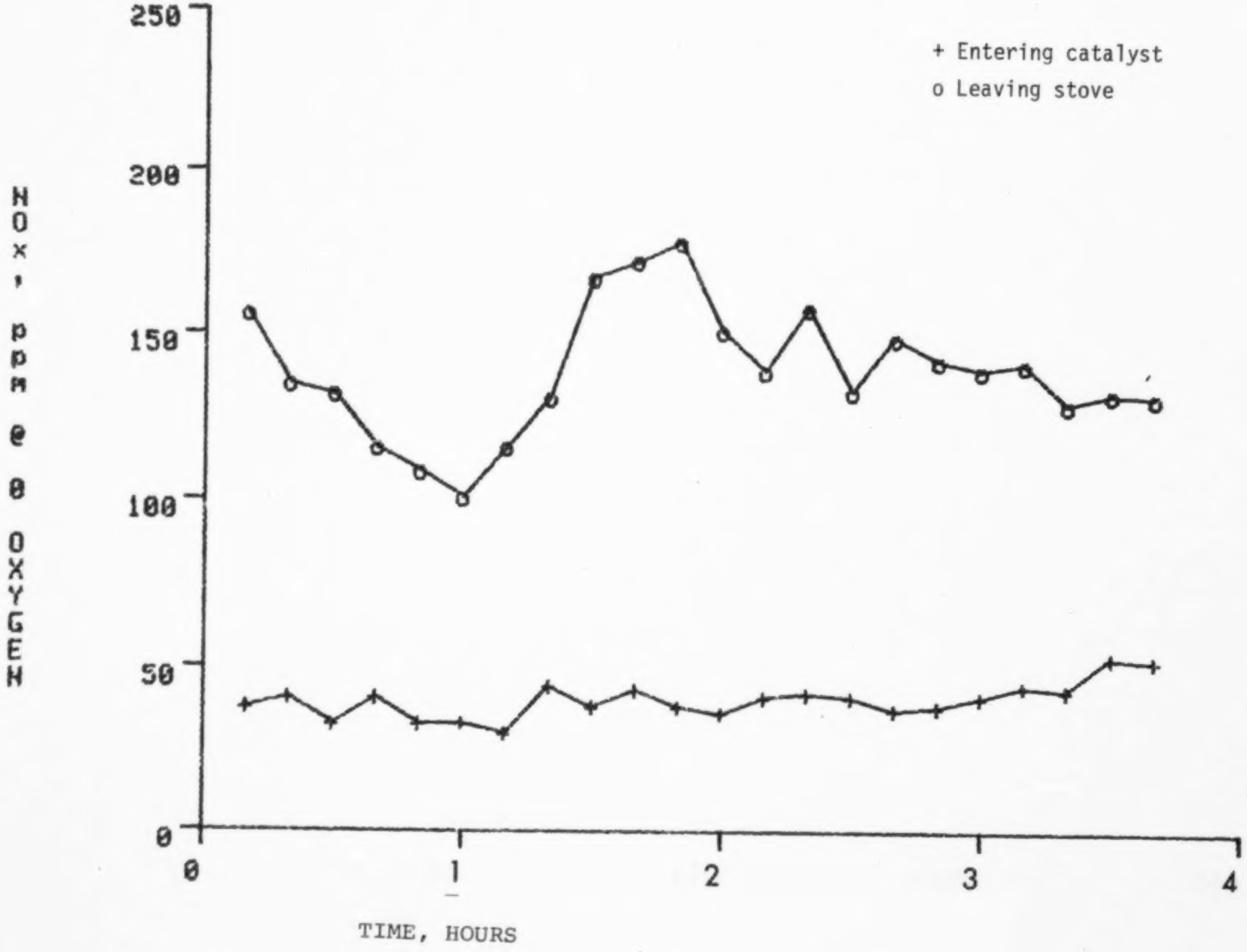

Figure 8. NO_x Emissions Normalized to Zero O_2, Active Catalyst Run No. 5.

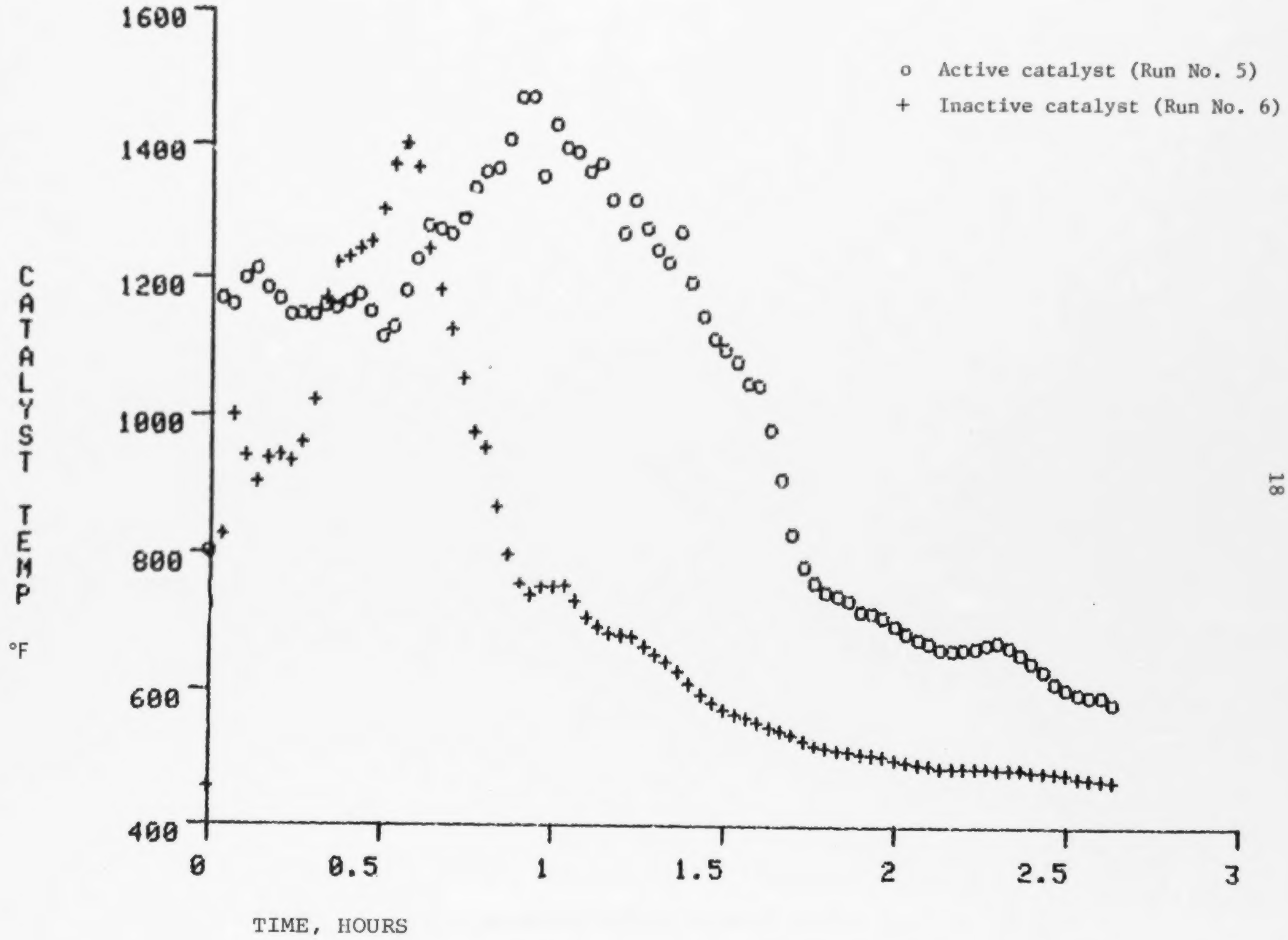

Figure 9. Temperature Within Catalyst

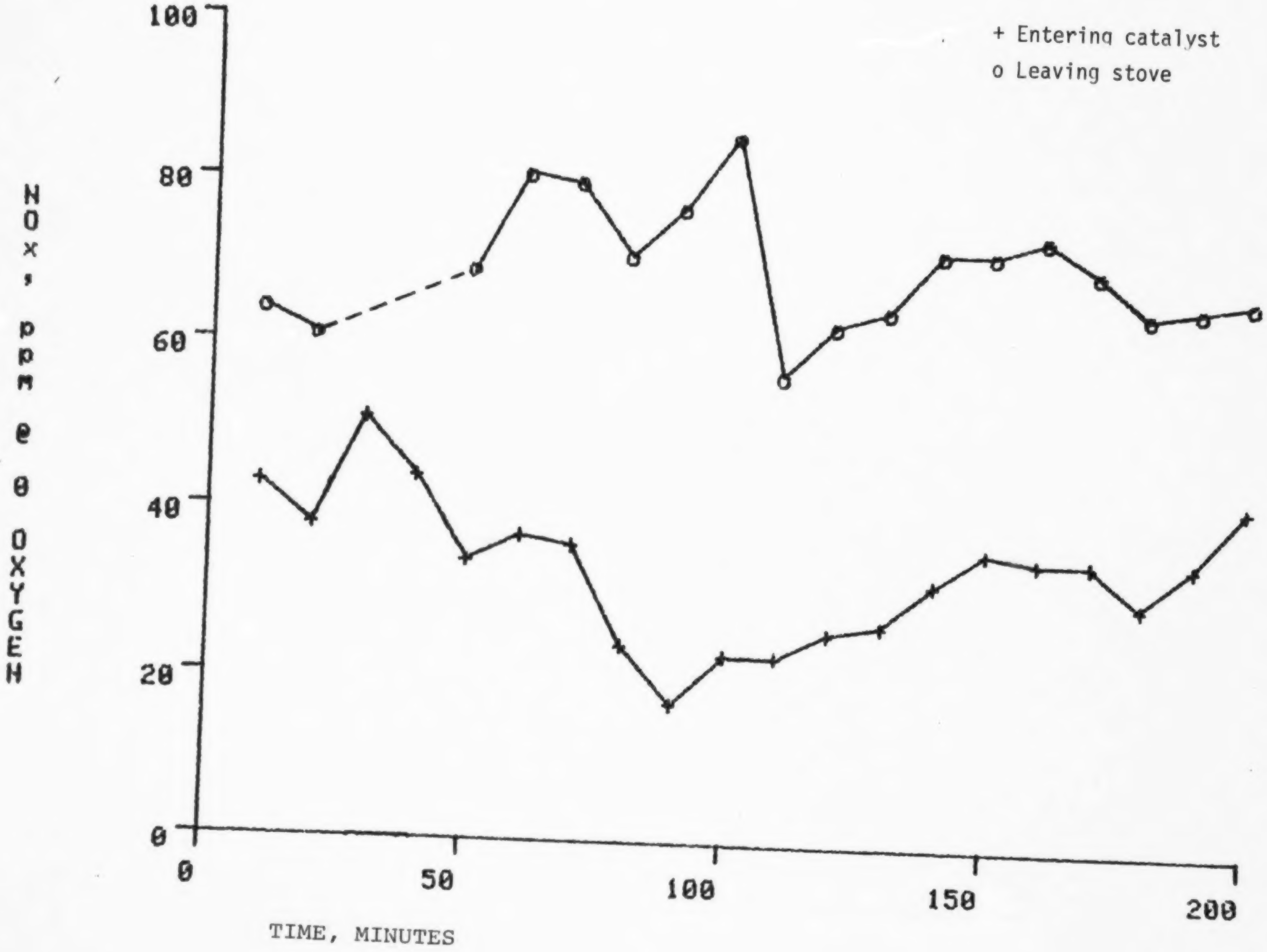

Figure 10. NO_x Emissions Normalized to Zero O_2, Inactive Catalyst Run No. 6.

APPENDIX A
LIST OF ATTENDEES

1982 JOINT SYMPOSIUM ON STATIONARY COMBUSTION NO$_X$ CONTROL
DALLAS, TEXAS, NOVEMBER 1-4, 1982

James H. Abbott
U.S. Environmental Protection Agency
IERL (MD-62B)
Research Triangle Park, NC 27711

John Allen
Battelle, Columbus Laboratories
505 King Avenue
Columbus, OH 43201

Ralph F. Altman
Electric Power Research Institute
516 Franklin Building
Chattanooga, TN 37411

Goroh Baba
Ihi, Tokyo, Japan c/o Foster Wheeler
110 South Orange Avenue
Livingston, NJ 07039

Gary E. Baker
PEDCO Environmental Inc.
11499 Chester Road
Cincinnati, OH 45246

M. A. Bambrough
Department of Environment, Canada
APCD 351 St. Joseph Blvd.
Mull, Quebec K1A1C8
CANADA

Joseph A. Barsin
Babcock & Wilcox Company
P.O. Box 351
Barberton, OH 44203

Timothy K. Bauer
Stearns-Roger Engineering Company
P.O. Box 5888
Denver, CO 80217

Jahanbakhsh Behnam
U.S. Environmental Protection Agency
1201 Elm Street
Dallas, TX 75270

Rod Beittel
Southern Research Institute
P.O. Box 3307-A
Birmingham, AL 35255

Charles E. Benson
Exxon Research & Engineering Company
P.O. Box 101
Florham Park, NJ 07932

Bahjat S. Beshty
Engelhard Corporation
Metro Park
Edison, NJ 08818

Gregory T. Bielawski
Babcock & Wilcox Company
20 South Van Buren Avenue
Barberton, OH 44203

D. Kerry Blamire
Nova Scotia Power Corporation
Duke Tower, Duke Street, P.O. Box 910
Halifax B3J2W5, Nova Scotia
CANADA

Lorenzo Boldware, Jr.
Texas Electric Service Company
P.O. Box 8368
Fort Worth, TX 76112-0368

Arthur A. Boni
Science Applications, Inc.
P.O. Box 2351
La Jolla, CA 92038

H. Boorsma
Stork Boilers
P.O. Box 20
7550 GB. Hengelo
THE NETHERLANDS

Robert H. Borgwardt
EPA Technical Center
MD-62B, ERC/RTP
Durham, NC 27711

T. D. Bornemann
Kon. Mij. De Schelde
Glacisstraat 65
4380 AA Vlissingen
THE NETHERLANDS

Joshua S. Bowen
U.S. Environmental Protection Agency
IERL (MD-65)
Research Triangle Park, NC 27711

Craig T. Bowman
Stanford University
Department of Mechanical Engineering
Stanford, CA 94305

Bernard P. Breen
Energy Systems Associates
2522 Chambers Road, Suite 213
Tustin, CA 92680

Willem T. Broer
N.V. Nederlandse Gasunie
P.O. Box 19, 9700 MA
Groningen
THE NETHERLANDS

John M. Burke
Radian Corporation
P.O. Box 9948
Austin, TX 78766

David Burre
Frito-Lay Inc.
7929 Brookriver Drive
Dallas, TX 75247

William Cain
U.S. Environmental Protection Agency
IERL-Ci
Cincinnati, OH 45268

Ivor E. Campbell
Smelter Control Research Association
150 E. Broad Street, Suite 310
Columbus, OH 43215

Robert B. Candelaria
Salt River Project
P.O. Box W
Page, AZ 86040

Robert Carr
Electric Power Research Institute
3412 Hillview Avenue, P.O. Box 10412
Palo Alto, CA 94303

Wallace A. Carter
KVB, Inc.
18006 Skypark Blvd.
Irvine, CA 92714

Carlo Castaldini
Acurex Corporation
555 Clyde Avenue, P.O. Box 7555
Mountain View, CA 94039

Paul R. Chaney
Mobil Chemical
One Greenway Plaza, Suite 1100
Houston, TX 77046

Charles S. Chang
Tosco Corporation
10100 Santa Monica Blvd.
Los Angeles, CA 90067

Steven S. Cherry
KVB, Inc.
P.O. Box 19518
Irvine, CA 92714

David Chorpening
Cleveland Electric Illuminating Company
P.O. Box 5000
Cleveland, OH 44101

M. Yaqub Chughtai
L & C Steinmüller GmbH
Postfach 1949/1960
D-5270 Gummersbach 1
WEST GERMANY

J. Edward Cichanowicz
Electric Power Research Institute
3412 Hillview Avenue
Palo Alto, CA 94303

Darryl D. Ciliberto
Tampa Electric Company
P.O. Box 111
Tampa, FL 33601

Clifford E. Clark
Exxon Nuclear Idaho Company Inc.
P.O. Box 2800
Idaho Falls, ID 83401

Peter E. Coffey
New York Power Pool
3890 Carman Road
Schenectady, NY 12303

Bob Collette
Combustion Engineering Inc.
1000 Prospect Hill Road
Windsor, CT 06095

John O. Copeland
U.S. Environmental Protection Agency
ESED (MD-13)
Research Triangle Park, NC 27711

Cheryl E. Cortright
Salt River Project
P.O. Box 1980
Phoenix, AZ 85001

William Cress
Allegheny Power Service Corporation
Cabin Hill Drive
Greensburg, PA 15601

John S. Cvicker
Foster Wheeler, Dept. C176
110 South Orange Avenue
Livingston, NJ 07039

Robert Dahlin
Southern Research Institute
P.O. Box 3307-A
Birmingham, AL 35255

Stuart Dalton
Electric Power Research Institute
3412 Hillview Avenue
Palo Alto, CA 94303

James Damon
Stearns-Roger Engineering Corporation
4500 Cherry Creek Drive
Denver, CO 80217

Lisa M. Daniels
Pennsylvania Power & Light
2 North 9th Street
Allentown, PA 18101

Kenneth L. Demerjian
U.S. Environmental Protection Agency
ESRL (MD-80)
Research Triangle Park, NC 27711

Bob DeRosier
Acurex Corporation
555 Clyde Avenue, P.O. Box 7555
Mountain View, CA 94039

Edward B. Dismukes
Southern Research Institute
P.O. Box 3307-A
Birmington, AL 35255

J. R. Donnelly
Bechtel Power Corporation
P.O. Box 2166
Houston, TX 77252-2166

Dennis C. Drehmel
U.S. Environmental Protection Agency
IERL (MD-62B)
Research Triangle Park, NC 27711

Owen W. Dykema
Rockwell International Energy Sys. Group
8900 DeSoto Avenue
Canoga Park, CA 91304

Henry T. Dziegiel
Department of Water & Power
111 North Hope Street, Room 667B
Los Angeles, CA 90051

Sherman Eaton
Coen Company, Inc.
1510 Rollins Road
Burlingame, CA 94010

John W. Eldridge
University of Massachusetts
Chemical Engineering Department
Amherst, MA 01003

Werner Emsperger
Kraftwerk Union A.G.
Hammerbacherstr. 12 + 14
8520 Erlangen
WEST GERMANY

David Eskinazi
Electric Power Research Institute
3412 Hillview Avenue
Palo Alto, CA 94303

Roger Etter
ARCO Petroleum Products Company
400 E. Sibley Blvd.
Harvey, IL 60430

Earl Evans
USDOE, Pittsburgh Energy Tech. Center
P.O. Box 10940
Pittsburgh, PA 15236

John E. Fairbanks
Babcock & Wilcox Company
20 South Van Buren Avenue
Barberton, OH 44203

John M. Ferraro
Exxon Research & Engineering Company
P.O. Box 101
Florham Park, NJ 07932

Blair A. Folsom
Energy & Environmental Research Corp.
18 Mason
Irvine, CA 92714

Louis B. Fournier
DuPont Company
Jackson Laboratory
Deepwater, NJ 08023

T. Fujimoto
Mitsui Miike Machinery Company
Mitsui Bldg., Nihonbashi Muromachi 2-1-1
Chuoku, Tokyo
JAPAN

K. Fujiyama
Electric Power Development Company, Ltd.
8-2 Marunouchi, 1-chome, Chiyoda-KU
Tokyo 100
JAPAN

Jim Gabrielson
Energy Systems Associates
2512 Chambers Road, Suite 101
Tustin, CA 92680

G. M. Gardetta
Southern California Gas Company
810 S. Flower Street
Los Angeles, CA 90017

Frederick C. Garman
U.S. Environmental Protection Agency
401 M. Street SW
Washington, DC 20560

Richard L. Gay
Rockwell International
8900 DeSoto Avenue
Canoga Park, CA 91304

James B. Gibson, Jr.
Tennessee Valley Authority
400 West Summit Hill Drive (W7D194)
Knoxville, TN 37902

Gerald B. Gilbert
Dynatech R/D Company
99 Erie Street
Cambridge, MA 02139

Lee K. Gilmer
Texaco USA
P.O. Box 1608
Port Arthur, TX 77640

Dan V. Giovanni
P.O. Box 990
Antioch, CA 94509

Harry A. Glander
Gilbert Associates, Inc.
P.O. Box 1498
Reading, PA 19603

Robert J. Gleason
Research-Cottrell, Inc.
P.O. Box 1500
Somerville, NJ 08876

John P. Gooch
Southern Research Institute
P.O. Box 3307-A
Birmingham, AL 35255

Alan Goodley
California Air Resources Board
P.O. Box 2815
Sacramento, CA 95812

Charles H. Goodman
Southern Company Services, Inc.
P.O. Box 2625
Birmingham, AL 35202

James R. Graham
Occidental Research Corporation
2100 S.E. Main Street, P.O. Box 19601
Irvine, CA 92713

Jack H. Greene
U.S. Environmental Protection Agency
IERL (MD-60)
Research Triangle Park, NC 27711

Robert E. Hall
U.S. Environmental Protection Agency
IERL (MD-65)
Research Triangle Park, NC 27711

Randy Hamilton
Texas Air Control Board
6330 Highway 290 East
Austin, TX 78723

Robert P. Hangebrauck
U.S. Environmental Protection Agency
IERL (MD-61)
Research Triangle Park, NC 27711

Joseph A. Harrington
Amoco Oil Company
P.O. Box 400 M/S H-9
Naperville, IL 60566

Marcus L. Hart
Cajun Electric Power Cooperative, Inc.
P.O. Box 15540
Baton Rouge, LA 70895

J. B. Headrick
Dallas Power & Light Company
1506 Commerce Street
Dallas, TX 75201

Michael P. Heap
Energy & Environmental Research Corp.
18 Mason
Irvine, CA 92714

Raymond Helion
ELF
BP 22
St. Symphorien D'Ozon 38200
FRANCE

Stuart Hersh
KVB, Inc.
175 Clearbrook Road
Elmsford, NY 10523

Scott Hill
Brigham Young University
270 Clyde Building
Provo, UT 84602

Deane A. Horne
Midland-Ross Corporation
900 N. Westwood
Toledo, OH 43696

Hann S. Huang
Argonne National Laboratory
9700 Cass Avenue
Argonne, IL 60439

S. C. (Kim) Hunter
KVB, Inc.
18006 Skypark Blvd.
Irvine, CA 92714

Boyd E. Hurst
Exxon Research & Engineering Company
P.O. Box 101
Florham Park, NJ 07932

Yung-Wo Jao
Ontario Hydro
700 University Avenue
Toronto, Ontario M5G 1X6
CANADA

Richard G. Johnson
Ventura Co. Air Pollution Control Dist.
800 South Victoria Avenue
Ventura, CA 93009

Stephen A. Johnson
Science Applications, Inc.
2011 Glamorgan Street
Alliance, OH 44601

Gary Jones
Radian Corporation
P.O. Box 9948
Austin, TX 78766

James Joubert
USDOE, Pittsburgh Energy Tech. Center
P.O. Box 10940
Pittsburgh, PA 15236

John Kayser
Chevron Research Company
576 Standard Avenue (Loc. 1651)
Richmond, CA 94802

John T. Kelly
Acurex Corporation
555 Clyde Avenue, P.O. Box 7555
Mountain View, CA 94039

Robert A. Kennedy
Texas Power & Light Company
P.O. Box 226331
Dallas, TX 75266

Stephen E. Kerho
KVB, Inc.
18006 Skypark Blvd.
Irvine, CA 92714

Harold A. Kerry
Southern California Edison Company
P.O. Box 800
Rosemead, CA 91770

John P. Kesselring
Alzeta Corporation
440 Clyde Avenue
Mountain View, CA 94043

Michael J. Kisha
Ohio Edison
76 South Main Street
Akron, OH 44308

Kent M. Kitchingman
U.S. Environmental Protection Agency
215 Fremont Street
San Francisco, CA 94105

William D. Knowles
Shell Oil Company
P.O. Box 3105
Houston, TX 77001

Bernard J. Koch
Conoco/Coal Research
4000 Brownsville Road
Pittsburgh, PA 15129

Angelos Kokkinos
Combustion Engineering
1000 Prospect Hill Road
Windsor, CT 06082

Michael D. Koplow
Thermo Electron Corporation
45 First Avenue
Waltham, MA 02254

J. D. Kuenzly
TRW EDG
One Space Park, R4/2158
Redondo Beach, CA 90277

Takeshi Kunimoto
Mitsubishi Heavy Industries, Ltd.
Shin-Tamachi Bldg., 34-6 Shiba, 5-chome 1
Minatoku, Tokyo
JAPAN

F. Richard Kurzynske
Gas Research Institute
8600 West Bryn Mawr Avenue
Chicago, IL 60559

David G. Lachapelle
U.S. Environmental Protection Agency
IERL (MD-62B)
Research Triangle Park, NC 27711

Howard Lange
KVB, Inc.
P.O. Box 19518
Irvine, CA 92714

W. Steven Lanier
U.S. Environmental Protection Agency
IERL (MD-65)
Research Triangle Park, NC 27711

Albert D. LaRue
Babcock & Wilcox Company
20 S. Van Buren
Barberton, OH 44203

George O. Layman
Gulf Power Company
P.O. Box 1151
Pensacola, FL 32520

Robert A. Lisauskas
Riley Stoker Corporation
P.O. Box 547
Worcester, MA 01613

Jack Don Lokey, Jr.
Tennessee Valley Authority
River Oaks Building
Muscle Shoals, AL 35660

Michael Lukasiewicz
Gas Research Institute
8600 West Bryn Mawr Avenue
Chicago, IL 60631

Kenneth L. Maloney
KVB, Inc.
P.O. Box 19518
Irvine, CA 92714

M. N. Mansour
KVB, Inc.
18006 Skypark Blvd., P.O. Box 19518
Irvine, CA 92714

Gregory A. Martel
Northeast Utilities Service Company
1866 River Road
Middletown, CT 06457

G. Blair Martin
U.S. Environmental Protection Agency
IERL (MD-62B)
Research Triangle Park, NC 27711

George V. Marusak
U.S. Environmental Protection Agency
1201 Elm Street
Dallas, TX 75270

Howard B. Mason
Acurex Corporation
555 Clyde Avenue, P.O. Box 7555
Mountain View, CA 94039

Charles C. Masser
U.S. Environmental Protection Agency
IERL (MD-62B)
Research Triangle Park, NC 27711

S. Matsushita
NGK-Locke, Inc.
767 Third Avenue
New York, NY 10017

James D. Maxwell
Tennessee Valley Authority
501 Chemical Engineering Building
Muscle Shoals, AL 35660

Mallory S. May
Gifford-Hill & Company, Inc.
8435 Stemmons Freeway
Dallas, TX 75247

Barry McDonald
Energy Systems Associates
2512 Chambers Road, Suite 101
Tustin, CA 92680

Michael W. McElroy
Electric Power Research Institute
3412 Hillview Avenue
Palo Alto, CA 94303

Richard D. McRanie
Southern Company Services, Inc.
P.O. Box 2625
Birmingham, AL 35202

John O. Milliken
U.S. Environmental Protection Agency
IERL (MD-62)
Research Triangle Park, NC 27711

Subroto Mitro
Potomac Electric Power Company
1900 Pennsylvania Avenue, NW
Washington, DC 20068

T. Miyasaka
Electric Power Development Company, Ltd.
8-2 Marunouchi, 1-chome, Chiyoda-ku
Tokyo 100
JAPAN

John E. Monacelli
Babcock & Wilcox Company
20 South Van Buren Avenue
Barberton, OH 44203

Ralph K. Mongeon
Riley Stoker Corporation
P.O. Box 547
Worcester, MA 01613

Keith A. Moore
Rockwell International
8900 DeSoto
Canoga Park, CA 91307

Shigeki Morita
Babcock-Hitachi K. K.
Kureworks 6-9, Takara-Machi
Kure-Shi, Hiroshima-Ken 737
JAPAN

Tom Morris
Babcock & Wilcox Company
1562 Beeson Street
Alliance, OH 44601

Per Morsing
A/S Niro Atomizer
305 Gladsaxevej, DK-2860 Soeborg
Copenhagen
DENMARK

Bernie G. Morton
KVB, Inc.
18006 Skypark Blvd., P.O. Box 19518
Irvine, CA 92714

William J. Morton
E. Keeler Company/Fiber Burner Division
238 West Street
Williamsport, PA 17701

Larry J. Muzio
KVB, Inc.
18006 Skypark Blvd.
Irvine, CA 92714

Robert Newell
Wisconsin Power & Light Company
222 W. Washington Avenue
Madison, WI 53701

Joseph T. Newman
Bechtel Group, Inc.
50 Beale Street
San Francisco, CA 94105

Hung D. Nguyen
UOP Process Division
20 UOP Plaza
Des Plaines, IL 60016

Grady B. Nichols
Southern Research Institute
P.O. Box 3307-A
Birmingham, AL 35255

William H. Nurick
Nurick and Associates
16 Willowbrook
Irvine, CA 92714

Daniel O'Leary
Rohm and Haas
P.O. Box 584
Bristol, PA 19007

Andrew T. O'Neill
Peabody Process Systems
5349 Amesbury, #407
Dallas, TX 75206

Raymond C. O'Sullivan
Orange and Rockland Utilities, Inc.
One Blue Hill Plaza
Pearl River, NY 10965

Shigeto Ohmine
Acurex Corporation
555 Clyde Avenue, P.O. Box 7555
Mountain View, CA 94039

James L. Olander
U.S. Environmental Protection Agency
1201 Elm Street
Dallas, TX 75270

Michael C. Osborne
U.S. Environmental Protection Agency
IERL (MD-65)
Research Triangle Park, NC 27711

Joseph H. Oxley
Battelle, Columbus Laboratories
505 King Avenue
Columbus, OH 43201

Roy Payne
Energy & Environmental Research Corp.
18 Mason
Irvine, CA 92714

David W. Pershing
University of Utah
Department of Chemical Engineering
Salt Lake City, UT 84112

Ellen Merrick Petrill
TRW
1 Space Park (MSR-2142)
Redondo Beach, CA 90278

Frances Phillips
U.S. Environmental Protection Agency
1201 Elm Street
Dallas, TX 75270

Bill Piske
Engineering Science
13740 Midway Drive
Dallas, TX 75234

Robert Ploss
Gibbs & Hill, Inc.
5501 LBJ Freeway
Dallas, TX 75080

John Pohl
Energy & Environmental Research Corp.
18 Mason
Irvine, CA 92714

Joseph Pullen
Air Quality State of Lousiana
P.O. Box 44066
Baton Rouge, LA 70804

Les J. Radak
Southern California Edison Company
P.O. Box 800
Rosemead, CA 91770

N. B. Rainer
Philip Morris
P.O. Box 26583
Richmond, VA 23261

Dee P. Rees
Utah Power & Light Company
P.O. Box 899
Salt Lake City, UT 84110

George Rey
U.S. Environmental Protection Agency
ORD-RD-681
Washington, DC 20460

Bruce W. Rising
Battelle, Columbus Laboratories
505 King Avenue
Columbus, OH 43201

J. Robert Rizza
Combustion Technology International
605 Stillson Road
Fairfield, CT 06430

Larry Rodgers
Babcock & Wilcox Company
1562 Beeson Street
Alliance, OH 44601

Demarest Romaine
Consolidated Edison Company
4 Irving Place
New York, NY 10003

Harvey S. Rosenberg
Battelle, Columbus Laboratories
505 King Avenue
Columbus, OH 43201

Abe Rosenstein
Engelhard Industries
2655 Route 22
Union, NJ 07083

Sam Ruggeri
American Electric Power Service Corp.
P.O. Box 487
Canton, OH 44701

Randall E. Rush
Southern Company Services, Inc.
P.O. Box 2625
Birmingham, AL 35202

Norman C. Samish
Shell Development Company
P.O. Box 1380
Houston, TX 77001

Henry Sanematsu
Los Angeles Dept. Water & Power
111 N. Hope Street
Los Angeles, CA 90051

Adel F. Sarofim
Massachusetts Institute of Technology
Department of Chemical Engineering
Cambridge, MA 02139

Robert W. Scheck
Stearns-Roger Engineering Corporation
4500 Cherry Creek Drive
Denver, CO 80217

C. E. Schleckser, Jr.
Exxon Research & Engineering Company
P.O. Box 101
Florham Park, NJ 07932

Herbert Schuster
Deutsche Babcock Werke AG
Duisburgerstrasse 375
D-4200 Oberhausen
WEST GERMANY

Phil Schwindt
U.S. Environmental Protection Agency
1201 Elm Street
Dallas, TX 75270

W. Randall Seeker
Energy & Environmental Research Corp.
18 Mason
Irvine, CA 92714

Chris Shafer
Riley Stoker Corporation
P.O. Box 547
Worcester, MA 01613

Gary H. Shiomoto
KVB, Inc.
P.O. Box 19518
Irvine, CA 92714

Eiji Shirakawa
Kobe Steel America Inc.
707 Wilshire Blvd., Suite 4300
Los Angeles, CA 90017

Dale E. Shore
KVB, Inc.
P.O. Box 19518
Irvine, CA 92714

W. Leigh Short
Environmental Research & Technology, Inc.
6666 Harwin Drive, Suite 600
Houston, TX 77072

James L. Shy
Allis Chalmers Corporation
1126 S. 70th Street
West Allis, WI 53214

Aziz A. Siddiqi
ARCO Petroleum Products Company
P.O. Box 2451
Houston, TX 77001

Terry D. Skidmore
Arizona Public Service
P.O. Box 21666, Station 1720
Phoenix, AZ 85036

Lowell L. Smith
KVB, Inc.
18006 Skypark Blvd.
Irvine, CA 92714

Terry Smith
Central Power and Light Company
P.O. Box 2121
Corpus Christi, TX 78403

Gerard de Soete
Institut Francais du Petrole
B.P. N 311
92506 Rueil-Malmaison Cedex
FRANCE

Todd M. Sommer
Babcock & Wilcox Company
20 South Van Buren Avenue
Barberton, OH 44203

John Stafford
Guaranty Performance
1120 E. Main
Independence, KS 67301

Seymour Stahl
Exxon Research & Engineering Company
60 Columbia Road, P.O. Box 390
Morristown, NJ 07960

Robert M. Statnick
Conoco/Coal Research
4000 Brownsville Road
Pittsburgh, PA 15129

N. J. Stevens
Research-Cottrell
P.O. Box 1500
Somerville, NJ 08876

Walter H. Stevenson
U.S. Environmental Protection Agency
(MD-13) ESED, OAQPS
Research Triangle Park, NC 27711

Bob Strain
Environment Reporter
1231 25th Street, NW
Washington, DC 20037

Joseph Strakey
U.S. Department of Energy
P.O. Box 10940
Pittsburgh, PA 15236

John O. Sudbury
CONOCO
4000 Brownsville
Library, PA 15129

Rick Sugarek
U.S. Environmental Protection Agency
215 Fremont Street
San Francisco, CA 94105

Henry R. Sung
Caltex Petroleum Corporation
125 East John Carpenter Freeway
Irving, TX 75062

Donald P. Teixeira
Pacific Gas & Electric
3400 Crow Canyon Road
San Ramon, CA 94583

Laurence R. Thomas
Johnson Matthey Inc.
1401 King Road
West Chester, PA 19380

Jack T. Thompson
Tennessee Valley Authority
705 Edney Building
Chattanooga, TN 37401

Paul F. Thompson
KVB, Inc.
3131 Briarpark Drive, Suite 250
Houston, TX 77042

Richard E. Thompson
KVB, Inc.
18006 Skypark Blvd.
Irvine, CA 92714

Kimishiro Tokuda
Mitsubishi Heavy Industries, Ltd.
1000 Prospect Hill Road
Windsor, CT 06095

Robert S. Truesdale
Research Triangle Institute
P.O. Box 12194
Research Triangle Park, NC 27709

Robert E. Trumbule
Congressional Research Service
Library of Congress, CRS/ENR
Washington, DC 20540

Arthur Y. Tso
Mobil Research and Development Corp.
P.O. Box 1026
Princeton, NJ 08540

K. Tsuji
Mitsui Mining Company
808 Hibikimachi, Wakamatsu
Kitakyushu City, Fukuoka Pref.,
JAPAN

Thomas K. Turner
Turner Engineering
P.O. Box 47004
Dallas, TX 75247

Richard M. Vaccaro
Exxon Research & Engineering Company
180 Park Avenue, Bldg. 102, C474
Florham Park, NJ 07932

Joel Vatsky
Foster Wheeler Energy Corporation
9 Peach Tree Hill Road
Livingston, NJ 07039

J. Veurink
Stork Boilers
P.O. Box 20
7550 GB. Hengelo
THE NETHERLANDS

Donald F. Walters
U.S. Environmental Protection Agency
OAQPS (MD-11)
Research Triangle Park, NC 27711

Hsuan-Hsien Wang
Union Carbide Corporation
P.O. Box 8361
South Charleston, WV 25303

Shih-Chung Wang
Bechtel Group, Inc.
50 Beale Street
San Francisco, CA 94105

John H. Wasser
U.S. Environmental Protection Agency
IERL (MD-65)
Research Triangle Park, NC 27711

Larry R. Waterland
Acurex Corporation
555 Clyde Avenue, P.O. Box 7555
Mountain View, CA 94039

Alexander Weir, Jr.
Southern California Edison Company
P.O. Box 800
Rosemead, CA 91770

David Wethington
Texas Power & Light Company
Box 226331
Dallas, TX 75266

Horace Whaley
CDN Combustion Research Laboratory
555 Booth Street
Ottawa, Ontario K1A0G1
CANADA

John Williams
USDOE, Pittsburgh Energy Tech. Center
P.O. Box 10940
Pittsburgh, PA 15236

Robert P. Wilson
Arthur D. Little, Inc.
Acorn Park
Cambridge, MA 02140

Cynthia M. Wood
Union Camp Corporation
Franklin, VA 23851

Dennis L. Wright
Texas Electric Service Company
P.O. Box 8368
Fort Worth, TX 76112-0368

Robert E. Yang
KVB, Inc.
18006 Skypark Boulevard
Irvine, CA 92714

Rick Yeh
Black, Sivalls & Bryson
8303 Southwest Freeway
Houston, TX 77074